THE EFFECT OF VAPOR GROWN CARBON NANOFIBER-MODIFIED ALKYD PAINT COATINGS ON THE CORROSION BEHAVIOR OF MILD STEEL

By

Sahar Mohamed Hassan Atwa

A Dissertation
Submitted to the Faculty of
Mississippi State University
in Partial Fulfillment of the Requirements
for the Degree of Doctor of Philosophy
in Chemistry
in the Department of Chemistry

Mississippi State, Mississippi

May 2010

THE EFFECT OF VAPOR GROWN CARBON NANOFIBER-MODIFIED ALKYD PAINT COATINGS ON THE CORROSION BEHAVIOR OF MILD STEEL

By

Sahar Mohamed Hassan Atwa

Approved:

David O. Wipf Professor of Chemistry (Director of Dissertation)	Charles U. Pittman, Jr. Professor Emeritus of Chemistry (Committee Member)
William P. Henry Associate Professor of Chemistry (Committee Member)	Steven Gwaltney Associate Professor of Chemistry (Committee Member)
Kang Xia Assistant Professor of Chemistry (Committee Member)	Stephen C. Foster Associate Professor of Chemistry and Graduate Coordinator
Gary Myers Dean of the College of Arts and Sciences	

Name: Sahar Mohamed Hassan Atwa

Date of Degree: May 01, 2010

Institution: Mississippi State University

Major Field: Chemistry

Major Professor: Dr. David O. Wipf

Title of Study: THE EFFECT OF VAPOR GROWN CARBON NANOFIBER-MODIFIED ALKYD PAINT COATINGS ON THE CORROSION BEHAVIOR OF MILD STEEL

Pages in Study: 454

Candidate for Degree of Doctor of Philosophy

Vapor grown carbon nanofibers (VGCNFs) are a class of carbon fibers that are produced by catalytic dehydrogenation of a hydrocarbon at high temperatures. Depending on the method of synthesis and the post-treatment processes, the diameter of the VGCNFs is normally in the 10-300 nm range. The small size, light weight, high aspect ratio, and unique physical, thermal, mechanical, and electrical properties of VGCNF make it an ideal reinforcing filler in organic coatings and polymer matrix nanocomposites.

The main objective of the current investigation was to study the corrosion protection offered by the incorporation of VGCNFs into a commercial alkyd paint matrix applied to the surface of mild steel coupons. The corrosion protection was investigated by immersing samples in 3% NaCl solution. The samples were studied by electrochemical impedance spectroscopy (EIS) along with other measurements, including electrochemical

(open circuit potential, cyclic voltammetry), chemical (salt spray test), electrical conductivity, and surface analysis techniques.

The study involved the investigation of the effect of the weight percent (wt %) of the VGCNF as well as the coating film thickness on the corrosion protection performance of the coated steel samples when exposed to the corrosive electrolyte. By way of contrast, the EIS behavior of steel coupons coated with a paint coating incorporating different weight percents of powdered silicon carbide (SiC) particles was also studied.

The electrical conductivity measurements showed that the incorporation of the VGCNFs or SiC microparticles in the alkyd paint formulation significantly enhances the electrical conductivity properties imparted by the coating. The nanoindentation measurements showed that the incorporation of VGCNF in the paint matrix improves the hardness up to 3%. On the other hand, increasing the SiC content improves the hardness of the paint matrix at all levels tested. The chemical and electrochemical measurements showed that VGCNF- and SiC-reinforced coatings are more stable than pure paint coatings.

Overall, the incorporation of a small amount of VGCNFs or SiC microparticles leads to significant improvements in the barrier properties of the paint matrix. Based on their anticorrosive properties, the three coatings systems are ranked as follows: VGCNF-reinforced coatings > SiC-reinforced coatings > pure paint coatings.

KEYWORDS:

Electrochemical impedance spectroscopy (EIS), mild steel, alkyd paints, organic coatings, vapor grown carbon nanofibers (VGCNFs), silicon carbide (SiC) particles, conductive polymers (CPs), open circuit potential (OCP), corrosion, corrosion protection, accelerated corrosion testing, salt spray test

DEDICATION

This work is dedicated to my mother, Mrs. Tawheeda Abbas. It is also dedicated to the souls of my father, Mr. Mohamed Atwa, and my mother-in-law, Mrs. Kareemah Kassem, may Allah have mercy on their souls.

ACKNOWLEDGEMENTS

First and foremost, I am deeply thankful and grateful to Allah, the Most Gracious, the Most Merciful, for his countless and endless blessings and bounties he (S.W.T.) has bestowed upon me and my family.

The list of people that I need to acknowledge in this work is very long. However, time and space constraints limit me to but some people who have been essential to my life and I wish to acknowledge their help at this time.

I wish to express my sincere appreciation to my advisor, Dr. David Wipf, for his guidance, encouragement, patience, and support throughout my graduate studies. I am deeply honored and extremely fortunate to have worked with him.

I would also like to extend my thanks to the members of my doctoral committee: Dr. Charles Pittman, Jr., Dr. William Henry, Dr. Steven Gwaltney, and Dr. Kang Xia for their priceless advice, comments, and suggestions. Your assistance in completing this work is greatly appreciated.

Special thanks go to Dr. Stephen Foster for his help with the administrative issues throughout my graduate studies. I also feel indebted to him for donating his time and effort to solve a time conflict issue with my dissertation defense.

I am also thankful to Dr. Pat Donohoe from the Department of Electrical and Computer Engineering for his help with the conductivity measurements. Many thanks are

also due to Richard Kuklinski from the Electron Microscope Center (EMC) for his assistance with the SEM imaging.

Special thanks are due to Dr. Haitham El Kadiri from the Department of Mechanical Engineering and Dr. Youssef Hammi from the Center for Advanced Vehicular Systems (CAVS) for their help with the surface hardness and nanoindentation measurements.

I would also like to express my gratitude and appreciation to my colleague Ekta Goel. Many thanks for her for friendship, invaluable help, support, and encouragements.

A very special expression of gratitude and appreciation is extended to Dr. El Barbary Hassan from the College of Forest Resources for his countless effort and time he dedicated in helping me with the paperwork especially in the final phase of this work. His sincere help saved me a lot of time and trouble.

I would also like to express my deepest affection and appreciation to my best friend Abeer Youssef who is as dear to me as my blood sister. Many thanks for her for friendship, hospitality, invaluable help and advice, support, and encouragements.

I would also like to express my indebtedness, deepest affection and appreciation to my mother for her endless love, encouragement, support, patience, and supplications throughout all the years I have been away from her. Without her support and encouragement, I would not have been able to finish this work.

I also acknowledge my father-in-law Mr. Mohamed El-Giar; my sister Azza and my brothers Jamal and Wael as well as their families for their limitless kindness and unfailing support throughout my graduate studies.

Finally, my deepest affection and gratitude are owed to my husband Emad, and my beloved children Ahmed, Dena, Dalia, and Kareem for their love, support, and sacrifice throughout this work. Without their love and help this endeavor would not have been possible.

TABLE OF CONTENTS

Page

LIST OF TABLES

LIST OF FIGURES

LIST OF ABBREVIATIONS AND SYMBOLS

Abb.*	Meaning	Abb.*	Meaning
A_d	Delaminated area	PANI	polyaniline
AC (ac)	Alternating current	R	Resistance
AFM	Atomic force microscope (microscopy)	R_{ct}	Charge transfer or polarization resistance of a polymer-coated substrate
C	Capacitance	$R_{ct}°$	Charge transfer resistance of an uncoated metal
C_o	Capacitance of dry coating	RE	Reference electrode
C_c	Coating capacitance	R_f	Carbon fiber resistance
C_{dl}	Double layer capacitance	R_p	Polarization resistance
$C_{dl}°$	Double layer capacitance of an uncoated metal	R_Ω	Ohmic (solution) resistance
CB	Carbon black	SCE	Saturated calomel electrode
CPs	Conductive polymers	SECM	Scanning electrochemical microscopy
CPE	Constant phase element	SEM	Scanning electron microscopy (microscope)
CV	Cyclic voltammetry (voltammogram)	SWNT	Single wall nanotube
D	Diffusion coefficient	VGCNF	Vapor grown carbon nanofiber
DC (dc)	Direct current	X	Reactance
E	Potential	XDS	X-ray diffraction spectroscopy
E_{ss}	Steady-state potential	Z	Impedance
EDS	Energy dispersive X-ray spectroscopy	Z_{im}	Reactive or imaginary component of the impedance
EIS	Electrochemical impedance spectroscopy	Z_r	Resistive or real component of the impedance
f	Frequency	ε	Dielectric constant of the coating
j	$\sqrt{-1}$	ε_0	Dielectric constant of vacuum
MWNT	Multi-walled nanotube	θ	Phase angle lag between perturbation and response
OCP	Open-circuit potential	ω	Angular frequency (= $2\pi f$)

*Abb. = abbreviation

CHAPTER 1

INTRODUCTION

1.1 Importance of Corrosion and Corrosion Control

Corrosion is defined as the involuntary deterioration and destruction of a substance (usually metal, alloy, or a mineral building material) or its properties as a result of its chemical or electrochemical interaction with its corrosive environment.[1-3] Corrosion is a very serious problem and is responsible for enormous economic losses all over the world.[4-6] It has a serious impact on all society on a daily basis, causing dangerous and expensive degradation and damage to everything including household appliances; automobiles; buildings; bridges; nuclear power and solar energy production and distribution systems; drinking water and sewage systems; underground oil pipeline systems; aircraft industry; pulp and paper industry; fertilizer plants; air pollution control systems; decorative platings; offshore and marine equipment; dairy and food industry; and much more.[1, 4, 7] Economic losses due to corrosion are quite high and are divided into direct losses, and indirect losses.[3] Direct losses due to corrosion include the costs of replacing, repainting, or modifying corroded parts or equipment while indirect losses include losses due to shutdown of plants and companies during maintenance periods. Although direct losses can be roughly estimated, indirect losses due to corrosion are difficult to estimate.[3, 5]

According to a report by the National Bureau of Standards (NBS), the estimated economic cost of direct and indirect corrosion in the United States (U.S.) in 1985 alone was $167 billion.[8, 9] A more recent study conducted in 1995 by NACE International (Figure 1.1) estimated the direct economic losses due to metallic corrosion in the U.S. to be $276 billion per year (about 3.1% of the U.S. Gross National Product (GNP)).[10] For other industrialized countries such as Canada, United Kingdom, Japan, and Australia, the cost of corrosion was estimated to be 3.0-5.0% of the GNP.[3, 4, 7, 10-12] These figures, when put into monetary terms, will lead to staggering amount of money which reflects the tremendous economic loss due to corrosion. Moreover, this huge cost is substantially escalating due to the fast growing industrialization, high energy costs, worldwide shortage of construction materials, and huge infrastructures required in polluted and corrosive environments especially in vital fields such as the oil production and refinery, and automotive industries.

The surveys on the causes of corrosion damages and failure have shown that over 40% of the damages and failures are due to improper selection of the metal or alloy, ineffective design measures, and non-use of efficient and durable protective coatings. Although corrosion is inevitable and cannot be completely eliminated, corrosion scientists and engineers believe that most of the causes of corrosion failure can be avoided and the cost of corrosion can be substantially reduced by the following: (i) use of optimum corrosion management practices, and (ii) use of proper corrosion prevention and protection techniques. Optimum management practices include: better understanding of

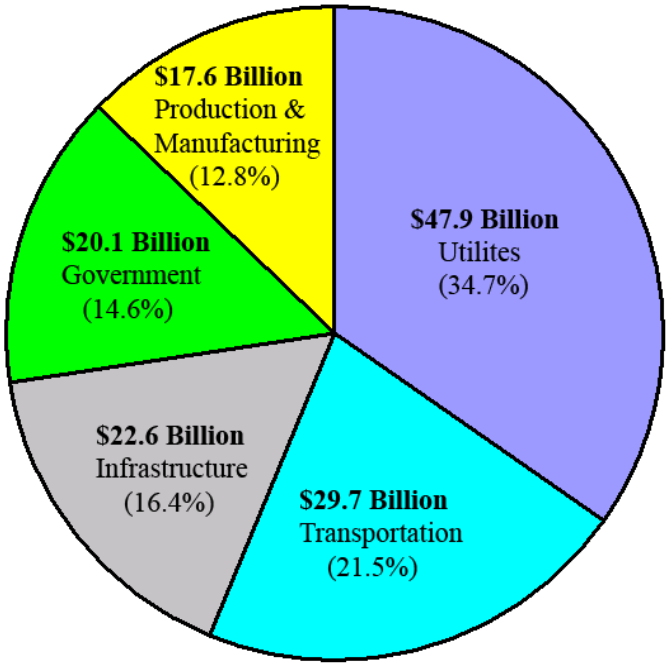

Figure 1.1 The annual corrosion cost per analyzed sector in the USA in 2001. The total corrosion cost was estimated to be $276 billion/year. (Adapted from Ref. No. 10)

the corrosion mechanisms; proper design and selection of materials for specific application; and good maintenance of equipment.

Corrosion protection techniques include cathodic protection;[13, 14] anodic protection;[15, 16] chemical modification of the corrosive environment (e.g., increasing the electrolyte pH or adding corrosion inhibitors and passivators);[17-21] use of microorganisms (e.g., bacteria);[22-25] use of pure or modified organic, inorganic, and metallic coating systems;[26-36] and the use of organic-inorganic hybrid materials.[1, 3, 37-39] Accordingly, most of the current research in the field of corrosion is directed toward the synthesis of corrosion resistant alloys as well as composite materials; synthesis of new chemical compounds that behave as better inhibitors or passivators better than the current inhibitors; and the development and testing of new, nontoxic, environmentally friendly, and better corrosion resistant paints.[40-48]

1.2 Corrosion of Iron and Carbon Steel Alloys

Iron and steel alloys are the most common and extensively used category of metallic materials worldwide. This is mainly due to their low manufacture cost. In addition, these materials offer a wide range of mechanical properties.[49, 50] Another advantage of steel alloys is that they can be produced to meet a wide range of applications through the control of the concentration of alloying elements.[51, 52] Accordingly, iron and steel alloys have been the major materials for the construction of structural features such as ships and offshore structures, bridges, buildings, oil and gas pipelines, railroad equipment, automobiles, and aircrafts.[53-55]

Mild steels or low-carbon steels are iron alloys containing 0.10 to 0.25% carbon content.[50] These alloys are the cheapest steels, have high strength, high hardness, superior formability, and are considered the most important engineering alloys.[50] Mild steels represent more than 90% of the total amount of steel shipped in the United States.[50, 54]

As a result of the economic importance of iron and steel alloys, it is not surprisingly that most of the corrosion losses are due to the corrosion of these alloys.[56] Corrosion usually starts naturally at any defective, damaged, or bare area on the surface of a metal or alloy. Anodic oxidation reactions start at these sites. Thus, at an anodic site on the surface of iron or carbon steel exposed to natural atmosphere, the following anodic reaction takes place:[1, 54, 56-58]

$$Fe \rightleftharpoons Fe^{2+} + 2e^{-} \quad (1.1)$$

This reaction is very rapid in most media. Thus, when iron or steel corrodes, the rate of corrosion is controlled by the much slower cathodic (reduction) reaction.

In the absence of oxygen, the hydrogen ion (H^+) reduction reaction is the main cathodic reaction in most of the corrosion reactions:

$$2H^{+} + 2e^{-} \rightleftharpoons H_2 \quad (1.2)$$

The accumulation of H_2 at the cathode would slow the process due to the depletion of H^+ at the cathode. However, the presence of oxygen (either from the atmosphere or dissolved in water) in aerobic corrosive media acts as a cathodic depolarizer and usually accelerates the reduction of H^+

$$2H^{+} + \tfrac{1}{2}O_2 + 2e^{-} \rightleftharpoons H_2O \quad (1.3)$$

Also,

$$H_2O \rightleftharpoons H^+ + OH^- \quad (1.4)$$

Adding equations 1.1, 1.3, and 1.4 gives:

$$Fe + \tfrac{1}{2}O_2 + H_2O \rightleftharpoons Fe(OH)_2 \quad (1.5)$$

Ferrous hydroxide is further oxidized to a hydrated ferric oxide as:

$$Fe(OH)_2 + O_2 \rightleftharpoons 2Fe_2O_3 \bullet H_2O + 2H_2O \quad (1.6)$$

For long term exposure of iron to natural atmosphere, the final corrosion product is ferric oxyhydride (orange-red to brownish-red in color) according to the following equation:

$$4Fe + 3O_2 + 2H_2O \rightleftharpoons 4FeOOH \quad (1.7)$$

$Fe_2O_3 \bullet H_2O$, and FeOOH constitute the main corrosion products (also referred to as rust) of iron and steel alloys and their formation means failure of the metal or the alloy. However, Equations 1.5 through 1.7 show that both water and dissolved oxygen (called the corrodents) is necessary for the corrosion of iron and mild steel alloys.[59]

1.3 Corrosion Protection by Organic Coatings

Several methods and techniques have been used to prevent or inhibit corrosion of metals and alloys. Among these methods are the following: selection of the proper metal or alloy for a particular corrosive service; changing the environment; control of the pH of the corrosive medium; use of proper inhibitors; modifying the designs of systems; use of cathodic or anodic protection; and use of barrier coatings.[15, 19, 60-73]

Paints, varnishes, lacquers, resins, glass coatings (e.g., vitreous enamels, glass linings, porcelain enamels), noble and sacrificial metal coatings, phosphate coatings, and other coatings have become among the most common, cost-effective methods to provide good corrosion protection against corrosive species and improve the durability as well as lifetime of metals and engineering alloys.[40, 56, 74] They are currently used in several industries including the aircraft, automotive, military equipment, and food and beverage packaging industries.[75, 76] As shown in Table 1.1, coatings are generally classified into four different groups, namely organic, inorganic, chemical conversion, and metallic coatings.[74, 77-79]

Coatings are applied either on the internal or external surfaces of metals and alloys to introduce a barrier to ionic transport and electrical conduction through the substrate surface. When applied to the internal surfaces of metals (e.g., when used as interior linings for food and beverage cans), the coatings provide corrosion protection for the substrate and flavor protection for the contents. On the other hand, when applied to external surfaces, coatings protect the substrate and improve its durability against atmospheric corrosion.[34]

If a thick and perfect barrier layer of paint or a coating is applied to a metal or alloy surface exposed to a corrosive environment, then neither water nor oxygen can reach the substrate surface and hence corrosion will be prevented. The performance and service life (durability) of any coating system depends mainly on the coating thickness, its physical and chemical properties, the surface characteristics of the metal substrate, the surface pretreatment, and the nature of the surrounding atmosphere.[62, 80]

Table 1.1 Classes of coatings.*

Organic Coatings	Inorganic Coatings	Chemical Conversion Coatings	Metallic Coatings
Phenolics	Glass	Molybdate	Electroplating
Acrylics	Silicates	Chromate	Vacuum vapor deposition
Urethanes	Ceramics	Anodizing	Galvanizing
Polyvinyls		Phosphating	Diffusion
Coal tars			
Epoxy			
Alkyds			
Polyethylene			

*Modified from Ref. No. 74.

Among the four classes of coatings, organic coatings have gained an increased interest in several industries over the past two decades especially for use as protective coatings for a wide range of metals and engineering alloys in many industries including the automotive, aircraft, domestic products and food packaging, marine, crude oil, building trade, and wastewater treatment industries.[29, 31, 56, 77-79, 81-88] This is mainly because organic coatings are corrosion resistant and easy to apply to various surfaces at a reasonable cost.[34, 59, 89] Organic coatings are typically highly resistant to ionic as well as water penetration, thus inhibiting the diffusion of ions and water to and from the substrate surface. Accordingly, the use of organic coatings to reduce the rate of corrosion of metals and engineering alloys has increased tremendously during the last decade. For example, in 1986,[1] it was estimated that the U.S. spends $2 billion per year on organic coatings, while in 2002, according to the *Current Industrial report-Paint and Coating Manufacturing*, the value of shipments of paint and allied coating products in the U.S. was $17.5 billion which increased to $19.9 billion in 2005.[56, 90]

In addition to their use with metals and alloys, organic coatings have also been applied to other substrate materials such as woods, plastics, composites, and ceramics. In addition, the use of organic coatings is not limited to the corrosion protection of the substrate, but they have also been applied for other purposes such as decorative or aesthetic appearance,[91, 92] packaging,[93-95] and electronic as well as other functional applications.[56, 96-98]

The basic constituents of any organic coating are binder, pigments, additives and fillers, and solvent. In addition, organic coating formula may contain corrosion inhibitors

to enhance the corrosion protection of the metal substrate.[59, 99] All of these components act together to provide good adhesion to the substrate surface, hinder the permeation of water and electrolytes, and increase the mechanical and electrical resistance of the coating, thus providing corrosion protection to the substrate against wear, abrasion, and corrosion attack by corrosive chemicals and/or atmospheric conditions for the longest possible time. A detailed discussion about the properties and functions of the components of organic coatings is beyond the scope of this dissertation. However, for further information, several specific references are available.[100-106]

Unfortunately, all paints and organic coatings are porous and permeable to oxygen and water to some degree and through-thickness microvoids and defects in the coatings cannot be avoided even for thick coatings.[3] Moreover, even if they are free of defects when new, organic coatings tend to become damaged during shipment or during the service life. Accordingly, pure paints and coatings are not perfect barriers against corrosion and eventually fail either through existing pinholes, craters, and other defects or sites of damage. Corrosion of coated metals starts by diffusion of corrodents through these defects followed by loss of adhesion then attack of the metal. For this reason, it is highly desirable to find other methods to improve the corrosion protection of the organic coatings. For this purpose, several methods have been investigated including:[107, 108]

(i) Incorporation of nano-sized or platelet-shaped barrier pigments (e.g., platy talcs, mica, glass flakes, micaceous iron oxides such as Fe_2O_3, leafed or regular Al, graphite, carbon black, TiO_2 nanoparticles, steel nanoparticles, Pb dust, Ca ferrite, Zn nanoparticles, SiC nanoparticles, and other metal flake pigments) into the organic coating

to reduce the permeability of the coating.[109-124] When mixed with the organic coatings, these pigments, after curing, tend to overlap and form several layers, thus creating longer and indirect pathways for the corrodents (water, oxygen, electrolytes) to go through before reaching the metal surface (Figure 1.2), thus reducing the rate of metal corrosion, and hence improving the barrier properties of the metal substrate.[59, 120-124] When dispersed in a polymer matrix as fillers or accessory ingredients, these pigments not only improve the barrier properties of the host matrix, but also improve the coating's mechanical strength, rheological property, and light resistance.[110, 125-128]

Surveying the literature shows that the properties of the host matrix depends on the weight percent of the added conductive filler.[129, 130] The literature data also shows that there is a threshold weight percent for the filler, above which the properties (e.g., the electrical conductivity) of the host matrix deteriorate. This threshold value depends on both the type of the conductive filler and the polymeric composite in which the filler is dispersed.[130] For example, the threshold value is about 7.5% for epoxy resins containing Fe[130] and 20-40% for epoxy resins reinforced with Ag, Sn, Pb, Cu, or Al.[131, 132] The threshold value is 5-6% for Cu particles in polyvinyl chloride[133] and Ni in polyethylene[134] while it is 1% and 8% for CB in polyvinyl alcohol,[110] and Araldite D,[135] respectively. The threshold value is 37% for Ag particles in Bakelite powder.[136]

(ii) Incorporation of sacrificial cathodically protective pigments into the coatings.[137-140] Usually these pigments contain zinc metal which acts as a sacrificial anode where it (Zn) dissolves in preference to the metal (e.g., iron) thus protecting the metal surface.

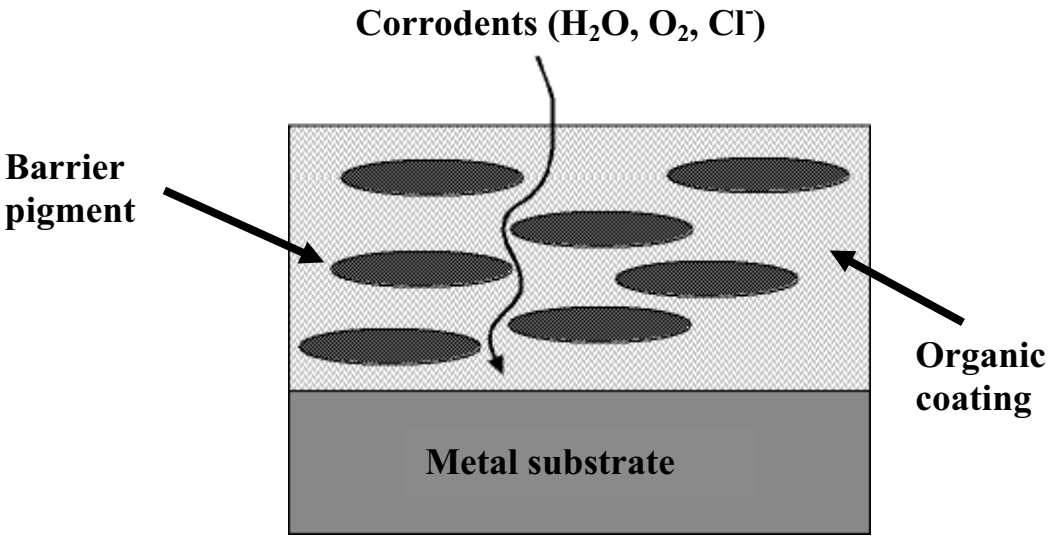

Figure 1.2 Effect of barrier pigments on the path of the corrodents (H_2O, O_2, and aggressive ions) on the barrier and passivation properties of an organic coating. (Modified from Ref. No. 59).

(iii) Use of organic corrosion inhibitors.[141-145] A wide range of organic compounds have been investigated for use as corrosion inhibitors including aromatics, amines, organic acids, nitrogen- and sulfur-containing compounds, and many other heterocyclic compounds.[146] When incorporated in the coatings, these inhibitors reduce the corrosion process by forming a passivating layer that either passivates the anodic or cathodic sites on the metal surface. These inhibitors can also show their protective action through the formation of a barrier layer that covers the entire metal surface. In either case, the incorporation of inhibitors into the coatings improves the corrosion resistance of the coating and prevents the corrodents from reaching the metal surface.

(iv) Addition of anticorrosive pigments into the coatings.[123, 147-152] This is the most commonly used method for improving the corrosion protection of organic coatings. These pigments show their protective action through their reaction with absorbed water in the coating and releasing inhibitive ions that penetrate the coating and reach the metal surface to passivate it with an inorganic layer.[42, 153] This family of inhibitive pigments is divided into oxidizing (e.g., chromates) and non-oxidizing (e.g., phosphates and molybdates) pigments. Non-oxidizing pigments require the presence of oxygen to show their inhibitive action while oxidizing ones do not. Although chromate and lead based pigments are the best corrosive resistant pigments; recently, there has been an interest for the replacement of these toxic pigments with low-toxic pigments such as phosphate, borate, and phosphosilicate pigments. However, although these pigments are less toxic, they show a much lower corrosion protection performance as compared with that of lead and chromate based pigments.

Currently, research is on going for the evaluation of new additive candidates that can be incorporated into the formulation of a coating to improve the corrosion resistance of the coating.[154, 155] In addition to offering excellent corrosion protection, these candidate additives should be inexpensive and environmentally friendly. They should also be able to be incorporated in a wide range of organic coatings, and improve the mechanical as well as the chemical properties of the pure coatings.

In the present study, and for the first time, the electrochemical impedance spectroscopy (EIS) technique was used to evaluate the corrosion behavior of mild steel samples coated with a layer of a commercial paint containing a known weight percent (wt %) of VGCNF. With its unique physical, electrical, and mechanical properties (vide infra), it anticipated that VGCNF would improve the barrier properties of the pure alkyd paint coatings. For comparison, the study also included the EIS behavior of steel samples coated with the paint containing a known weight of SiC powder. The EIS experiments were conducted in aqueous solutions of 3% NaCl in water at room temperature. This solution was chosen as the immersion electrolyte because it imitates an industrial atmospheric environment.[156]

The aim of the present work was to evaluate the effect of incorporation of VGCNF in the commercial paint matrix on the protective properties of the coatings applied to the surface of the mild steel. The barrier properties of both pure and VGCNF-incorporated coatings have been investigated using the EIS technique along with other electrochemical measurements such as cyclic voltammetry (CV) and open circuit potential (OCP) measurements. In addition, the investigation involved accelerated

corrosion studies (salt spray test), electrical conductivity measurements, surface analysis measurements (e.g., SEM, optical profilometery) and mechanical measurements (nanoindentation).

1.4 Mechanism of Protection by Organic Coatings

Many researchers have investigated the mechanism of the corrosion protection provided by organic or inorganic coatings applied to the surfaces of metals or alloys.[157-164] It is now well known that the degradation of a coated metal occurs along the metal/coating interface and usually starts as a localized corrosion at the defects in the coating which provide contact between the metal and the corrosive electrolyte.[80, 165] Thus, for a coated metal or alloy to corrode, the following five elements are required: (i) an anodic site on the metal surface (e.g., a defect in the coating) for the anodic dissolution to occur, (ii) a cathodic site, (iii) an electrolyte (e.g., water), (iv) oxygen or another reducible species, and (v) an electrolytic path between the cathode and anode.

The corrosion process occurring for a metallic substrate beneath a coating is similar to that occurring for a bare uncoated substrate. However, for a coated substrate, the following steps are involved in the corrosion process before the deterioration of the metal substrate occurs: (i) diffusion of corrodents (oxygen, water, ions) through the coating, (ii) development of an aqueous layer at the coating/substrate interface, (iii) initiation of the anodic and cathodic reaction on the substrate surface, and (iv) damage of the bonds at the substrate/coating interface.[74]

Accordingly, the role of a good protective coating is to reduce the rate of the corrosion of the metallic substrate through limiting or eliminating the effect of any of the above mentioned elements or steps. Organic coatings offer protection through the following mechanisms:

(i) Providing a thick protective barrier against the transport of aggressive substances, water, oxygen, and soluble salts.

(ii) Creating a highly resistive electrolytic path between the anode and the cathode.

(iii) Providing a sacrificial anode for the dissolution reaction

(iv) Providing a passive layer with soluble pigments

1.5 Diffusion Phenomena in Organic Coatings

As mentioned earlier, the atmospheric corrosion of a coated metal or alloy starts at the defects in the coating in the presence of both water and oxygen.[31, 56, 59, 74] In addition, the presence of soluble salts and aggressive ions, such as chloride ions, significantly accelerate the rate of corrosion.

1.5.1 Oxygen Diffusion

In aerated neutral solutions, the oxygen reduction is usually the cathodic reaction in a corrosion reaction:

$$\tfrac{1}{2}O_2 + H_2O + 2e^- \rightleftharpoons 2OH^- \qquad (1.8)$$

The above cathodic reaction occurs at the metal surface. Therefore, oxygen permeation through the coating is a must for the initiation and propagation of corrosion at the metal surface underneath the coating.[166]

Several authors have determined the oxygen permeability in different organic coatings and paint films including epoxy resins, alkyd, and rubber films. The studies showed that the oxygen permeability through these organic coatings is in the range of 1.0×10^{-8} - 4.0×10^{-6} L/cm^2/d.[167] It has been determined that although the oxygen transport is a crucial step in the corrosion of the metal beneath the coating, this step is not the rate-determining step in the corrosion reaction of a coated system.[161, 167-169] Moreover, studies showed that the amount of oxygen necessary for steel corrosion to occur at a rate of 70 mg Fe/cm^2/year is 30 mg/cm^2/yr which is much less than the amount of oxygen that can diffuse through the organic coating.[170] A review on the oxygen transport through organic coatings is available.[88]

1.5.2 Water Diffusion

As mentioned earlier, the main electrochemical corrosion reaction is the cathodic reduction of oxygen (as shown in Equation1.5), in the presence of water, along with the localized anodic dissolution of the metal substrate.[59, 78, 89, 171]

Water permeation through organic coatings occurs mainly due to the strong adsorption forces between the water molecules and the paint. The studies on the diffusion of water through organic coatings have shown that the average amount of water that can

diffuse through an organic coating with a reasonable thickness is always greater than the amount of water necessary for corrosion to occur.

Similar to the oxygen diffusion, the amounts of water necessary for steel corrosion to occur at a rate of 70 mg Fe/cm^2/yr was estimated to be 11 mg/cm^2/yr.[170] The studies also showed that water diffusion is not the rate-determining step in the corrosion process of coated metals and alloys.

Recent studies on the corrosion behavior of coated steel have shown that the degree of protection against corrosion is not only controlled by the barrier and passivation properties of the coating film but also by other factors such as the electrical conductivity of the coating as well as the strength of the adhesion forces between the coating and the substrate.[40, 172-180] In this regard, when exposed to corrodents, coatings with poor adhesion would grow blisters on the metal surface faster and hence deteriorate at a higher rate than coatings with good adhesion.[31, 56, 59, 181, 182]

1.6 Testing the Stability of Organic Coatings

The stability and durability of organic coatings are evaluated using two general methods, namely (i) short-term (also known as accelerated) measurements and (ii) long-term measurements.

(i) Short-term (accelerated) measurements are usually used to compare the corrosion resistance of different paint/metal systems and decide which system would provide the longest time durability and best corrosion protection. These accelerated tests depend on the application of specific stresses (such as high temperature, UV light, high corrosive

salt concentration, and high humidity, either individually or using a combination of them) at levels higher than those encountered under normal atmospheric conditions to produce aging or failure of the paint/metal system at a shorter time than under normal conditions but without changing the degradation mechanisms.[82, 183] As shown in Equation 1.5, both dissolved oxygen and water (or any electrolyte) are necessary for the degradation of any paint coating and the corrosion of a metal or alloy. The drastic and unusual conditions used in accelerated tests, such as high temperature, enhance the transport of the corrodents through the coating film and hence accelerates the corrosion reactions.[184] Because of the lack of sufficient direct correlation between natural degradation and the weathering device, accelerated tests are currently used only in quality control to compare the anti-corrosive properties of different coating systems.[185, 186] In other cases, the results of these tests are used to give a rough prediction about the long-term stability of the system under investigation.[187-189]

(ii) Long-term measurements allow for a comprehensive evaluation of the overall corrosion behavior of any given system. In addition, these tests allow for the determination of the corrosion kinetics (e.g., measurement of the corrosion rate) of the test samples at different time intervals. In long-term measurements, the system under investigation is kept under normal atmospheric conditions and the corrosion behavior of the system is monitored over time using DC and/or AC electrochemical techniques. As the name implies, the time frame for the conclusion of these test measurements ranges from few months to several years.[190-195]

Among the electrochemical techniques used for studying the corrosion behavior, EIS and the salt spray test are the most frequently used techniques for the evaluation of behavior of organic coatings in aggressive media.[196-201] In addition to these two main approaches, other techniques are also used as complementary techniques for the characterization of organic coatings as well as coated metals and alloys such as electrochemical noise measurements (ENM);[202-205] scanning electron microscopy (SEM);[206-212] X-ray techniques (e.g., X-ray diffraction, X-ray photoelectron spectroscopy, energy dispersive X-ray);[213-219] polarization and cyclic voltammetry;[218, 220, 221] ellipsometry;[222-225] and the scanning probe microscopy (SPM)[226-228] techniques such as the scanning Kelvin probe (SKP),[229-232] the scanning vibrating electrode technique (SVET),[233-236] the atomic force microscope (AFM),[232, 237-242] scanning tunneling microscope (STM),[243, 244] and the scanning electrochemical microscope (SECM).[226, 245-248]

1.7 Electrochemical Impedance Spectroscopy (EIS)

EIS is a widely used technique in a large number of research areas including corrosion studies and corrosion control by coatings and/or inhibitors;[37, 249-254] monitoring of microbiologically influenced corrosion;[255-260]
study of the kinetics and elucidation of transport phenomena in electrochemical systems;[261-269] evaluation of the mechanism and efficiency of inhibitors;[270] measurements in batteries and fuel cell-related systems;[271-275] electrochemical characterization of ultramicroelectrodes;[276, 277] and monitoring the properties of conducting and ionic

polymers.[278-284] Moreover, the EIS technique can also be used for measurements in harsh and low conductivity media.[285-289] The EIS experiment offers a wealth of electrochemical information that can be interpreted and modeled as an equivalent electrical circuit (vide infra).[37, 199, 251, 290-292]

In addition to its chemistry applications, impedance spectroscopy has become a multi-discipline science that has been applied in biology,[293, 294] semiconductors and electronics,[295-297] biomedical sensors,[298, 299] biomaterials,[300] drug research,[301-304] and biotechnology and tissue engineering.[293, 305-307] Several proceedings, symposia, books, book chapters, and review articles provide evidence of the different successful applications of EIS.[37, 251, 308-315]

The use of EIS in the evaluation of the properties of polymer coated metals and alloys and their changes during exposure to corrosive environments has been the topic of a large number of investigations during the last two decades.[82, 316-320] In this regard, the technique has been extensively used for the electrochemical evaluation of anti-corrosive properties and the early detection of the degradation of paints as well as organic coatings on metals and alloys under different conditions including both normal atmospheric conditions and in aggressive media.[37, 177, 286, 287, 321-324] The results of an EIS experiment for a coated substrate in a corrosive medium provide useful information about the system under investigation such as corrosion stability, presence of defects, reactivity of the interface, and adhesion and barrier properties to water. Having this information greatly helps in determining the approximate lifetime of an in-service system.

The EIS technique involves the measurement of the impedance (Z) of an electrochemical system (e.g., a three electrode electrochemical cell) as a function of frequency (f) of an applied perturbation in an alternating current (AC) circuit. The perturbation signal is a small AC potential (E) on the order of 5-10 mV (peak-to-peak) in the form of sine waves over a frequency range of several decades. The resulting AC current (I) and the phase shift (θ) of the output signal are measured. Z is determined from Ohm's law:

$$Z = E/I \tag{1.9}$$

which can be calculated over a wide frequency range.

Z is a complex value (planar vector quantity) that differs from the resistance (R) in that it takes phase differences into account (See Figure 1.3). Z_{Total}, or simply Z, is expressed at each f value by its resistive or real (Z_r) component and reactive or imaginary (Z_{im}) component.

In rectangular coordinates:

$$Z_r = Z' = |Z_{Total}| \cos \theta \tag{1.10a}$$

$$Z_{im} = Z'' = |Z_{Total}| \sin \theta \tag{1.10b}$$

$$\theta = \tan^{-1} (Z_{im}/Z_r) \tag{1.11}$$

$$Z = Z_{Total} = Z_r + jZ_{im} = R - jX;\ X = 1/\omega C; \qquad \omega = 2\pi f, \qquad j = \sqrt{-1} \tag{1.12}$$

The modulus of the impedance $|Z|$ is:

$$|Z| = \sqrt{(Z_r^2 + Z_{im}^2)} \tag{1.13}$$

where:

R = resistance, X = reactance, C = capacitance, ω = the applied angular frequency

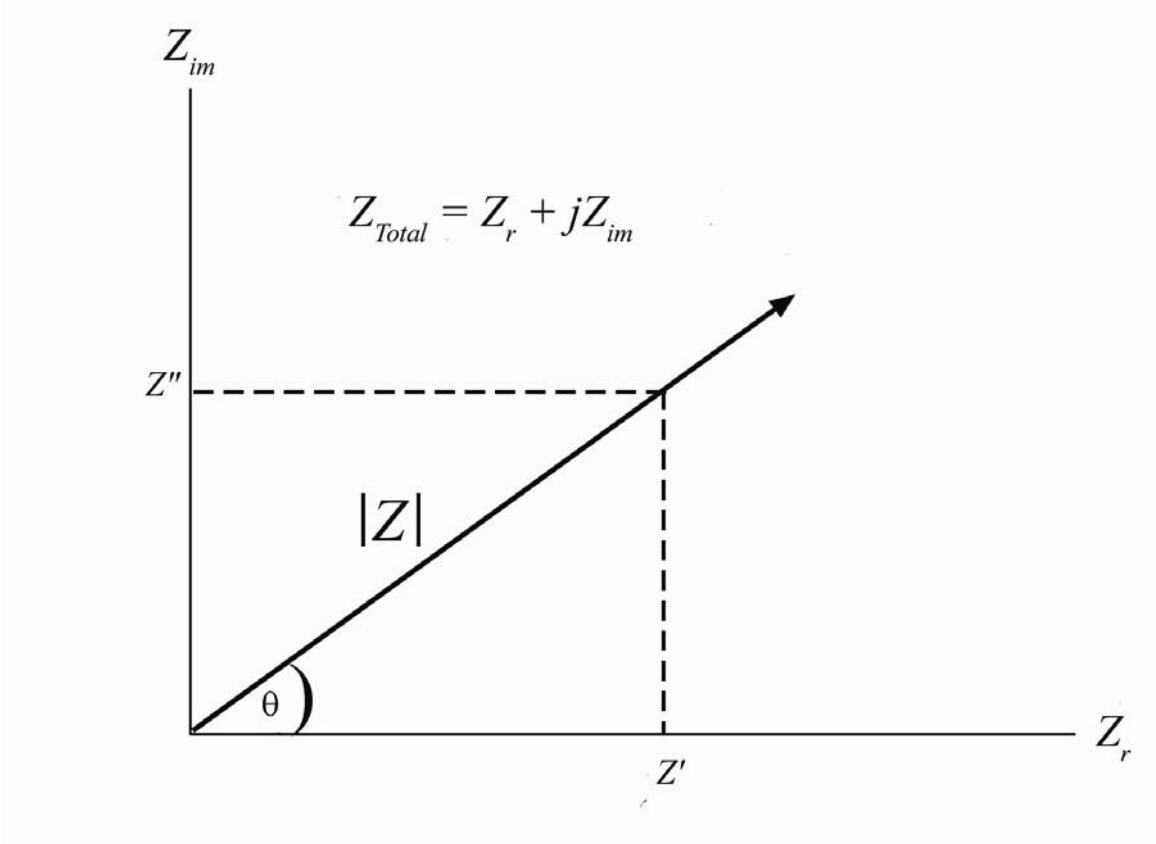

Figure 1.3 The impedance ($|Z|$) plotted as a planar vector in terms of real (Z') and imaginary (Z'') components using rectangular and polar coordinates.

The impedance spectra are usually expressed in one of two formats, namely Bode plots and Nyquist plots. Examples for both plot formats are given for the Randles cell (shown in Figure 1.4.a). This cell is one of the simplest and most common cell models. As shown in Figure 1.4.a, the equivalent circuit of the Randles cell includes a solution resistance (R_Ω) (also known as the uncompensated resistance between the reference and working electrodes), a double layer capacitance (C_{dl}), and a polarization resistance (R_p) (also known as the charge transfer resistance).

(i) A Bode plot shows the variation of the phase angle (θ) and the logarithm of the total (absolute or modulus) impedance Z ($\log |Z|$) vs. $\log f$ at each f value. As shown in Figure 1.4.b, the Bode plot can provide values of R_p and R_Ω. C_{dl} can also be calculated from the Bode plot by extrapolation of the middle line to $\log |Z| = 0$. At this $\log |Z|$ value, $|Z| = 1/C_{dl}$. Moreover, the minima and maxima of θ and their positions on the Bode plot are indicators of system characteristics.[37]

(ii) A Nyquist plot (also known as a Cole-Cole plot or a complex plan plot) shows the variation of the imaginary component of the impedance (Z_{im}) (ordinate) vs. the real component (Z_r) (abscissa) at each excitation frequency (Figure 1.5). As shown in Figure 1.3, the overall impedance can be represented as a vector of length $|Z|$ with θ is the angle between this vector and the x axis. In the Nyquist plot shown in Figure 1.5, at very high frequency (on the left side of the plot), Z_{im} vanishes, leaving only R_Ω. At very low frequency, Z_{im} again disappears, leaving a sum of R_Ω and R_p. Thus the value of R_p can be calculated by subtraction of the impedance value measured at very high frequency from the impedance value measured at very low frequency. It should be mentioned that the

(a)

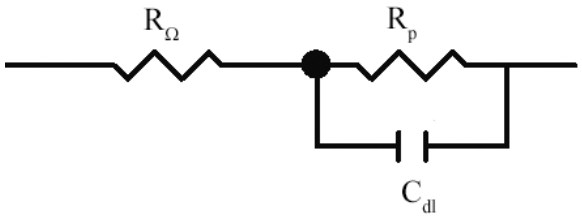

(b)

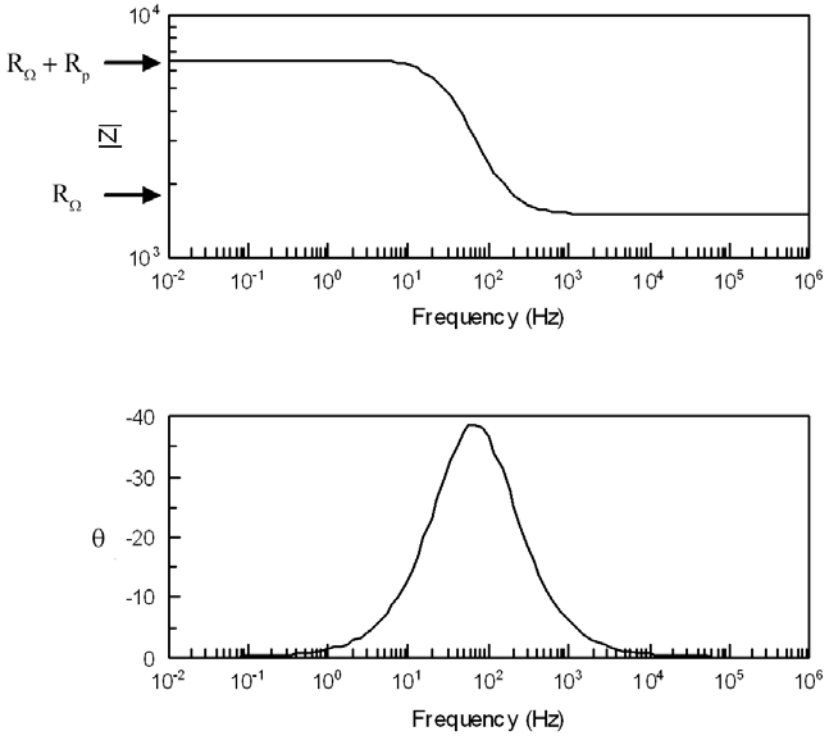

Figure 1.4 Equivalent circuit (a) and Bode plot (b) for a simple electrochemical cell (Randles cell). R = Ohmic (solution) resistance; R_p = polarization (charge transfer) resistance; and C_{dl} = the electrode double layer capacitance.

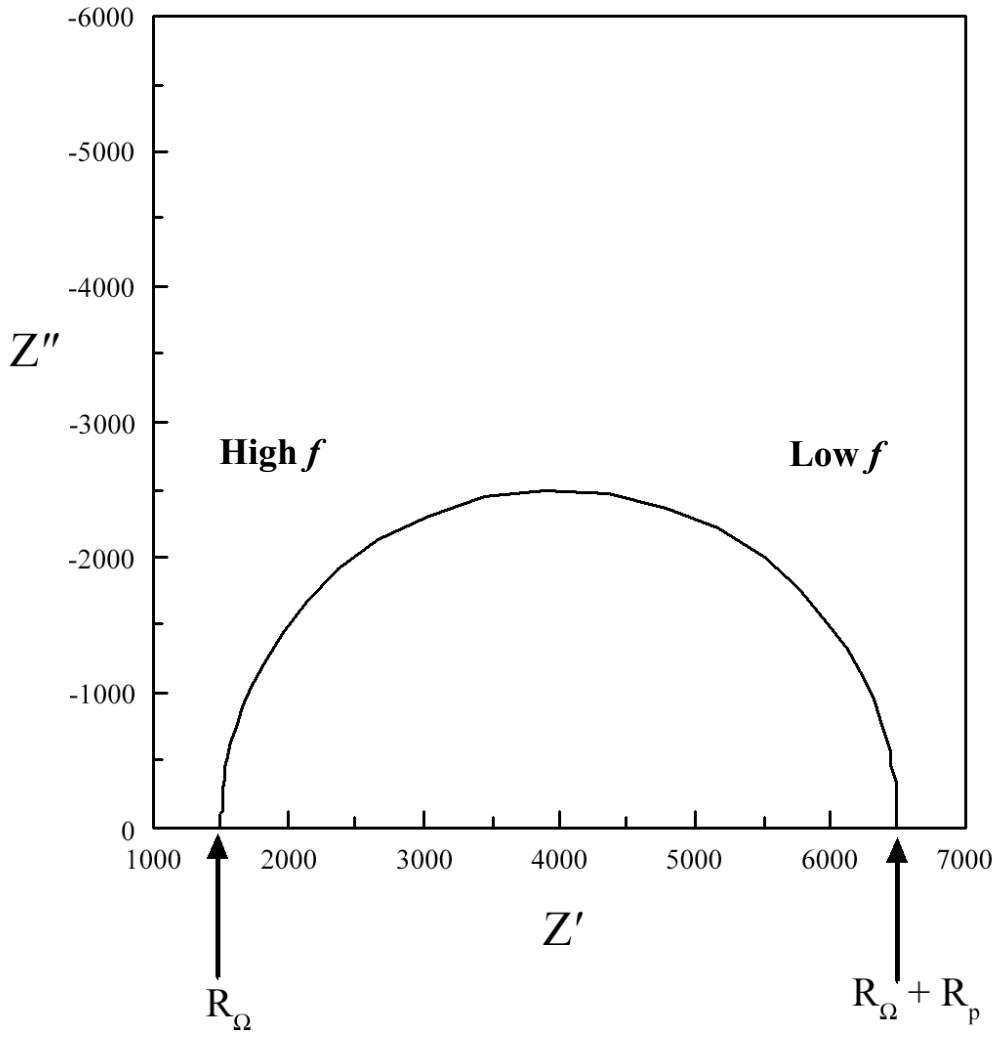

Figure 1.5 Nyquist plot for the electrochemical system shown in Figure 1.4.a.

value of R_p calculated from the Nyquist plot has been used to determine the rate of corrosion where R_p is inversely proportional to the rate of corrosion (see Equation 3.1 in Chapter 3).[325-328]

1.8 Advantages and Limitations of EIS

As mentioned previously, impedance spectroscopy has become a very popular and convenient analytical tool in a wide range of fields. This popularity is reflected in the increased number of research articles, monograms, reviews, and books annually published. When compared to other techniques used for the assessment of the properties and performance of coated metals and alloys, EIS has several advantages including the following: (i) it is an in situ nondestructive technique that provides direct and accurate information about the system under investigation; (ii) it provides a simple and easy to handle setup with the possibility of automation; (iii) it provides a wealth of kinetic and mechanistic information that can be easily used to characterize metals, alloys, and coatings as well as calculate several electrical, chemical, and electrochemical parameters such as corrosion rates, dielectric properties, electrode capacitance, kinetic parameters of reactions (e.g., reaction rate constants, transfer coefficients, diffusion coefficients, etc.) in both aqueous and solid state electrochemistry; (iv) it imposes only infinitesimally small perturbation on the system under investigation with respect to the steady state. This characteristic is one of the great advantages of the EIS over other electrochemical techniques such as cyclic voltammetry; and (v) it can easily and accurately predict the

performance, the lifetime, and/or the behavior of a wide range of systems including fuel cells, chemical sensors, and biological systems.[177, 252, 282, 291, 309, 319, 329-335]

However, such as the case with any other technique, EIS has also some limitations. The EIS data are always explained using a modeling program that uses electrical components to build an equivalent circuit to fit a given electrochemical system. Macdonald mentioned two main limitations for the EIS technique.[252, 336] The first one is the difficulty to interpret and possible misinterpretation of the EIS spectra if a wrong equivalent circuit or circuit elements are selected, especially for unknown systems. Another source of error is that for some electrochemical systems, the use of ideal equivalent circuit elements does not result in good fitting for the observed EIS data.[252] In addition to these two limitations, the EIS results and calculations depend on the area of the system under investigation, thus the EIS measurements require an accurate control of the area of the system. However, with the constant efforts of the experienced electrochemists and corrosion engineers, these limitations can be controlled. For example, the inclusion of distributed impedance elements such as the constant-phase elements (CPEs) in the modeled equivalent circuits greatly improves the fitting process.

1.9 Equivalent Circuit Modeling and EIS Data Modeling

As mentioned above, one of the great advantages of the EIS technique is that the experimental data can be interpreted, even for complex electrochemical systems, using theoretical equivalent electrical circuits (models). An equivalent electrical circuit is a combination of typical electrical components such as resistors and capacitors along with

some other electrochemical elements such as Warburg diffusion elements (Z_w) and CPEs; arranged in logical series and parallel combinations. Numerous theoretical equivalent circuit models have been developed to interpret the experimental data for several chemical as well as electrochemical systems.[337-339]

An acceptable model should satisfy both of the following two conditions:[292]

(i) All elements in the model should have a real physical meaning with respect to the characteristics of the electrochemical system under investigation.

(ii) The model has to be as simple as possible and must generate modeled spectra that fit to or correlate with the experimental data with minimal error.

Currently, all commercially available EIS measurement instruments are equipped with software packages that allow the user to either build a model or use sample models from a library for EIS data fitting and analysis.[340-342]

Figure 1.6 shows the general and most commonly used equivalent electrical circuits to fit the experimental EIS data for the degradation of polymer-coated substrates in corrosive environments (metal/organic coating/electrolyte system).[287, 319, 329, 343-345] According to the models shown in Figure 1.5, the Nyquist plot could show two semi-circles, corresponding to two time constants, one due to the bare metal ($R_p \times C_{dl}$) and another one due to the organic coating ($R_c \times C_c$) where R_c and C_c represent the resistance and capacitance of the polymer film, respectively. Normally, the semi-circle due to the organic film appears in the Nyquist plot in the high frequency (HF) range while the semi-circle due to the corrosion process appears in the low to medium frequency (LF-MF)

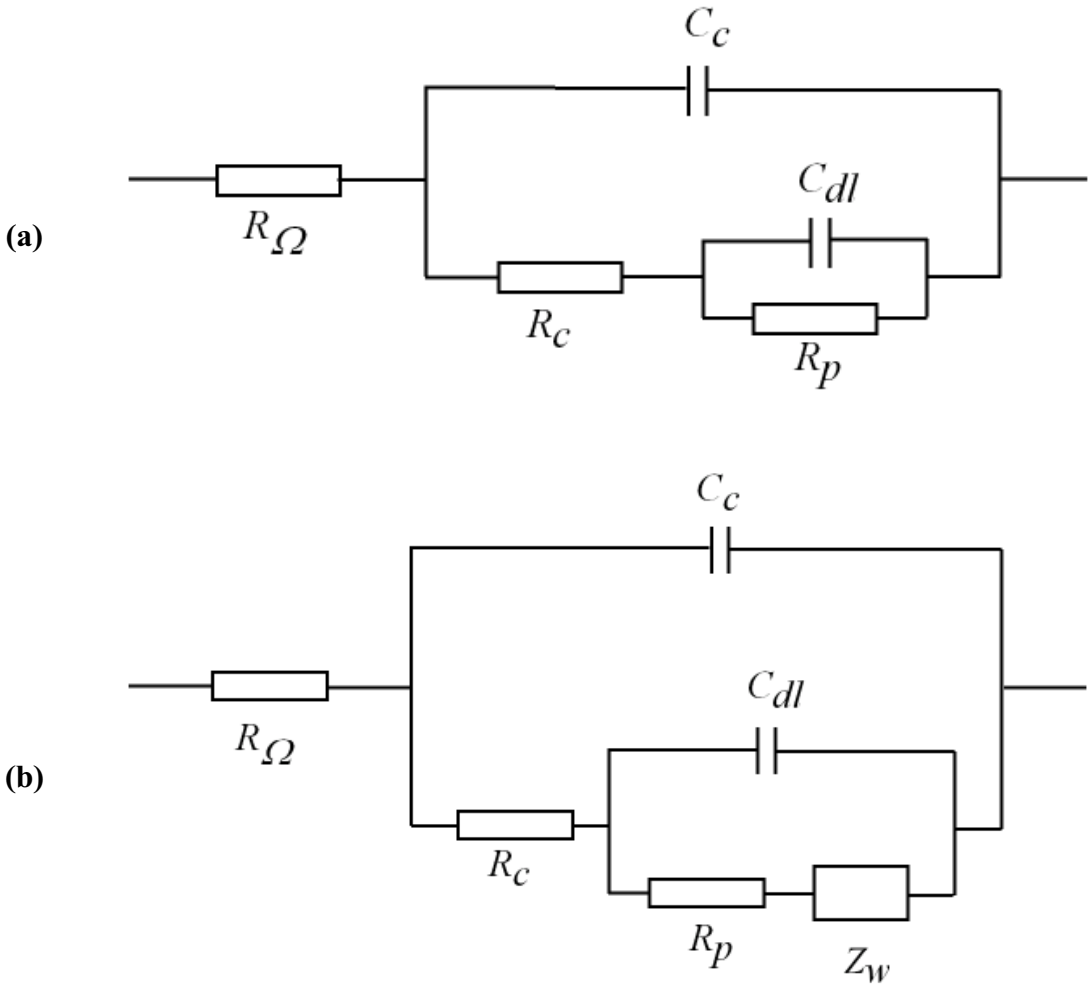

Figure 1.6 Schematic drawings for the general equivalent electrical circuits for a polymer-coated metal. R_Ω = Ohmic (solution) resistance; C_{dl} = the electrode double layer capacitance; C_c = coating capacitance; R_c = coating pore resistance; R_p = polarization (charge transfer) resistance, and Z_w = Warburg diffusional impedance.

range. At very low frequency range, the Warburg impedance (W) appears as a diffusion tail in the Nyquist plot.[334, 335, 346, 347]

In addition to the models shown in Figure 1.5, several other equivalent circuits have also been suggested.[348-353] In some of these novel circuits,[348] both R_c and R_p are connected in series instead of the usual hierarchical connection shown in Figure 1.5. In other proposed circuits CFEs replaced C_c and C_{dl} because of the depressed semi-circle.[29, 354, 355] In addition, some other circuits include other supplementary elements such as inductive elements.[351, 356]

1.10 Applications of EIS to Study Stability of Organic Coatings

EIS has been widely used for the evaluation of the anti-corrosive performance of both organic and inorganic coatings and paints applied to a wide range of metals and alloys such as iron, zinc, aluminum, copper, magnesium, titanium, platinum, mild steel, brass, and bronze sculptures.[148, 201, 220, 253, 319, 329, 357-366] EIS is a very sensitive technique that can provide highly accurate data that relates to the quality of the coating and also predict any possible damage that may occur for the coating before the damage is visible. Moreover, the use of EIS for the characterization of coated metals and alloys in corrosive electrolytes not only measure the deterioration of the coating film, but also measures the corrosion rate of the substrate under the coating film as well.[361, 367, 368]

Three factors contribute to the total electrochemical impedance (Z_{Total}) of a metal/coating system; namely (1) the solution resistance (R_Ω), (2) the coating resistance (R_c) and capacitance (C_c), and (3) the charge transfer or polarization resistance (R_{ct} *or* R_p)

and the double layer capacitance (C_{dl}) of the bare metal substrate. For a coated substrate exposed to a corrosive medium, as the exposure time increases, the defects in the coating increase in number and size, thus allowing dissolved oxygen, water, and other corrosive electrolytes (e.g., Cl^-, SO_4^{2-} ions) to diffuse through the coating to the metal surface. These interactions lead to changes in the above mentioned variables and hence a change in Z_{Total}. Thus, one of the characteristics of a good protective coating is that it delays the diffusion process for the longest possible time.

1.11 Vapor Grown Carbon Nanofiber (VGCNF)

Carbon has several allotropies including high structure carbon black (CB), pitch-based and polyacrylonitrile-based carbon fibers (CFs), vapor grown carbon nanofibers (VGCNFs), and the relatively new and intriguing carbon nanotubes (CNTs) such as single-wall nanotubes (SWNTs) and multi-walled nanotubes (MWNTs).[369-372]

VGCNFs are a class of carbon fibers that are produced by catalytic dehydrogenation of a hydrocarbon (e.g., methane, ethane, propane, ethylene, acetylene, benzene, naphthalene, etc.) or carbon monoxide in the gas phase at high temperatures (around 950-1500 °C) in presence of small catalytic particles of a transition metal (e.g., iron, cobalt, nickel, gold) or metal alloy (e.g., Fe-Ni, Ni-Cu) under reducing conditions in a flow system.[373-380] Recently, these fibers were produced by microwave pyrolysis chemical vapor deposition without any catalyst.[381] Depending on the synthesis method and post-treatment technique, these fibers may be of several microns to several centimeters in length but only 10-300 nm in diameter.[374, 382-384]

VGCNFs differ from the other types of carbon fiber not only in their method of production, but also in their physical as well as mechanical properties.[385] VGCNFs are high aspect ratio (length/width) nanofibers that exhibit excellent thermal conductivity and the lowest electrical resistivity among all types of carbon fibers.[370, 371, 375-377, 385-390] Moreover, although inferior to CNTs, VGCNFs have good mechanical properties that are comparable to those of conventional CFs.[385, 391-396] In addition, due to their small size and their production from natural gas or coal as feedstock, VGCNFs have the advantage of low cost and high availability.

The small size, light weight, high aspect ratio, and unique physical, thermal, mechanical, and electrical properties of VGCNFs make them an ideal reinforcing filler in polymer matrix nanocomposites to enhance the mechanical properties of the pure polymeric material in high performance applications, especially in the automotive, battery, sensors, catalysis, aircraft, electronics, and sports industries.[375, 392, 396-404] According to the literature, the addition of VGCNFs to polymer matrix composites (both thermoplastics and thermoset), aluminum matrix composites, and concrete improves both the mechanical and physical properties of the composite such as the tensile properties (e.g., flexural strength, tensile strength, tensile modulus, flexural toughness, free-thaw durability, and shear bond strength), thermal conductivity, and electrical conductivity.[392, 394, 396, 405-413]

Another important application of VGCNFs is their use as conductive material in electromagnetic interference (EMI) shielding for radio frequency sources and electronics, and electrostatic discharge (ESD) protection.[385, 414, 415] In this regard, several polymer

matrices reinforced with VGCNFs have been investigated for use as materials for EMI shielding. Among these materials are VGCNF-reinforced liquid crystal polymer (LCP) composites,[416] polyesterpolyol shape memory polymer (SMP) composites,[417] and VGCNF-reinforced polyethylene composites.[385]

In addition to their use as reinforcing agents, VGCNFs are also used as adsorbents and conductive fillers.[418-420] More recently, they have been also used in batteries (e.g., alkaline batteries, lithium-ion batteries, lithium polymer batteries) as electrocatalyst supports in the production of electrodes and separators.[375, 421-425]

1.12 Aims and Scope of the Current Dissertation

Over the past few decades, considerable progress has been made in the development of fast, cost- and energy-efficient, and easy to implement methods for the protection of metals and alloys. Among these methods is the incorporation of additives in organic paint matrices to improve the corrosion properties of these coatings for high performance systems. Currently, research in coating technology is focused on finding efficient, anticorrosive, environmentally acceptable additives that are neither as toxic nor carcinogenic as the chromate-based additives nor generate high amounts of sludge as in the phosphatation process. Another requirement in these new additives is that they should produce similar or better protection than the currently-used additives.

Conductive additives such as zinc dust,[426, 427] silver powders,[428-430] copper powders,[431] iron powder,[432] cationic agents (e.g., quaternary ammonium salts),[433] and carbon black[434-437] have been used to improve the mechanical, electrical, and/or thermal

properties of insulating and/or conducting polymers, paints, adhesives, and coatings for several applications.[438-442]

As mentioned above, the thermal, electrical, and mechanical properties of VGCNFs make them good candidates as additives to improve the mechanical properties of thermoset and thermoplastic composites as well as epoxy resins and paints applied to metals.[391, 394, 398, 406, 410, 413, 443-449] Accordingly, the main goal of the present research was to study the effect of added VGCNFs on the corrosion protection of mild steel samples spin-coated with commercial alkyd paints reinforced with VGCNF. To the best of our knowledge, there is no single report on the evaluation of VGCNFs as an additive to alkyd paints for the corrosion protection of any metal or alloy.

Therefore, this research involved the use of the EIS technique to evaluate the corrosion protection behavior of the VGCNF-reinforced coatings, as compared to the behavior of the pure coatings, in corrosive medium of 3% NaCl aqueous solution. By way of contrast, the EIS behavior of steel coupons coated with paint coating containing powdered silicon carbide (SiC) microparticles with different weight percent was also studied. SiC was selected based on its electrical (semi-conductive) properties (see Chapter 4). In the current investigation, the EIS measurements involved studying the effect of the paint thickness, the percent of the VGCNF, and immersion time on the rate of corrosion of the coatings. The study also involved the surface characterization of the samples using optical microscopy; scanning electron microscopy and energy dispersive X-ray spectroscopy (SEM/EDS); atomic force microscopy (AFM), nanoindentation measurements, and two- and three-dimensional optical profilometry. In addition, the

study involved an accelerated corrosion (salt spray) test to compare the anticorrosion stabilities of pure paint, VGCNF/alkyd paint, and SiC/alkyd paint coatings.

In this dissertation, Chapter 1 presents an overview of the current research relevant to the present study, including a short discussion on the importance of the corrosion studies and corrosion control; followed by a brief discussion on iron and steel alloys with special emphasis on economic and strategic importance as well as applications of mild steel. This section concludes with the mechanism of atmospheric corrosion of iron and steel. Chapter 1 also briefly covers the importance of organic coatings and their applications for corrosion protection and/or decoration of metals and alloys. In addition, Chapter 1 also provides a short survey on the EIS technique, its importance, advantages, and limitations. Finally, a brief discussion about the advantages of VGCNFs and their industrial applications especially as fillers in composites is given.

Chapter 2 is devoted to the characterization of the dry alkyd paint coatings with different weight percent of VGCNF and film thicknesses. Accordingly, this chapter focuses on the study of the electrical and mechanical properties of these coatings deposited on steel as well as poly(methyl methacrylate) substrates. In addition, some surface analysis measurements such as optical profilometry, scanning electron microscopy (SEM), and atomic force microscopy (AFM) have been performed.

Chapter 3 is devoted to the investigation of the EIS behavior of a coating layer composed of a commercial alkyd paint containing VGCNFs of different weight percent and applied to the surface of mild steel coupons using the spin-coating technique. In addition to studying the effect of the VGCNF wt %, the investigation also includes

studying the effect of the coating thickness on the corrosion protective properties of the paint coating. EIS measurements were performed at the open circuit potential (OCP) of the system in a quiescent aerated 3% NaCl aqueous solution at ambient temperature. In addition to the EIS measurements, the investigation also included OCP and cyclic voltammetry (CV) measurements. The chapter ends with some conclusions regarding the effect of the incorporation of VGCNF on the corrosion protection properties of the paint and the most corrosion resistant VGCNF-alkyd paint mixture.

Chapter 4 deals with the EIS behavior of SiC-containing alkyd paint coated mild steel samples in 3% NaCl solution under the same conditions used in Chapter 3. In Chapter 4, a brief introduction on the importance of SiC and its applications is given. Then, the OCP and the EIS data are presented and compared. The chapter also includes a comparison between the EIS behavior of alkyd paint films containing SiC particles vs. the behavior of alkyd paint containing VGCNF of the same thickness and weight percent both applied to the surface of mild steel samples.

In Chapter 5, the salt spray test is used to evaluate and compare the stability and corrosion resistance of VGCNF-reinforced alkyd paint coatings vs. those of SiC-reinforced alkyd paint coatings, both applied to mild steel coupons. The chapter starts with a brief introduction on the importance, merits, and applications of the salt spray test as a desirable accelerated corrosion test. The discussion is followed by a short section on the experimental setup used to perform the salt spray test based on the specifications given in the ASTM B117 protocol. The results of the test are then given in the form of digital photos, tables, and graphs showing the gradual change in the morphology of the

paint film layer, the extent of degradation, and the time elapsed before the coating films failed and the corrosion products were visual. The chapter ends with some conclusions based on the results of the test.

Chapter 6 provides a proposed mechanism for the corrosion protection offered as a result of the incorporation of VGCNFs or SiC in the alkyd paint matrix. The chapter also draws some conclusions and suggests research goals that should be carried out in the future to produce VGCNF-reinforced coatings with uniform distribution of the nanofibers in the paint matrix, thus improving the performance of the coating in aggressive media.

1.13 References

(1) Fontana, M. G. *Corrosion Engineering*, 3rd ed.; McGraw-Hill, Inc.: New York, 1986.

(2) Kelly, R. G.; Scully, J. R.; Shoesmith, D.; Buchheit, R. G. *Electrochemical Techniques in Corrosion Science and Engineering;* Marcel Dekker, Inc.: New York, 2002.

(3) Uhlig, H. H.; Revie, R. W. *Corrosion and Corrosion Control: An Introduction to Corrosion Science and Engineering*, 3rd ed.; John Wiley & Sons, Inc.: New York, 1985.

(4) Biezma, M. V.; San Cristobal, J. R. *Corrosion Engineering, Science and Technology,* **2005**, *40*, 344-352.

(5) Brasunas, A. D., Ed. *NACE Basic Corrosion Course*, 2nd ed.; NACE: Houston, TX, 1971.

(6) Slater, J. E. *Materials Performance* **1979**, *18*, 34-37.

(7) Biezma, M. V.; San Cristobal, J. R. *Corrosion* **2006**, *62*, 1051-1055.

(8) Edyvean, R. G. J.; A., V. H. In *Recent Advances in Biodeterioration and Biodegradation*; Garg, K. L., Garg, N., Mukerji, K. J., Eds.: Naya Prokash, Calcutta, India, 1994; Vol. 2, pp 81-116.

(9) Moran, G. C.; Labine, P., Eds. *Corrosion Monitoring in Industrial Plants Using Nondestructive Testing and Electrochemical Methods*; ASTM International: West Conshohocken, PA, 1996.

(10) http://www.corrosioncost.com/home.html (accessed Dec 2009).

(11) Cherry, B. W. *Materials Forum* **1995**, *19*, 1-7.

(12) Sastri, V. S.; Elboujdaini, M.; Perumareddi, J. R. In *Proceedings of the 2nd International Symposium on Environmental Degradation of Materials and Corrosion Control in Metals*: Vancouver, BC, Canada, 2003, pp 321-328.

(13) Ashworth, V.; Booker, C. J. L. *Cathodic Protection: Theory and Practice;* Ellis Horwood Publishing Limited: West Sussex, U.K., 1986.

(14) von Baeckmann, W.; Schwenk, W.; Prinz, W. *Handbook of Cathodic Corrosion Protection: Theory and Practice of Electrochemical Protection Processes,* 3rd ed.; Gulf Professional Publishing: Houston, TX, 1997.

(15) Mudali, U. K.; Khatak, H. S.; Raj, B. *Encyclopedia of Electrochemistry* **2003**, *4*, 393-434.

(16) Riggs, O. L., Jr.; Locke, C. E. *Anodic Protection. Theory and Practice in the Prevention of Corrosion*; Plenum Press: New York, 1981.

(17) Babic-Samardzija, K.; Hackerman, N. *Journal of Solid State Electrochemistry* **2005**, *9*, 483-497.

(18) Bellakhal, N.; Dachraoui, M. *Materials Chemistry and Physics* **2004**, *85*, 366-369.

(19) Magnussen, O. M. *Encyclopedia of Electrochemistry* **2003**, *4*, 435-459.

(20) Metikos-Hukovic, M.; Babic, R.; Paic, I. *Journal of Applied Electrochemistry* **2000**, *30*, 617-624.

(21) Ranney, M. W., Ed. *Corrosion Inhibitors - Manufacture and Technology;* Noyes Data Corp. : Park Ridge, NJ, 1976.

(22) Hernandez, G.; Kucera, V.; Thierry, D.; Pedersen, A.; Hermansson, M. *Corrosion* **1994**, *50*, 603-608.

(23) Pedersen, A.; Hermansson, M. *Biofouling* **1991**, *3*, 1-11.

(24) Ponmariappan, S.; Maruthamuthu, S.; Palaniswamy, N.; Palaniappan, R. *Corrosion Reviews* **2004**, *22*, 307-323.

(25) Volkland, H. P.; Harms, H.; Kaufmann, K.; Wanner, O.; Zehnder, A. J. B. *Corrosion Science* **2001**, *43*, 2135-2146.

(26) Athey, R. D., Jr. *European Coatings Journal* **1999**, 56-59.

(27) Athey, R. D., Jr. In *Coatings Technology Handbook* 2nd ed.; Satas, D., Tracton, A. A., Eds.; Marcel Dekker, Inc.: New York, 2001, pp 787-794.

(28) Carter, V. E. *Metallic Coatings for Corrosion Control*; Newnes-Butterworths Ltd.: London, U.K., 1977.

(29) de Wit, J. H. W.; van der Weijde, D. H.; Ferrari, G. In *Corrosion Mechanisms in Theory and Practice,* 2nd ed.; Marcus, P., Ed.; Marcel Dekker, Inc.: New York, 2002, pp 683-729.

(30) Dislich, H. *Organic Coatings* **1984**, *6*, 517-534.

(31) Forsgren, A. *Corrosion Control Through Organic Coatings;* CRC Press: Boca Raton, FL, 2006.

(32) Harding, W. B.; Di Bari, G. A., Eds. *ASTM Special Technical Publication, No. 947. Testing of Metallic and Inorganic Coatings*; ASTM: Philadelphia, PA, 1987.

(33) Munger, C. G. *Materials Performance* **1991**, *30*, 34-38.

(34) Perez, C.; Izquierdo, M.; Abreu, C. M.; Collazo, A.; Merino, P. *Recent Research Developments in Electrochemistry* **2002**, *5*, 115-144.

(35) Sidky, P. S.; Hocking, M. G. *British Corrosion Journal* **1999**, *34*, 171-183.

(36) Simpson, T. C.; Townsend, H. E. *Corrosion Tests and Standards* **1995**, 513-524.

(37) Mansfeld, F. In *Analytical Methods in Corrosion Science and Engineering*; Marcus, P., Mansfeld, F., Eds.; CRC Press: Boca Raton, FL, 2006, pp 463-505.

(38) Smith, A. *Anti-Corrosion Methods and Materials* **1979**, *26*, 15-16.

(39) Voevodin, N. N.; Balbyshev, V. N.; Khobaib, M.; Donley, M. S. *Progress in Organic Coatings* **2003**, *47*, 416-423.

(40) Buchheit, R. G. In *Handbook of Environmental Degradation of Materials*; Kutz, M., Ed.; William Andrew, Inc.: Norwich, NY, 2005, pp 367-385.

(41) Iannuzzi, M.; Young, T.; Frankel, G. S. *Journal of the Electrochemical Society* **2006**, *153*, B533-B541.

(42) Kendig, M.; Hon, M.; Warren, L. *Progress in Organic Coatings* **2003**, *47*, 183-189.

(43) Knag, M. *Journal of Dispersion Science and Technology* **2006**, *27*, 587-597.

(44) Mathiyarasu, J.; Pathak, S. S.; Yegnaraman, V. *Corrosion Reviews* **2006**, *24*, 307-321.

(45) Nakatsugawa, I.; Dai, F., In *Magnesium Technology in the Global Age*, Proceedings of the International Symposium on Magnesium Technology in the Global Age, Montreal, QC, Canada, Oct. 1-4, 2006; 519-532.

(46) Povetkin, V. V.; Shibleva, T. G. *Protection of Metals* **2006**, *42*, 516-519.

(47) Tallman, D. E.; Spinks, G.; Dominis, A.; Wallace, G. G. *Journal of Solid State Electrochemistry* **2002**, *6*, 73-84.

(48) Zheludkevich, M. L.; Salvado, I. M.; Ferreira, M. G. S. *Journal of Materials Chemistry* **2005**, *15*, 5099-5111.

(49) Smith, C. A. *Anti-Corrosion Methods and Materials* **1981**, *28*, 14-15.

(50) Smith, W. F. *Structure and Properties of Engineering Alloys*; McGraw-Hill Co.: New York, 1981.

(51) Bardes, B. P., Ed. *Matals Handbook, Vol. 1: Properties and Selection: Irons and Steels*, 9th ed.; American Society of Metals: Metals Park, OH, 1978.

(52) Luce, W. A.; Peacock, J. H. *Industrial and Engineering Chemistry* **1967**, *59*, 57-61.

(53) Cunat, P.-J. *Stainless Steel Industry* **2002**, *30*, 9-11.

(54) Davis, J. R., Ed. *Carbon and Alloy Steels*; ASM International: Materials Park, OH, 1996.

(55) Svistunova, T. V.; Shlyamnev, A. P. *Protection of Metals* **1996**, *32*, 342-347.

(56) Wicks, Z. W. J.; Jones, F. N.; Pappas, S. P. *Organic Coatings - Science and Technology Vol 2. Applications, Properties and Performance,* 3rd ed.; John Wiley & Sons, Inc.: Hoboken, NJ, 2007.

(57) Craig, B. *Corrosion Technology* **2001**, *15*, 1-30.

(58) Sangaj, N. S.; Malshe, V. C. *Progress in Organic Coatings* **2004**, *50*, 28-39.

(59) Grundmeier, G.; Simoes, A. *Encyclopedia of Electrochemistry* **2003**, *4*, 500-566.

(60) Augustyn, M. *European Coatings* **2004**, *80*, 37-45.

(61) Evitts, R. W. In *Handbook of Environmental Degradation of Materials*; Kutz, M., Ed.; William Andrew, Inc.: Norwich, NY, 2005, pp 229-241.

(62) Hare, C. H. In *Coatings Technology Handbook,* 2nd ed.; Satas, D., Tracton, A. A., Eds.; Marcel Dekker, Inc.: New York, 2001, pp 795-805.

\

(63) Juchniewicz, R.; Jankowski, J.; Darowicki, K. *Materials Science and Technology* **2000**, *19*, 383-470.

(64) Mansfeld, F. *NATO ASI Series, Series E: Applied Sciences* **1991**, *203*, 521-544.

(65) Munro, J. I.; Shim, W. W. *Materials Performance* **2001**, *40*, 22-25.

(66) Paul, L.; Rebak, R. B.; Crook, P. In *Proceedings of the International Conference on Incineration and Thermal Treatment Technologies,* Orlando, FL 1999, pp 785-789.

(67) Polder, R. B. *Corrosion in Reinforced Concrete Structures* **2005**, 215-241.

(68) Raghavan, M. *Corrosion Science and Technology* **2002**, *31*, 63-69.

(69) Rohrbach, K. P. *Advanced Materials & Processes* **1995**, *148*, 37-40.

(70) Schweitzer, P. A.; Ed. *Corrosion and Corrosion Protection Handbook. 2nd ed*, 1989.

(71) Subramania, A.; Sundaram, N. T. K.; Priya, R. S.; Muralidharan, V. S.; Vasudevan, T. *Bulletin of Electrochemistry* **2004**, *20*, 49-58.

(72) Szabo, S.; Bakos, I. *Corrosion Reviews* **2006**, *24*, 231-280.

(73) Yunovich, M.; Thompson, N. G.; Virmani, Y. P. *International Journal of Materials & Product Technology* **2005**, *23*, 269-285.

(74) Schweitzer, P. A., Ed. *Paint and Coatings: Applications and Corrosion Resistance*; CRC Press: New York, 2006.

(75) Fettis, G., Ed. *Automotive Paints and Coatings;* Wiley-VCH Verlag GmbH: New York, 1995.

(76) Lacaze, P.-C., Ed. *Organic Coatings. (53rd International Meeting of Physical Chemistry, Ministere de la Recherche, Paris, France, January 1995.)*; AIP Press: Woodbury, NY, 1996.

(77) de Wit, J. H. W. In *Corrosion Technology Volume 8: Corrosion Mechanisms in Theory and Practice*; Marcus, P., Oudar, J., Eds.; Marcel Dekker, Inc.: New York, 1995, pp 581-628.

(78) Leidheiser, H., Jr., Ed. *Corrosion Control by Organic Coatings*; NACE: Houston, TX, 1981.

(79) van Ooij, W. J.; Bierwagen, G. P.; Skerry, B. S.; Mills, D. *Corrosion Control of Metals by Organic Coatings*; CRC Press: Boca Raton, FL, 1999.

(80) Rammelt, U.; Reinhard, G. *Progress in Organic Coatings* **1992**, *21*, 205-226.

(81) Bierwagen, G.; Shedlosky, T. J.; Stanek, K. *Progress in Organic Coatings* **2003**, *48*, 289-296.

(82) Bierwagen, G.; Tallman, D.; Li, J.; He, L.; Jeffcoate, C. *Progress in Organic Coatings* **2003**, *46*, 148-157.

(83) Hare, C. H. In *Coatings Technology Handbook,* 3rd ed.; Tracton, A. A., Ed.; CRC Press: Boca Raton, FL, 2006, pp 102/101-102/109.

(84) Carruth, G. F., Ed. *Organic coatings*; Marcel Dekker, Inc.: New York, 1979.

(85) Deflorian, F.; Rossi, S.; Vadillo, M. D. C.; Fedel, M. *Journal of Applied Electrochemistry* **2009**, *39*, 2151-2157.

(86) Khanna, A. S., Ed. *High-Performance Organic Coatings: Selection, Application and Evaluation*; CRC Press: Boca Raton, FL, 2008.

(87) Schoff, C. K. *Progress in Organic Coatings* **2005**, *52*, 21-27.

(88) Walter, G. W. *Corrosion Science* **1986**, *26*, 27-38.

(89) Grundmeier, G.; Schmidt, W.; Stratmann, M. *Electrochimica Acta* **2000**, *45*, 2515-2533.

(90) U.S. Census Bureau Home Page. http://www.census.gov/manufacturing/cir/historical_data/ma325f/index.html (accessed Dec 2009)

(91) Urban, D.; Takamura, K., Eds. *Polymer Dispersions and Their Industrial Applications* Wiley-VCH Verlag GmbH & Co. KGaA: Weinheim, Denmark, 2002.

(92) Wood, K. A.; Gaboury, S. R. *Surface Coatings International, Part B: Coatings Transactions* **2006**, *89*, 231-235.

(93) Barilli, F.; Fragni, R.; Gelati, S.; Montanari, A. *Progress in Organic Coatings* **2003**, *46*, 91-96.

(94) Lange, J.; Wyser, Y. *Packaging Technology & Science* **2003**, *16*, 149-158.

(95) Robertson, G. L. *Food Packaging: Principles and Practice*, 2nd ed.; Marcel Dekker, Inc.: New York, 1993.

(96) Broer, D. J. *Advances in Organic Coatings Science and Technology Series* **1989**, *11*, 219-228.

(97) Ghosh, S. K., Ed. *Functional Coatings: By Polymer Microencapsulation;* Wiley-VCH Verlag GmbH & Co. KGaA: Weinheim, Denmark, 2006.

(98) Licari, J. J. *Coating Materials for Electronic Applications: Polymers, Processes, Reliability, Testing* Noyes Publications/ William Andrew, Inc.: Norwich, NY, 2003.

(99) Wicks, Z. W., Jr.; Jones, F. N.; Pappas, S. P. *Organic Coatings: Science and Technology, Vol. 2: Film Formation, Components, and Appearance*; Wiley-Interscience: New York, 1992.

(100) Jones, D. A., Ed. *Principles and Prevention of Corrosion*, 2nd ed.; Prentice Hall: Norwell, MA, 1996.

(101) Lambourne, R.; Strivens, T. A., Eds. *Paint and Surface Coatings--Theory and Practice*, 2nd ed.; Woodhead Publishing Ltd.: Cambridge, U.K., 1999.

(102) Mellor, B. G., Ed. *Surface Coatings for Protection Against Wear*; CRC Press: Boca Raton, FL, 2006.

(103) Nylen, P.; Sunderland, E. *Modern Surface Coatings: A Textbook of the Chemistry and Technology of Paints, Varnishes, and Lacquers*; Interscience Publishers: New York, 1965.

(104) Rickerby, D. S.; Matthews, A., Eds. *Advanced Surface Coatings: A Handbook of Surface Engineering*; Blackie Academic and Professional: London, U.K., 1991.

(105) Roberge, P. R. *Handbook of Corrosion Engineering*; McGraw-Hill: New York, 2000.

(106) Shreir, L. L., Ed. *Corrosion, Vol. 2: Corrosion Control*; Newnes-Butterworths: London, U.K., 1976.

(107) Florio, J. J.; Miller, D. J., Eds. *Handbook of Coatings Additives*, 2nd ed.; CRC Press: Boca Raton, FL 2004.

(108) Matienzo, L. J.; Shaffer, D. K.; Moshier, W. C.; Davis, G. D. *ACS Symposium Series* **1986**, *322*, 234-249.

(109) Praveen, B. M.; Venkatesha, T. V. *Journal of Alloys and Compounds* **2009**, *482*, 53-57.

(110) Zhang, W.-G.; Li, L.; Yao, S.-W.; Zheng, G.-Q. *Corrosion Science* **2007**, *49*, 654-661.

(111) Ataee-Esfahani, H.; Vaezi, M. R.; Nikzad, L.; Yazdani, B.; Sadrnezhaad, S. K. *Journal of Alloys and Compounds* **2009**, *484*, 540-544.

(112) Ramalingam, S.; Muralidharan, V. S.; Subramania, A. *Journal of Solid State Electrochemistry* **2009**, *13*, 1777-1783.

(113) Ma, J.; Shi, Y.; Di, J.; Yao, Z.; Liu, H. *Materials and Corrosion* **2009**, *60*, 274-279.

(114) Zamblau, I.; Varvara, S.; Bulea, C.; Muresan, L. M. *Chemical and Biochemical Engineering Quarterly* **2009**, *23*, 43-52.

(115) Wang, S.-C.; Tseng, C.-H. *Advanced Materials Research* **2008**, *51*, 131-139.

(116) Zhou, Y. B.; Qian, B. Y.; Zhang, H. J. *Thin Solid Films* **2009**, *517*, 3287-3291.

(117) Xu, J.; Tao, J.; Jiang, S. *Materials Chemistry and Physics* **2008**, *112*, 966-972.

(118) Chu, X. Y.; Hong, X.; Zhang, X. T.; Zou, P.; Liu, Y. C. *Journal of Physical Chemistry C* **2008**, *112*, 15980-15984.

(119) Praveen, B. M.; Venkatesha, T. V.; Arthoba Naik, Y.; Prashantha, K. *Surface and Coatings Technology* **2007**, *201*, 5836-5842.

(120) Bieganska, B.; Zubielewicz, M.; Smieszek, E. *Progress in Organic Coatings* **1988**, *16*, 219-229.

(121) Funke, W. *Journal of Coatings Technology* **1983**, *55*, 31-38.

(122) Gonzalez, S.; Mirza Rosca, I. C.; Souto, R. M. *Progress in Organic Coatings* **2001**, *43*, 282-285.

(123) Kalendova, A.; Snuparek, J. *FATIPEC Congress* **2000**, *25th*, 21-42.

(124) Kalendova, A.; Sapurina, I.; Stejskal, J.; Vesely, D. *Corrosion Science* **2008**, *50*, 3549-3560.

(125) Stamatakis, P.; Palmer, B. R.; Salzman, G. C.; Bohren, C. F.; Allen, T. B. *Journal of Coatings Technology* **1990**, *62*, 95-98.

(126) Hu, Z. S.; Dong, J. X.; Chen, G. X.; He, J. Z. *Wear* **2000**, *243*, 43-47.

(127) Nasu, A.; Otsubo, Y. *Colloids and Surfaces, A: Physicochemical and Engineering Aspects* **2008**, *326*, 92-97.

(128) Li, F.; Zhou, S.; Gu, G.; You, B.; Wu, L. *Journal of Applied Polymer Science* **2005**, *96*, 912-918.

(129) Kouloumbi, N.; Tsangaris, G. M.; Kyvelidis, S. T. *Journal of Coatings Technology* **1994**, *66*, 83-88.

(130) Kouloumbi, N.; Tsangaris, G. M.; Skordos, A.; Kyvelidis, S. *Progress in Organic Coatings* **1996**, *28*, 117-124.

(131) De Araujo, F. F. T.; Rosenberg, H. M. *Journal of Physics D: Applied Physics* **1976**, *9*, 1025-1030.

(132) Aharoni, S. M. *Journal of Applied Physics* **1972**, *43*, 2463-2465.

(133) Bhattacharyya, S. K.; De, S. K.; Basu, S. *Polymer Engineering and Science* **1979**, *19*, 533-539.

(134) Malliaris, A.; Turner, D. T. *Journal of Applied Physics* **1971**, *42*, 614-618.

(135) Miane, J. L.; Achour, M. E.; Carmona, F. *Physica Status Solidi A: Applied Research* **1984**, *81*, K71-K76.

(136) Gurland, J. In *Powder metallurgy in the nuclear age;* Metallwerk Plansee AG & Co.: Reutte/Tyrol, Austria, 1962; Vol. 1962, pp 507-518.

(137) Brooman, E. W. *Metal Finishing* **2002**, *100*, 48-52.

(138) Li, Y. *Bulletin of Materials Science* **2001**, *24*, 355-360.

(139) Schmidt, D. P.; Shaw, B. A.; Sikora, E.; Shaw, W. W. *Corrosion* **2006**, *62*, 323-339.

(140) Schmidt, D. P.; Shaw, B. A.; Sikora, E.; Shaw, W. W.; Laliberte, L. H. *Progress in Organic Coatings* **2006**, *57*, 352-364.

(141) Coughlin, R. In *Handbook of Coatings Additives,* 2nd ed.; Florio, J. J., Miller, D. J., Eds.; Marcel Dekker, Inc.: New York, 2004, pp 127-144.

(142) Hosseini, M. G.; Ehteshamzadeh, M.; Shahrabi, T. *Electrochimica Acta* **2007**, *52*, 3680-3685.

(143) Khramov, A. N.; Balbyshev, V. N.; Mantz, R. A. *Materials Science Forum* **2006**, *519-521*, 661-666.

(144) Lebrini, M.; Lagrenee, M.; Vezin, H.; Traisnel, M.; Bentiss, F. *Corrosion Science* **2007**, *49*, 2254-2269.

(145) Brooman, E. W. *Metal Finishing* **2002**, *100*, 42, 44-47, 49-53.

(146) Brooman, E. W. *Metal Finishing* **2002**, *100*, 104-110.

(147) Skerry, B. S.; Chen, C. T.; Ray, C. J. *Journal of Coatings Technology* **1992**, *64*, 77-86.

(148) Deflorian, F.; Felhosi, I. *Corrosion* **2003**, *59*, 112-120.

(149) Kalendova, A. *Anti-Corrosion Methods and Materials* **2002**, *49*, 364-372.

(150) Kalendova, A.; Snuparek, J. *Macromolecular Symposia* **2002**, *187*, 97-107.

(151) Kalendova, A.; Vesely, D.; Sapurina, I.; Stejskal, J. *Progress in Organic Coatings* **2008**, *63*, 228-237.

(152) Liu, W. M. *Materials and Corrosion* **1998**, *49*, 576-584.

(153) Sinko, J. *Progress in Organic Coatings* **2001**, *42*, 267-282.

(154) Matsuzaki, A.; Yamaji, T.; Yamashita, M. *Surface and Coatings Technology* **2003**, *169-170*, 655-657.

(155) Nomura, S.; Sakai, H.; Miki, K.; Nakamura, K. *KOBELCO Technology Review* **1989**, *6*, 24-27.

(156) Gelling, V. J.; Wiest, M. M.; Tallman, D. E.; Bierwagen, G. P.; Wallace, G. G. *Progress in Organic Coatings* **2001**, *43*, 149-157.

(157) Cook, A.; Gabriel, A.; Laycock, N. *Journal of the Electrochemical Society* **2004**, *151*, B529-B535.

(158) Leidheiser, H., Jr. *Progress in Organic Coatings* **1979**, *7*, 79-104.

(159) Leidheiser, H., Jr. *Corrosion* **1983**, *39*, 189-201.

(160) Lu, J. L.; Liu, N. J.; Wang, X. H.; Li, J.; Jing, X. B.; Wang, F. S. *Synthetic Metals* **2003**, *135-136*, 237-238.

(161) Mayne, J. E. O. In *Corrosion,* 2nd ed.; Shreir, L. L., Ed.; Newnes Butterworths: Boston, MA, 1976; Vol. 2, pp 15:24-15:37.

(162) Nguyen, T. D.; Nguyen, T. A.; Pham, M. C.; Piro, B.; Normand, B.; Takenouti, H. *Journal of Electroanalytical Chemistry* **2004**, *572*, 225-234.

(163) Plieth, W.; Bund, A. *Encyclopedia of Electrochemistry* **2003**, *4*, 567-592.

(164) Seegmiller, J. C.; Pereira da Silva, J. E.; Buttry, D. A.; Cordoba de Torresi, S. I.; Torresi, R. M. *Journal of the Electrochemical Society* **2005**, *152*, B45-B53.

(165) Nguyen, T.; Hubbard, J. B.; Pommersheim, J. M. *Journal of Coatings Technology* **1996**, *68*, 45-56.

(166) Guruviah, S. *Journal of the Oil and Colour Chemists' Association* **1970**, *53*, 669-679.

(167) Feser, R.; Stratmann, M. *Steel Research* **1990**, *61*, 482-489.

(168) Haagen, H.; Funke, W. *Journal of the Oil and Colour Chemists' Association* **1975**, *58*, 359-364.

(169) Kittelberger, W. W.; Elm, A. C. *Journal of Industrial and Engineering Chemistry* **1952**, *44*, 326-329.

(170) Mayne, J. E. O. *Official Digest, Federation of Paint and Varnish Production Clubs* **1952**, *325*, 127-136.

(171) Leidheiser, H., Jr. *Journal of Coatings Technology* **1981**, *53*, 29-39.

(172) Fang, J.; Xu, K.; Zhu, L.; Zhou, Z.; Tang, H. *Corrosion Science* **2007**, *49*, 4232-4242.

(173) Gonzalez-Garcia, Y.; Gonzalez, S.; Souto, R. M. *Corrosion Science* **2007**, *49*, 3514-3526.

(174) Gonzalez-Rodriguez, J. G.; Lucio-Garcia, M. A.; Nicho, M. E.; Cruz-Silva, R.; Casales, M.; Valenzuela, E. *Journal of Power Sources* **2007**, *168*, 184-190.

(175) Jorcin, J.-B.; Aragon, E.; Merlatti, C.; Pebere, N. *Corrosion Science* **2006**, *48*, 1779-1790.

(176) Kendig, M.; Mansfeld, F. *Materials Research Society Symposium Proceedings* **1988**, *125*, 293-320.

(177) Kendig, M.; Mansfeld, F.; Tsai, S. *Corrosion Science* **1983**, *23*, 317-329.

(178) Monetta, T.; Bellucci, F.; Nicodemo, L.; Nicolais, L. *Progress in Organic Coatings* **1993**, *21*, 353-369.

(179) Rohwerder, M.; Michalik, A. *Electrochimica Acta* **2007**, *53*, 1300-1313.

(180) Tallman, D. E.; Bierwagen, G. P. In *Handbook of Conducting Polymers,* 3rd ed.; Skotheim, T. A., Reynolds, J., Eds.; Marcel Dekker, Inc.: New York, 2007; Vol. 2, pp 15/11-15/53.

(181) McGill, W. J. *Journal of the Oil and Colour Chemists' Association* **1977**, *60*, 121-126.

(182) Deflorian, F.; Fedrizzi, L. *Journal of Adhesion Science and Technology* **1999**, *13*, 629-645.

(183) Sherbondy, V. D. In *Paint and Coating Testing Manual-Fourteenth Edition of the Gardner-Sward Handbook*; Koleske, J. V., Ed.; ASTM Manual Series: Philadelphia, PA, 1995, pp 643-653.

(184) Olivier, M. *Chimie Nouvelle* **2001**, *19*, 3310-3314.

(185) Goering, W.; Koesters, E.; Muenster, R. In *Corrosion Control by Organic Coatings*; Leidheiser, H., Ed.; National Association of Corrosion Engineers: Houston, TX, 1981, pp 255-262.

(186) Rengaswamy, N. S.; Vedhalakshmi, R.; Balakrishnan, K. *Anti-Corrosion Methods and Materials* **1995**, *42*, 7-9.

(187) Kim, J.-G.; Yu, Y.-J.; Yoo, J.-K. *Metals and Materials International* **2005**, *11*, 209-214.

(188) Shah, B. K.; Gurumurthy, K. R.; Choudhuri, G. *Metals, Materials and Processes* **2006**, *18*, 95-106.

(189) Edwards, M.; Ferguson, J. F. *Proceedings - Water Quality Technology Conference* **1993**, 759-775.

(190) de la Fuente, D.; Castano, J. G.; Morcillo, M. *Corrosion Science* **2007**, *49*, 1420-1436.

(191) Blekkenhorst, F.; Ferrari, G. M.; Van der Wekken, C. J.; Ijsseling, F. P. *British Corrosion Journal* **1986**, *21*, 163-176.

(192) Blekkenhorst, F.; Ferrari, G. M.; Van der Wekken, C. J.; Ijsseling, F. P. *British Corrosion Journal* **1988**, *23*, 165-171.

(193) Arganis-Juarez, C. R.; Malo, J. M.; Uruchurtu, J. *Nuclear Engineering and Design* **2007**, *237*, 2283-2291.

(194) Kim, K. Y.; Hwang, Y. H.; Yoo, J. Y. *Corrosion* **2002**, *58*, 570-583.

(195) Van Westing, E. P. M.; Ferrari, G. M.; De Wit, J. H. W. *Electrochimica Acta* **1994**, *39*, 899-910.

(196) Hammouda, N.; Boudinar, Y.; Touiker, M.; Belmokre, K. *Materials and Corrosion* **2006**, *57*, 338-344.

(197) Lambert, M. R.; Townsend, H. E.; Hart, R. G.; Frydrych, D. J. *Industrial & Engineering Chemistry Product Research and Development* **1985**, *24*, 378-384.

(198) Skerry, B. S.; Simpson, C. H. *Corrosion* **1993**, *49*, 663-674.

(199) Bonnel, K.; Le Pen, C.; Pebere, N. *Electrochimica Acta* **1999**, *44*, 4259-4267.

(200) van der Weijde, D. H.; van Westing, E. P. M.; de Wit, J. H. W. *Electrochimica Acta* **1996**, *41*, 1103-1107.

(201) Deflorian, F.; Rossi, S. *Electrochimica Acta* **2006**, *51*, 1736-1744.

(202) Eden, D. A.; Hoffman, M.; Skerry, B. S. *ACS Symposium Series* **1986**, *322*, 36-47.

(203) Jeyaprabha, C.; Muralidharan, S.; Venkatachari, G.; Raghavan, M. *Corrosion Reviews* **2001**, *19*, 301-313.

(204) Metikis-Hukovic, M.; Stupnisek-Lisac, E.; Loncar, M. *Bulletin of Electrochemistry* **1991**, *7*, 128-132.

(205) Mills, D. J.; Mabbutt, S. *Progress in Organic Coatings* **2000**, *39*, 41-48.

(206) Arslan, O.; Arpac, E.; Sayilkan, F.; Sayilkan, H. *Journal of Materials Science* **2007**, *42*, 2138-2142.

(207) Colak, N.; Oezyilmaz, A. T. *Polymer-Plastics Technology and Engineering* **2005**, *44*, 1547-1558.

(208) Holsworth, R. M. *Advances in Chemistry Series* **1983**, *203*, 363-382.

(209) Wolfe, K. L.; Kimbrough, K. L.; Dillard, J. G.; Harp, S. R.; Grant, J. W. *Journal of Adhesion* **1995**, *55*, 109-122.

(210) Lan, W.; Sun, J.; Zhou, A.; Zhang, D. *Materials Science Forum* **2009**, *610-613*, 880-883.

(211) Wu, M.; Gao, P.; Liu, Y.; Xiao, H. *Materials Science Forum* **2009**, *610-613*, 211-214.

(212) Dominguez-Crespo, M. A.; Garcia-Murillo, A.; Torres-Huerta, A. M.; Carrillo-Romo, F. J.; Onofre-Bustamante, E.; Yanez-Zamora, C. *Electrochimica Acta* **2009**, *54*, 2932-2940.

(213) Almeida, E.; Pereira, D.; Figueiredo, O. *Progress in Organic Coatings* **1989**, *17*, 175-189.

(214) Hinder, S. J.; Lowe, C.; Maxted, J. T.; Perruchot, C.; Watts, J. F. *Progress in Organic Coatings* **2005**, *54*, 20-27.

(215) Horner, M. R.; Boerio, F. J. *Journal of Adhesion* **1990**, *32*, 141-156.

(216) Lenormand, P.; Lecomte, A.; Babonneau, D.; Dauger, A. *Thin Solid Films* **2005**, *495*, 224-231.

(217) Malzbender, J.; De With, G. *Journal of Materials Science* **2000**, *35*, 4809-4814.

(218) Sinapi, F.; Lejeune, I.; Delhalle, J.; Mekhalif, Z. *Electrochimica Acta* **2007**, *52*, 5182-5190.

(219) Watts, J. F. *Microchimica Acta* **2009**, *164*, 379-385.

(220) Branzoi, V.; Pilan, L.; Branzoi, F. *WIT Transactions on Engineering Sciences* **2005**, *51*, 269-277.

(221) Wilson, B.; Fink, N.; Grundmeier, G. *Electrochimica Acta* **2006**, *51*, 3066-3075.

(222) Goossens, V.; Van Gils, S.; De Strycker, J.; Finsy, R.; Terryn, H. *Thin Solid Films* **2005**, *493*, 35-40.

(223) Ritter, J. J. *Journal of Coatings Technology* **1982**, *54*, 51-57.

(224) Roseler, A.; Korte, E.-H. *Thin Solid Films* **1998**, *313-314*, 708-712.

(225) Tsankov, D.; Hinrichs, K.; Roseler, A.; Korte, E. H. *Physica Status Solidi A: Applied Research* **2001**, *188*, 1319-1329.

(226) Ghorbal, A.; Grisotto, F.; Charlier, J.; Palacin, S.; Goyer, C.; Demaille, C. *ChemPhysChem* **2009**, *10*, 1053-1057.

(227) Hwang, J.-H.; Lee, B. I.; Klep, V.; Luzinov, I. *Materials Research Bulletin* **2008**, *43*, 2652-2657.

(228) Paulussen, S.; Rego, R.; Goossens, O.; Vangeneugden, D.; Rose, K. *Journal of Physics D: Applied Physics* **2005**, *38*, 568-575.

(229) Posner, R.; Wapner, K.; Stratmann, M.; Grundmeier, G. *Electrochimica Acta* **2009**, *54*, 891-899.

(230) Rohwerder, M.; Stratmann, M. *Proceedings of the Electrochemical Society* **2000**, *99-28*, 302-315.

(231) Rohwerder, M.; Stratmann, M.; Leblanc, P.; Frankel, G. S. In *Analytical Methods in Corrosion Science and Engineering*; Marcus, P., Mansfeld, F., Eds.; CRC Press: Boca Raton, FL, 2006, pp 605-648.

(232) Frankel, G. S.; Leblanc, P. *Corrosion Science and Technology* **2002**, *31*, 419-425.

(233) Bohm, S.; McMurray, H. N.; Powell, S. M.; Worsley, D. A. *Electrochimica Acta* **2000**, *45*, 2165-2174.

(234) Worsley, D. A.; Williams, D.; Ling, J. S. G. *Corrosion Science* **2001**, *43*, 2335-2348.

(235) Bohm, S.; Challis, M.; Heatley, T.; Worsley, D. A. *Transactions of the Institute of Metal Finishing* **2001**, *79*, 16-21.

(236) McMurray, H. N.; Williams, D.; Worsley, D. A. *ECS Transactions* **2006**, *1*, 153-164.

(237) Fian, A.; Haase, A.; Stadlober, B.; Jakopic, G.; Matsko, N. B.; Grogger, W.; Leising, G. *Analytical and Bioanalytical Chemistry* **2008**, *390*, 1455-1461.

(238) Spirkova, M.; Slouf, M.; Blahova, O.; Farkacova, T.; Benesova, J. *Journal of Applied Polymer Science* **2006**, *102*, 5763-5774.

(239) Smith, J. R.; Breakspear, S.; Fletcher, R. J. R.; Campbell, S. A. *Transactions of the Institute of Metal Finishing* **2005**, *83*, 63-67.

(240) Brus, J.; Spirkova, M. *Macromolecular Symposia* **2005**, *220*, 155-164.

(241) Karbach, A.; Drechsler, D. *Surface and Interface Analysis* **1999**, *27*, 401-409.

(242) Zhang, F.; Liu, J.; Li, X.; Guo, M. *Journal of Applied Polymer Science* **2008**, *109*, 1890-1899.

(243) Green, J. B. D.; McDermott, C. A.; McDermott, M. T.; Porter, M. D. In *Imaging of Surfaces and Interfaces*; Lipkowski, J., Ross, P., Eds.; Wiley-VCH: New York, 1999, pp 249-303.

(244) Buchholz, S.; Fuchs, H.; Rabe, J. P. *Advanced Materials* **1991**, *3*, 51-54.

(245) Eckhard, K.; Erichsen, T.; Stratmann, M.; Schuhmann, W. *Chemistry-A European Journal* **2008**, *14*, 3968-3976.

(246) Bastos, A. C.; Simoes, A. M.; Gonzalez, S.; Gonzalez-Garcia, Y.; Souto, R. M. *Progress in Organic Coatings* **2005**, *53*, 177-182.

(247) Simoes, A. M.; Battocchi, D.; Tallman, D. E.; Bierwagen, G. P. *Corrosion Science* **2007**, *49*, 3838-3849.

(248) Souto, R. M.; Gonzalez-Garcia, Y.; Gonzalez, S. *Corrosion Science* **2005**, *47*, 3312-3323.

(249) Alagta, A.; Felhoesi, I.; Bertoti, I.; Kalman, E. *Corrosion Science* **2008**, *50*, 1644-1649.

(250) Hamlaoui, Y.; Pedraza, F.; Tifouti, L. *Corrosion Science* **2008**, *50*, 1558-1566.

(251) Macdonald, D. D. *Electrochimica Acta* **2006**, *51*, 1376-1388.

(252) Macdonald, J. R.; Johnson, W. B. In *Impedance Spectroscopy: Theory, Experiment, and Applications,* 2nd ed.; Barsoukov, E., Macdonald, J. R., Eds.; John Wiley & Sons, Inc.: Hoboken, NJ, 2005, pp 1-26.

(253) Mansfeld, F. *Electrochimica Acta* **1990**, *35*, 1533-1544.

(254) Rammelt, U.; Koehler, S.; Reinhard, G. *Corrosion Science* **2008**, *50*, 1659-1663.

(255) Horn, J.; Jones, D. In *Manual of Environmental Microbiology,* 2nd ed.; Hurst, C. J., Crawford, R. L., Knudsen, G. R., McInerney, M. J., Stetzenbach, L. D., Eds.; ASM Press: Washington, DC, 2002, pp 1072-1083.

(256) Little, B. J.; Wagner, P. A. *ASTM Special Technical Publication* **1994**, *STP 1232*, 1-11.

(257) Little, B. J.; Wagner, P. A. *Modern Aspects of Electrochemistry* **2001**, *34*, 205-246.

(258) Mansfeld, F. *Materials and Corrosion* **2003**, *54*, 489-502.

(259) Sequeira, C. A. C. *Biology of World Resources Series* **1995**, *1*, 307-325.

(260) Videla, H. A.; Herrera, L. K. *International Microbiology* **2005**, *8*, 169-180.

(261) Brito, R.; Tremont, R.; Cabrera, C. R. *Journal of Electroanalytical Chemistry* **2004**, *574*, 15-22.

(262) Co, A. C.; Xia, S. J.; Birss, V. I. *Journal of the Electrochemical Society* **2005**, *152*, A570-A576.

(263) Diard, J.-P.; Glandut, N.; Montella, C.; Sanchez, J.-Y. *Journal of Electroanalytical Chemistry* **2005**, *578*, 247-257.

(264) Gimenez-Romero, D.; Garcia-Jareno, J. J.; Vicente, F. *Electrochemistry Communications* **2003**, *5*, 722-727.

(265) Gregori, J.; Gimenez-Romero, D.; Garcia-Jareno, J. J.; Vicente, F. *Journal of Solid State Electrochemistry* **2006**, *10*, 920-928.

(266) Kumar, P. S.; Lakshminarayanan, V. *Langmuir* **2007**, *23*, 1548-1554.

(267) Lasia, A. *Modern Aspects of Electrochemistry* **2002**, *35*, 1-49.

(268) Sakly, H.; Mlika, R.; Bonnamour, I.; Aouni, F.; Ben Ouada, H.; Renault, N. J. *Electrochimica Acta* **2007**, *52*, 3697-3703.

(269) Sundfors, F.; Bobacka, J.; Ivaska, A.; Lewenstam, A. *Electrochimica Acta* **2002**, *47*, 2245-2251.

(270) Quraishi, M. A.; Rawat, J. *Corrosion Reviews* **2001**, *19*, 273-299.

(271) Gomadam, P. M.; Weidner, J. W. *International Journal of Energy Research* **2005**, *29*, 1133-1151.

(272) Jiang, S. P.; Love, J. G.; Badwal, S. P. S. *Key Engineering Materials* **1997**, *125-126*, 81-132.

(273) Morita, H.; Nakano, H.; Mugikura, Y.; Izaki, Y.; Watanabe, T.; Uchida, I. *Journal of the Electrochemical Society* **2003**, *150*, A1693-A1698.

(274) Schulze, M.; Wagner, N.; Kaz, T.; Friedrich, K. A. *Electrochimica Acta* **2007**, *52*, 2328-2336.

(275) Wiezell, K.; Gode, P.; Lindbergh, G. *Journal of the Electrochemical Society* **2006**, *153*, A759-A764.

(276) Gabrielli, C.; Keddam, M.; Portail, N.; Rousseau, P.; Takenouti, H.; Vivier, V. *Journal of Physical Chemistry B* **2006**, *110*, 20478-20485.

(277) Aaboubi, O.; Los, P.; Amblard, J.; Chopart, J. P.; Olivier, A. *Journal of the Electrochemical Society* **2003**, *150*, E125-E130.

(278) Benyaich, A.; Deslouis, C.; El Moustafid, T.; Musiani, M. M.; Tribollet, B. *Electrochimica Acta* **1996**, *41*, 1781-1785.

(279) Chiu, C.-Y.; Yen, Y.-J.; Kuo, S.-W.; Chen, H.-W.; Chang, F.-C. *Polymer* **2007**, *48*, 1329-1342.

(280) Deslouis, C.; El Moustafid, T.; Musiani, M. M.; Tribollet, B. *Electrochimica Acta* **1996**, *41*, 1343-1349.

(281) Ehrenbeck, C.; Juttner, K.; Ludwig, S.; Paasch, G. *Electrochimica Acta* **1998**, *43*, 2781-2789.

(282) Musiani, M. M. *Electrochimica Acta* **1990**, *35*, 1665-1670.

(283) Rossberg, K.; Dunsch, L. *Electrochimica Acta* **1999**, *44*, 2061-2071.

(284) Tarola, A.; Dini, D.; Salatelli, E.; Andreani, F.; Decker, F. *Electrochimica Acta* **1999**, *44*, 4189-4193.

(285) Duprat, M.; Lafont, M. C.; Dabosi, F.; Moran, F. *Electrochimica Acta* **1985**, *30*, 353-365.

(286) Kendig, M. *AIChE Symposium Series* **1990**, *86*, 61-70.

(287) Mansfeld, F.; Kendig, M. W.; Tsai, S. *Corrosion Science* **1982**, *22*, 455-471.

(288) Stewart, K. C.; Kolman, D. G.; Taylor, S. R. *ASTM Special Technical Publication* **1993**, *STP 1188*, 73-93.

(289) Hilbert, L. R. *Corrosion Science* **2006**, *48*, 3907-3923.

(290) Orazem, M. E.; Tribollet, B. *Electrochemical Impedance Spectroscopy*; John Wiley & Sons, Inc.: Hoboken, NJ, 2008.

(291) Lasia, A. *Modern Aspects of Electrochemistry* **1999**, *32*, 143-248.

(292) Bonora, P. L.; Deflorian, F.; Fedrizzi, L. *Electrochimica Acta* **1996**, *41*, 1073-1082.

(293) K'Owino, I. O.; Sadik, O. A. *Electroanalysis* **2005**, *17*, 2101-2113.

(294) Li, D.; Zou, X.; Shen, Q.; Dong, S. *Electrochemistry Communications* **2007**, *9*, 191-196.

(295) Jansen, A. N.; Orazem, M. E. *Journal of the Electrochemical Society* **1992**, *139*, 1463-1469.

(296) Peter, L. M. *Comprehensive Chemical Kinetics* **1999**, 223-280.

(297) Viscor, P.; Vedde, J. *Surface Science* **1993**, *287-288*, 510-513.

(298) Ariza, E.; Rocha, L. A. *Materials Science Forum* **2005**, *492-493*, 189-194.

(299) Gonzalez, J. E. G.; Mirza-Rosca, J. C. *Journal of Electroanalytical Chemistry* **1999**, *471*, 109-115.

(300) Hubrecht, J. In *Metals as Biomaterials*; Helsen, J. A., Breme, H. J., Eds.; John Wiley & Sons, Inc.: New York, 1998, pp 405-466.

(301) Liu, Q.; Yu, J.; Xiao, L.; Tang, J. C. O.; Zhang, Y.; Wang, P.; Yang, M. *Biosensors & Bioelectronics* **2009**, *24*, 1305-1310.

(302) Jauhari, S.; Mehta, G. N.; Pai, K. B. *Transactions of the SAEST* **2003**, *38*, 155-156.

(303) Malkia, A.; Liljeroth, P.; Kontturi, K. *Electrochemistry Communications* **2003**, *5*, 473-479.

(304) Smith, G.; Heidari, S.; Suherman, P.; Bell, R. *Drug Development and Industrial Pharmacy* **2002**, *28*, 151-156.

(305) Moisel, M.; Lorenzo de Mele, M. A. F.; Mueller, W.-D. *Advanced Engineering Materials* **2008**, *10*, B33-B46.

(306) Silva, M. G.; Helali, S.; Esseghaier, C.; Suarez, C. E.; Oliva, A.; Abdelghani, A. *Sensors and Actuators, B: Chemical Sensors* **2008**, *B135*, 206-213.

(307) Panke, O.; Balkenhohl, T.; Kafka, J.; Schafer, D.; Lisdat, F. *Advances in Biochemical Engineering/Biotechnology* **2008**, *109*, 195-237.

(308) Deflorian, F., Ed. *Special Issue on Electrochemical Impedance Spectroscopy. (Proceedings of a Symposium held June 2001 in Marilleva, Italy.) [In: Electrochimica Acta, 2002; 47(13-14) pp. 2025-2361]*, 2002.

(309) Gabrielli, C. *Physical Electrochemistry* **1995**, 243-292.

(310) Macdonald, D. D. *Proceedings of the Electrochemical Society* **1991**, *91-6*, 1-43.

(311) Macdonald, D. D., Ed. *Special Issue: EIS-1992: The 2nd International Symposium on Electrochemical Impedance Spectroscopy (held 12-17 July 1992 in Santa Barbara, CA.) [In Electrochimica Acta, 1993; 38(14) pp. 1797-2143]*, 1993.

(312) Mattos, O. R. *Electrochimica Acta* **1999**, *44*, 4113-4464.

(313) Orazem, M. E., Ed. *Special Issue: Electrochemical Impedance Spectroscopy. (Selection of Papers from the 6th International Symposium (EIS 2004) held 16-21 May 2004 in Cocoa Beach, FL.) [In: Electrochimica Acta, 2006; 51(8-9) pp. 1375-1904]*, 2006.

(314) Pejcic, B.; De Marco, R. *Electrochimica Acta* **2006**, *51*, 6217-6229.

(315) Vereecken, J.; Editor *Electrochimica Acta* **1996**, *41*, 953-1409

(316) Fernandez-Sanchez, C.; McNeil, C. J.; Rawson, K. *TrAC, Trends in Analytical Chemistry* **2005**, *24*, 37-48.

(317) Taylor, S. R. *Progress in Organic Coatings* **2001**, *43*, 141-148.

(318) Mansfeld, F.; Han, L. T.; Lee, C. C.; Zhang, G. *Electrochimica Acta* **1998**, *43*, 2933-2945.

(319) Amirudin, A.; Thierry, D. *Progress in Organic Coatings* **1995**, *26*, 1-28.

(320) Angelini, E.; Grassini, S.; Rosalbino, F.; Fracassi, F.; d'Agostino, R. *Progress in Organic Coatings* **2003**, *46*, 107-111.

(321) Beaunier, L.; Epelboin, I.; Lestrade, J. C.; Takenouti, H. *Surface Technology* **1976**, *4*, 237-254.

(322) Kendig, M.; Scully, J. *Corrosion* **1990**, *46*, 22-29.

(323) Marchebois, H.; Joiret, S.; Savall, C.; Bernard, J.; Touzain, S. *Surface and Coatings Technology* **2002**, *157*, 151-161.

(324) Perez, C.; Izquierdo, M.; Abreu, C. M. In *Trends in Electrochemistry and Corrosion at the Beginning of the 21st Century*; Brillas, E., Cabot, P.-L., Eds.; Universitat de Barcelona Publications: Barcelona, Spain, 2004, pp 923-946.

(325) Stern, M. *Journal of the Electrochemical Society* **1957**, *104*, 559-563.

(326) Stern, M.; Geavy, A. L. *Journal of the Electrochemical Society* **1957**, *104*, 56-63.

(327) Silverman, D. C. *Electrochimica Acta* **1993**, *38*, 2075-2078.

(328) Silverman, D. C.; Carrico, J. E. *Corrosion* **1988**, *44*, 280-287.

(329) Amirudin, A.; Barreau, C.; Hellouin, R.; Thierry, D. *Progress in Organic Coatings* **1995**, *25*, 339-355.

(330) Chen, C. T.; Skerry, B. S. *Corrosion* **1991**, *47*, 598-611.

(331) Mansfeld, F.; Kendig, M. W. *ASTM Special Technical Publication* **1985**, *866*, 122-142.

(332) Mansfeld, F.; Kendig, M. W.; Tsai, S. *Corrosion* **1982**, *38*, 478-485.

(333) Urquidi-Macdonald, M.; Egan, P. C. *Corrosion Reviews* **1997**, *15*, 169-194.

(334) Walter, G. W. *Corrosion Science* **1986**, *26*, 681-703.

(335) Walter, G. W. *Corrosion Science* **1991**, *32*, 1059-1084.

(336) Boukamp, B. A. *Technisches Messen* **2004**, *71*, 454-459.

(337) Macdonald, D. D. *Corrosion* **1990**, *46*, 229-242.

(338) Macdonald, D. D. *NATO ASI Series, Series E: Applied Sciences* **1991**, *203*, 31-68.

(339) Raistrick, I. D.; Franceschetti, D. R.; Macdonald, J. R. In *Impedance Spectroscopy: Theory, Experiment, and Applications,* 2nd ed.; Barsoukov, E., Macdonald, J. R., Eds.; John Wiley & Sons: Hoboken, NJ, 2005, pp 27-128.

(340) Instruments, G.; Gamry Instruments: Warminster, PA, 2009; Vol. 2009.

(341) Research, A. P. A., 2009; Vol. 2009.

(342) Scribner Associates, I., 2009.

(343) Amirudin, A.; Thierry, D. *British Corrosion Journal* **1995**, *30*, 214-220.

(344) McIntyre, J. M.; Pham, H. Q. *Progress in Organic Coatings* **1996**, *27*, 201-207.

(345) Murray, J. N.; Hack, H. P. *Corrosion* **1991**, *47*, 480-489.

(346) Feliu, S.; Galvan, J. C.; Morcillo, M. *Corrosion Science* **1990**, *30*, 989-998.

(347) Mansfeld, F.; Kendig, M. W.; Tsai, S. *Corrosion* **1982**, *38*, 570-580.

(348) Cavalcanti, E.; Ferraz, O.; Di Sarli, A. R. *Progress in Organic Coatings* **1993**, *23*, 185-200.

(349) Compere, C.; Hechler, J. J.; Cole, K. *Progress in Organic Coatings* **1992**, *20*, 187-198.

(350) Haruyama, S.; Asari, M.; Tsuru, T. *Proceedings of the Electrochemical Society* **1987**, *87-2*, 197-207.

(351) Narain, S.; Bonanos, N.; Hocking, M. G. *Journal of the Oil and Colour Chemists' Association* **1983**, *66*, 48-52.

(352) Pebere, N.; Picaud, T.; Duprat, M.; Dabosi, F. *Corrosion Science* **1989**, *29*, 1073-1086.

(353) Vogelsang, J.; Strunz, W. *Electrochimica Acta* **2001**, *46*, 3817-3826.

(354) Compere, C.; Frechette, E.; Ghali, E. *Corrosion Science* **1993**, *34*, 1259-1274.

(355) Frechette, E.; Compere, C.; Ghali, E. *Corrosion Science* **1992**, *33*, 1067-1081.

(356) Grandle, J. A.; Taylor, S. R. *Corrosion* **1994**, *50*, 792-803.

(357) Amirudin, A.; Thierry, D. *British Corrosion Journal* **1995**, *30*, 128-134.

(358) Bonora, P. L.; Deflorian, F.; Fedrizzi, L.; Rossi, S. *Special Publication - Royal Society of Chemistry* **1998**, *177*, 163-180.

(359) Hara, M.; Ichino, R.; Okido, M.; Wada, N. *Surface and Coatings Technology* **2003**, *169-170*, 679-681.

(360) Kumar, S. A.; Alagar, M.; Mohan, V. *Journal of Materials Engineering and Performance* **2002**, *11*, 123-129.

(361) Loveday, D.; Peterson, P.; Rodgers, B. *Journal of Coatings Technology* **2004**, *1*, 88-93.

(362) Mansfeld, F.; Lin, S.; Kim, S.; Shih, H. *Journal of the Electrochemical Society* **1990**, *137*, 78-82.

(363) Mansfeld, F.; Shih, H.; Postyn, A.; Devinny, J.; Islander, R.; Chen, C. L. *Corrosion* **1991**, *47*, 369-376.

(364) Mansfeld, F.; Sun, Z.; Hsu, C. H. *Electrochimica Acta* **2001**, *46*, 3651-3664.

(365) Rossi, S.; Deflorian, F.; Fontanari, L.; Cambruzzi, A.; Bonora, P. L. *Progress in Organic Coatings* **2005**, *52*, 288-297.

(366) Titz, J.; Wanger, G. H.; Spahn, H.; Ebert, M.; Juttner, K.; Lorenz, W. J. *Corrosion* **1990**, *46*, 220-221.

(367) Loveday, D.; Peterson, P.; Rodgers, B. *Journal of Coatings Technology* **2004**, *1*, 46-52.

(368) Loveday, D.; Peterson, P.; Rodgers, B. *Journal of Coatings Technology* **2005**, *2*, 22-27.

(369) Breuer, O.; Chen, H.; Lin, B.; Sundararaj, U. *Journal of Applied Polymer Science* **2005**, *97*, 136-142.

(370) Tibbetts, G. G.; Lake, M. L.; Strong, K. L.; Rice, B. P. *Composites Science and Technology* **2007**, *67*, 1709-1718.

(371) Winey, K. I.; Vaia, R. A. *MRS Bulletin* **2007**, *32*, 314-322.

(372) Maruyama, B.; Alam, K. *SAMPE Journal* **2002**, *38*, 59-70.

(373) Chung, D. D. L. *Carbon* **2001**, *39*, 1119-1125.

(374) Ci, L.; Wei, J.; Wei, B.; Liang, J.; Xu, C.; Wu, D. *Carbon* **2001**, *39*, 329-335.

(375) Endo, M.; Kim, Y. A.; Hayashi, T.; Nishimura, K.; Matusita, T.; Miyashita, K.; Dresselhaus, M. S. *Carbon* **2001**, *39*, 1287-1297.

(376) Endo, M.; Kim, Y. A.; Matusita, T.; Hayashi, T. *NATO Science Series, Series E: Applied Sciences* **2001**, *372*, 51-61.

(377) Endo, M.; Kim, Y. A.; Takeda, T.; Hong, S. H.; Matusita, T.; Hayashi, T.; Dresselhaus, M. S. *Carbon* **2001**, *39*, 2003-2010.

(378) Ngo, Q.; Cassell, A. M.; Radmilovic, V.; Li, J.; Krishnan, S.; Meyyappan, M.; Yang, C. Y. *Carbon* **2007**, *45*, 424-428.

(379) Paredes, J. I.; Martinez-Alonso, A.; Tascon, J. M. D. *Carbon* **2001**, *39*, 1575-1587.

(380) Van Hattum, F. W. J.; Bernardo, C. A.; Tibbetts, G. G. *NATO Science Series, Series E: Applied Sciences* **2001**, *372*, 245-254.

(381) Zou, J.-z.; Zeng, X.-r.; Xiong, X.-b.; Tang, H.-l.; Li, L.; Liu, Q.; Li, Z.-q. *Carbon* **2007**, *45*, 828-832.

(382) Lakshminarayanan, P. V.; Toghiani, H.; Pittman, C. U. *Carbon* **2004**, *42*, 2433-2442.

(383) Romero, A.; Garrido, A.; Nieto-Marquez, A.; De la Osa, A. R.; De Lucas, A.; Valverde, J. L. *Applied Catalysis, A: General* **2007**, *319*, 246-258.

(384) Zhou, J.-H.; Sui, Z.-J.; Li, P.; Chen, D.; Dai, Y.-C.; Yuan, W.-K. *Carbon* **2006**, *44*, 3255-3262.

(385) Al-Saleh, M. H.; Sundararaj, U. *Carbon* **2009**, *47*, 2-22.

(386) Breuer, O.; Sundararaj, U. *Polymer Composites* **2004**, *25*, 630-645.

(387) Moniruzzaman, M.; Winey, K. I. *Macromolecules* **2006**, *39*, 5194-5205.

(388) Heremans, J. *Carbon* **1985**, *23*, 431-436.

(389) Ishioka, M.; Okada, T.; Matsubara, K. *Journal of Materials Research* **1992**, *7*, 3019-3022.

(390) Mordkovich, V. Z. *Theoretical Foundations of Chemical Engineering* **2003**, *37*, 429-438.

(391) Jacobsen, R. L.; Tritt, T. M.; Guth, J. R.; Ehrlich, A. C.; Gillespie, D. J. *Carbon* **1995**, *33*, 1217-1221.

(392) Lake, M. L.; Ting, J.-M. In *Carbon Materials for Advanced Technologies*; Burchell, T. D., Ed.; Elsevier Science Ltd.: Oxford, U.K., 1999, pp 139-167.

(393) Miyagawa, H.; Misra, M.; Mohanty, A. K. *Journal of Nanoscience and Nanotechnology* **2005**, *5*, 1593-1615.

(394) Patton, R. D.; Pittman, C. U., Jr.; Wang, L.; Hill, J. R. *Composites, Part A: Applied Science and Manufacturing* **1999**, *30A*, 1081-1091.

(395) Tibbetts, G. G. *Carbon* **1989**, *27*, 745-747.

(396) Tibbetts, G. G. *NATO Science Series, Series E: Applied Sciences* **2001**, *372*, 1-9.

(397) Alig, R.; Lake, M.; Guth, J.; Burton, D. *Proceedings of the 11th Annual International Pittsburgh Coal Conference* **1994**, *1*, 180-187.

(398) Finegan, I. C.; Tibbetts, G. G. *Journal of Materials Research* **2001**, *16*, 1668-1674.

(399) Lee, J.-T.; Chu, Y.-J.; Wang, F.-M.; Yang, C.-R.; Li, C.-C. *Journal of Materials Science* **2007**, *42*, 10118-10123.

(400) Subramanian, V.; Zhu, H.; Wei, B. *Journal of Physical Chemistry B* **2006**, *110*, 7178-7183.

(401) Tibbetts, G. G.; McHugh, J. J. *Journal of Materials Research* **1999**, *14*, 2871-2880.

(402) Ting, J. M.; Lake, M. L. *Microelectronics International* **1995**, *38*, 30-31.

(403) Tsubokawa, N.; Chen, J.; Wei, G.; Mikuni, M.; Fujiki, K. *Polymer Preprints* **2003**, *44*, 429-430.

(404) Zhang, H.-L.; Zhang, Y.; Zhang, X.-G.; Li, F.; Liu, C.; Tan, J.; Cheng, H.-M. *Carbon* **2006**, *44*, 2778-2784.

(405) Day, R. J.; Lovell, P. A.; Wazzan, A. A. *Composites Science and Technology* **2001**, *61*, 41-56.

(406) Lozano, K.; Bonilla-Rios, J.; Barrera, E. V. *Journal of Applied Polymer Science* **2001**, *80*, 1162-1172.

(407) Shibuya, M.; Sakurai, M.; Takahashi, T. *Composites Science and Technology* **2007**, *67*, 3338-3344.

(408) Thongruang, W.; Spontak, R. J.; Balik, C. M. *Polymer* **2002**, *43*, 2279-2286.

(409) Tibbetts, G. G. *NATO Science Series, Series E: Applied Sciences* **2001**, *372*, 63-73.

(410) Tibbetts, G. G.; Finegan, I. C.; Kwag, C. *Molecular Crystals and Liquid Crystals Science and Technology, A: Molecular Crystals and Liquid Crystals* **2002**, *387*, 129-133.

(411) Xu, J.; Donohoe, J. P.; Pittman, C. U., Jr. *Composites, Part A* **2004**, *35A*, 693-701.

(412) Yudin, V. E.; Svetlichnyi, V. M.; Shumakov, A. N.; Schechter, R.; Harel, H.; Marom, G. *Composites, Part A: Applied Science and Manufacturing* **2008**, *39*, 85-90.

(413) Zhou, Y.; Pervin, F.; Jeelani, S. *Journal of Materials Science* **2007**, *42*, 7544-7553.

(414) Al-Saleh, M. H.; Sundararaj, U. *Annual Technical Conference - Society of Plastics Engineers* **2008**, *66th*, 34-38.

(415) Katsumata, M.; Yamanashi, H.; Ushijima, H. *Proceedings of SPIE-The International Society for Optical Engineering* **1993**, *1916*, 140-148.

(416) Yang, S.; Lozano, K.; Lomeli, A.; Foltz, H. D.; Jones, R. *Composites, Part A: Applied Science and Manufacturing* **2005**, *36A*, 691-697.

(417) Zhang, C.-S.; Ni, Q.-Q.; Fu, S.-Y.; Kurashiki, K. *Composites Science and Technology* **2007**, *67*, 2973-2980.

(418) Gordeyev, S. A.; Ferreira, J. A.; Bernardo, C. A.; Ward, I. M. *Materials Letters* **2001**, *51*, 32-36.

(419) Tzeng, S.-S.; Hung, K.-H.; Ko, T.-H. *Carbon* **2006**, *44*, 859-865.

(420) Wu, G.; Asai, S.; Sumita, M. *Macromolecules* **1999**, *32*, 3534-3536.

(421) Abe, H.; Murai, T.; Zaghib, K. *Journal of Power Sources* **1999**, *77*, 110-115.

(422) Alcantara, R.; Lavela, P.; Ortiz, G. F.; Tirado, J. L.; Stoyanova, R.; Zhecheva, E.; Merino, C. *Carbon* **2004**, *42*, 2153-2161.

(423) Kuwahara, A.; Suzuki, S.; Miyayama, M. *Key Engineering Materials* **2006**, *301*, 159-162.

(424) Tatsumisago, M.; Mizuno, F.; Hayashi, A. *Journal of Power Sources* **2006**, *159*, 193-199.

(425) Zaghib, K.; Tatsumi, K.; Abe, H.; Ohsaki, T.; Sawada, Y.; Higuchi, S. *Journal of the Electrochemical Society* **1998**, *145*, 210-215.

(426) Faidi, S. E.; Scantlebury, J. D.; Bullivant, P.; Whittle, N. T.; Savin, R. *Corrosion Science* **1993**, *35*, 1319-1328.

(427) Gervasi, C. A.; Di Sarli, A. R.; Cavalcanti, E.; Ferraz, O.; Bucharsky, E. C.; Real, S. G.; Vilche, J. R. *Corrosion Science* **1994**, *36*, 1963-1972.

(428) El-Sawy, S. M.; Morsi, I. M.; Abdel-Mohdy, F. A. *Pigment & Resin Technology* **1983**, *12*, 11-13.

(429) Rusev, D.; Radev, D.; Karaivanov, S. *Metal Finishing* **1983**, *81*, 27-30.

(430) Xia, W.; Wang, L. *Polymeric Materials Science and Engineering* **1987**, *56*, 695-698.

(431) Samui, A. B.; Chavan, J. G.; Hande, V. R. *Progress in Organic Coatings* **2006**, *57*, 301-306.

(432) Kouloumbi, N.; Tsangaris, G. M.; Kyvelidis, S. T.; Psarras, G. C. *British Corrosion Journal* **1999**, *34*, 267-272.

(433) Davis, B. In *Coatings Technology Handbook,* 2nd ed.; Satas, D., Tracton, A. A., Eds.; Marcel Dekker, Inc.: New York, 2001, pp 559-563.

(434) Grunlan, J. C.; Gerberich, W. W.; Francis, L. F. *Polymer Engineering and Science* **2001**, *41*, 1947-1962.

(435) Grunlan, J. C.; Jang, W.-S.; McConnell, E. P.; Jan, C. J. *PMSE Preprints* **2005**, *93*, 728-729.

(436) Psarras, G. C. *Journal of Polymer Science, Part B* **2007**, *45*, 2535-2545.

(437) Zhang, B.; Fu, R.; Zhang, M.; Dong, X.; Zhao, B.; Wang, L.; Pittman, C. U. *Composites, Part A: Applied Science and Manufacturing* **2006**, *37A*, 1884-1889.

(438) Bourdo, S. E.; Viswanathan, T. *Polymer Preprints* **2004**, *45*, 236-237.

(439) Rwei, S. P.; Ku, F. H.; Cheng, K. C. *Colloid and Polymer Science* **2002**, *280*, 1110-1115.

(440) Smith, J. G.; Delozier, D. M.; Connell, J. W.; Watson, K. A. *Polymer* **2004**, *45*, 6133-6142.

(441) Wong, C. P.; Bollampally, R. S. *Journal of Applied Polymer Science* **1999**, *74*, 3396-3403.

(442) Yi, X.-S.; Wu, G.; Ma, D. *Journal of Applied Polymer Science* **1998**, *67*, 131-138.

(443) Caldeira, G.; Maia, J. M.; Carneiro, O. S.; Covas, J. A.; Bernardo, C. A. *Polymer Composites* **1998**, *19*, 147-151.

(444) Carneiro, O. S.; Maia, J. M. *Polymer Composites* **2000**, *21*, 970-977.

(445) Carneiro, O. S.; Maia, J. M. *Polymer Composites* **2000**, *21*, 960-969.

(446) Guo, H.; Kumar, S. *PMSE Preprints* **2006**, *94*, 492-493.

(447) Lozano, K. *JOM* **2000**, *52*, 34-36.

(448) Shim, B. S.; Starkovich, J.; Kotov, N. *Composites Science and Technology* **2006**, *66*, 1174-1181.

(449) Van Hattum, F. W. J.; Bernardo, C. A.; Finegan, J. C.; Tibbetts, G. G.; Alig, R. L.; Lake, M. L. *Polymer Composites* **1999**, *20*, 683-688.

CHAPTER 2

ELECTRICAL AND MECHANICAL PROPERTIES OF VGCNF-REINFORCED ALKYD PAINT-COATED MILD STEEL SAMPLES

2.1 Introduction

As mentioned in Chapter 1, steel alloys have the widest application range among all engineering alloys. The applications of steel alloys range from domestic and household appliances to construction, automotive, marine and offshore equipment, power and energy components, and agricultural equipment. Accordingly, the corrosion of steel structures, especially mild steel ones, is of great economical importance and has a huge impact on several industries. Thus, the last century has witnessed enormous efforts towards the development of more efficient and environmentally compliant methods for the corrosion protection of mild steel structures. In this regard, the most common techniques used to reduce the rate of corrosion are anodic protection, cathodic protection, and organic coatings.[1, 2]

Organic coatings are effective for providing reliable long-term protection to a wide range of substrate materials and structures against corrosion not only for domestic applications, but also for a wide range of industrial applications in all possible environments.[3-6] Thus, along with the increased use of construction materials such as plastics, composites, ceramics, metals, and engineering alloys, the last two decades have

witnessed an increased interest in the investigation and quantification of the stability, corrosion protection properties, and lifetime of organic coatings applied to these materials.[7-13]

The efficiency of an organic coating in protecting a metal substrate against corrosion depends on several factors including the properties of the coating (e.g., its thickness, permeability, electrical, thermal, mechanical, and barrier properties), the adhesion properties of the coating with the substrate, the composition of the coating (e.g., presence of sacrificial pigments), the nature of the substrate surface pretreatment, the coating application method, and the environmental conditions (degree of aggressiveness of the environment).[14, 15]

The last few years have witnessed an increased interest in the development and investigation of novel additives to improve the corrosion protection properties of pure paints and coatings applied to metals and alloys.[16] These additives should also be environmentally acceptable and abide by legislative limitations. Among these novel additives are anticorrosive pigments;[17-19] inhibitors;[20, 21] modified clays;[22, 23] electrically conductive polymers (CPs);[16, 24, 25] and carbon as well as metallic powders such as carbon black,[26-30] aluminum powder,[31] copper powder,[32] silver powder,[33-35] zinc dust,[36-40] iron powder,[41] cationic agents (e.g., quaternary ammonium salts),[42] gold nanoparticles,[43-45] and mixtures of metals (e.g., Ni, Cu, Fe).[46]

The use of CPs as corrosion-resistant coating systems to replace the environmentally harmful chromate-based coatings is of current interest. In addition to their conductivity, CPs exhibit redox activities with typical potentials positive of iron and aluminum.[47, 48] Accordingly, a large number of studies have been reported on the use of

CP coatings for corrosion protection of metal and alloy substrates.[49-54] The advantages of such organic coatings include good adhesion to the metallic surface, good electrical conductivity, ease of deposition, low toxicity, and good corrosion protection. Among these CPs, polypyrrol (PPy),[55-59] polyaniline (PANI),[60-68] and polythiophene (PTh)[69-72] were the most widely used materials in these studies.

The use of carbon materials (such as carbon black, short carbon fiber, graphite) as conductive fillers in organic coatings and composites is gaining more interest especially for applications that require lightweight construction materials. Although carbon materials are less conductive relative to metal powders, carbon materials are more attractive as conductive pigments mainly because they are light and inexpensive. Moreover, carbon materials are also effective as shielding coatings and have good physical and mechanical properties.[73]

Among the carbon materials that are currently investigated as additives in organic coatings and composite materials are VGCNFs, SWNTs, and MWNTs. VGCNFs are unique as they are considered the bridge between the large conventional carbon fibers and the smaller SWNTs and MWNTs.[74] Compared to the nanotubes (NTs), VGCNFs have the advantages of low price, availability, and excellent electrical properties.[75-82] Moreover, the thermal and mechanical properties of VGCNFs are similar to those of the NTs.[75, 83, 84] Thus, VGCNFs are a cheap alternative to NTs. These unique properties make VGCNFs good filler candidates to improve the properties of polymer composites especially those used in industries such as aircraft, automotive, batteries, and electronics.[85-93] Moreover, VGCNFs are currently used to replace the heavy metallic materials as fillers in polymer composites, especially for applications that require light

structural materials.[94] In addition, the incorporation of VGCNF was found to improve the thermal and electrical conductivities of metal matrix composites[95-97] as well as several polymer-based composites including: high-density polyethylene (HDPE),[98] silicon oxycarbide ceramic composites,[99] polypropylene (PP),[100-105] epoxy-based composites,[106-108] phenol-formaldehyde and other phenolic resins,[90, 109, 110] polycarbonate,[111] polyacrylonitrile (PAN),[112] poly(vinyl alcohol) (PVA),[113] liquid crystal polymer (LCP) composites;[114] vinyl ester composites,[115] polyether;[116] and polystyrene.[117]

Alkyd resin-based coatings are a group of environmentally friendly paints that were introduced in the 1930s.[118] Until the 1960s, they were mainly used by the automotive and appliance industries.[119] These paints are very resistant to normal wear and tear and provide chemically tough and weather resistant coatings at relatively low cost.[119, 120]

The increased interest in VGCNF-reinforced composites in several industries along with the low cost, light weight, high aspect ratio, availability, and unique properties of the VGCNFs motivated this research group to use the EIS technique to evaluate the effect of the incorporation of VGCNFs in a commercial alkyd paint matrix on the protective properties of the paint when applied to mild steel samples immersed in air-saturated 3% NaCl solution. The hypothesis was that, due to its excellent electrical and mechanical properties, VGCNF would behave similar to CPs, and hence the presence of the VGCNF in the paint matrix would improve the mechanical as well as the corrosion protection properties of the matrix. If the proposed hypothesis turns out to be true, then VGCNF-reinforced polymer coatings should be better and have a wider application range than CPs-reinforced ones. This is mainly because, even with the current advances in CPs

technology, some of the CPs have seen limited applications due to high cost of production, complex preparation process, poor processability and solubility, difficult syntheses, and loss of conductivity when exposed to corrosive atmospheres.[73, 121] In addition, some of the CPs (e.g., polypyrrole) tend to have poor mechanical properties and require modification of the polymer structure which usually results in a decreased conductivity.[47] On the other hand, VGCNFs are relatively cheap, have a range of dimensions, structure, thermal, mechanical, and electrical properties depending on the method of production and post-treatment.[75, 122]

The work presented in this chapter focuses on studying the mechanical and electrical properties of dry alkyd paint coatings, with different VGCNF weight percent and paint thicknesses, applied to the surface of either mild steel or poly(methyl methacrylate) substrates. In addition, the study involved surface analysis measurements such as AFM, SEM, and optical profilometry measurements.

2.2 Experimental

2.2.1 Chemicals and Reagents

VGCNF (PR-19-HT, Pyrograph III™) material was ~ 120-200 nm in diameter, 30-100 μm in length, and had 21 m^2/g total surface area. The VGCNF material was donated by Applied Sciences, Inc. (Cedarville, OH). Silicon carbide whiskers (1.5 μm in diameter, 18 μm in length, density = 3.217 g/cm^3) were obtained from Alfa Aesar (Ward Hill, MA). A commercial oil-based paint (Gloss White 7792, Rust-Oleum, Vernon Hills,

IL) was purchased locally. Commercial poly(methyl methacrylate) (PMMA) (4.5 mm thick Plexiglas) sheets were also purchased locally.

2.2.2 Electrodes and Instrumentation

The steel samples were flat coupons in a square shape of ~ 8 cm × 8 cm, cut from 1.51 mm thick mild steel sheets. After cutting, the coupons were first polished through wet grinding with successive grades of 80 to 1000 grit SiC sandpaper. No further polishing was done to maintain a good surface roughness. The coupons were, then, cleaned using a commercial degreaser (Greased Lightning, A&M Cleaning Products, Inc., Clemson, SC) to remove any grease and polishing debris. The coupons were then rinsed with tap water, deionized water, and acetone. The coupons were allowed to dry in a dust-free environment.

The PMMA samples were also cut in a square shape of ~ 8 cm × 8 cm from 4.5 mm thick sheets. The coupons were, then, rinsed with tap water, deionized water, and ethanol. The coupons were then allowed to dry in a dust-free environment.

After being dried, the steel and PMMA substrates were coated with pure and VGCNF-reinforced alkyd paint films using the spin coating method (vide infra). The coated substrates were then allowed to dry before being cut to suitable dimensions as needed for the different experiments.

Adhesion is the most crucial factor in determining the long-term performance, durability, and the corrosion resistance of any coating.[123, 124] Mechanical adhesion of any coating depends on the metal surface roughness. Thus, roughening the substrate surface (e.g., by sanding) increases the number of pores, scratches, and pits on the surface of the

bare sample. This increases the bonding between the coating and the alloy and hence the adhesion of the coating.[119]

2.2.3 Spin Coating of the Samples

Mixing the VGCNFs with the composite material is the most crucial variable that determines the mechanical properties of the VGCNF-reinforced organic matrix composite.[90] Accordingly, in the current study, the VGCNF was first mixed thoroughly with the paint. The mixture was then stirred using a magnetic stirrer for at least 12 h at a high stirring rate (in rpm), depending on the wt % of the VGCNF, in a closed bottle, to ensure that the fibers are well-dispersed in the paint. For samples containing high wt % (3% or higher) of VGCNF, the viscosity of the paint/VGCNF mixture was very high. To lower the viscosity for these mixtures, a few milliliters of acetone was added. The VGCNF-incorporated paint mixtures were then applied to the mild steel coupons using a spin coater (Model WS-400-6NPP-Lite, Laurell Technologies Corporation, North Wales, PA). The spin-coating conditions were varied depending on the viscosity of the mixture to give the most homogeneous coating with a constant and uniform film thickness all over the substrate surface. The coated samples were prepared in identical sets of 2-4 samples.

2.2.4 Drying the Coating

The spin-coated mild steel coupons were allowed to dry at room temperature (25 ºC) in a dust-free place for at least 7 d. The process of drying is an important step and has to be done before any measurements occur. During the drying period, several physical

and/or chemical changes occur such as solvent evaporation, oxidation, crosslinking, polymerization, and curing.[125]

2.2.5 Coating Thickness Measurements

The thicknesses of the dry coatings were measured by two different methods, (i) using a digital micrometer (caliper), and (ii) using an optical profiling system. Both methods were used to determine the coating thickness for the data presented in this work.

2.2.5.1 Using a Digital Micrometer (Caliper)

In this method, a flake of the coating was carefully freed from the surface of the coated mild steel sample (using a blade) and its thickness was measured directly using an electronic digital caliper with 0.1 μm accuracy (Model 14-648-17, Control Company, Friendswood, TX). The reported thickness data are the average of 4-5 flakes freed from different areas on the substrate surface. Alternatively, the thickness of the bare substrate was measured, and then the total thickness of the coated mild steel substrate was measured. This method has the advantage of being non-destructive as it does not require the removal of the coating. The coating thickness is the difference between the two measurements.

2.2.5.2 Using an Optical Profiling System

This method was used to measure the thickness of some random coated samples to check for the validity of the thickness data measured using the caliper. In addition to the coating thickness measurements, the optical profilometry measurements provide an

estimate of the average surface roughness of the coating. In this case, the thickness as well as the surface roughness of the paint coatings on the mild steel samples was determined using an optical profiling system (WYKO NT 1100, Veeco Metrology Group, Tucson, AZ). Both film thickness and surface roughness were determined using the vertical scanning interferometry (VSI) mode with 20× and 50× objectives, respectively. In this method, a blade is used to carefully remove a flake of the coating from the surface of the coated mild steel sample. Then, a laser beam is used to scan the region between the coated and non-coated regions on the surface of the steel sample.

2.2.6 Scanning Electron Microscopy (SEM) and Energy Dispersive X-ray Spectroscopy (EDS) Measurements

The surface morphology and composition (elemental analysis) of the coatings without and with VGCNFs was studied by SEM micrographs using a field emission scanning electron microscope (FE-SEM, Model JSM-6500F, JEOL, Inc., Peabody, MA). For these studies, the paint-coated mild steel coupons were coated with a 20 nm thick Au/Pd layer deposited by sputtering (using a Model E5100 Polaron SEM coating system, Polaron Instruments, Inc., Hatfield, PA) for 15 s using a low voltage and current of 2.4 kV, and 20 mA, respectively. For SEM imaging, the samples were examined under low acceleration voltage conditions (5 kV). The energy dispersive X-ray spectroscopy (EDS) measurements were performed using an Oxford Instruments detector (Model EDS 7558 INCAx-sight, Oxford Instruments, Oxfordshire, U.K.), attached to the SEM. These measurements were carried out to detect and image the presence of the VGCNFs at the mild steel/paint coating interface. In addition, the EDS technique is a very useful

technique for the determination of elemental composition and hence the identification of inorganic pigments and fillers in any paint matrix.

2.2.7 Atomic Force Microscopy (AFM) Measurements

AFM micrographs for the paint coatings without and with VGCNF were recorded at ambient temperature using a Topometrix Explorer AFM (from Thermomicroscopes, now Veeco, Santa Barbara, CA) in the contact/noncontact mode. For these studies, 5 mm square samples were cut from the paint-coated steel panels.

2.2.8 Microhardness and Nanoindentation Measurements

The mechanical properties of any coating applied to the surface of a metal are of great importance in determining the stability as well as the service life of the coating film. In the current investigation, the mechanical properties of the coatings were measured using an Ultra-Micro Indentation System (UMIS). This system works by making a controlled indentation with its diamond indenter tip. With indenter displacement continuously monitored, the system measures important mechanical properties such as substrate hardness, Young's modulus, and fracture behavior. Depth-sensing microhardness tests were performed using a Hysitron multi-range probe nanoindentation system (Hysitron, Inc., Minneapolis, MN). A Berkovich diamond indenter was used for all indenters. The nanoindentation tests were carried out in load control mode. For all samples, a variable loading amplitude scheme was achieved over a square shaped grid of 25 imprints interspaced by 50 μm. The maximum load for the first imprint was 100 μN, and this load was increased by 10% imprint up to the last one. The loading scheme

followed a loading rate of 10 μN/s, a dwelling time of 5 s and an unloading rate of 10 μN/s for all samples.

The alkyd paint-coated steel samples were cut using an automatic precision cut-off machine (Model Minitom, Strikers, Westlake, OH). The specimens were then vertically potted in a non-conducting epoxy resin in rubber septa approximately 30 mm in diameter and 15 mm tall. The specimens were then allowed to cure at room temperature overnight. After curing, the paint-steel interface (edge) surface was exposed by wet grinding with successive grades of SiC particle sizes up to 0.5 μm on cloth using a grinding-polishing wheel (Metaserv, Buehler, Lake Bluff, IL). Between polishing steps and after final polishing, the specimens were sonicated in deionized water.

2.2.9 Electrical Conductivity Measurements

The electrical conductivity of the pure paint and VGCNF/paint coatings was measured using two different methods. In the first method, a high-impedance digital electrometer (Model 6512, Keithley Instruments, Inc., Cleveland, OH) was used to measure the conductivity of the paint coatings applied to the surface of mild steel coupons. In the second method, the electrical resistivity (ρ) of the coatings applied to the surface of electrically insulating PMMA coupons was measured using the van der Pauw technique. The van der Pauw technique is a four-point probe technique that is based on calculating ρ of a given sample using four isolated contacts on the boundary of a flat, arbitrary shaped sample.[126] The technique involves the application of a DC current between two terminals (using a Model 220 Keithley current source) and the measurement of the resulting DC voltage between the other two terminals (using a Model 6512

Keithley multimeter). The technique gives the average of two computed resistivity values. In order to use the van der Pauw method, the sample thickness must be known and must be less than the width and length of the sample. In addition, the sample surface has to be flat without any isolated holes.[126] More details about the method are given in the results and discussion section.

2.3 Results and Discussion

2.3.1 Preliminary Dry Paint Film Characterization

In this section, the results of the initial properties of the paint coatings, without and with VGCNFs, are presented. Properties such as physical appearance and morphology, film thickness, surface hardness, surface roughness, film homogeneity and integration, for both pure and VGCNF-reinforced paint coatings, were characterized with the optical microscopy, SEM, optical profilometry, and nanoindentation measurements.

2.3.1.1 Physical Appearance

Figure 2.1 shows digital photos recorded for pure as well as VGCNF-containing paint films before immersion in any solution. As shown in the figure, the pure film is white while the VGCNF-containing films are slightly gray with the color becoming darker as the VGCNF % increases in the film. The texture of the pure paint film, as determined by touch, is smooth while VGCNF-containing paint films are less smooth. It is also visually evident from Figure 2.1 that as the VGCNF content increases in the film, the film becomes rougher.

(a)

(b)

(c)

Figure 2.1 Digital photos showing the physical appearance of the (a) pure, (b) 1% VGCNF-reinforced, and (c) 3% VGCNF-reinforced paint coatings before immersion in NaCl solutions.

2.3.1.2 SEM Measurements

Alkyd paint-coated mild steel samples without and with VGCNFs were examined both visually and by SEM and EDS. The SEM and EDS images were recorded with Au/Pd coated samples. Examination of the SEM micrographs (Figures 2.2 through 2.7) for both pure as well as VGCNF-incorporated paint samples (before immersion) indicates that the coating films are relatively flat. The VGCNFs are very obvious in the figures as cylindrical strands (e.g., Figures 2.3, 2.4, and 2.6). The hollow nature of the VGCNFs can also be seen in the SEMs (e.g., Figure 2.4.b). The diameter measurements of different VGCNFs in the paint coating (Figure 2.4.b) show that the fibers have diameters in the range of 80-200 nm in accordance with the diameters provided by the vendor (Applied Sciences, Inc.).

In addition, SEM micrographs (Figures 2.3 through 2.5) showed that the low VGCNF-loaded paint coatings are more homogeneous in the distribution of the VGCNFs in the paint matrix than paint matrices containing 5% VGCNFs. Figure 2.6 shows the SEM micrographs for 5% VGCNF-incorporated paint samples. As shown in the figure, the fibers are not uniformly distributed throughout the paint matrix. Instead, some areas of the surface showed higher fiber concentration nests or clumps while other regions showed lower fiber concentration. These results are in agreement with those reported by Pittman et al. and others[127, 128]

The EDS measurements were conducted for the elemental analysis of the VGCNF-loaded alkyd paint coatings. An example of an EDS spectrum for a 5% VGCNF-incorporated sample is shown in Figure 2.7.b. As depicted in the figure, in addition to carbon, the alkyd paint contains Ti metal (usually in the form of TiO_2) as one

(a)

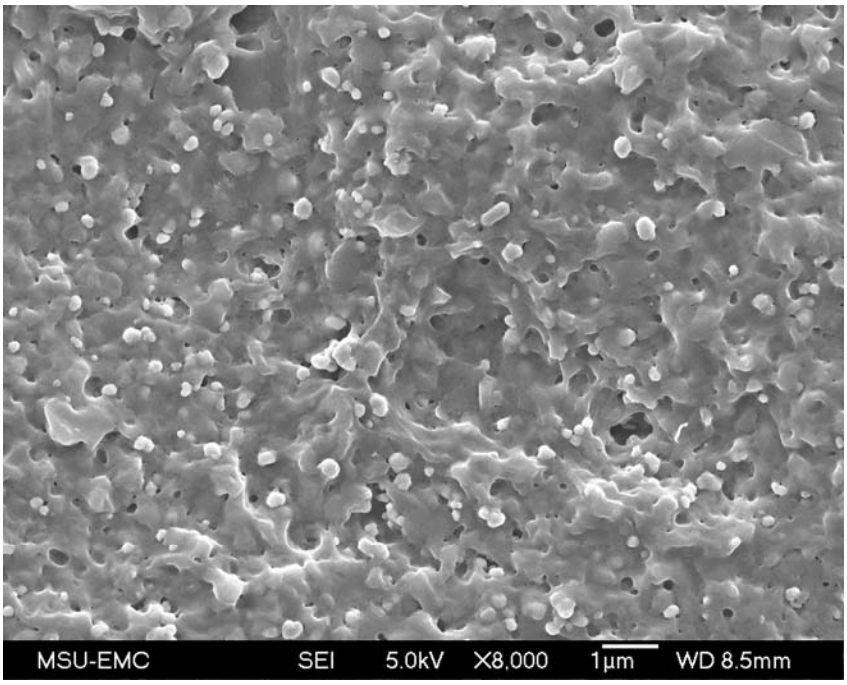

(b)

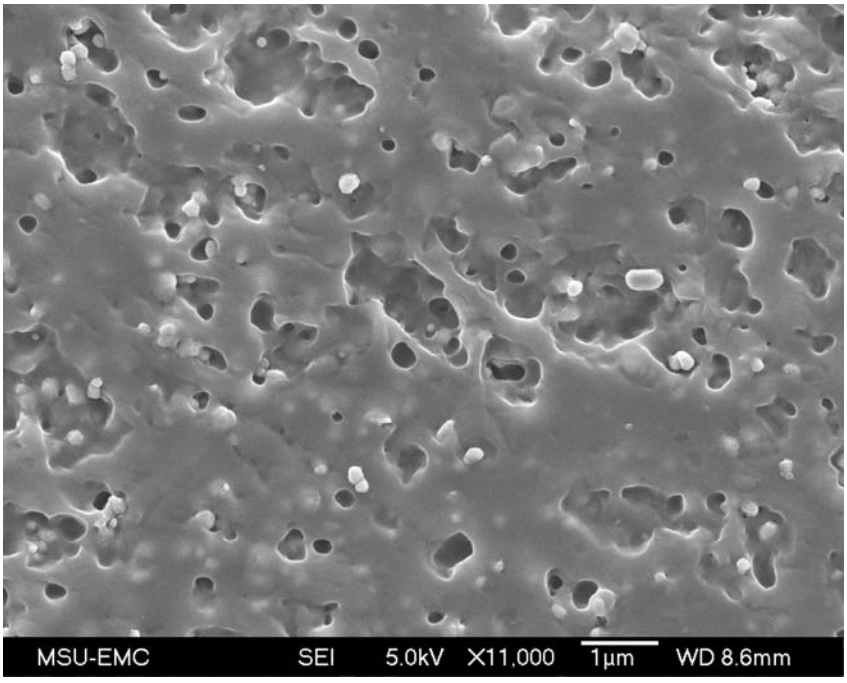

Figure 2.2 Scanning electron micrographs of a pure alkyd paint coating at different magnifications.

(a)

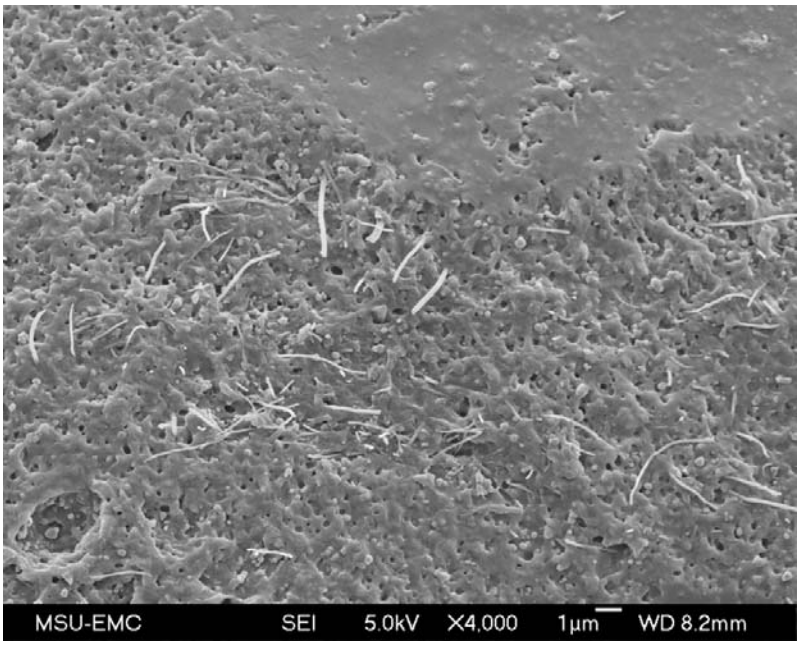

(b)

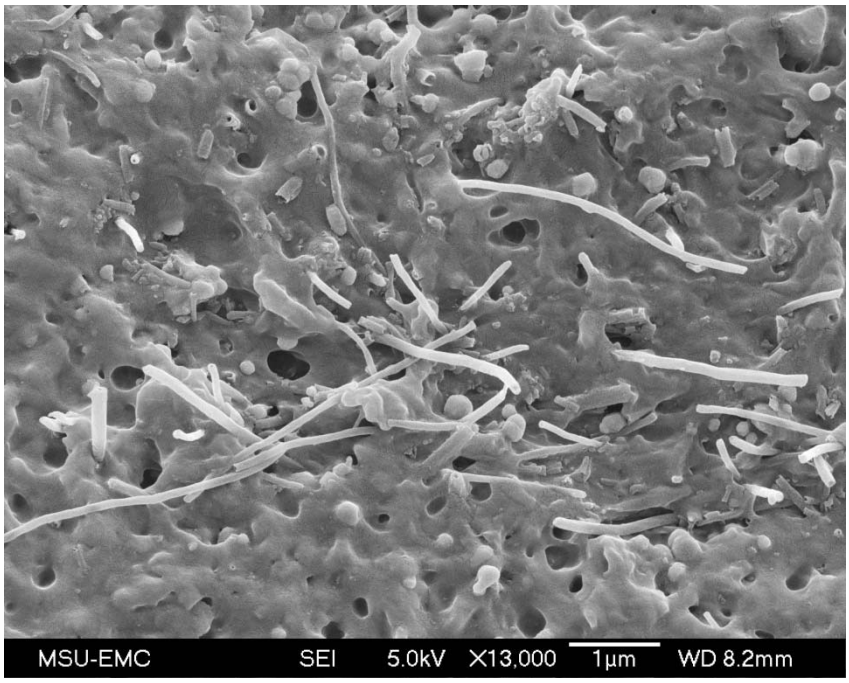

Figure 2.3 Scanning electron micrographs of a 0.5 wt % VGCNF-incorporated alkyd paint coating at different magnifications.

(a)

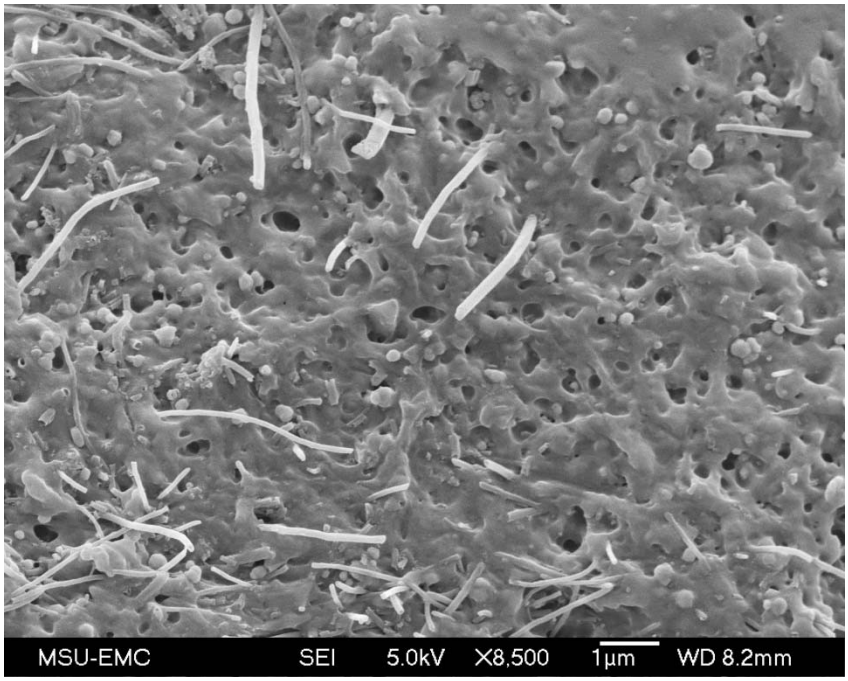

(b)

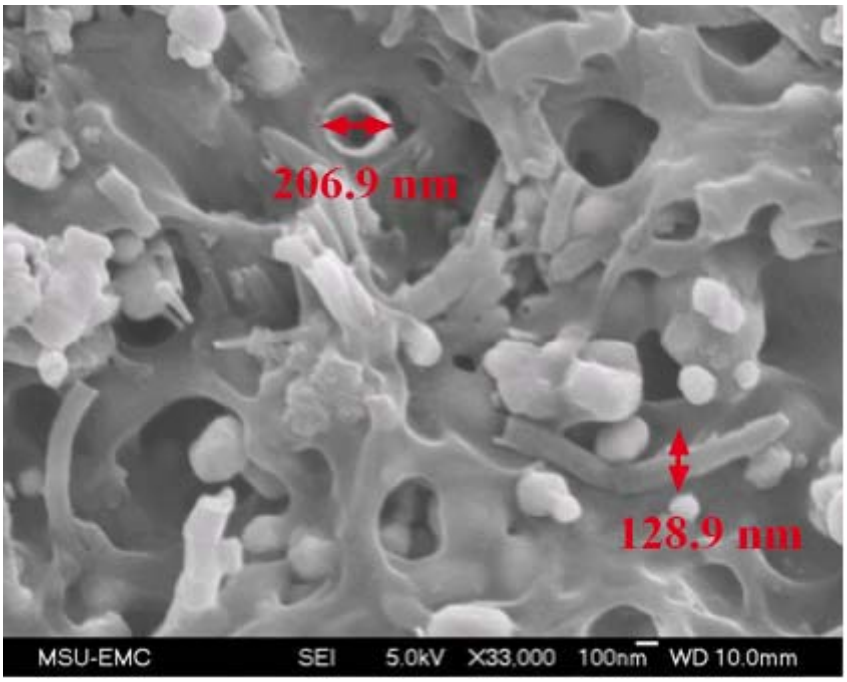

Figure 2.4 Scanning electron micrographs of a 1 wt % VGCNF-incorporated alkyd paint coating at different magnifications.

(a)

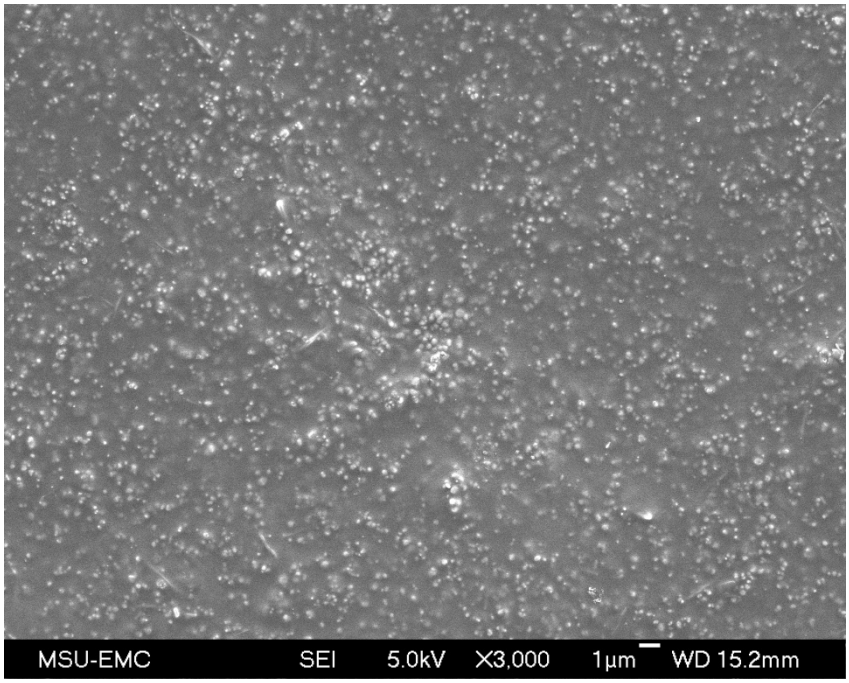

(b)

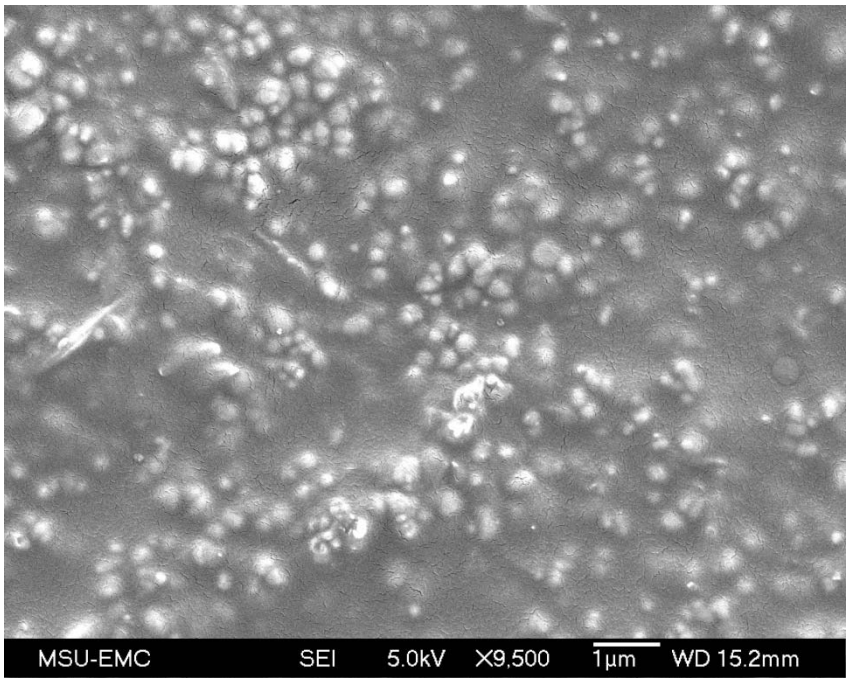

Figure 2.5 Scanning electron micrographs of a 3 wt % VGCNF-incorporated alkyd paint coating at different magnifications.

(a)

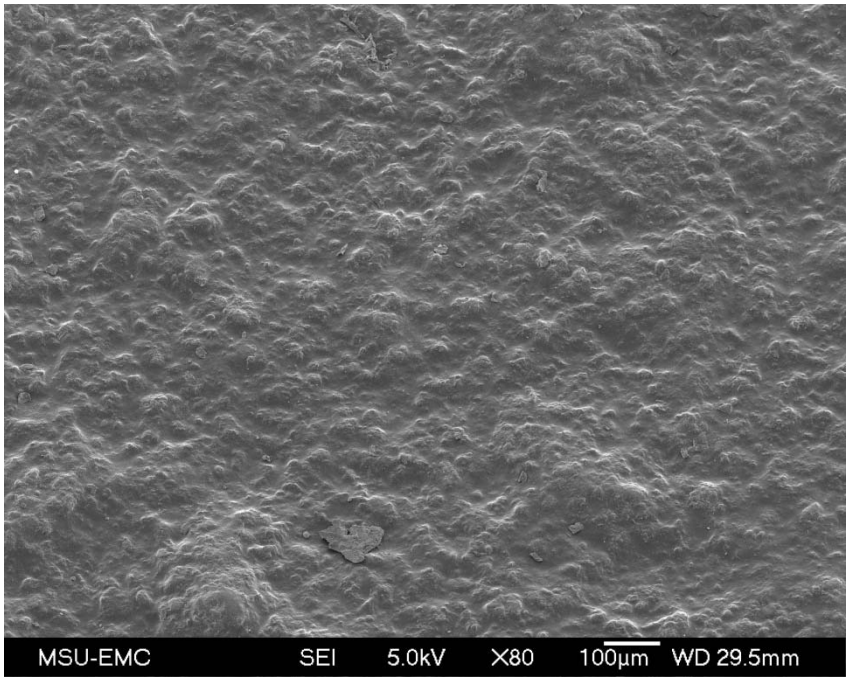

(b)

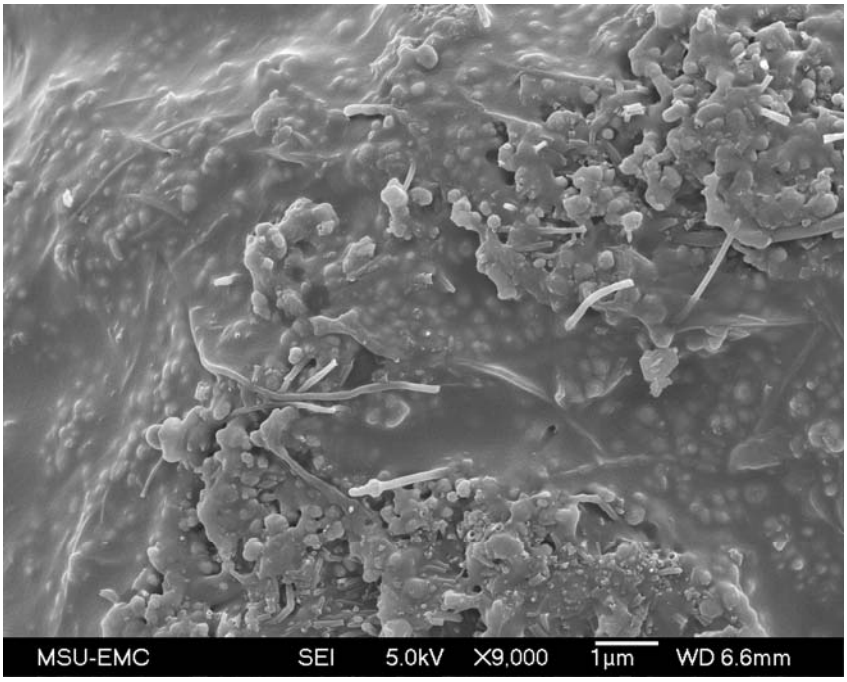

Figure 2.6 Scanning electron micrographs of a 5 wt % VGCNF-incorporated commercial alkyd paint at different magnifications.

(c)

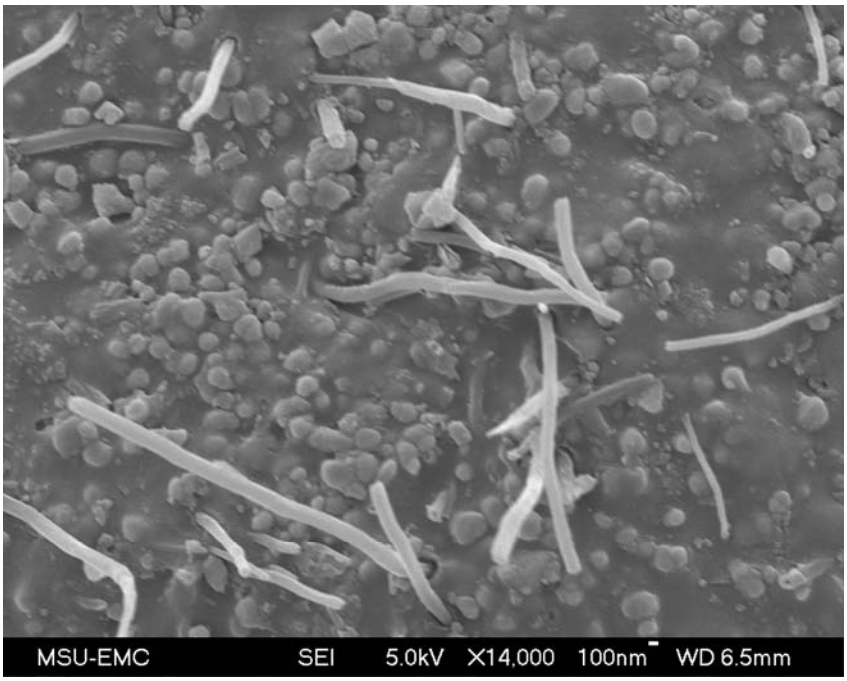

Figure 2.6 Continued.

(a)

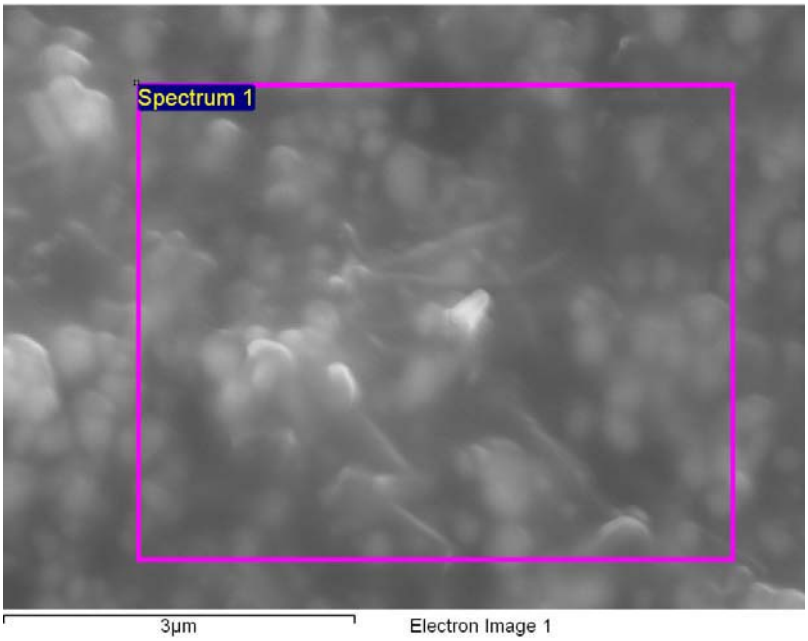

(b)

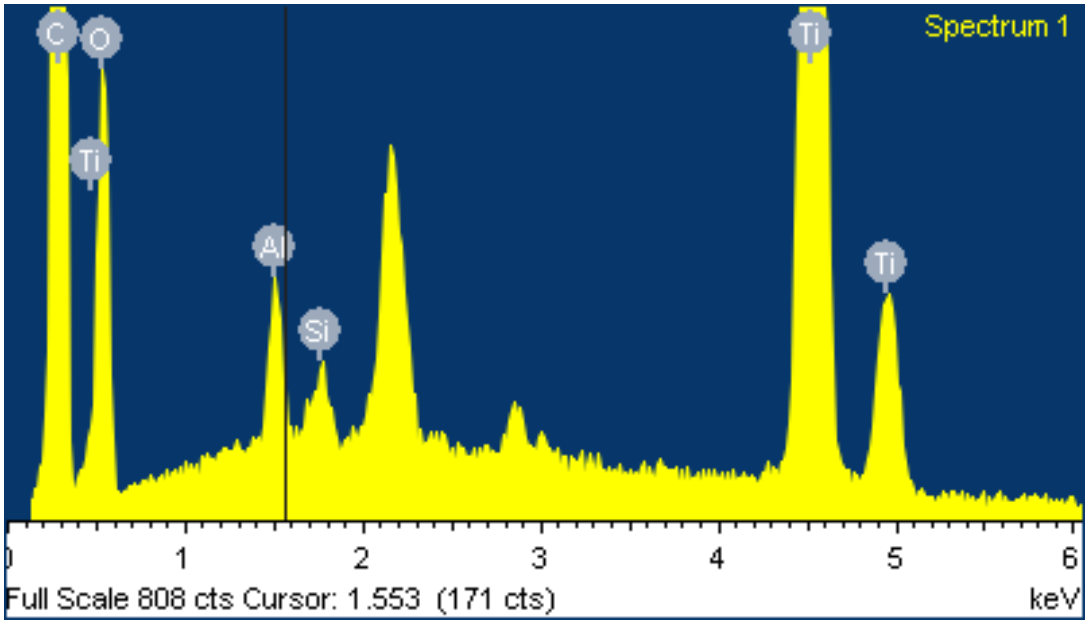

Figure 2.7 (a) SEM and (b) EDS spectra for a 5% VGCNF-incorporated alkyd paint coating applied to the surface of a mild steel sample.

of the paint additives or pigments. The peaks in Figure 2.7.b also indicate that Ti is present in a high concentration. It should be mentioned that, the peaks of sputtered Pd and Au metals were omitted to clarify the EDS spectrum.

2.3.2 Optical Profilometry and Atomic Force Microscopy (AFM) Measurements

Among the factors that affect the performance and service life of any organic coating are the paint thickness and its uniformity. The more uniform and even the coating is, the better its performance.

Optical profilometry is a rapid, non-destructive, non-contact, and highly accurate optical surface analysis technique to obtain 2- and 3-dimensional topographies of surfaces. In addition, the technique does not require any special sample preparation.[129-136] The technique uses a scanning laser beam to measure the amount of light reflected from the surface of substrate.[131, 137] The amount of light reflected at any point from a surface depends on the depth of the material in that point. Accordingly, scanning the edge region between two surfaces with different thicknesses would provide an estimate of the height difference.

Optical profilometry was used to measure the thickness as well as the surface roughness of the paint coating films with and without VGCNF. The profilometer measures the coating film thickness as the difference in height (depth) between a bare substrate region and a paint-coated region. Accordingly, for thickness measurements, the paint film was removed from a small area of the steel surface to expose the bare substrate surface and the border between the coated and the bare areas is scanned using the profilometer. The thickness of a coating is measured as the difference in height (depth)

between the two plateaus for the bare and coated regions. Figure 2.8 shows the 2- and 3-D profilers for a mild steel sample coated with a film of the paint without any VGCNF. The values of the thickness measured using the profilometer are close to those measured using the caliper.

The surface roughness images (Figure 2.9) show that the higher the wt % of the VGCNF content, the higher the surface roughness. As shown in Figure 2.9, a film containing 1% VGCNF (Figure 2.9.a) is less rough than a film containing 5% VGCNF (Figure 2.9.b). These results are in agreement with the visual as well as the digital photos.

Figures 2.10 through 2.12 show some AFM height images recorded for the paint coatings with and without VGCNF before immersion in the electrolyte. The results revealed non-uniformities in the structures of the coatings along with some characteristic features of polishing lines for polished samples. Some hillocks are also randomly distributed in the paint film. The hillocks are very obvious especially for paint samples containing higher (5 wt %) VGCNF content. These hillocks are believed to be a result of the uneven distribution of the VGCNF in the coating matrix during the spin coating step. These hillocks are also obvious in the SEM micrographs. Although these features are obvious in both AFM as well as SEM images, the EIS data for the coating samples with high VGCNF content showed that these hillocks have no effect on the corrosion protection performance of the coatings.

2.3.3 Surface Hardness Measurements

Several factors contribute to a perfect corrosion protection attainable by any coating on the surface of a metal or alloy. Among those factors are the adhesion

(a)

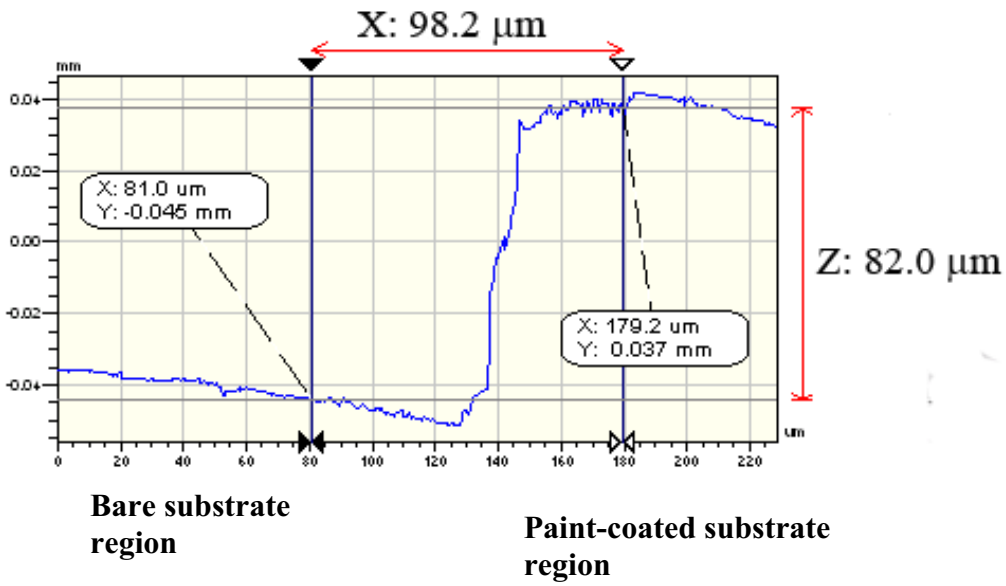

(b)

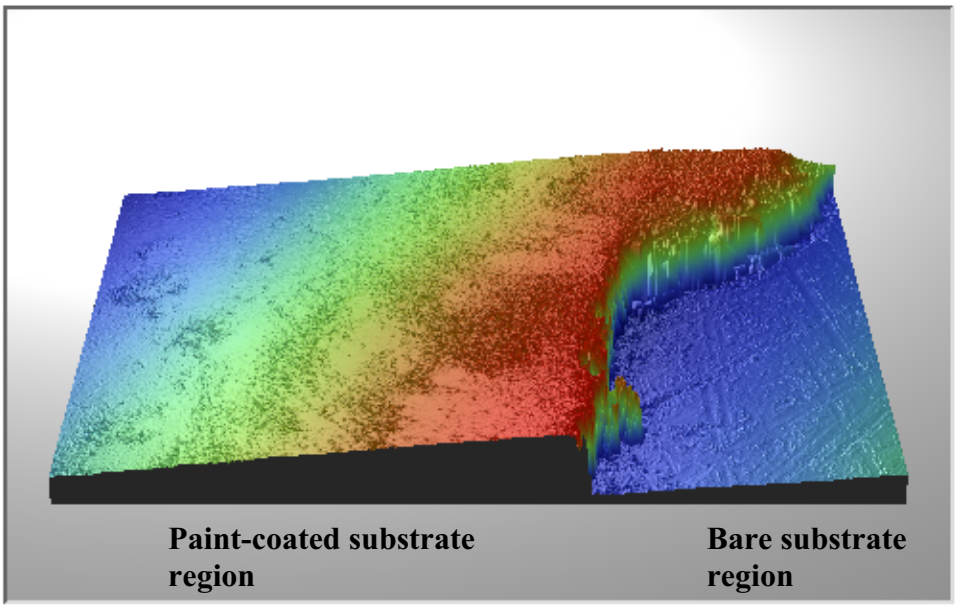

Figure 2.8 Two- (a) and three- (b) dimensional optical profilers for a mild steel sample coated with an 80 µm thick layer of a pure commercial alkyd paint sample applied to the surface of a mild steel coupon. Profiler (a) shows that the actual coating thickness is 82 µm.

(a)

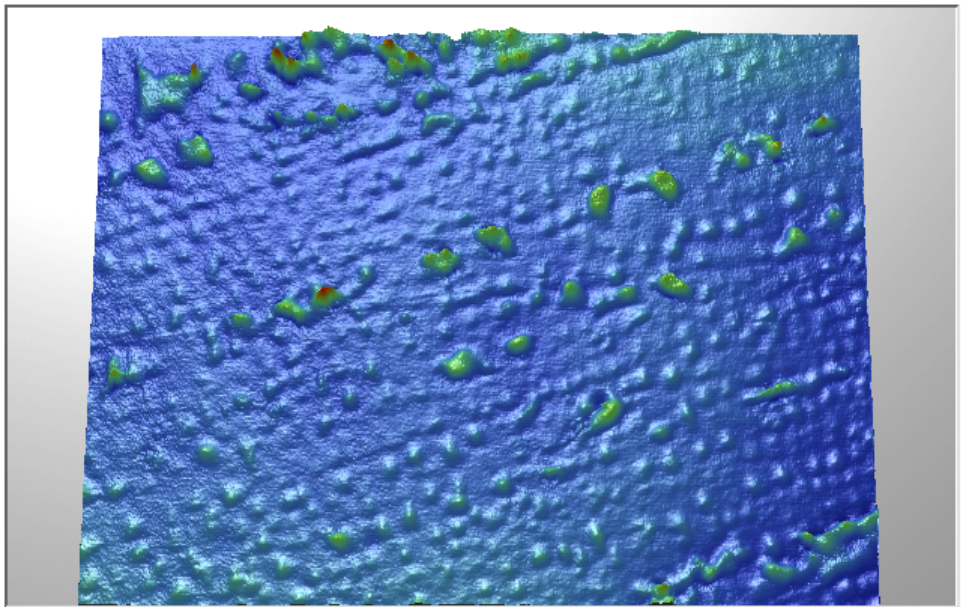

(b)

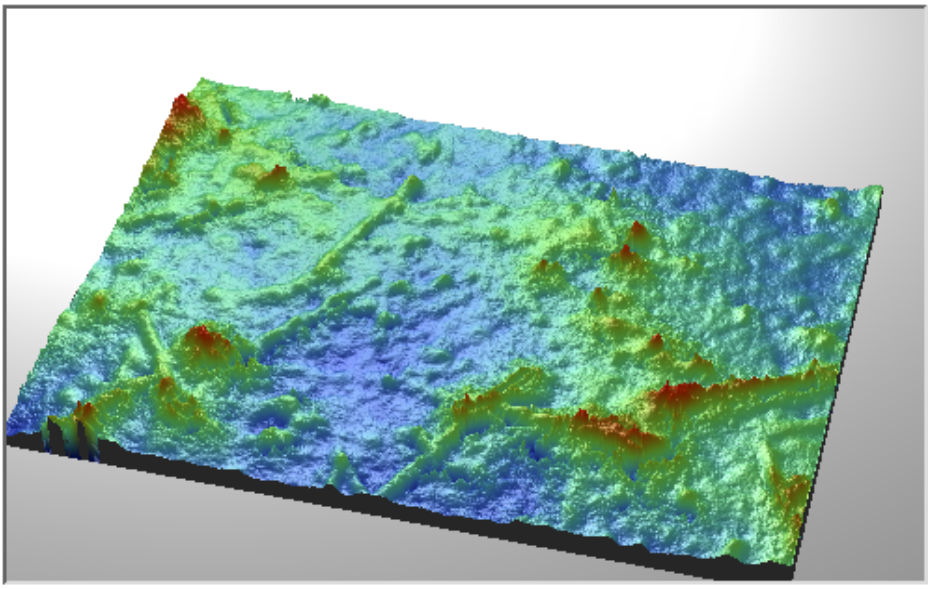

Figure 2.9 Two-dimensional optical profilers showing the surface roughness of a VGCNF-incorporated commercial alkyd paint coating applied to the surface of mild steel substrates. (a) 1 wt % loading of VGCNF and (b) 5 wt % loading of VGCNF.

(a)

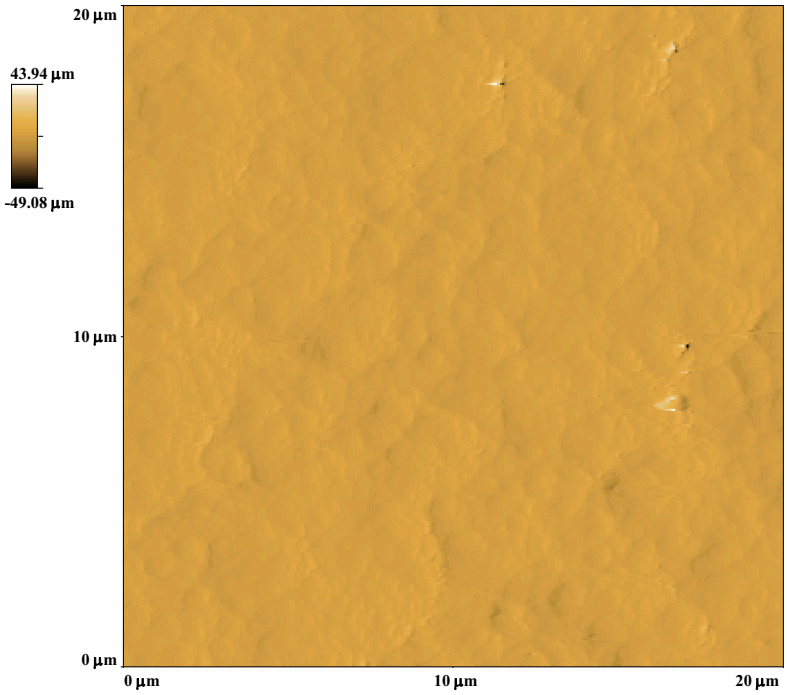

(b)

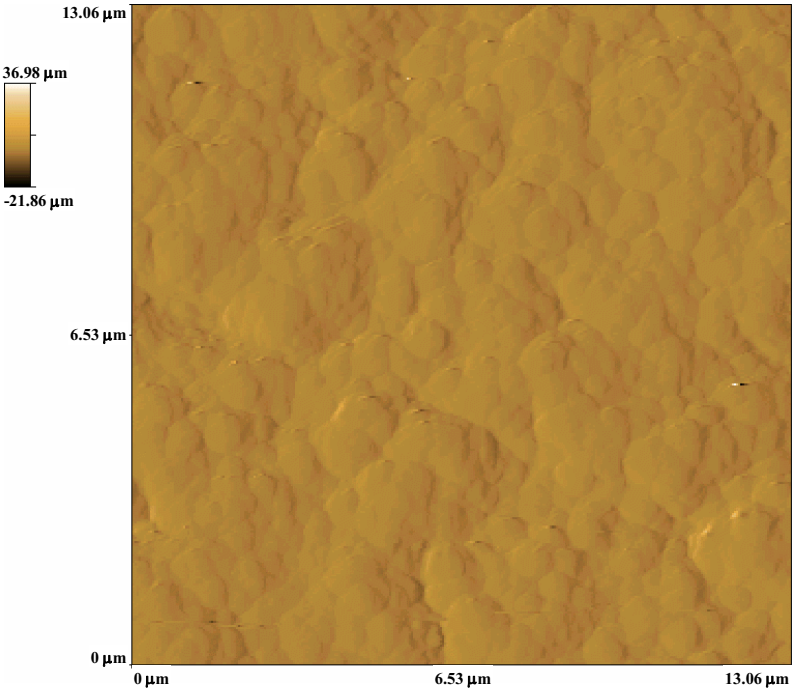

Figure 2.10 AFM height images for two different areas on mild steel panels coated with a pure commercial alkyd paint film.

(a)

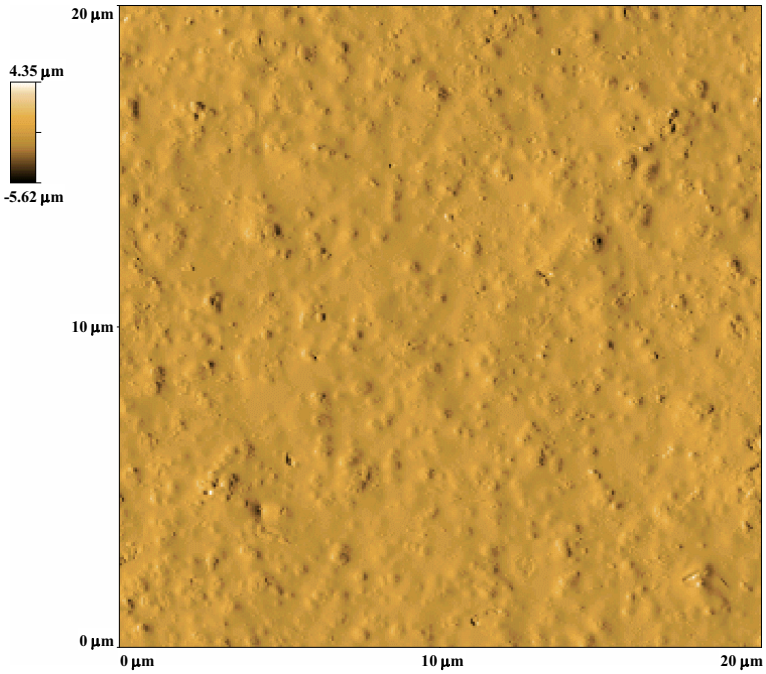

(b)

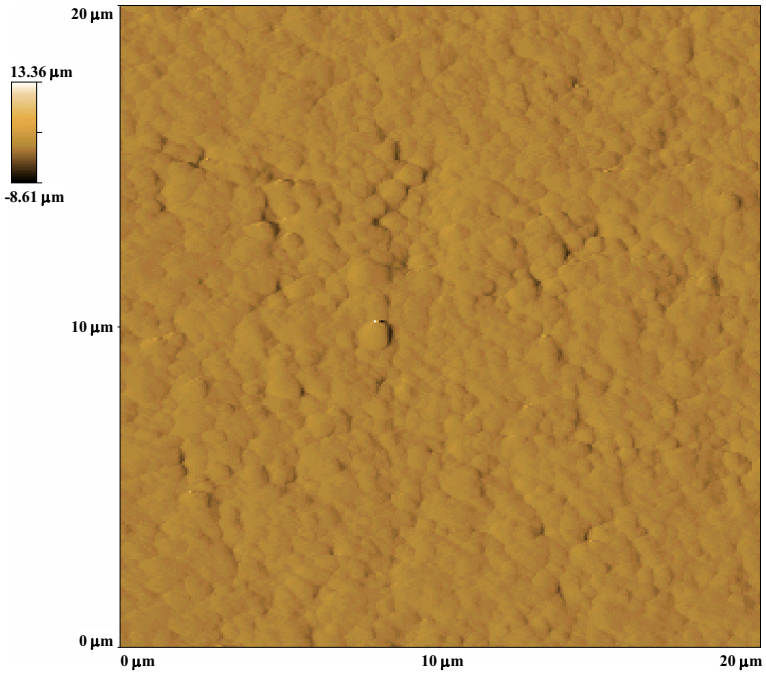

Figure 2.11 AFM height images for mild steel panels coated with a commercial alkyd paint film containing 0.5 wt % VGCNF. Image (b) was collected after the sample was polished with alumina slurry.

(a)

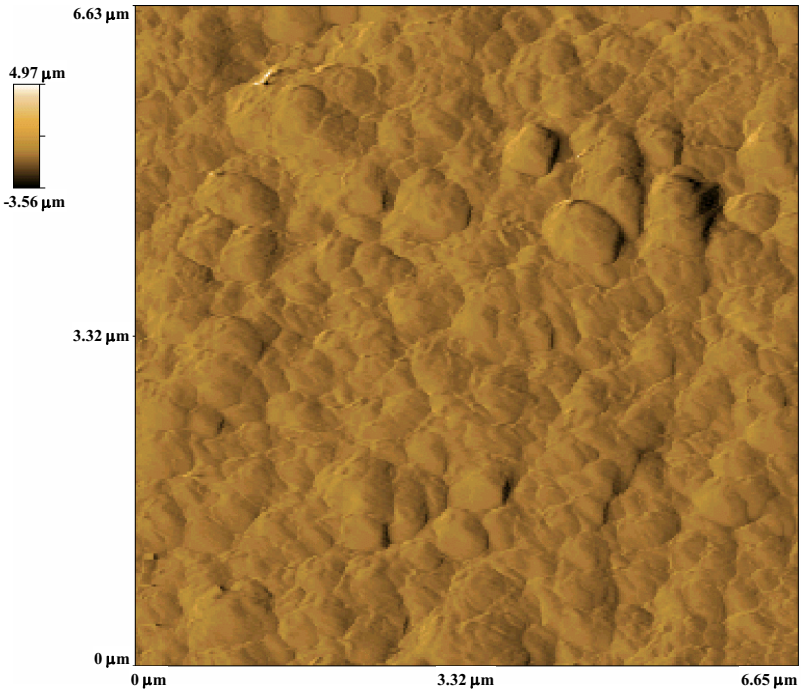

(b)

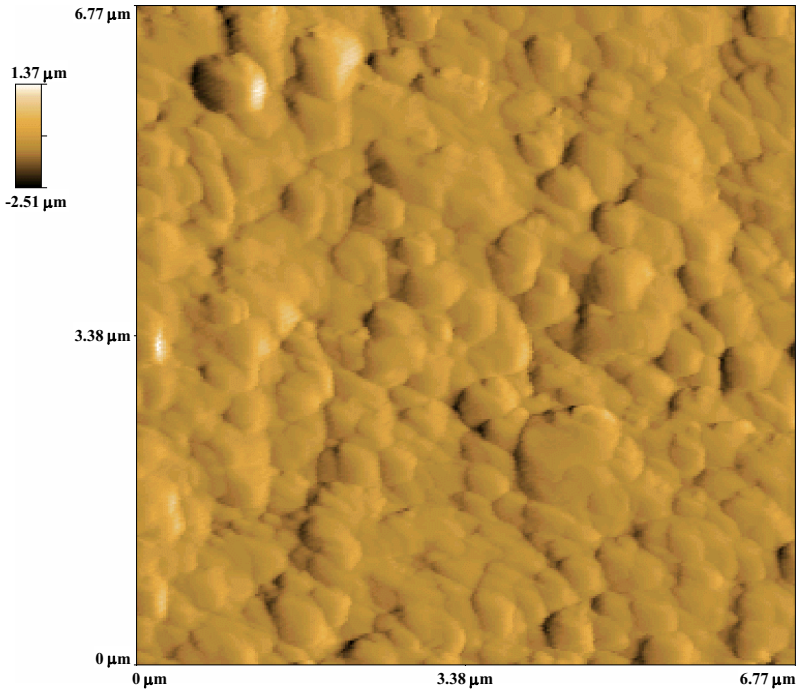

Figure 2.12 AFM height images for two different areas on a mild steel panel coated with a commercial alkyd paint film containing 5 wt % VGCNF.

properties between the metal and the coating.[138-145] No matter how excellent the other properties of a coating are, it would be only useful if it shows acceptable adhesion properties. The adhesion is a matter of both the interface and the mechanical properties of the coat itself.

The coating hardness is another important factor that affects the corrosion protection properties and hence the service life of a coating. The hardness of a material is defined as its resistance to localized deformation.[146-148] Hardness is a measure of the ability of a substrate to resist permanent deformation when an increasing load is applied to it.[149] A material can deform as a result of cutting, scratching, abrasion, or indentation.[146] The greater the hardness of a material, the better is its resistance to deformation, and hence the higher its strength.

In the current study, the hardness properties between the steel substrate and the alkyd paint, with and without VGCNFs, were investigated through the use of a Hysitron-type nanoindentation system to measure the change in the Vickers microhardness vs. maximum applied load. Nanoindentation hardness measurements are useful in ranking coatings on rigid substrates for their resistance to mechanical deformation.[150, 151]

Nanoindentation is a depth-sensing testing in the submicrometer range. The technique offers a unique method for in situ probing the interphase properties of both bulk solids and thin films (e.g., thin metal films, polymers, and organic coatings).[150, 152-157] This technique is currently well recognized as a high-resolution surface analysis method to probe the mechanical properties of thin films and solid materials in a wide range of fields including biology; human dental structures and

medical implants; polymers and polymer composites; organic coatings; microelectronics; microelectromechanical systems (MEMS); and ceramics.[151, 158-165]

In nanoindentation tests, a nanosized probe tip is controllably pressed on the material surface and then retracted at a constant rate, thus providing direct quantification of the mechanical properties of the indented material on the nanoscale.[149, 152, 159, 166, 167] The result of these tests are commonly provided as a force-displacement curve that encompasses the local mechanical properties of the indented material. Thorough reviews on the use of the nanoindentation technique for studying the mechanical behavior of polymers and organic coatings are available.[151, 158-162, 168-173]

Figure 2.13 demonstrates the typical loading scheme followed in all of the indentation experiments for VGCNF-reinforced as well as SiC-reinforced alkyd paint coatings applied to the surface of mild steel coupons. In this scheme, the maximum indent load was 50 mN, the holding period was 15 s, and both the loading and unloading rates were 15 mN/s. For each panel, twenty five replications of the nanoindentation experiments were performed repeatedly with the same loading sequence, rate, and hold period but with different maximum load. The maximum load was varied from one imprint to another in an effort to characterize the creep properties.

The hardness as a function of the displacement of the indenter was measured from the loading/unloading of the indenter. Figure 2.14 shows a typical load-penetration depth curve of a nanoindentation test of a VGCNF-reinforced alkyd paint coating applied to the surface of mild steel panels. As shown from the loading/unloading portions in the figure, during the early stage of loading, the indentation depth is very small and the paint film follows the Hertzian contact theory and hence shows elastic deformation

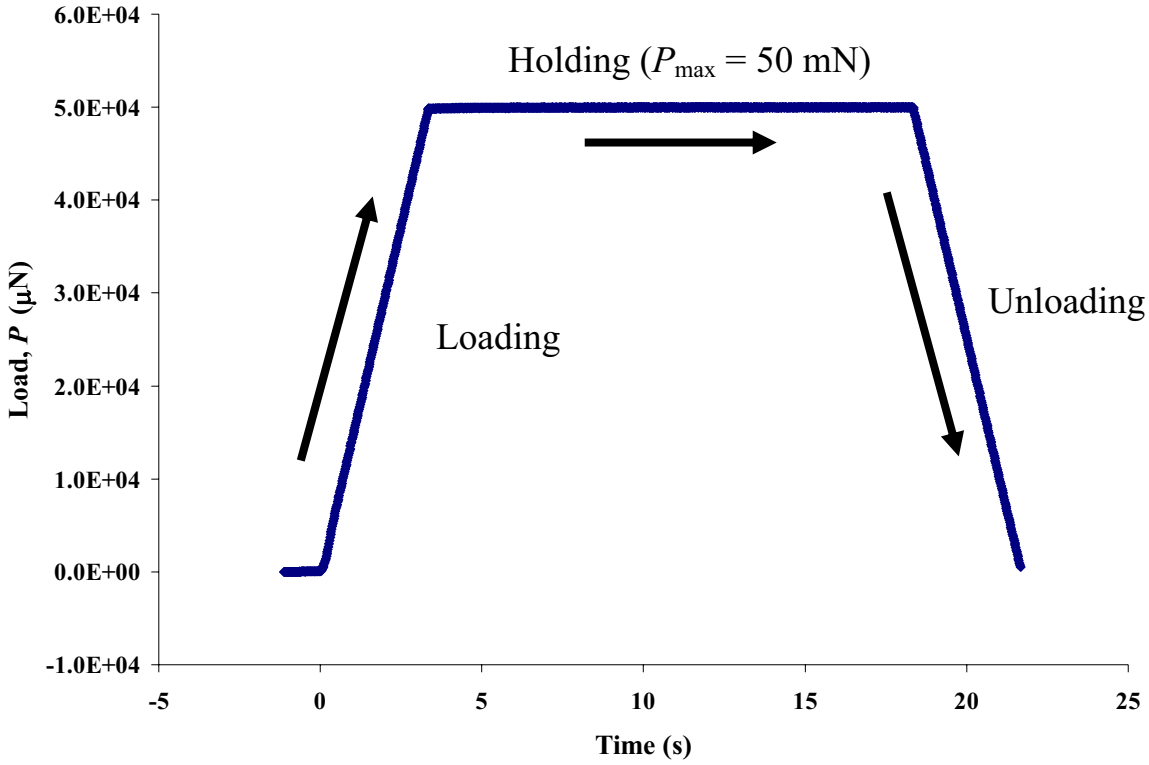

Figure 2.13 Typical load-time curve for a nanoindentation experiment for a mild steel panel coated with a 5% VGCNF-incorporated alkyd paint film (40 μm thick).

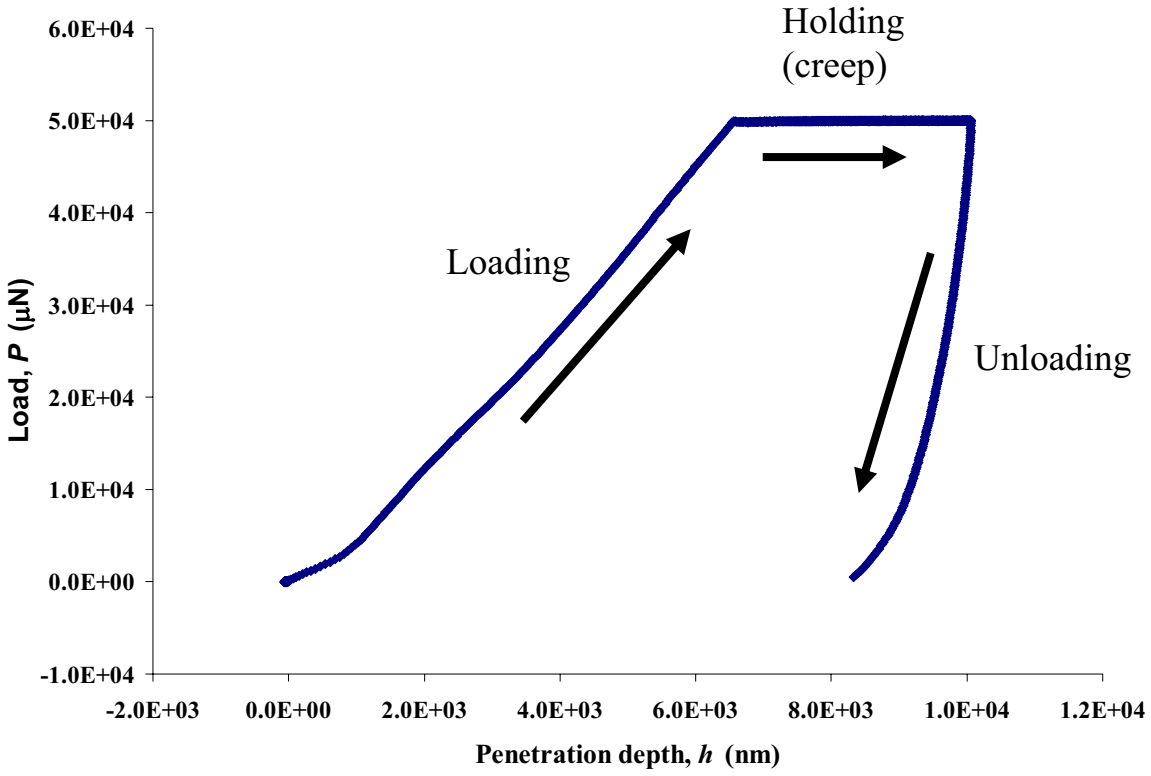

Figure 2.14 Typical load-penetration depth curve for a nanoindentation experiment for a mild steel panel coated with a 5% VGCNF-incorporated alkyd paint film (40 μm thick).

(yielding).[174-176] As the applied load increases, the indentation depth also increases, and the deformation behavior deviates from the Hertzian behavior. Accordingly, at the late stage of loading, the paint film shows an elastoplastic deformation. On the other hand, the unloading step shows an elastic yielding in accordance with the Hertzian theory.[174, 177-179]

Figure 2.15 shows the variation of the coating hardness (in Vickers) vs. the maximum load (P_{max}) for alkyd paint coatings containing 0, 1, 3, and 5 wt % VGCNF, respectively. It can be seen from the figure that, at constant paint thickness, increasing the VGCNF content improves the hardness of the alkyd paint matrix up to 3% and then it decreases the hardness for VGCNF content above 3%. This behavior is common in the literature.[180] An explanation of this decrease in the hardness at high VGCNF wt % is that at VGCNF content higher than 3%, the fibers agglomerate in the coating. This agglomeration impairs the properties of the coating film and promotes damage and higher deformation upon loading,. and hence decreases the coating hardness.

Surveying the literature shows that, when a metallic filler is added to an organic coating or a composite material, the properties of the host matrix depends on the weight percent of the added filler.[46, 180] The literature data also shows that there is a threshold weight percent for the filler, above which the properties (e.g., the electrical conductivity) of the host matrix deteriorate. This threshold value depends on both the type of the conductive filler and the polymeric composite in which the filler is dispersed.[180] For example, the threshold value is about 7.5% for epoxy resins containing Fe[180] and 20-40% for epoxy resins reinforced with Ag, Sn, Pb, Cu, or Al.[181, 182] The threshold value is 5-6% for Cu particles in polyvinyl chloride[183] and Ni in polyethylene[184] while it is 1% and 8%

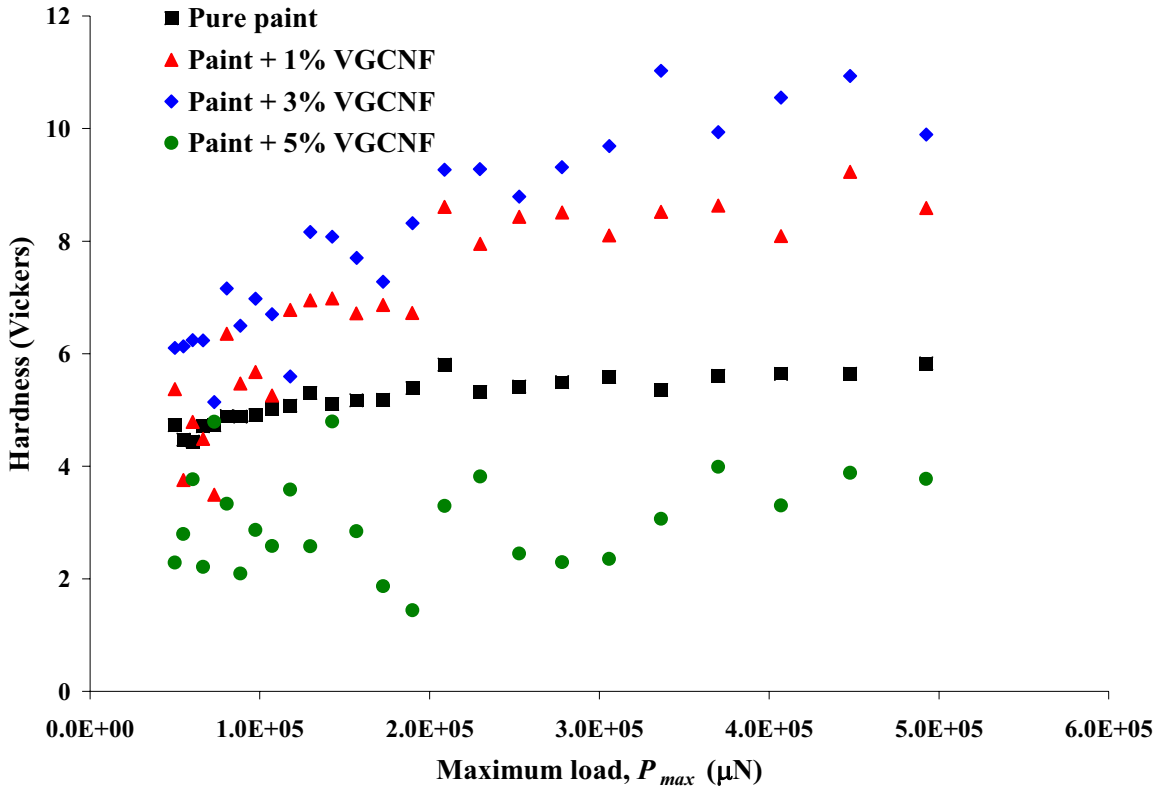

Figure 2.15 Variation of the indentation hardness (Vickers) vs. the maximum load (P_{max}) for VGCNF-reinforced alkyd paint coatings with different VGCNF wt %. ■ = pure paint, ▲ = paint + 1% VGCNF, ◆ = paint + 3% VGCNF, and ● = paint + 5% VGCNF. All samples have a thickness of ~ 40 μm.

for CB in polyvinyl alcohol,[30] and Araldite D,[185] respectively. The threshold value is 37% for Ag particles in Bakelite powder.[186]

For comparison, the hardness behavior of alkyd paint coatings containing SiC whiskers (1.5 μm in diameter, 18 μm in length, density = 3.217 g/cm^3) applied to the surface of mild steel coupons has been studied under the same conditions used for VGCNF-reinforced samples. Figure 2.16 depicts the variation of the hardness vs. the maximum load for alkyd paint coatings containing 0, 5, and 10 wt % SiC. As shown in the figure, in contrast to the behavior of the VGCNF, increasing the SiC content improves the hardness of the alkyd paint matrix at all levels tested. These results are in agreement with those reported by others.[187] However, it can be seen that the hardness obtained with 10 wt % SiC is almost the same as the hardness obtained with 3 wt % VGCNF. This indicates that VGCNF is more effective in improving the hardness than SiC.

Viscoelasticity is another mechanical property of polymers, paint coatings, and polymer-based composites.[188-191] The viscoelastic behavior of polymers depends on the properties of the polymeric material (e.g., polymer structure, length of the polymeric chain, average molecular weight, density, etc) and processing history.[192-194] Based on its properties, a polymeric material could show some non-linear recoverable strain with an extent of residual strain.[195-197] The way to understand this behavior is to perform creep tests under constant load for a range of loads.[188, 189, 198] Naturally, the loads should not surpass the limit where the indentation depth approaches the maximum thickness of the paint.

As shown in Figures 2.13 and 2.14, when the maximum load (P_{max}) is reached, this load is kept constant for a short period of time. During that constant-load period, the

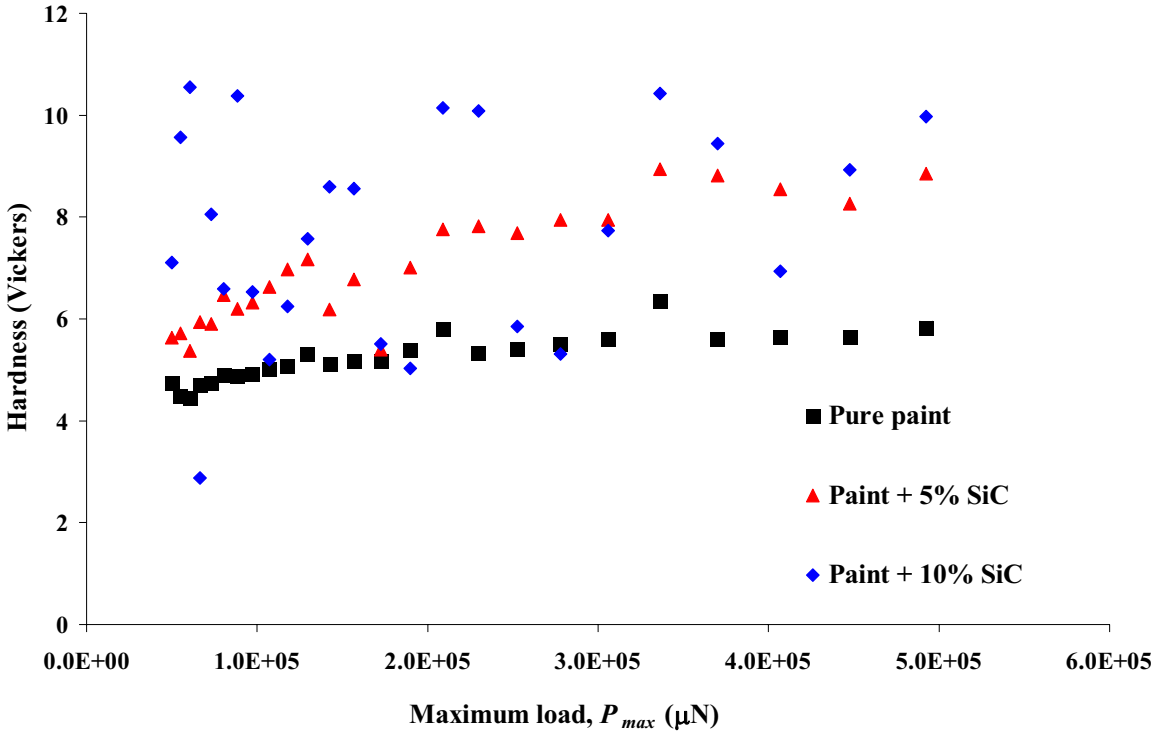

Figure 2.16 Variation of the indentation hardness (Vickers) vs. the maximum load (P_{max}) for SiC-reinforced alkyd paint coatings with different SiC wt %. ■ = pure paint, ▲ = paint + 5% SiC, and ◆ = paint + 10% SiC. All samples have a thickness of ~ 40 μm.

paint film continues to deform. This type of deformation at constant load is called "creep". The creep rate is defined as the rate of deformation of a solid material or a polymer film under the influence of a constant stress. The creep rate of any material depends on several factors including the microstructure properties of the material, the temperature, the magnitude of the load, and the exposure time. The creep behavior of an organic coating applied to the surface of a metal or alloy is one of the important parameters that strongly influence the working reliability of the coating.[199-204]

Figures 2.17 and 2.18 display examples for the variation of the creep rate vs. maximum load (P_{max}) obtained for a 5 wt % VGCNF- and a 1 wt % SiC-reinforced alkyd paint coatings. As shown in both figures, the creep rate decreases with increasing load, which is atypical behavior but also common in the literature.[200] However, this behavior is consistent with variation in hardening with increasing VGCNF or SiC content in the paint matrix. The overall range of creep rate values is much lower for SiC than for VGCNF. This could be explained by the higher aspect ratio and smaller diameter of the VGCNFs compared to the SiC whiskers. Having a smaller diameter, the VGCNF fiber would offer a smaller resistance to the flow of the paint. Also, having a high aspect ratio, the resistance of the VGCNF would be more directional so the flow could be a lot easier in one direction, in contrast to the SiC whiskers that will show minimal rotation for alignment with the deformation flow direction.

2.3.4 Electrical Conductivity Measurements

According to the literature, the incorporation of carbon fiber (e.g., polyacrylonitrile (PAN) carbon fiber, VGCNF, and CNTs) in thermoplastic polymer

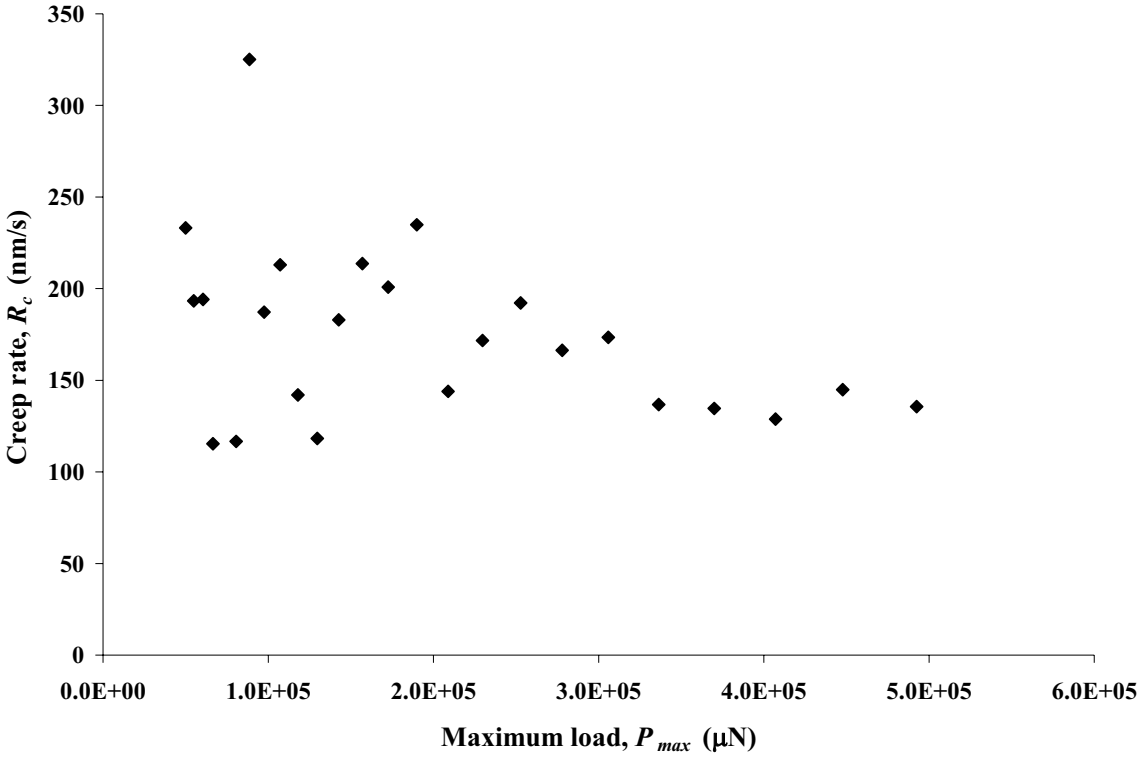

Figure 2.17 Variation of the creep rate (R_c) with maximum load for mild steel panels coated with a 5% VGCNF-incorporated commercial paint film (40 μm thick).

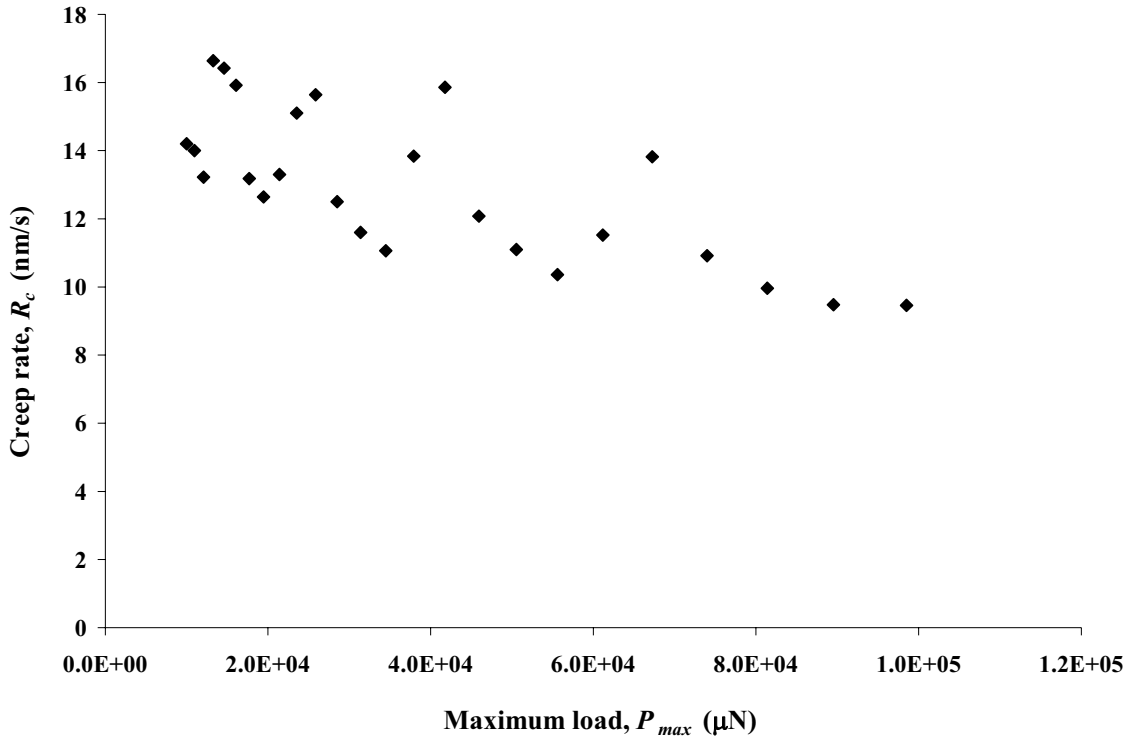

Figure 2.18 Variation of the creep rate (R_c) with maximum load for mild steel panels coated with a 1% SiC-incorporated commercial paint film (40 μm thick).

composites such as polyethylene, PVC, polyetheretherketone (PEEK), polypropylene, and polyethersulfone (PES) composites enhances the electrical conductivity of the polymer matrix by up to 11 orders of magnitude.[75, 102, 205-213] The data reported in the literature shows that when a conductive filler is added to a non-conducting matrix, the conductivity increases abruptly at a critical loading (known as the percolation threshold) of the conductive filler.[214, 215] At the filler concentration equal to the percolation threshold, the conductive filler forms a three-dimensional conductive network inside the insulating polymer (paint) matrix. Increasing the concentration of conductive filler added to an insulating polymer (composite) matrix above the percolation threshold has little effect on the conductivity of the polymer matrix.[29, 216]

Because of the strong adhesion of the VGCNF/paint coating to the mild steel surface, it was not possible to remove the paint film from the substrate surface to measure its conductivity and the measurements were performed on the as-deposited coatings applied to the mild steel substrates using a voltmeter. In this experiment, the resistivity was measured with probes ~ 1 cm apart on the surface of the coating. Accordingly, the measured conductivity values were expected to be inaccurate and higher than those values for freestanding VGCNF/paint films due to the effect of the underlying conductive substrate surface. Nevertheless, the measured conductivity values are useful for the qualitative ranking of different organic coatings.[217] As shown in Table 2.1, the higher the VGCNF wt % in the paint matrix, the higher the conductivity of the paint film.

To avoid the errors in the measured conductivity values due to the underlying conductive substrate, the VGCNF/paint coatings were also deposited, via spin coating, on

Table 2.1 Conductivity measurements for a commercial alkyd paint containing different VGCNF weight percent (wt %) and film thickness applied to the surface of mild steel panels.

wt % of VGCNF	Coating Thickness (μm)	Conductance (μS)	Resistivity (ρ, Ω.cm)	Conductivity (σ, $\Omega^{-1}.cm^{-1}$)
1	30	11.1	270	3.7×10^{-3}
3	50	27.0	185	5.4×10^{-3}
5	20	26.3	76	1.3×10^{-2}
	30	32.3	93	1.1×10^{-2}
	55	44.8	123	8.1×10^{-3}
	80	58.8	136	7.3×10^{-3}
	90	71.4	126	7.9×10^{-3}
	150	76.9	195	5.1×10^{-3}
10	30	3330.0	0.9	1.1
	100	10000.0	1.0	1.0

the insulating PMMA sheets. The conductivity (resistivity) values of these samples were determined using the van der Pauw technique.

The van der Pauw method, a version of the four-point probe technique, is a method commonly used to measure the electrical resistivity (sheet resistivity, ρ) for conducting as well as semiconducting samples that are flat, homogeneous in thickness, do not contain holes, and have arbitrary shapes.[218] This method has many applications including the semiconductor industry, the determination of the electrical characteristics of foils, ceramics, and superconductors.[219-226]

The van der Pauw method involves the use of two pairs of isolated leads for the measurement of the sheet resistivity of any sample. One pair of leads is used to force a constant electric current (I) through the sample while the second pair is used to measure the voltage drop (V). The method requires the use of a current source as well as a sensitive voltmeter.[218]

Figure 2.19 is a diagram of the van der Pauw set-up for resistivity measurements. As shown in the figure, for accurate measurements, the contacts should be small and placed on the boundary of the sample. A total of eight measurements are made around the sample as shown in Figure 2.19. The average resistivity (ρ_{AVG}) is determined by combining the readings of all measurements as follows:

Two values of sheet resistivity, ρ_A and ρ_B, are computed as follows:

$$\rho_A \quad \frac{\pi}{\ln 2} f_A t_s \frac{(V_2 + V_4 - V_1 - V_3)}{4I} \tag{2.1}$$

$$\rho_B \quad \frac{\pi}{\ln 2} f_B t_s \frac{(V_6 + V_8 - V_5 - V_7)}{4I} \tag{2.2}$$

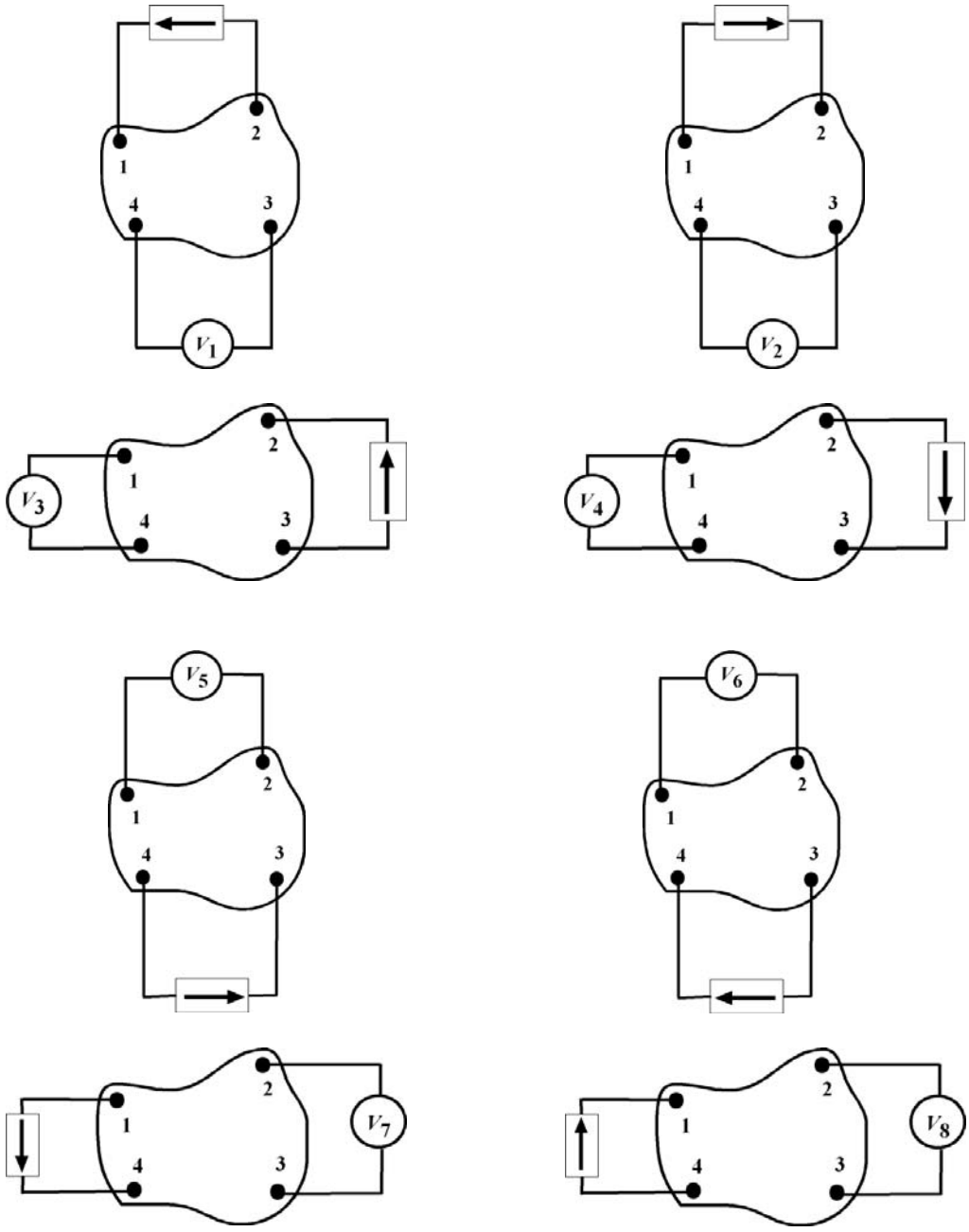

Figure 2.19 Schematic drawing of the van der Pauw resistivity measurement connections.

Where: ρ_A and ρ_B are resistivities in ohm-cm;

t_s is the sample thickness in cm;

V_1 through V_8 represent the voltages measured by the voltmeter;

I is the current forced through the sample in amperes;

f_A and f_B are geometrical factors based on sample symmetry. For samples having perfect symmetry, $f_A = f_B = 1$

The average resistivity (ρ_{AVG}) is determined as follows:

$$\rho_{AVG} \quad \frac{\rho_A + \rho_B}{2} \tag{2.3}$$

Table 2.2 shows the variation of the resistivity of VGCNF/alkyd paint coatings with the wt % of VGCNF and film thickness. The results indicate that the electrical resistivity of the VGCNF/paint coating decreases with increasing the VGCNF loading. These results are in agreement with the literature results.[73, 107, 112, 117, 227]

The data shown in Table 2.2 also clearly indicate that there is a remarkable continuous decrease in the electrical resistivity of the alkyd paint matrix with increasing the filler loading above the percolation threshold. As depicted in the table, coating samples containing 10% VGCNF showed a slightly big difference in the resistivity values for samples with 200 and 230 μm thicknesses. It is expected that both films would have the same resistivity. However, this difference could be attributed to the heterogeneity in the distribution of the VGCNF and the film thickness for the 10% VGCNF-reinforced coating. As mentioned above, the van der Pauw method requires that the sample be flat, homogeneous, and free of voids and holes.

Table 2.2 Resistivity measurements for commercial alkyd paint coatings containing different weight percents of VGCNF and different film thicknesses applied to the surface of a PMMA substrate.

wt % of VGCNF	Coating Thickness (μm)	Number of Trials (N)	Average Resistivity (ρ, Ω.cm)	Average Conductivity (σ, $\Omega^{-1}.cm^{-1}$)
3	50	2	33.8	2.96×10^{-2}
5	100	3	18.2 ± 0.877	5.50×10^{-2}
10	200	1	0.862	2.67×10^{-1}
10	230	1	3.74	1.16

According to the literature, the decrease in the resistivity of the VGCNF/paint composite is mainly due to either tunneling or direct contact between the filler particles.[228, 229] Conduction through tunneling is the dominant mechanism when the filler particles are less than 10 nm apart from each other.[230] To determine the exact mechanism, the current-voltage (*I-V*) relationship for the composite is examined. A linear *I-V* relationship (Ohm's law) indicates that the composite conductivity is mainly due to direct contact of particles. On the other hand, for composites having a power law *I-V* relation, the tunneling mechanism is the dominant mechanism.[228, 231]

Figures 2.20 and 2.21 show examples of the *I-V* relationship for alkyd paint films containing different VGCNF loadings, namely 3 and 5 wt %, respectively with the same thickness (~ 50 μm). These figures were obtained by applying a constant voltage to the coating film and recording the corresponding current using the four-point probe technique. The voltage was then varied and a new current value was recorded. Examining the two figures indicates that the there is a linear *I-V* relationship for the VGCNF-reinforced alkyd paint coatings indicating that the conductivity is due to direct contact of the VGCNF particles in the paint matrix. It can also be noticed from the slopes of the two graphs that the average resistance *R* ($R = 10^6$/slope Ω) of the paint containing 5% VGCNF (Figure 2.21) is ~ 700 Ω while the value for the coating containing 3% is ~ 1000 Ω. These results indicate that the higher the VGCNF content, the smaller the average resistance of the coating which is consistent with the data presented in Table 2.2.

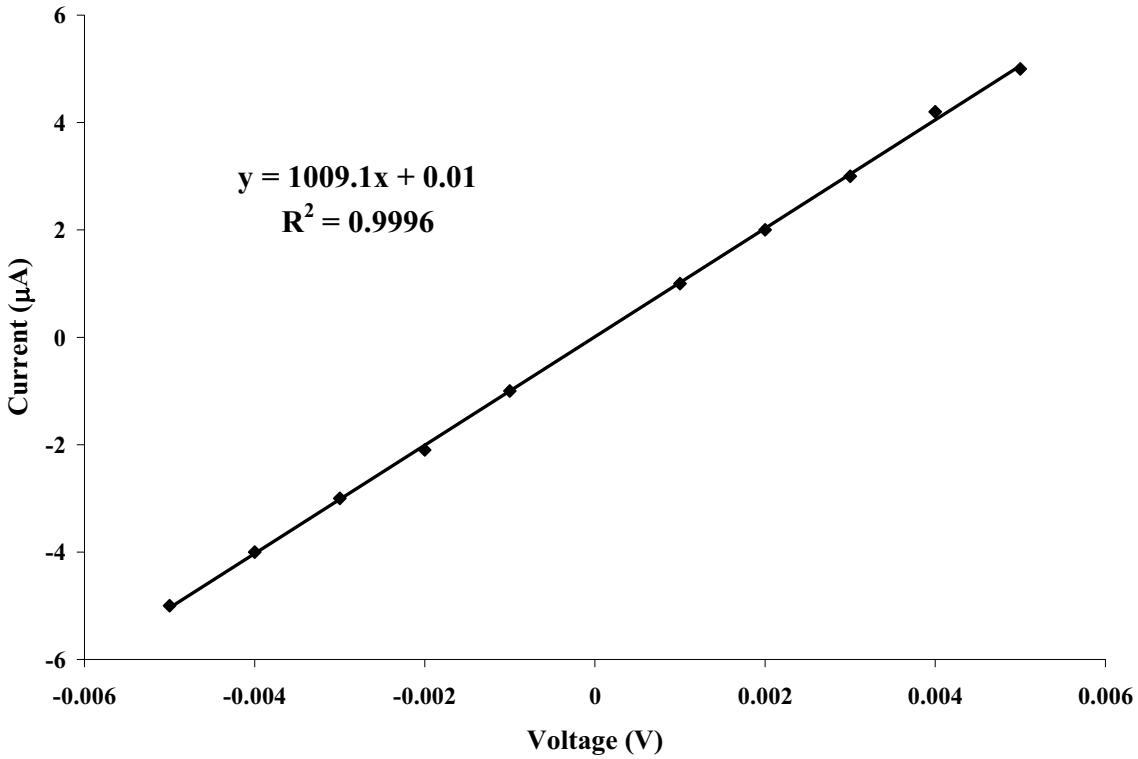

Figure 2.20 Current (*I*)-voltage (*V*) relationship, recorded using the four-point probe technique, for a 3 wt % VGCNF-incorporated commercial alkyd paint film (50 μm thick) applied to the surface of a PMMA substrate.

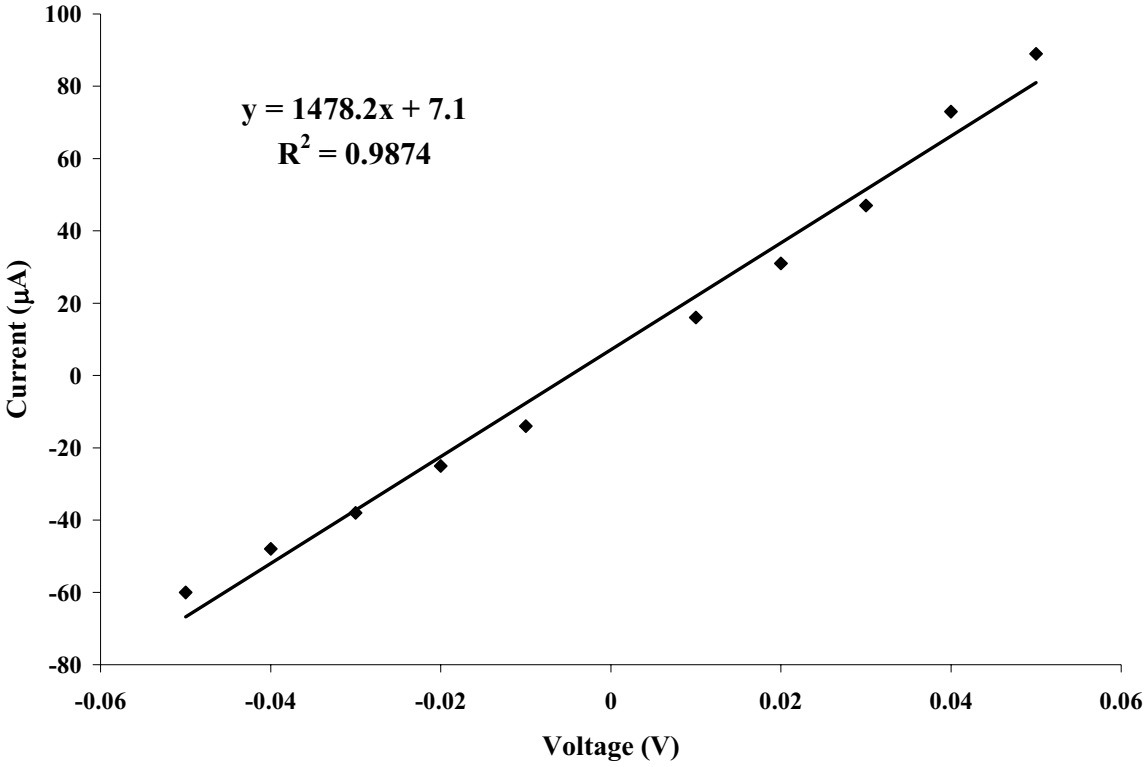

Figure 2.21 Current (*I*)-voltage (*V*) relationship, recorded using the four-point probe technique, for a 5 wt % VGCNF-incorporated commercial alkyd paint film (55 μm thick) applied to the surface of a PMMA substrate.

2.4 Conclusions

In this chapter, the surface, mechanical, and electrical properties of commercial alkyd paint coatings containing different loadings of VGCNF and applied to the surface of steel and poly(methyl methacrylate) substrates were investigated. In addition, the investigation involved optical as well as visual inspections. The results showed that the incorporation of the VGCNF in the alkyd paint formulation significantly enhances the electrical conductivity properties imparted by the coating. On the other hand, the nanoindentation measurements showed that the incorporation of VGCNF in the paint matrix improves the hardness up to 3 wt % and then it deteriorates the hardness for VGCNF content higher than 3%.

2.5 References

(1) Forsgren, A. *Corrosion Control Through Organic Coatings;* CRC Press: Boca Raton, FL, 2006.

(2) Wicks, Z. W. J.; Jones, F. N.; Pappas, S. P. *Organic Coatings - Science and Technology Vol 2. Applications, Properties and Performance,* 3rd ed.; John Wiley & Sons, Inc.: Hoboken, NJ 2007.

(3) Bierwagen, G. P. *Progress in Organic Coatings* **1996**, *28*, 43-48.

(4) Bierwagen, G. P.; Jeffcoate, C. S.; Li, J.; Balbyshev, S.; Tallman, D. E.; Mills, D. J. *Progress in Organic Coatings* **1996**, *29*, 21-30.

(5) Leidheiser, H., Jr. *Corrosion* **1982**, *38*, 374-383.

(6) Walter, G. W. *Corrosion Science* **1986**, *26*, 27-38.

(7) Bierwagen, G.; Li, J.; He, L.; Tallman, D. *ACS Symposium Series* **2002**, *805*, 316-350.

(8) Bierwagen, G. P.; Tallman, D. E.; Zlotnick, J.; Jeffcoate, C. S. *ACS Symposium Series* **1998**, *689*, 123-136.

(9) Branzoi, V.; Pilan, L.; Branzoi, F. *WIT Transactions on Engineering Sciences* **2005**, *51*, 269-277.

(10) de Wit, J. H. W.; van der Weijde, D. H.; Ferrari, G. In *Corrosion Mechanisms in Theory and Practice,* 2nd ed.; Marcus, P., Ed.; Marcel Dekker, Inc.: New York, 2002, pp 683-729.

(11) Koch, R. R. *Organic Coatings and Plastics Chemistry* **1980**, *42*, 98-101.

(12) Perez, C.; Izquierdo, M.; Abreu, C. M.; Collazo, A.; Merino, P. *Recent Research Developments in Electrochemistry* **2002**, *5*, 115-144.

(13) Singh, A. J.; Bhide, S. P. *Journal of the Colour Society* **1982**, *21*, 25-30.

(14) Groseclose, R. G.; Frey, C. M.; Floyd, F. L. *Journal of Coatings Technology* **1984**, *56*, 31-41.

(15) Lambourne, R.; Strivens, T. A., Eds. *Paint and Surface Coatings--Theory and Practice*, 2nd ed.; Woodhead Publishing Ltd.: Cambridge, U.K., 1999.

(16) Armelin, E.; Oliver, R.; Liesa, F.; Iribarren, J. I.; Estrany, F.; Aleman, C. *Progress in Organic Coatings* **2007**, *59*, 46-52.

(17) Blustein, G.; Di Sarli, A. R.; Jaen, J. A.; Romagnoli, R.; Del Amo, B. *Corrosion Science* **2007**, *49*, 4202-4231.

(18) del Amo, B.; Deya, C.; Zalba, P. *Microporous and Mesoporous Materials* **2005**, *84*, 353-356.

(19) Deya, C.; Romagnoli, R.; del Amo, B. *Journal of Coatings Technology and Research* **2007**, *4*, 167-175.

(20) Elsener, B.; Buchler, M.; Bohni, H. *European Federation of Corrosion Publications* **1998**, *25*, 54-59.

(21) Goldie, B. P. F. *Paint & Resin* **1985**, *55*, 16, 18-20.

(22) Hang, T. T. X.; Truc, T. A.; Nam, T. H.; Oanh, V. K.; Jorcin, J.-B.; Pebere, N. *Surface and Coatings Technology* **2007**, *201*, 7408-7415.

(23) Sugama, T. *Materials Letters* **2006**, *60*, 2700-2706.

(24) Iribarren, J. I.; Armelin, E.; Liesa, F.; Casanovas, J.; Aleman, C. *Materials and Corrosion* **2006**, *57*, 683-688.

(25) Ocampo, C.; Armelin, E.; Liesa, F.; Aleman, C.; Ramis, X.; Iribarren, J. I. *Progress in Organic Coatings* **2005**, *53*, 217-224.

(26) Grunlan, J. C.; Gerberich, W. W.; Francis, L. F. *Polymer Engineering and Science* **2001**, *41*, 1947-1962.

(27) Grunlan, J. C.; Jang, W.-S.; McConnell, E. P.; Jan, C. J. *PMSE Preprints* **2005**, *93*, 728-729.

(28) Psarras, G. C. *Journal of Polymer Science, Part B* **2007**, *45*, 2535-2545.

(29) Zhang, B.; Fu, R.; Zhang, M.; Dong, X.; Zhao, B.; Wang, L.; Pittman, C. U. *Composites, Part A: Applied Science and Manufacturing* **2006**, *37A*, 1884-1889.

(30) Zhang, W.-g.; Li, L.; Yao, S.-w.; Zheng, G.-q. *Corrosion Science* **2007**, *49*, 654-661.

(31) Gonzalez, S.; Caceres, F.; Fox, V.; Souto, R. M. *Progress in Organic Coatings* **2003**, *46*, 317-323.

(32) Samui, A. B.; Chavan, J. G.; Hande, V. R. *Progress in Organic Coatings* **2006**, *57*, 301-306.

(33) El-Sawy, S. M.; Morsi, I. M.; Abdel-Mohdy, F. A. *Pigment & Resin Technology* **1983**, *12*, 11-13.

(34) Rusev, D.; Radev, D.; Karaivanov, S. *Metal Finishing* **1983**, *81*, 27-30.

(35) Xia, W.; Wang, L. *Polymeric Materials Science and Engineering* **1987**, *56*, 695-698.

(36) Faidi, S. E.; Scantlebury, J. D.; Bullivant, P.; Whittle, N. T.; Savin, R. *Corrosion Science* **1993**, *35*, 1319-1328.

(37) Gervasi, C. A.; Di Sarli, A. R.; Cavalcanti, E.; Ferraz, O.; Bucharsky, E. C.; Real, S. G.; Vilche, J. R. *Corrosion Science* **1994**, *36*, 1963-1972.

(38) Kalendova, A. *Anti-Corrosion Methods and Materials* **2002**, *49*, 173-180.

(39) Marchebois, H.; Keddam, M.; Savall, C.; Bernard, J.; Touzain, S. *Electrochimica Acta* **2004**, *49*, 1719-1729.

(40) Marchebois, H.; Savall, C.; Bernard, J.; Touzain, S. *Electrochimica Acta* **2004**, *49*, 2945-2954.

(41) Kouloumbi, N.; Tsangaris, G. M.; Kyvelidis, S. T.; Psarras, G. C. *British Corrosion Journal* **1999**, *34*, 267-272.

(42) Davis, B. In *Coatings Technology Handbook,* 2nd ed.; Satas, D., Tracton, A. A., Eds.; Marcel Dekker, Inc.: New York, 2001, pp 559-563.

(43) Ogoshi, T.; Umeda, K.; Yamagishi, T.-a.; Nakamoto, Y. *Polymer Journal* **2008**, *40*, 942-943.

(44) Fei, B.; Qian, B.; Yang, Z.; Wang, R.; Liu, W. C.; Mak, C. L.; Xin, J. H. *Carbon* **2008**, *46*, 1795-1797.

(45) Joseph, Y.; Guse, B.; Vossmeyer, T.; Yasuda, A. *Journal of Physical Chemistry C* **2008**, *112*, 12507-12514.

(46) Kouloumbi, N.; Tsangaris, G. M.; Kyvelidis, S. T. *Journal of Coatings Technology* **1994**, *66*, 83-88.

(47) Gelling, V. J.; Wiest, M. M.; Tallman, D. E.; Bierwagen, G. P.; Wallace, G. G. *Progress in Organic Coatings* **2001**, *43*, 149-157.

(48) Lu, W.-K.; Basak, S.; Elsenbaumer, R. L. In *Handbook of Conducting Polymers,* 2nd ed.; Skotheim, T. A., Elsenbaumers, R. L., Reynolds, J. R., Eds.; Marcel Dekker, Inc.: New York, 1998, pp 881-920.

(49) Rohwerder, M.; Michalik, A. *Electrochimica Acta* **2007**, *53*, 1300-1313.

(50) Tan, C. K.; Blackwood, D. J. *Corrosion Science* **2002**, *45*, 545-557.

(51) Kilmartin, P. A.; Trier, L.; Wright, G. A. *Synthetic Metals* **2002**, *131*, 99-109.

(52) Breslin, C. B.; Fenelon, A. M.; Conroy, K. G. *Materials & Design* **2005**, *26*, 233-237.

(53) Sitaram, S. P.; Yu, P.; O'Keefe, T.; Stoffer, J. O.; Kinlen, P. *Polymeric Materials Science and Engineering* **1996**, *75*, 352-353.

(54) Thompson, K. G.; Benicewicz, B. C. *Polymer Preprints* **2000**, *41*, 1731-1732.

(55) Mollahosseini, A.; Noroozian, E. *Synthetic Metals* **2009**, *159*, 1247-1254.

(56) Bereket, G.; Huer, E. *Progress in Organic Coatings* **2009**, *65*, 116-124.

(57) Mazario, E.; Cabrera, L.; Herrasti, P. *Journal of Advances in Engineering Science* **2007**, 37-44.

(58) Selvaraj, M.; Palraj, S.; Maruthan, K.; Rajagopal, G.; Venkatachari, G. *Synthetic Metals* **2008**, *158*, 888-899.

(59) Gelling, V. J.; Vetter, C.; Somayajula, S. V. K.; Qi, X. *Polymer Preprints* **2008**, *49*, 642-643.

(60) Riaz, U.; Ahmad, S.; Ashraf, S. M. *Materials and Corrosion* **2009**, *60*, 280-286.

(61) Armelin, E.; Aleman, C.; Iribarren, J. I. *Progress in Organic Coatings* **2009**, *65*, 88-93.

(62) Wang, X. H.; Lu, J. L.; Chen, Y.; Li, J.; Wang, F. S. *Journal of Advances in Engineering Science* **2007**, 45-62.

(63) Sathiyanarayanan, S.; Jeyaram, R.; Muthukrishnan, S.; Venkatachari, G. *Journal of the Electrochemical Society* **2009**, *156*, C127-C134.

(64) Radhakrishnan, S.; Sonawane, N.; Siju, C. R. *Progress in Organic Coatings* **2009**, *64*, 383-386.

(65) Ozyilmaz, A. T.; Erbil, M.; Yazici, B. *Thin Solid Films* **2006**, *496*, 431-437.

(66) Tallman, D. E.; Pae, Y.; Bierwagen, G. P. *Corrosion* **2000**, *56*, 401-410.

(67) Tallman, D. E.; Pae, Y.; Bierwagen, G. P. *Corrosion* **1999**, *55*, 779-786.

(68) Huerta-Vilca, D.; Siefert, B.; Moraes, S. R.; Pantoja, M. F.; Motheo, A. J. *Molecular Crystals and Liquid Crystals* **2004**, *415*, 229-238.

(69) Tueken, T.; Yazici, B.; Erbil, M. *Progress in Organic Coatings* **2004**, *51*, 205-212.

(70) Bazzaoui, M.; Bazzaoui, E. A.; Martins, J. I.; Martins, L. *Materials Science Forum* **2004**, *455-456*, 484-488.

(71) Kousik, G.; Pitchumani, S.; Renganathan, N. G. *Progress in Organic Coatings* **2001**, *43*, 286-291.

(72) Barsch, U.; Beck, F. *Synthetic Metals* **1993**, *55*, 1638-1643.

(73) Wang, T.; Chen, G.; Wu, C.; Wu, D. *Progress in Organic Coatings* **2007**, *59*, 101-105.

(74) Cordoba, J. M.; Tamayo-Ariztondo, J.; Molina-Aldareguia, J. M.; Elizalde, M. R.; Oden, M. *Corrosion Science* **2009**, *51*, 926-930.

(75) Al-Saleh, M. H.; Sundararaj, U. *Carbon* **2009**, *47*, 2-22.

(76) Ebbesen, T. W. *Journal of Physics and Chemistry of Solids* **1996**, *57*, 951-955.

(77) Endo, M.; Kim, Y. A.; Hayashi, T.; Nishimura, K.; Matusita, T.; Miyashita, K.; Dresselhaus, M. S. *Carbon* **2001**, *39*, 1287-1297.

(78) Heremans, J. *Carbon* **1985**, *23*, 431-436.

(79) Ruoff, R. S.; Lorents, D. C. *Carbon* **1995**, *33*, 925-930.

(80) Treacy, M. M. J.; Ebbesen, T. W.; Gibson, J. M. *Nature* **1996**, *381*, 678-680.

(81) Iijima, S.; Brabec, C.; Maiti, A.; Bernholc, J. *Journal of Chemical Physics* **1996**, *104*, 2089-2092.

(82) Saito, R.; Fujita, M.; Dresselhaus, G.; Dresselhaus, M. S. *Applied Physics Letters* **1992**, *60*, 2204-2206.

(83) Chung, D. D. L. *Carbon* **2001**, *39*, 1119-1125.

(84) Eisenmenger-Sittner, C.; Schrank, C.; Neubauer, E.; Eiper, E.; Keckes, J. *Applied Surface Science* **2006**, *252*, 5343-5346.

(85) Hammel, E.; Tang, X.; Trampert, M.; Schmitt, T.; Mauthner, K.; Eder, A.; Potschke, P. *Carbon* **2004**, *42*, 1153-1158.

(86) Kuriger, R. J.; Alam, M. K.; Anderson, D. P. *HTD* **2000**, *366-3*, 349-354.

(87) Lake, M. L.; Ting, J.-M. In *Carbon Materials for Advanced Technologies*; Burchell, T. D., Ed.; Elsevier Science Ltd.: Oxford, U.K., 1999, pp 139-167.

(88) Lozano, K. *Jom* **2000**, *52*, 34-36.

(89) Lozano, K.; Bonilla-Rios, J.; Barrera, E. V. *Journal of Applied Polymer Science* **2001**, *80*, 1162-1172.

(90) Patton, R. D.; Pittman, C. U., Jr.; Wang, L.; Hill, J. R. *Composites, Part A: Applied Science and Manufacturing* **1999**, *30A*, 1081-1091.

(91) Van Hattum, F. W. J.; Bernardo, C. A.; Tibbetts, G. G. *NATO Science Series, Series E: Applied Sciences* **2001**, *372*, 245-254.

(92) Yudin, V. E.; Svetlichnyi, V. M.; Shumakov, A. N.; Schechter, R.; Harel, H.; Marom, G. *Composites, Part A: Applied Science and Manufacturing* **2008**, *39*, 85-90.

(93) Zhu, D.; Bin, Y.; Matsuo, M. *Journal of Polymer Science, Part B: Polymer Physics* **2007**, *45*, 1037-1044.

(94) Alias, M. N.; Brown, R. *Corrosion Science* **1993**, *35*, 395-402.

(95) Guth, J. R.; Lake, M. L.; Cornie, J. A.; Zhang, S. *NASA Conference Publication* **1994**, *3235*, 31-42.

(96) Ting, J.-M. *Journal of Materials Science* **1999**, *34*, 229-233.

(97) Ting, J. M.; Tang, C.; Lake, P. *Materials Research Society Symposium Proceedings* **1999**, *551*, 281-284.

(98) Thongruang, W.; Spontak, R. J.; Balik, C. M. *Polymer* **2002**, *43*, 2279-2286.

(99) Shibuya, M.; Sakurai, M.; Takahashi, T. *Composites Science and Technology* **2007**, *67*, 3338-3344.

(100) Bernardo, C. A.; van Hattum, F. W. J.; Carneiro, O. S.; Maia, J. M. *NATO Science Series, Series E: Applied Sciences* **2001**, *372*, 289-300.

(101) Finegan, I. C.; Tibbetts, G. G. *Journal of Materials Research* **2001**, *16*, 1668-1674.

(102) Gordeyev, S. A.; Ferreira, J. A.; Bernardo, C. A.; Ward, I. M. *Materials Letters* **2001**, *51*, 32-36.

(103) Gordeyev, S. A.; Macedo, F. J.; Ferreira, J. A.; Van Hattum, F. W. J.; Bernardo, C. A. *Physica B: Condensed Matter* **2000**, *279*, 33-36.

(104) Jiang, X.; Bin, Y.; Kikyotani, N.; Matsuo, M. *Polymer Journal* **2006**, *38*, 419-431.

(105) Tibbetts, G. G.; Finegan, I. C.; Kwag, C. *Molecular Crystals and Liquid Crystals Science and Technology, A: Molecular Crystals and Liquid Crystals* **2002**, *387*, 129-133.

(106) Choi, Y.-K.; Sugimoto, K.-i.; Song, S.-M.; Gotoh, Y.; Ohkoshi, Y.; Endo, M. *Carbon* **2005**, *43*, 2199-2208.

(107) Katsumata, M.; Endo, M.; Ushijima, H.; Yamanashi, H. *Journal of Materials Research* **1994**, *9*, 841-843.

(108) Kotaki, M.; Wang, K.; Toh, M. L.; Chen, L.; Wong, S. Y.; He, C. *Macromolecules* **2006**, *39*, 908-911.

(109) Ko, T.-H.; Hu, H.-L.; Kuo, W.-S.; Wang, S.-H. *Journal of Applied Polymer Science* **2006**, *102*, 1531-1538.

(110) Patton, R. D.; Pittman, C. U.; Wang, L.; Hill, J. R.; Day, A. *Composites, Part A: Applied Science and Manufacturing* **2001**, *33A*, 243-251.

(111) Choi, Y.-K.; Sugimoto, K.-i.; Song, S.-M.; Endo, M. *Composites, Part A: Applied Science and Manufacturing* **2006**, *37A*, 1944-1951.

(112) Guo, H.; Kumar, S. *PMSE Preprints* **2006**, *94*, 492-493.

(113) Bin, Y.; Mine, M.; Koganemaru, A.; Jiang, X.; Matsuo, M. *Polymer* **2006**, *47*, 1308-1317.

(114) Yang, S.; Lomeli, A.; Borrego, M.; Jones, R.; Lozano, K. *International SAMPE Technical Conference* **2003**, *35*, 535-540.

(115) Xu, J.; Donohoe, J. P.; Pittman, C. U., Jr. *Composites, Part A* **2004**, *35A*, 693-701.

(116) Shui, X.; Chung, D. D. L. *International SAMPE Symposium and Exhibition* **1993**, *38*, 1869-1875.

(117) Enomoto, K.; Yasuhara, T.; Ohtake, N.; Kato, K. *JSME International Journal, Series A: Solid Mechanics and Material Engineering* **2003**, *46*, 353-358.

(118) Boxall, J. *Paint & Resin* **1983**, *53*, 48-49.

(119) Schweitzer, P. A., Ed. *Paint and Coatings: Applications and Corrosion Resistance*; CRC Press: New York, 2006.

(120) Buchheit, R. G. In *Handbook of Environmental Degradation of Materials*; Kutz, M., Ed.; William Andrew, Inc.: Norwich, NY, 2005, pp 367-385.

(121) Johnson, J. A.; Barbato, M. J.; Hopkins, S. R.; O'Malley, M. J. *Progress in Organic Coatings* **2003**, *47*, 198-206.

(122) Van Hattum, F. W. J.; Serp, P. H.; Figueiredo, J. L.; Bernardo, C. A. *Carbon* **1997**, *35*, 860-863.

(123) Kittel, J.; Celati, N.; Keddam, M.; Takenouti, H. *Progress in Organic Coatings* **2001**, *41*, 93-98.

(124) Marsh, J.; Scantlebury, J. D.; Lyon, S. B. *Corrosion Science* **2001**, *43*, 829-852.

(125) Koleske, J. V., Ed. *Paint and Coating Testing Manual: Fourteenth Edition of the Gardner-Sward Handbook*; ASTM: Philadelphia, PA, 1995.

(126) Schuetze, A. P.; Lewis, W.; Brown, C.; Geerts, W. J. *American Journal of Physics* **2004**, *72*, 149-153.

(127) Lakshminarayanan, P. V.; Toghiani, H.; Pittman, C. U. *Carbon* **2004**, *42*, 2433-2442.

(128) Armelin, E.; Pla, R.; Liesa, F.; Ramis, X.; Iribarren, J. I.; Aleman, C. *Corrosion Science* **2008**, *50*, 721-728.

(129) Power, J. F. *Review of Scientific Instruments* **2002**, *73*, 4057-4141.

(130) Grove, G.; Grove, M. J. In *Handbook of Cosmetic Science and Technology*; Barel, A. O., Paye, M., Maibach, H. I., Eds.; Marcel Dekker, Inc.: New York, 2001, pp 829-835.

(131) Dey, S. K.; Perry, T. A.; Alpas, A. T. *Wear* **2009**, *267*, 515-524.

(132) Berman, M.; Coward, D. A.; Whitbourn, L. B.; Osborne, B. G.; Evans, C. J.; Connor, P. M.; Beare, R. J.; Phillips, R. N.; Quodling, R. *Cereal Chemistry* **2007**, *84*, 282-284.

(133) Yung, K. C.; Wang, J.; Yue, T. M. *Journal of Adhesion Science and Technology* **2007**, *21*, 363-377.

(134) Vernani, D.; Pareschi, G.; Mazzoleni, F.; Spiga, D.; Valtolina, R. *Materials Structure in Chemistry, Biology, Physics and Technology* **2006**, *13*, 71-75.

(135) Bushman, S.; Celii, F.; Martin, S.; Tristan, L. *AIP Conference Proceedings* **2005**, *788*, 427-431.

(136) Thissell, W. R.; Zurek, A. K.; Rivas, J. M.; Tonks, D. L.; Hixson, R. S. *Microstructural Science* **1999**, *26*, 497-505.

(137) Verberne, G.; Merkher, Y.; Halperin, G.; Maroudas, A.; Etsion, I. *Wear* **2009**, *266*, 1216-1223.

(138) Deflorian, F.; Fedrizzi, L. *Journal of Adhesion Science and Technology* **1999**, *13*, 629-645.

(139) Deflorian, F.; Fedrizzi, L.; Rossi, S. *Corrosion* **1999**, *55*, 1003-1011.

(140) Dickie, R. A. *Journal of Coatings Technology* **1994**, *66*, 29-37.

(141) Dickie, R. A. *Progress in Organic Coatings* **1994**, *25*, 3-22.

(142) Maeda, S. *Progress in Organic Coatings* **1996**, *28*, 227-238.

(143) van Westing, E. P. M.; Ferrari, G. M.; de Wit, J. H. W. *Corrosion Science* **1994**, *36*, 979-994.

(144) van Westing, E. P. M.; Ferrari, G. M.; de Wit, J. H. W. *Corrosion Science* **1994**, *36*, 957-977.

(145) Van Westing, E. P. M.; Ferrari, G. M.; De Wit, J. H. W. *Electrochimica Acta* **1994**, *39*, 899-910.

(146) Jennett, N. M.; Gee, M. G. In *Surface Coatings for Protection against Wear*; Millor, B. G., Ed.; CRC Press: Boca Raton, FL, 2006, pp 58-78.

(147) Klansky, J. *Characterization of Materials* **2003**, *1*, 316-323.

(148) Oliver, W. C.; Pharr, G. M. *Journal of Materials Research* **2004**, *19*, 3-20.

(149) Seo, M. In *Analytical Methods In Corrosion Science and Engineering;* Marcus, P., Mansfeld, F. B., Eds.; CRC Press: Boca Raton, FL, 2006, pp 335-360.

(150) Bull, S. J. *Journal of Physics D: Applied Physics* **2005**, *38*, R393-R413.

(151) VanLandingham, M. R.; Villarrubia, J. S.; Guthrie, W. F.; Meyers, G. F. *Macromolecular Symposia* **2001**, *167*, 15-43.

(152) Nix, W. D. *Materials Science & Engineering, A: Structural Materials: Properties, Microstructure and Processing* **1997**, *A234-236*, 37-44.

(153) Chowdhury, S.; Laugier, M. T.; Rahman, I. Z.; Serantoni, M. *Surface and Coatings Technology* **2004**, *177-178*, 537-544.

(154) Pharr, G. M. *Materials Science & Engineering, A: Structural Materials: Properties, Microstructure and Processing* **1998**, *A253*, 151-159.

(155) Saha, R.; Nix, W. D. *Materials Science & Engineering, A: Structural Materials: Properties, Microstructure and Processing* **2001**, *A319-321*, 898-901.

(156) Bhushan, B. In *Handbook of Micro/Nano Tribology,* 2nd ed.; Bhushan, B., Ed.; CRC Press LLC: Boca Raton, FL, 1999, pp 433-524.

(157) Bhushan, B. *Wear* **2005**, *259*, 1507-1531.

(158) Bhushan, B.; Li, X. *International Materials Reviews* **2003**, *48*, 125-164.

(159) Fischer-Cripps, A. C. *Nanoindentation*, 2nd ed.; Springer: New York, 2004.

(160) Fischer-Cripps, A. C. *Surface and Coatings Technology* **2006**, *200*, 4153-4165.

(161) Lin, D. C.; Horkay, F. *Soft Matter* **2008**, *4*, 669-682.

(162) Mammeri, F.; Le Bourhis, E.; Rozes, L.; Sanchez, C. *Journal of Materials Chemistry* **2005**, *15*, 3787-3811.

(163) Mann, A. B. In *Springer Handbook of Nanotechnology,* 2nd ed., 2007, pp 1137-1166.

(164) Matzke, H. *Key Engineering Materials* **1991**, *56-57*, 365-392.

(165) Zeng, K. In *Handbook of Theoretical and Computational Nanotechnology*; Rieth, M., Schommers, W., Eds.; American Scientific Publishers: Stevenson Ranch, CA, 2006; Vol. 4, pp 387-461.

(166) Mann, A. B. In *Surfaces and Interfaces for Biomaterials*; Vadgama, P., Ed.; CRC Press: Boca Raton, FL, 2005, pp 225-247.

(167) Schuh, C. A. *Materials Today* **2006**, *9*, 32-40.

(168) Tan, E. P. S.; Lim, C. T. *Composites Science and Technology* **2006**, *66*, 1102-1111.

(169) VanLandingham, M. R.; Villarrubia, J. S.; Meyers, G. F. *Polymer Preprints* **2000**, *41*, 1412-1413.

(170) Etienne-Calas, S.; Duri, A.; Etienne, P. *Journal of Non-crystalline Solids* **2004**, *344*, 60-65.

(171) Lee, T.-H.; Kang, E.-S.; Bae, B.-S. *Journal of Sol-Gel Science and Technology* **2003**, *27*, 23-29.

(172) Spirkova, M.; Slouf, M.; Blahova, O.; Farkacova, T.; Benesova, J. *Journal of Applied Polymer Science* **2006**, *102*, 5763-5774.

(173) Ballarre, J.; Lopez, D. A.; Cavalieri, A. L. *Thin Solid Films* **2008**, *516*, 1082-1087.

(174) Johnson, K. L. *Contact mechanics*; Cambridge University Press: New York, 1985.

(175) Chang, S.-Y.; Lee, Y.-S.; Chang, T.-K. *Materials Science & Engineering, A* **2006**, *A423*, 52-56.

(176) Chang, S.-Y.; Chang, T.-K.; Lee, Y.-S. *Journal of the Electrochemical Society* **2005**, *152*, C657-C663.

(177) McGuiggan, P. M.; Wallace, J. S.; Smith, D. T.; Sridhar, I.; Zheng, Z. W.; Johnson, K. L. *Journal of Physics D* **2007**, *40*, 5984-5994.

(178) Johnson, K. L. *Wear* **1995**, *190*, 162-170.

(179) Montagne, A.; Tromas, C.; Audurier, V.; Woirgard, J. *Journal of Materials Research* **2009**, *24*, 883-889.

(180) Kouloumbi, N.; Tsangaris, G. M.; Skordos, A.; Kyvelidis, S. *Progress in Organic Coatings* **1996**, *28*, 117-124.

(181) De Araujo, F. F. T.; Rosenberg, H. M. *Journal of Physics D: Applied Physics* **1976**, *9*, 1025-1030.

(182) Aharoni, S. M. *Journal of Applied Physics* **1972**, *43*, 2463-2465.

(183) Bhattacharyya, S. K.; De, S. K.; Basu, S. *Polymer Engineering and Science* **1979**, *19*, 533-539.

(184) Malliaris, A.; Turner, D. T. *Journal of Applied Physics* **1971**, *42*, 614-618.

(185) Miane, J. L.; Achour, M. E.; Carmona, F. *Physica Status Solidi A: Applied Research* **1984**, *81*, K71-K76.

(186) Gurland, J. In *Powder metallurgy in the nuclear age;* Metallwerk Plansee AG & Co.: Reutte/Tyrol, Austria, 1962; Vol. 1962, pp 507-518.

(187) Zhang, S.; Han, K.; Cheng, L. *Surface and Coatings Technology* **2008**, *202*, 2807-2812.

(188) Liu, X.; Huang, Y.; Deng, C.; Wang, X.; Tong, W.; Liu, Y.; Huang, J.; Yang, Q.; Liao, X.; Li, G. *Polymer Engineering & Science* **2009**, *49*, 1375-1382.

(189) O'Connell, P. A.; Hutcheson, S. A.; McKenna, G. B. *Journal of Polymer Science, Part B: Polymer Physics* **2008**, *46*, 1952-1965.

(190) Guedes, R. M. *Composites Science and Technology* **2007**, *67*, 2574-2583.

(191) Shen, L.; Wang, L.; Liu, T.; He, C. *Macromolecular Materials and Engineering* **2006**, *291*, 1358-1366.

(192) Lee, L. S. *Durability of Composites for Civil Structural Applications* **2007**, 150-169.

(193) Scott, D. W.; Lai, J. S.; Zureick, A. H. *Journal of Reinforced Plastics and Composites* **1995**, *14*, 588-617.

(194) Payne, A. R. *Progress in High Polymers* **1968**, *2*, 1-93.

(195) Akay, G. *Polymer Engineering and Science* **1975**, *15*, 811-816.

(196) Falahatgar, S. R.; Salehi, M.; Aghdam, M. M. *Journal of Reinforced Plastics and Composites* **2009**, *28*, 1793-1811.

(197) Shaito, A.; Fairbrother, D.; Sterling, J.; D'Souza, N. A. *Annual Technical Conference - Society of Plastics Engineers* **2008**, *66th*, 728-732.

(198) Beake, B. D.; Bell, G. A.; Brostow, W.; Chonkaew, W. *Polymer International* **2007**, *56*, 773-778.

(199) Atanacio, A. J.; Latella, B. A.; Barbe, C. J.; Swain, M. V. *Surface and Coatings Technology* **2005**, *192*, 354-364.

(200) Koukal, J.; Sondel, M.; Schwarz, D.; Foldyna, V. *Welding in the World* **2008**, *52*, 81-85.

(201) Lukas, P. *NATO Science Series, Series E* **2000**, *367*, 67-81.

(202) Rodriguez, P.; Mannan, S. L.; Mathew, M. D. *Metals, Materials and Processes* **1999**, *11*, 271-288.

(203) Tai, Q.; Mocellin, A. *Ceramics International* **1999**, *25*, 395-408.

(204) Davis, L. C. *NIST Special Publication* **1996**, *910*, 51-58.

(205) Agari, Y.; Uno, T. *Journal of Applied Polymer Science* **1985**, *30*, 2225-2235.

(206) Clingerman, M. L.; King, J. A.; Schulz, K. H.; Meyers, J. D. *Journal of Applied Polymer Science* **2002**, *83*, 1341-1356.

(207) King, J. A.; Keith, J. M.; Smith, R. C.; Morrison, F. A. *Polymer Composites* **2007**, *28*, 168-174.

(208) McNally, T.; Boyd, P.; McClory, C.; Bien, D.; Moore, I.; Millar, B.; Davidson, J.; Carroll, T. *Journal of Applied Polymer Science* **2008**, *107*, 2015-2021.

(209) Saleem, A.; Frormann, L.; Iqbal, A. *Polymer Composites* **2007**, *28*, 785-796.

(210) Guo, H.; Rasheed, A.; Minus, M. L.; Kumar, S. *Journal of Materials Science* **2008**, *43*, 4363-4369.

(211) Li, Y.; Shimizu, H. *Macromolecules* **2008**, *41*, 5339-5344.

(212) Yue, H.; Huang, X.; Yang, Y. *Materials Letters* **2008**, *62*, 3388-3390.

(213) Bal, S. *Journal of Scientific & Industrial Research* **2007**, *66*, 752-756.

(214) Bigg, D. M. *Polymer Engineering and Science* **1977**, *17*, 842-847.

(215) Bueche, F. *Journal of Applied Physics* **1972**, *43*, 4837-4838.

(216) Zhang, B.; Fu, R.; Zhang, M.; Dong, X.; Wang, L.; Pittman, C. U. *Materials Research Bulletin* **2006**, *41*, 553-562.

(217) Strzelec, K.; Pospiech, P. *Progress in Organic Coatings* **2008**, *63*, 133-138.

(218) Yeager, J.; Hrusch-tupta, M. A., Eds. *Low Level Measurements: Precison DC Current, Voltage and Resistance Measurements*, 5th ed.; Keithley Instruments, Inc.: Cleveland, OH, 1998.

(219) Demircan, O.; Xu, C.; Zondlo, J.; Finklea, H. O. *Journal of Power Sources* **2009**, *194*, 214-219.

(220) Dzakula, R.; Savic, S.; Stojanovic, G. *Processing and Application of Ceramics* **2008**, *2*, 33-37.

(221) Lai, F.; Lin, L.; Gai, R.; Lin, Y.; Huang, Z. *Thin Solid Films* **2007**, *515*, 7387-7392.

(222) Din, M.; Gould, R. D. *Applied Surface Science* **2006**, *252*, 5508-5511.

(223) Takahashi, M.; Muramatsu, Y.; Watanabe, M.; Wakita, K.; Miyuki, T.; Ikeda, S. *Journal of the Electrochemical Society* **2002**, *149*, C311-C316.

(224) Woltgens, H. W.; Friedrich, I.; Njoroge, W. K.; Theiss, W.; Wuttig, M. *Thin Solid Films* **2001**, *388*, 237-244.

(225) Masuda, H.; Fujino, T.; Sato, N.; Yamada, K. *Materials Research Bulletin* **1999**, *34*, 1291-1300.

(226) Wentworth, S. M. *Characterization of Materials* **2003**, *1*, 401-411.

(227) Katsumata, M.; Endo, M.; Yamanashi, H.; Ushijima, H. *Journal of Materials Research* **1994**, *9*, 1829-1833.

(228) Bar, H.; Narkis, M.; Boiteux, G. *Polymer Composites* **2005**, *26*, 12-19.

(229) Yui, H.; Wu, G.; Sano, H.; Sumita, M.; Kino, K. *Polymer* **2006**, *47*, 3599-3608.

(230) Strumpler, R.; Glatz-Reichenbach, J. *Journal of Electroceramics* **1999**, *3*, 329-346.

(231) Chekanov, Y.; Ohnogi, R.; Asai, S.; Sumita, M. *Journal of Materials Science* **1999**, *34*, 5589-5592.

CHAPTER 3

ELECTROCHEMICAL IMPEDANCE SPECTROSCOPY (EIS) OF VGCNF-REINFORCED ALKYD PAINT-COATED MILD STEEL SAMPLES IN 3% NaCl

3.1 Introduction

As mentioned in Chapter 1, several classical DC and AC electrochemical analysis methods are used to monitor and evaluate the corrosion protection abilities of polymer coatings on corrodible metals and their degradation during exposure to corrosive environments.[1, 2] These methods include potentiodynamic polarization measurements,[3, 4] chronopotentiometry,[5, 6] chronoamperometry,[5, 6] cyclic voltammetry,[7, 8] and EIS.[9-13]

Among all of these methods, EIS is the most predominant and least perturbing technique. In addition, DC methods are not preferred for such studies due to the high resistance of the polymer coating.[14-19] In this regard, EIS has been extensively used to study polymer-coated metals in different natural as well as artificial corrosive environments to evaluate water uptake, predict the lifetime of corrosion protection, estimate corrosion rates, identify corrosion mechanisms, evaluate the effects of mechanical deformation on the behavior of the coating, compare the performance of different coatings, and develop equivalent circuit models for the performance of different coating/metal systems.[9, 12, 14, 15, 20-30]

As mentioned in Chapter 2, the unique properties of VGCNF motivated this research group to investigate the effect of incorporating the VGCNF into a commercial alkyd paint on the insulation (corrosion protection) properties of the coating materials when applied to the surface of mild steel panels. As shown in Chapter 2, the reinforcement of the alkyd paint with VGCNF improved both the electrical and mechanical properties of the paint matrix. However, for a complete investigation of the stability, service lifetime, and behavior of the coating film in corrosive media, some electrochemical measurements, such as EIS measurements, are required.

The work presented in this chapter focuses on the use of electrochemical techniques to study the effect of increasing the VGCNF loading and the coating thickness on the protective behavior of alkyd paint coatings on mild steel substrates in 3% NaCl solutions. The investigation included the use of the OCP, cyclic voltammetry (CV), and EIS electrochemical techniques. Based on the EIS measurements, different electrochemical parameters were calculated and correlated to the stability of coating films

3.2 Experimental

3.2.1 Chemicals and Reagents

Sodium chloride, potassium ferricyanide, and acetone were purchased from Fisher Scientific (Pittsburgh, PA). Hexaammineruthenium(III) chloride was purchased from Aldrich Chemicals (Milwaukee, WI). All chemicals used in this work were of reagent grade and were used as received from the manufacturer. All solutions were prepared as needed using 18 MΩ-cm ultra-pure water (Milli-Q, Millipore Corp., Bedford, MA).

All other materials, chemicals, reagents, and substrates used in the preparation of the paint coatings are as mentioned in Chapter 2.

3.2.2 Electrodes and Instrumentation

Square-shaped steel and PMMA coupons (~ 8 cm × 8 cm × 1.51 mm) were cut, cleaned, and coated with pure and VGCNF-reinforced alkyd paint films with different thicknesses and VGCNF wt % as mentioned in Chapter 2. The steel-coated coupons were used for the EIS measurements whereas the PMMA-coated coupons were used for cyclic voltammetry measurements.

An undivided, three-electrode electrochemical cell was obtained by gluing a cylindrical poly(vinyl chloride) (PVC) pipe (~ 4 cm in both diameter and height) to the surface of a coated mild steel coupon using a clear silicone sealant (80242 Clear Silicone Sealant, Loctite, Rocky Hill, CT). Then, the volume inside the PVC pipe was filled with the test solution (3% NaCl). The electrode area inside the PVC pipe was 7.1 cm^2. All measurements were done in air saturated stagnant solution. Unless otherwise stated, all potentials were measured and referred to a saturated calomel reference electrode (SCE = +241 mV vs. SHE). A 1 mm diameter Pt wire (Goodfellow, Cambridge Science Park, U.K.) served as the auxiliary electrode.

3.2.3 Coating Preparation and Thickness Measurements

VGCNF-reinforced alkyd paint-coated mild steel samples with different coating thicknesses and VGCNF wt % have been prepared using the spin coating method under

the same conditions as mentioned in Chapter 2. The thicknesses of the dry coatings were measured using the same methods mentioned in Chapter 2.

3.2.4 Cyclic Voltammetry (CV) Measurements

To study the cyclic voltammetric behavior of the VGCNF-incorporated paint coatings, the paint was spun deposited on insulating PMMA sheets (8 cm × 8 cm) to avoid the interference of the mild steel substrate in the measurements. The PMMA sheets were spin-coated using the same conditions used for coating the mild steel samples. The coated PMMA sheets were then allowed to dry at room temperature in a dust-free place for at least 7 d and then cut into strips (8 cm × 1 cm) to be used as the working electrode for the CV experiments. The cyclic voltammograms (CVs) were collected either in 2.0 mM $Ru(NH_3)_6Cl_3$ in 3% NaCl solution or in 2 mM $K_3Fe(CN)_6$ in 3% NaCl solution at 10 mV/s sweep rate. The CV measurements were conducted with an electrochemical interface (Model SI 1287, Solartron, Hampshire, UK) in a three-electrode cell. A saturated calomel electrode (SCE) and a Pt wire were used as reference and counter electrodes, respectively. To study the effect of immersion time on the voltammetric behavior of coatings, the CVs were collected at different immersion times in the $Ru(NH_3)_6Cl_3$-NaCl solution.

3.2.5 Electrochemical Impedance Spectroscopy (EIS) Measurements

The corrosion protection properties of the coated steel coupons were evaluated by EIS. The experimental setup for the EIS is shown in Figure 3.1. The measurements were performed at the open circuit potential (OCP) of the coated steel coupons with a three-

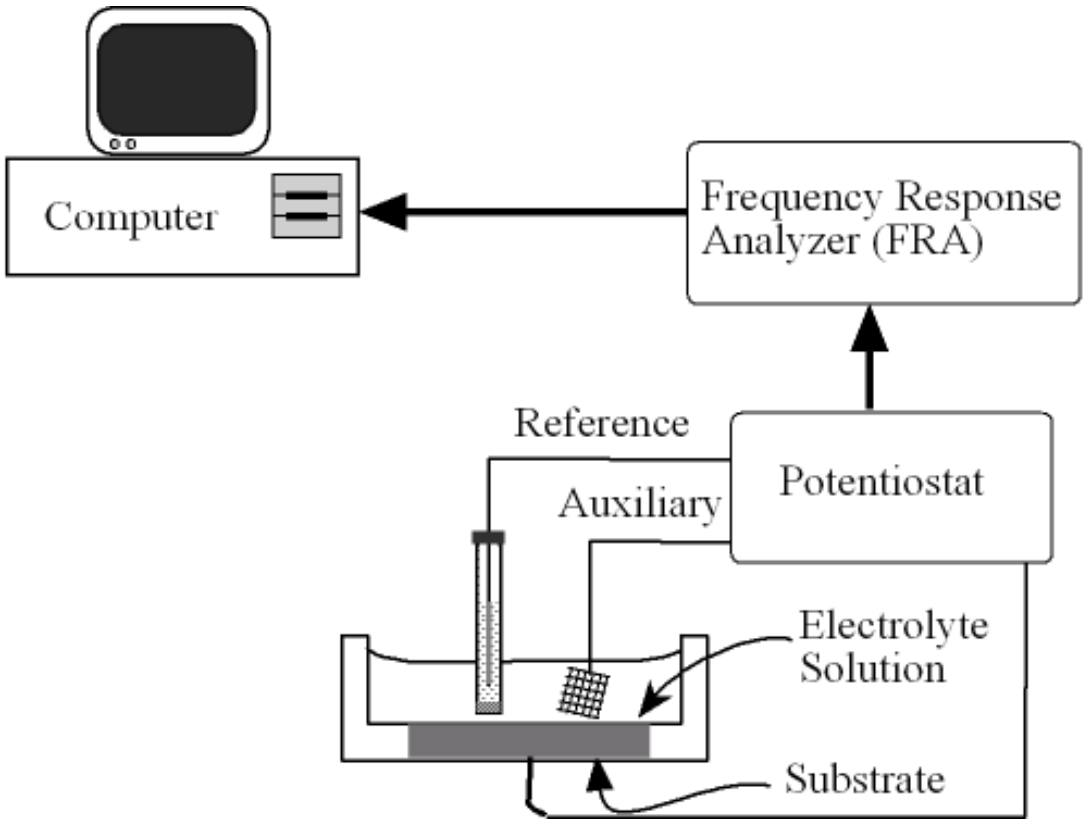

Figure 3.1 Schematic drawing of the EIS experimental setup.

electrode cell in which the steel sample is the working electrode, the platinum wire as the counter electrode, and the SCE as the reference electrode. The impedance spectra were recorded in the 0.01 Hz to 100 kHz frequency range using a frequency response analyzer (Model SI 1250, Solartron) connected to an electrochemical interface (Model SI 1287, Solartron). EIS measurements were performed using ZPlot impedance software (Scribner Associates Inc., Southern Pines, NC). The measurements were carried out using a sinusoidal AC voltage of 10 mV as the amplitude inside a Faraday cage in order to minimize external interferences. The impedance spectra were then analyzed in terms of equivalent electrical circuits and fitting models using ZView impedance software (Scribner Associates Inc.). All experiments were carried out at room temperature of (23 ± 2) °C in quiescent naturally aerated 3% (by weight) NaCl aqueous solutions, simulating the aggressive marine environment. The electrolyte solution was changed periodically with a freshly prepared solution. EIS measurements were conducted until significant changes in the impedance behavior or physical changes on the coating and/or the substrate surface were visually observed. Measurements up to 5 years (1880 d) of immersion were recorded for some samples.

3.3 Results and Discussions

The rate of corrosion of any coated material (e.g., metal, alloy, composite) depends on several factors including the coat nature, composition, and thickness; the activity of the bare material; and the composition and aggressiveness of the environment (solution composition), relative humidity, and temperature.[17, 31-33]

In this section, the results of the electrochemical measurements in 3% NaCl solutions are presented.

3.3.1 Cyclic Voltammetry (CV) Measurements

The CV measurements for the VGCNF/alkyd paint/PMMA electrodes containing different VGCNF loadings were performed in air-saturated $Ru(NH_3)_6Cl_3$-3% NaCl or $K_3Fe(CN)_6$-3% NaCl solutions at a scan rate of 10 mV/s. Voltammograms recorded for the pure paint coatings and paint coatings containing 0.5 or 1% VGCNF in these redox systems showed no measureable currents indicating redox inactivity.

Figure 3.2 shows the voltammograms for the reduction of $Ru(NH_3)_6Cl_3$ at the surface of alkyd paint samples loaded with 3, 5, and 10 wt % VGCNF, respectively. As depicted in the figure, a reduction peak centered at ~ 0.7-0.8 (vs. SCE) starts to appear, increases in size, and shifts to a more anodic potential as the VGCNF loading increases. Moreover, the shape of the CV for the paint coating containing 10% VGCNF indicates a more reversible process with both cathodic and anodic peaks centered at ~ -0.03 and -0.02 V, respectively.

As shown in Chapter 2, the electrical resistance of the VGCNF-reinforced coatings depend on the wt % of the VGCNF. The lower the VGCNF wt %, the higher the resistance of the coating film. When the coating is a part of an electrochemical cell, electrical resistance of the film is part of the Ohmic resistance, R_Ω, (also known as the solution resistance or uncompensated resistance). The main effect of R_Ω on an electrochemical experiment is that the potential imposed on an electrode/solution interface is less than that supplied by the potentiostat.[34, 35] In a CV experiment, the effects

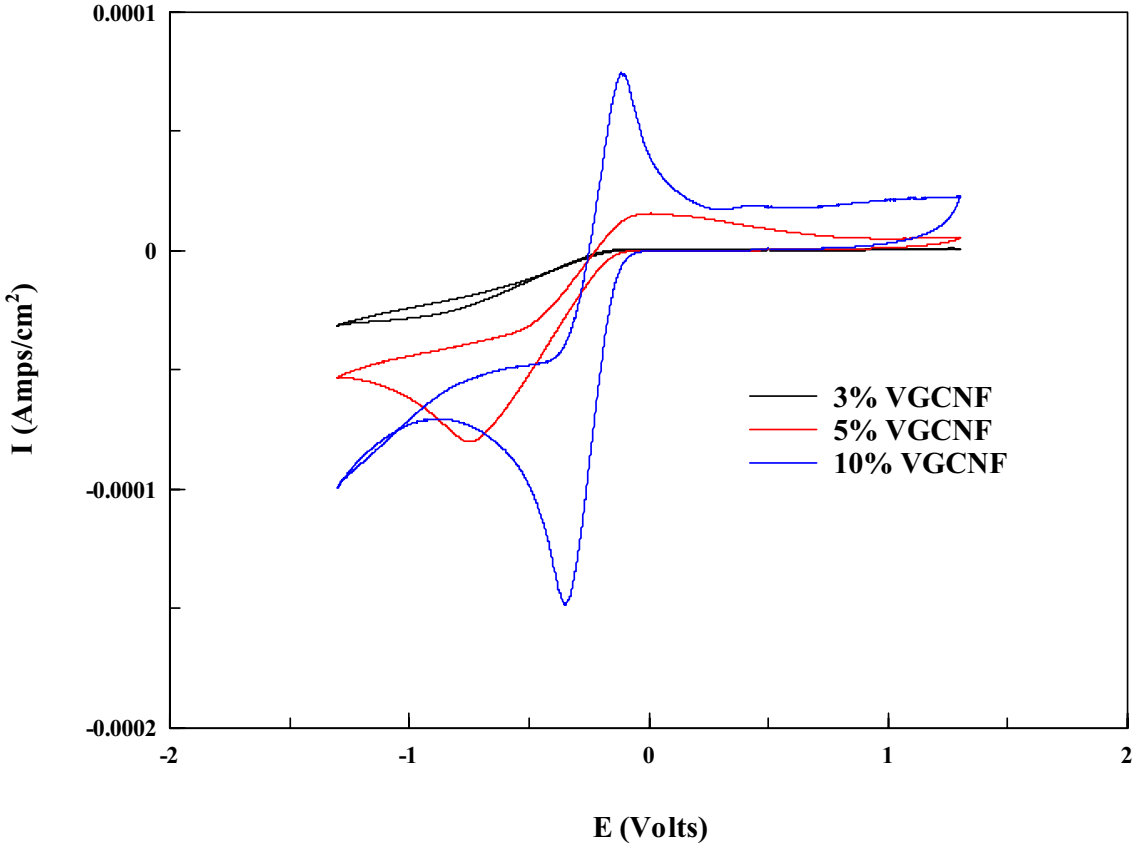

Figure 3.2 Cyclic voltammetry profiles, recorded at 10 mV/s, for VGCNF-incorporated alkyd paint films spun-coated on poly(methyl methacrylate) (PMMA) immersed in unstirred aerated 2 mM $Ru(NH_3)_6Cl_3$-3% NaCl solution.

of R_{Ω} on the shape of the CV of an electroactive film include (i) enlarged peak width, and (ii) increased peak-to-peak potential, thus suggesting a non-reversible behavior.[36-38]

The CV behavior of VGCNF-reinforced coatings shown in Figure 3.2 is mainly due to Ohmic potential drop in the coating film. The distortion in the shape of the voltammograms in Figure 3.2 is very common in the literature for conventional (normal size) electodes.[35, 39-42] As shown in Figure 3.2, the reverse peaks are small because it takes a long time to get back to the oxidation potential. In addition, this behavior could also be due to the VGCNFs in the film acting as an array of microelectrodes.

These results shown in Figure 3.2 are supported by following the effect of aging on the CV behavior of paint coatings containing 3, 5, and 10% VGCNF in $Ru(NH_3)_6Cl_3$ (Figure 3.3 through 3.5). As shown in Figure 3.3, for 3% VGCNF-loaded paint samples, for all immersion times, the shape of the CVs is the same with no reversible peaks. For paint coatings containing 5% VGCNF (Figure 3.4), as the immersion time increases, the peaks become less distinct and the peak currents (both anodic and cathodic) decrease. In addition, the cathodic peak potential gets slightly more negative. On the other hand, for paint coatings containing 10% (Figure 3.5), the voltammograms approach the shape of a CV for a reversible system.[43-49] As shown in Figure 3.5, the behavior of the 10% VGCNF-loaded paint matrix is similar to that of the 5% VGCNF-loaded paint sample. However, it is clear in Figure 3.4 that the cathodic and anodic peaks are well distinct and none of them diminishes with time.

Figure 3.6 shows the CVs for the reduction of $K_3Fe(CN)_6$ in 3% NaCl at the surface of VGCNF-incorporated alkyd paint spun-coated on PMMA substrates. The results indicate that paint samples containing less than 10% VGCNF show

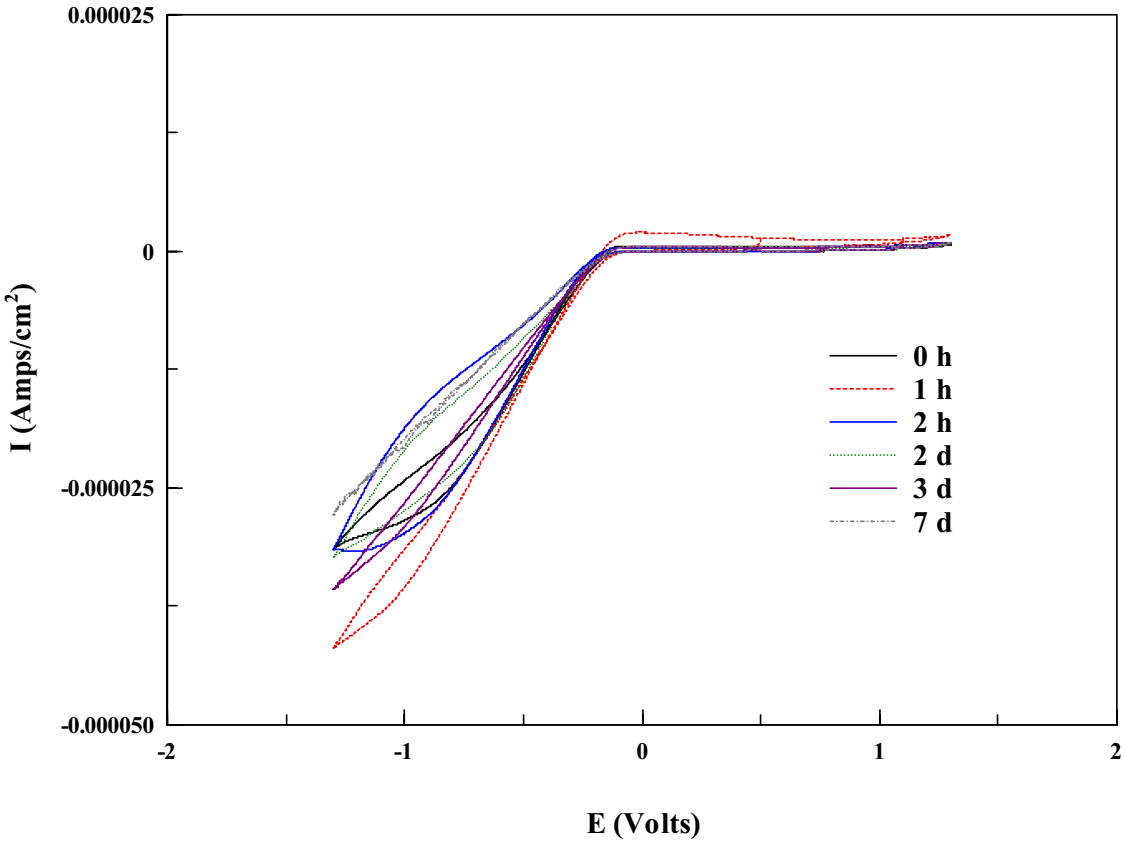

Figure 3.3 Effect of immersion time on the cyclic voltammetry behavior of 3 wt % VGCNF-incorporated alkyd paint films spun-coated on poly(methyl methacrylate) immersed in unstirred aerated 2 mM $Ru(NH_3)_6Cl_3$-3% NaCl solution. Scan rate is 10 mV/s.

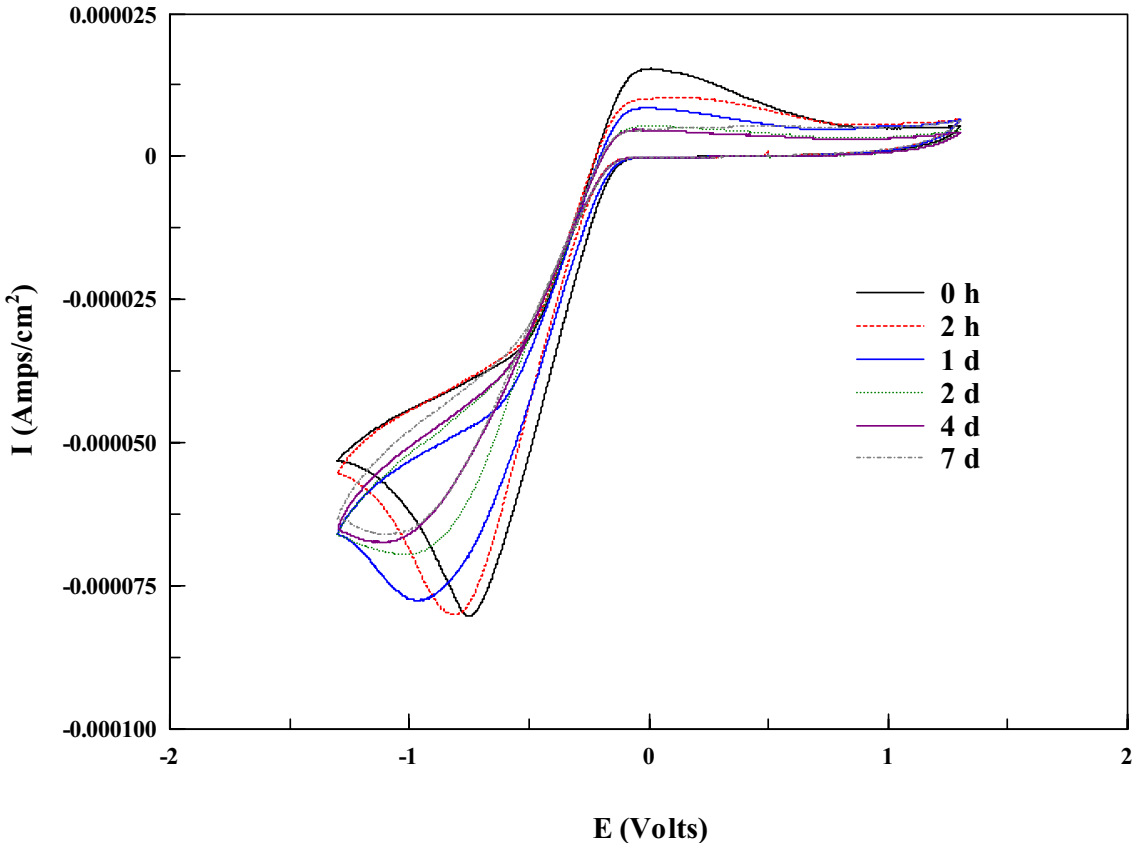

Figure 3.4 Effect of immersion time on the cyclic voltammetry behavior of 5 wt % VGCNF-incorporated alkyd paint films spun-coated on poly(methyl methacrylate) (PMMA) immersed in unstirred aerated 2 mM $Ru(NH_3)_6Cl_3$-3% NaCl solution. Scan rate is 10 mV/s.

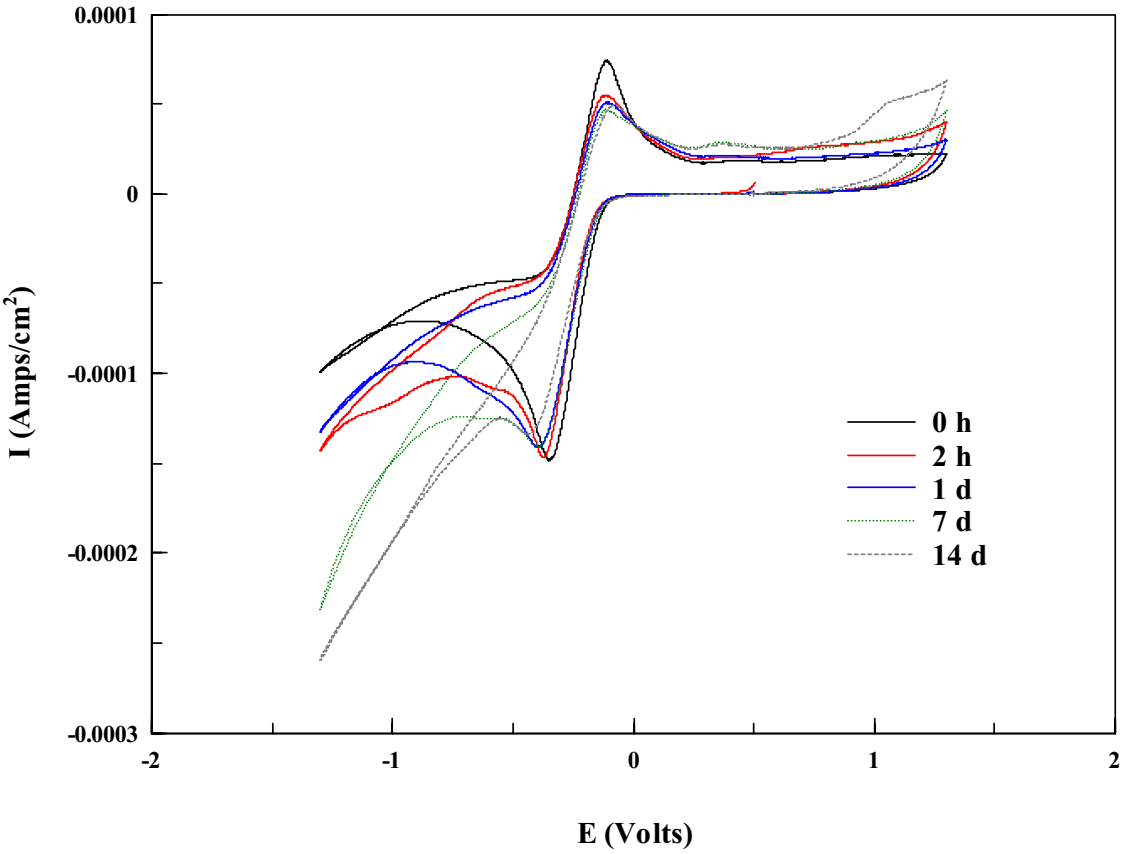

Figure 3.5 Effect of immersion time on the cyclic voltammetry behavior of 10 wt % VGCNF-incorporated alkyd paint films spun-coated on poly(methyl methacrylate) immersed in unstirred aerated 2 mM $Ru(NH_3)_6Cl_3$-3% NaCl solution. Scan rate is 10 mV/s.

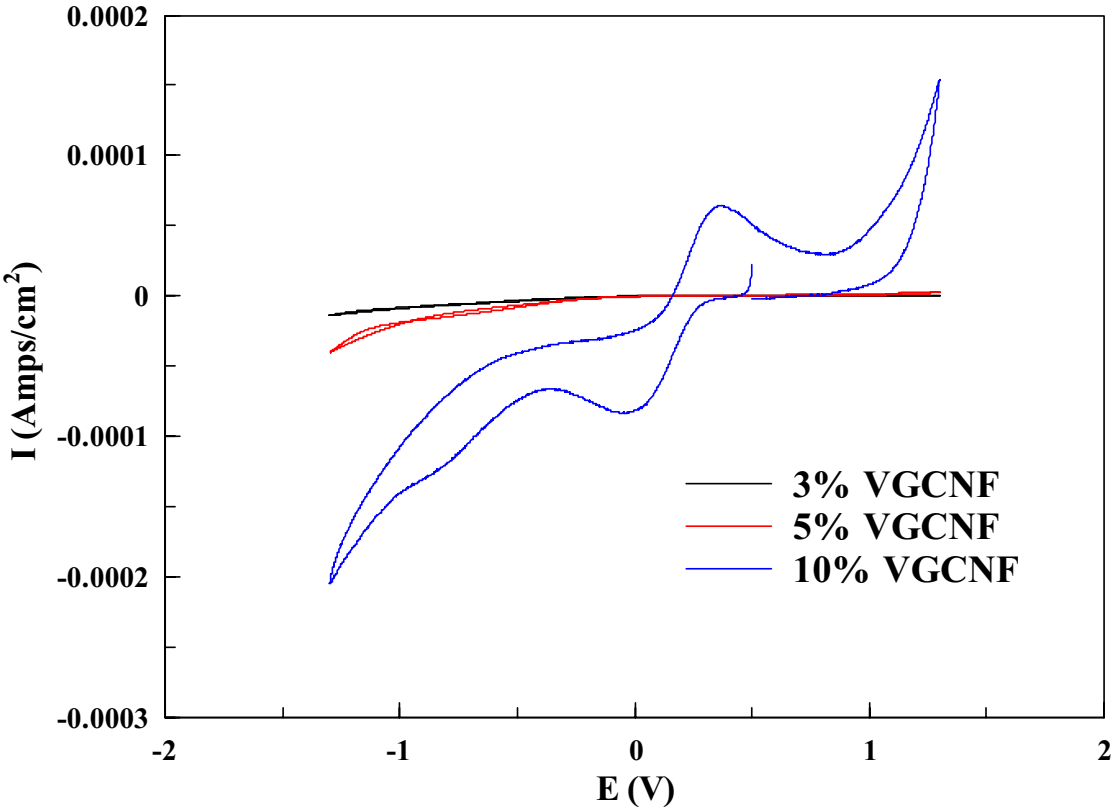

Figure 3.6 Cyclic voltammetry profiles, recorded at 10 mV/s, for VGCNF-incorporated alkyd paint films spun-coated on poly(methyl methacrylate) (PMMA) immersed in unstirred aerated 2 mM $K_3Fe(CN)_6$-3% NaCl solution.

voltammograms similar to those of irreversible electrodes with a small cathodic peak. However, for paint samples containing 10% VGCNF, the CV shows a behavior close to that of a quasi-reversible electrode with a cathodic and anodic peak centered at 0.0, and 0.4 V (vs. SCE), respectively. These results are consistent with the CV behavior of the same electrodes in $Ru(NH_3)_6Cl_3$ shown in Figure 3.2. Accordingly, all of the CV measurements indicate that the incorporation of the VGCNF in the paint matrix increases the conductivity of the matrix and as the wt % of the VGCNF increases, the conductivity of the paint film increases. The VGCNF/paint/PMMA electrode behaves as a quasi-reversible electrode system (peak separation > 59 mV).

3.3.2 Open Circuit Potential (OCP) Measurements

The OCP is the spontaneous potential assumed by any electrode immersed in an electrolyte. An OCP measurement is considered the simplest and cheapest electrochemical method to monitor the corrosion of metals and alloys in a corrosive electrolyte.[50] The OCP is a non-invasive test that involves following the change in the electrode potential vs. a reference electrode for a certain period of time. This test provides complementary information to the EIS results.

In this study, the OCP behavior of the coated mild steel panels was followed over a period of up to 5 years (1880 d) in naturally aerated 3% NaCl aqueous solutions. Because of the large number of samples studied, it is not convenient to reproduce graphs for the effect of the immersion time on the OCP for all of the measured samples. Instead, some typical examples for the variation of the OCP with immersion time at various VGCNF loadings and film thickness will be given.

As shown in Figures 3.7 through 3.12, for all of the given coating samples, the starting values of the OCP were positive values (about +0.3 to +0.2 V vs. SCE).[51] The steady-state potential (E_{ss}) of the bare mild steel in the same electrolyte solution is about -0.6 V (vs. SCE).[52] Accordingly, it is clear that the application of the coating, with or without VGCNF, shifts the initial OCP of the bare substrate to a more positive value indicating the protective characters of the coatings. As shown in the figures, as the immersion time increased, the OCP of the coated substrates shifted toward more negative values before it reached the E_{ss} value of the bare steel alloy. The decrease in the OCP with time indicates that the chloride ions from the electrolyte penetrate through the coating pores causing a continuous degradation of the film coating. E_{ss} is reached when the coating film completely degrades and the corrosion of the bare substrate occurs.

Figures 3.7 through 3.9 show the variation of the OCP with time for mild steel coupons coated with different thicknesses of paint containing 0, 1, and 5 wt % VGCNF, respectively. On the other hand, Figures 3.10 through 3.12 show the variation of the OCP with immersion time for coating samples having the same thickness (30, 40, and 50 μm) but with different wt % (0, 1, 5, and 10%) of the VGCNF.

The results show that the worst OCP behavior was observed for the pure paint coatings with a thickness of 30 μm (Figure 3.7) where E_{ss} was achieved in a very short period of time (~ 25 d) indicating that the electrolyte easily penetrated the coating film and hence caused rapid damage of the coating film. The results also show that the thicker the coating the longer the time needed to achieve the E_{ss} (see Figures 3.7 through 3.9) Moreover, the incorporation of the VGCNF into the paint matrix extends the time needed to achieve the E_{ss} value and hence improves the corrosion protection properties of the

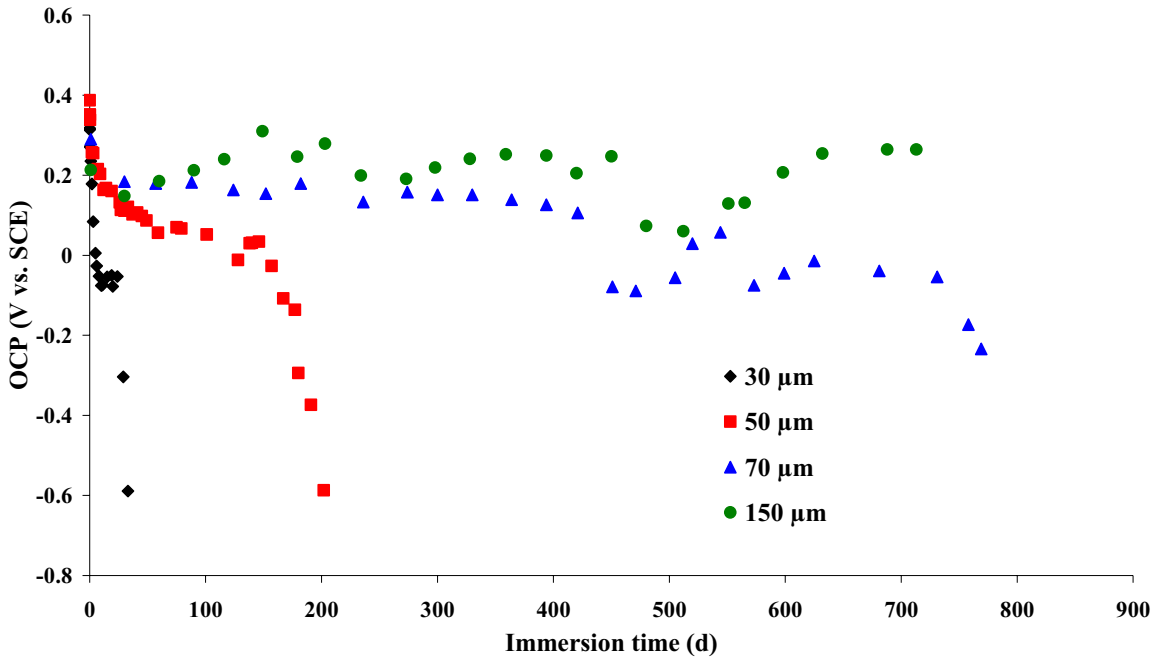

Figure 3.7 Long term OCP-immersion time curves for mild steel panels coated with pure commercial alkyd paint in 3% NaCl solution. ◆ = 30 µm, ■ = 50 µm, ▲ = 70 µm, and ● = 150 µm.

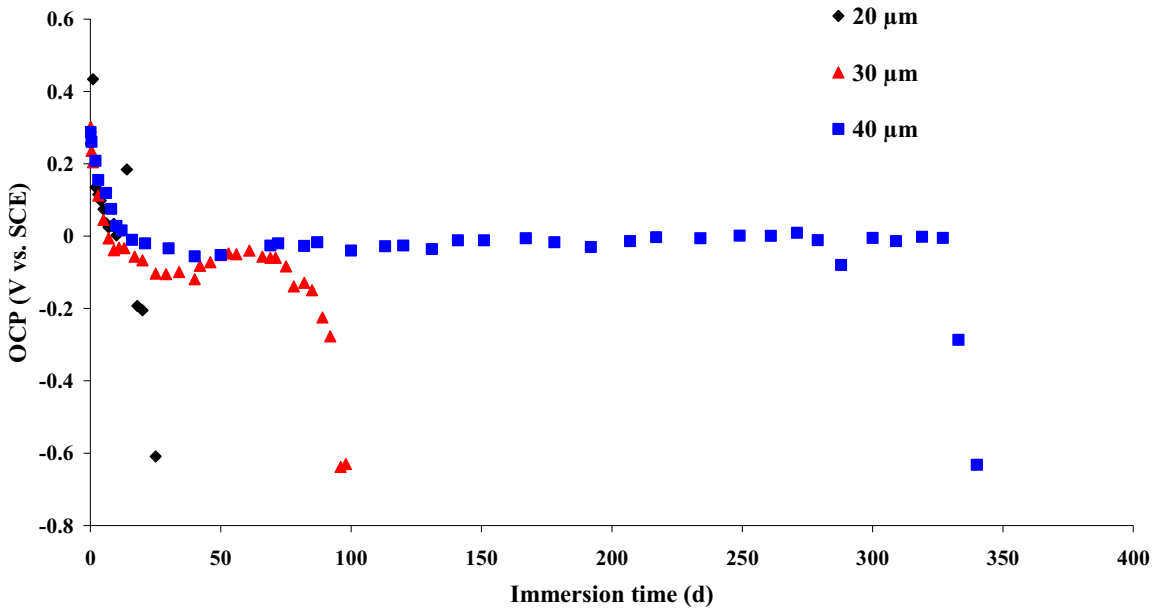

Figure 3.8 Long term OCP-immersion time curves for mild steel panels coated with a commercial alkyd paint film containing 1 wt % VGCNF in 3% NaCl solution. ◆ = 20 µm, ▲ = 30 µm, and ■ = 40 µm.

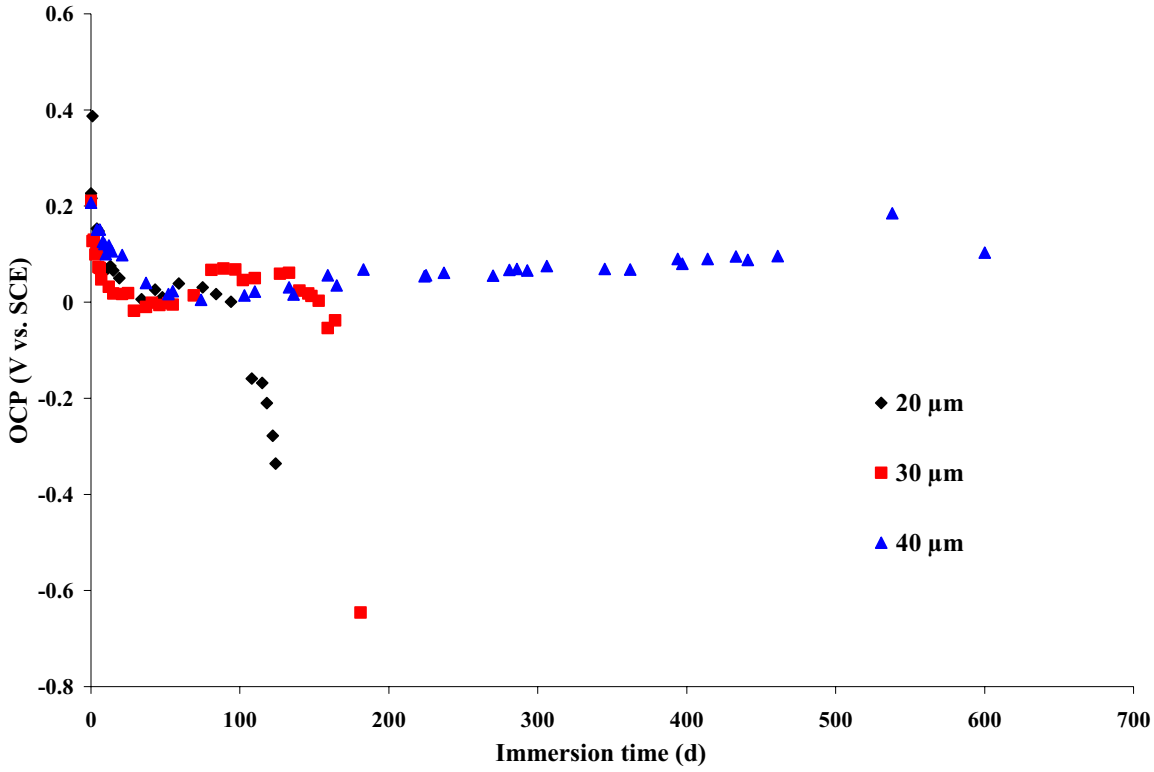

Figure 3.9 Long term OCP-immersion time curves for mild steel panels coated with a commercial alkyd paint film containing 5 wt % VGCNF in 3% NaCl solution. ◆ = 20 µm, ■ = 30 µm, and ▲ = 40 µm.

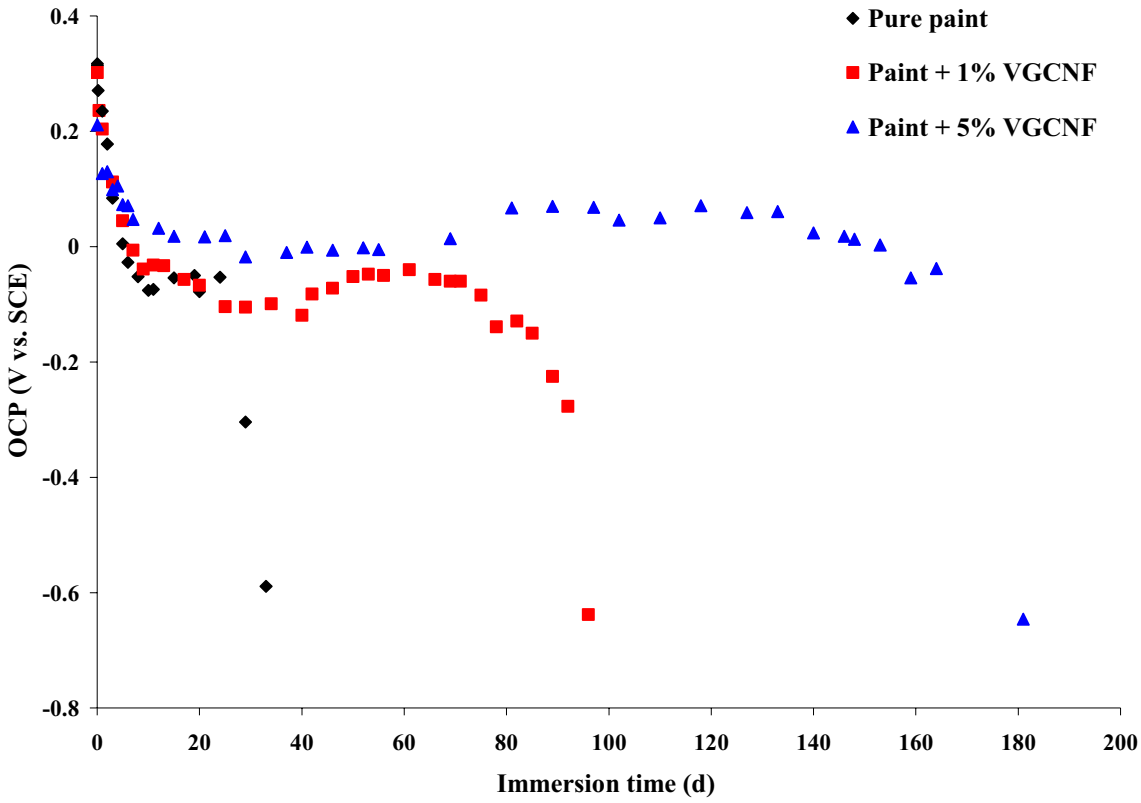

Figure 3.10 Long term OCP-immersion time curves for mild steel panels coated with a commercial alkyd paint film (30 μm in thickness) with different VGCNF content (wt % loading) in 3% NaCl solution. ◆ = pure paint, ■ = paint + 1% VGCNF, and ▲ = paint + 5% VGCNF.

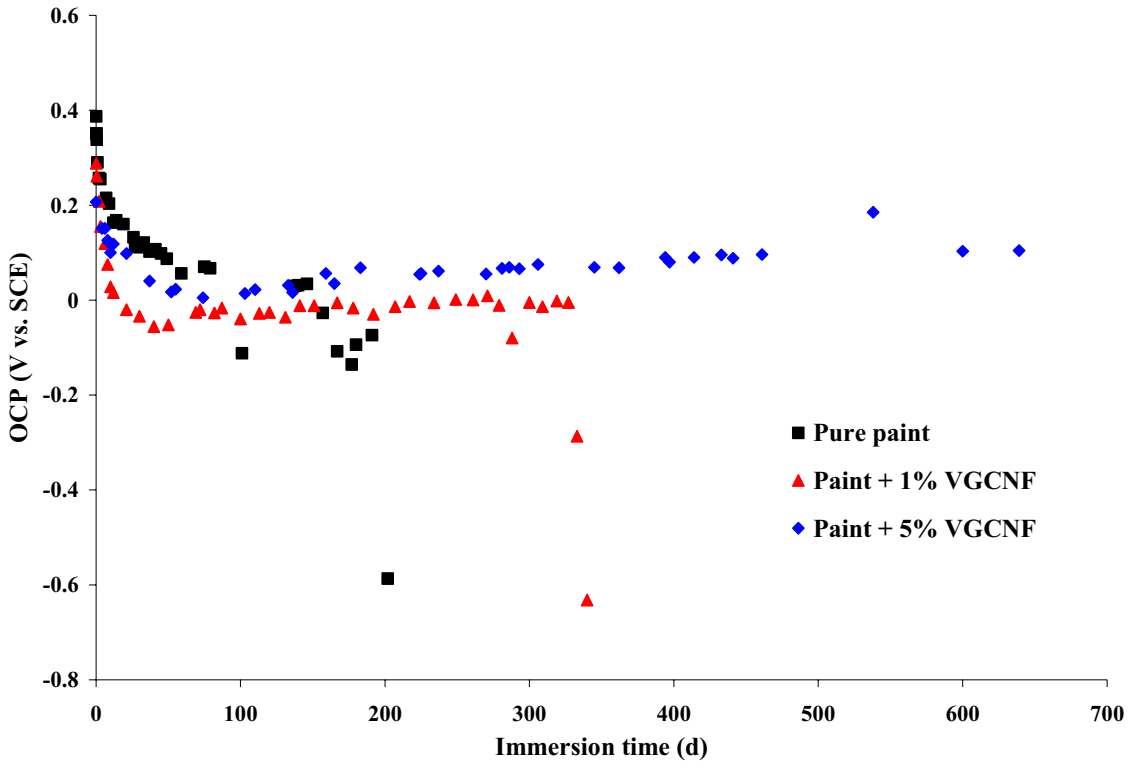

Figure 3.11 Long term OCP-immersion time curves for mild steel panels coated with a commercial alkyd paint film (40 μm in thickness) with different VGCNF content (wt % loading) in 3% NaCl solution. ■ = pure paint, ▲ = paint + 1% VGCNF, and ◆ = paint + 5% VGCNF.

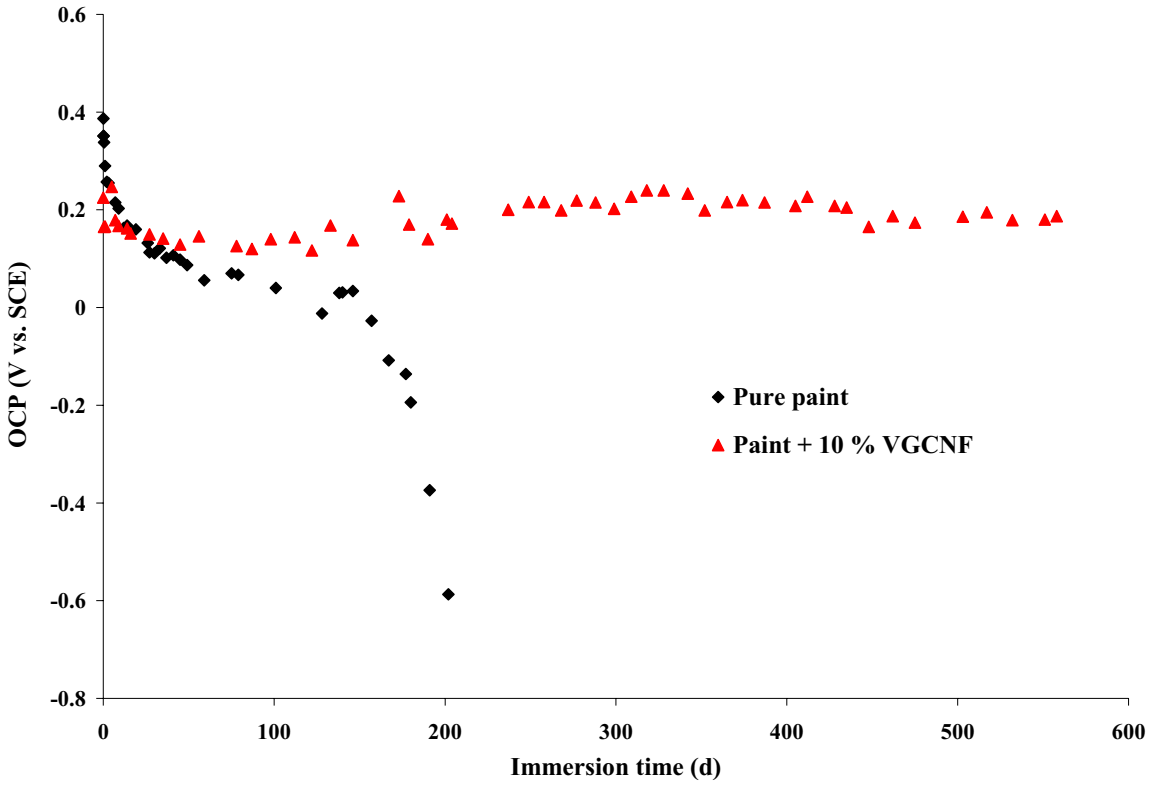

Figure 3.12 Long term OCP-immersion time curves for mild steel panels coated with a commercial alkyd paint film (50 μm thick) in 3% NaCl solution. The wt % of VGCNF is marked in the figure legend. ◆ = pure paint, and ▲ = paint + 10% VGCNF.

pure coating. In addition, Figures 3.10 through 3.12 also show that the higher the wt % of the VGCNF, the longer the time needed to reach E_{ss} and hence the better the corrosion protection offered by the coating film. Furthermore, the data depicted in Figures 3.10 and 3.12 show that the best behavior was associated with the paint coatings having 10% VGCNF where the OCP was the highest (~ +200 mV vs. SCE) among all of the coating samples assayed. Moreover, Figure 3.12 depicts that after almost 600 d (~ 20 months), the OCP of steel panels coated with a 50 μm thick coating containing 10% VGCNF was still almost +200 mV.

Table 3.1 and Figure 3.13 show the time to coating failure or end of testing (in d) based on the OCP measurements and visual observations for some of the studied coatings with different thicknesses and VGCNF loadings. It should be mentioned that, all coating films that showed no failure at the end of testing had variable OCP values that were more positive than the E_{ss} value. Moreover, among these coatings, the very thick ones and the ones with the higher VGCNF wt % showed the most positive OCP values at the end of testing. Based on the results depicted in Figures 3.7 through 3.13 and Table 3.1, it can be concluded that the 50 μm thick paint coating containing 10% VGCNF is the most passive and hence the slowest to reach E_{ss}.

3.3.3 Electrochemical Impedance Spectroscopy (EIS) Measurements

As mentioned in Chapter 1, the main role of the EIS in the electrochemical characterization of organic coatings is to collect information about the coating system and its barrier properties and also determine the onset and progression of the corrosion processes on the metal substrate underneath the coating.[53] In the current investigation, the

Table 3.1 Time to coating failure or end of testing based on open circuit potential (OCP) measurements for pure and VGCNF-reinforced alkyd paint coatings with different thicknesses and VGCNF loadings.

Coating Specification	Film Thickness (μm)	Time to Coating Failure or End of Testing (d)
Pure paint	30	33
	50	202
	70	1814*
	150	1882*
Paint + 0.5 % VGCNF	95	1751*
	150	1848*
	180	1804*
Paint + 1% VGCNF	20	25
	30	98
	40	340
Paint + 5% VGCNF	20	124
	30	181
	40	842*
Paint + 10% VGCNF	50	1734*

*Testing ended with no failure.

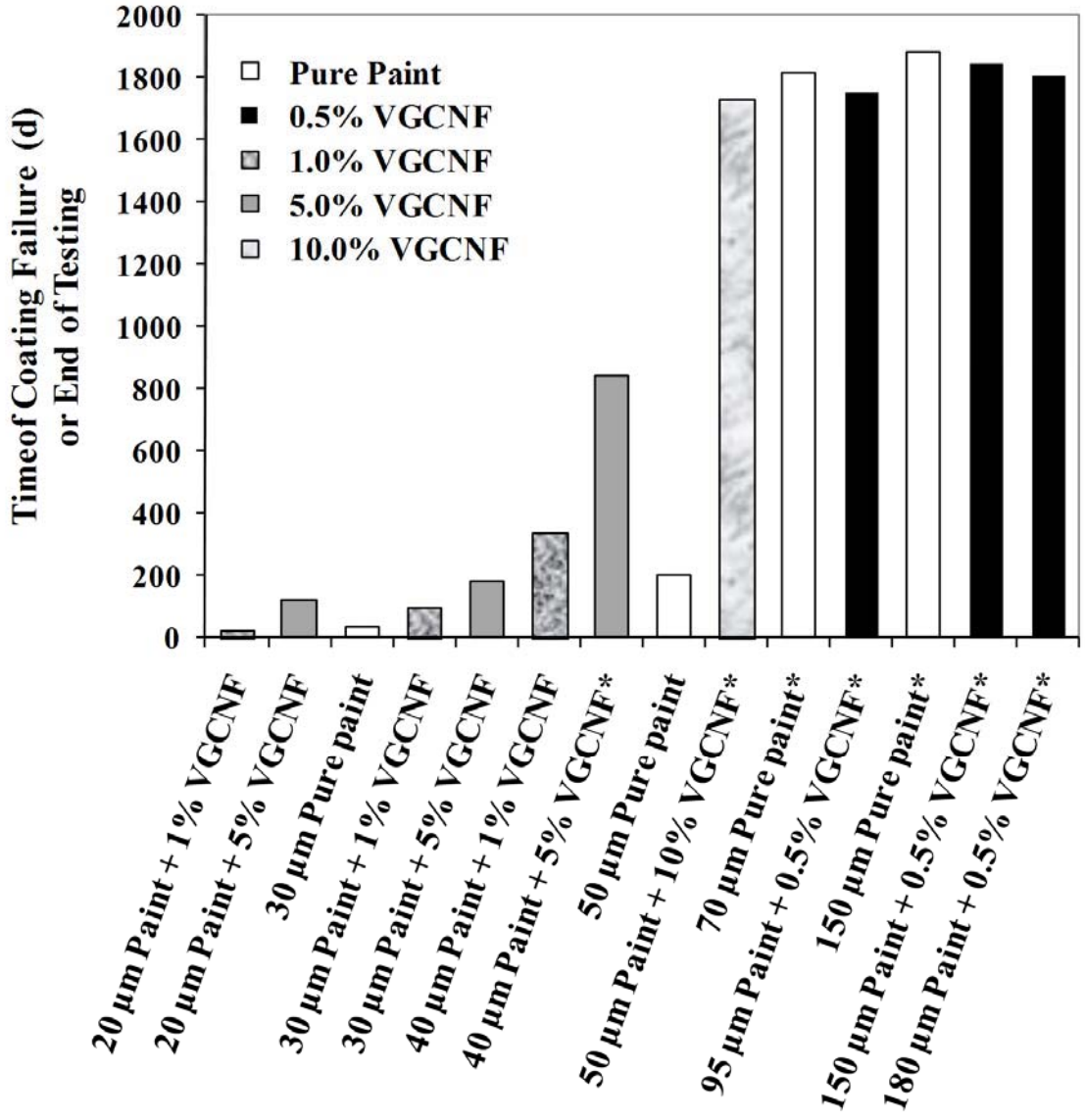

Figure 3.13 Time to coating failure or end of testing based on open circuit potential (OCP) measurements for pure and VGCNF-reinforced alkyd paint coatings with different thicknesses and VGCNF loadings. *Testing ended with no failure.

EIS behavior of the alkyd paint-coated mild steel coupons, with and without VGCNF, was followed by recording the Bode and Nyquist plots in 3% NaCl aqueous solution for an exposure period of up to 27 months. To avoid any significant changes in the possible equilibria established at the coating/electrolyte solution interface, the EIS spectra were recorded at the OCP of the substrates. The experimental EIS spectra shown in these figures were modeled to theoretical equivalent electrical circuits using the ZView software.

Figure 3.14 shows the general equivalent circuit proposed for the breakdown of the corrosion protection provided by a polymer coating applied to the surface of a metallic substrate.[54] Depending on the characteristics of the metal and/or the coating, few changes have been reported for the general circuit shown in Figure 3.14.[55-60] Kendig and Mansfeld have used the model shown in Figure 3.14 to analyze impedance spectra obtained for steel and Al alloys coated with polybutadiene.[12, 54, 61, 62]

Corrosion of substrates under coatings usually takes place in stages.[33] The shapes of the Bode and Nyquist plots for a polymer-coated metal or alloy depend on the state of the paint coating.[57, 63-65] At the early stage of exposure of the polymer coating to a corrosive solution, the polymer film is in good contact with the substrate surface and protects the surface from being attacked by the aggressive ions. Accordingly, the impedance spectra only characterize the insulating properties of the coating. Thus, the coating resistance (R_c) is extremely high while the coating capacitance (C_c) is very low. At this stage, perfectly protective and intact coatings show a straight line with a slope of -1 in the Bode plot and a capacitive arc in the Nyquist plot (Figure 3.15.a) indicating that the coating has excellent barrier properties and behaves as a pure capacitor.

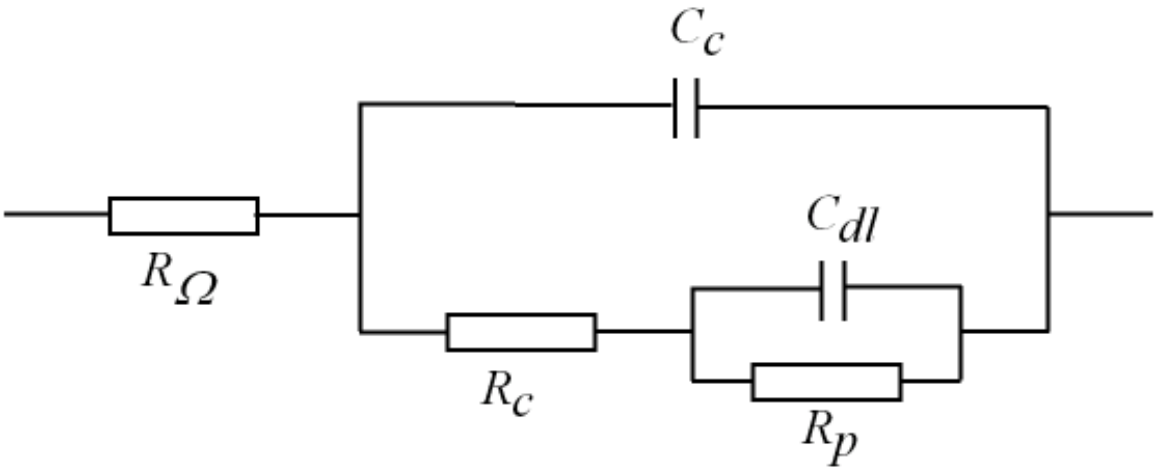

Figure 3.14 Schematic drawing for the general equivalent electrical circuit for a polymer-coated metal. R = Ohmic (solution) resistance; C_{dl} = the electrode double layer capacitance; C_c = coating capacitance; R_c = coating pore resistance; and R_p = polarization (charge transfer) resistance.

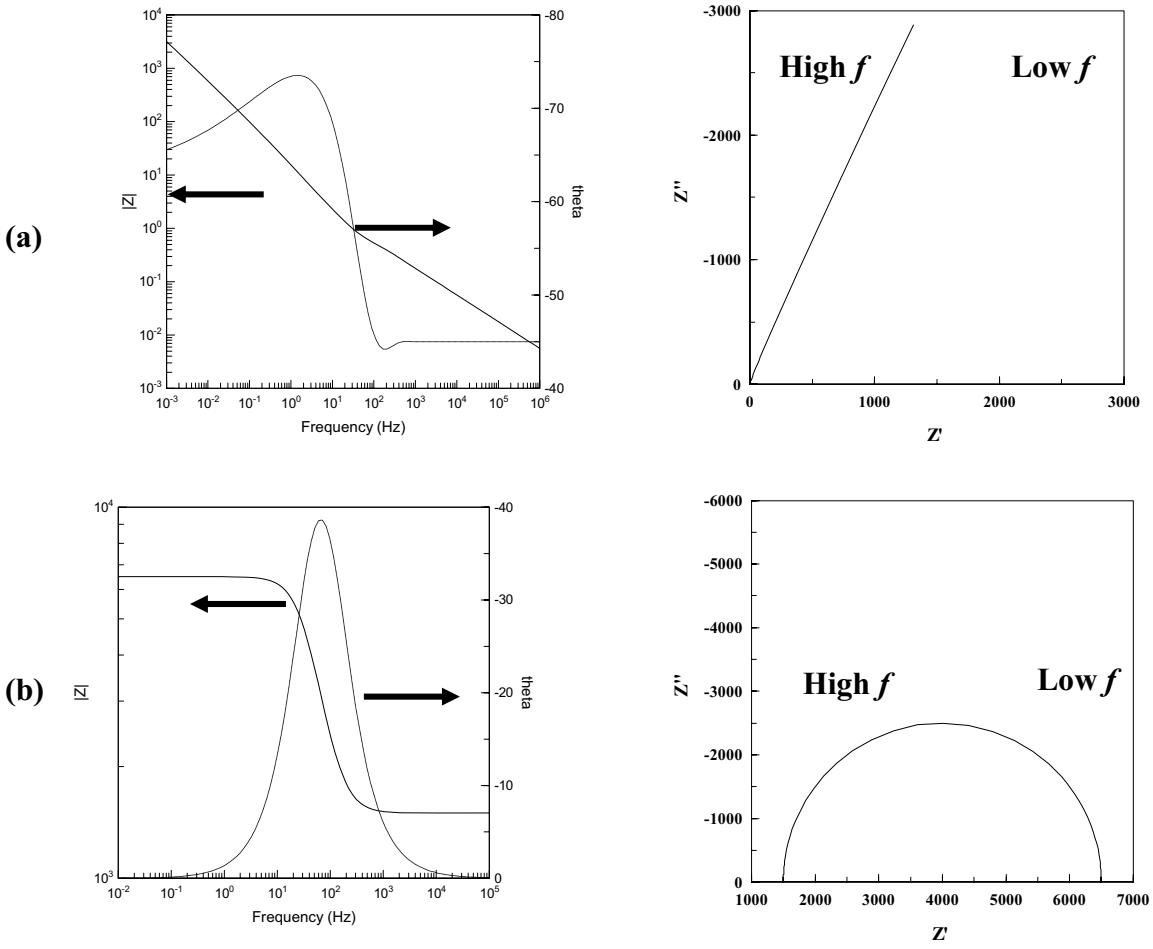

Figure 3.15 Different Bode and Nyquist plots for a paint-coated metal at different states of degradation. (a) An intact undamaged coating with absorbed water, (b) a coating that is developing a low coating resistance, (c) a coating that has suffered major damage, and a (d) a damage coating with a diffusion-controlled degradation process.

(c)

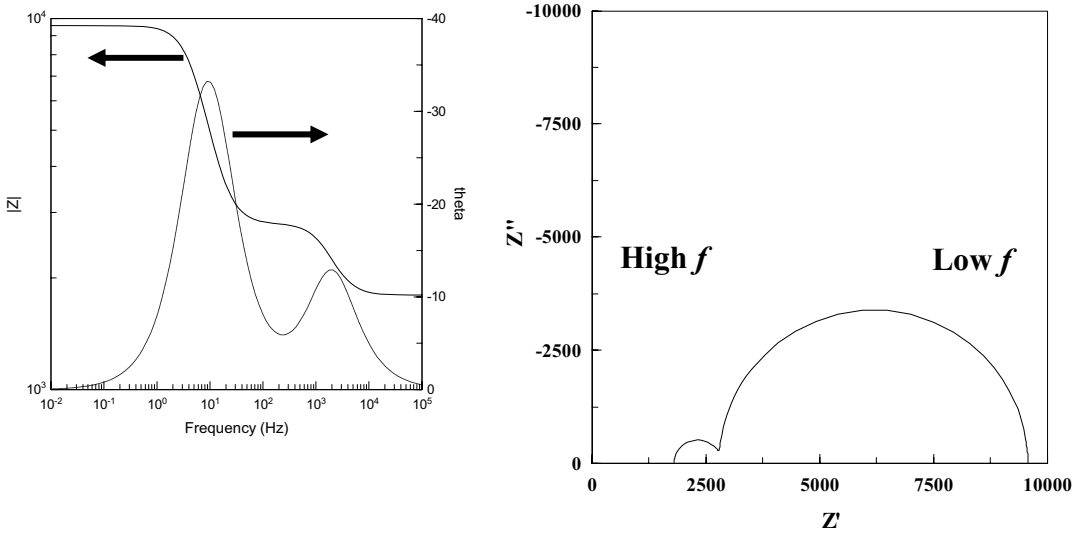

(d)

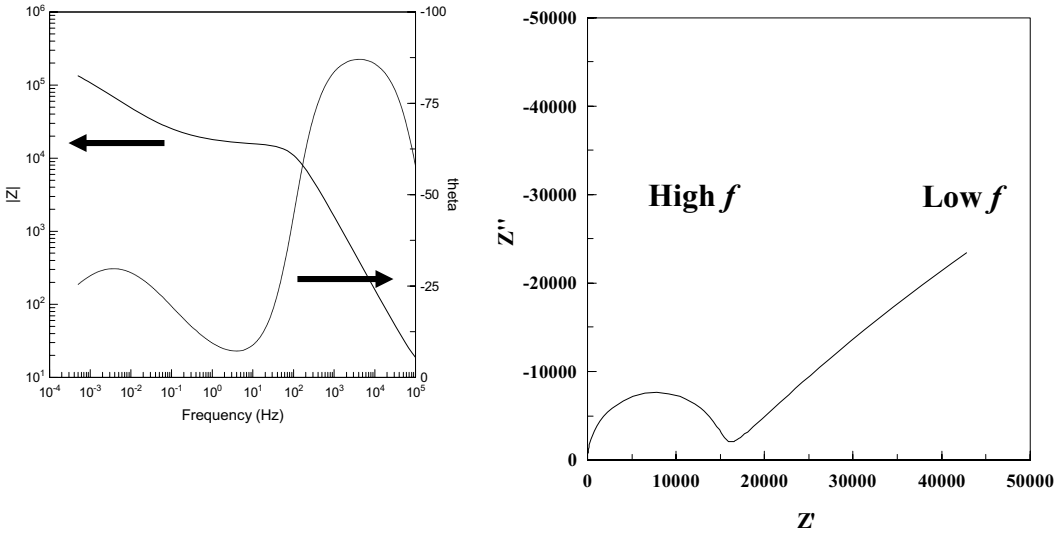

Figure 3.15 Continued.

As the immersion time increases, water and other electrolytes diffuse through the coating and the impedance from the Bode plot decreases due to the water and electrolyte absorption and creation of electrolytic paths to the metal surface. In that case, R_c is much lower than its value when the coating was initially immersed in the electrolyte. The coating resistance results in a frequency-independent plateau at low frequencies in the Bode plot. On the other hand, the arc in the Nyquist plot becomes a semi-circle (Figure 3.15.b). The x-intercept at high frequency (to the left) is the uncompensated resistance (R_Ω) and the x-intercept at low frequencies is the sum of the uncompensated and polarization resistances ($R_\Omega + R_p$). At this stage, there is no significant corrosion of the metal substrate.

At a later stage of exposure to the electrolyte, the electrolyte reaches the metal/paint interface and a larger area of the metal substrate is exposed to the electrolyte and corrosion is initiated at the substrate surface. As the exposed substrate area increases, the polarization resistance (R_p) decreases and double layer capacitance (C_{dl}) increases. In this case, faradaic processes occur and the Bode plot becomes more complex and shows two breaks or two "time constants". The Nyquist plot displays two semi-circles corresponding to the two time constants.(Figure 3.15.c) The smaller semi-circle at high frequency (to the left) is due to the coating capacitance while the bigger semi-circle at lower frequency (to the right) is due to the double layer capacitance. For some coatings, as the exposure time increases, the degradation process becomes diffusion-controlled. The Nyquist plot shows a semi-circle in the higher frequency region with a straight line angled at 45º to the real axis in the lower frequency region (Figure 3.15.d). The straight line in the Nyquist plot is an indicator of a diffusion-controlled process.

At a very late stage of exposure to the electrolyte, the coating is severely damaged and most of the metal substrate is exposed to the electrolyte and the measured impedance is dominated by the general corrosion of the substrate. The shape of the Bode plot looks like the one shown in Figures 3.15.c and 3.15.d but with much lower total $|Z|$ values at the low frequencies. The value of $|Z|$ measured in this stage could be 5-6 orders of magnitude less than the value recorded at the initial immersion time. In this final stage of coating damage, the two semi-circles in the Nyquist plot are more defined than earlier in the degradation process.

As shown above, the EIS spectra for organic coatings applied to the surface of metallic substrates are usually characterized by two frequency domains (i.e. two parts or time constants). The high-frequency (HF) domain corresponds to the organic coating while the low-frequency (LF) one is related to the reactions occurring at the metal substrate surface due to the diffusion of the electrolyte through the pores and defects in the coating.[63, 66] The resistance values extracted from the HF part (either in the Bode or Nyquist plots) correspond to the corrosion resistance of the organic coating. Accordingly, those resistance values have been used to follow the degradation of different organic coatings applied to metals with time in corrosive media.[67-69]

Representative impedance spectra (both Bode and Nyquist plots) obtained for mild steel samples covered with alkyd paint coatings with and without VGCNF are shown in Figures 3.16 through 3.27. Figures 3.16.a through 3.20 present the Bode plots obtained for mild steel samples coated with pure alkyd paint. Examining these plots shows that longer immersion times produce smaller $|Z|$ values (e.g., Figures 3.16.a and 3.17.a). In addition, the thinner the coating, the higher the rate of the drop in the

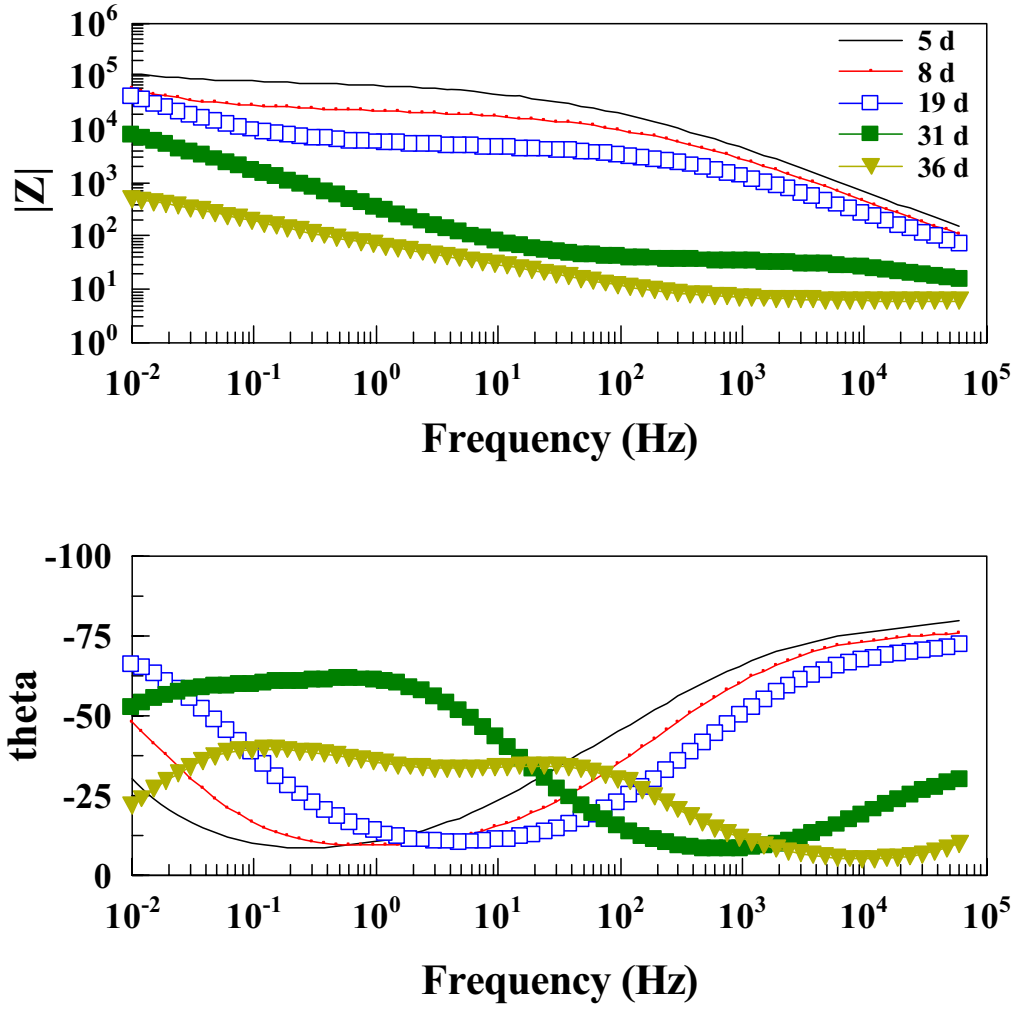

(a)

Figure 3.16 Bode (a) and Nyquist (b) plots for mild steel panels coated with a pure commercial alkyd paint film (30 μm thick) at different immersion times in 3% NaCl solution.

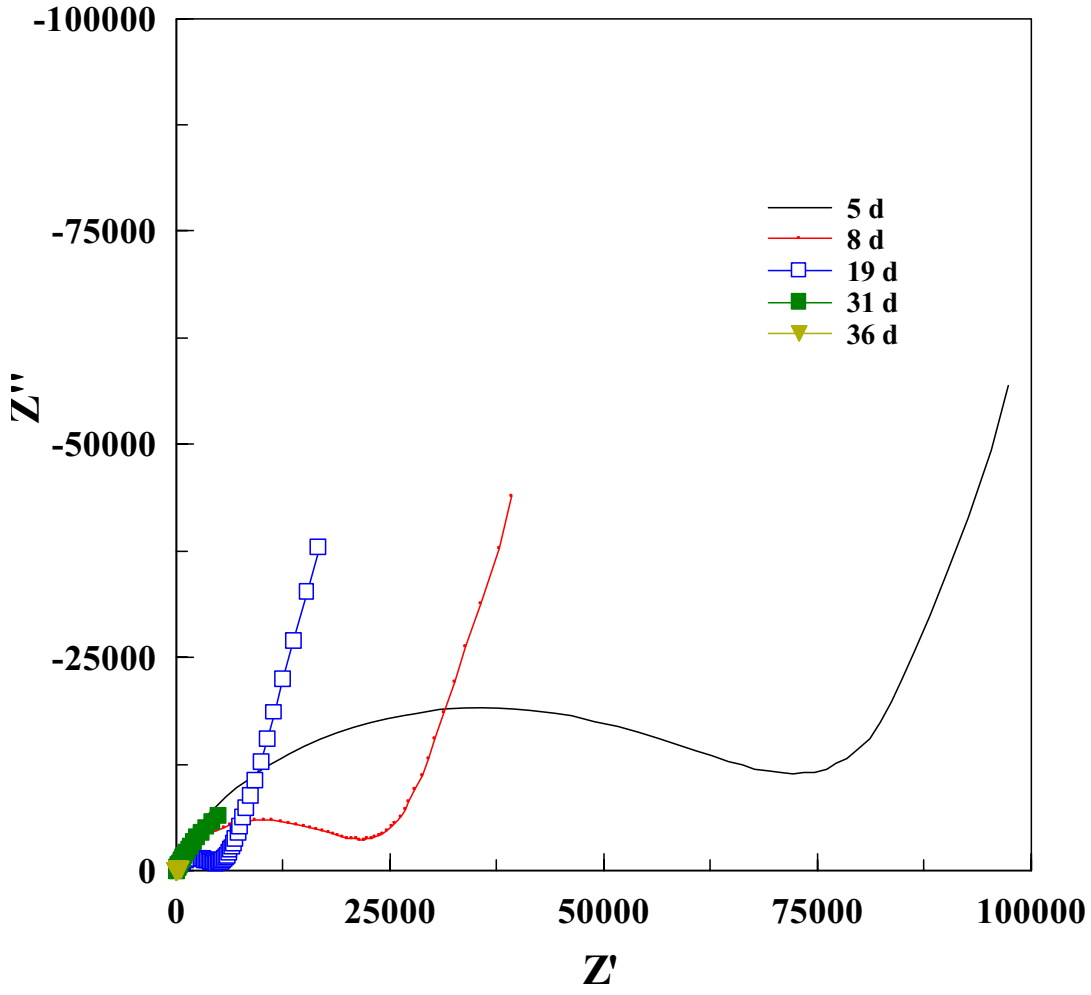

(b)

Figure 3.16 Continued.

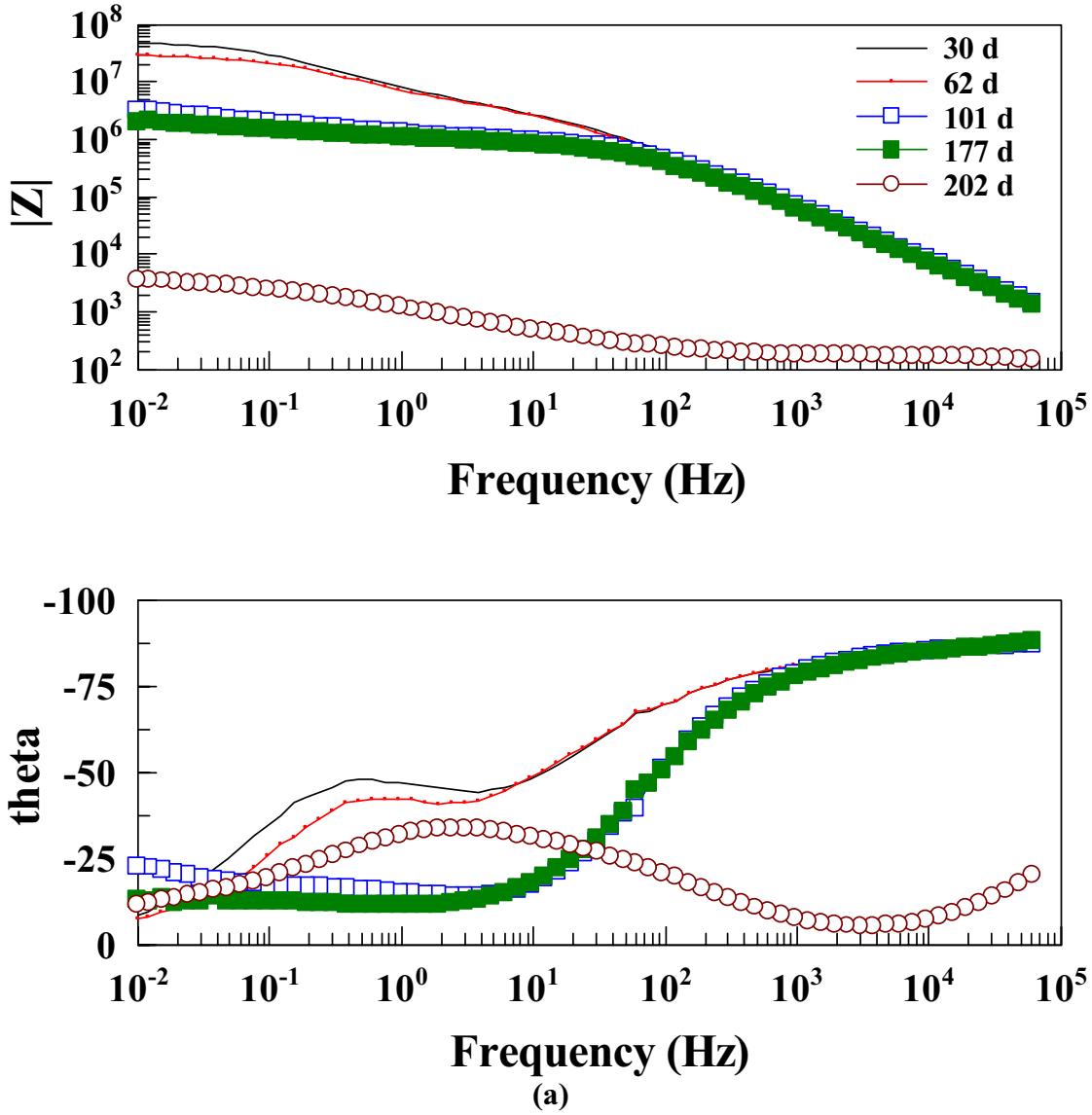

Figure 3.17 Bode (a) and Nyquist (b) plots for mild steel panels coated with a pure commercial alkyd paint film (40-50 μm thick) at different immersion times in 3% NaCl solution.

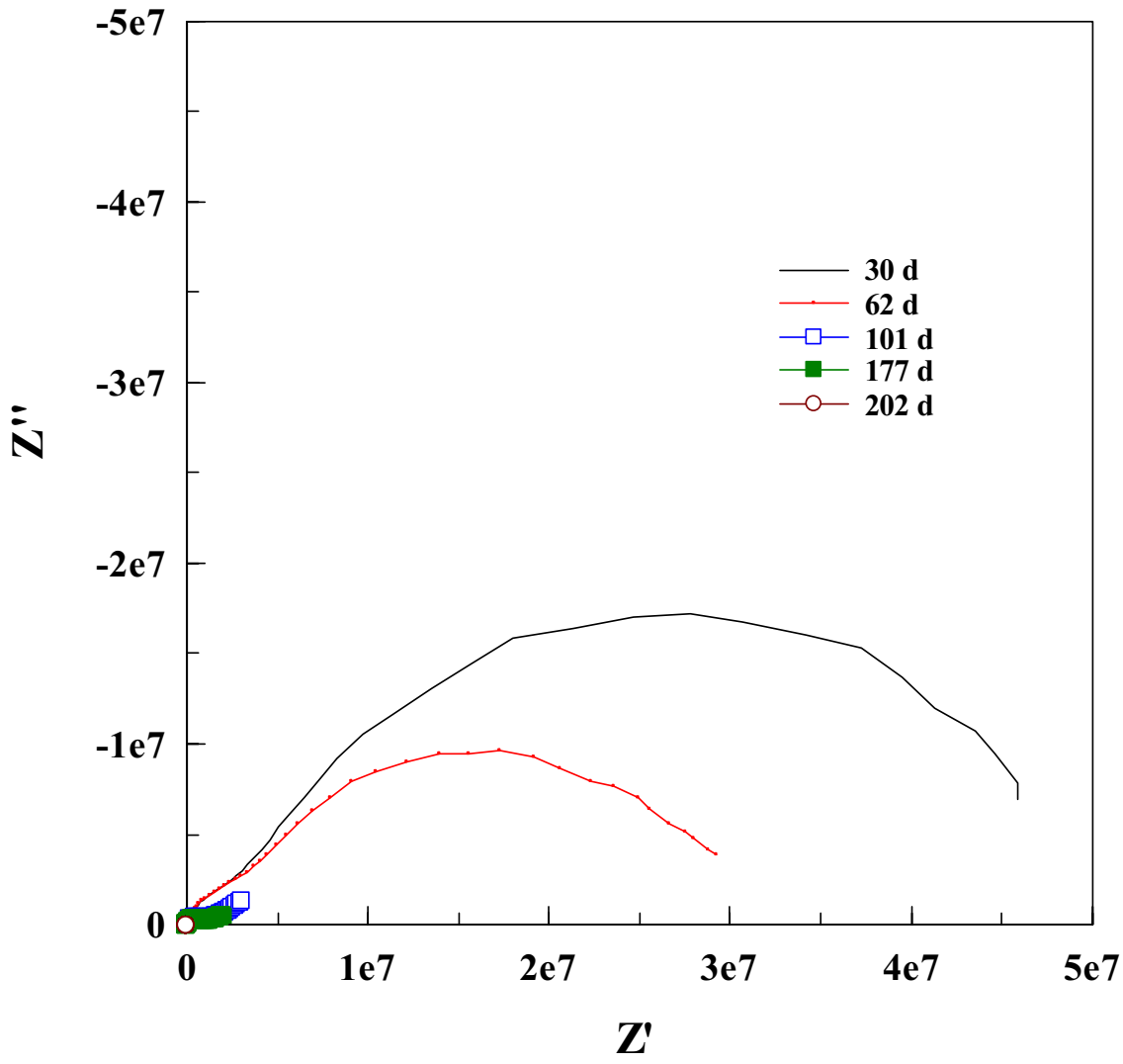

(b)

Figure 3.17 Continued.

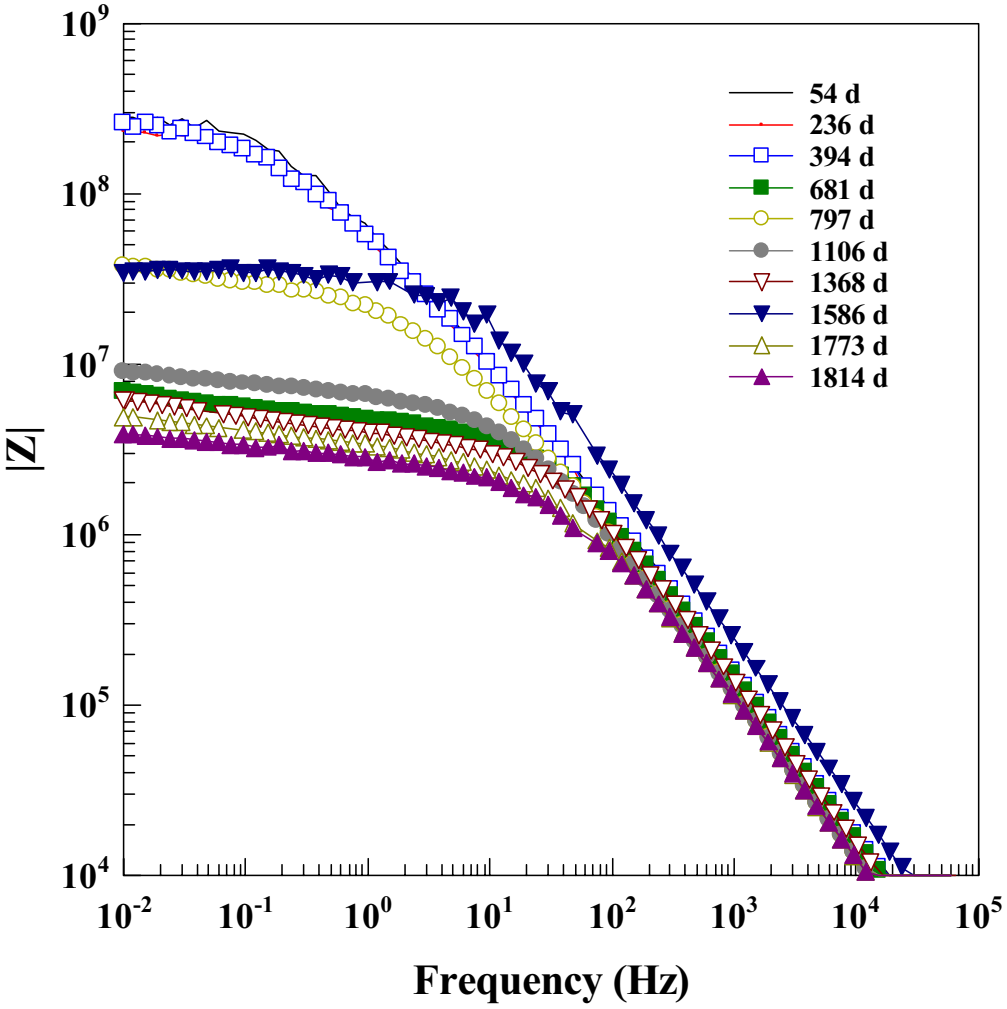

Figure 3.18 Bode plots for mild steel panels coated with pure commercial alkyd paint film (70 μm thick) at different immersion times in 3% NaCl solution.

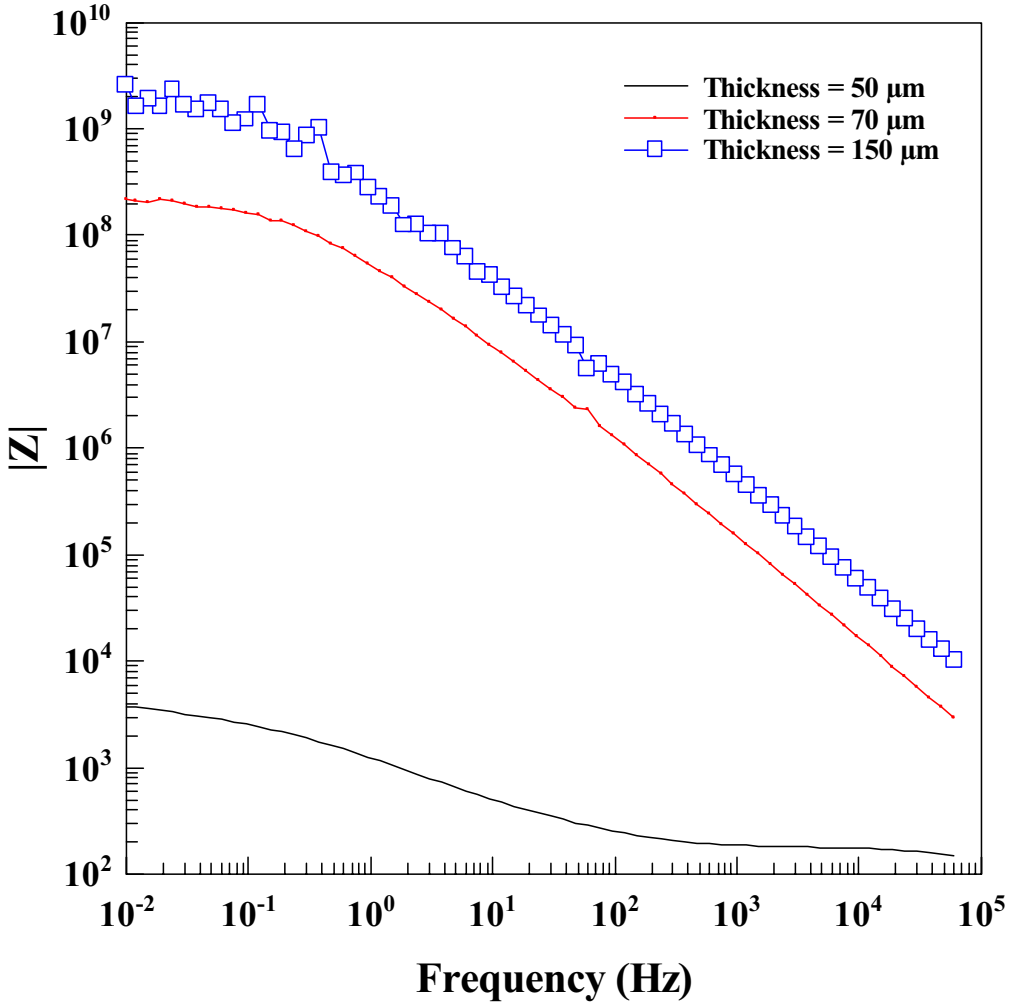

Figure 3.19 Bode plots for mild steel panels coated with pure commercial alkyd paint film (with different thicknesses) after 200 d of immersion in 3% NaCl solution. The coating thickness is shown in the legend.

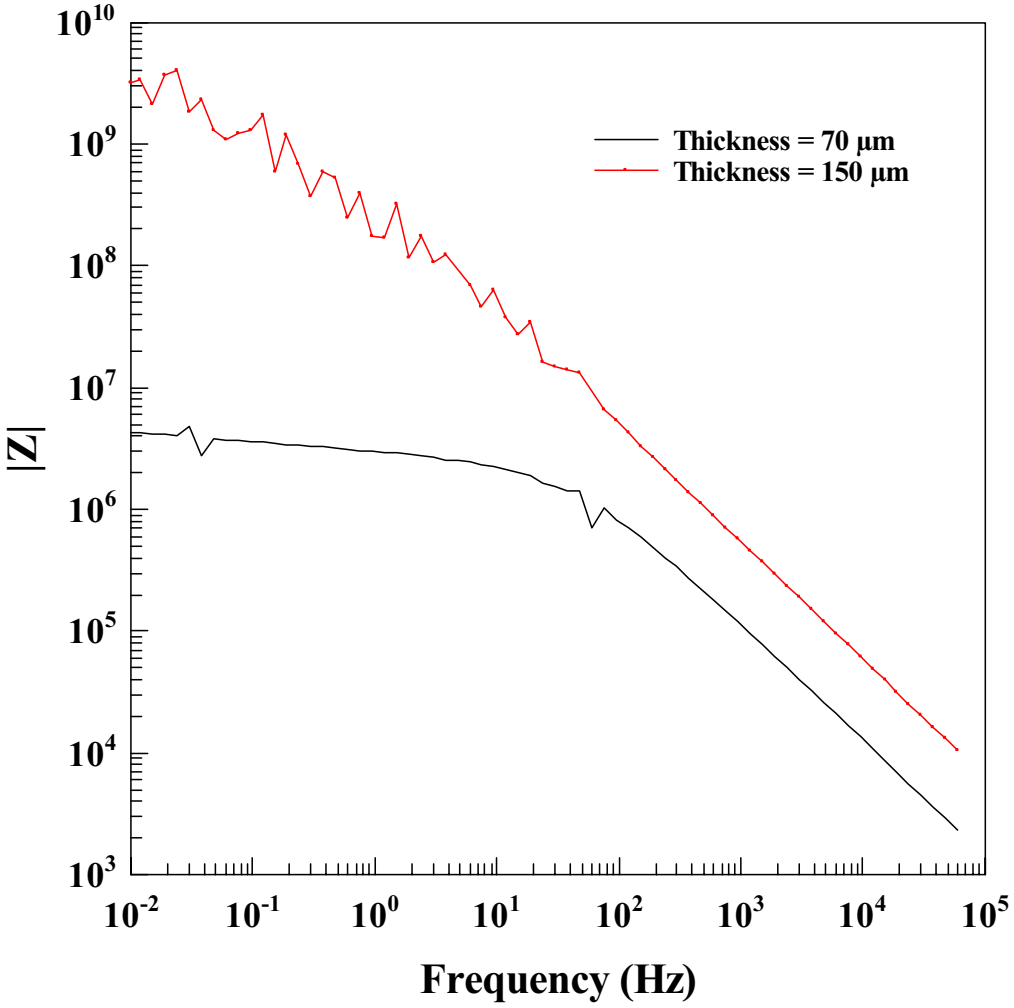

Figure 3.20 Bode plots for mild steel panels coated with pure commercial alkyd paint film (with different thicknesses) after 1800 d of immersion in 3% NaCl solution. The coating thickness is shown in the legend.

impedance is, and hence the faster the rate of degradation of the film (e.g., Figures 3.16.a and 3.17.a).

As shown in Figure 3.16.a for a 30 μm thick pure paint film, in the first 19 days of immersion, the Bode plot shows a short frequency-independent plateau at low frequencies with an initial $|Z|$ value in the 10^4 to 10^5 Ω range. This plateau is associated with inherent film quality.[70-72] This plateau is also is an indication of water and electrolyte absorption in the coating and the initiation of corrosion. For immersion times longer than 19 days, the initial $|Z|$ values are less than 10^4 Ω and the plateau disappears indicating a higher rate electrolyte absorption, higher rate of corrosion, and hence a higher rate of damage of the paint film. On the other hand, the Nyquist plots in Figure 3.16.b show a capacitive semi-circle in the higher frequency region and a diffusion tail in the lower frequency region in agreement with the literature.[73] As shown in the figure, the capacitive semi-circle progressively decreases as the immersion time increases indicating degradation of the paint coating and the diffusion tail starts at a higher frequency indicating a higher rate of electrolyte diffusion through the paint film.

For a 40-50 μm thick pure paint film (Figure 3.17), the Bode plot (Figure 3.17.a) shows that the initial $|Z|$ value is in the 10^6 to 10^8 Ω range and the low-frequency plateau stays for a period of 177 d before it disappears. On the other hand, the Nyquist plots (Figure 3.17.b) show only a capacitive arc with no diffusion tail for up to 177 d. These results indicate that a thick pure paint film is more stable than a thin film.

For a 70 μm thick paint film (Figure 3.18), the Bode plots show that the initial $|Z|$ value higher than 1.0×10^6 Ω even after 1814 d (~ 5 yr) of constant immersion in 3 % NaCl solution. In addition, the low-frequency plateau is very evident in the Bode plot

after this long period of immersion indicating better barrier properties for the film. Moreover, as depicted in Figures 3.19 and 3.20, the $|Z|$ values for the 150 μm thick coatings are the highest among all of the studied coating thicknesses indicating the high stability of these coatings.

As shown in Figure 3.19 and 3.20, thicker coatings are characterized by very high $|Z|$ values in the LF part of the Bode plot which lead to low current and high noise in the low-frequency range of the measurement. This noise, as well as data scatter, is very common in the literature especially in the early period of immersion in the corrosive electrolyte.[72, 74, 75] MacDonald attributed this noise to the difficulty that the frequency response analyzer (FRA) is having in defining the sinusoidal variation in the current due to the impedance being very high at low frequency.[76] According to the literature, thick, high quality coatings are characterized by very high resistance (R_c) and very low capacitance (C_c) indicating high corrosion resistance.[77, 78] The very high resistance results in very small currents, especially at low frequencies where resistive elements in the system under investigation dominate.[79]

The Bode and Nyquist plots for VGCNF-reinforced coatings are shown in Figures 3.21 through 3.27. These plots collectively show that the incorporation of the VGCNF in the alkyd paint matrix increases the $|Z|$ values and lowers its rate of decrease with immersion time indicating better corrosion protection properties relative to the unmodified paint matrix. The data also reveals that the higher the VGCNF content, the higher and more stable the $|Z|$ values over a long period of immersion in the corrosive electrolyte.

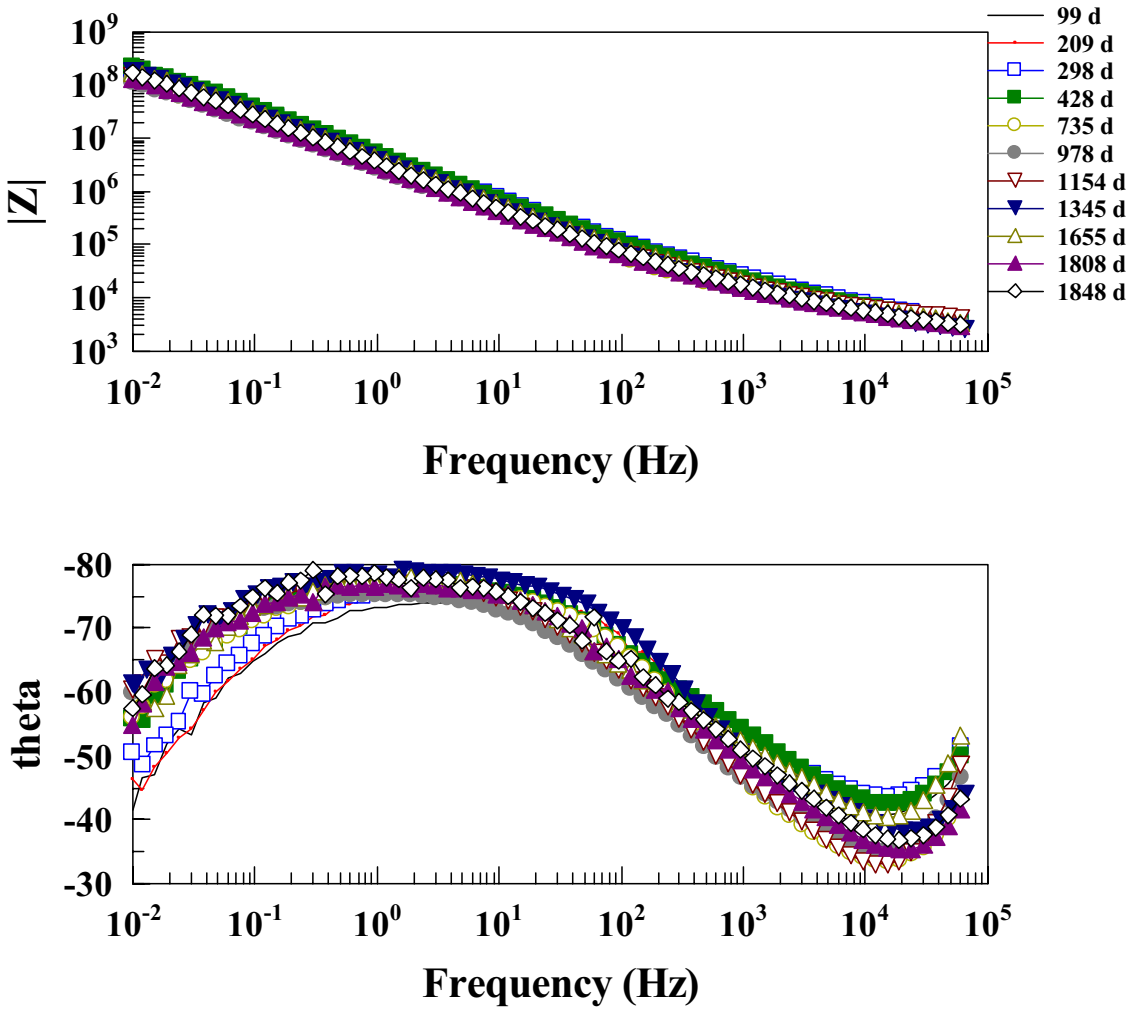

Figure 3.21 Bode (a) and Nyquist (b) plots for mild steel panels coated with 0.5 wt % VGCNF-incorporated commercial alkyd paint film (150 µm thick) at different immersion times in 3% NaCl solution.

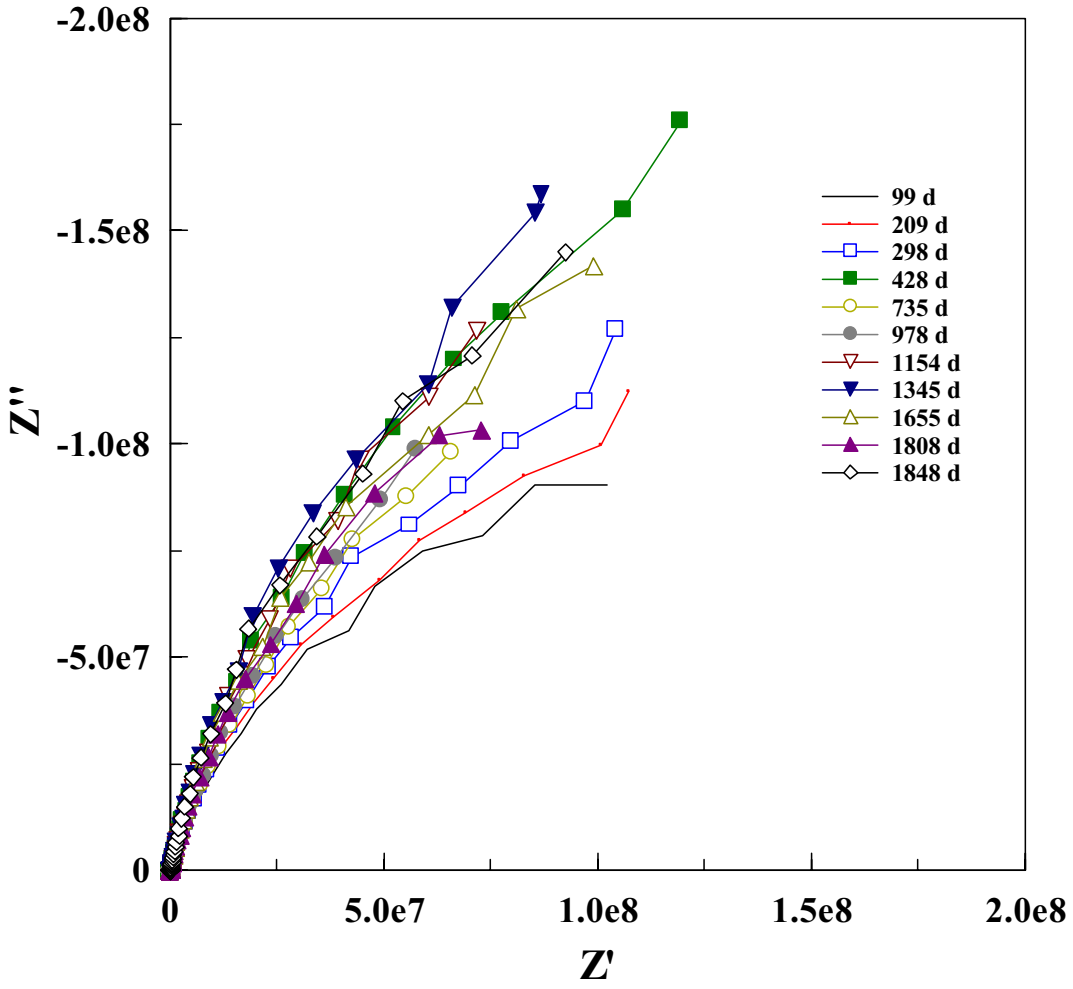

(b)

Figure 3.21 Continued.

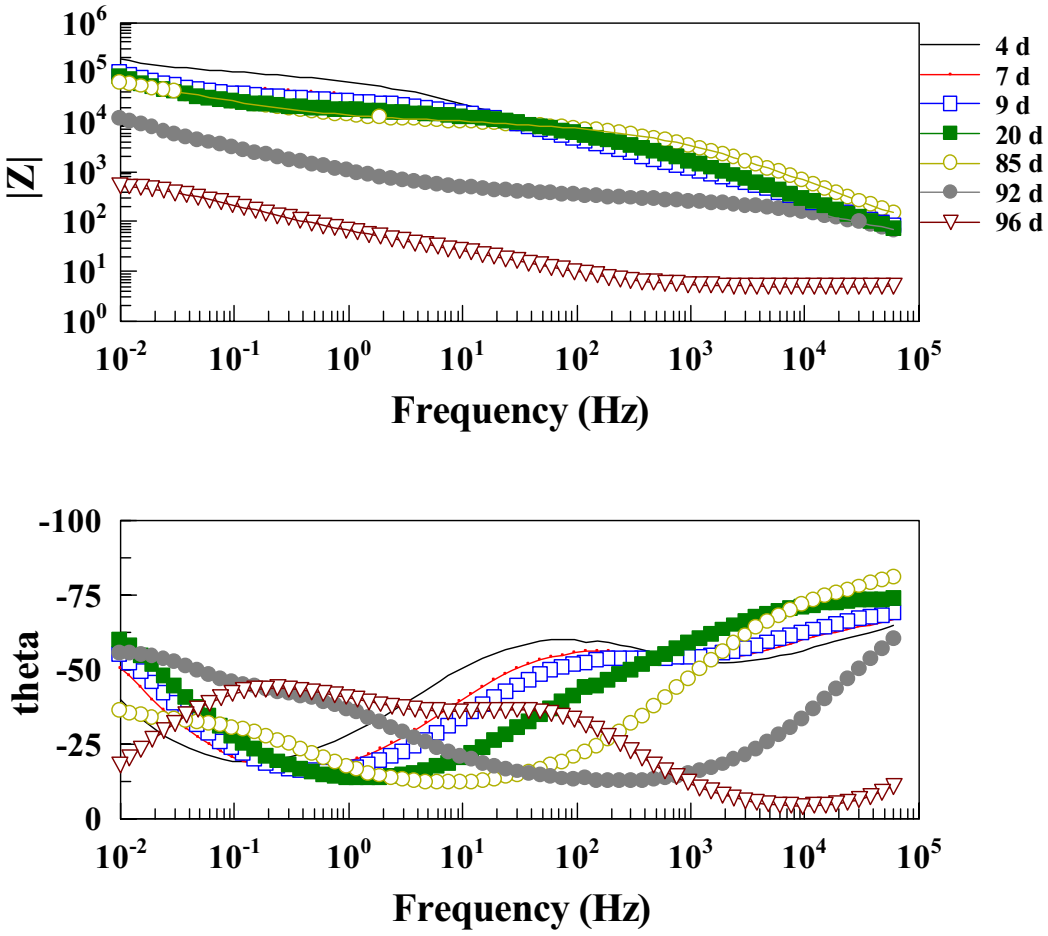

Figure 3.22 Bode (a) and Nyquist (b) plots for mild steel panels coated with 1 wt % VGCNF-incorporated commercial alkyd paint films (30 μm thick) at different immersion times in 3% NaCl solution.

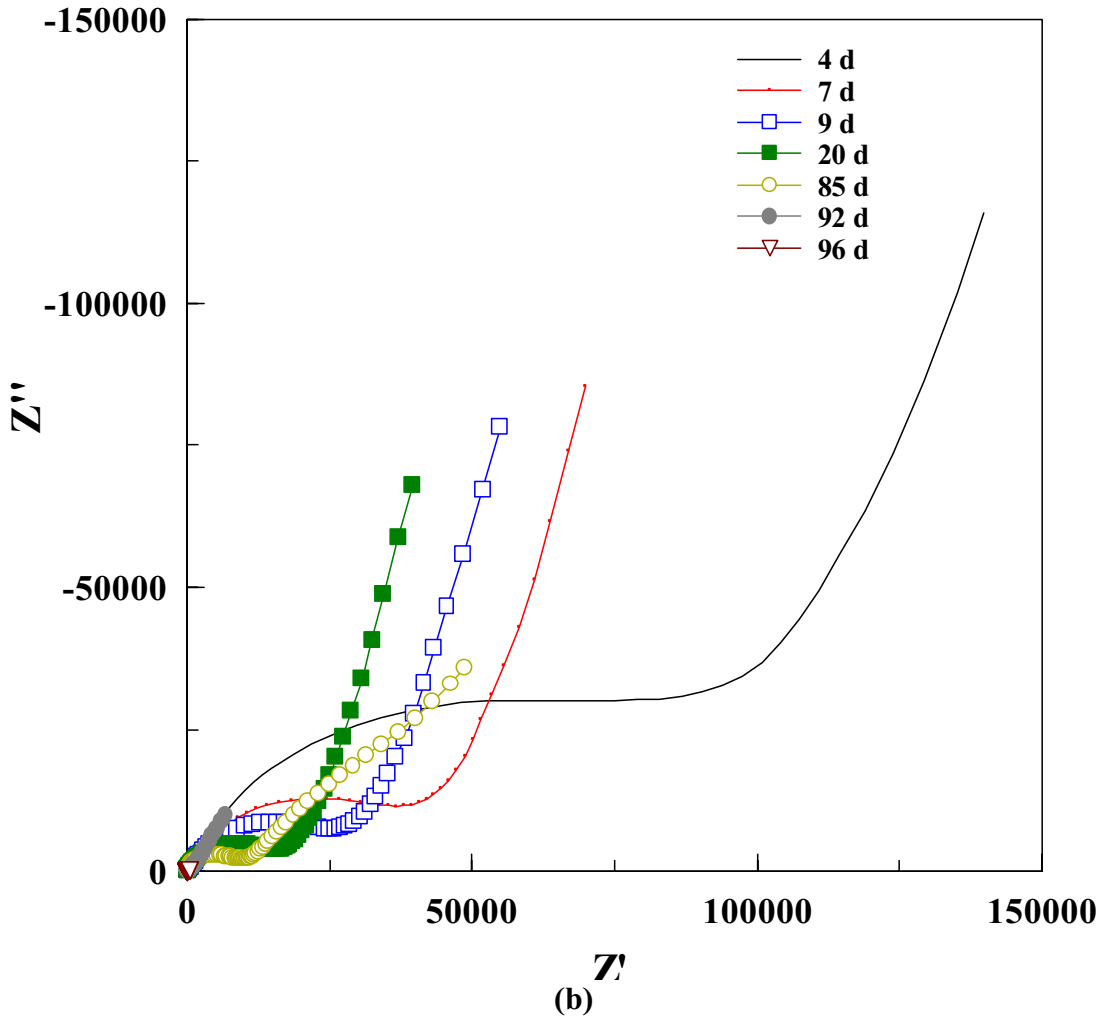

Figure 3.22 Continued.

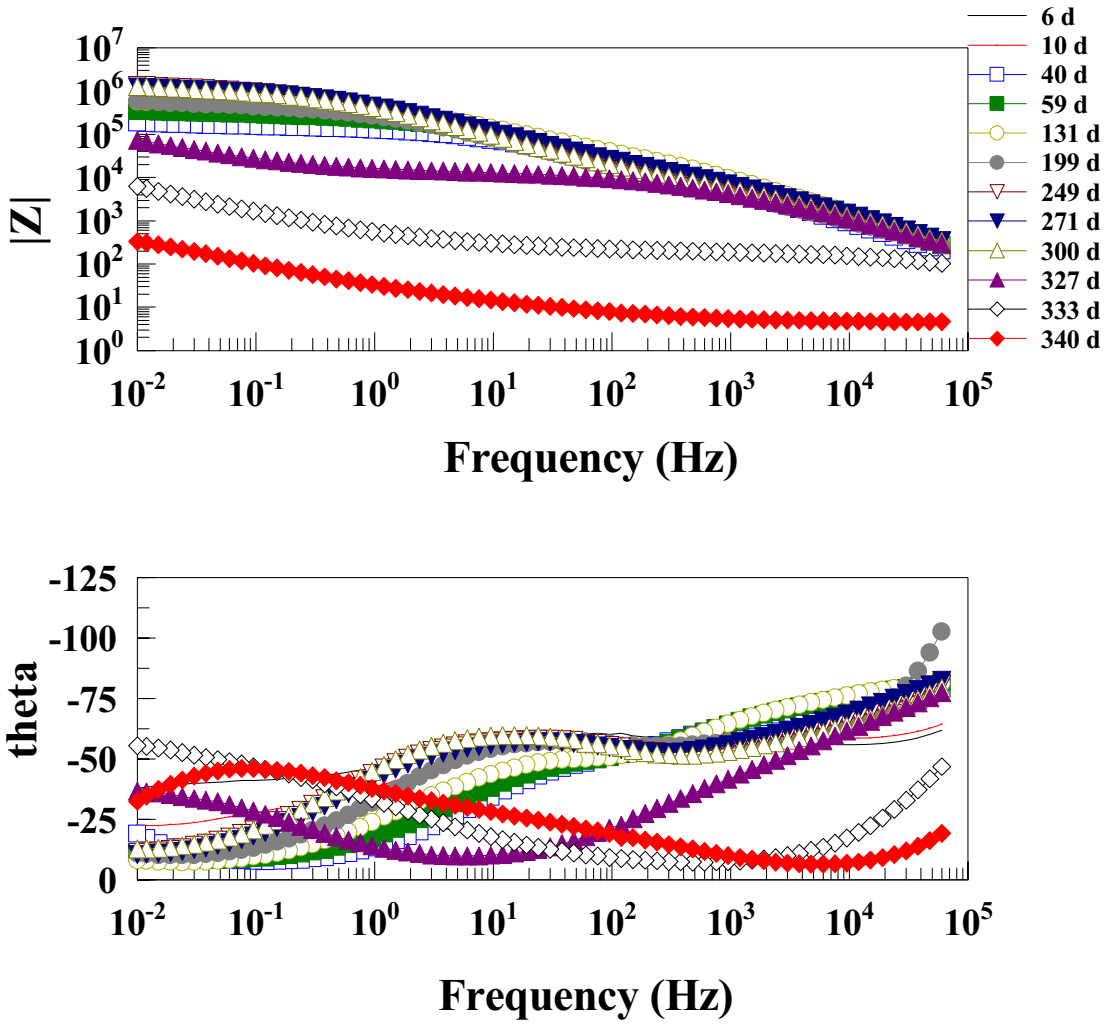

(a)

Figure 3.23 Bode (a) and Nyquist (b) plots for mild steel panels coated with 1 wt % VGCNF-incorporated commercial alkyd paint films (40-50 μm thick) at different immersion times in 3% NaCl solution.

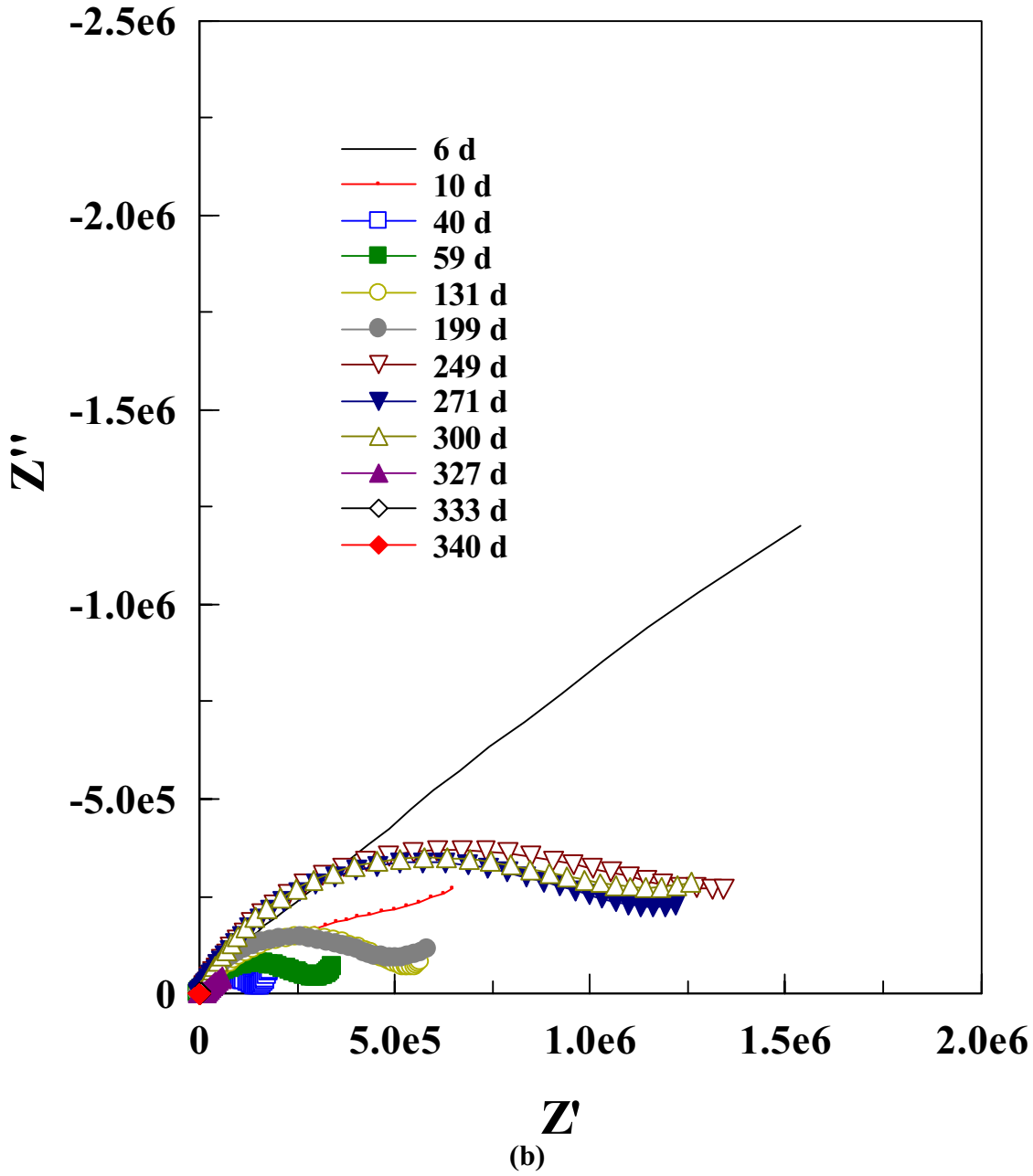

Figure 3.23 Continued.

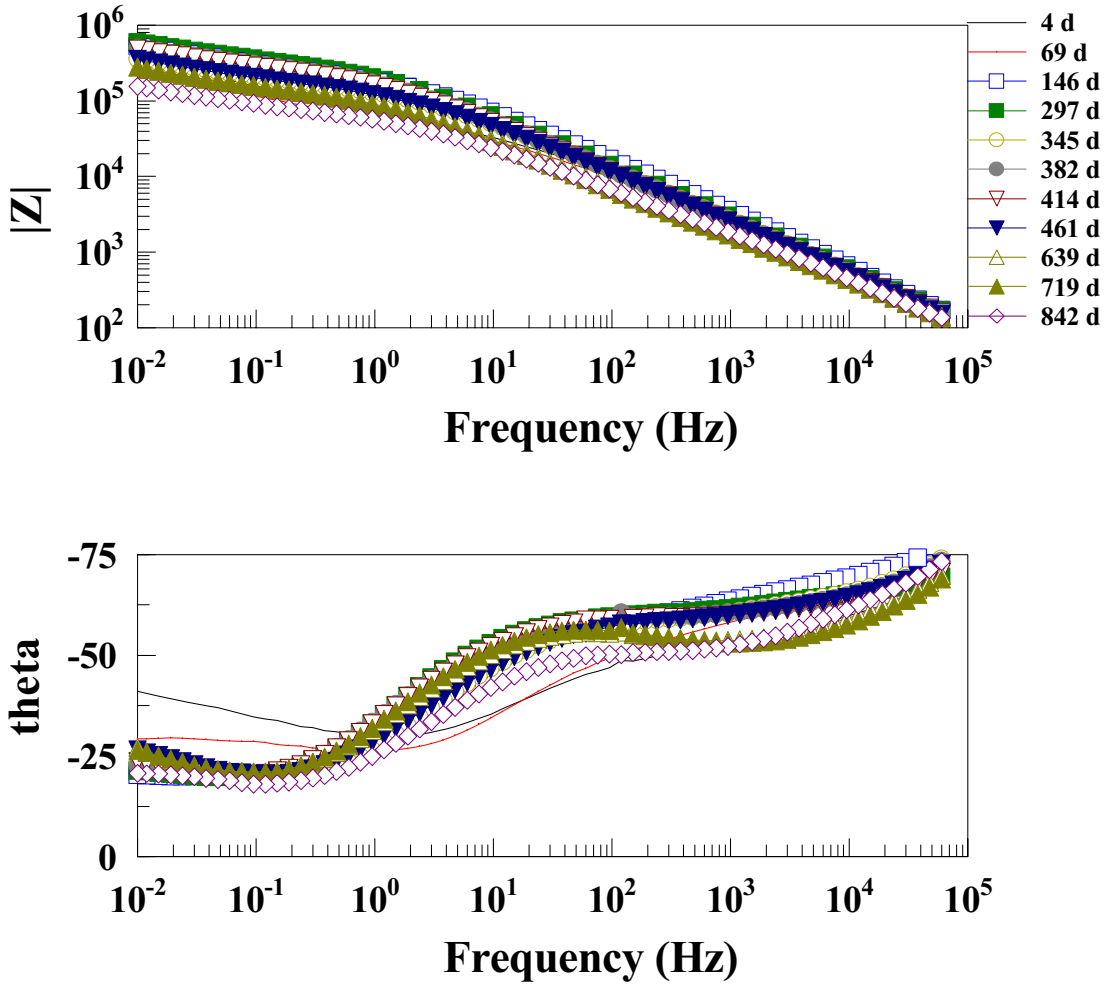

(a)

Figure 3.24 Bode (a) and Nyquist (b) plots for mild steel panels coated with 5 wt % VGCNF-incorporated commercial alkyd paint films (40-50 μm thick) at different immersion times in 3% NaCl solution.

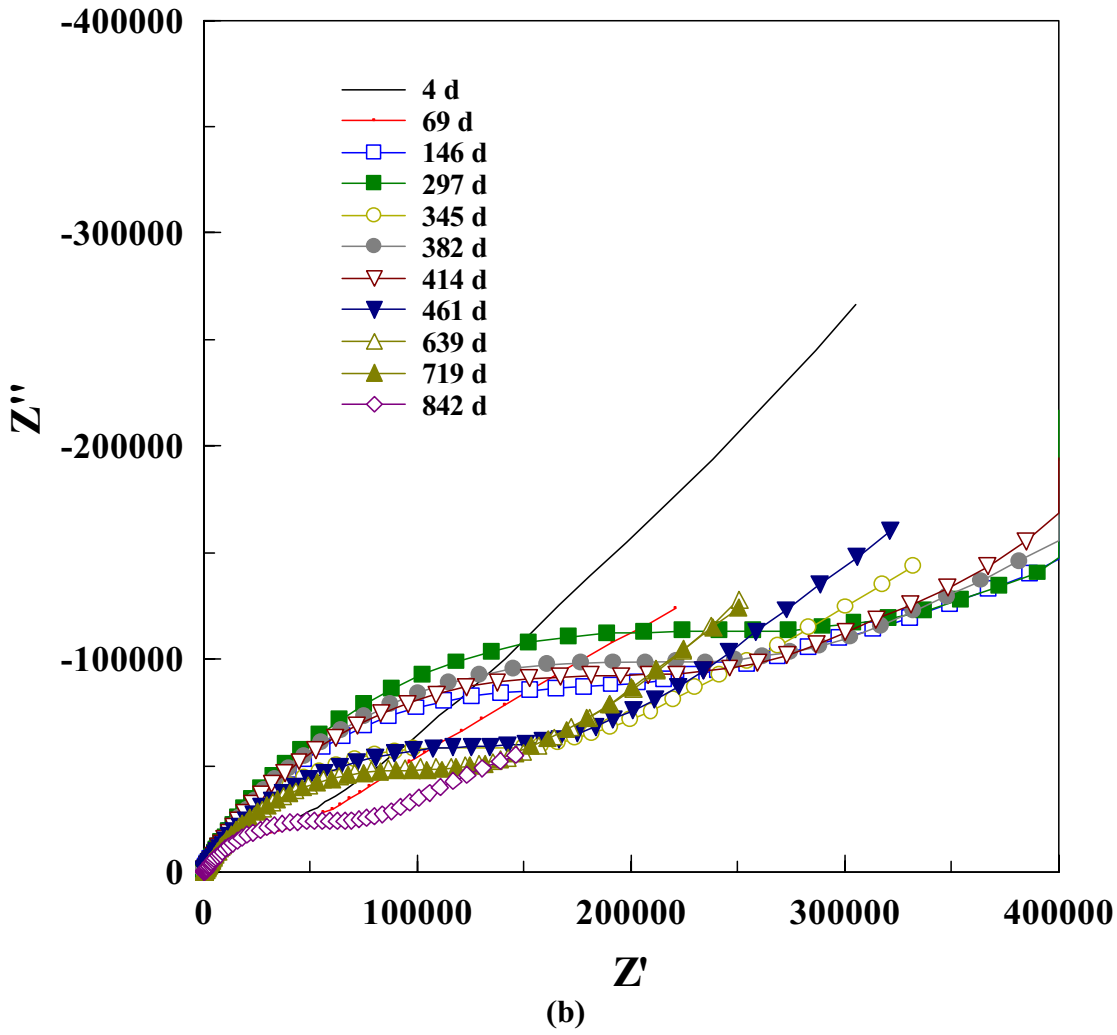

Figure 3.24 Continued.

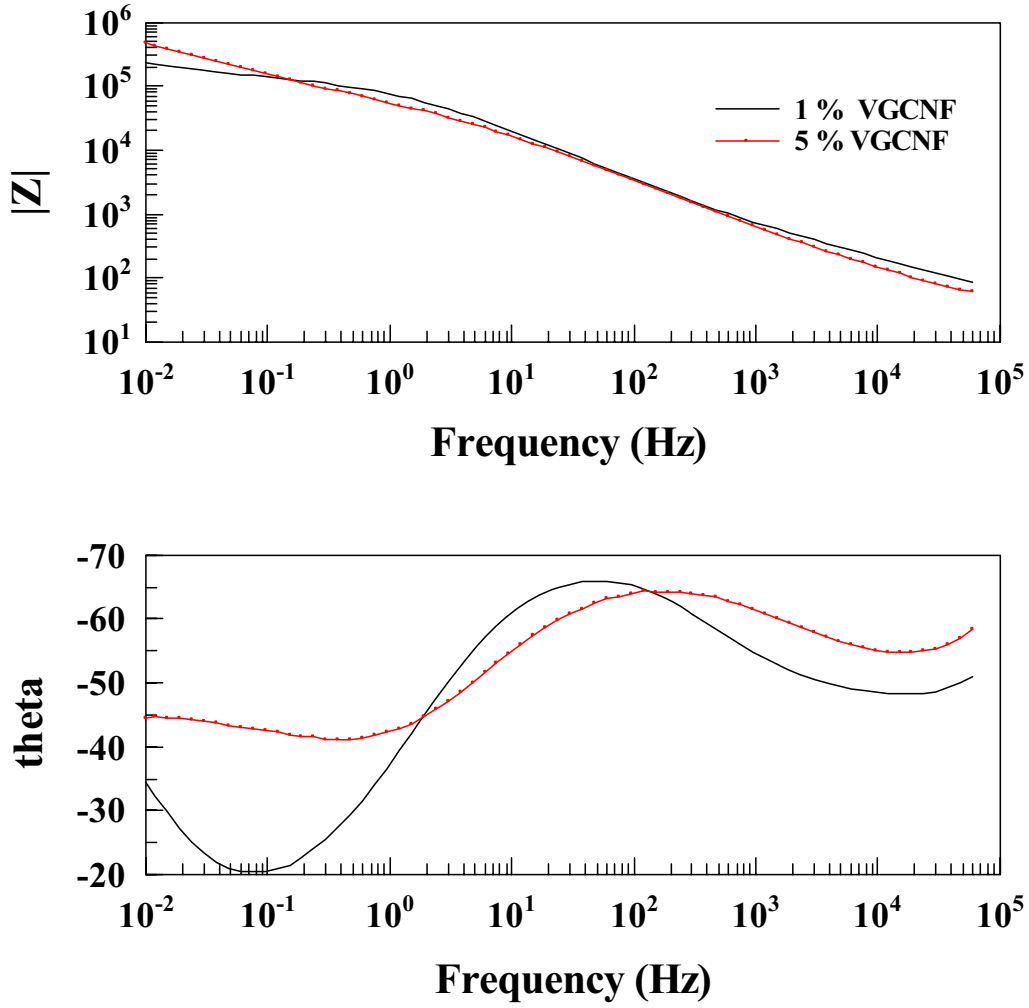

Figure 3.25 Bode (a) and Nyquist (b) plots for mild steel panels coated with VGCNF-incorporated commercial alkyd paint film (20 μm thick) after 4 d of immersion in 3% NaCl solution. The VGCNF loading is shown in the legend.

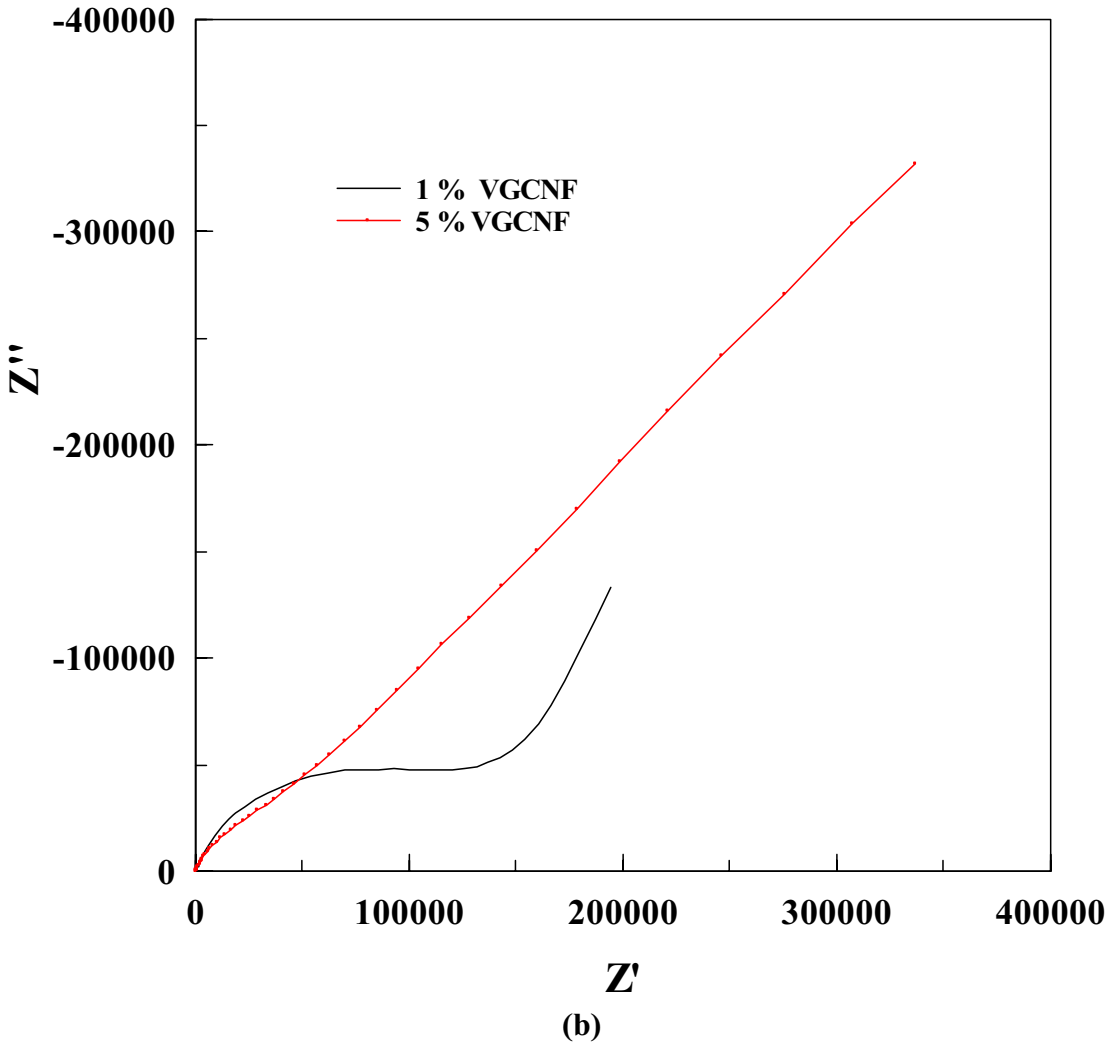

Figure 3.25 Continued.

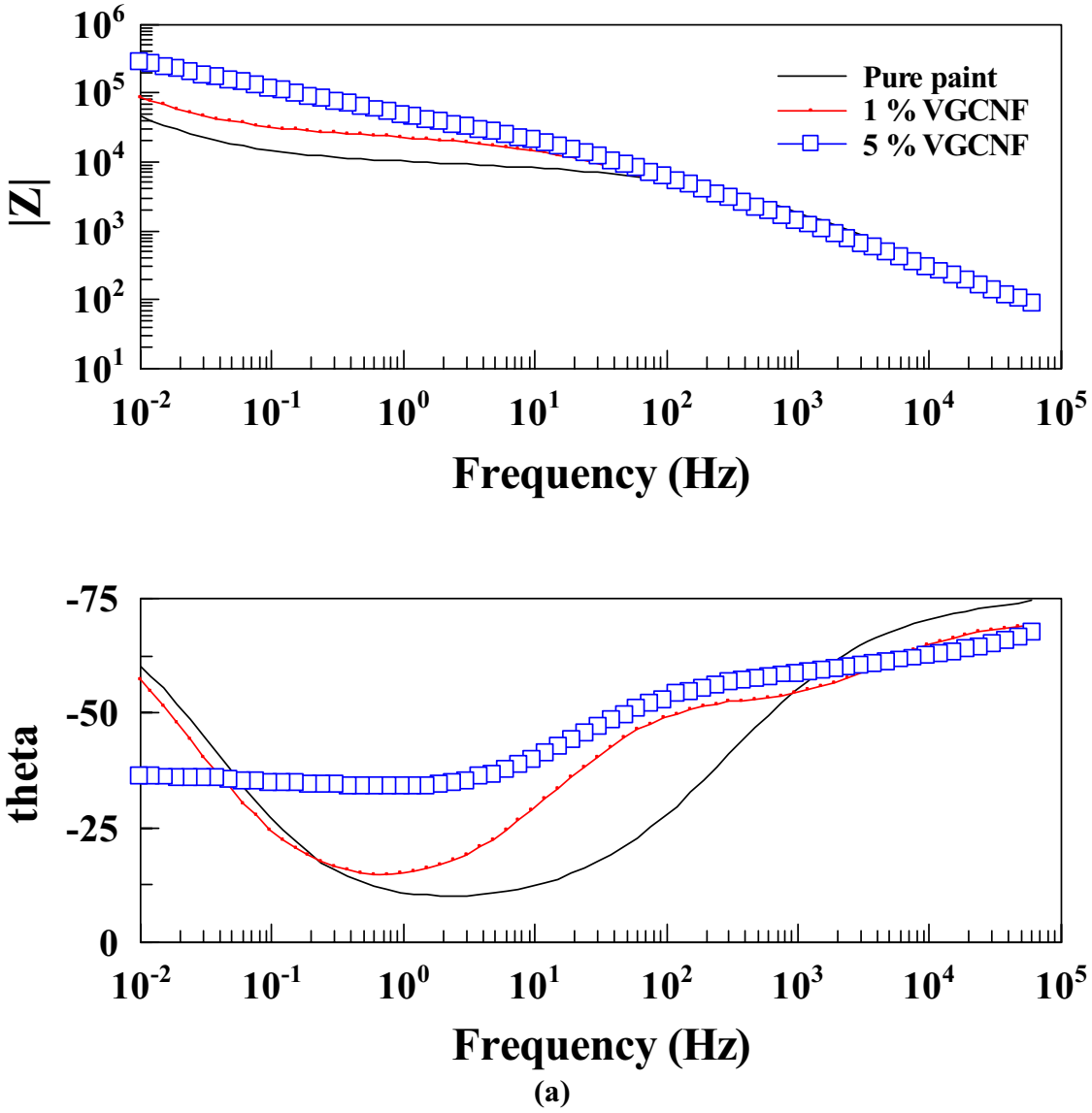

Figure 3.26 Bode (a) and Nyquist (b) plots for mild steel panels coated with VGCNF-incorporated commercial alkyd paint films (30 μm thick) after 11 d of immersion in 3% NaCl solution. The VGCNF loading is shown in the legend.

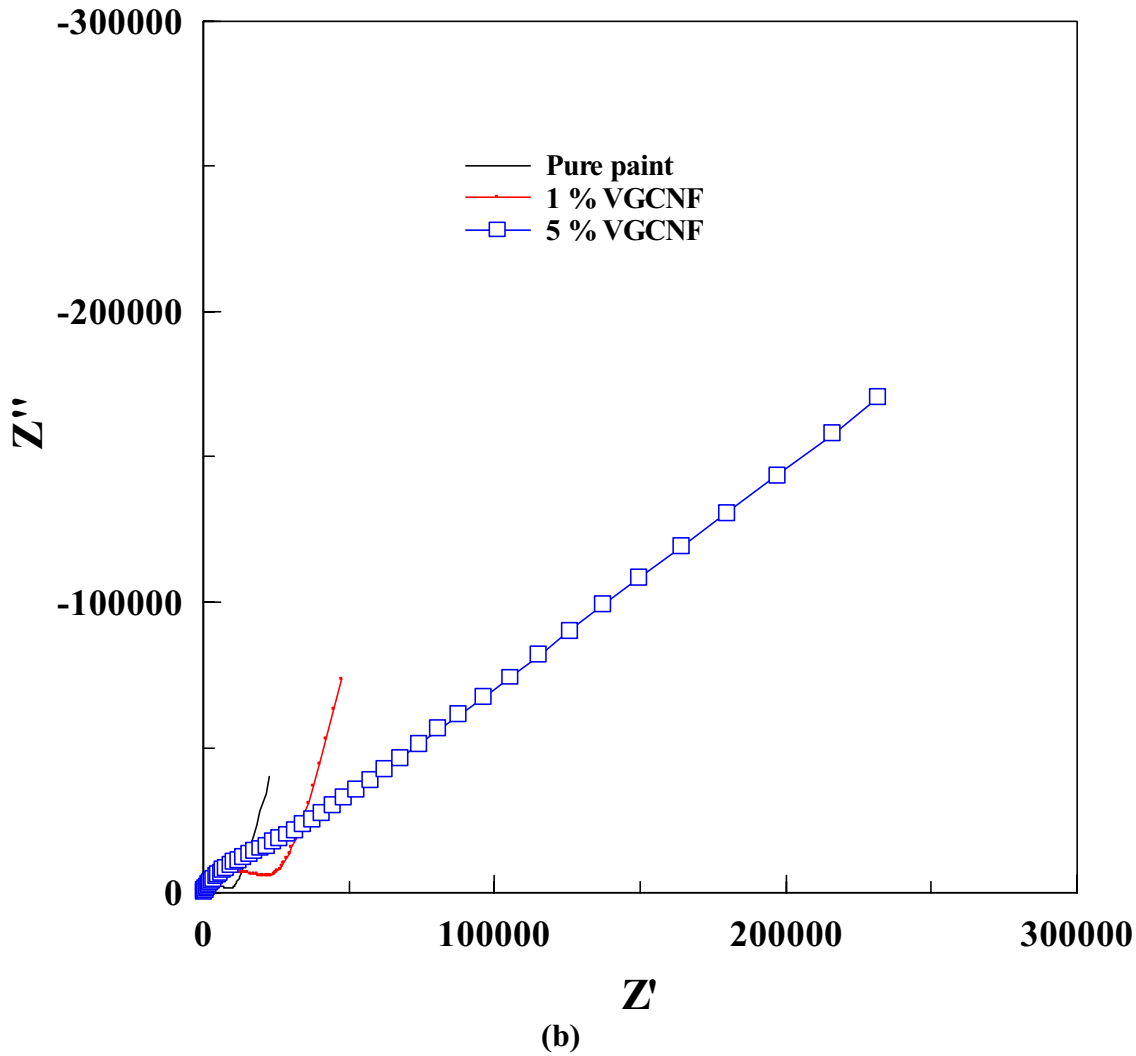

Figure 3.26 Continued.

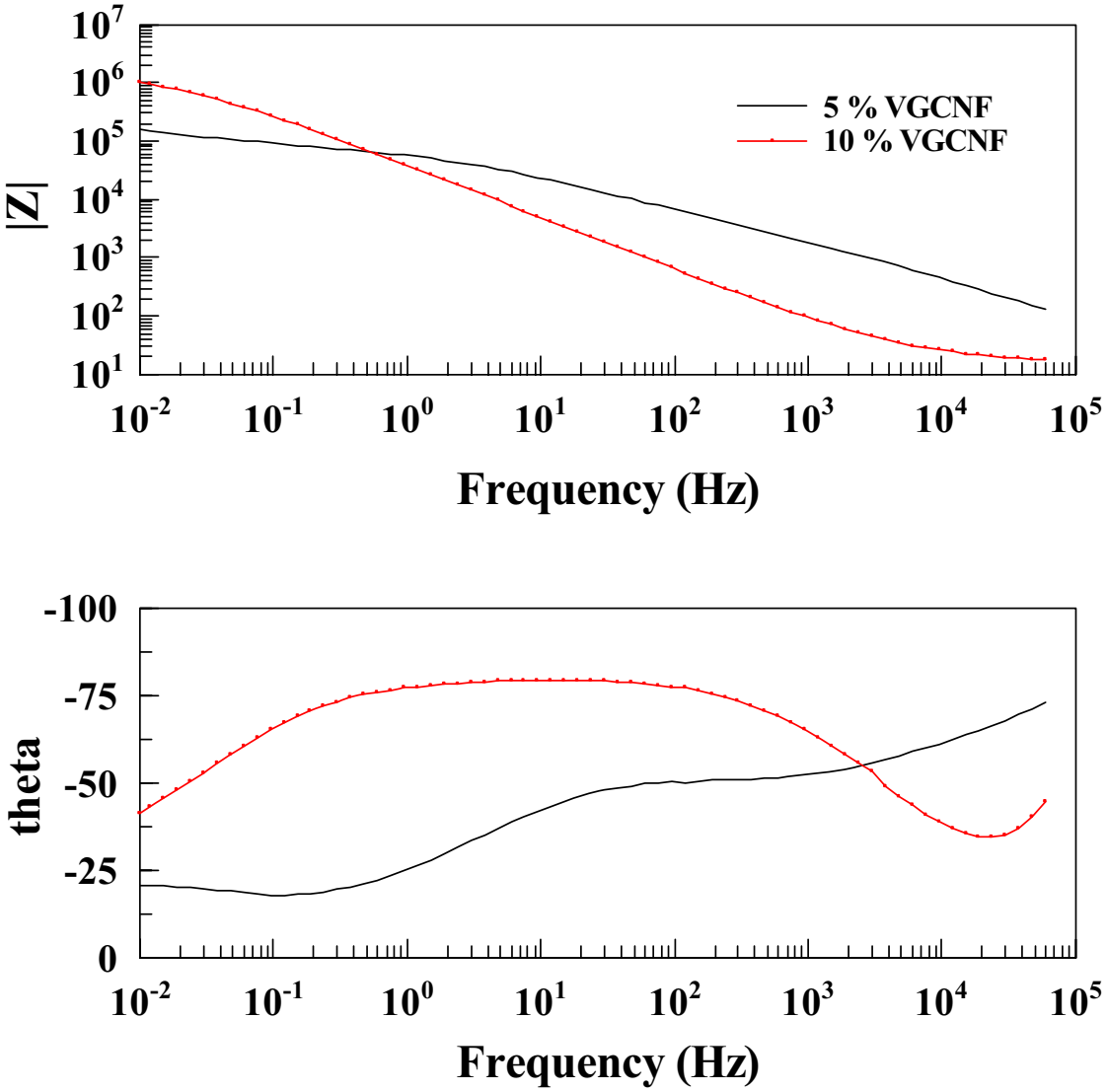

(a)

Figure 3.27 Bode (a) and Nyquist (b) plots for mild steel panels coated with VGCNF-incorporated commercial alkyd paint film (40-50 μm thick) after 840 d of immersion in 3% NaCl solution. The VGCNF loading is shown in the legend.

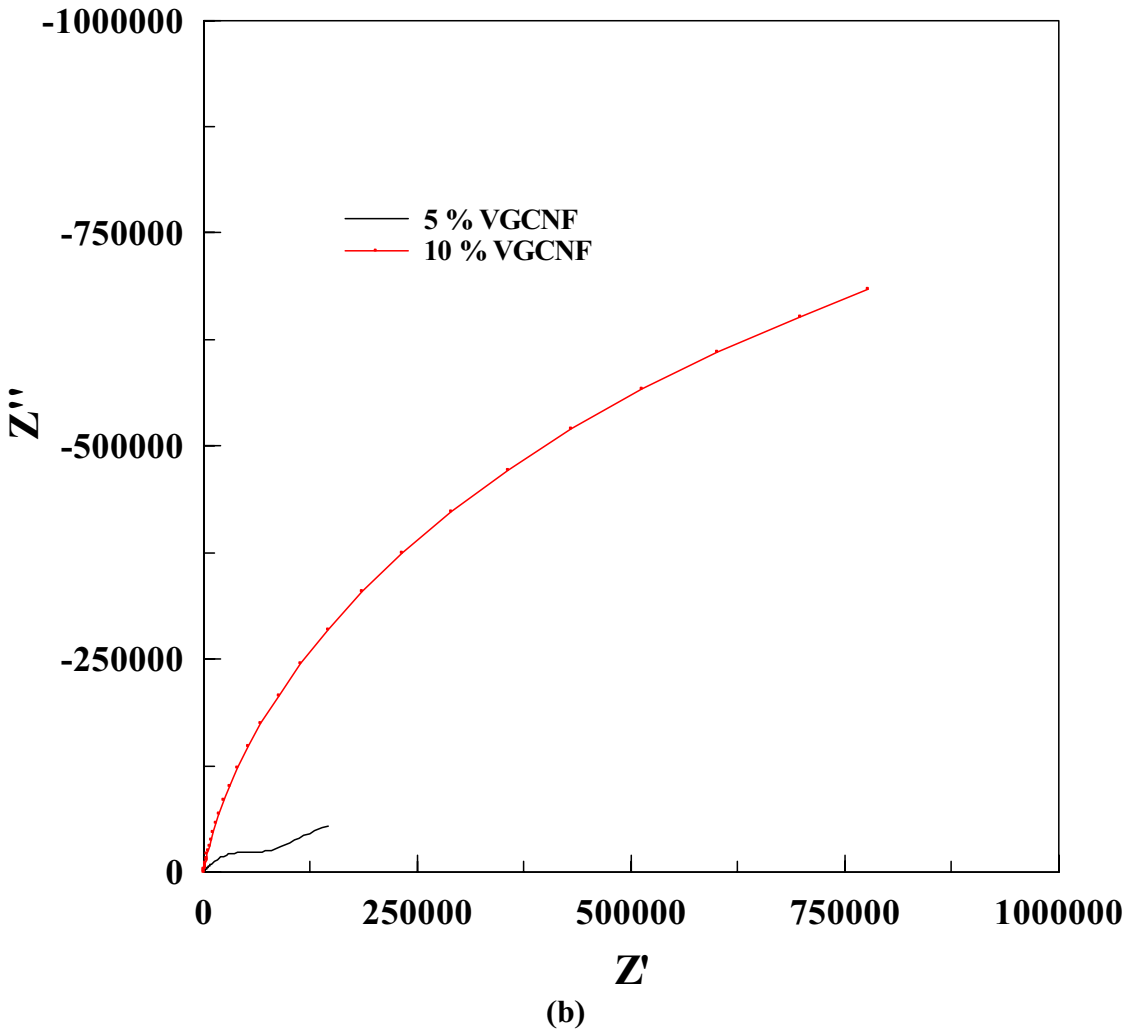

Figure 3.27 Continued.

Figure 3.21 shows the Bode and Nyquist plots for a 150 μm thick paint film containing 0.5% VGCNF. As shown in Figure 3.21.a, the initial $|Z|$ values are almost the same as the values for a pure paint film with the same thickness (Figures 3.19 and 3.20). However, for an immersion period of 1848 d (over 5 yr), the Bode plots for a 0.5% VGCNF-incorporated paint matrix show the characteristic straight line for a perfectly insulating and intact polymer film. In addition, the Nyquist plot (Figure 3.21.b) shows a capacitive arc that slightly increases with increasing the immersion time.

Figure 3.22 depicts the Bode and Nyquist plots for a 30 μm thick alkyd paint film containing 1% VGCNF. As shown in Figure 3.22.a, in the first 10 d of immersion in the electrolyte, the initial $|Z|$ values is close to 1.0×10^5 Ω. This low $|Z|$ value is normal for thin paint films. The Bode plots also show no frequency-independent plateau and the rate of decrease in the $|Z|$ values increases with increase in immersion time. On the other hand, the Nyquist plot (Figure 3.22.b) shows a capacitive semi-circle in the higher frequency region and a diffusion tail in the lower frequency region. As shown in the figure, as the immersion time increases, the semi-circle progressively decreases and the diffusion tail starts at a higher frequency indicating a higher rate of electrolyte diffusion through the paint film and degradation of the coating.

Figure 3.23 shows the Bode and Nyquist plots for a 40-50 μm thick alkyd paint film containing 1% VGCNF. It is obvious from the Bode plot (Figure 3.23.a) that the initial $|Z|$ values are one order of magnitude higher than the corresponding values in Figure 3.22.a indicating that a 40-50 μm thick paint coating is more stable than a 30 μm one. Moreover, the Bode plots in Figure 3.23.a show that the frequency-independent plateau gradually disappears as the immersion time increases. The behavior is confirmed

in the Nyquist plots. As shown in Figure 3.23.b, in the first few days of immersion in the electrolyte, the Nyquist plot shows a capacitive line indicating a perfectly insulating coating film. At a later stage of immersion, the capacitive line becomes a capacitive semi-circle in the HF region followed by a diffusion tail. With further increase in the immersion time, semi-circle decreases and the diffusion tail starts at a higher frequency indicating the electrolyte diffusion and damage of the coating.

Figures 3.24 through 2.27 show that the higher the VGCNF content, the higher the initial $|Z|$ values and hence the more stable the coating is. Furthermore, for alkyd paint samples containing 10% VGCNF with a thickness in the 40-50 μm range, the Nyquist plots show only a capacitive loop even after 840 d of immersion indicating the stability of the coating (Figure 3.27.b).

3.3.4 Equivalent Electrical Circuits and Data Fitting

As mentioned in Chapter 1, one of the great advantages of the EIS measurements is the ability to model the experimental EIS data, even for complex electrochemical systems, using pure theoretical equivalent electrical circuits that represent the physical process occurring in the system under investigation.[80-82] The equivalent circuits can also support or rule out mechanistic models and enable the calculation of the corrosion parameters for the system being studied.[83-85] In this regard, an acceptable model is one that is as simple as possible and generates model spectra that correlates very well with the experimental EIS data with minimal error. In addition, all elements of the model should have physical meaning.[86]

In the current investigation, the experimental EIS spectra were fit to theoretical equivalent electrical circuits using the ZView software. The fitting process usually starts with selecting a suitable model based on similar previous research work published in the literature and/or using one of the simple models provided by the software that is close to the experimental data presented in the research under investigation. The model is then tested and modified, as necessary, to meet the criteria for an acceptable model as mentioned above. Once a model is selected, the next step will be to run the fitting program which requires the input of initial values for all parameters related to the electrochemical system under investigation. As shown in Tables 3.2 through 3.4, some of these parameters are fixed while the rest are variable. The fixed parameters (e.g., R_s, R_p) are initially estimated from the experimental Bode and Nyquist plots. The fitting program is then run where the algorithm makes changes in several or all of the parameter values and evaluates the resulting fit. If the change improves the fit, the new parameter value is accepted. If the change worsens the fit, the old parameter value is retained. The process is then repeated with another parameter until a good fitting spectrum is obtained or all of the trials are exhausted.[87] As mentioned above, the best model curve is one that is almost superimposed on the experimental one and shows the minimum uncertainty (% error) in the calculated parameters. One of the parameters that are used as a measure for the "goodness of fit" is the chi-squared parameter (χ^2). The smaller the value of χ^2, the better the goodness of fit is. In addition, according to Boukamp, the value of χ^2 should decrease by tenfold if a new circuit element is introduced into the model. If the value does not decrease, then the element should be eliminated and either another element is introduced or a different circuit model is tried.[87]

Figures 3.28 through 3.30 and Tables 3.2 through 3.4 show the fitting spectra and data, including the percent error for the elements in the models, along with the experimental EIS spectra for a mild steel sample coated with a layer of a 30 μm thick pure alkyd paint film. The selection of a wrong model and/or the estimated values for the fixed parameters always gives poor fitting results either in the form of fitting spectra that are non-superimposed on the experimental ones or high percent errors in the fitting data. The modeled data presented in Figures 3.28 through 3.30 and Tables 3.2 through 3.4 were generated using the same model (Figure 3.31.a) but with different initial values for the fixed parameters. For example, Figure 3.28 and Table 3.2 show the fitted spectra and data for a poor modeling obtained for a mild steel sample coated with a 30 μm thick pure paint film after 3 d of immersion in NaCl solution. As shown in Figure 3.28, the fitted spectra are not superimposable on the experimental ones. In addition, Table 3.2 shows that the % error is as high as 9.7×10^{19} and the χ^2 is also high (0.18). The data presented in Figure 3.29 and Table 3.3 show still poor but better fitting data than that presented in Figure 3.28 and Table 3.2. As shown in Figure 3.29, the deviation between the modeled spectrum and the data spectrum is smaller than in Figure 3.28. Also, the uncertainties in the fitting parameters (Table 3.3) are still high (as high as 3.9×10^{8}) but better than those shown in Table 3.2. Moreover, the χ^2 value (0.019) is better than the value shown in Table 3.2. On the other hand, Figure 3.30 and Table 3.4, show the best fit among the three given examples. It is evident from Figure 3.30 that the modeled spectrum is more superimposed on the experimental ones than the other two. In addition, Table 3.4 clearly indicates that the maximum uncertainty in the fitting data is less than 6% and the χ^2 value is as low as 0.0011. These results indicate that the suggested circuit model shown in

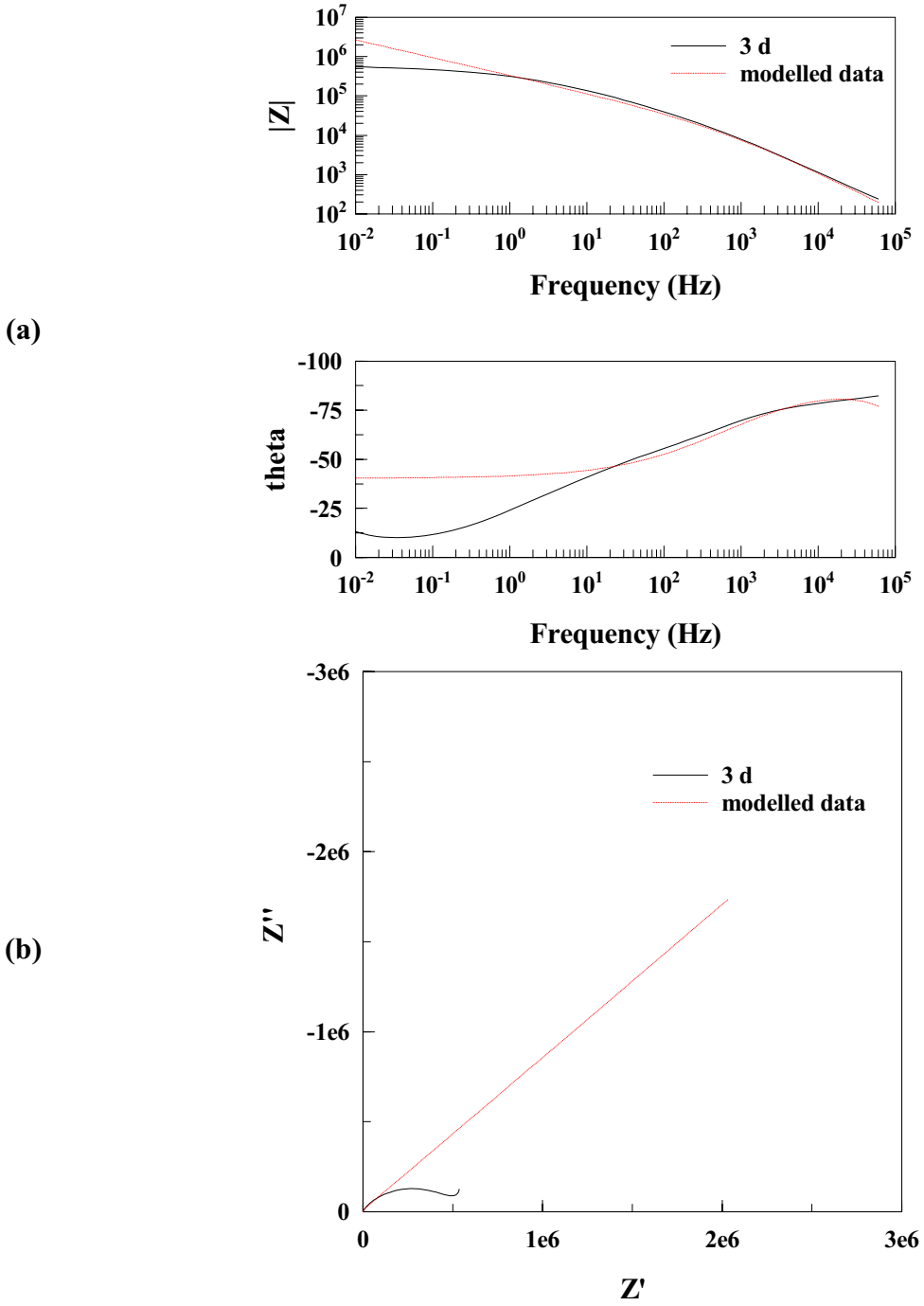

Figure 3.28 Experimental and a very poor fitting; (a) Bode, and (b) Nyquist plots for a pure alkyd paint coating film (30 μm thick) applied to the surface of a mild steel coupon after 3 d of immersion in aqueous 3% NaCl solution.

Table 3.2 Data for a very poor fitting model for a pure alkyd paint coating film (30 μm thick) applied to the surface of a mild steel coupon after 3 d of immersion in aqueous 3% NaCl solution.

Element	Freedom	Value	Error	Error %
R_s	Fixed (X)	32.27	N/A	N/A
C_c-T	Free (+)	1.30×10^{-8}	3.95×10^{-9}	30.33
C_c-P	Fixed (X)	1	N/A	N/A
R_c	Free (+)	4.77×10^{-3}	7.38×10^{3}	1.55×10^{8}
DE1	Fixed (X)	2-CPE #1		
DE1-R	Fixed (X)	5.74E5	N/A	N/A
DE1-T	Free (+)	9.01×10^{-7}	1.36×10^{-7}	15.14
DE1-P	Free (+)	4.49×10^{-1}	1.76×10^{-2}	3.92
DE1-U	Free (+)	1.35×10^{-4}	1.30×10^{14}	9.70×10^{19}
Chi-Squared		**0.182**		
Weighted sum of squares		24.253		

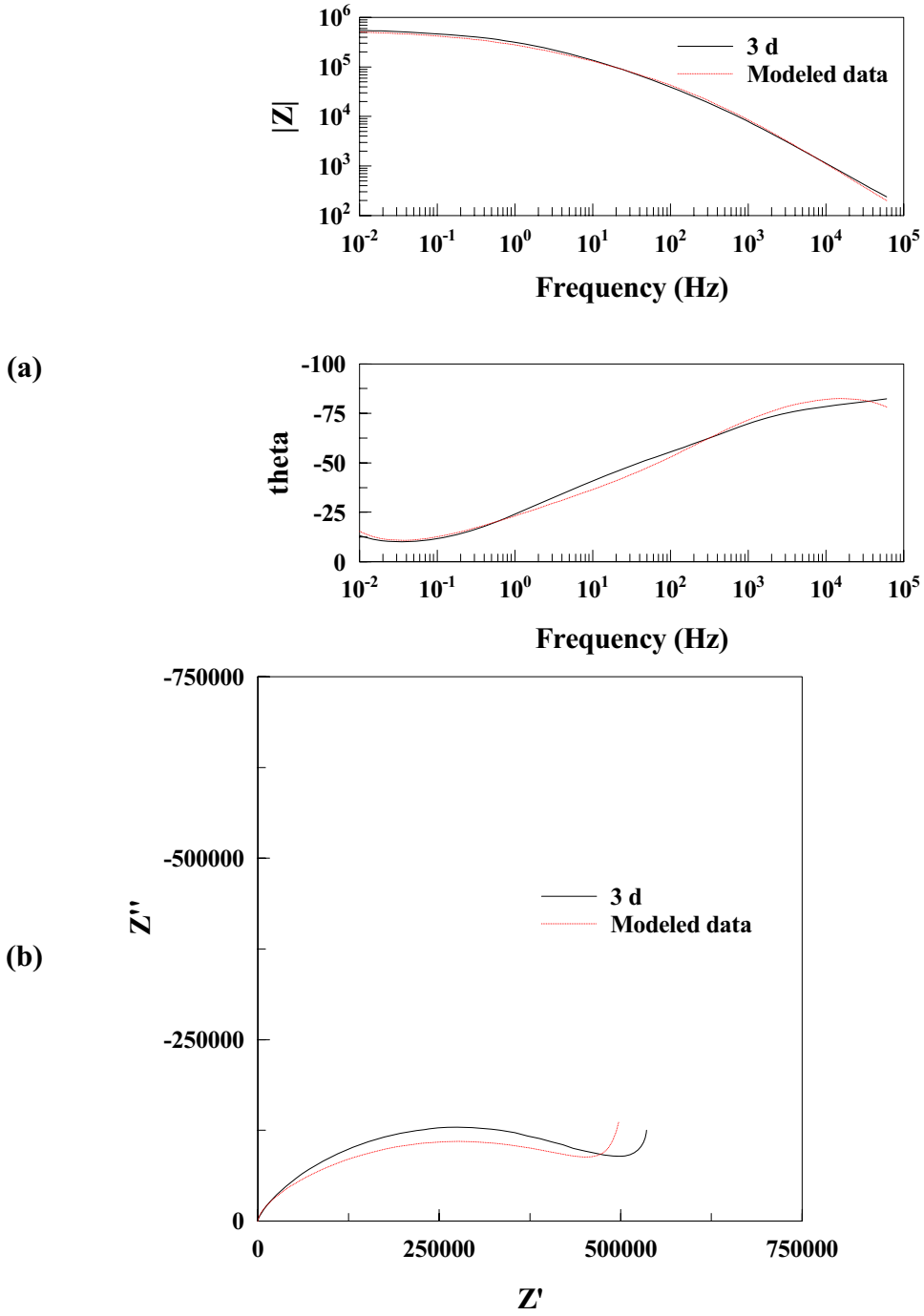

Figure 3.29 Experimental and poor fitting; (a) Bode, and (b) Nyquist plots for a pure alkyd paint coating film (30 μm thick) applied to the surface of a mild steel coupon after 3 d of immersion in aqueous 3% NaCl solution.

Table 3.3 Data for a poor fitting model for a pure alkyd paint coating film (30 μm thick) applied to the surface of a mild steel coupon after 3 d of immersion in aqueous 3% NaCl solution.

Element	Freedom	Value	Error	Error %
R_s	Fixed (X)	32.27	N/A	N/A
C_c-T	Free (+)	1.30×10^{-8}	4.40×10^{-10}	3.379
C_c-P	Fixed (X)	1	N/A	N/A
R_c	Free (+)	2.48×10^{-4}	966.02	3.90×10^{8}
DE1	Fixed (X)	2-CPE #1		
DE1-R	Fixed (X)	5.74×10^{5}	N/A	N/A
DE1-T	Free (+)	9.01×10^{-7}	2.98×10^{-8}	3.306
DE1-P	Free (+)	4.49×10^{-1}	7.06×10^{-3}	1.573
DE1-U	Free (+)	1.36×10^{-4}	3.34×10^{-5}	24.843
Chi-Squared		**0.019**		
Weighted sum of squares		2.527		

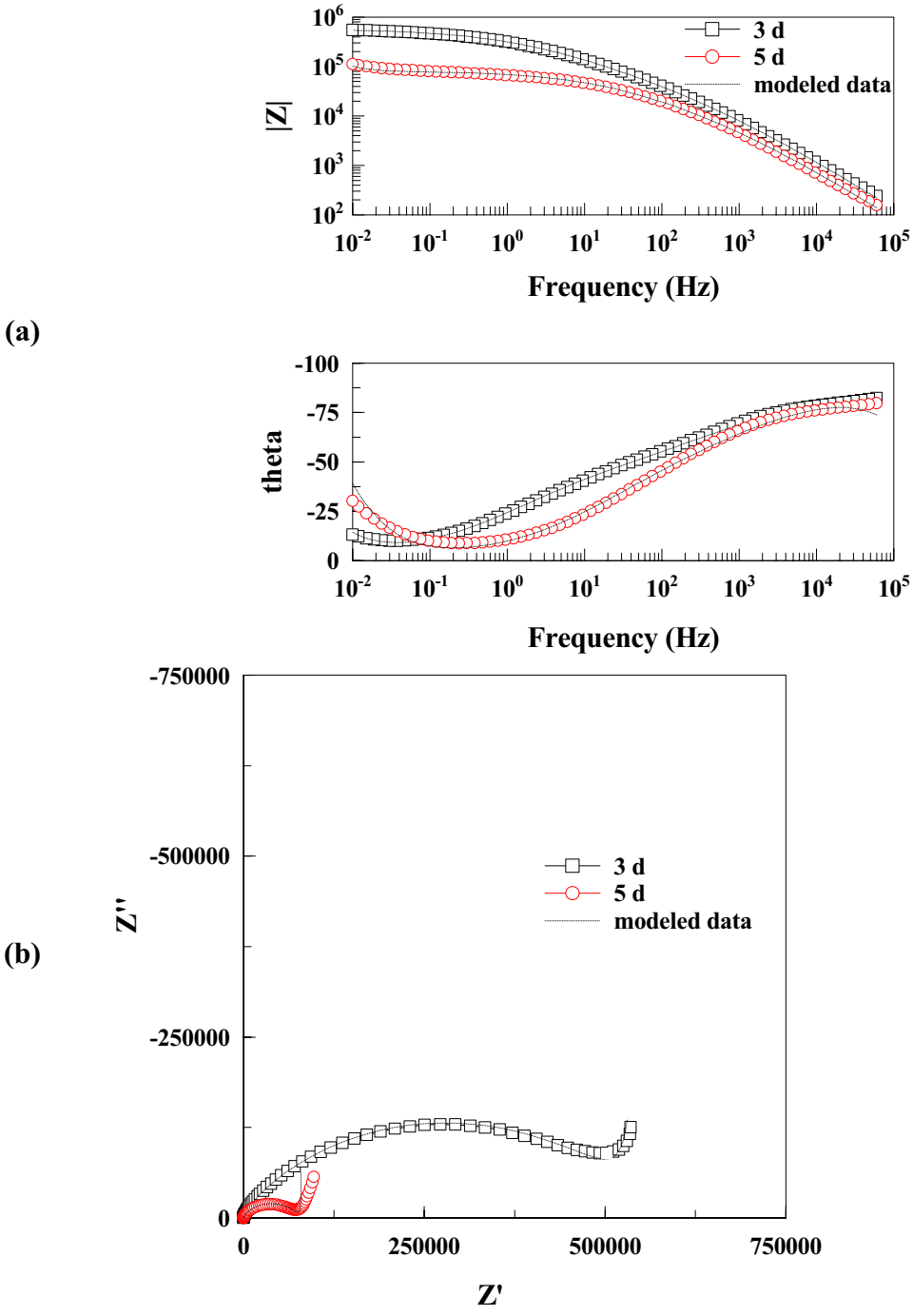

Figure 3.30 Experimental and good fitting; (a) Bode, and (b) Nyquist plots for a pure alkyd paint coating film (30 μm thick) applied to the surface of a mild steel coupon after 3 and 5 d of immersion in aqueous 3% NaCl solution.

Table 3.4 Data for a good fitting model for a pure alkyd paint coating (30 μm thick) applied to the surface of a mild steel coupon after 3 and 5 d of immersion in aqueous 3% NaCl solution.

Element	Freedom	Value	Error	Error %
R_s	Fixed (X)	32.27	N/A	N/A
C_c-T	Free (+)	1.16×10^{-8}	3.47×10^{-10}	2.995
C_c-P	Fixed (X)	1	N/A	N/A
R_c	Free (+)	623.10	59.869	9.608
DE1	Fixed (X)	2-CPE #1		
DE1-R	Fixed (X)	5.74×10^{5}	N/A	N/A
DE1-T	Free (+)	6.34×10^{-7}	5.87×10^{-9}	0.926
DE1-P	Free (+)	0.449	$1.76\ 10^{-3}$	0.333
DE1-U	Free (+)	1.35×10^{-4}	7.65×10^{-6}	5.684
Chi-Squared		**0.001**		
Weighted sum of squares		0.143		

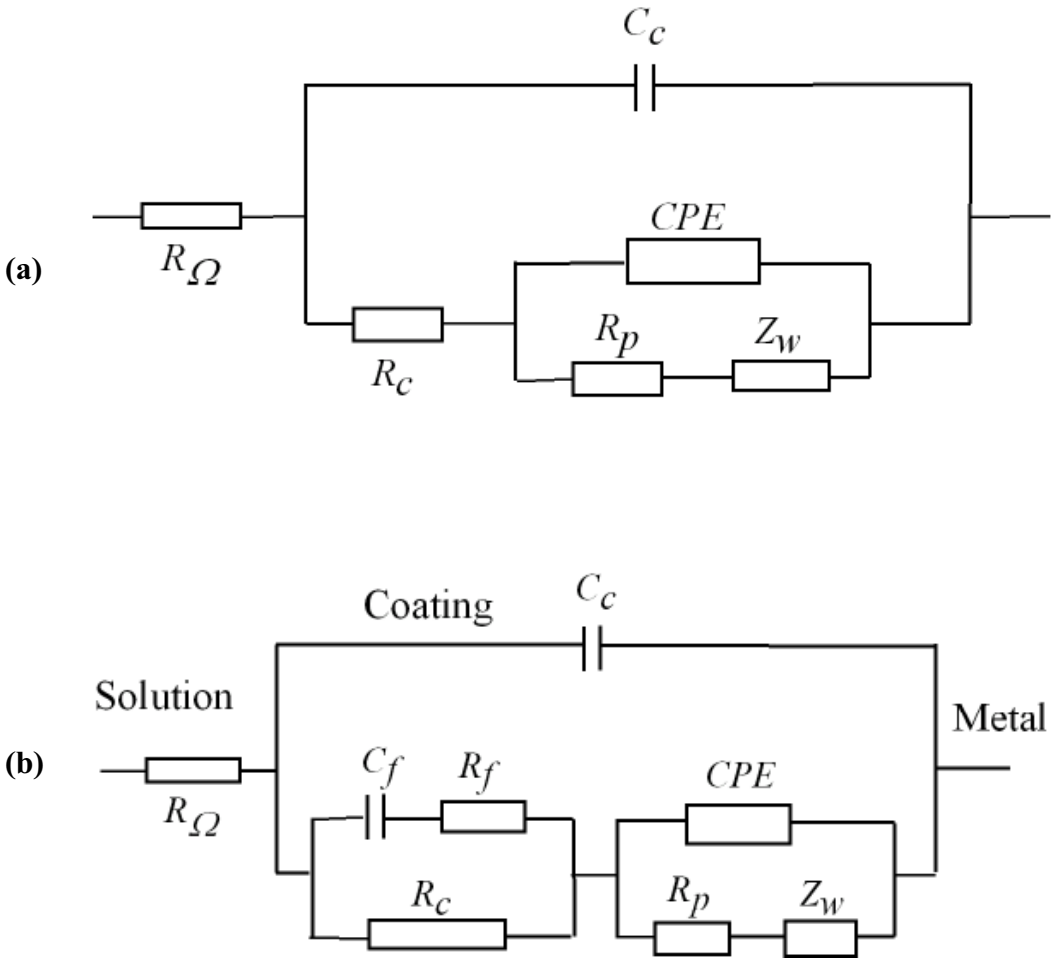

Figure 3.31 The electrical equivalent circuits used to fit the experimental data for (a) pure alkyd paint coatings, and (b) VGCNF-incorporated alkyd paint coatings applied to the surface of mild steel coupons immersed in 3% NaCl solution. R = Ohmic (solution) resistance, C_{dl} = the electrode double layer capacitance, C_c = coating capacitance, R_c = coating pore resistance, R_p = polarization (charge transfer) resistance, Z_w = Warburg diffusional impedance, CPE = constant phase element, R_f = carbon fiber resistance, and C_f = carbon fiber capacitance.

Figure 3.31.a meets the required criteria for a good model for the experimental data (vide infra).

Figure 3.31 shows the equivalent electrical circuit models used to analyze the behavior of the pure (Figure 3.31.a) as well as VGCNF-incorporated (Figure 3.31.b) alkyd paint coatings applied to the surface of mild steel samples immersed in 3% NaCl solution. The elements in these circuits are the Ohmic (solution) resistance (R); the electrode double layer capacitance (C_{dl}); the coating capacitance (C_c); the coating resistance (R_c); the polarization (charge transfer) resistance (R_p); the Warburg diffusional impedance (Z_w); the constant phase element (CPE); the carbon fiber resistance (R_f); and the carbon fiber capacitance (C_f). The values of several system parameters were calculated based on these two equivalent circuit models (vide infra).

Representative experimental EIS data along with the fitted curves for pure as well as VGCNF-incorporated alkyd paint coatings are shown in Figures 3.32 through 3.34. The fitted curves for pure paint coatings correspond to the equivalent circuit in Figure 3.31.a while the modeled spectra for VGCNF-incorporated paint coatings correspond to the equivalent circuit in Figure 3.31.b. As depicted in the figures, the suggested fitting models reproduce fitting spectra that are almost superimposed on the experimental spectra.

Plots of variation of the calculated values of system parameters such as the impedance modulus ($|Z|$), the polarization resistance (R_p), the double layer capacitance (C_{dl}), the coating resistance (R_c), the coating capacitance (C_c), the percent water uptake, the delaminated area (A_d), the VGCNF resistance (R_f), and the VGCNF capacitance (C_f) with exposure time are presented in Figures 3.35 through 3.81.

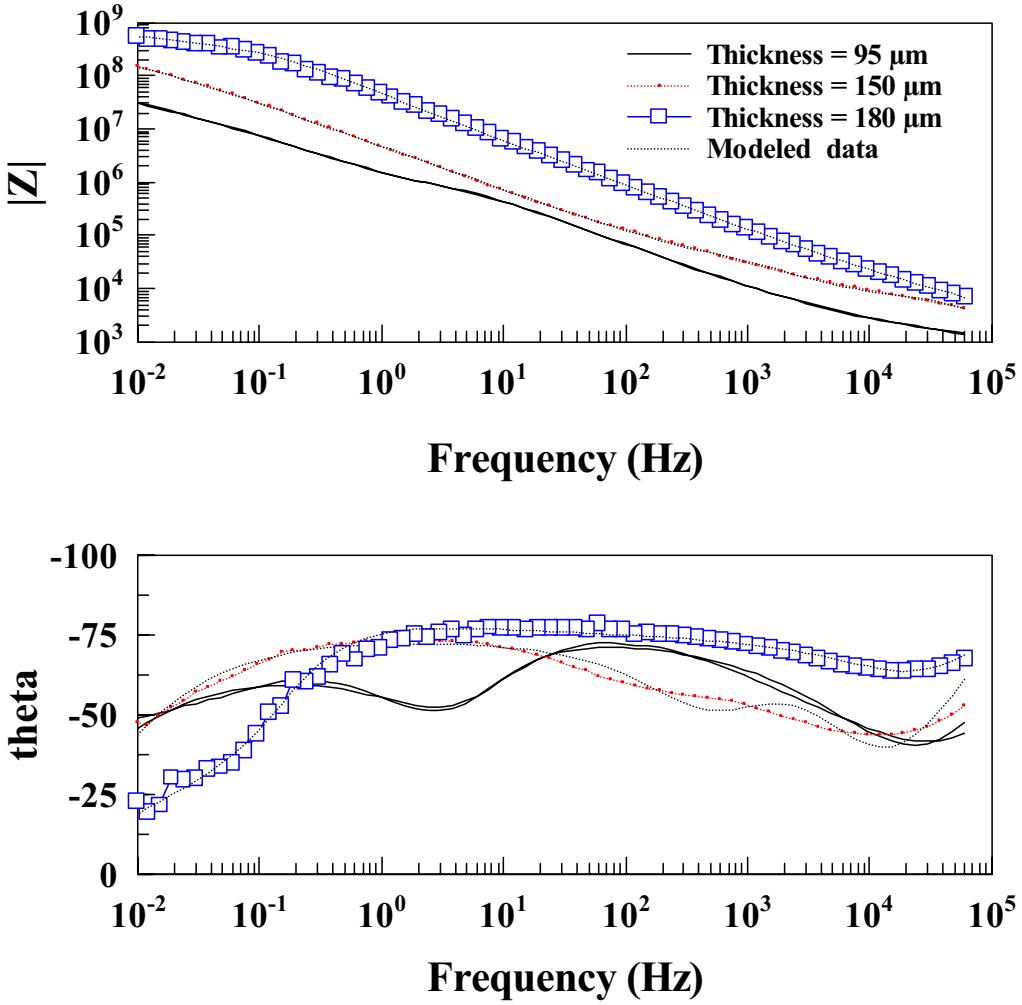

Figure 3.32 Bode (a) and Nyquist (b) plots with fittings for mild steel panels coated with 0.5 wt % VGCNF-incorporated commercial alkyd paint film (with different film thickness) after 100 d of immersion in 3% NaCl solution.

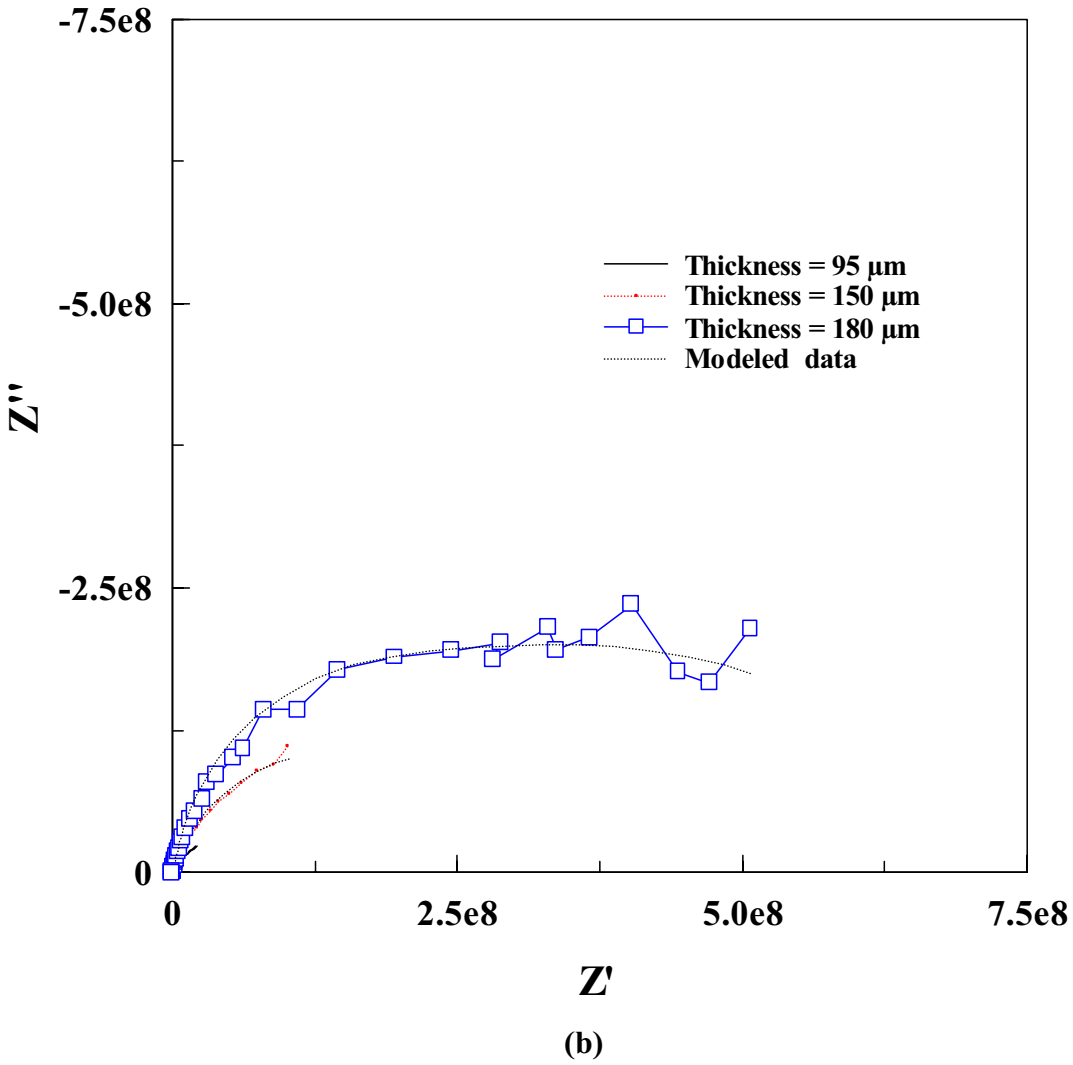

Figure 3.32 Continued.

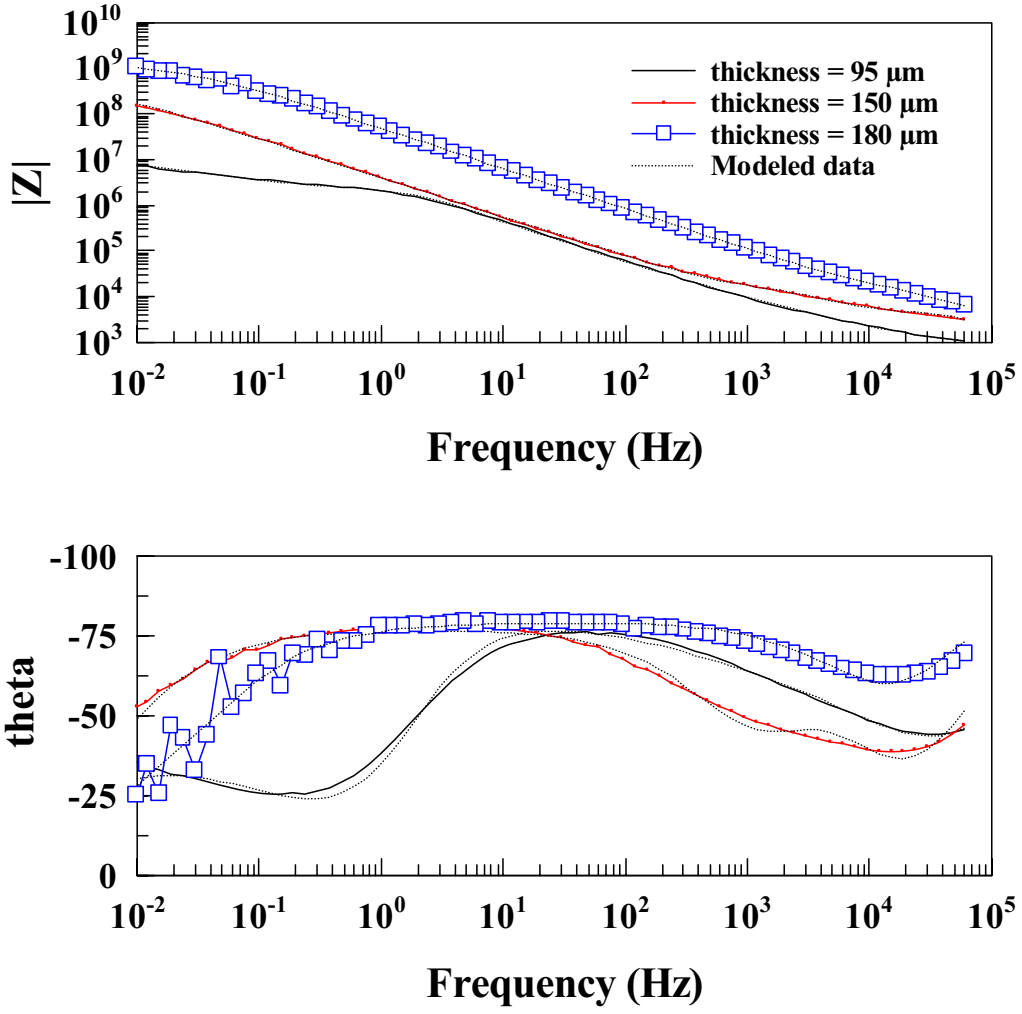

Figure 3.33 Bode (a) and Nyquist (b) plots for mild steel panels coated with 0.5 wt % VGCNF-incorporated commercial alkyd paint films after 500 d of immersion in 3% NaCl solution. The coating thickness is shown in the legend.

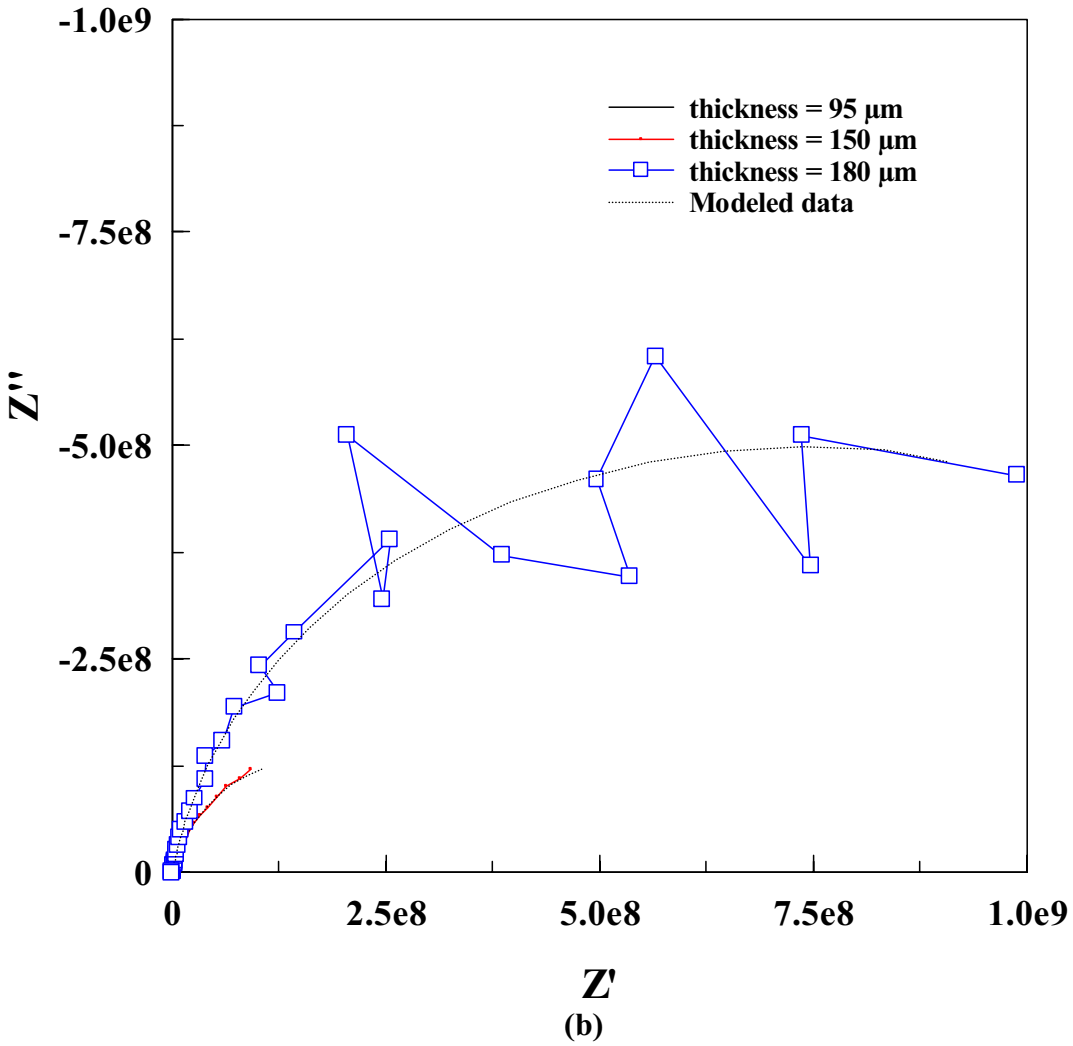

Figure 3.33 Continued.

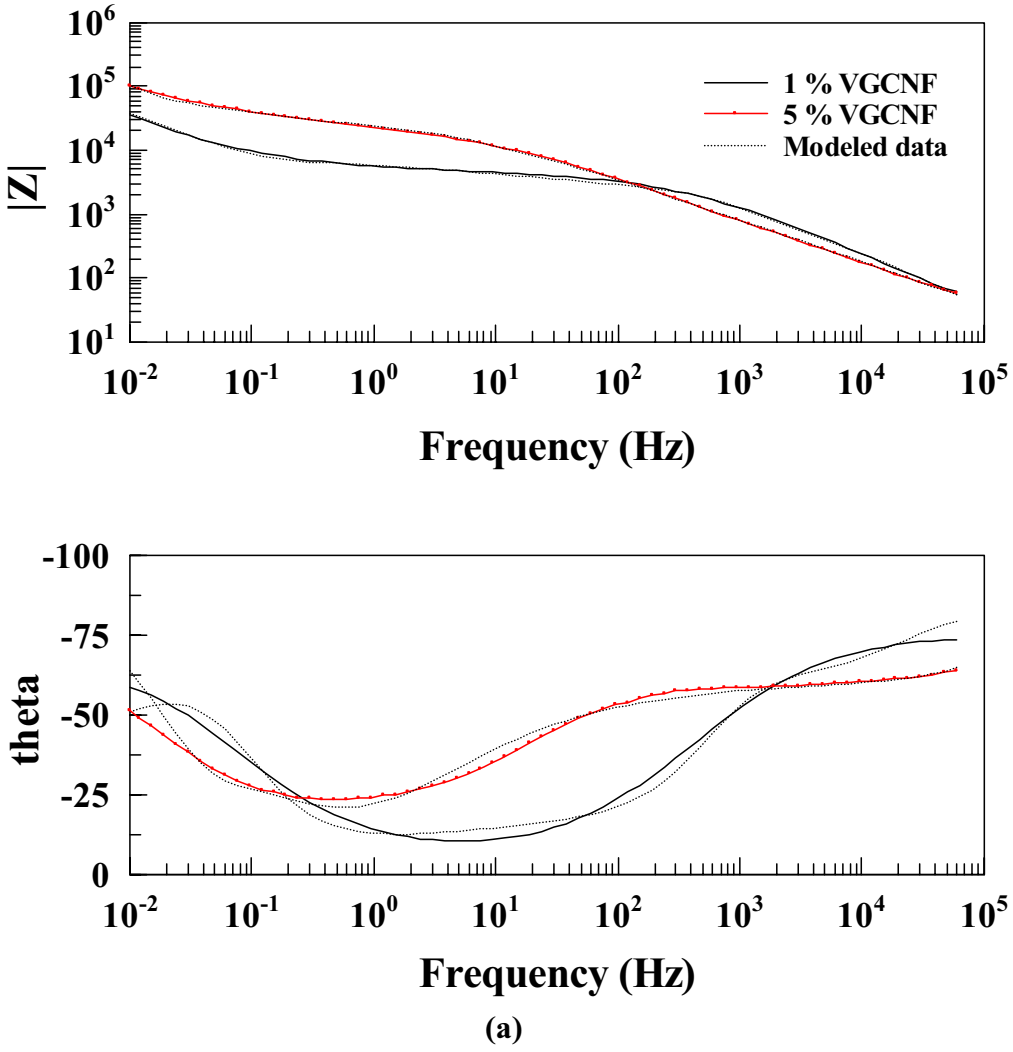

Figure 3.34 Bode (a) and Nyquist (b) plots with fittings for mild steel panels coated with VGCNF-incorporated commercial alkyd paint films (20 μm thick) after 18 d of immersion in 3% NaCl solution. The VGCNF loading is shown in the legend.

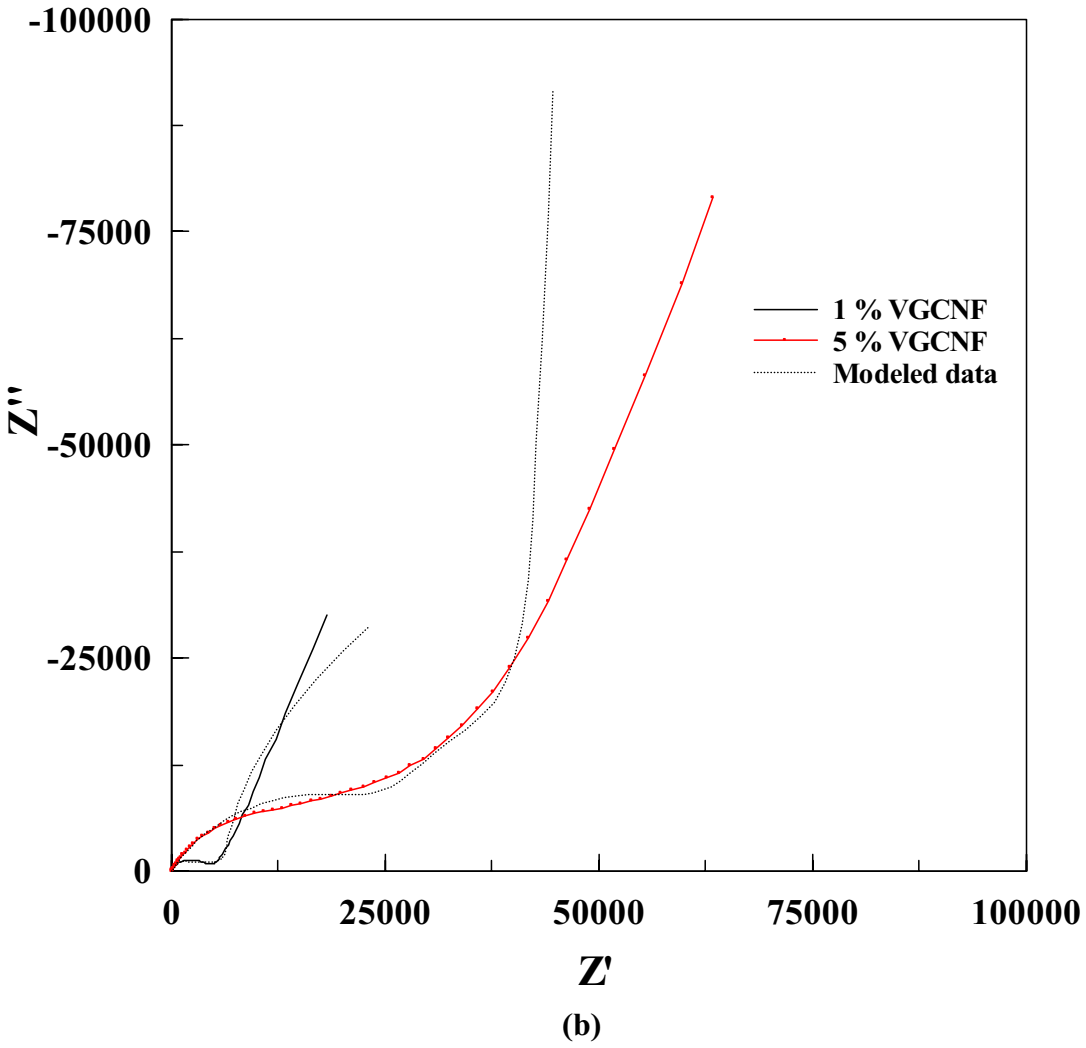

Figure 3.34 Continued.

3.3.5 Total Impedance (|*Z*|) Measurements

Representative plots of |*Z*| vs. immersion time are shown in Figures 3.35 through 3.41 for both pure and VGCNF-incorporated paint coatings with different film thicknesses. Traditionally, the impedance values in these plots are the measured |*Z*| values at the minimum frequency. These |*Z*| values are usually the maximum impedance values in the Bode plots. The data depicted in Figures 3.35 through 3.41 show the |*Z*| values measured at 1.0×10^{-2} Hz. The data show high |*Z*| values for all coatings upon initial immersion in the NaCl solution in the range of 10^6 to 10^9 Ω which decrease with immersion time due to the degradation of the coating film in the corrosive solution. These results are consistent with those in the literature.[57, 88-95]

Examining Figures 3.35 through 3.38 clearly shows that the thicker the coating film, the higher the impedance is and hence the more protective the film is. These results are also consistent with the literature.[96] In addition, the results also show that for thick paint coatings with or without VGCNF with a thickness of 95 μm or above, the coating impedance is at least 10^7 Ω (Figures 3.35 and 3.36) over an immersion period of 800 d. Moreover, a close look at Figures 3.41 shows that, at constant coating thickness, the impedance data for paint coatings containing 5 and 10% VGCNF are almost the same and stable for a long immersion period (600 d) indicating that there is a threshold VGCNF mass percent above which the |*Z*| value does not appreciably increase with increasing the fiber loading.

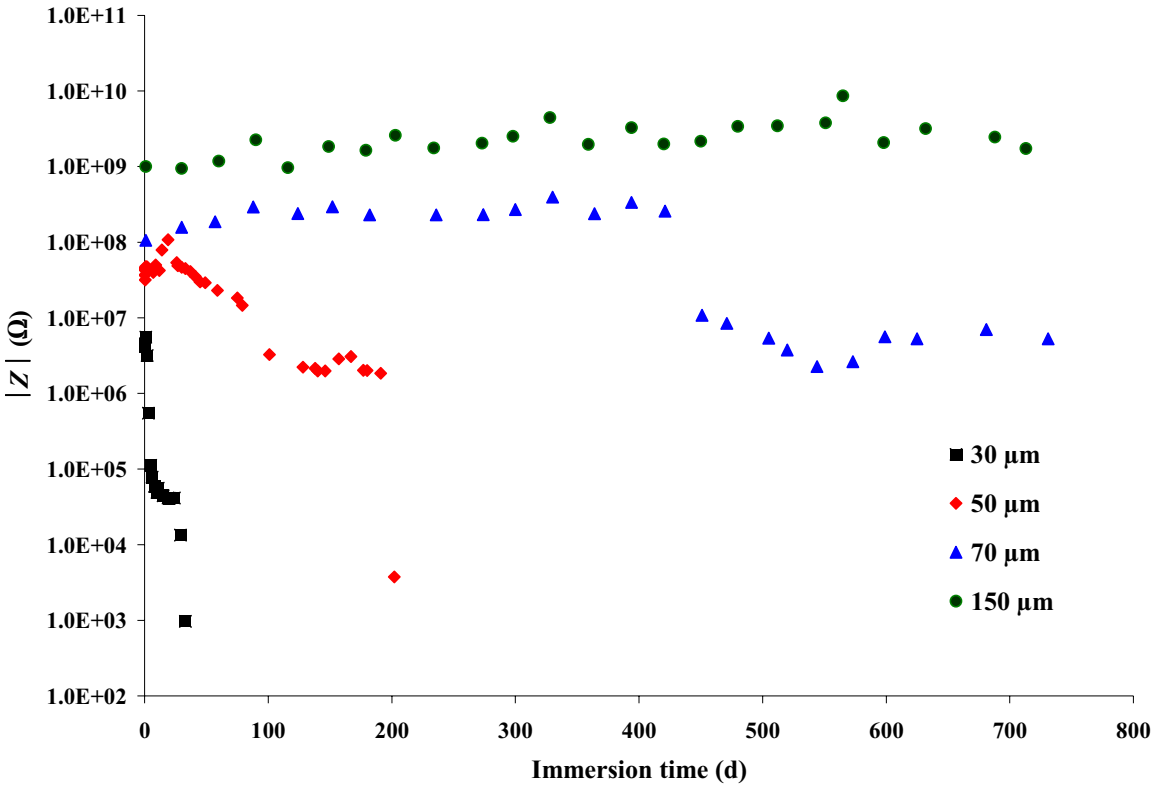

Figure 3.35 Variation of the absolute impedance ($|Z|$), measured at 1.0×10^{-2} Hz, with immersion time for mild steel panels coated with a pure commercial alkyd paint film and exposed to 3% NaCl solution. ◆ = 30 µm, ■ = 50 µm, ▲ = 70 µm, and ● = 150 µm.

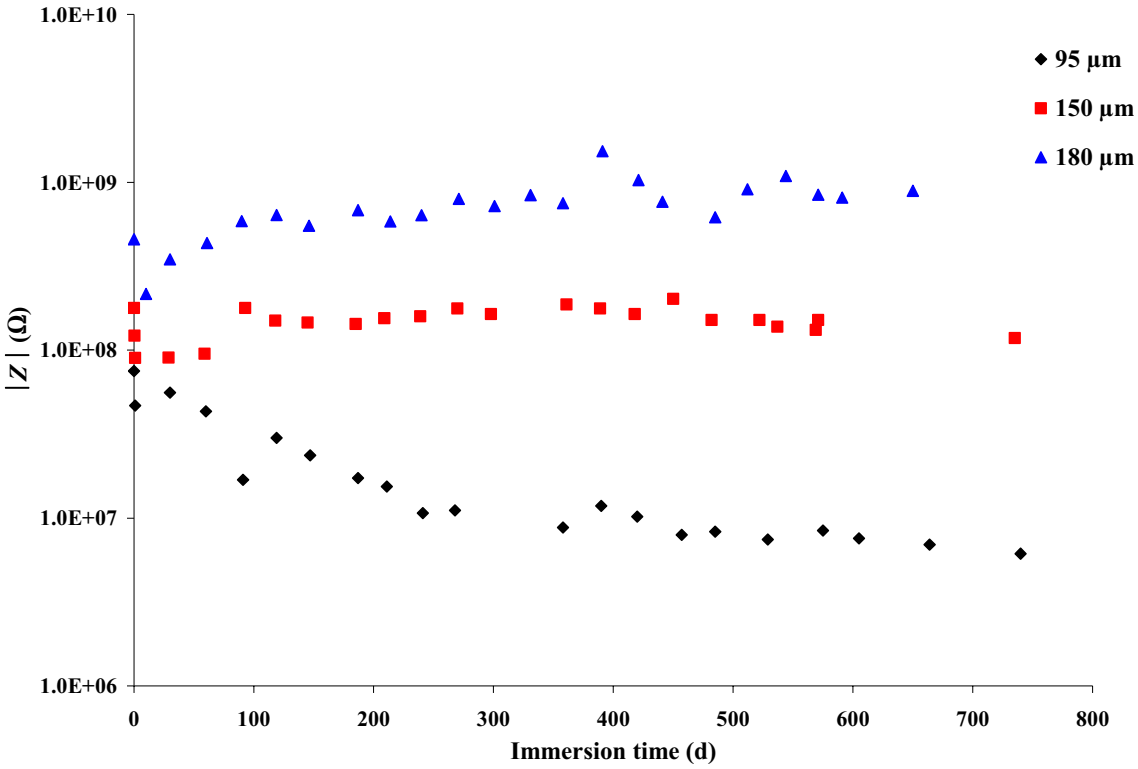

Figure 3.36 Variation of the absolute impedance ($|Z|$), measured at 1.0×10^{-2} Hz, with immersion time for mild steel panels coated with a commercial alkyd paint film containing 0.5 wt % VGCNF and exposed to 3% NaCl solution.
◆ = 95 µm, ■ = 150 µm, and ▲ = 180 µm.

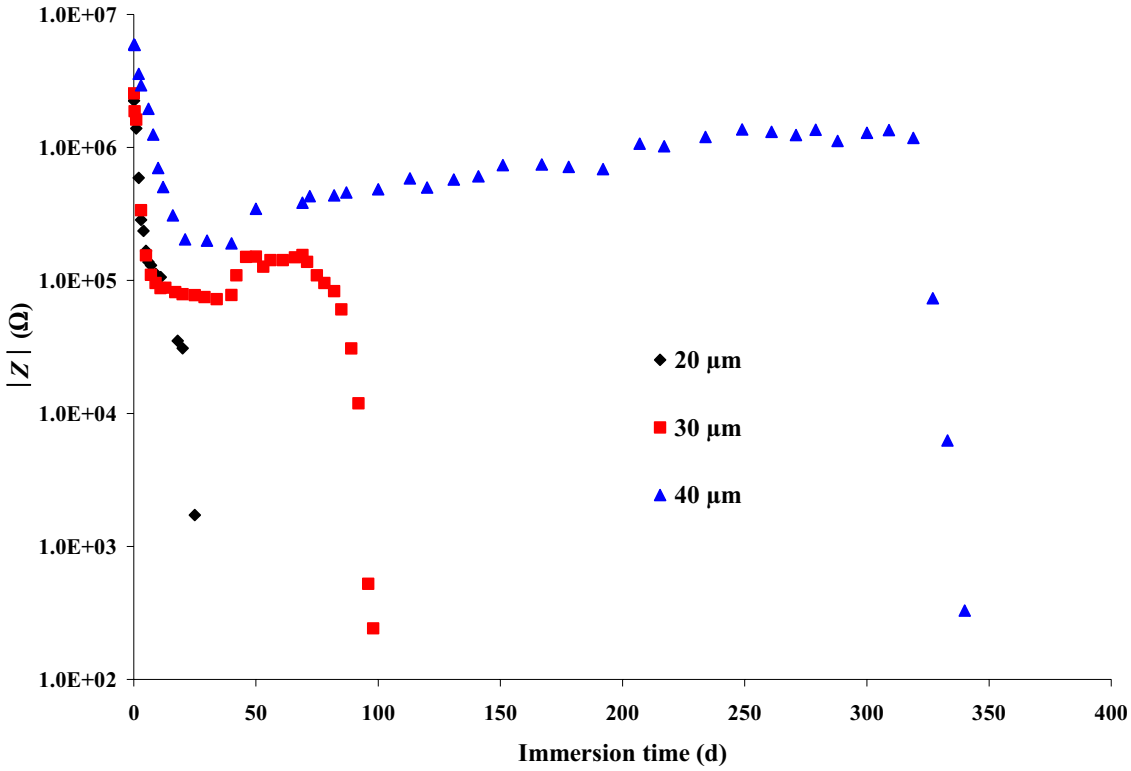

Figure 3.37 Variation of the absolute impedance ($|Z|$), measured at 1.0×10^{-2} Hz, with immersion time for mild steel panels coated with a commercial alkyd paint film containing 1 wt % VGCNF and exposed to 3% NaCl solution.

◆ = 20 µm, ■ = 30 µm, and ▲ = 40 µm.

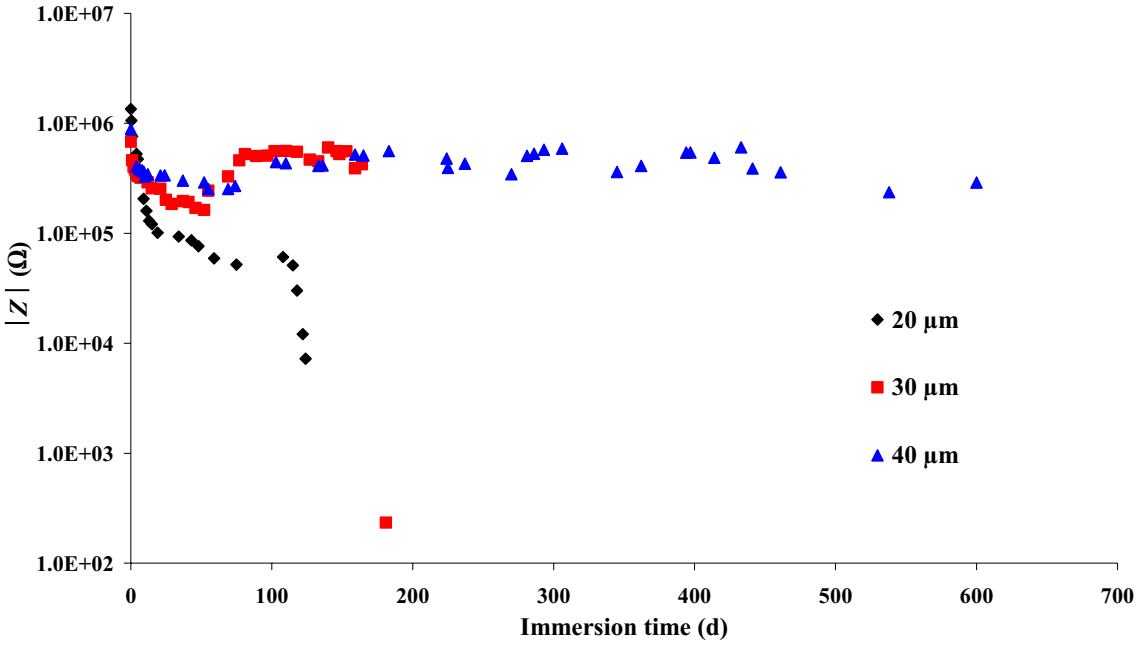

Figure 3.38 Variation of the absolute impedance ($|Z|$), measured at 1.0×10^{-2} Hz, with immersion time for mild steel panels coated with a commercial alkyd paint film containing 5 wt % VGCNF and exposed to 3% NaCl solution.

◆ = 20 µm, ■ = 30 µm, and ▲ = 40 µm.

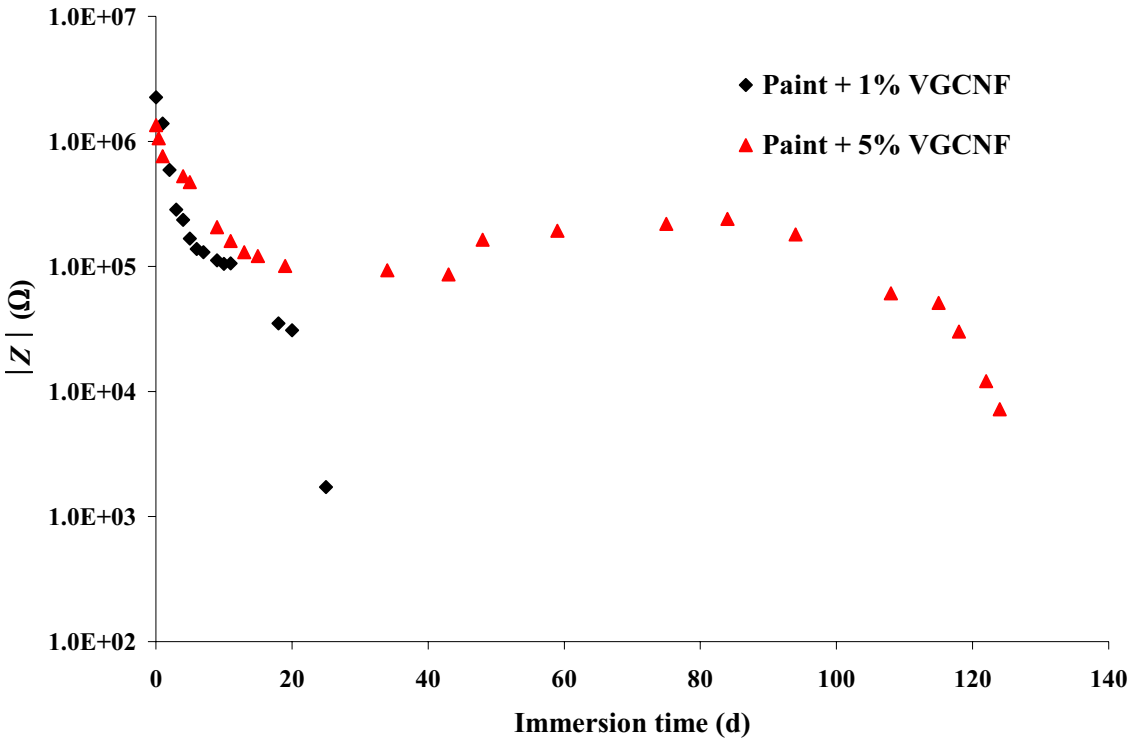

Figure 3.39 Variation of the absolute impedance ($|Z|$), measured at 1.0×10^{-2} Hz, with immersion time for mild steel panels coated with a VGCNF-incorporated commercial alkyd paint film (20 μm thick) and exposed to 3% NaCl solution. ◆ = paint + 1% VGCNF, and ▲ = paint + 5% VGCNF.

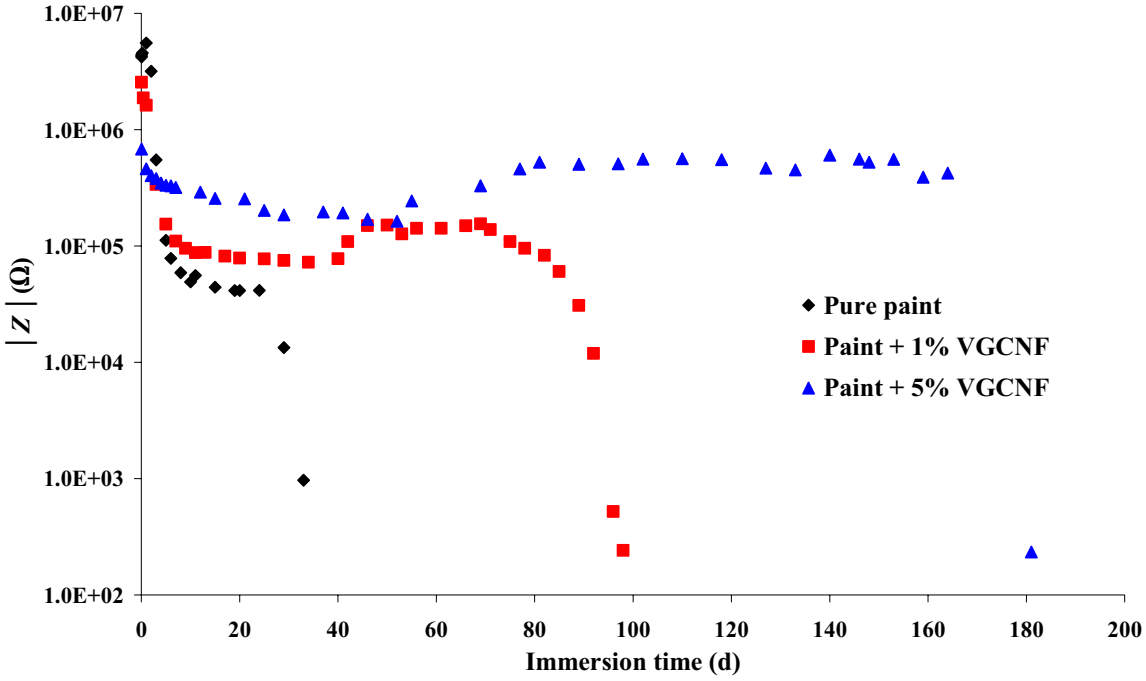

Figure 3.40 Variation of the absolute impedance ($|Z|$), measured at 1.0×10^{-2} Hz, with immersion time for mild steel panels coated with a VGCNF-incorporated commercial alkyd paint film (30 μm thick) and exposed to 3% NaCl solution. ◆ = pure paint, ■ = paint + 1% VGCNF, and ▲ = paint + 5% VGCNF.

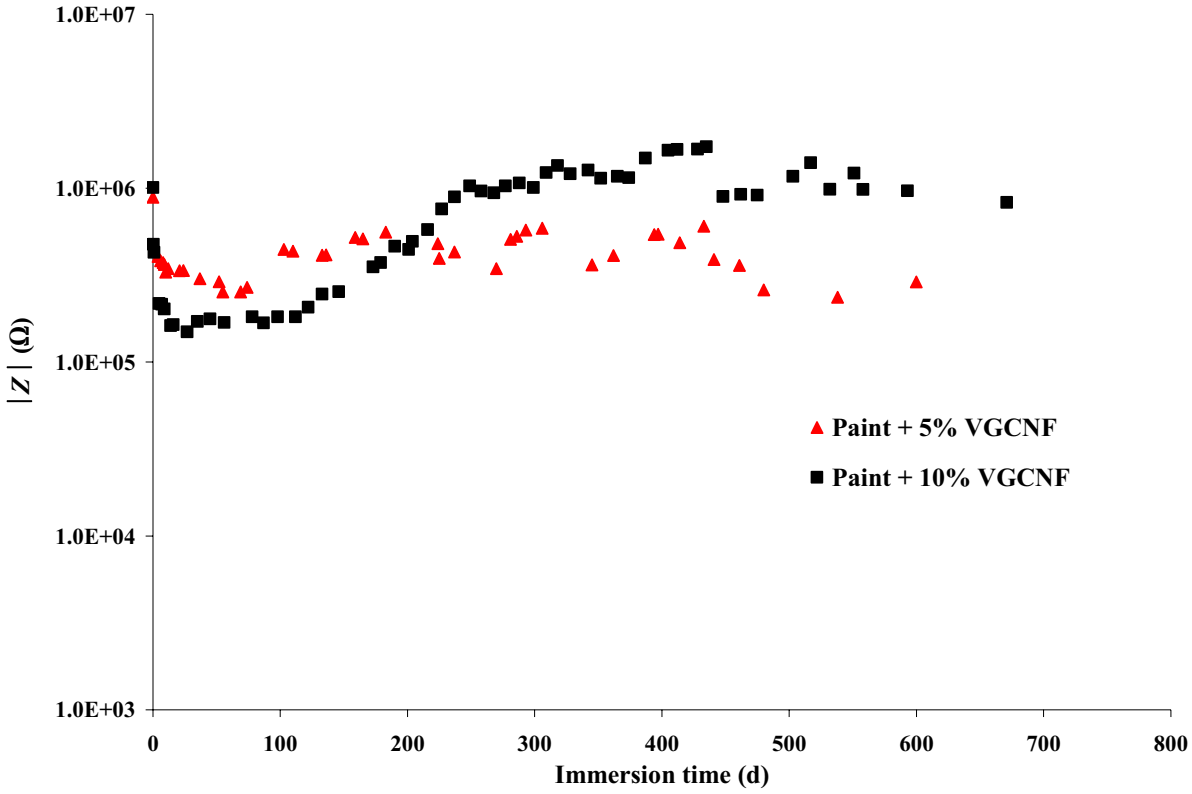

Figure 3.41 Variation of the absolute impedance ($|Z|$), measured at 1.0×10^{-2} Hz, with immersion time for mild steel panels coated with a VGCNF-incorporated commercial alkyd paint film (45 μm thick) and exposed to 3% NaCl solution. ■ = paint + 5% VGCNF, and ▲ = paint + 10% VGCNF.

3.3.6 Polarization Resistance (R_p) Measurements

The polarization resistance (R_p), also known as the charge transfer resistance (R_{ct}), is the resistance between the reference and working electrodes. R_p is one of the important parameters used in the characterization of any electrochemical system under corrosion. It should be mentioned that R_p is inversely proportional to the rate of corrosion and the rate of corrosion is directly proportional to the corrosion current (i_{corr}). According to Stern and Geary, corrosion currents (and hence corrosion rates) can be calculated from the values of R_p as:[97, 98]

$$i_{corr} = K/R_p \tag{3.1}$$

where K is a constant. R_p is determined from the low frequency limit of the real part of the Nyquist plot (vide supra).

Figures 3.42 through 3.47 show the variation of R_p with immersion time for mild steel coupons spin-coated with VGCNF-incorporated commercial alkyd paint with different thicknesses and VGCNF loadings. As shown in the figures, for all of the tested coatings, the initial R_p values are high (in the range of 10^6 to 10^{11} Ω) and decrease with immersion time. The relatively high initial R_p values imply that the coatings are initially largely intact and stable. However, as the immersion time increases, defects and pores in the coating initiate and grow in number and size. The growth of these active sites is accompanied by significant decrease in the R_p of the system and hence an increase in the corrosion rate. This interpretation is confirmed by the visual inspection of the specimens at the end of the exposure period to the aggressive NaCl solution. The visual inspection showed a roughened surface, with localized cracks, holes, and corrosion products on the coating surface in addition to rust formation underneath the coating due to the loss of

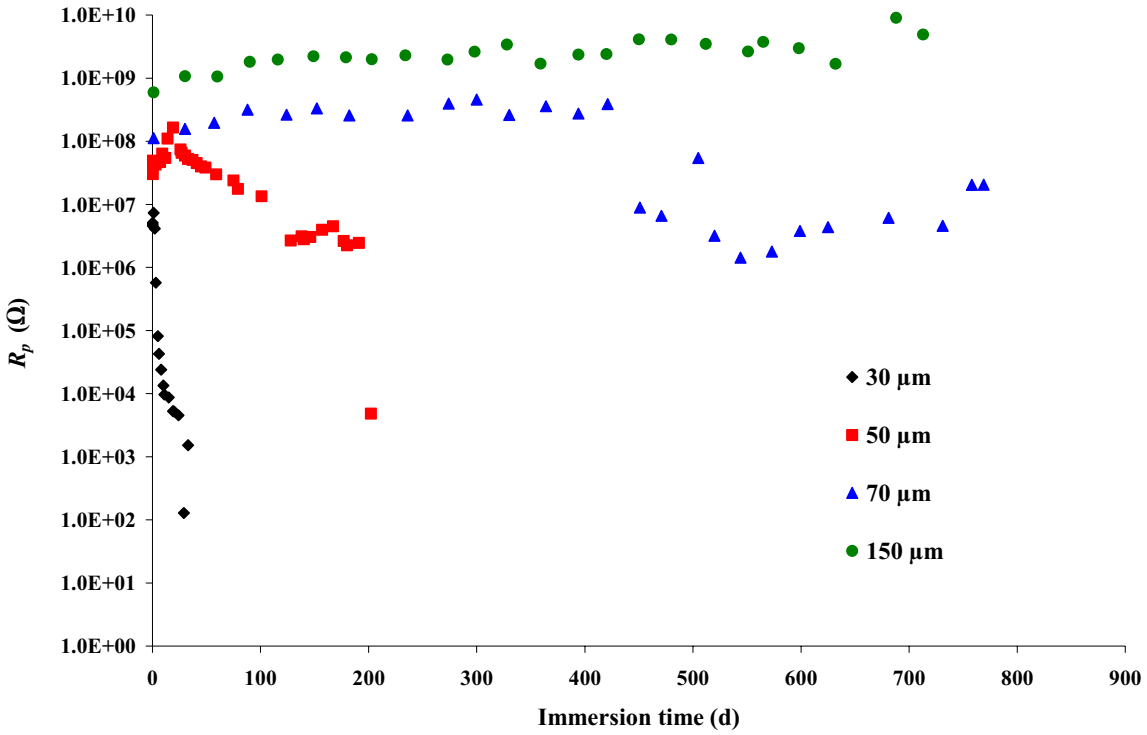

Figure 3.42 Variation of the polarization resistance (R_p) with immersion time for mild steel panels coated with a pure commercial alkyd paint film and exposed to 3% NaCl solution. ◆ = 30 µm, ■ = 50 µm, ▲ = 70 µm, and ● = 150 µm.

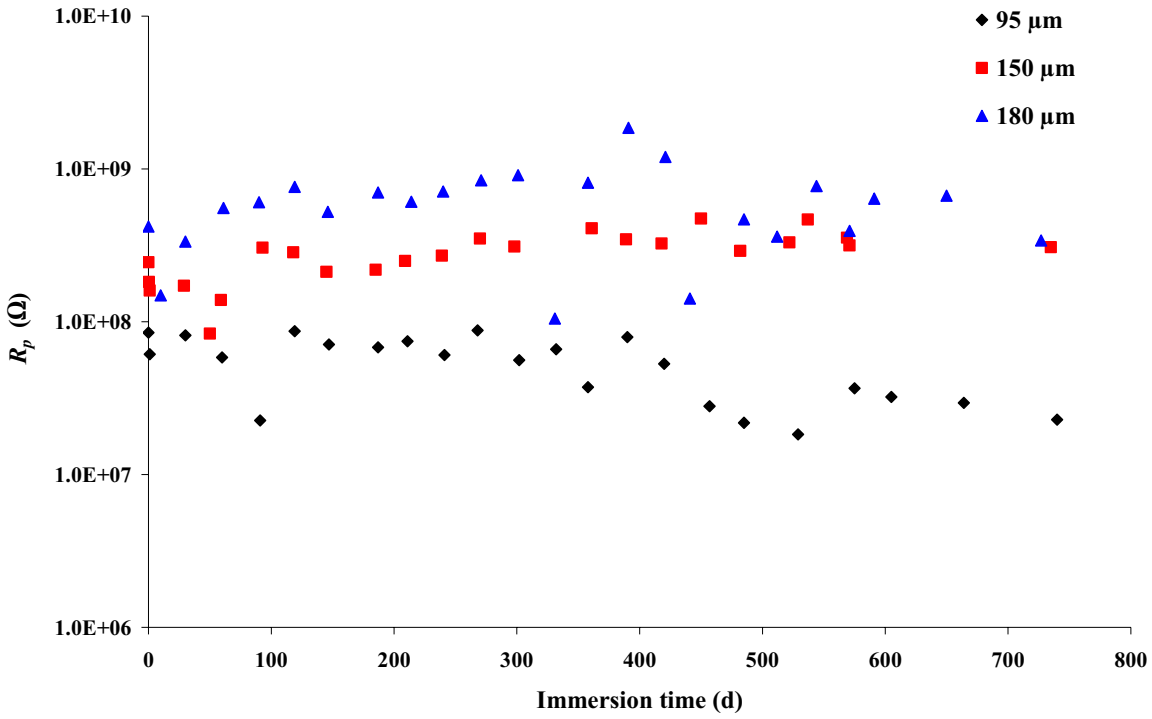

Figure 3.43 Variation of the polarization resistance (R_p) with immersion time for mild steel panels coated with a commercial alkyd paint film containing 0.5 wt % VGCNF in 3% NaCl solution. ◆ = 95 µm, ■ = 150 µm, and ▲ = 180 µm.

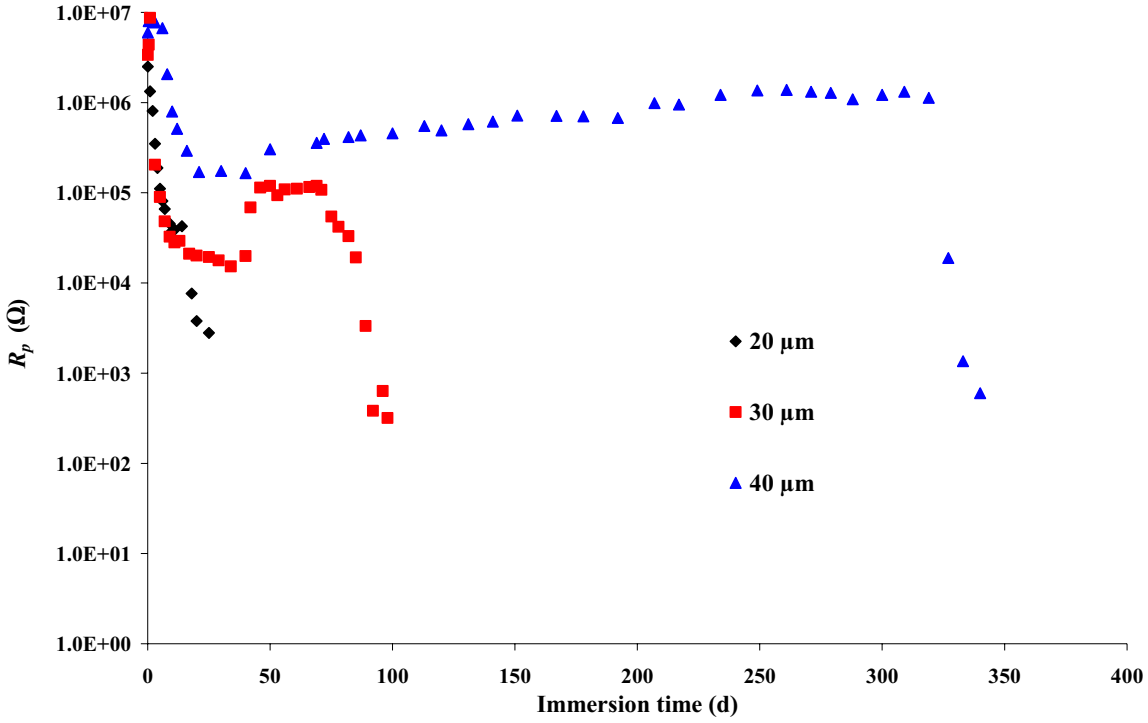

Figure 3.44 Variation of the polarization resistance (R_p) with immersion time for mild steel panels coated with a commercial alkyd paint film containing 1 wt % VGCNF in 3% NaCl solution. ◆ = 20 µm, ■ = 30 µm, and ▲ = 40 µm.

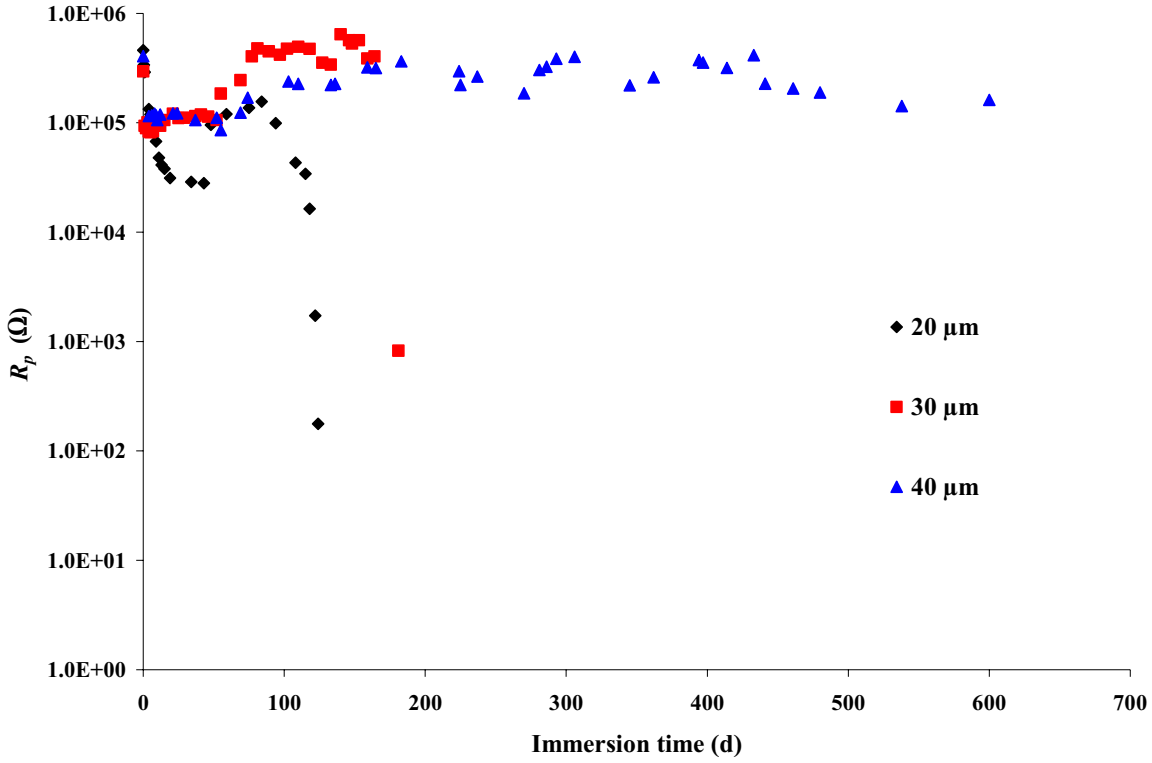

Figure 3.45 Variation of the polarization resistance (R_p) with immersion time for mild steel panels coated with a commercial alkyd paint film containing 5 wt % VGCNF in 3% NaCl solution. ◆ = 20 µm, ■ = 30 µm, and ▲ = 40 µm.

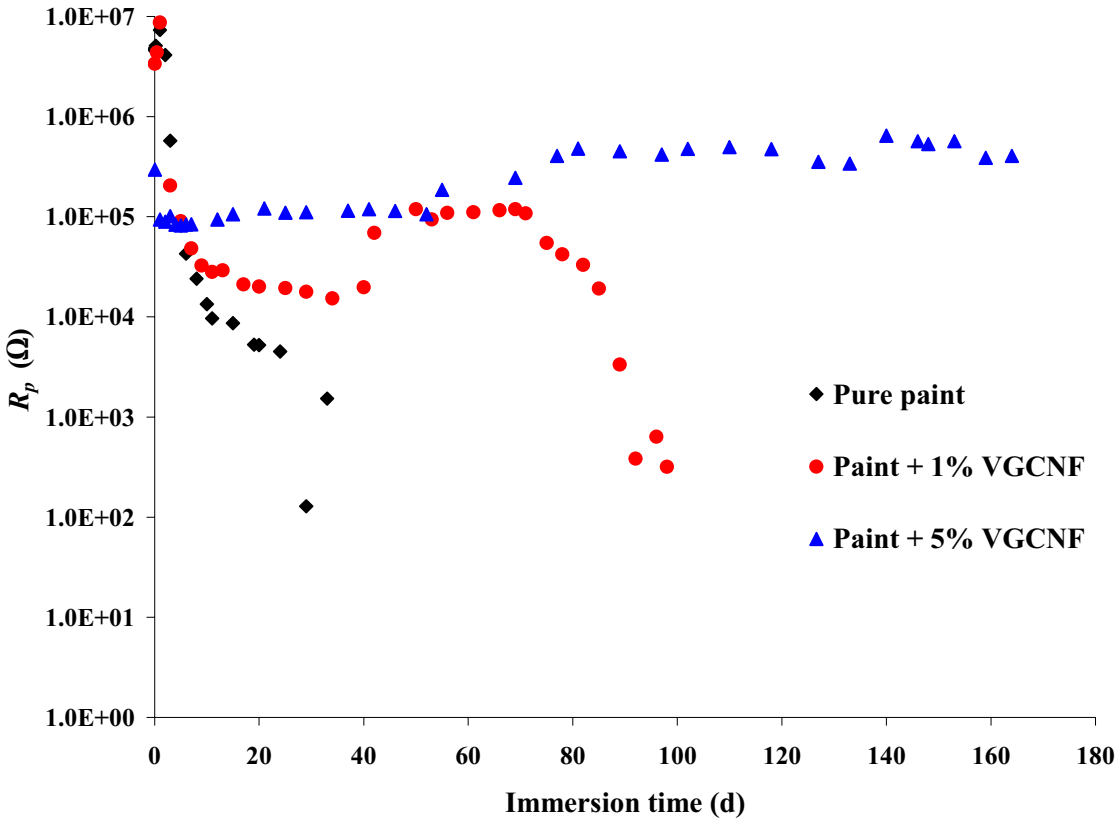

Figure 3.46 Variation of the polarization resistance (R_p) with immersion time for mild steel panels coated with a VGCNF-incorporated commercial alkyd paint film (30 μm thick) and exposed to 3% NaCl solution. ◆ = pure paint, ● = paint + 1% VGCNF, and ▲ = paint + 5% VGCNF.

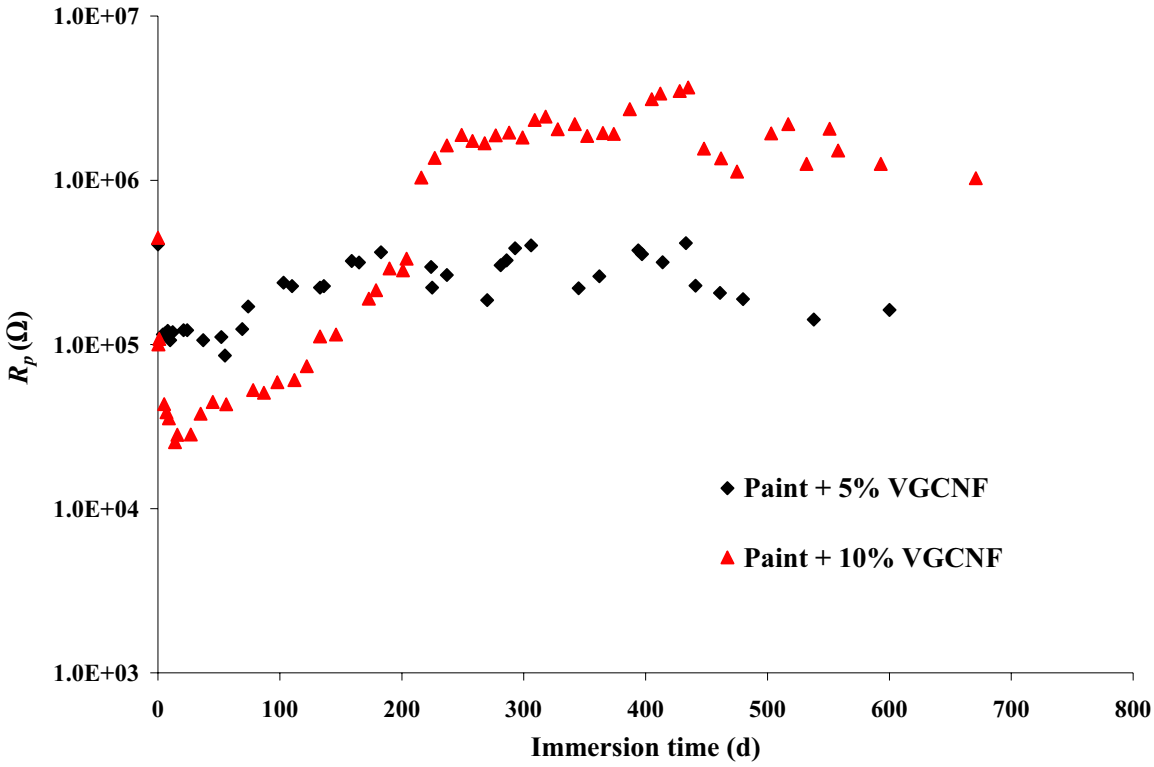

Figure 3.47 Variation of the polarization resistance (R_p) with immersion time for mild steel panels coated with a VGCNF-incorporated commercial alkyd paint film (45 μm thick) and exposed to 3% NaCl solution. ◆ = paint + 5% VGCNF, and ▲ = paint + 10% VGCNF.

adherence of the coating to the substrate. Additional confirmation of the coating failure was provided by the measurement of the OCP at the end of the exposure time. The OCP values were close to -600 mV (vs. SCE) as shown in the regular OCP measurements (vide supra).

The data depicted in Figures 3.42 through 3.45 show that, for film coatings having the same weight percent of VGCNF, the thicker the coating film, the higher the initial R_p value and the slower the rate of decrease in R_p with immersion time and hence the longer the time needed for the coating film to breakdown. In addition, the data show that the steepest decrease in R_p, and the fastest corrosion rate occurs for the pure coatings with thin film thicknesses (< 50 μm). This denotes a fast diffusion of the electrolyte into these pure coatings and hence a fast degradation of the paint films.

For thick coating films containing high VGCNF content, the results shown in Figures 3.43 through 3.47 indicate that there is an initial decrease in R_p (in the first 10 d of immersion) followed by a plateau for a long period of immersion, then followed by a sudden decrease of R_p indicating the film breakdown. Moreover, Figure 3.46 shows that the incorporation of the VGCNF, even for samples with a coating thickness as small as 30 μm, increases the lifetime of the coating film and consequently improves the protection properties of the coating. The results shown in Figures 3.45 and 3.47 also depict that after ~ 700 d of immersion in NaCl solution, thick paint coatings (≥ 40 μm) containing 5 and 10% VGCNFs are still stable and protective with R_p values almost constant.

3.3.7 Double-Layer Capacitance (C_{dl}) Measurements

The double-layer capacitance (C_{dl}) at the electrolyte/metal substrate is another factor that reflects the barrier properties of an organic coating. The values of C_{dl} are taken as a measure of the area over which the coating has disbonded.[53] Figures 3.48 through 3.53 show the variation of C_{dl} with the immersion time for some coating systems with different thicknesses and wt % of VGCNF. The increase in C_{dl} with immersion time indicates an increase of the disbonded area (wet area) over the mild steel surface under the coating.[52]

As shown in Figures 3.48 through 3.53, for all of the tested coatings, the initial C_{dl} values are low (as low as 1.0×10^{-10} F/cm^2) and increases with immersion time. The relatively low initial C_{dl} values imply that the coatings are initially largely bonded to the substrate surface. However, as the immersion time increases the values of C_{dl} increase for a short period of time, denoting the entry of the electrolyte into the paint coating. After that initial period of increase, the value of C_{dl} remain unchanged for the long exposure time until the film finally fails and corrosion occurs at the steel substrate surface and the value of C_{dl} increases rapidly. It can also be noted that the thicker the coating film, the lower the initial value of the C_{dl} indicating a good protective film with greater corrosion stability (see Figures 3.48 through 3.50). On the other hand, the data shows that during the first few days (1-3 d) of immersion, coatings containing VGCNF show an increase in the C_{dl} values. However, after this initial period, the value of C_{dl} decreases to a stable value and remains unchanged for a long period of immersion in the corrosive solution (Figures 3.52 and 3.53). These results are also in good agreement with the R_p measurements (vide supra).

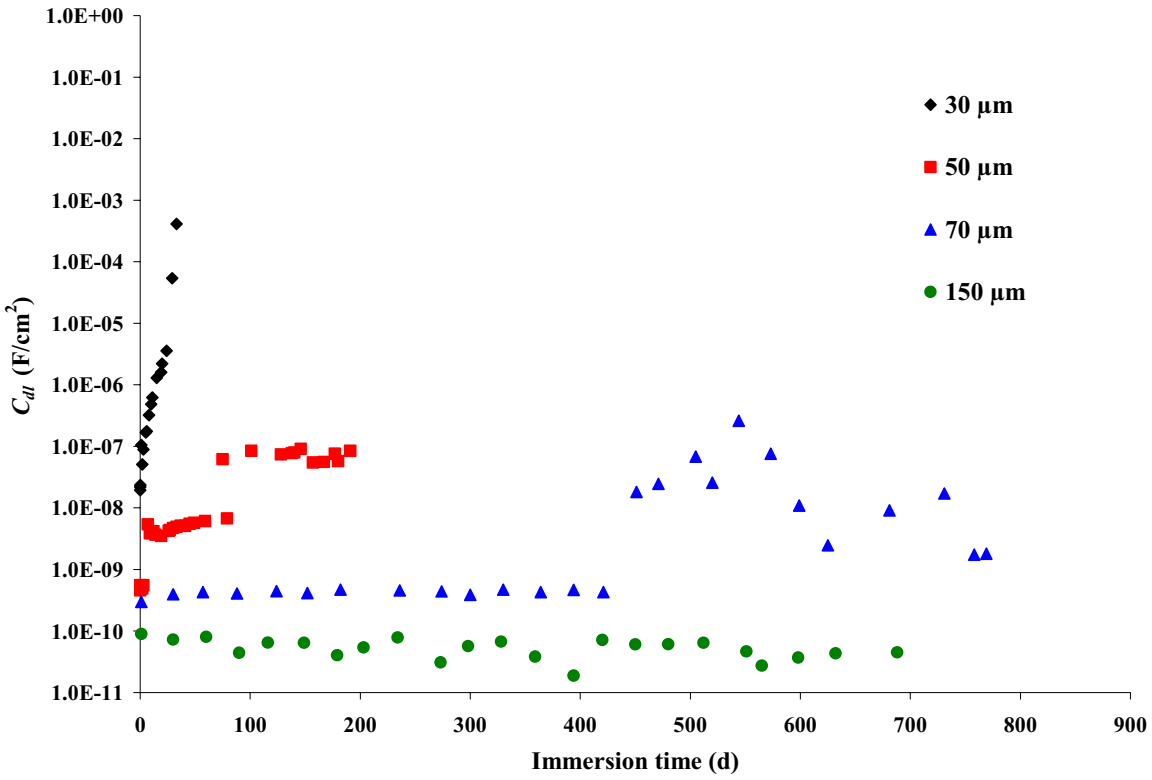

Figure 3.48 Variation of the double layer capacitance (C_{dl}) with immersion time for mild steel panels coated with a pure commercial alkyd paint film and exposed to 3% NaCl solution. ◆ = 30 µm, ■ = 50 µm, ▲ = 70 µm, and ● = 150 µm.

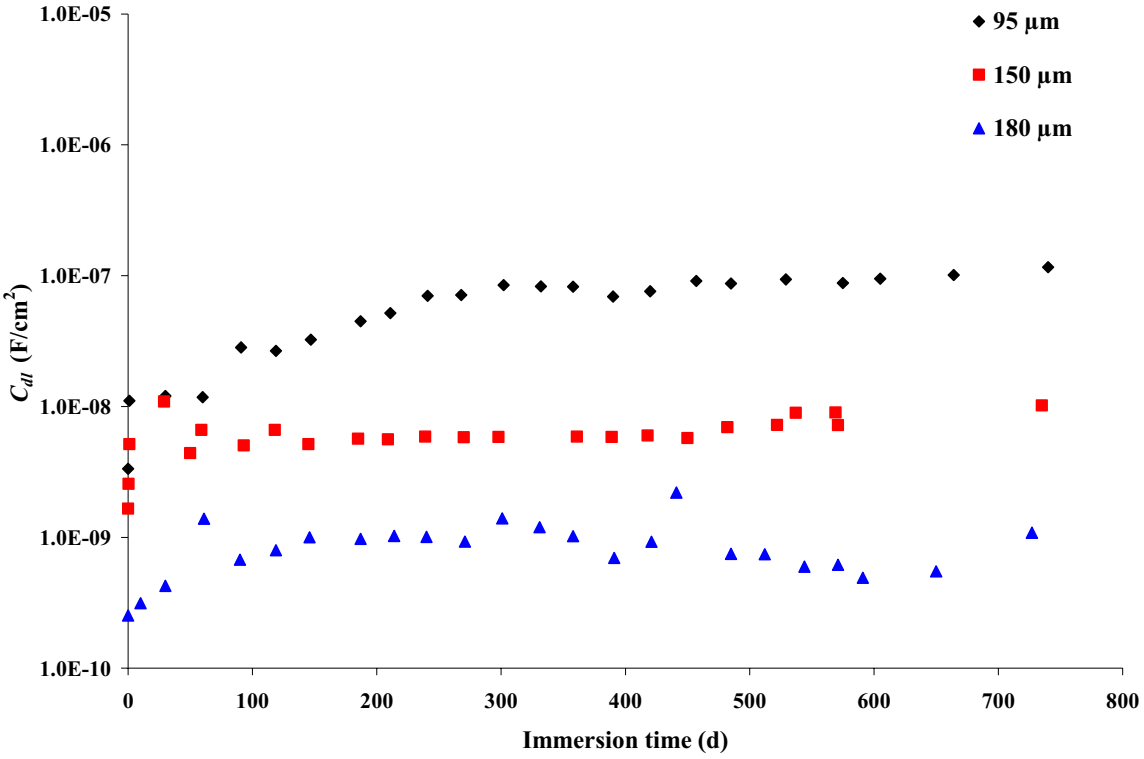

Figure 3.49 Variation of the double layer capacitance (C_{dl}) with immersion time for mild steel panels coated with a commercial alkyd paint film containing 0.5 wt % VGCNF in 3% NaCl solution. ◆ = 95 µm, ■ = 150 µm, and ▲ = 180 µm.

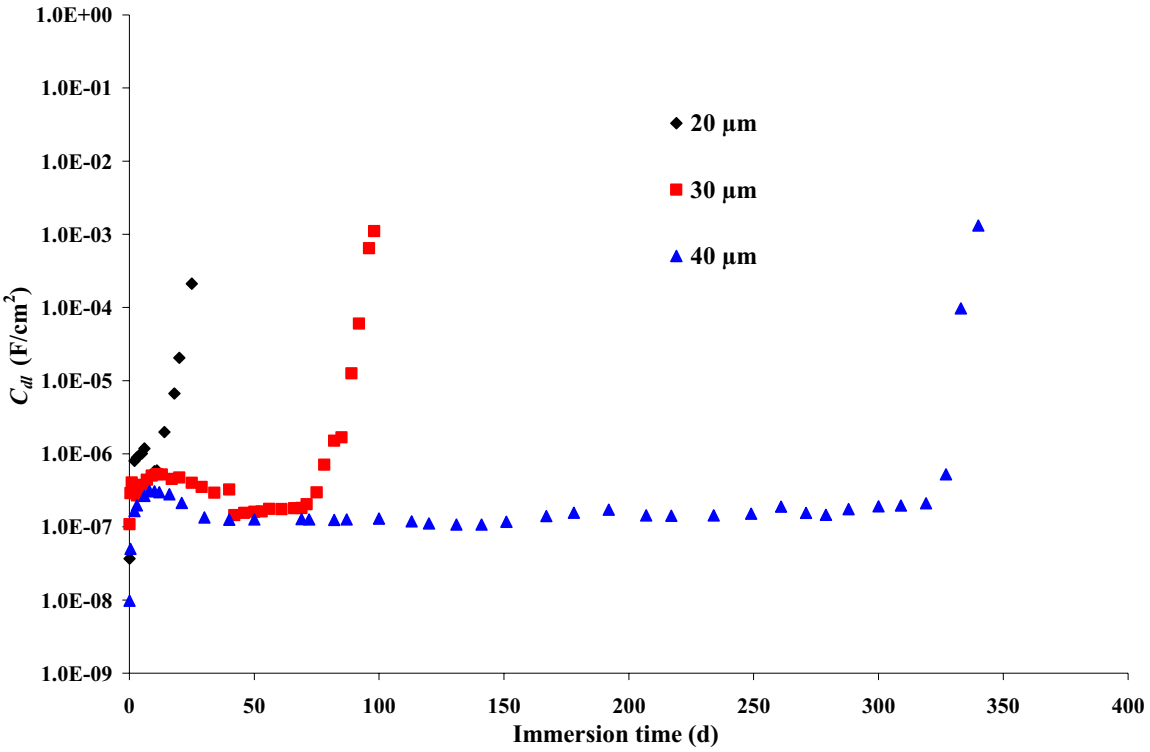

Figure 3.50 Variation of the double layer capacitance (C_{dl}) with immersion time for mild steel panels coated with a commercial alkyd paint film containing 1 wt % VGCNF in 3% NaCl solution. ◆ = 20 µm, ■ = 30 µm, and ▲ = 40 µm.

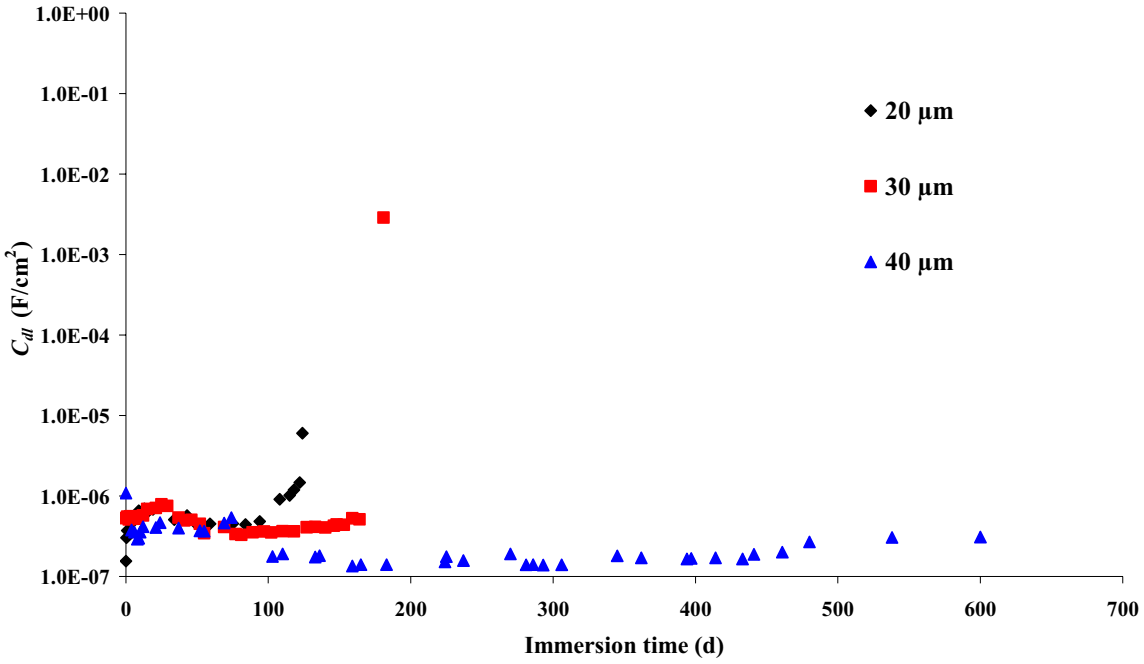

Figure 3.51 Variation of the double layer capacitance (C_{dl}) with immersion time for mild steel panels coated with a commercial alkyd paint film containing 5 wt % VGCNF in 3% NaCl solution. ◆ = 20 µm, ■ = 30 µm, and ▲ = 40 µm.

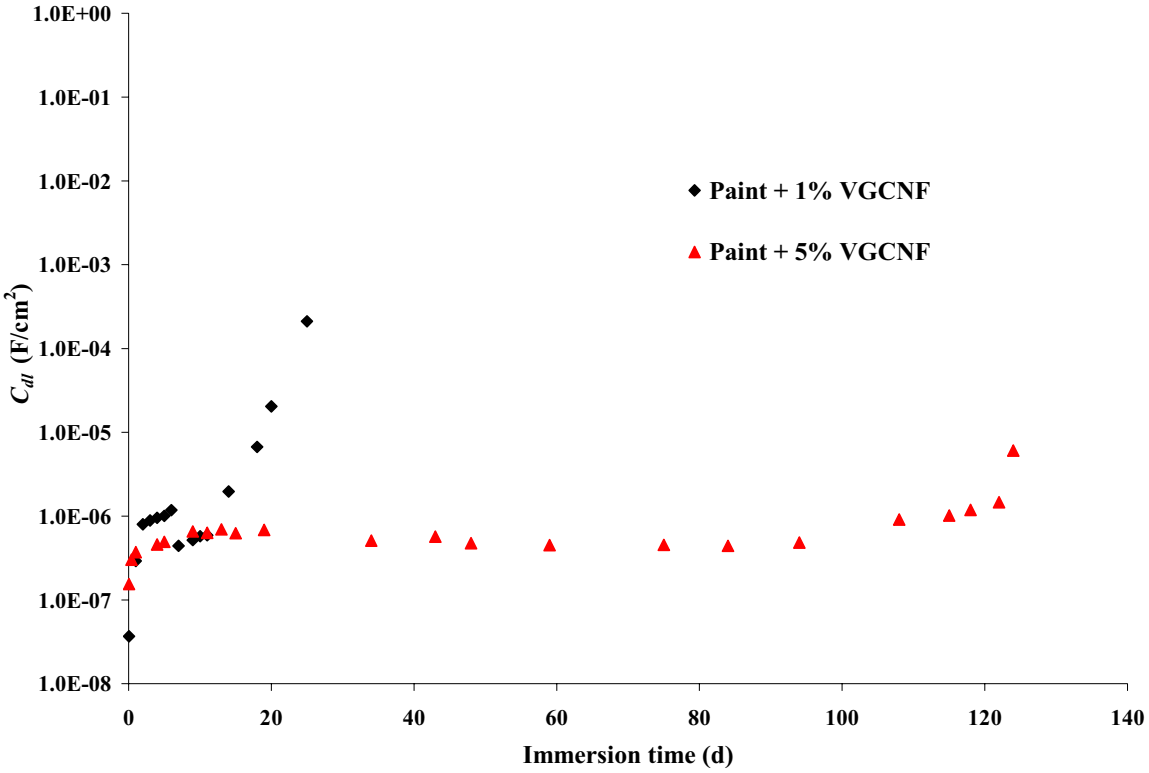

Figure 3.52 Variation of the double layer capacitance (C_{dl}) with immersion time for mild steel panels coated with a VGCNF-incorporated commercial alkyd paint film (20 μm thick) and exposed to 3% NaCl solution. ◆ = paint + 1% VGCNF, and ▲ = paint + 5% VGCNF.

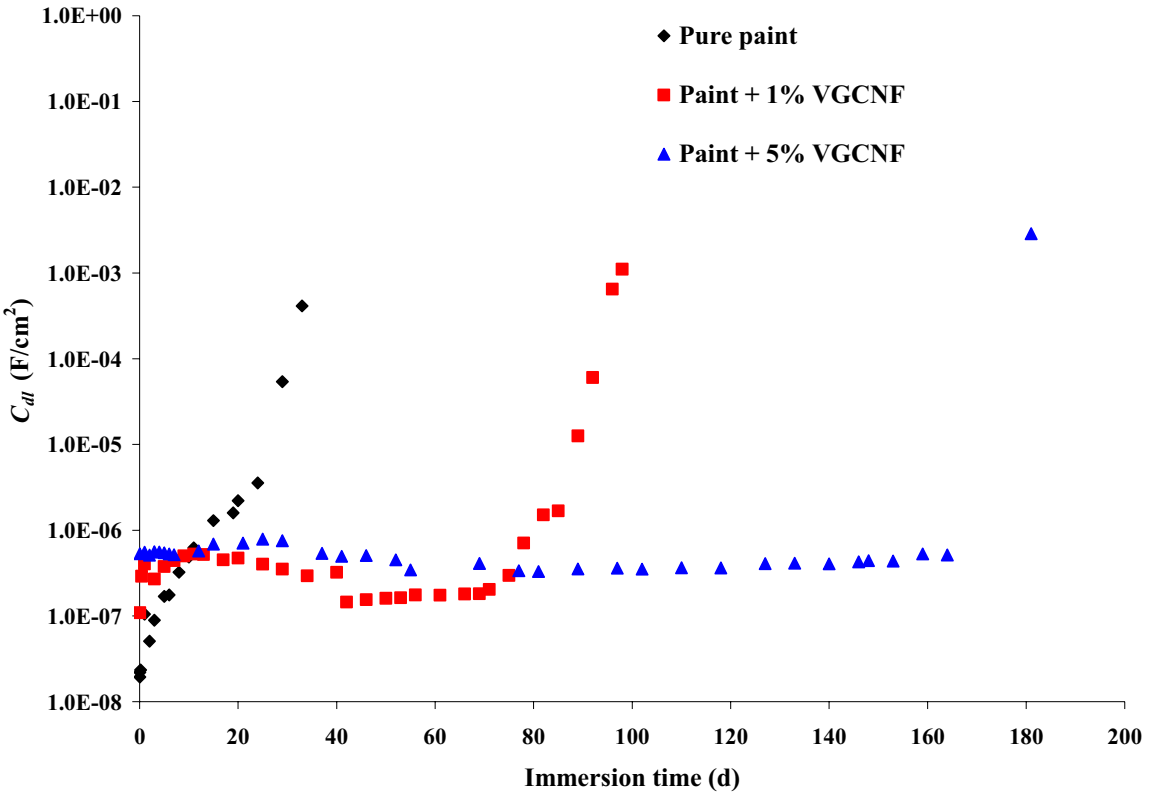

Figure 3.53 Variation of the double layer capacitance (C_{dl}) with immersion time for mild steel panels coated with a VGCNF-incorporated commercial alkyd paint film (30 μm thick) and exposed to 3% NaCl solution. ◆ = pure paint, ■ = paint + 1% VGCNF, and ▲ = paint + 5% VGCNF.

3.3.8 Coating Resistance (R_c) Measurements

The estimated values of the coating resistance (R_c) along with the coating capacitance (C_c) are generally considered the best measures for the stability of the organic coatings.[93, 99] R_c is also defined as the pore resistance of the coating resulting from the penetration of the electrolyte. It is well known that a decrease in R_c and increase in C_c during exposure to the corrosive medium imply degradation of the coating.[14, 15]

The variation of the R_c with immersion time is shown in Figures 3.54 through 3.59 for pure and VGCNF-incorporated alkyd paint coatings applied to mild steel substrates. The data show that, depending on the coating thickness and the VGCNF weight percent, the initial R_c values for all coatings are in the range of 10^4 to 10^8 Ω. The data also show that, for coatings having the same film thickness, the initial R_c values for the VGCNF-incorporated coatings samples are at least one order of magnitude higher than the corresponding values for pure paint (e.g., compare Figures 3.54, 3.56, 3.57 and 3.58 for the 30 μm thick coatings).

The data shown in Figures 3.54 through 3.59 depict that, for all coatings, R_c decreases in the first few days of exposure to NaCl solution, denoting the entry of the electrolyte into the alkyd paint coating. This is the first step of electrolyte diffusion through an organic coating.[100, 101] After this initial period, the value of R_c reaches a plateau and remains almost constant over a long immersion time period before R_c significantly drops indicating a film breakdown and corrosion of the metallic substrate. The length of the immersion time before film breakdown occurs is an indication of the stability of the organic coating. The longer the immersion time before film breakdown, the greater the corrosion protection properties of the coating film.

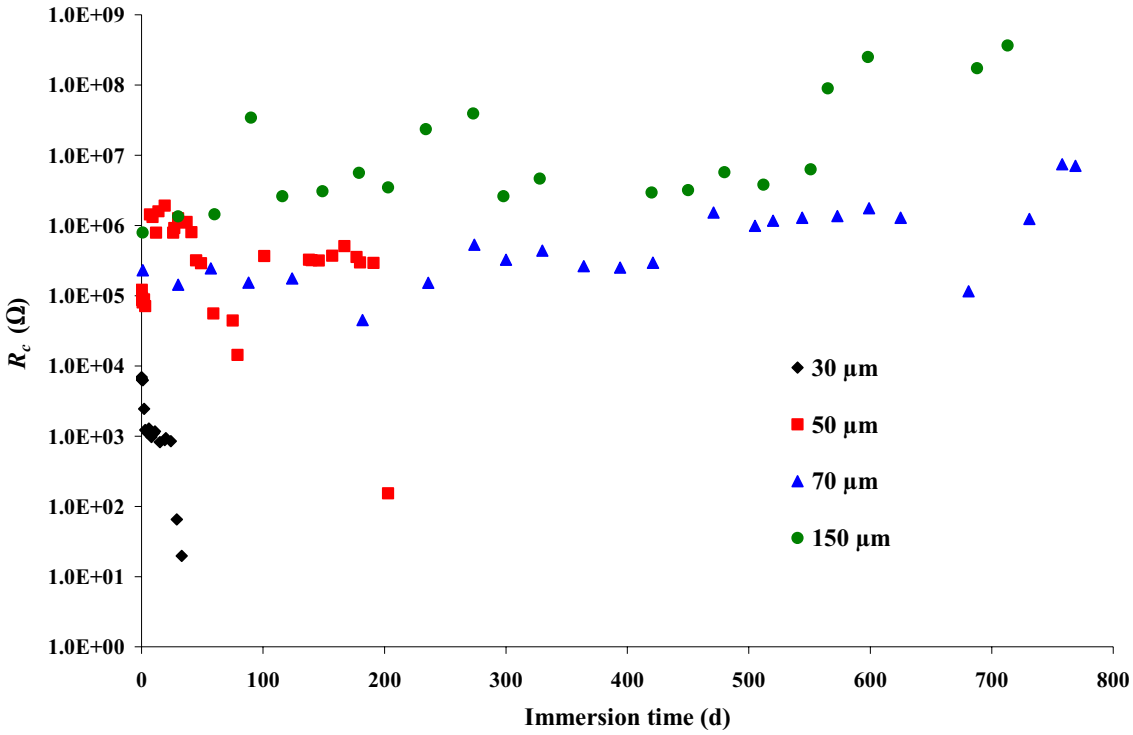

Figure 3.54 Variation of the coating resistance (R_c) with immersion time for mild steel panels coated with a pure commercial alkyd paint film and exposed to 3% NaCl solution. ◆ = 30 µm, ■ = 50 µm, ▲ = 70 µm, and ● = 150 µm.

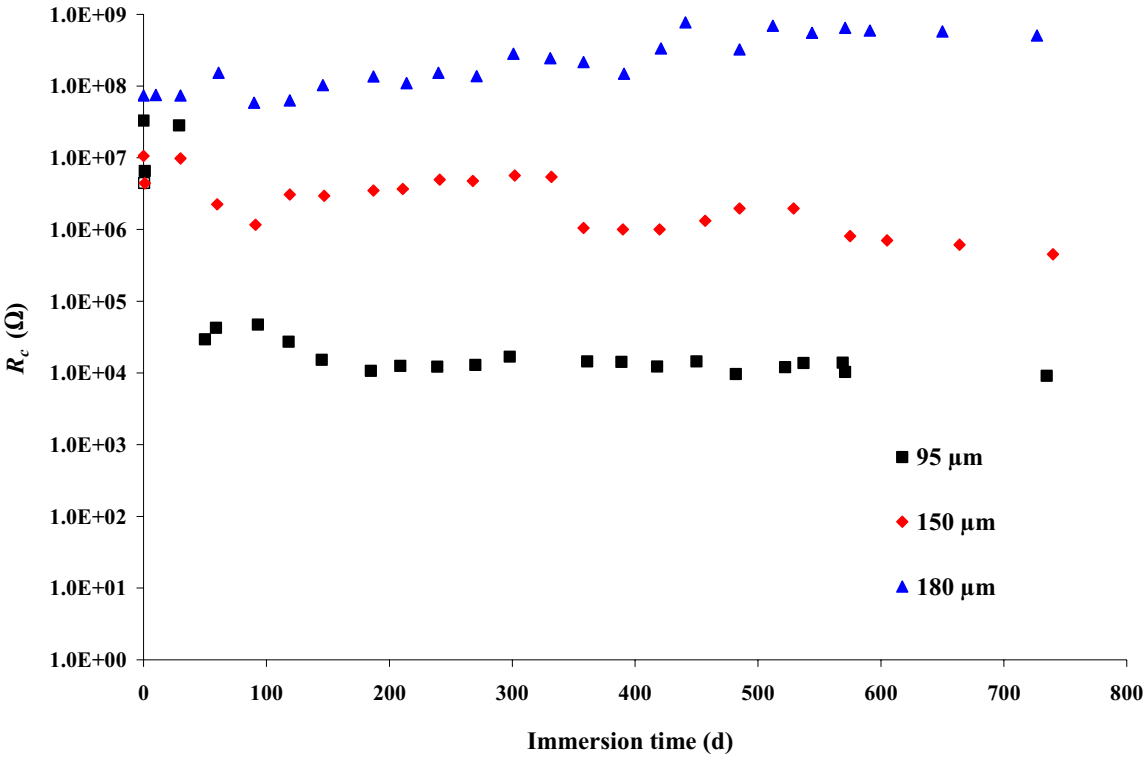

Figure 3.55 Variation of the coating resistance (R_c) with immersion time for mild steel panels coated with a commercial alkyd paint film containing 0.5 wt % VGCNF in 3% NaCl solution. ■ = 95 µm, ◆ = 150 µm, and ▲ = 180 µm.

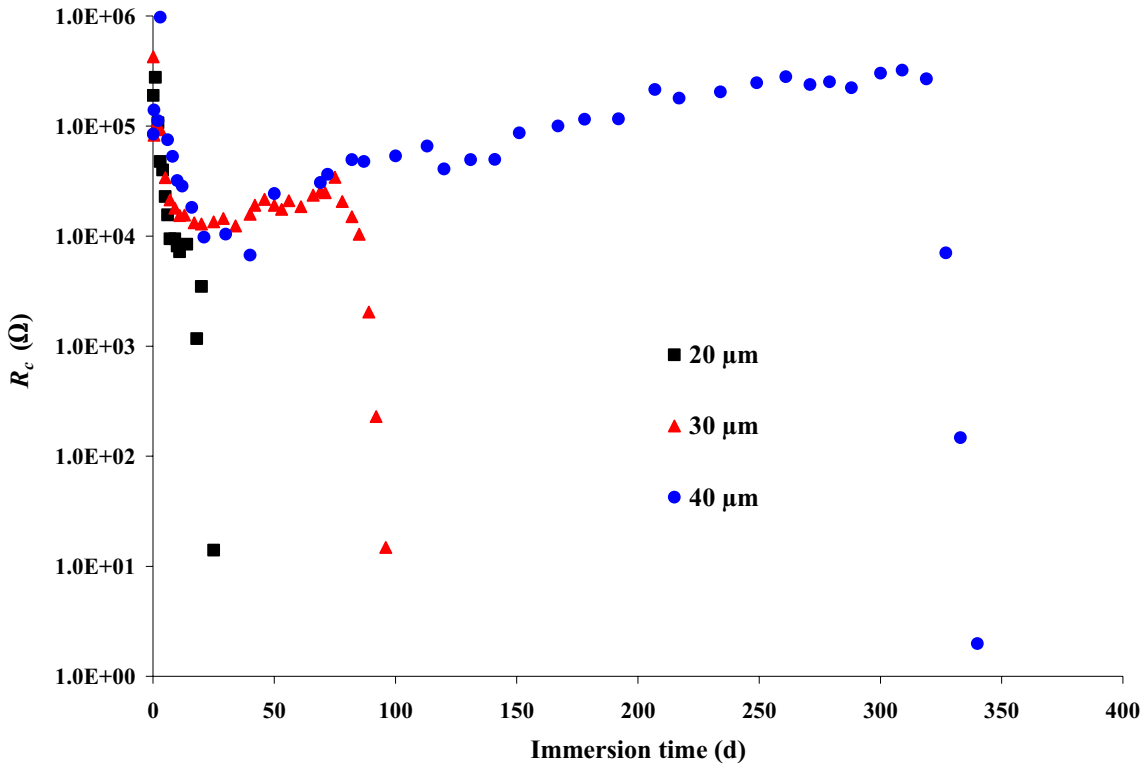

Figure 3.56 Variation of the coating resistance (R_c) with immersion time for mild steel panels coated with a commercial alkyd paint film containing 1wt % VGCNF in 3% NaCl solution. ■ = 20 µm, ▲ = 30 µm, and ● = 40 µm.

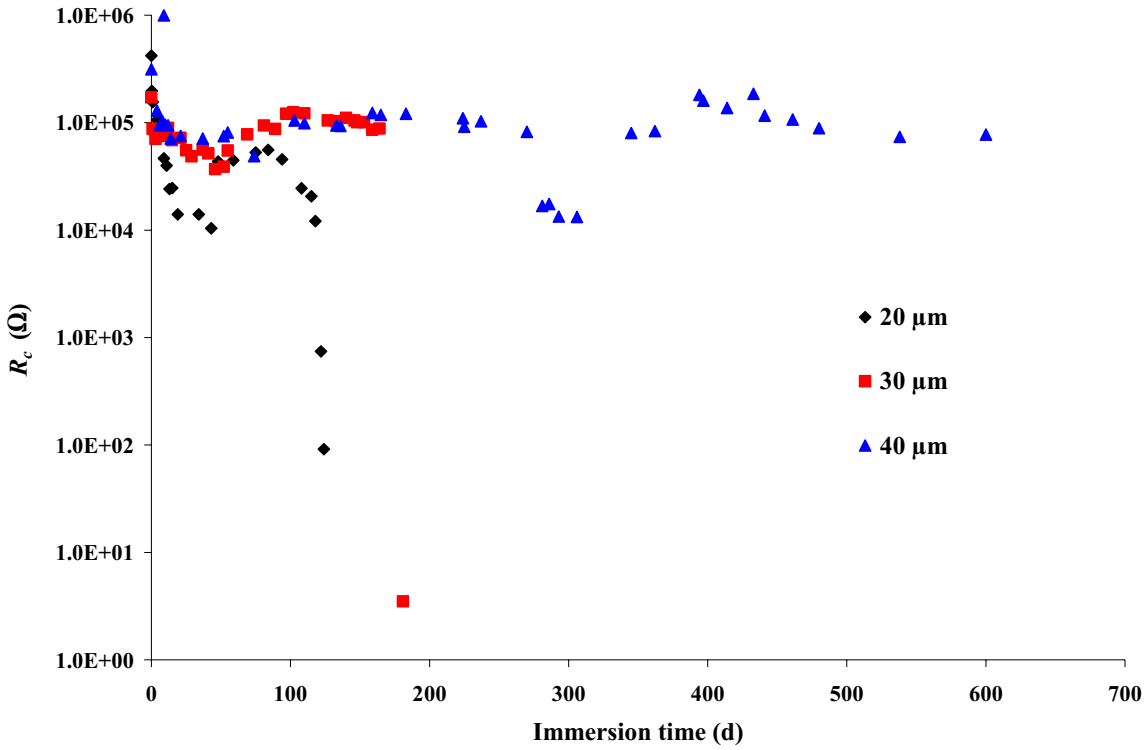

Figure 3.57 Variation of the coating resistance (R_c) with immersion time for mild steel panels coated with a commercial alkyd paint film containing 5 wt % VGCNF in 3% NaCl solution. ■ = 20 µm, ◆ = 30 µm, and ▲ = 40 µm.

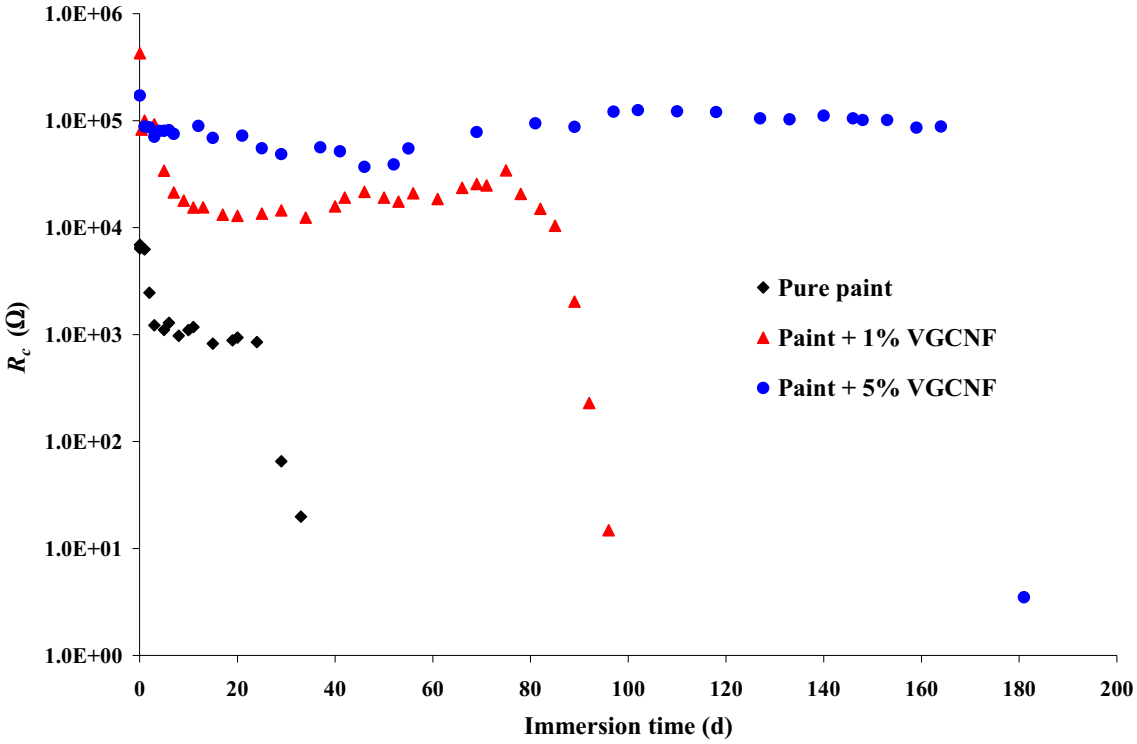

Figure 3.58 Variation of the coating resistance (R_c) with immersion time for mild steel panels coated with a VGCNF-incorporated commercial alkyd paint film (30 μm thick) and exposed to 3% NaCl solution. ■ = pure paint, ▲ = paint + 1% VGCNF, and ● = paint + 5% VGCNF.

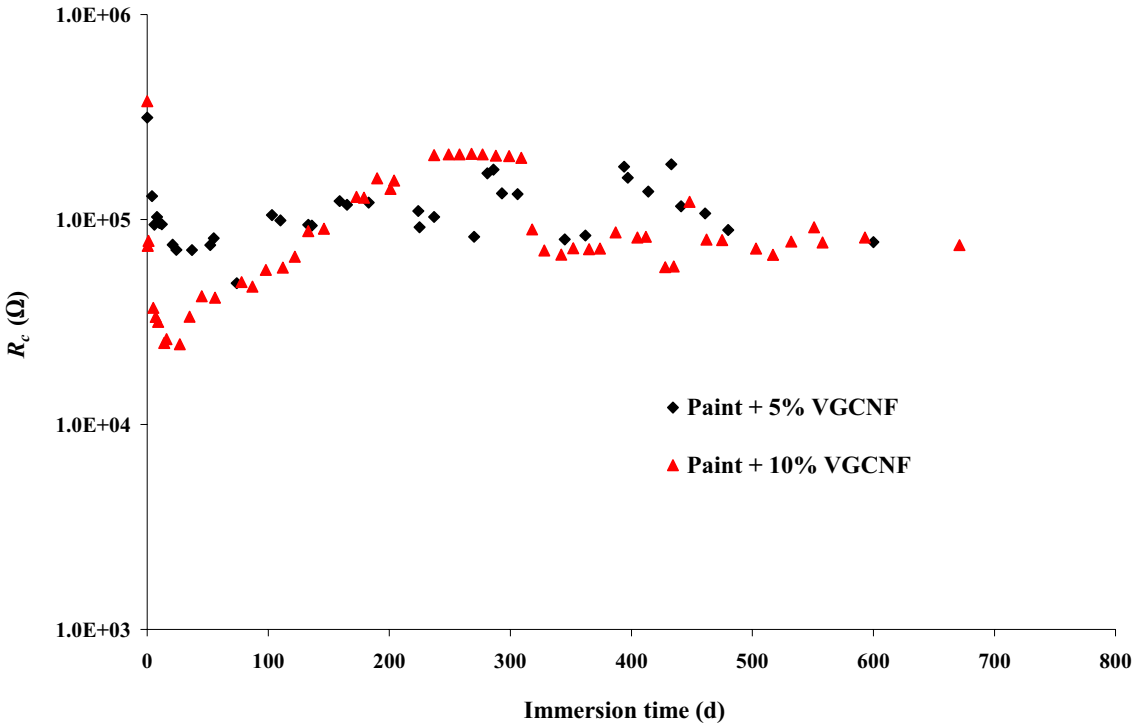

Figure 3.59 Variation of the coating resistance (R_c) with immersion time for mild steel panels coated with a VGCNF-incorporated commercial alkyd paint film (45 μm thick) and exposed to 3% NaCl solution. ◆ = paint + 5% VGCNF, and ▲ = paint + 10% VGCNF.

As shown in Figure 3.54, for paint coatings containing no VGCNFs, the R_c value for the thin (30 μm thick) film sample is high at early immersion times and decreases appreciably in a very short time. However, for the 50 μm thick paint films, the value of R_c remained high up to ~ 200 d before the values started to decrease. On the other hand, for thick pure (70 and 150 μm thick) pure paint coatings, the value of R_c remained high for the whole study time (800 d). These results clearly indicate that the corrosion protection ability of the pure paint coating increases as the paint film thickness increases.

Figure 3.58 depicts that the incorporation of the VGCNFs into the alkyd paint matrix improves the corrosion protection properties of the film coating. Moreover, the higher the wt % of the VGCNF, the longer the period in which the value of R_c remains high and hence the more stable and the better the anticorrosive properties of the coating film.

Figure 3.59 shows a comparison between the behavior of two coatings having the same thickness (45 μm) but different VGCNF weight percent (5% and 10%). As shown in the figure, the behavior of the two coatings is almost the same with the R_c values for the 10% VGCNF-containing coating slightly lower than those for the 5% VGCNF-containing coatings. This result could be attributed to a threshold VGCNF weight percent, above which the protection properties of the coating film do not appreciably increase with increasing the VGCNF loading (as shown with the mechanical properties in Chapter 2). However, this R_c behavior is identical to the previously studied system parameters such as $|Z|$ and R_p.

3.3.9 Coating Capacitance (C_c) Measurements

The coating capacitance (C_c) is generally used as a measure of the total amount of water in the coating (i.e., C_c is related to the percent water uptake), and, in theory, its value is expected to increase with immersion time.[102-104] Figures 3.60 through 3.65 present the variation of C_c with immersion time for both pure and VGCNF-incorporated paint coatings. As shown in the figures, in the first few days of exposure to the electrolyte, the value of C_c increases with increased immersion time indicating the absorption of water in the coatings until it reaches a plateau and remains almost unchanged for a longer period of exposure to the corrosive environment. When the film breakdown time is reached, the corrosive electrolyte reaches the substrate surface and metallic corrosion occurs which is indicated by a sudden increase in C_c coating.

The data shows that, for pure coatings (e.g., Figures 3.60 and 3.64); the rate of initial increase in the value of C_c is very fast especially for the thin film (30 μm) coatings. The results also show that the thicker the coating film, the more stable the film and the longer the immersion time period in which the value of C_c remains constant (e.g., Figure 3.60). These results are in good agreement with both the water uptake measurements (vide supra) and the literature results.[102-104]

The value of C_c (in F) is given by:[105]

$$C_c \quad \varepsilon\varepsilon^{\circ}\frac{A}{d} \tag{3.2}$$

where ϵ is the relative dielectric constant of the coating, ϵ^o is the dielectric constant of the vacuum (8.85×10^{-14} F.cm^{-1}), A is the coating surface area in contact with the electrolyte (cm^2) and d is the coating thickness (cm).

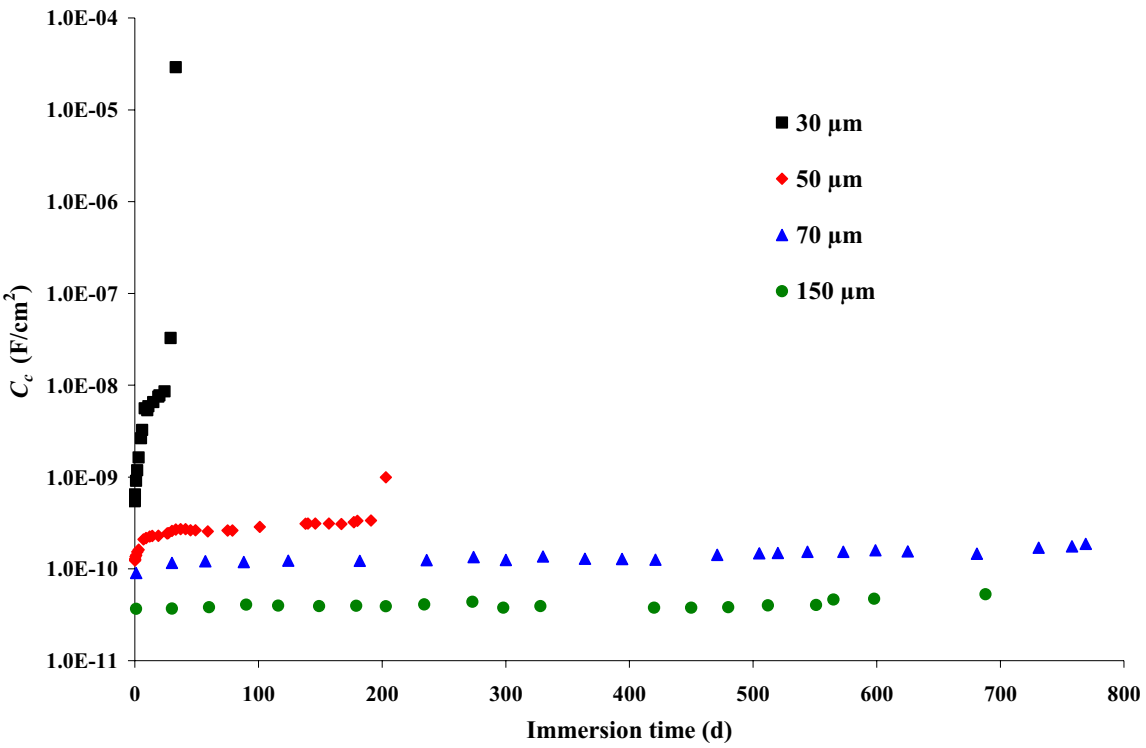

Figure 3.60 Variation of the coating capacitance (C_c) with immersion time for mild steel panels coated with a pure commercial alkyd paint film and exposed to 3% NaCl solution. ◆ = 30 µm, ■ = 50 µm, ▲ = 70 µm, and ● = 150 µm.

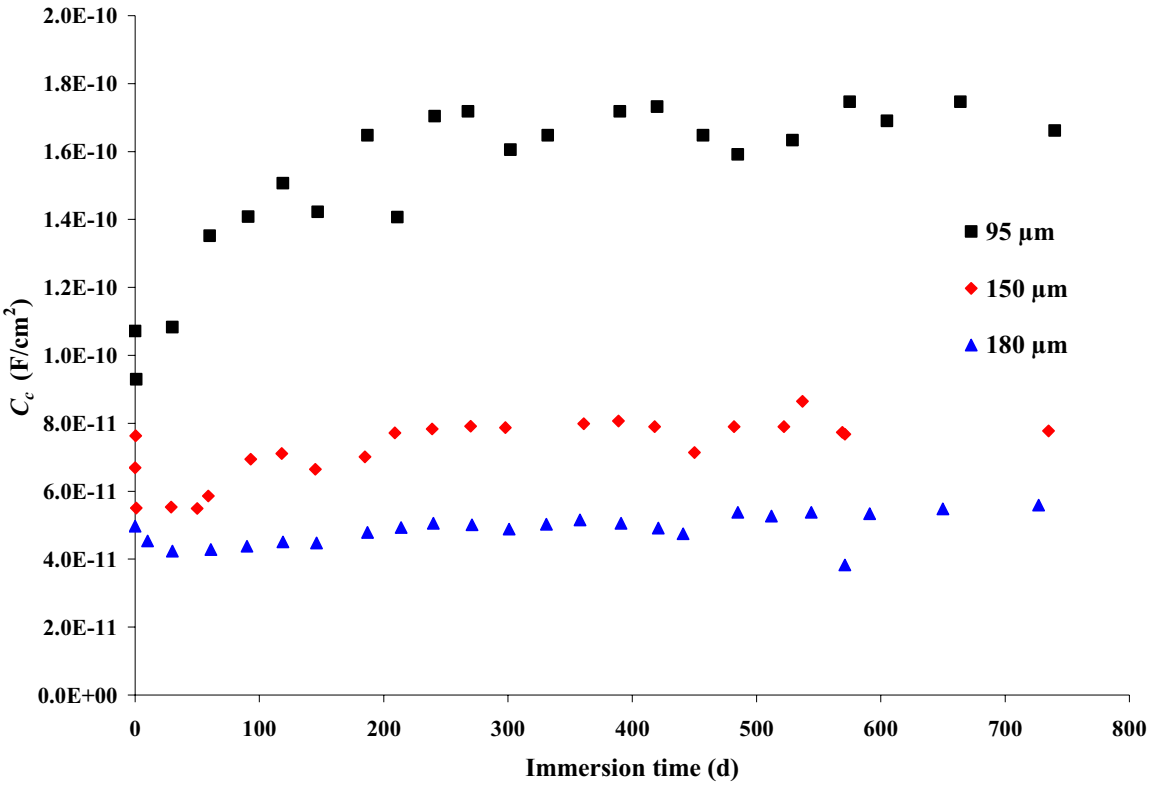

Figure 3.61 Variation of the coating capacitance (C_c) with immersion time for mild steel panels coated with a commercial alkyd paint film containing 0.5 wt % VGCNF in 3% NaCl solution. ◆ = 95 µm, ■ = 150 µm, and ▲ = 180 µm.

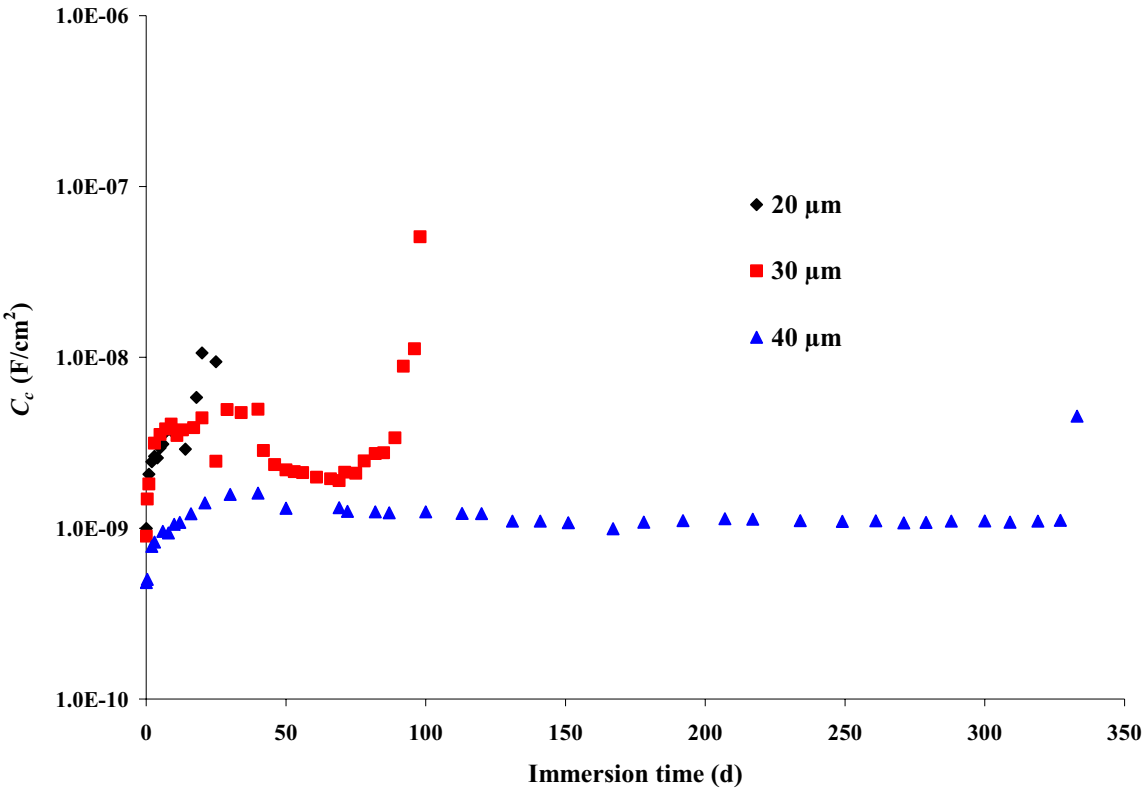

Figure 3.62 Variation of the coating capacitance (C_c) with immersion time for mild steel panels coated with a commercial alkyd paint film containing 1 wt % VGCNF in 3% NaCl solution. ◆ = 20 µm, ■ = 30 µm, and ▲ = 40 µm.

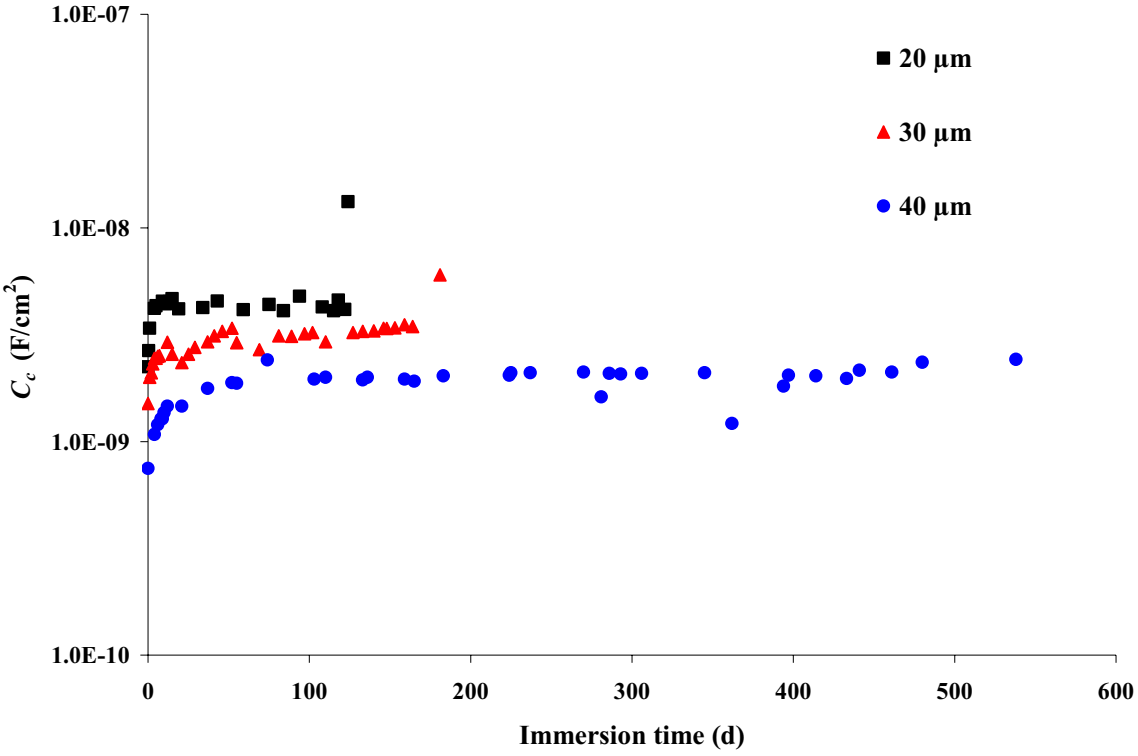

Figure 3.63 Variation of the coating capacitance (C_c) with immersion time for mild steel panels coated with a commercial alkyd paint film containing 5 wt % VGCNF in 3% NaCl solution. ■ = 20 µm, ▲ = 30 µm, and ● = 40 µm.

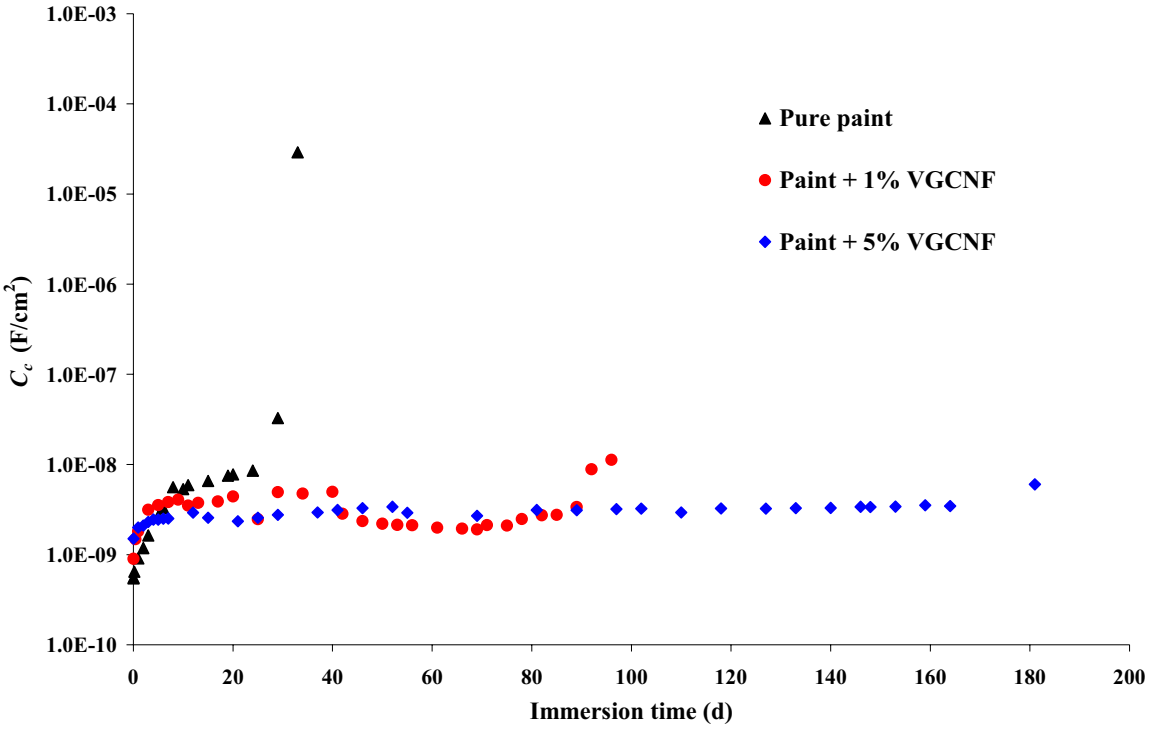

Figure 3.64 Variation of the coating capacitance (C_c) with immersion time for mild steel panels coated with a VGCNF-incorporated commercial alkyd paint film (30 μm thick) and exposed to 3% NaCl solution. ▲ = pure paint, ● = paint + 1% VGCNF and ◆ = paint + 5% VGCNF.

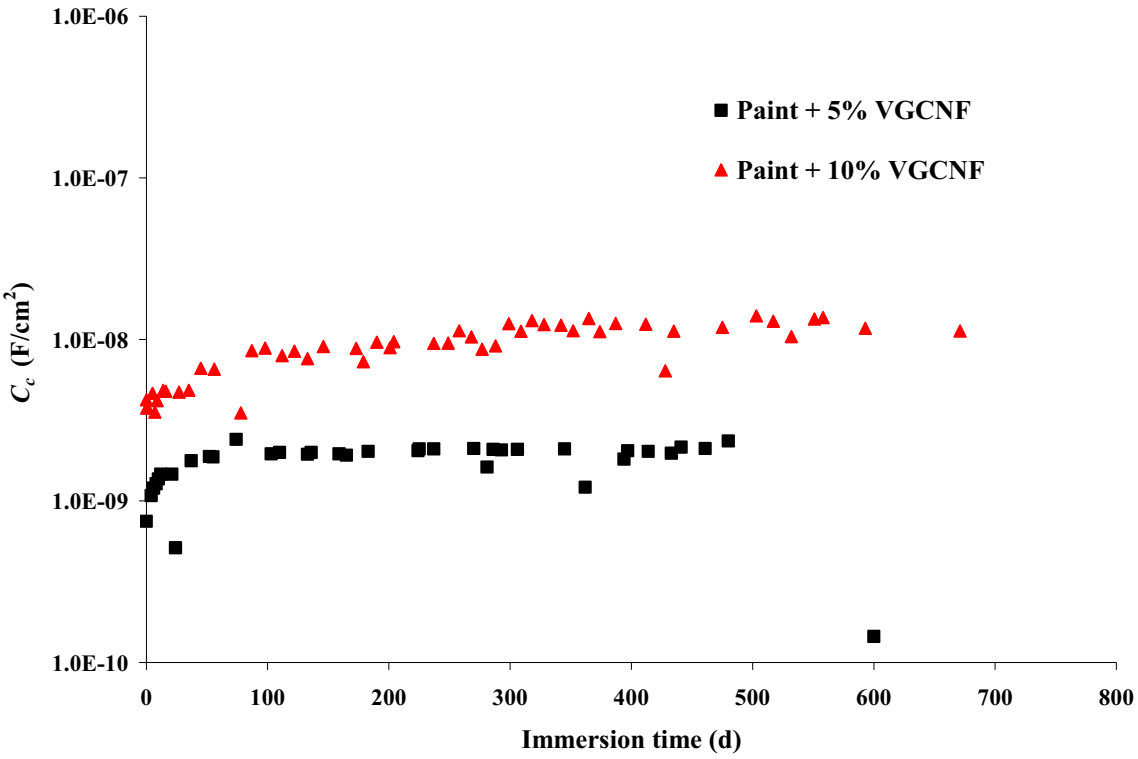

Figure 3.65 Variation of the coating capacitance (C_c) with immersion time for mild steel panels coated with a VGCNF-incorporated commercial alkyd paint film (45 μm thick) and exposed to 3% NaCl solution. ■ = paint + 5% VGCNF, and ▲ = paint + 10% VGCNF.

The absorption of water causes an increase in the dielectric constant of the coating (ϵ) with a corresponding increase in C_c as indicated from Equation 3.2. The data in Figures 3.64 and 3.65 also show that the increase in C_c is lowest in the case of the 5% VGCNF-incorporated paint system which also stays stable for the longest period of time (~ 800 d) indicating that this system has the lowest rate of corrosion. On the other hand, the increase in C_c is highest for the pure paint coating systems (Figure 3.60) with film thickness of 30 μm, indicating that the rate of corrosion is highest for the that system.

It can also be noted from Figure 3.65 that coating systems containing 10% VGCNFs have higher capacitance values than coating systems containing 5% VGCNF. This behavior is consistent with the R_c measurements for the same coating systems which imply a threshold VGCNF wt content. These results are also consistent with the VGCNF resistance (R_f) and capacitance (C_f) measurements (vide infra).

3.3.10 Water Uptake Measurements

Water uptake (also known as water penetration, water diffusion, and water transport) into an anticorrosive coating applied to the surface of a metal or alloy is an important parameter that affects both the barrier and the adhesion properties of the coating to the substrate surface.[106] Water uptake is considered the primary factor that controls the service life of any organic coating and the degradation of a polymer-coated metal occurs after water penetrates the coating layer.[18] The water uptake can be evaluated using several methods including EIS.[14, 15, 18, 102, 107-113]

In the current investigation, the water uptake was studied by the EIS technique. The percent water absorbed by the coating was calculated from the coating capacitance values using the Brasher-Kingsbury equation:[103]

$$\% \text{ Water uptake} = 100[\log(C_c/C_o)/\log(80)] \quad (3.3)$$

where C_c is the coating capacitance, C_o is the coating capacitance of the dry coating (determined at immersion time, t, = 0), and 80 is the dielectric constant of water.[93, 114]

Figures 3.66 through 3.71 display the variation of the percent water uptake with film thickness, and % VGCNF incorporated in the coating, respectively, for paint-coated mild steel coupons immersed in 3% NaCl solution. The results show that as the exposure time increases, the water uptake increases and hence the film coating resistance decreases until the film is totally destroyed where the electrolyte reaches the substrate surface and corrosion products are formed. The data show that the increase in water uptake starts gradually for all of the tested panels followed by a rapid increase that corresponds to the complete loss of adhesion and onset of blistering in the coating films.

The data depicted in Figures 3.66 and 3.67 show that the highest and steepest increase in the water uptake values occurs for the pure coatings denoting a fast diffusion of water into these coatings. As shown in Figure 3.66, the thicker the coating film, the less water absorbed, the slower the permeability of the electrolyte, and hence the longer the time needed for the coating breakdown. Moreover, for samples with high wt % of VGCNF (e.g., Figures 3.67 through 3.71), the water uptake reaches a plateau after the initial increase. Although, in some cases, the plateau for the paint coating containing higher VGCNF content is higher than with less or no VGCNFs, the results depict that the higher the VGCNF wt %, the longer the immersion time elapsed before the coating film

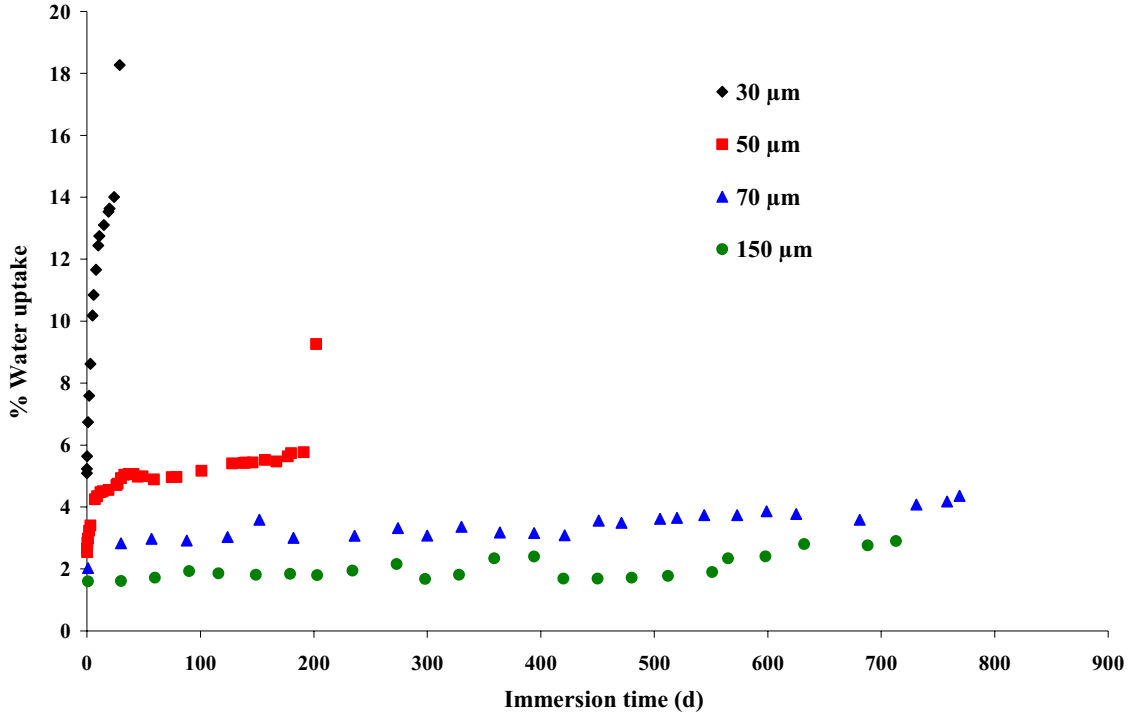

Figure 3.66 Variation of % water uptake with immersion time for mild steel panels coated with a pure commercial alkyd paint film and exposed to 3% NaCl solution. ◆ = 30 µm, ■ = 50 µm, ▲ = 70 µm, and ● = 150 µm.

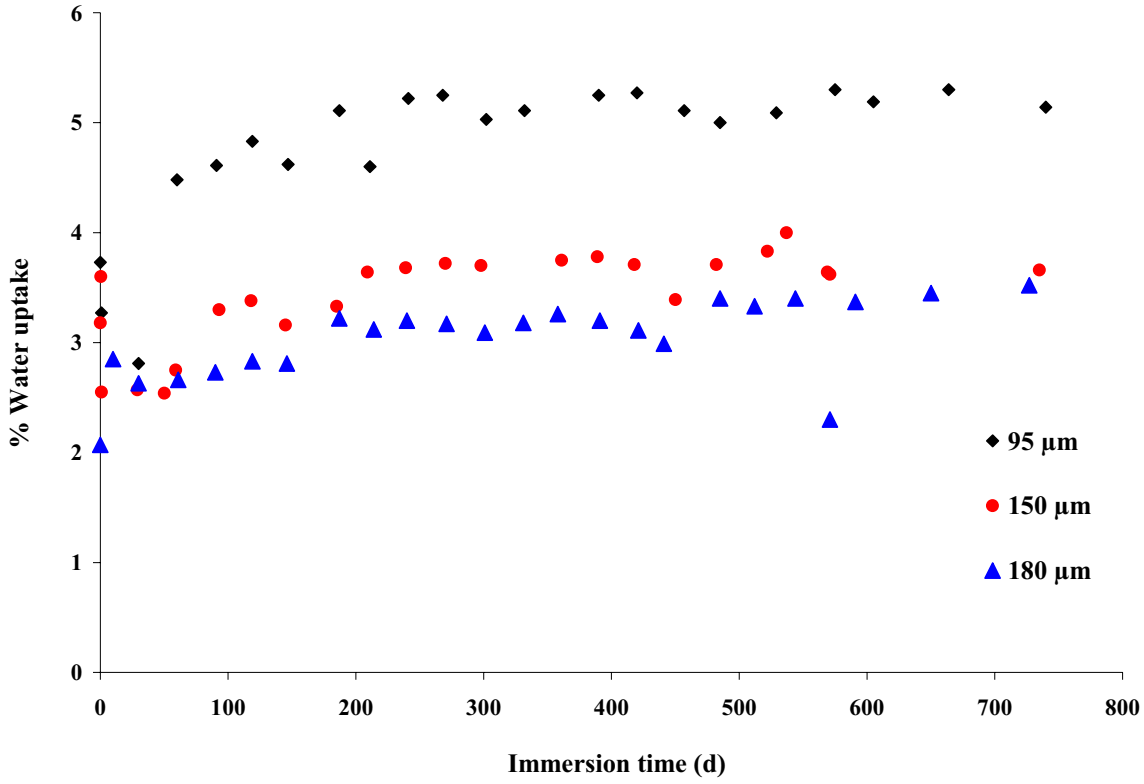

Figure 3.67 Variation of % water uptake with immersion time for mild steel panels coated with a commercial alkyd paint film containing 0.5 wt % VGCNF and exposed to 3% NaCl solution. ◆ = 95 µm, ● = 150 µm, and ▲ = 180 µm.

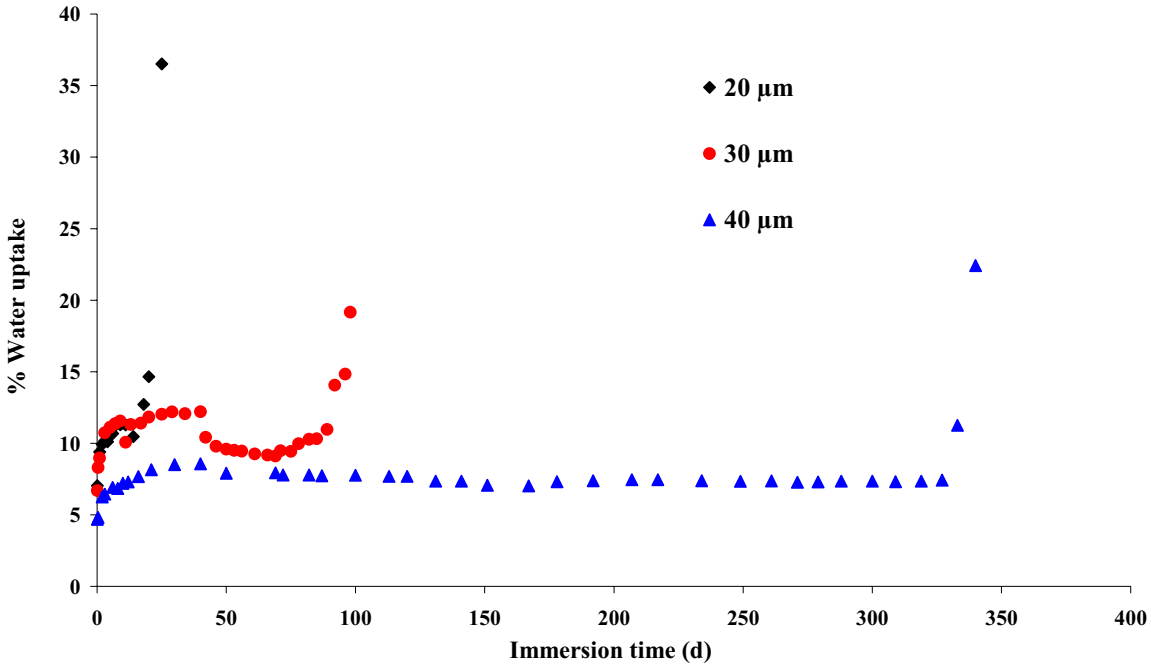

Figure 3.68 Variation of % water uptake with immersion time for mild steel panels coated with a commercial alkyd paint film containing 1 wt % VGCNF and exposed to 3% NaCl solution. ◆ = 20 µm, ● = 30 µm, and ▲ = 40 µm.

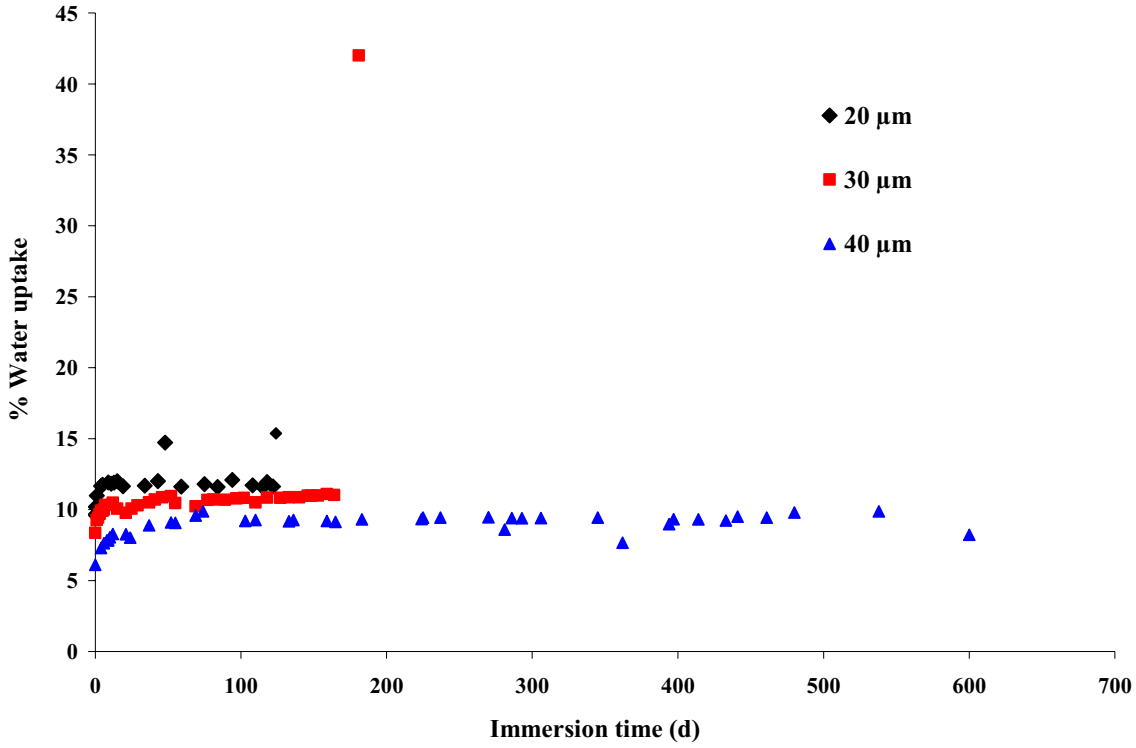

Figure 3.69 Variation of % water uptake with immersion time for mild steel panels coated with a commercial alkyd paint film containing 5 wt % VGCNF and exposed to 3% NaCl solution. ◆ = 20 µm, ■ = 30 µm, and ▲ = 40 µm.

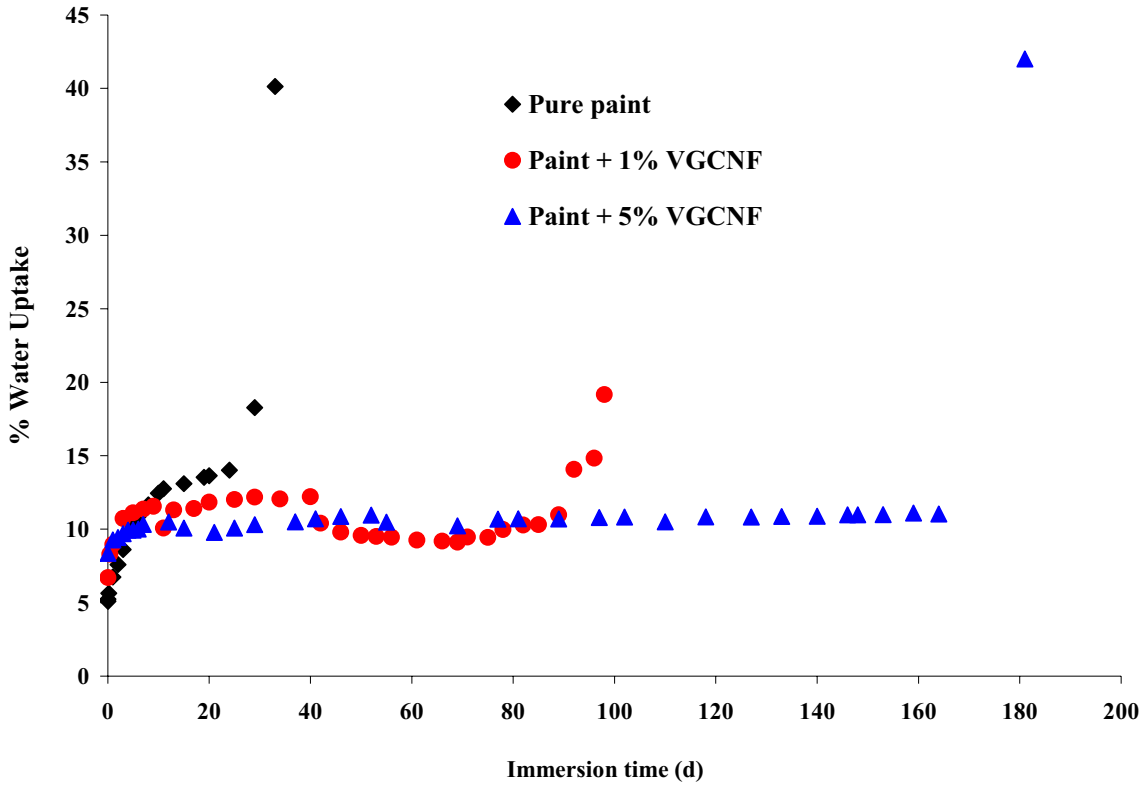

Figure 3.70 Variation of % water uptake with immersion time for mild steel panels coated with a VGCNF-incorporated commercial alkyd paint film (30 μm thick) in 3% NaCl solution. ◆ = pure paint, ● = paint + 1% VGCNF, and ▲ = paint + 5% VGCNF.

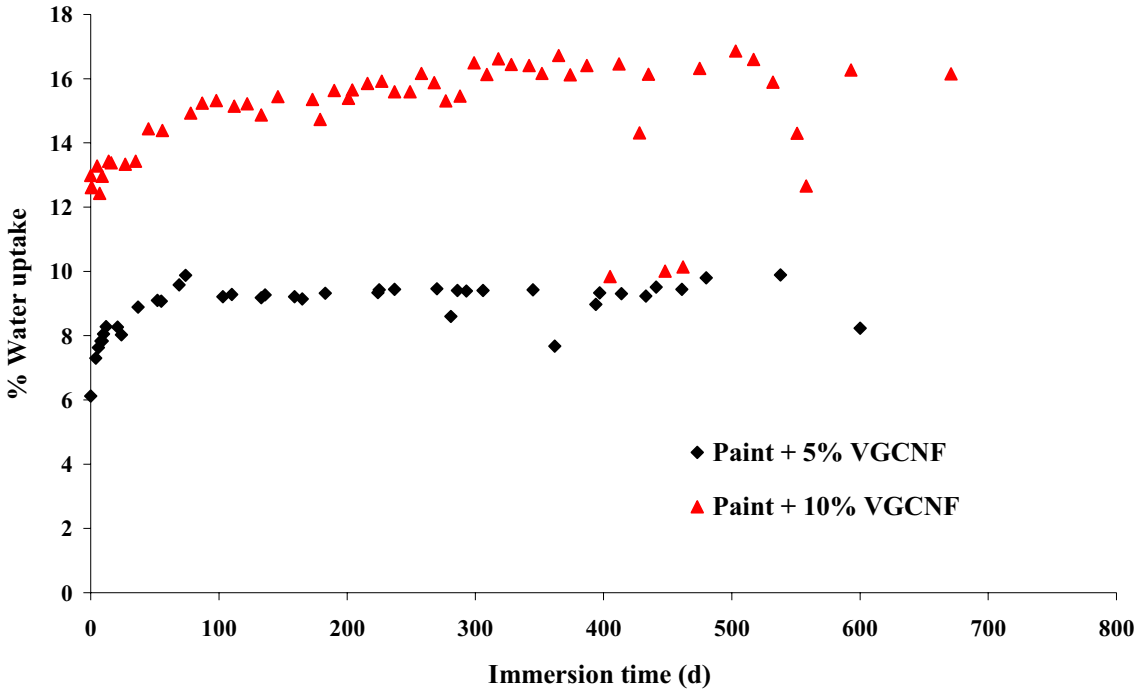

Figure 3.71 Variation of % water uptake with immersion time for mild steel panels coated with a VGCNF-incorporated commercial alkyd paint film (45 μm thick) in 3% NaCl solution. ◆ = paint + 5% VGCNF, and ▲ = paint + 10% VGCNF.

breakdown occurs. These results are also consistent with the previous results such as $|Z|$, R_c, C_c, and C_{dl}.

3.3.11 Delaminated Area (A_d) Measurements

The delaminated area (A_d) is the electrochemically active area under the coating. Delamination of a coated metal substrate immersed in an electrolyte solution occurs as a result of the diffusion of water, along with oxygen and ions in the electrolyte solution, through the polymer coating until it finally gets in direct contact with the bare metal substrate where the electrochemical corrosion reactions take place at the bare metal/electrolyte interface. Accordingly, delamination leads to loss of the adhesion and protective properties of the coating.[115] If a part of the coating is removed (e.g., by scratches), ions will have direct access to the bare metal substrate and corrosion will occur immediately.[116-121] Due to all of these processes, delamination will occur and, in theory, A_d is expected to increase with immersion time.

Four different methods, based on the EIS measurements, have been proposed in the literature to calculate A_d.[122, 123] According to Haruyama et al., A_d is determined using the following equation:[124]

$$A_d = R_{ct}^{\circ}/R_{ct} = C_{dl}/C_{dl}^{\circ} \qquad (3.4)$$

where R_{ct} and C_{dl} are the charge-transfer resistance and the double-layer capacitance for the polymer-coated substrate, respectively while R_{ct}° and C_{dl}° are the charge-transfer resistance, and the double-layer capacitance of the uncoated metal, respectively. The superscript (°) denotes the area-specific values for the charge-transfer resistance ($\Omega.cm^2$) and the double layer capacitance (F/cm^2). All of the parameters in Equation 3.4 are

obtained from the EIS measurements along with the dielectric constant. In the current investigation, the values of $R_{ct}°$ and $C_{dl}°$ for the bare mild steel samples immersed in 3% NaCl solution are 186.5 ($\Omega.cm^2$) and 3.875×10^{-3} (F/cm^2), respectively.

The percent of the delaminated area ($\%A_d$) is calculated using the following equation:

$$\%A_d = (A_d \text{ /electrode area}) \times 100 \qquad (3.5)$$

Figures 3.72 through 3.77 present the variation of $\%A_d$ with immersion time for both pure and VGCNF-incorporated paint coatings. As shown in the figures, the value of $\%A_d$ increases with increased immersion time indicating the absorption of water in the coatings. In the case of the pure coatings (Figures 3.72 and 3.76), the increase in the value of $\%A_d$ is very fast especially for the thin film (30 μm) coatings. These results are in agreement with the fact that thin coating films can be easily penetrated by small molecules such as water and oxygen molecules.[125-128] The results in Figure 3.72 also show that for thick coatings (70 μm and up), $\%A_d$ stabilizes at a constant value after a few days. As shown in the figure, the thicker the coating film, the more stable the film and longer the immersion time period in which the value of A_d remains constant.

For VGCNF-reinforced paint coatings (Figures 3.73 through 2.75), it can be noticed that thick coatings are characterized by a longer immersion time period in which $\%A_d$ remains unchanged. In addition, the data in Figure 3.76 shows that the higher the VGCNF content in the coating, the smaller the value of $\%A_d$ and the longer the immersion period in which $\%A_d$ remains constant indicating a more stable polymer film. These results are in accordance with both the water uptake measurements (vide supra) and the literature results.[129]

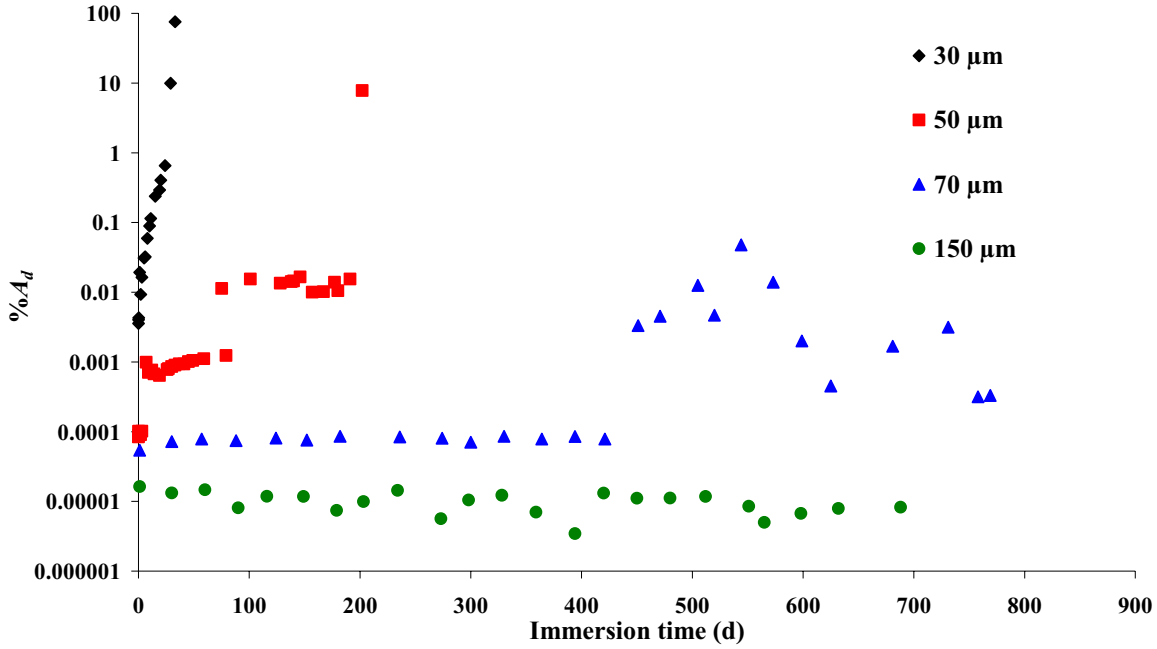

Figure 3.72 Variation of the percent delaminated area (%A_d) with immersion time for mild steel panels coated with a pure commercial alkyd paint film and exposed to 3% NaCl solution. ◆ = 30 µm, ■ = 50 µm, ▲ = 70 µm, and ● = 150 µm.

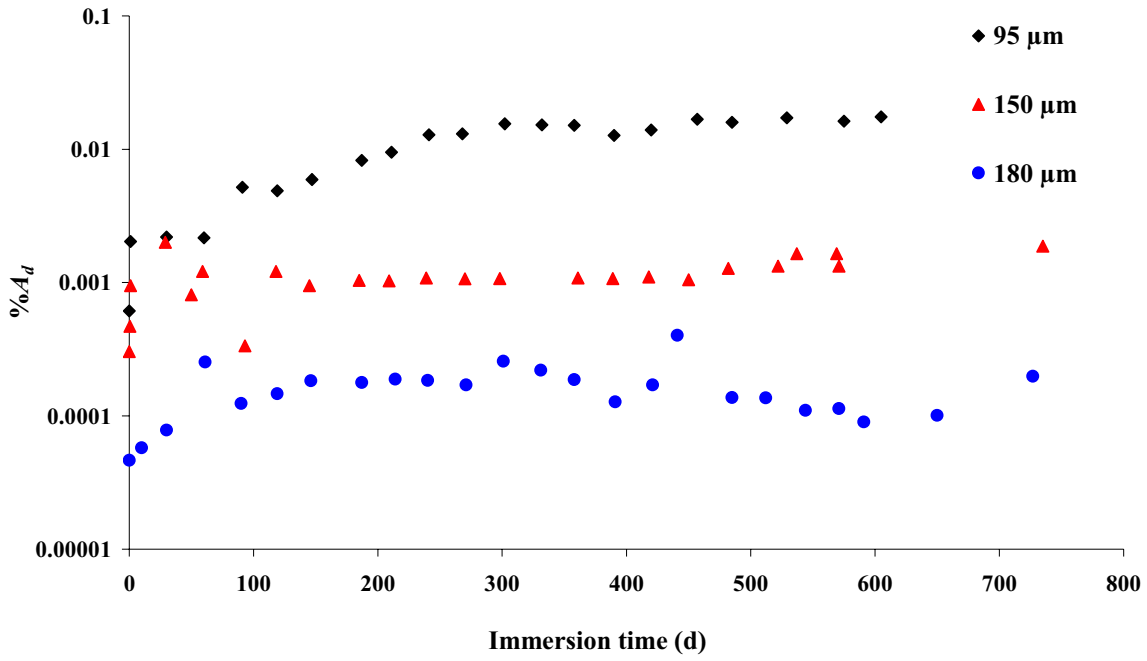

Figure 3.73 Variation of the percent delaminated area (%A_d) with immersion time for mild steel panels coated with a commercial alkyd paint film containing 0.5 wt % VGCNF and exposed to 3% NaCl solution. ◆ = 95 µm, ▲ = 150 µm, and ● = 180 µm.

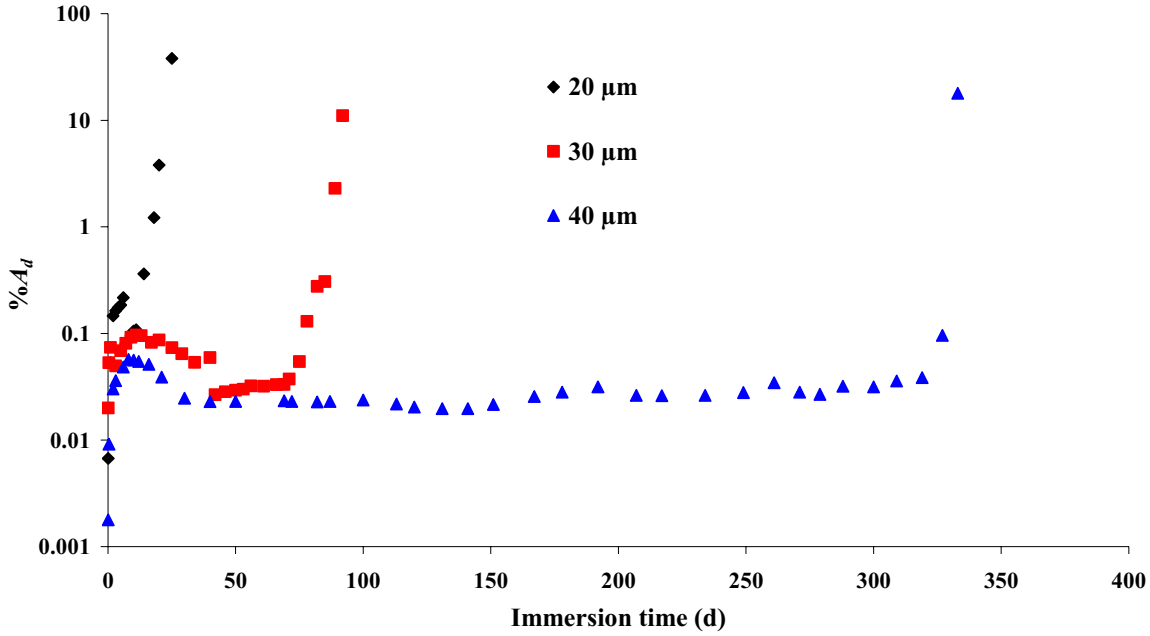

Figure 3.74 Variation of the percent delaminated area (%A_d) with immersion time for mild steel panels coated with a commercial alkyd paint film containing 1 wt % VGCNF and exposed to 3% NaCl solution. ◆ = 20 µm, ■ = 30 µm, and ▲ = 40 µm.

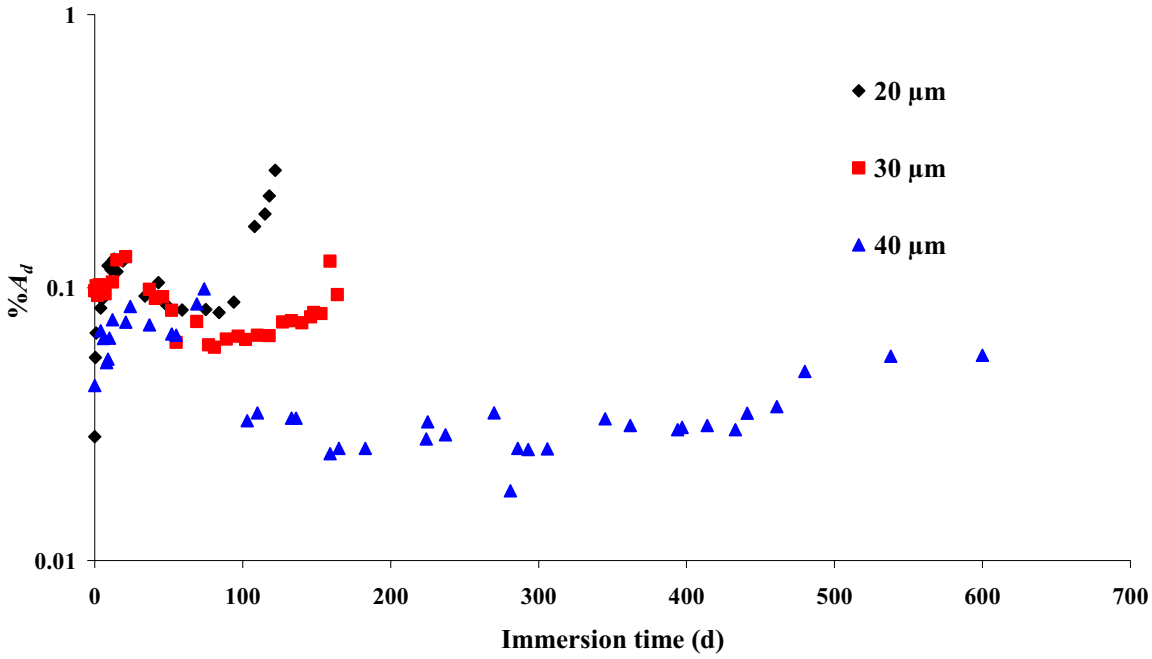

Figure 3.75 Variation of the percent delaminated area (%A_d) with immersion time for mild steel panels coated with a commercial alkyd paint film containing 5 wt % VGCNF and exposed to 3% NaCl solution. ◆ = 20 µm, ■ = 30 µm, and ▲ = 40 µm.

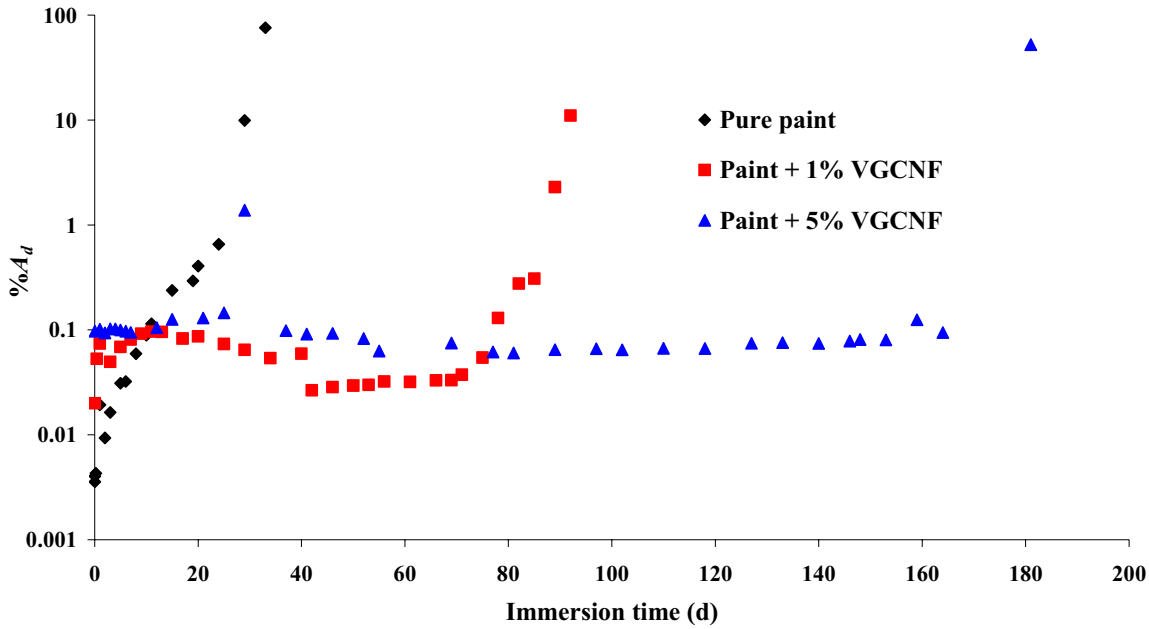

Figure 3.76 Variation of the percent delaminated area (%A_d) with immersion time for mild steel panels coated with a VGCNF-incorporated commercial alkyd paint film (30 μm thick) and exposed to 3% NaCl solution. ◆ = pure paint, ■ = paint + 1% VGCNF, and ▲ = paint + 5% VGCNF.

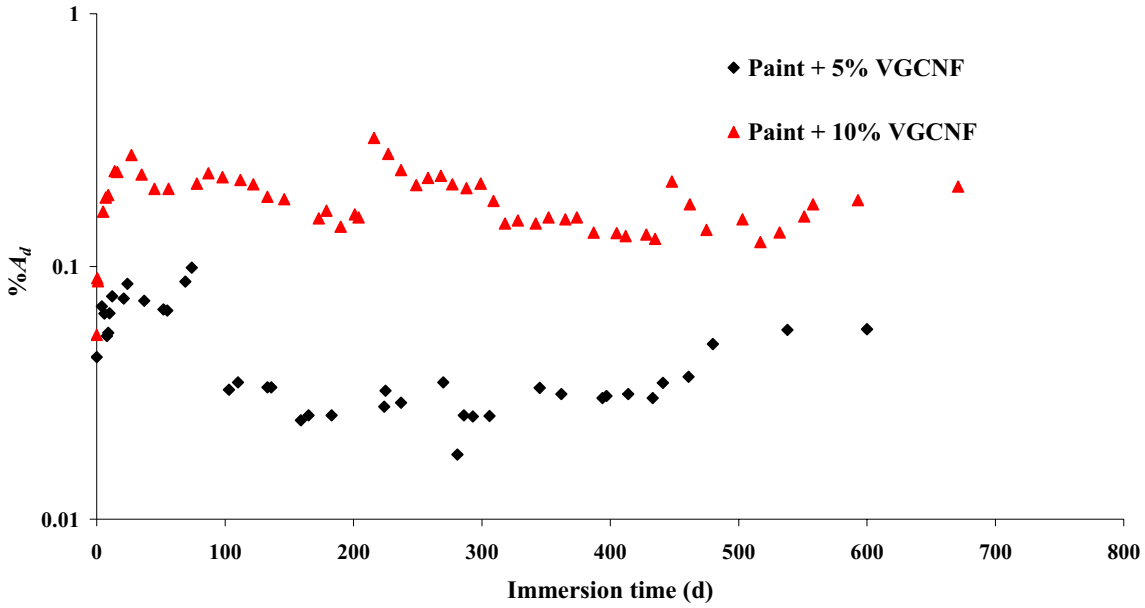

Figure 3.77 Variation of the percent delaminated area (%A_d) with immersion time for mild steel panels coated with a VGCNF-incorporated commercial alkyd paint film (45 μm thick) and exposed to 3% NaCl solution. ◆ = paint + 5% VGCNF, and ▲ = paint + 10% VGCNF.

3.3.12 Carbon Nanofiber Resistance (R_f)

The carbon fiber resistance (R_f) and capacitance (C_f) are two parameters added to the equivalent circuit shown in Figure 3.31.b to account for the behavior of the VGCNFs in the alkyd paint coating. Figures 3.78 and 3.79 show the variation of R_f with immersion time for alkyd paint coatings having different thicknesses (Figure 3.78) and VGCNF loadings (Figure 3.79). It can be noticed that the initial R_f values are generally small and in the range of 100 – 1000 Ω depending on the coating thickness and VGCNF content. . The data presented in Figures 3.78 and 3.79 show that, after an initial fluctuation during the early stages of immersion in the NaCl solution, the value of R_f remains more or less constant throughout the lifetime of the coating film until the film is completely destroyed. In addition, Figure 3.78 shows that as the paint film thickness increases, the value of R_f becomes stable for a longer period of immersion time, indicating good barrier properties for the thicker coating.

Examining Figure 3.79 clearly shows that a paint coating containing 5% VGCNF is less resistive (more conductive) than a coating having 1% VGCNF. This result is consistent with the nature of VGCNF as a conductive material. The result is also consistent with the electrical conductivity measurements presented in Chapter 2 as well as the literature.[130-134]

3.3.13 Carbon Nanofiber Capacitance (C_f)

The capacitance of the VGCNFs is the second parameter added to the equivalent circuit shown in Figures 3.31.b. As shown with R_c and C_c for the coating, a decrease in the value of R_f and an increase in the value of C_f during exposure to the NaCl solution

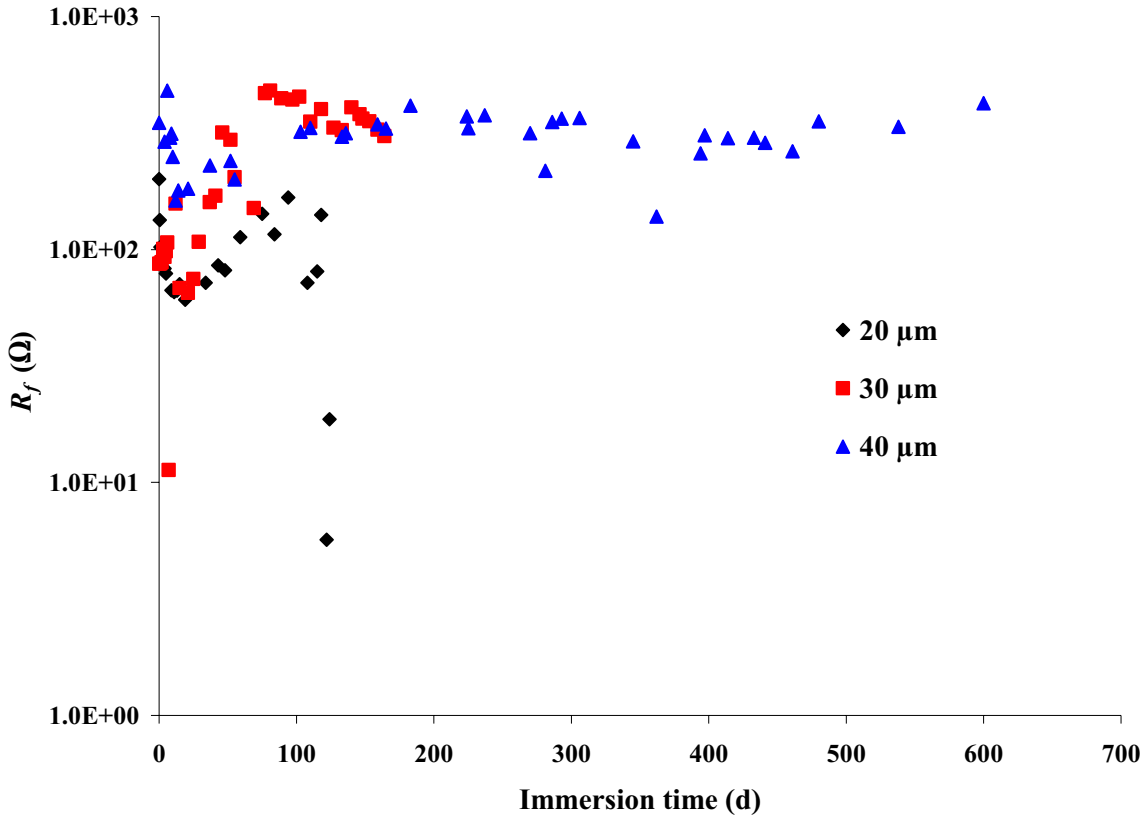

Figure 3.78 Variation of the VGCNF resistance (R_f) with immersion time for mild steel panels coated with a commercial alkyd paint film containing 5 wt % of VGCNF in 3% NaCl solution. ◆ = 20 µm, ■ = 30 µm, and ▲ = 40 µm.

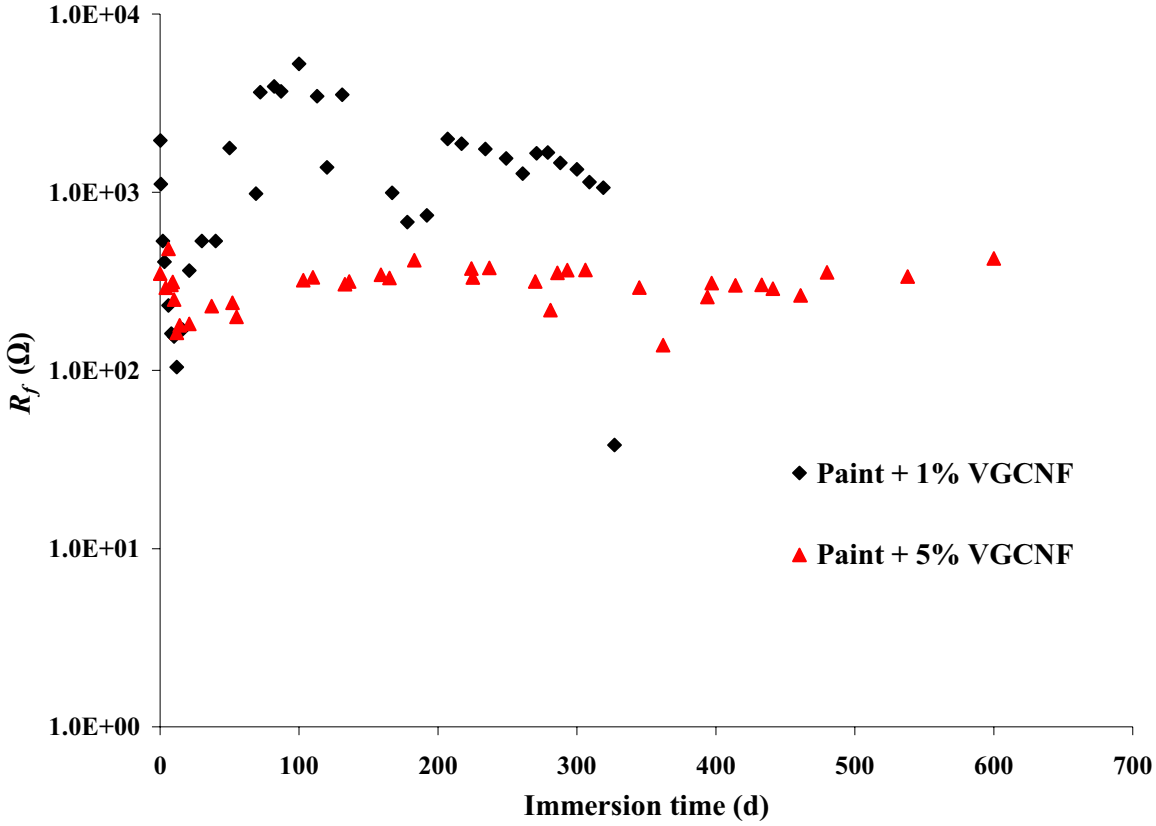

Figure 3.79 Variation of the VGCNF resistance (R_f) with immersion time for mild steel panels coated with a VGCNF-incorporated commercial alkyd paint film (40 μm thick) and exposed to 3% NaCl solution. ◆ = paint + 1% VGCNF, and ▲ = paint + 5% VGCNF.

imply degradation of the coating film. Figures 3.80 and 3.81 show the variation of C_f with immersion time for paint coatings containing VGCNFs with different thicknesses (Figure 3.80) and loadings (Figure 3.81). As shown in Figure 3.80, after a short initial period of immersion in which the fiber capacitance is not stable, the fiber capacitance C_f becomes more or less constant for a period of time before it increases indicating the degradation of the paint film. The longer the time elapsed before degradation occurs, the better the barrier properties of the coating film. Figure 3.80 shows that for thin coatings (20 μm), C_f increased in a short time. On the other hand, for thick coatings (40 μm), C_f remained constant for more than 600 d of immersion in the corrosive medium indicating the good barrier properties of the thick coating.

Figure 3.81 shows the effect of the VGCNF wt % on the value of C_f. As shown in the figure, alkyd paint coating containing 5% VGCNFs have higher capacitance and more stable than coatings containing 1% VGCNFs. These results are also consistent with the R_f measurements shown above.

3.3.14 The Role of VGCNF in the Corrosion Protection Mechanism of the Paint Coatings

Conducting polymers (CPs) (e.g., polyaniline, poly(*o*-methoxyaniline), poly(*o*-ethoxyaniline), polypyrrole, poly(3-methylthoiphene), poly(aromatic amines)) protect the surface of metal and alloy substrates through stabilizing the substrate potential in the passive region.[135-139] Several research papers have been reported on the use of CPs for corrosion protection of different metal and alloys such as iron,[140-147] copper,[148-155] zinc,[156-158] aluminum,[159-164] brass,[165] stainless steel,[166-172] and mild steel.[173-179] Depending

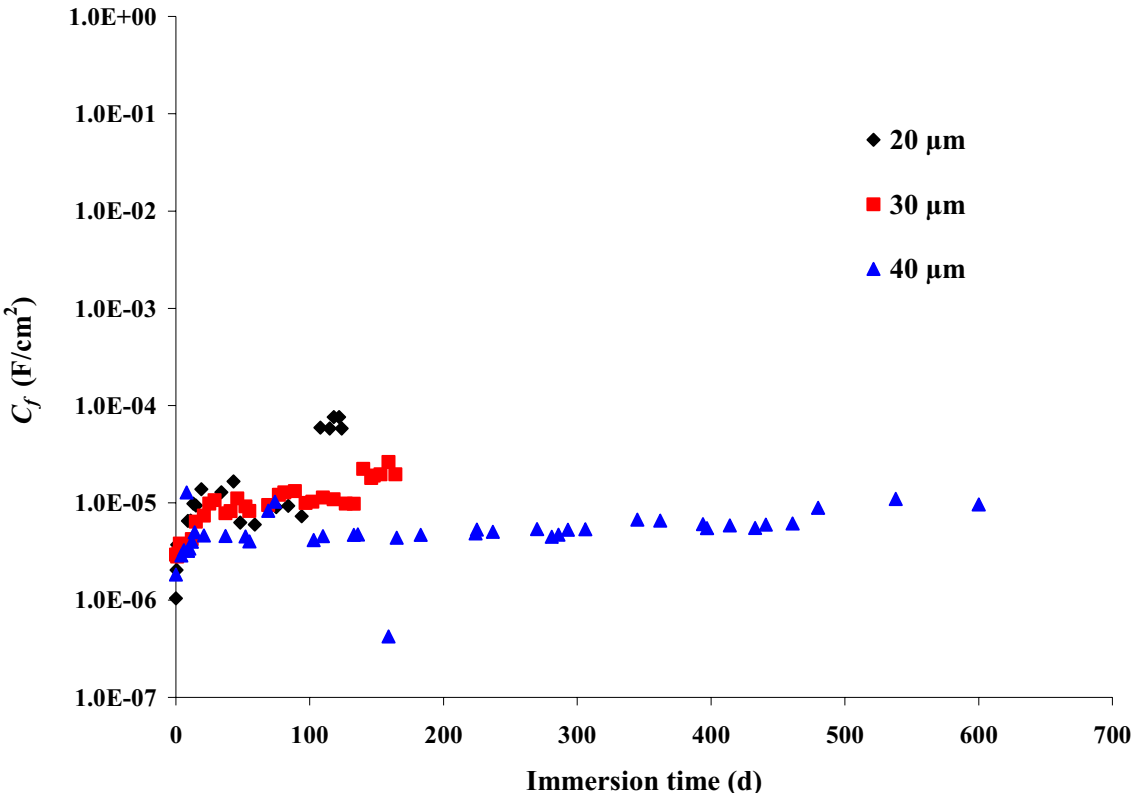

Figure 3.80 Variation of the VGCNF capacitance (C_f) with immersion time for mild steel panels coated with a commercial alkyd paint film containing 5 wt % of VGCNF in 3% NaCl solution. ◆ = 20 µm, ■ = 30 µm, and ▲ = 40 µm.

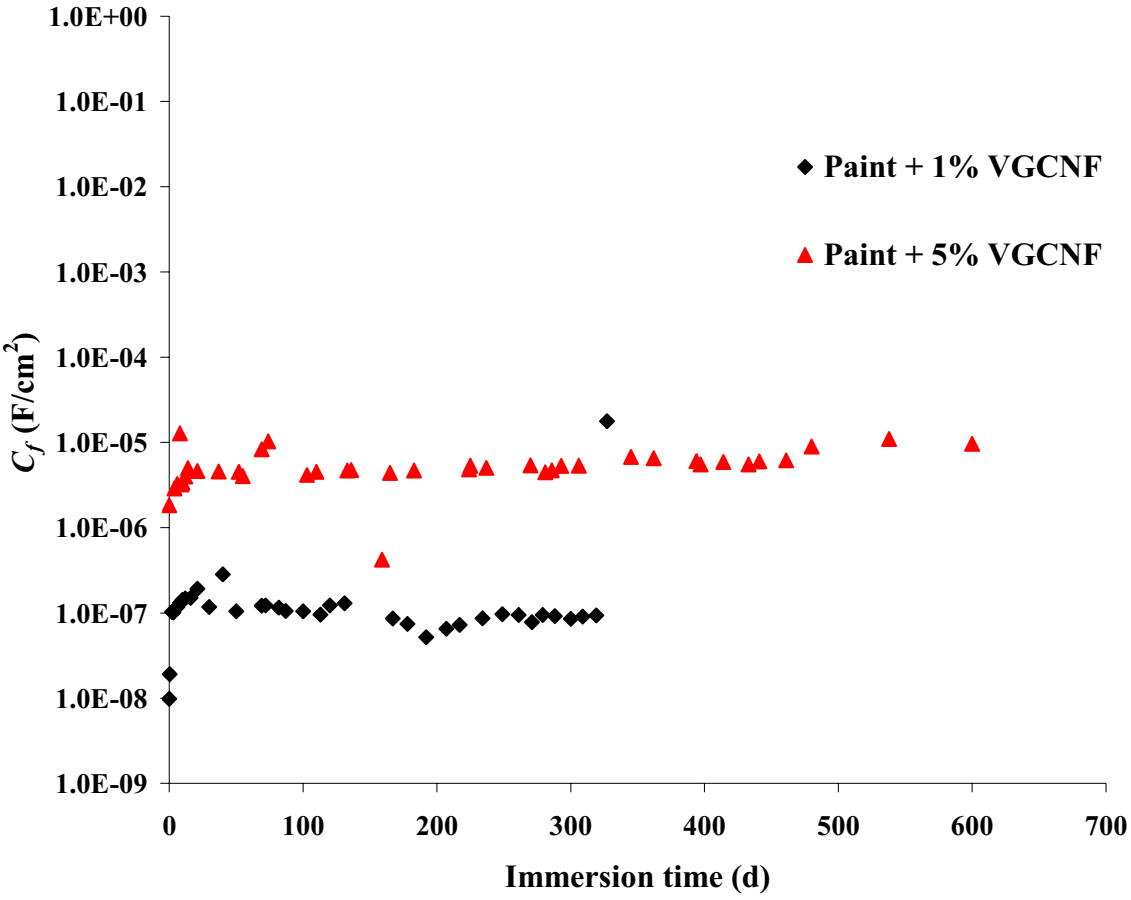

Figure 3.81 Variation of the VGCNF capacitance (C_f) with immersion time for mild steel panels coated with a VGCNF-incorporated commercial alkyd paint film (40 μm thick) and exposed to 3% NaCl solution. ◆ = paint + 1% VGCNF, and ▲ = paint + 5% VGCNF.

on the level of their conductivity, CPs are generally classified as semiconductor materials. Apart from their electrical properties, CPs have other advantages over inorganic semiconductors. Among these advantages, and perhaps the most important one, is the ability of the CPs to change their molecular structures and properties in a reaction depending on the reaction conditions and environment.[180] Another advantage is the relatively low density of CPs as compared to inorganic semiconductors.

The last decade has witnessed several papers on the protection mechanism promoted by conducted polymers applied to metals surfaces. For example, the protection mechanism of polyaniline applied to the surface of iron and steel substrates has been studied by several authors.[180-189] The studies showed that polyaniline has both barrier and electrochemical protection effects.[181] The electrochemical protection is caused by the formation of a passive layer on the substrate surface and the positive shift in the corrosion potential of the metal substrate due to the redox properties of polyaniline.[190]

As shown above, the mechanical, electrical, and electrochemical measurements have indicated that the incorporation of the conductive VGCNFs into the alkyd paint has improved the corrosive protective properties of the pure paint matrix applied to the surface of the mild steel samples. These results indicate that VGCNF acts as an excellent conductive filler as mentioned in the literature.[132, 134]

According to Pittman et al., the incorporation of VGCNF into the matrix of an insulating polymer (paint or organic coating) the fibers disperse more or less uniformly in the polymer matrix and form different bridge-like conductive networks in the polymer matrix which renders the matrix electrically conductive.[132, 134, 191] This observation was

again confirmed in the current study through the electrical conductivity measurements presented herein.

To the best of my knowledge, there is no single paper on the electrochemical behavior of VGCNF-incorporated alkyd paint coatings. The OCP measurements showed that the incorporation of the VGCNF in the paint matrix increases the immersion time period elapsed (service life) before the OCP drops to the corrosion potential (E_{ss}) of the bare steel substrate. These observations indicate an increase in the anticorrosion properties of the paint coating upon addition of VGCNFs. Based on the results presented in this chapter; it is believed that VGCNF has a barrier protection effect (e.g., Figures 3.8 through 3.13 and Table 3.1). More details on the corrosion protection mechanism offered by the incorporation of VGCNFs or SiC microparticles in the paint matrix are given in Chapter 6.

3.4 Conclusions

In this chapter, the EIS behavior of mild steel coupons coated with a commercial alkyd paint containing different loadings of VGCNF in 3% NaCl solution was investigated. The samples studied include pure paint and VGCNF-loaded paint with 0.5, 1, 3, 5, and 10 wt % VGCNF. In addition to the EIS, the study involved OCP, and CV measurements. The results showed that the incorporation of the VGCNF in the alkyd paint formulation significantly enhances the anticorrosive properties imparted by the coating. These results are in agreement with the proposed hypothesis that VGCNF would behave similar to conductive polymers. Furthermore, the results also showed that the highest barrier properties and the lowest corrosion rates were obtained for the paint

coatings containing 5 wt % VGCNF. Coatings with higher VGCNF (e.g., 10%) did not show any appreciable improvement in the protection properties of the coating film.

3.5 References

(1) Murray, J. N. *Progress in Organic Coatings* **1997**, *30*, 225-233.

(2) Popova, S. N.; Popov, B. N.; White, R. E.; Drazic, D. *Corrosion* **1990**, *46*, 1007-1014.

(3) Kumar, S. A.; Alagar, M.; Mohan, V. *Surface Coatings International, Part B: Coatings Transactions* **2001**, *84*, 43-47.

(4) Momose, Y.; Tomii, M.; Maruyama, T.; Shimoda, T.; Motohashi, Y. *Surface and Coatings Technology* **2003**, *169-170*, 682-685.

(5) Duan, H.; Du, K.; Yan, C.; Wang, F. *Electrochimica Acta* **2006**, *51*, 2898-2908.

(6) Lux, L.; Galova, M. *Chemical Papers* **1988**, *42*, 291-298.

(7) Petrovic, Z.; Metikos-Hukovic, M.; Babic, R. *Progress in Organic Coatings* **2008**, *61*, 1-6.

(8) Sinapi, F.; Lejeune, I.; Delhalle, J.; Mekhalif, Z. *Electrochimica Acta* **2007**, *52*, 5182-5190.

(9) Mansfeld, F. In *Analytical Methods in Corrosion Science and Engineering*; Marcus, P., Mansfeld, F., Eds.; CRC Press: Boca Raton, FL, 2006, pp 463-505.

(10) Orazem, M. E.; Tribollet, B. *Electrochemical Impedance Spectroscopy*; John Wiley & Sons, Inc.: Hoboken, NJ, 2008.

(11) Silverman, D. C.; Carrico, J. E. *Corrosion* **1988**, *44*, 280-287.

(12) Mansfeld, F.; Kendig, M. W. *ASTM Special Technical Publication* **1985**, *866*, 122-142.

(13) Loveday, D.; Peterson, P.; Rodgers, B. *Journal of Coatings Technology* **2005**, *2*, 22-27.

(14) Amirudin, A.; Thierry, D. *Progress in Organic Coatings* **1995**, *26*, 1-28.

(15) Amirudin, A.; Thierry, D. *British Corrosion Journal* **1995**, *30*, 128-134.

(16) Bierwagen, G.; Tallman, D.; Li, J.; He, L.; Jeffcoate, C. *Progress in Organic Coatings* **2003**, *46*, 148-157.

(17) Bierwagen, G. P.; Tallman, D. E.; Zlotnick, J.; Jeffcoate, C. S. *ACS Symposium Series* **1998**, *689*, 123-136.

(18) Walter, G. W. *Corrosion Science* **1986**, *26*, 681-703.

(19) Walter, G. W.; Nguyen, D. N.; Madurasinghe, M. A. D. *Electrochimica Acta* **1992**, *37*, 245-262.

(20) Macdonald, D. D. *Electrochimica Acta* **1990**, *35*, 1509-1525.

(21) Macdonald, D. D. *Electrochimica Acta* **2006**, *51*, 1376-1388.

(22) Macdonald, J. R.; Johnson, W. B. In *Impedance Spectroscopy: Theory, Experiment, and Applications,* 2nd ed.; Barsoukov, E., Macdonald, J. R., Eds.; John Wiley & Sons, Inc.: Hoboken, NJ, 2005, pp 1-26.

(23) Mansfeld, F. *Electrochimica Acta* **1990**, *35*, 1533-1544.

(24) Lasia, A. *Modern Aspects of Electrochemistry* **1999**, *32*, 143-248.

(25) Park, S.-M.; Yoo, J.-S. *Analytical Chemistry* **2003**, *75*, 455A-461A.

(26) Van Westing, E. P. M.; Ferrari, G. M.; De Wit, J. H. W. *Electrochimica Acta* **1994**, *39*, 899-910.

(27) Koleva, D. A.; van Breugel, K.; de Wit, J. H. W.; Fraaij, A. L. A.; Boshkov, N. *ECS Transactions* **2007**, *2*, 51-62.

(28) Rammelt, U.; Reinhard, G. *Progress in Organic Coatings* **1992**, *21*, 205-226.

(29) To, X. T.; Pebere, N.; Pelaprat, N.; Boutevin, B.; Hervaud, Y. *Materials Science Forum* **1998**, *289-292*, 1193-1203.

(30) Van Der Weijde, D. H.; Van Westing, E. P. M.; Ferrari, G. M.; De Wit, J. H. W. *ACS Symposium Series* **1998**, *689*, 45-57.

(31) Fontana, M. G. *Corrosion Engineering*, 3rd ed.; McGraw-Hill, Inc.: New York, 1986.

(32) Forsgren, A. *Corrosion Control Through Organic Coatings* CRC Press: Boca Raton, FL, 2006.

(33) Schweitzer, P. A., Ed. *Paint and Coatings: Applications and Corrosion Resistance*; CRC Press: New York, 2006.

(34) Trijueque, J.; Garcia-Jareno, J. J.; Navarro-Laboulais, J.; Sanmatias, A.; Vicente, F. *Electrochimica Acta* **1999**, *45*, 789-795.

(35) Wipf, D. O.; Wightman, R. M. *Analytical Chemistry* **1988**, *60*, 2460-2464.

(36) de Vries, W. T.; van Dalen, E. *Journal of Electroanalytical Chemistry* **1965**, *10*, 183-190.

(37) Fan, F. R. F.; Mirkin, M. V.; Bard, A. J. *ournal of Physical Chemistry* **1994**, *98*, 1475-1481.

(38) Roullier, L.; Laviron, E. *Journal of Electroanalytical Chemistry and Interfacial Electrochemistry* **1983**, *157*, 193-203.

(39) Lewandowski, A.; Waligora, L.; Galinski, M. *Electroanalysis* **2009**, *21*, 2221-2227.

(40) Baron, R.; Kershaw, N. M.; Donohoe, T. J.; Compton, R. G. *Journal of Physical Organic Chemistry* **2009**, *22*, 247-253.

(41) Fleming, B. D.; Zhang, J.; Elton, D.; Bond, A. M. *Analytical Chemistry* **2007**, *79*, 6515-6526.

(42) Jiang, J.-H.; Wu, B.-L.; Cha, C.-s. *Journal of Electroanalytical Chemistry* **1996**, *417*, 89-93.

(43) Evans, D. H.; O'Connell, K. M.; Petersen, R. A.; Kelly, M. J. *Journal of Chemical Education* **1983**, *60*, 290-293.

(44) Elvington, M. C.; Brewer, K. J. In *Applications of Physical Methods to Inorganic and Bioinorganic Chemistry*; Scott, R. A., Ed.; John Wiley & Sons, Ltd.: Hoboken, NJ, 2007, pp 17-38.

(45) Hammerich, O. In *Investigation of Organic Reactions and Their Mechanisms*; Maskill, H., Ed.; Blackwell Publishing Ltd.: Oxford, UK, 2006, pp 127-166.

(46) Henze, G. In *Handbook of Analytical Techniques*; Günzler, H., Williams, A., Eds.; Wiley-VCH: Weinheim, Germany, 2001; Vol. 2, pp 785-825.

(47) Rusling, J. F.; Suib, S. L. *Advanced Materials* **1994**, *6*, 922-930.

(48) Kapoor, R. C. In *Facets of Coordination Chemistry*; Agarwala, B. V., Munshi, K. N., Eds.; World Scientific Publishing Co. Pte. Ltd.: River Edge, NJ, 1993, pp 118-122.

(49) Heineman, W. R.; Kissinger, P. T. *Current Separations* **1989**, *9*, 15-18.

(50) Ahadi, M. M.; Attar, M. M. *Scientia Iranica* **2007**, *14*, 369-372.

(51) Ramirez, D.; Vera, R.; Gomez, H.; Conajahua, C. *Journal of the Chilean Chemical Society* **2005**, *50*, 489-494.

(52) Chaudhari, S.; Patil, P. P. *Journal of Applied Polymer Science* **2007**, *106*, 400-410.

(53) Bajat, J. B.; Dedic, O. *Journal of Adhesion Science and Technology* **2007**, *21*, 819-831.

(54) Mansfeld, F.; Kendig, M. W.; Tsai, S. *Corrosion* **1982**, *38*, 478-485.

(55) Liu, C.; Bi, Q.; Leyland, A.; Matthews, A. *Corrosion Science* **2003**, *45*, 1257-1273.

(56) Liu, C.; Bi, Q.; Leyland, A.; Matthews, A. *Corrosion Science* **2003**, *45*, 1243-1256.

(57) Loveday, D.; Peterson, P.; Rodgers, B. *Journal of Coatings Technology* **2004**, *1*, 88-93.

(58) Loveday, D.; Peterson, P.; Rodgers, B. *Journal of Coatings Technology* **2004**, *1*, 46-52.

(59) Meroufel, A.; Touzain, S. *Progress in Organic Coatings* **2007**, *59*, 197-205.

(60) Urquidi-Macdonald, M.; Egan, P. C. *Corrosion Reviews* **1997**, *15*, 169-194.

(61) Kendig, M.; Mansfeld, F.; Tsai, S. *Corrosion Science* **1983**, *23*, 317-329.

(62) Mansfeld, F.; Lin, S.; Chen, Y. C.; Shih, H. *Journal of the Electrochemical Society* **1988**, *135*, 906-907.

(63) Beaunier, L.; Epelboin, I.; Lestrade, J. C.; Takenouti, H. *Surface Technology* **1976**, *4*, 237-254.

(64) Macedo, M. C. S. S.; Margarit-Mattos, I. C. P.; Fragata, F. L.; Jorcin, J. B.; Pebere, N.; Mattos, O. R. *Corrosion Science* **2009**, *51*, 1322-1327.

(65) Amirudin, A. M.Ph.D. Thesis, The Royal Institute of Technology, Stockholm, Sweden, 1994.

(66) Pebere, N.; Duprat, M.; Dabosi, F.; De Savignac, A. *Materials Science Forum* **1989**, *44-45*, 97-107.

(67) Hang, T. T. X.; Truc, T. A.; Nam, T. H.; Oanh, V. K.; Jorcin, J.-B.; Pebere, N. *Surface and Coatings Technology* **2007**, *201*, 7408-7415.

(68) Le Pen, C.; Lacabanne, C.; Pebere, N. *Progress in Organic Coatings* **2003**, *46*, 77-83.

(69) Truc, T. A.; Pebere, N.; Hang, T. T. X.; Hervaud, Y.; Boutevin, B. *Progress in Organic Coatings* **2004**, *49*, 130-136.

(70) Leidheiser, H., Jr. *Progress in Organic Coatings* **1979**, *7*, 79-104.

(71) Leidheiser, H., Jr.; Granata, R. D. *IBM Journal of Research and Development* **1988**, *32*, 582-590.

(72) Kamarchik, P. *ASTM Special Technical Publication* **1993**, *STP 1188*, 463-474.

(73) Liu, J.; Gong, G.; Yan, C. *Electrochimica Acta* **2005**, *50*, 3320-3332.

(74) Zubielewicz, M.; Gnot, W. *Progress in Organic Coatings* **2004**, *49*, 358-371.

(75) Mahdavian, M.; Attar, M. M. *Progress in Organic Coatings* **2005**, *53*, 191-194.

(76) Macdonald, D. D.Personal communication, 2009.

(77) Pebere, N.; Picaud, T.; Duprat, M.; Dabosi, F. *Corrosion Science* **1989**, *29*, 1073-1086.

(78) Miskovic-Stankovic, V. B.; Drazic, D. M.; Acamovic, N. M. *Journal of Coatings Technology* **1991**, *63*, 25-29.

(79) Gamry Instruments Home Page. http://www.gamry.com/App_Notes/EIS_Of_Coatings/EIS_Of_Coatings.htm (accessed Dec 2009)

(80) Macdonald, D. D. *Corrosion* **1990**, *46*, 229-242.

(81) Macdonald, D. D. *NATO ASI Series, Series E: Applied Sciences* **1991**, *203*, 31-68.

(82) Raistrick, I. D.; Franceschetti, D. R.; Macdonald, J. R. In *Impedance Spectroscopy: Theory, Experiment, and Applications,* 2nd ed.; Barsoukov, E., Macdonald, J. R., Eds.; John Wiley & Sons: Hoboken, NJ, 2005, pp 27-128.

(83) Badawy, W. A.; Ismail, K. M.; Fathi, A. M. *Journal of Applied Electrochemistry* **2005**, *35*, 879-888.

(84) Badawy, W. A.; Ismail, K. M.; Fathi, A. M. *Electrochimica Acta* **2005**, *50*, 3603-3608.

(85) Badawy, W. A.; Ismail, K. M.; Fathi, A. M. *Electrochimica Acta* **2006**, *51*, 4182-4189.

(86) Bonora, P. L.; Deflorian, F.; Fedrizzi, L. *Electrochimica Acta* **1996**, *41*, 1073-1082.

(87) Instruments, G.; Gamry Instruments Home Page. http://www.gamry.com/App_Notes/EIS_Primer/EIS_Primer.htm (accessed Dec 2009)

(88) Deflorian, F.; Fedrizzi, L. *Journal of Adhesion Science and Technology* **1999**, *13*, 629-645.

(89) Deflorian, F.; Fedrizzi, L.; Bonora, P. L. *Progress in Organic Coatings* **1993**, *23*, 73-88.

(90) Bonnel, K.; Le Pen, C.; Pebere, N. *Electrochimica Acta* **1999**, *44*, 4259-4267.

(91) Simpson, T. C.; Moran, P. J.; Hampel, H.; Davis, G. D.; Shaw, B. A.; Arah, C. O.; Fritz, T. L.; Zankel, K. L. *ASTM Special Technical Publication* **1990**, *1000*, 397-412.

(92) Kendig, M. W.; Jeanjaquet, S.; Lumsden, J. *ASTM Special Technical Publication* **1993**, *STP 1188*, 407-427.

(93) Scully, J. R. *Journal of the Electrochemical Society* **1989**, *136*, 979-990.

(94) Carbonini, P.; Monetta, T.; Nicodemo, L.; Mastronardi, P.; Scatteia, B.; Bellucci, F. *Progress in Organic Coatings* **1996**, *29*, 13-20.

(95) Itagaki, M.; Ono, A.; Watanabe, K.; Katayama, H.; Noda, K. *ECS Transactions* **2006**, *1*, 215-222.

(96) Brown, R.; Alias, M. N.; Fontana, R. *Surface and Coatings Technology* **1993**, *62*, 467-473.

(97) Stern, M. *Journal of the Electrochemical Society* **1957**, *104*, 559-563.

(98) Stern, M.; Geavy, A. L. *Journal of the Electrochemical Society* **1957**, *104*, 56-63.

(99) Kendig, M.; Mansfeld, F. *Materials Research Society Symposium Proceedings* **1988**, *125*, 293-320.

(100) Miskovic-Stankovic, V. B.; Drazic, D. M.; Teodorovic, M. J. *Corrosion Science* **1995**, *37*, 241-252.

(101) Lazarevic, Z. Z.; Miskovic-Stankovic, V. B.; Kacarevic-Popovic, Z.; Drazic, D. M. *Corrosion Science* **2005**, *47*, 823-834.

(102) Bellucci, F.; Nicodemo, L. *Corrosion* **1993**, *49*, 235-247.

(103) Brasher, D. M.; Kingsbury, A. H. *Journal of Applied Chemistry* **1954**, *4*, 62-72.

(104) Lindqvist, S. A. *Corrosion* **1985**, *41*, 69-75.

(105) Mansfeld, F.; Tsai, C. H. *Corrosion* **1991**, *47*, 958-963.

(106) Deflorian, F.; Fedrizzi, L.; Bonora, P. L. *British Corrosion Journal* **1997**, *32*, 145-149.

(107) Castela, A. S.; Simoes, A. M. *Progress in Organic Coatings* **2003**, *46*, 130-134.

(108) Castela, A. S.; Simoes, A. M. *Corrosion Science* **2003**, *45*, 1631-1646.

(109) Hulden, M.; Hansen, C. M. *Progress in Organic Coatings* **1985**, *13*, 171-194.

(110) Perera, D. Y.; Selier, P. *Progress in Organic Coatings* **1973**, *2*, 57-80.

(111) Walter, G. W. *Journal of Electroanalytical Chemistry and Interfacial Electrochemistry* **1981**, *118*, 259-273.

(112) Miszczyk, A.; Darowicki, K.; Schauer, T. *Journal of Solid State Electrochemistry* **2005**, *9*, 909-913.

(113) Miszczyk, A.; Schauer, T. *Progress in Organic Coatings* **2005**, *52*, 298-305.

(114) Amirudin, A.; Thierry, D. *British Corrosion Journal* **1991**, *26*, 195-201.

(115) Leng, A.; Streckel, H.; Stratmann, M. *Corrosion Science* **1999**, *41*, 547-578.

(116) Brewis, D. M.; Briggs, D., Eds. *Industrial Adhesion Problems*; Wiley-Interscience: Malden, MA, 1985.

(117) Dickie, R. A. *ACS Symposium Series* **1986**, *322*, 136-154.

(118) Grundmeier, G.; Schmidt, W.; Stratmann, M. *Electrochimica Acta* **2000**, *45*, 2515-2533.

(119) Grundmeier, G.; Simoes, A. *Encyclopedia of Electrochemistry* **2003**, *4*, 500-566.

(120) Koehler, E. L. *Corrosion* **1984**, *40*, 5-8.

(121) Leidheiser, H., Jr. *Journal of Coatings Technology* **1981**, *53*, 29-39.

(122) McCluney, S. A.; Popova, S. N.; Popov, B. N.; White, R. E.; Griffin, R. B. *Journal of the Electrochemical Society* **1992**, *139*, 1556-1560.

(123) McIntyre, J. M.; Pham, H. Q. *Progress in Organic Coatings* **1996**, *27*, 201-207.

(124) Haruyama, S.; Asari, M.; Tsuru, T. *Proceedings of the Electrochemical Society* **1987**, *87-2*, 197-207.

(125) Nicodemo, L.; Bellucci, F.; Marcone, A.; Monetta, T. *Journal of Membrane Science* **1990**, *52*, 393-403.

(126) Deflorian, F.; Felhosi, I. *Corrosion* **2003**, *59*, 112-120.

(127) Deflorian, F.; Rossi, S. *Electrochimica Acta* **2006**, *51*, 1736-1744.

(128) Deflorian, F.; Rossi, S.; Fedrizzi, L.; Bonora, P. L. *Journal of Testing and Evaluation* **2003**, *31*, 91-97.

(129) Kousik, G.; Pitchumani, S.; Renganathan, N. G. *Progress in Organic Coatings* **2001**, *43*, 286-291.

(130) Wu, M.-S.; Lee, J.-T.; Chiang, P.-C. J.; Lin, J.-C. *Journal of Materials Science* **2007**, *42*, 259-265.

(131) Al-Saleh, M. H.; Sundararaj, U. *Carbon* **2009**, *47*, 2-22.

(132) Zhang, B.; Fu, R.; Zhang, M.; Dong, X.; Zhao, B.; Wang, L.; Pittman, C. U. *Composites, Part A: Applied Science and Manufacturing* **2006**, *37A*, 1884-1889.

(133) Guo, H.; Kumar, S. *PMSE Preprints* **2006**, *94*, 492-493.

(134) Zhang, B.; Fu, R.; Zhang, M.; Dong, X.; Wang, L.; Pittman, C. U. *Materials Research Bulletin* **2006**, *41*, 553-562.

(135) Tallman, D. E.; Bierwagen, G. P. In *Handbook of Conducting Polymers,* 3rd ed.; Skotheim, T. A., Reynolds, J., Eds.; Marcel Dekker, Inc.: New York, 2007; Vol. 2, pp 15/11-15/53.

(136) Liepins, R. In *Coatings Technology Handbook,* 3rd ed.; Tracton, A. A., Ed.; CRC Press: Boca Raton, FL, 2006, pp 91/91-91/99.

(137) Black, H. *Chemistry & Industry* **2005**, 16-17.

(138) Sitaram, S. P.; Stoffer, J. O.; O'Keefe, T. J. *Journal of Coatings Technology* **1997**, *69*, 65-69.

(139) Tallman, D. E.; Spinks, G.; Dominis, A.; Wallace, G. G. *Journal of Solid State Electrochemistry* **2002**, *6*, 73-84.

(140) Bernard, M. C.; Hugot-Le Goff, A.; Joiret, S.; Dinh, N. N.; Toan, N. N. *Journal of the Electrochemical Society* **1999**, *146*, 995-998.

(141) Bernard, M. C.; Hugot-LeGoff, A.; Joiret, S.; Dinh, N. N.; Toan, N. N. *Synthetic Metals* **1999**, *102*, 1383-1384.

(142) Fenelon, A. M.; Breslin, C. B. *Surface and Coatings Technology* **2004**, *190*, 264-270.

(143) Nguyen Thi Le, H.; Garcia, B.; Deslouis, C.; Le Xuan, Q. *Electrochimica Acta* **2001**, *46*, 4259-4272.

(144) Sazou, D.; Georgolios, C. *Journal of Electroanalytical Chemistry* **1997**, *429*, 81-93.

(145) Yagan, A.; Pekmez, N. O.; Yildiz, A. *Surface and Coatings Technology* **2007**, *201*, 7339-7345.

(146) Yagan, A.; Pekmez, N. O.; Yildiz, A. *Electrochimica Acta* **2008**, *53*, 5242-5251.

(147) Yano, J.; Nakatani, K.; Harima, Y.; Kitani, A. *Materials Letters* **2007**, *61*, 1500-1503.

(148) Chaudhari, S.; Patil, P. P. *Electrochimica Acta* **2007**, *53*, 927-933.

(149) Fedrizzi, L.; Deflorian, F.; Bonora, P. *Electrochimica Acta* **1999**, *44*, 4251-4258.

(150) Fenelon, A. M.; Breslin, C. B. *Electrochimica Acta* **2002**, *47*, 4467-4476.

(151) Herrasti, P.; del Rio, A. I.; Recio, J. *Electrochimica Acta* **2007**, *52*, 6496-6501.

(152) Redondo, M. I.; Breslin, C. B. *Corrosion Science* **2007**, *49*, 1765-1776.

(153) Shinde, V.; Gaikwad, A. B.; Patil, P. P. *Surface and Coatings Technology* **2008**, *202*, 2591-2602.

(154) Shinde, V.; Mandale, A. B.; Patil, K. R.; Gaikwad, A. B.; Patil, P. P. *Surface and Coatings Technology* **2006**, *200*, 5094-5101.

(155) Tueken, T.; Yazici, B.; Erbil, M. *Surface and Coatings Technology* **2006**, *200*, 4802-4809.

(156) Aeiyach, S.; Zaid, B.; Lacaze, P. C. *Electrochimica Acta* **1999**, *44*, 2889-2898.

(157) Hermelin, E.; Petitjean, J.; Lacroix, J.-C.; Chane-Ching, K. I.; Tanguy, J.; Lacaze, P.-C. *Chemistry of Materials* **2008**, *20*, 4447-4456.

(158) Vatsalarani, J.; Geetha, S.; Trivedi, D. C.; Warrier, P. C. *Journal of Power Sources* **2006**, *158*, 1484-1489.

(159) Cecchetto, L.; Ambat, R.; Davenport, A. J.; Delabouglise, D.; Petit, J. P.; Neel, O. *Corrosion Science* **2007**, *49*, 818-829.

(160) Gelling, V. J.; Tallman, D. E.; Bierwagen, G. P.; Wallace, G. G. *Polymer Preprints* **2000**, *41*, 1770-1771.

(161) Racicot, R.; Brown, R.; Yang, S. C. *Synthetic Metals* **1997**, *85*, 1263-1264.

(162) Racicot, R.; Clark, R. L.; Liu, H. B.; Yang, S. C.; Alias, M. N.; Brown, R. *Proceedings of SPIE-The International Society for Optical Engineering* **1995**, *2528*, 251-258.

(163) Tallman, D. E.; Pae, Y.; Bierwagen, G. P. *Corrosion* **2000**, *56*, 401-410.

(164) Yang, S. C.; Brown, R.; Racicot, R.; Lin, Y.; McClarnon, F. *ACS Symposium Series* **2003**, *843*, 196-206.

(165) Oezyilmaz, A. T.; Colak, N.; Ozyilmaz, G.; Sanguen, M. K. *Progress in Organic Coatings* **2007**, *60*, 24-32.

(166) Maouche, N.; Nessark, B. *Corrosion* **2008**, *64*, 315-324.

(167) Nicho, M. E.; Hu, H.; Gonzalez-Rodriguez, J. G.; Salinas-Bravo, V. M. *Journal of Applied Electrochemistry* **2006**, *36*, 153-160.

(168) Ren, S.; Barkey, D. *Journal of the Electrochemical Society* **1992**, *139*, 1021-1026.

(169) Santos, J. R., Jr.; Mattoso, L. H. C.; Motheo, A. J. *Electrochimica Acta* **1997**, *43*, 309-313.

(170) Sazou, D.; Kosseoglou, D. *Electrochimica Acta* **2006**, *51*, 2503-2511.

(171) Sazou, D.; Kourouzidou, M.; Pavlidou, E. *Electrochimica Acta* **2007**, *52*, 4385-4397.

(172) Zhang, T.; Zeng, C. L. *Electrochimica Acta* **2005**, *50*, 4721-4727.

(173) Ashrafi, A.; Golozar, M. A.; Mallakpour, S. *Journal of Applied Electrochemistry* **2008**, *38*, 225-229.

(174) Camalet, J. L.; Lacroix, J. C.; Aeiyach, S.; Chane-Ching, K.; Lacaze, P. C. *Journal of Electroanalytical Chemistry* **1996**, *416*, 179-182.

(175) Camalet, J. L.; Lacroix, J. C.; Nguyen, T. D.; Aeiyach, S.; Pham, M. C.; Petitjean, J.; Lacaze, P. C. *Journal of Electroanalytical Chemistry* **2000**, *485*, 13-20.

(176) Ding, K.; Jia, Z.; Ma, W.; Jiang, D.; Zhao, Q.; Cao, J.; Tong, R. *Protection of Metals* **2003**, *39*, 71-76.

(177) Hur, E.; Bereket, G.; Duran, B.; Ozdemir, D.; Sahin, Y. *Progress in Organic Coatings* **2007**, *60*, 153-160.

(178) Kinlen, P. J.; Ding, Y.; Silverman, D. C. *Corrosion* **2002**, *58*, 490-497.

(179) Lu, W.-K.; Elsenbaumer, R. L.; Wessling, B. *Synthetic Metals* **1995**, *71*, 2163-2166.

(180) Kalendova, A.; Vesely, D.; Stejskal, J.; Trchova, M. *Progress in Organic Coatings* **2008**, *63*, 209-221.

(181) Olad, A.; Rashidzadeh, A. *Progress in Organic Coatings* **2008**, *62*, 293-298.

(182) Gabriel, A.; Laycock, N. J.; McMurray, H. N.; Williams, G.; Cook, A. *ECS Transactions* **2006**, *1*, 37-46.

(183) Gabriel, A.; Laycock, N. J.; McMurray, H. N.; Williams, G.; Cook, A. *Electrochemical and Solid-State Letters* **2006**, *9*, B57-B60.

(184) Kamaraj, K.; Sathiyanarayanan, S.; Muthukrishnan, S.; Venkatachari, G. *Progress in Organic Coatings* **2009**, *64*, 460-465.

(185) Riaz, U.; Ashraf, S. M.; Ahmad, S. *Anti-Corrosion Methods and Materials* **2008**, *55*, 308-316.

(186) Alam, J.; Riaz, U.; Ashraf, S. M.; Ahmad, S. *Journal of Coatings Technology and Research* **2008**, *5*, 123-128.

(187) Syed Azim, S.; Sathiyanarayanan, S.; Venkatachari, G. *Progress in Organic Coatings* **2006**, *56*, 154-158.

(188) Galkowski, M. T.; Kulesza, P. J.; Miecznikowski, K.; Chojak, M.; Bala, H. *Journal of Solid State Electrochemistry* **2004**, *8*, 430-434.

(189) Huh, J. H.; Oh, E. J.; Cho, J. H. *Synthetic Metals* **2003**, *137*, 965-966.

(190) Wessling, B. *Paintindia* **2001**, *51*, 49-50,52.

(191) Xu, J.; Donohoe, J. P.; Pittman, C. U., Jr. *Composites, Part A* **2004**, *35A*, 693-701.

CHAPTER 4

ELECTROCHEMICAL IMPEDANCE SPECTROSCOPY (EIS) OF SiC-REINFORCED ALKYD PAINT-COATED MILD STEEL SAMPLES IN 3% NaCl

4.1 Introduction

Silicon carbide (SiC) is a wide-bandgap semiconductor material that has many applications in the semiconductor electronics industry.[1-7] The first use of SiC was as an abrasive for metallurgical applications.[8] The properties of SiC include good optical properties, high voltage switching characteristics, excellent physical and chemical stability, low thermal-expansion coefficient, excellent high-temperature properties, and high thermal-shock resistance.[9-14] All of these characteristics made SiC an ideal candidate for a wide range of applications including advanced energy systems,[15-18] high temperature, high power, and high frequency microelectronic devices,[19, 20] high power microwave devices,[21, 22] microelectromechanical systems (MEMS),[23-27] optoelectronic devices (e.g., light emitting diodes (LEDs), optical detectors, and lightweight mirrors)[28-31], and the transportation industry.[32-35]

SiC fibers and particles (in the micron and sub-micron range) are currently used as a reinforcing material in several ceramic microstructures, metal matrix composites (MMCs), and composite-based alloy coatings (e.g., such as Ni, Co, Mg, Al, and Ni-W-Co matrices).[36-46] Incorporation of SiC particles in MMCs improves the physical,

mechanical, and machinability properties of the composites and leads to superior properties such as high corrosion resistance especially in highly oxidizing and aggressive environments, good radiation stability, high-temperature fracture and creep, and improved friction and wear resistance.[47-51]

As mentioned in Chapters 1 and 3, EIS is a very useful, rapid, non-invasive, convenient, and relatively cheap technique for corrosion studies including rapid estimation of corrosion rates, assessment of corrosion inhibitors, and evaluation of organic and inorganic coatings.[52-59] Surveying the literature showed that there are only a few reports on the electrochemical behavior of SiC-reinforced MMCs (e.g., Mg- and Al-based composites), and metal-based coatings (e.g., Cr-, and Ni-based coatings).[60-67] However, to the best of our knowledge, there are no reported studies on the electrochemical behavior of SiC-reinforced alkyd paint coatings.

In the current investigation, the EIS technique, along with OCP measurements, has been used to evaluate the corrosion protection performance of SiC-reinforced commercial alkyd paint films, with different thicknesses and SiC content, applied to the surface of mild steel coupons immersed in 3% NaCl solution. The primary objective of this study was to assess and compare the effect of incorporation of SiC in the alkyd paint matrix with the effect of the incorporation of VGCNF in the same paint material on the insulating properties of the paint coatings.

4.2 Experimental

4.2.1 Chemicals and Reagents

Silicon carbide whiskers (1.5 μm in diameter, 18 μm in length, density = 3.217 g/cm^3) were obtained from Alfa Aesar (Ward Hill, MA). All other chemicals, reagents, and materials, including the commercial alkyd paint, used in the preparation of the SiC/paint-coated mild steel samples are as mentioned in Chapters 2 and 3.

All chemicals used in this work were of reagent grade and were used as received from the manufacturer. All solutions were prepared as needed using 18 MΩ-cm ultra-pure water (Milli-Q, Millipore Corp., Bedford, MA).

4.2.2 Electrodes and Instrumentation

The spin-coating procedure used to deposit the SiC-reinforced coating films on mild steel substrates is as mentioned in Chapter 2. The setup for EIS measurements is also similar to that described in Chapter 3.

4.3 Results and Discussions

4.3.1 Open Circuit Potential (OCP) Measurements

In this study, the OCP behavior of mild steel panels coated with alkyd paint films containing different weight content of SiC and having different thicknesses was followed over a period of up to 350 d in naturally aerated 3% NaCl aqueous solutions. Representative data are presented in Figures 4.1 through 4.5 for paint coatings containing 1 and 5 wt % SiC with film thicknesses in the 20 to 50 μm range.

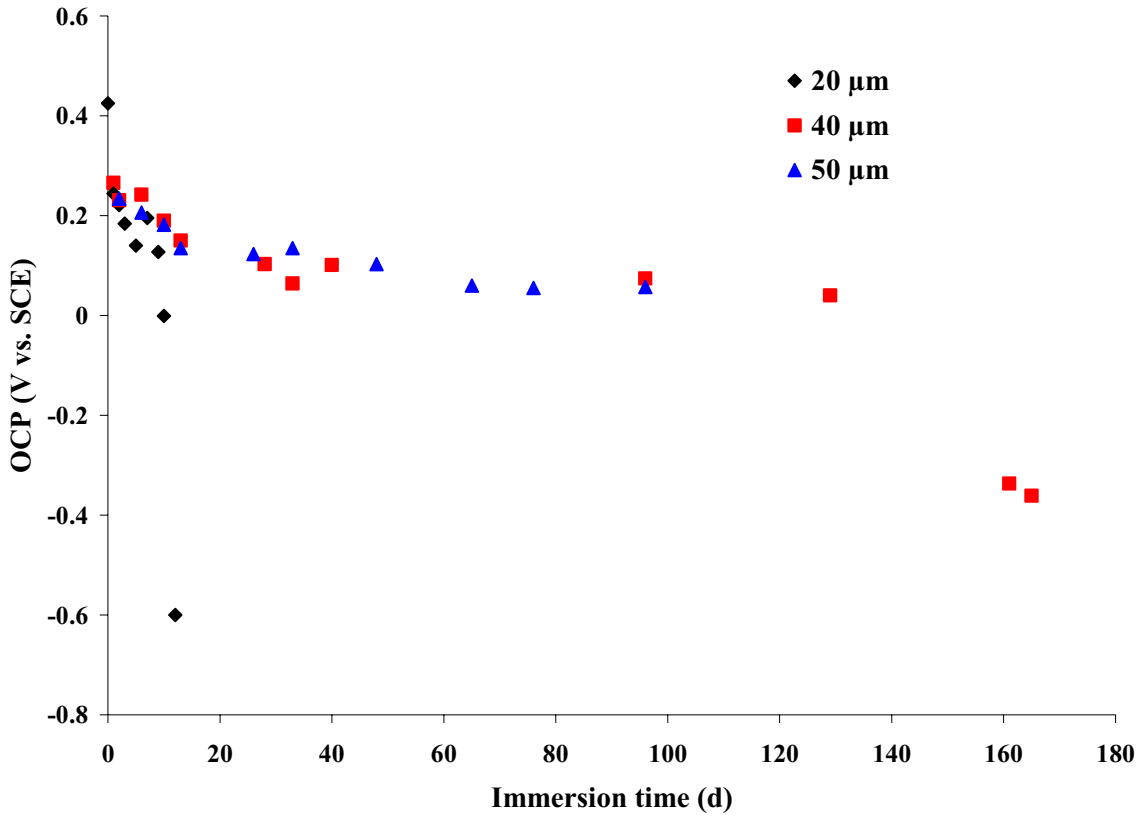

Figure 4.1 Long term OCP-immersion time curves for mild steel panels coated with a commercial alkyd paint film containing 1 wt % SiC in 3% NaCl solution. ◆ = 20 µm, ■ = 40 µm, and ▲ = 50 µm.

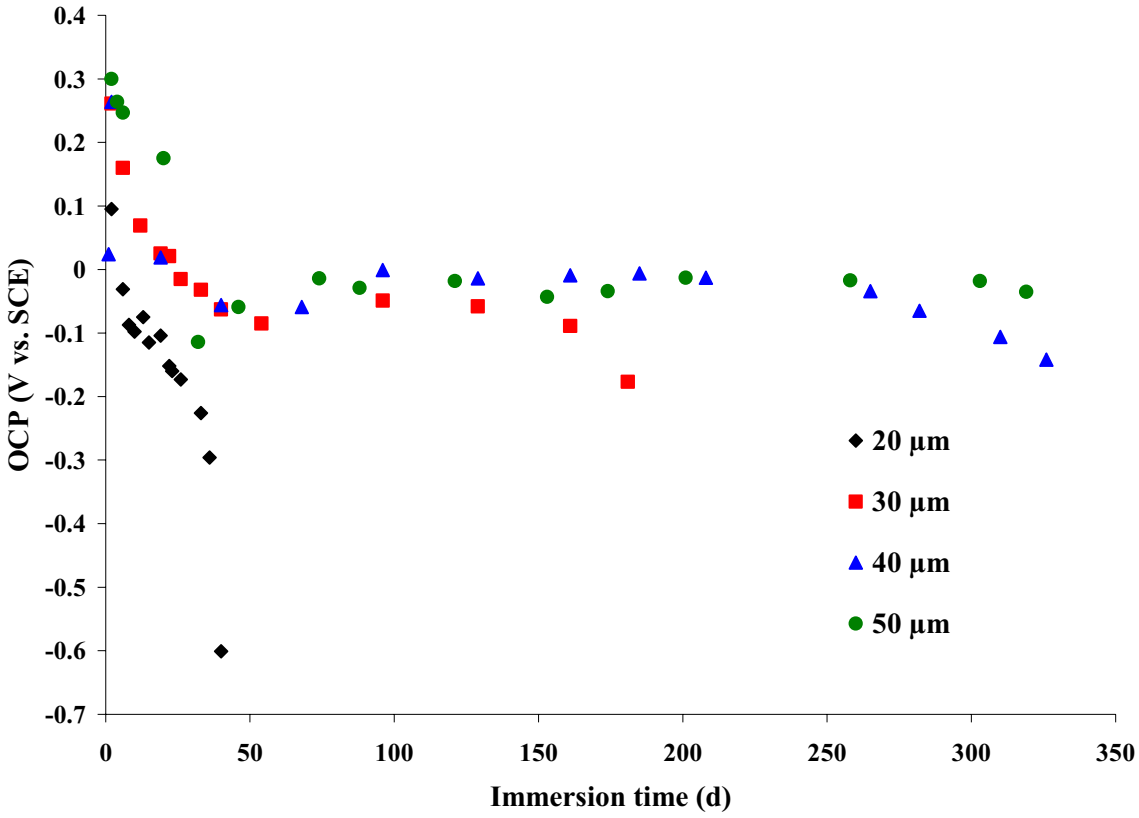

Figure 4.2 Long term OCP-immersion time curves for mild steel panels coated with a commercial alkyd paint film containing 5 wt % SiC in 3% NaCl solution. ◆ = 20 µm, ■ = 30 µm, ▲ = 40 µm, and ● = 50 µm.

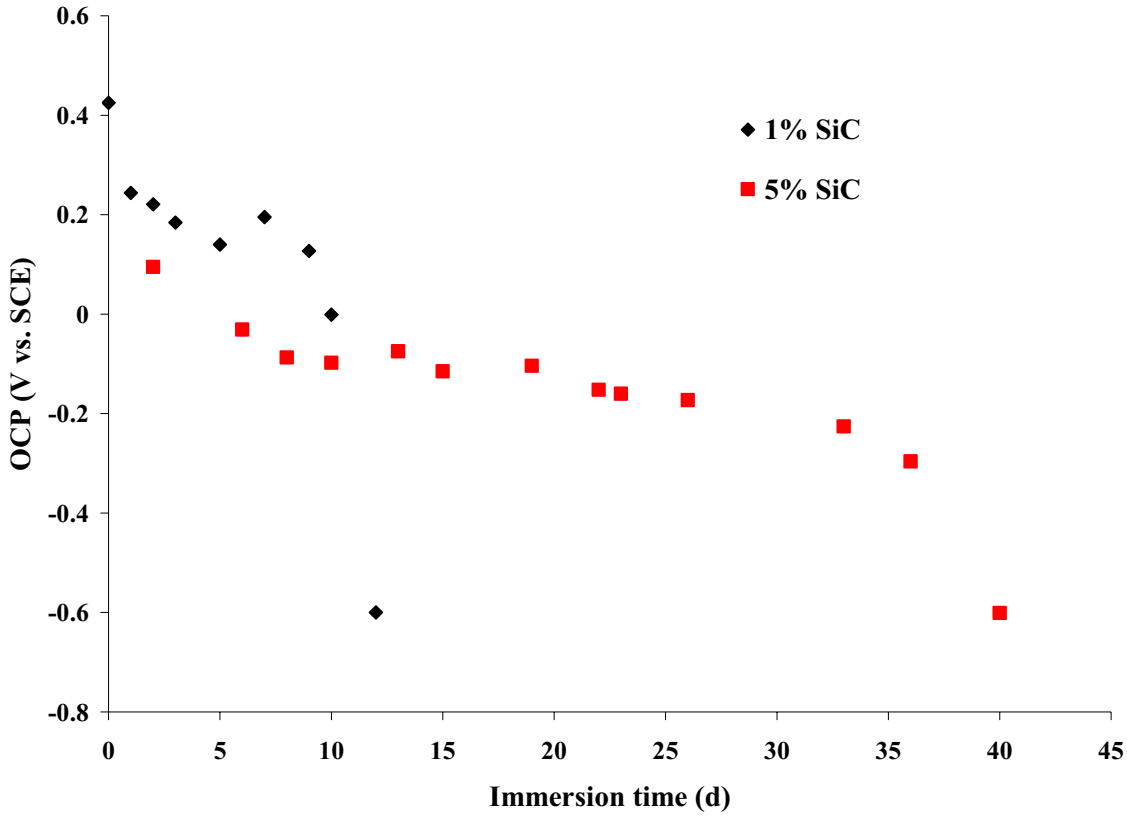

Figure 4.3 Long term OCP-immersion time curves for mild steel panels coated with a commercial alkyd paint film (20 μm in thickness) with different SiC loadings in 3% NaCl solution. ◆ = paint + 1% SiC, and ■ = paint + 5% SiC.

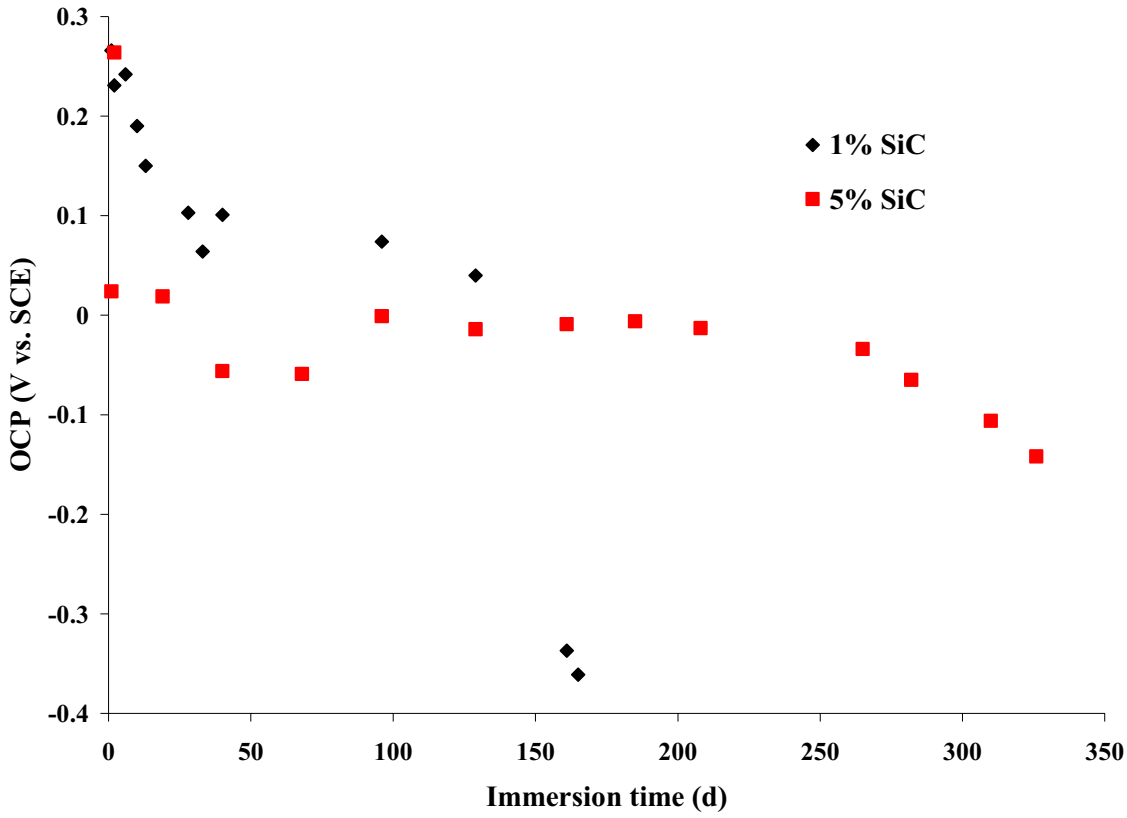

Figure 4.4 Long term OCP-immersion time curves for mild steel panels coated with a commercial alkyd paint film (40 μm in thickness) with different SiC loadings in 3% NaCl solution. ◆ = paint + 1% SiC, and ■ = paint + 5% SiC.

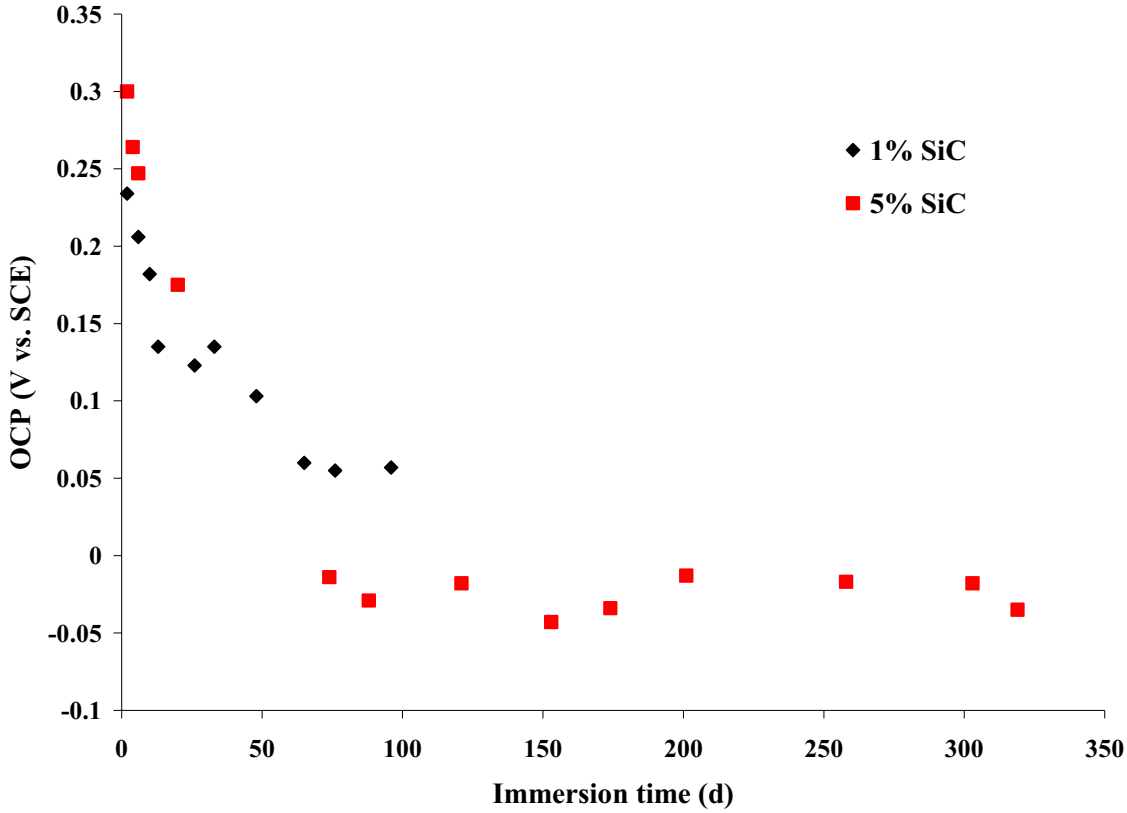

Figure 4.5 Long term OCP-immersion time curves for mild steel panels coated with a commercial alkyd paint film (50 μm in thickness) with different SiC loadings in 3% NaCl solution. ◆ = paint + 1% SiC, and ■ = paint + 5% SiC.

As shown in Figures 4.1 through 4.5, the initial OCP values were positive values (about +0.43 to +0.23 V vs. SCE). As mentioned in Chapter 3, the steady-state potential (E_{ss}) of the bare mild steel in the same electrolyte solution is about -0.60 V (vs. SCE).[68] These results indicate that the application of the SiC-incorporated coating shifts the initial OCP of the bare substrate to a more positive value indicating the protective characters of the coatings. As shown in the figures, as the immersion time increased, the OCP of the coated substrates shifted toward more negative values before it reached the E_{ss} value of the bare steel alloy. As depicted in Figure 4.1 and 4.2, the thicker the film coating, the longer the immersion period before the onset of the substrate corrosion (when E_{ss} is achieved and the corrosion products are clearly seen in the electrochemical cell). Figures 4.3 through 4.5 show that coatings containing 5 wt % SiC are more stable and require a longer time to reach E_{ss} than coatings containing 1 wt % SiC indicating better corrosion protection offered by the former coatings. For example, Figure 4.3 shows that for 20 μm thick coatings, the 5% SiC-incorporated film failed after 40 d while the 1% SiC-incorporated film failed after 12 d. These results are similar to those found with VGCNF-reinforced coatings presented in Chapter 3.

Table 4.1 and Figure 4.6 summarize the time to coating failure or end of testing (in d) for some of the studied samples based on the OCP measurements and visual observations for some of the studied coatings with different thicknesses and SiC loadings. For comparison, the results for pure coatings are also presented in the Table 4.1 and Figure 4.6. The data presented in Table 4.1 and Figure 4.6 also shows that a 50 μm thick coating containing 10 wt % SiC failed after 36 d of immersion in the electrolyte solution. This behavior can be attributed to variation in the coating thickness and the

Table 4.1 Time to coating failure or end of testing based on open circuit potential (OCP) measurements for pure and SiC-reinforced alkyd paint coatings with different thicknesses and SiC loadings.

Coating Specification	Film Thickness (μm)	Time to Coating Failure or End of Testing (d)
Pure paint	30	33
	50	202
	70	1814*
	150	1882*
Paint + 1 % SiC	20	12
	40	165
	50	129*
Paint + 5% SiC	20	40
	30	181
	40	326*
	50	319*
Paint + 10% SiC	50	36

*Testing ended with no failure.

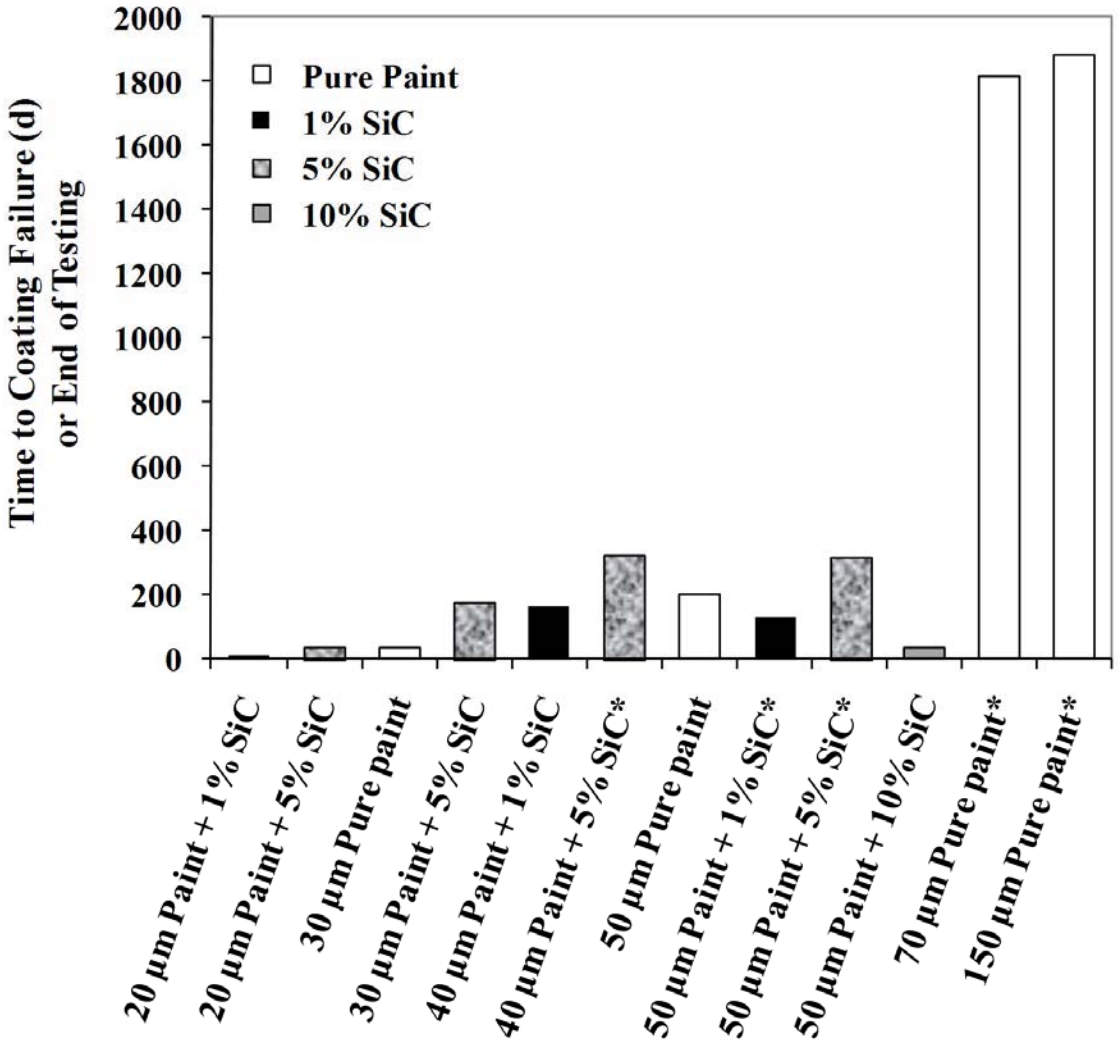

Figure 4.6 Time to coating failure or end of testing based on open circuit potential (OCP) measurements for pure and SiC-reinforced alkyd paint coatings with different thicknesses and SiC loadings. *Testing ended with no failure.

inhomogeneous distribution of the SiC particles in the coating film due to the higher viscosity of the SiC-paint matrix. As a result of the coating inhomogeneity, several voids and defects readily formed and the sample failed earlier than other coatings with the same thickness but less SiC content.

4.3.2 Electrochemical Impedance Spectroscopy (EIS) Measurements

Figure 4.7 through 4.22 show representative impedance spectra (both Bode and Nyquist plots) obtained for mild steel samples covered with alkyd paint coatings containing 1 and 5 SiC wt % with different coating thicknesses. The dotted lines in the spectra represent the modeled data. The Bode plots in Figures 4.7 through 4.13 show that the low frequency (LF) $|Z|$ value is in the range of 10^4 to 10^7 Ω depending on the coating thickness, the SiC wt %, and the immersion time. Furthermore, the figures also show that, for paint coatings having the same thickness, the longer the immersion time, the smaller the LF $|Z|$ value is, indicating a higher rate of electrolyte absorption, higher rate of corrosion, and hence a higher rate of damage of the paint film.

The Bode plot in Figure 4.7 shows that, for thin coatings (20-30 μm) containing 1 wt % SiC, as the immersion time increases, the short frequency-independent plateau at LF gets shorter indicating a faster rate of degradation. On the other hand, as shown in Figures 4.8 through 4.13, for thick coatings (> 30 μm) and coatings containing 5 wt % SiC, the plateau remains almost constant for a very long period of immersion in the electrolyte (as long as 326 d for the 40 μm thick coating shown in Figure 4.12) reflecting good corrosion protection for the coating film.

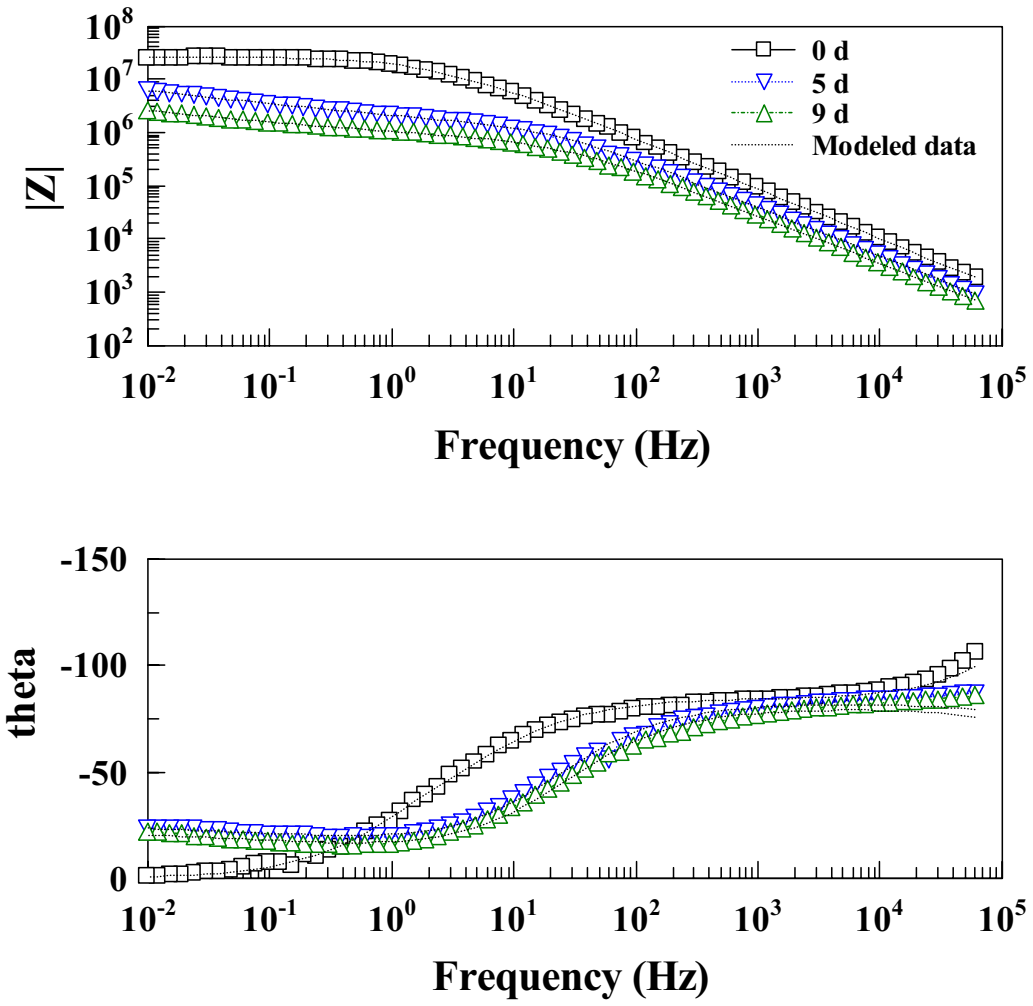

(a)

Figure 4.7 Bode (a) and Nyquist (b) plots with fittings for mild steel panels coated with 1 wt % SiC-incorporated commercial alkyd paint film (20-30 μm thick) at different immersion times in 3% NaCl solution.

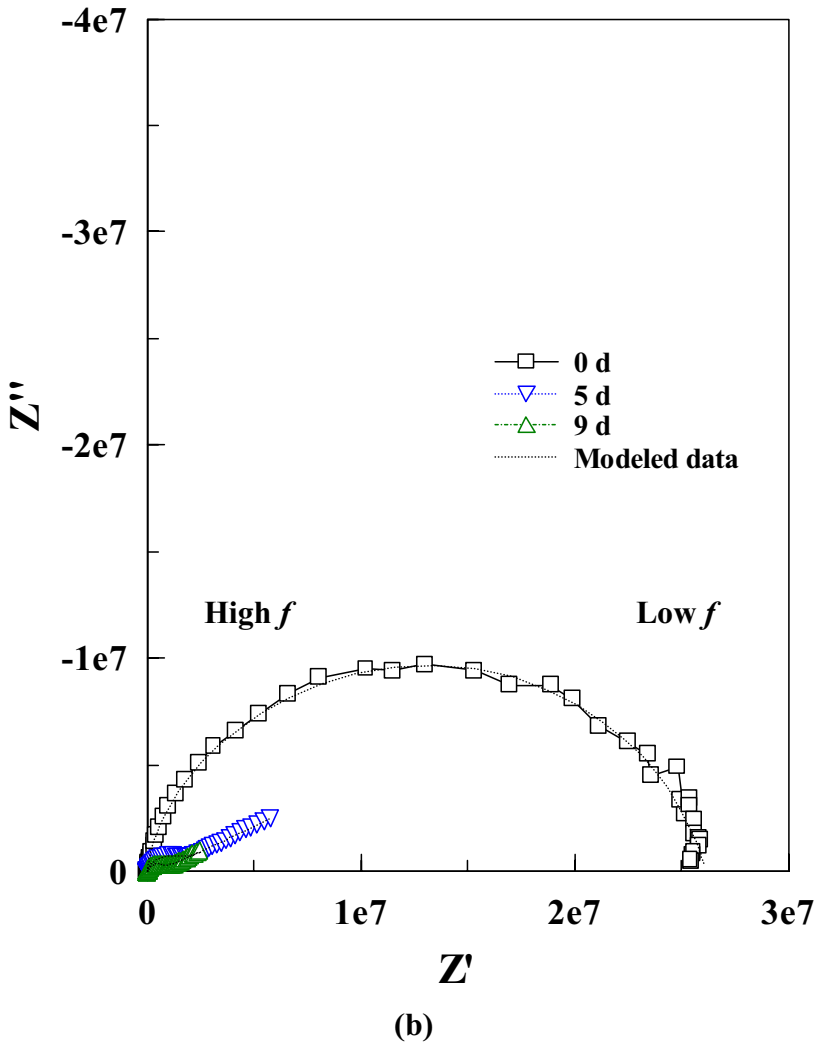

Figure 4.7 Continued.

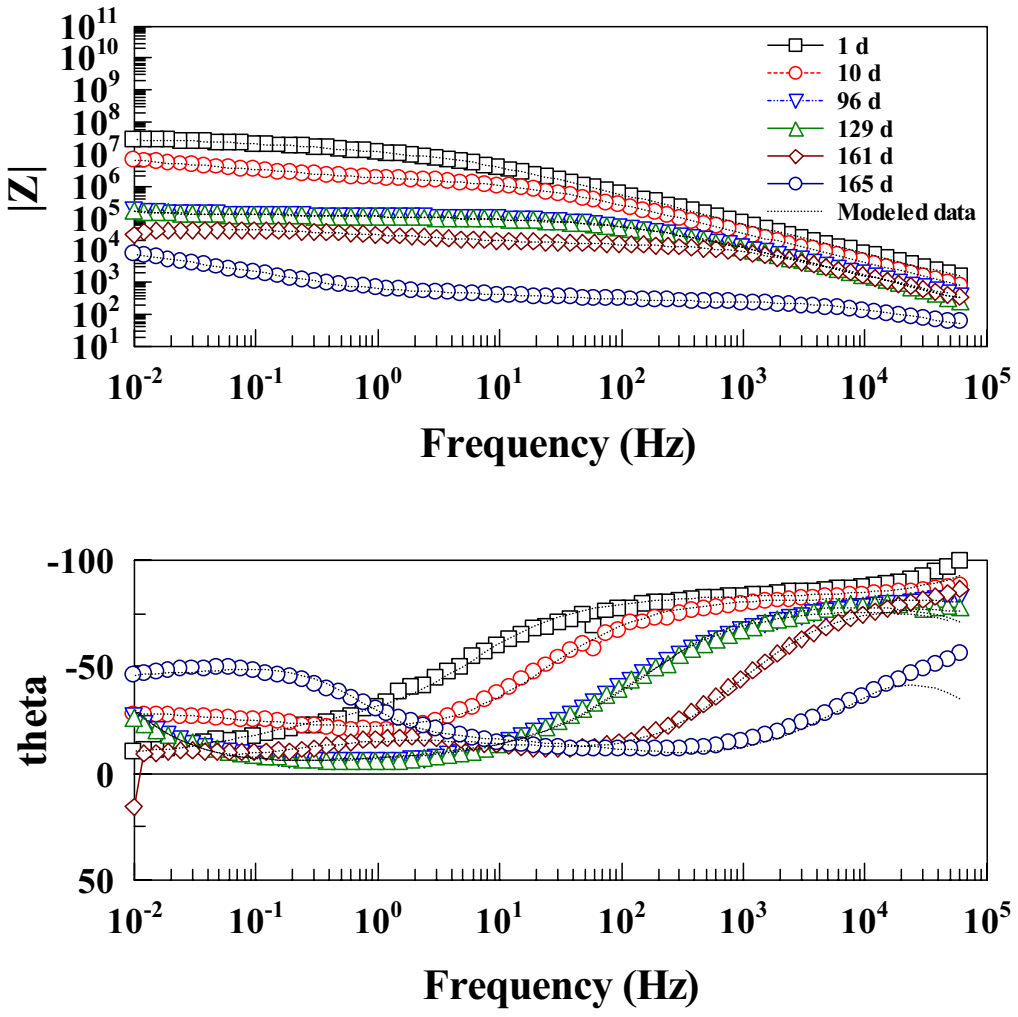

(a)

Figure 4.8 Bode (a) and Nyquist (b) plots with fittings for mild steel panels coated with 1 wt % SiC-incorporated commercial alkyd paint film (30-40 μm thick) at different immersion times in 3% NaCl solution.

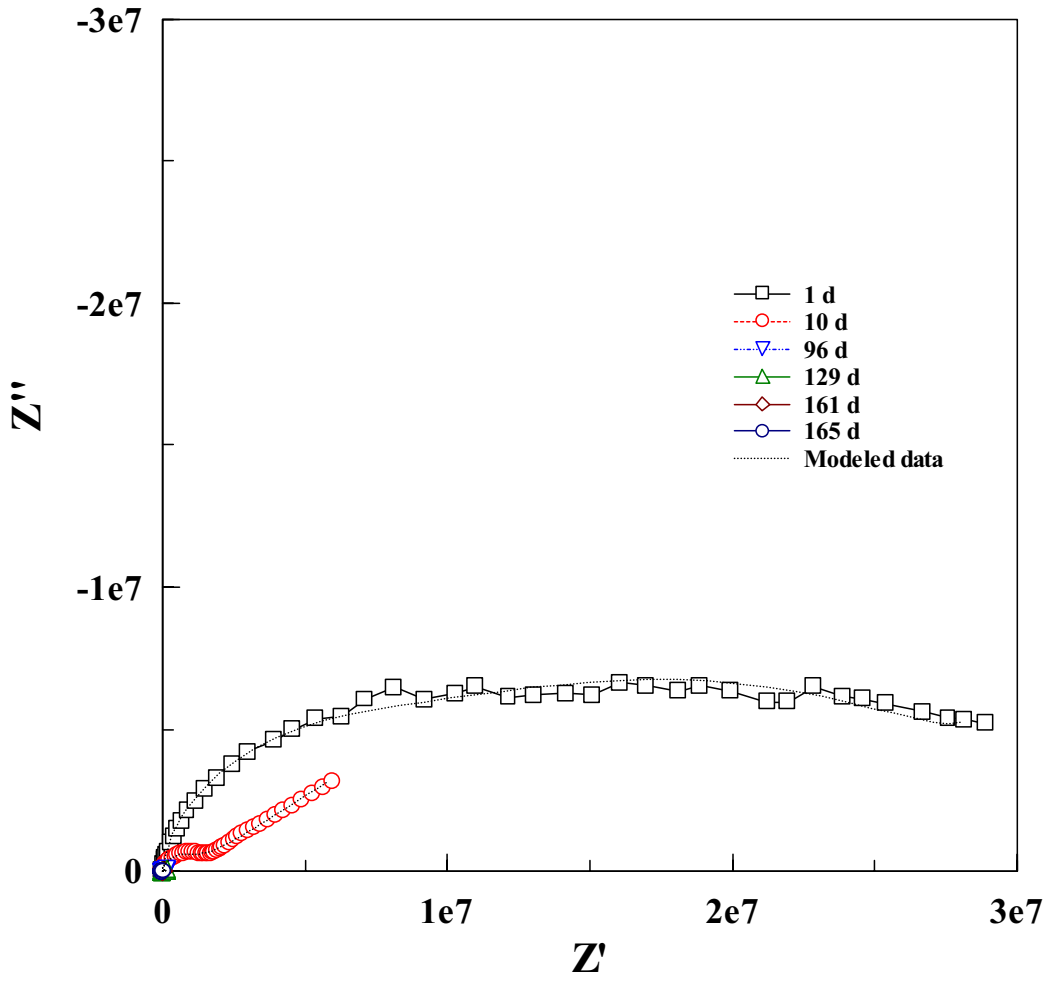

(b)

Figure 4.8 Continued.

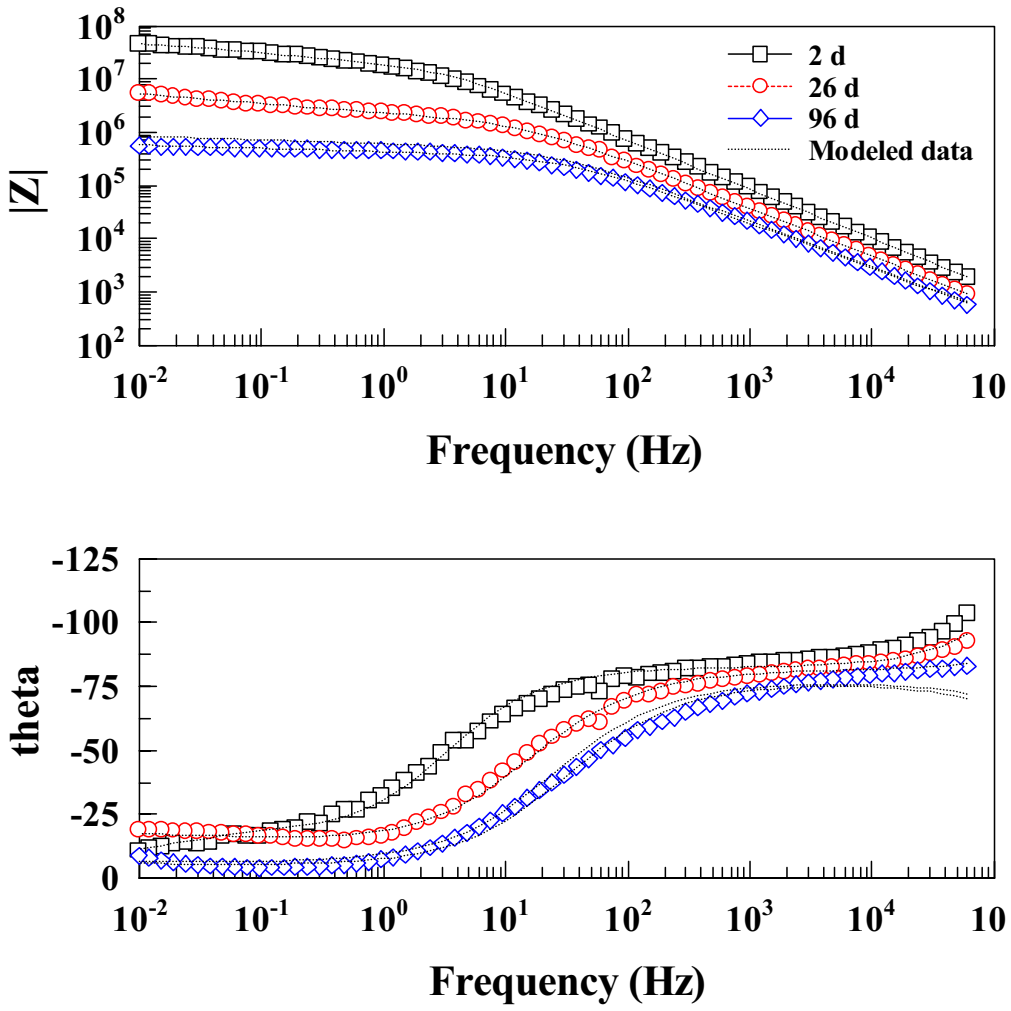

(a)

Figure 4.9 Bode (a) and Nyquist (b) plots with fittings for mild steel panels coated with 1 wt % SiC-incorporated commercial alkyd paint film (40-50 μm thick) at different immersion times in 3% NaCl solution.

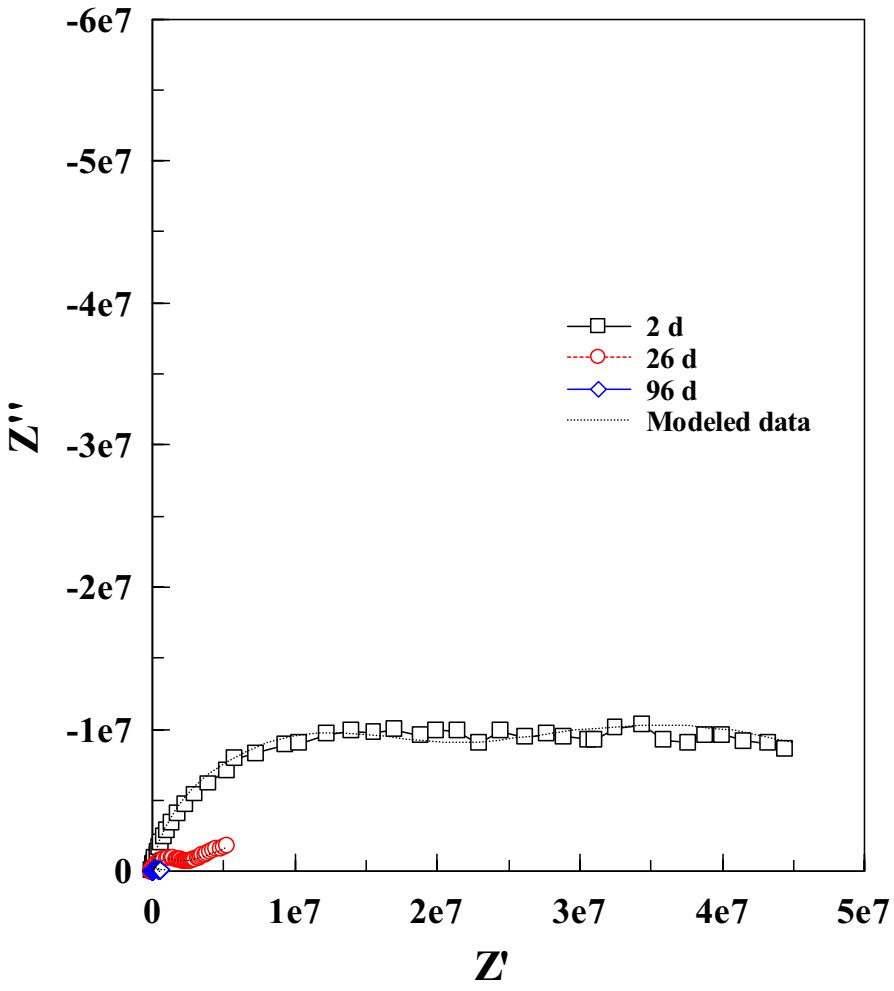

(b)

Figure 4.9 Continued.

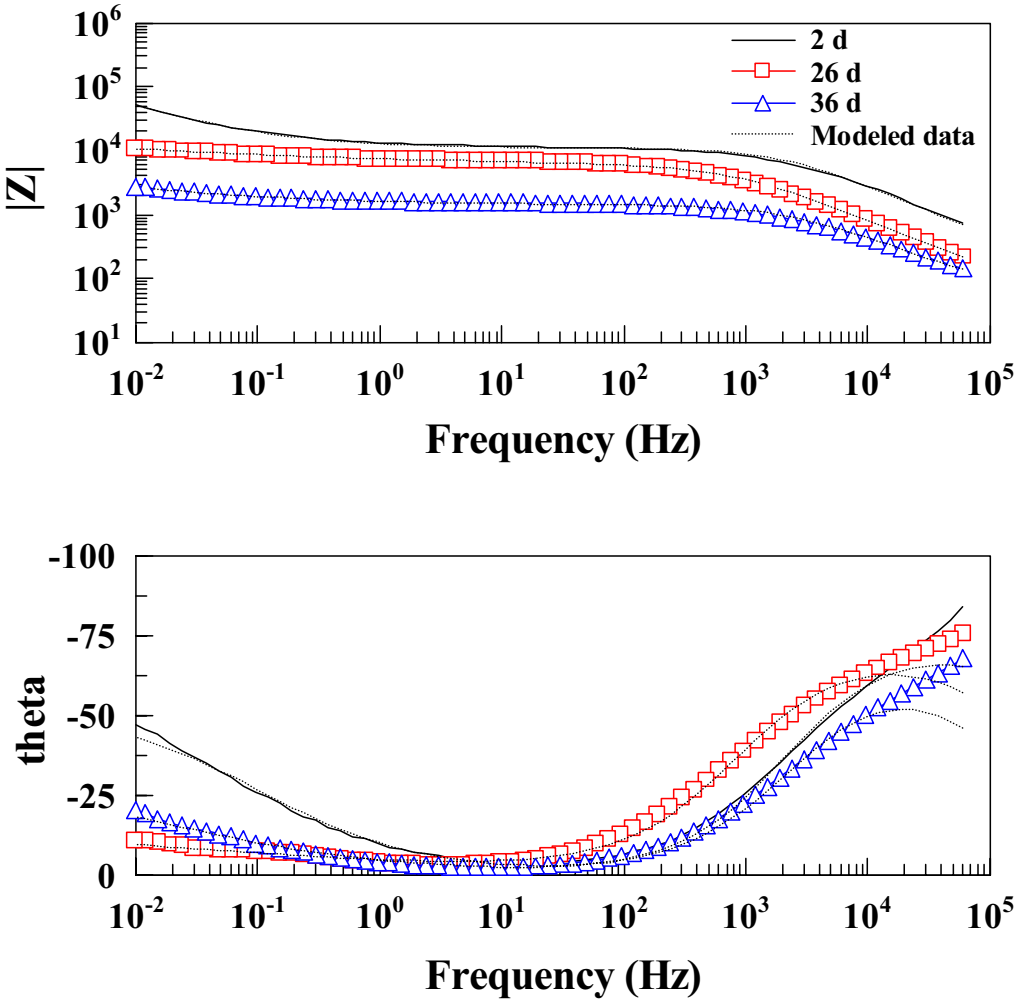

Figure 4.10 Bode (a) and Nyquist (b) plots with fittings for mild steel panels coated with 5 wt % SiC-incorporated commercial alkyd paint film (20 μm thick) at different immersion times in 3% NaCl solution.

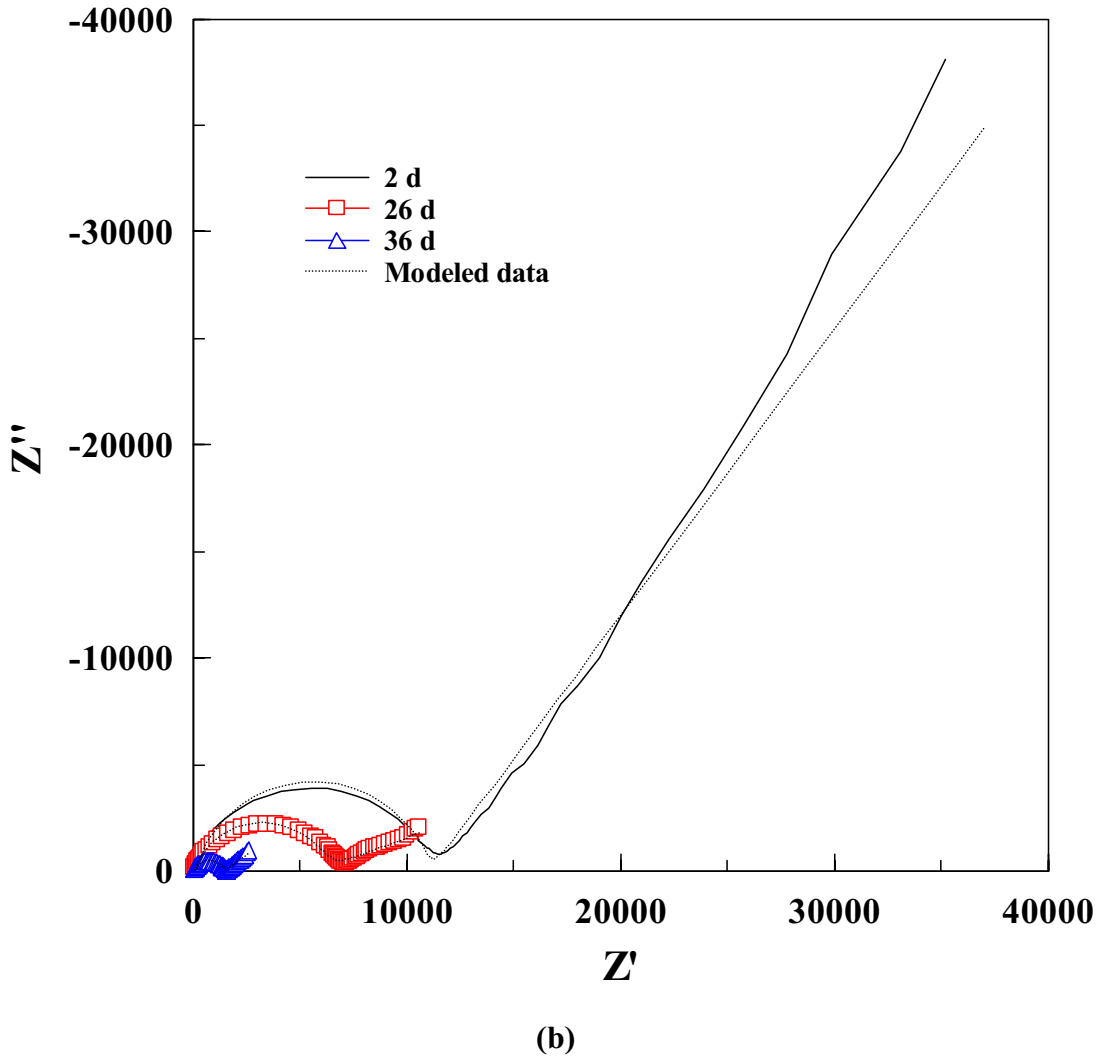

(b)

Figure 4.10 Continued.

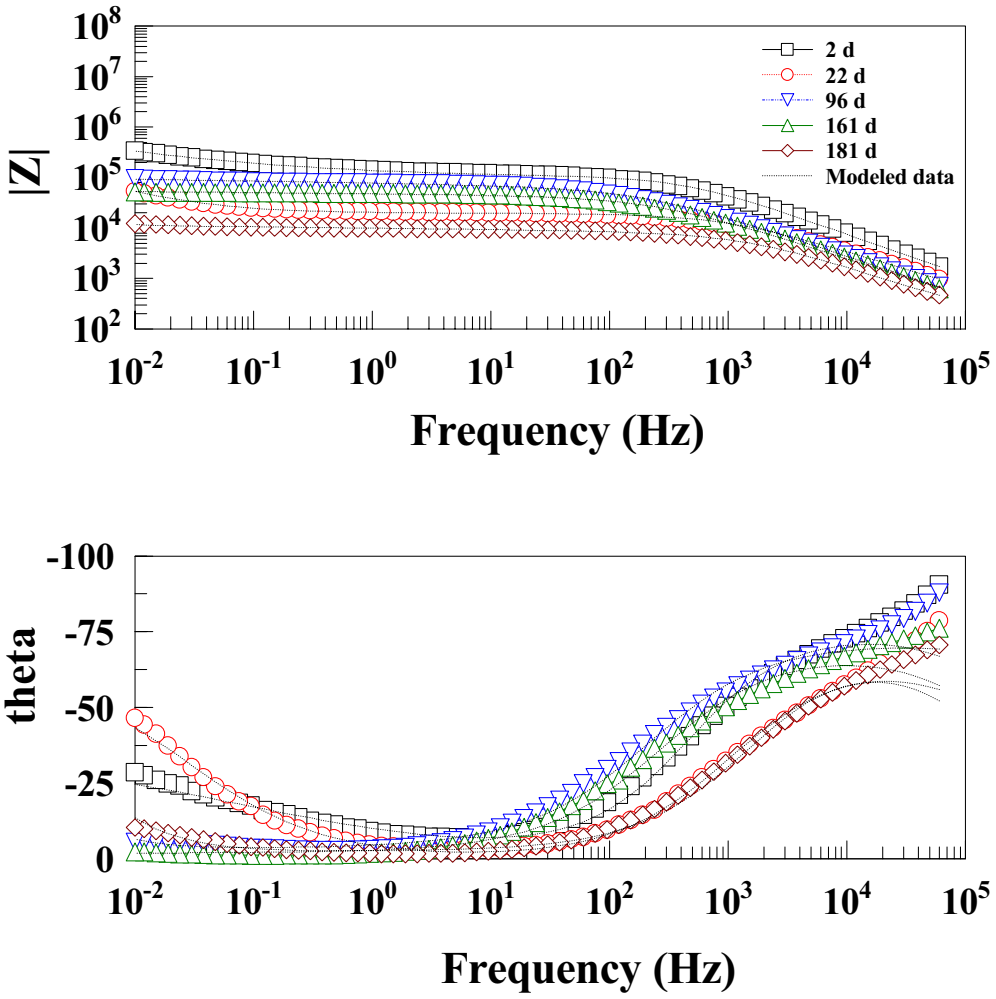

(a)

Figure 4.11 Bode (a) and Nyquist (b) plots with fittings for mild steel panels coated with 5 wt % SiC-incorporated commercial alkyd paint film (30 μm thick) at different immersion times in 3% NaCl solution.

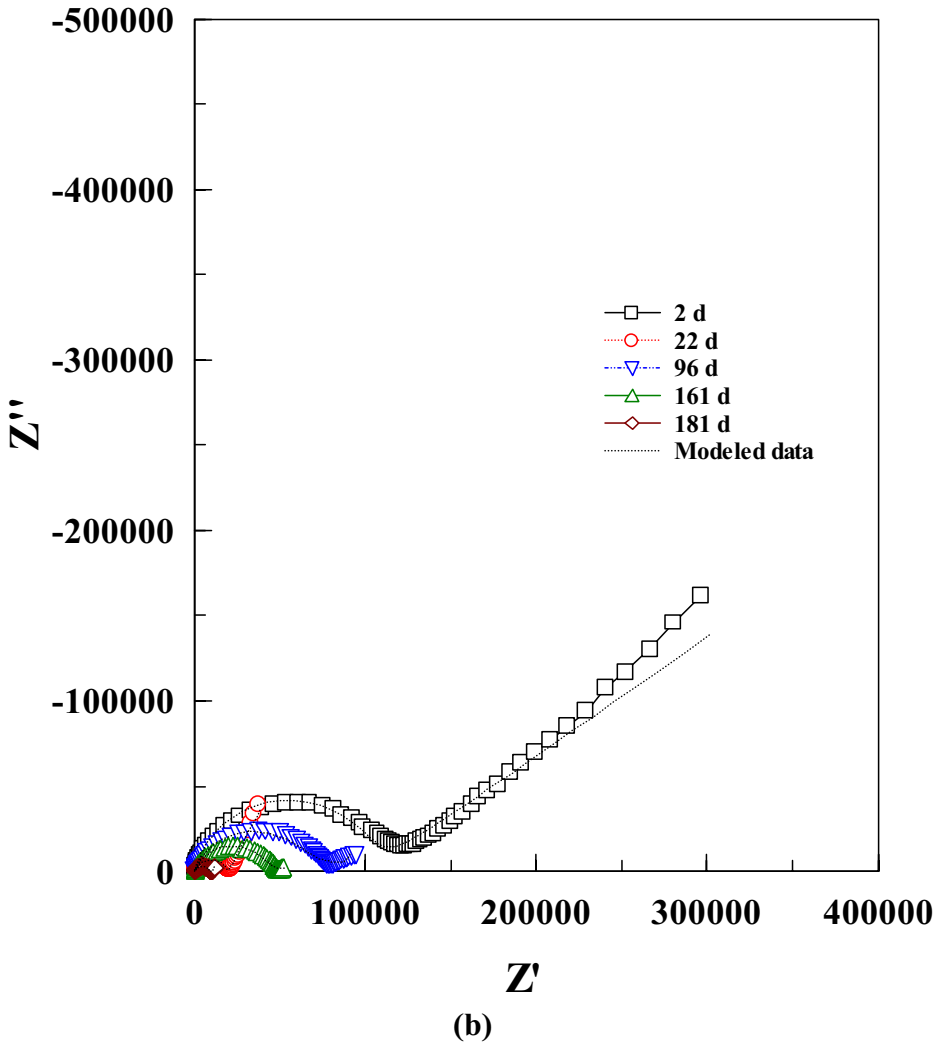

Figure 4.11 Continued.

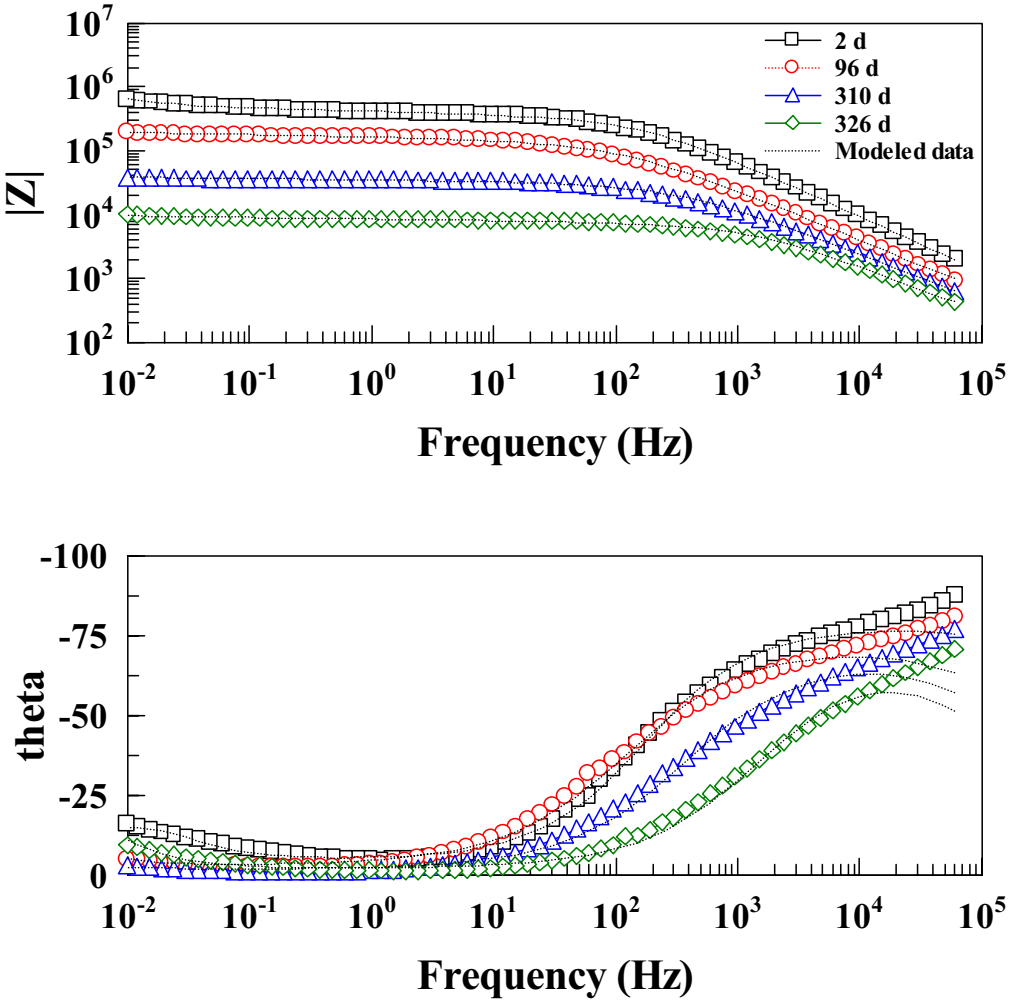

(a)

Figure 4.12 Bode (a) and Nyquist (b) plots with fittings for mild steel panels coated with 5 wt % SiC-incorporated commercial alkyd paint film (40 μm thick) at different immersion times in 3% NaCl solution.

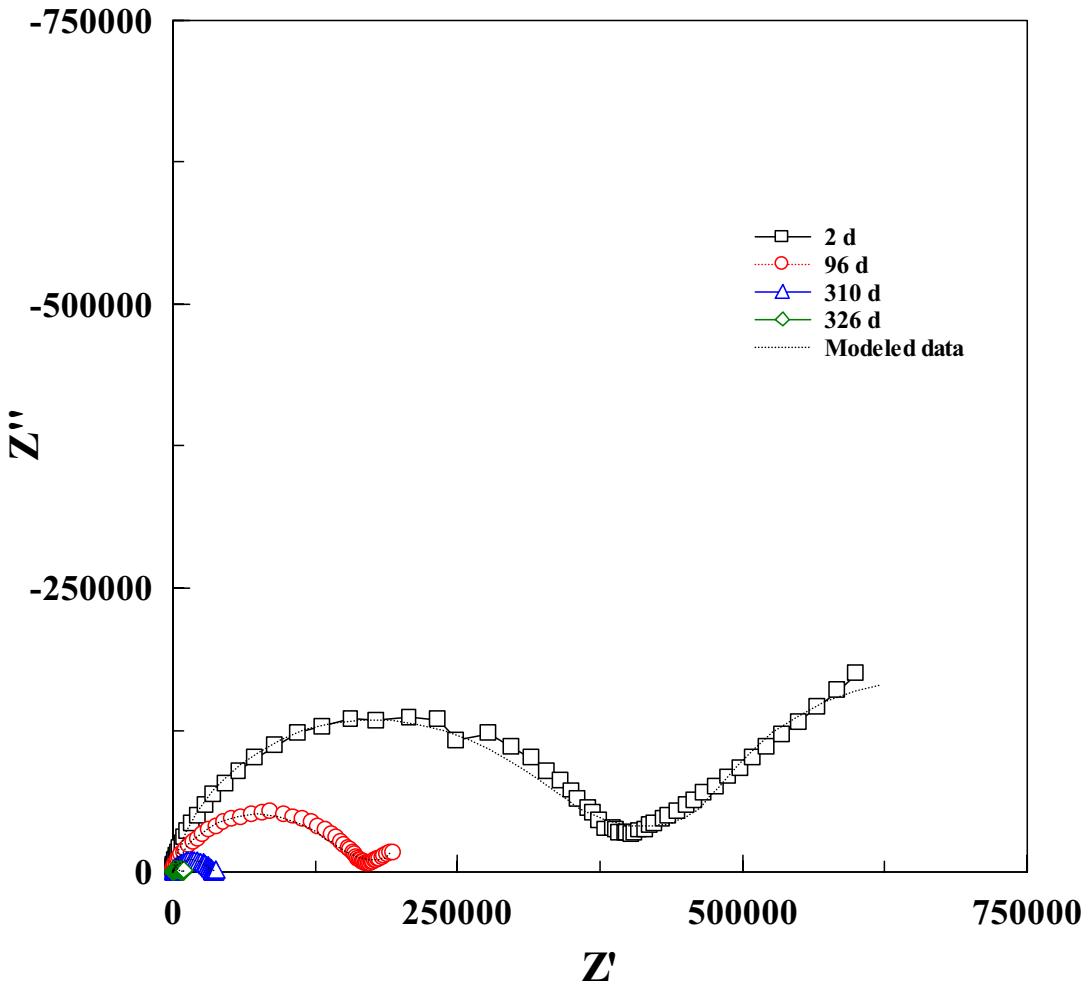

(b)

Figure 4.12 Continued.

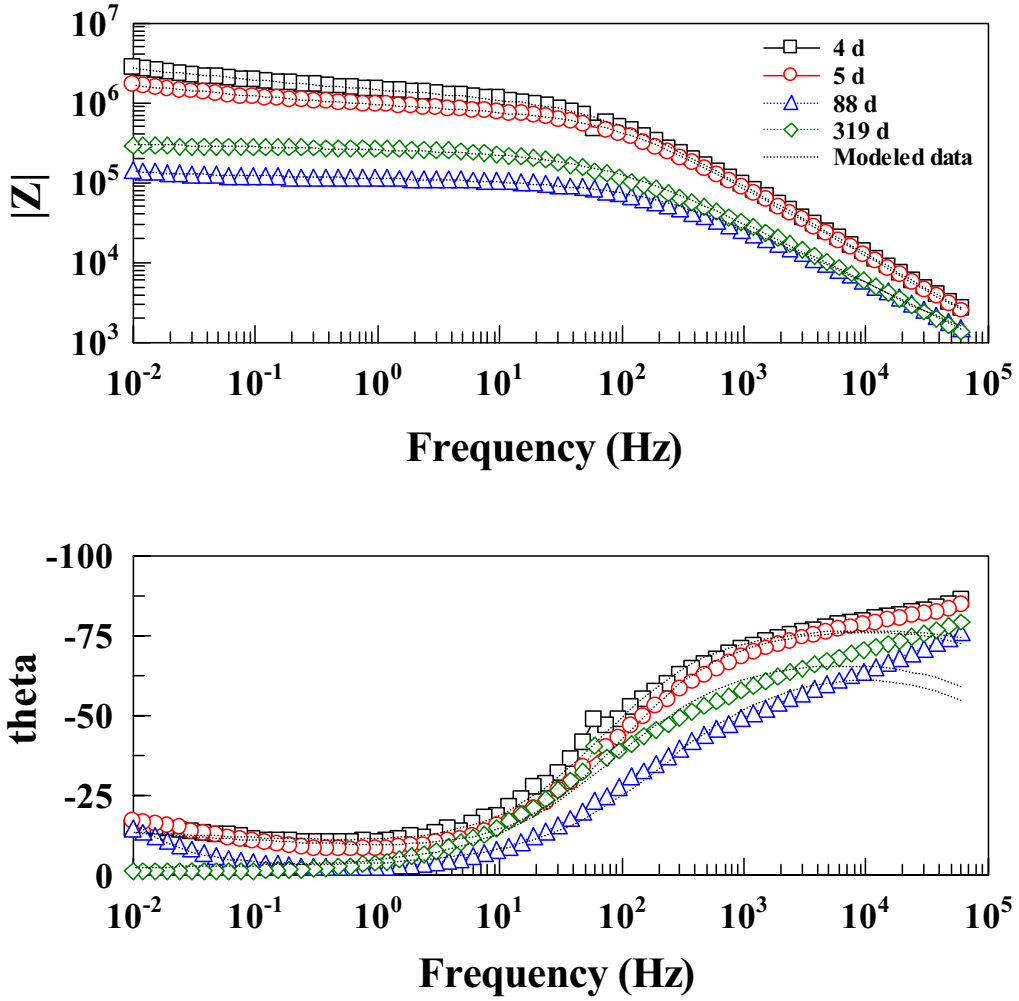

(a)

Figure 4.13 Bode (a) and Nyquist (b) plots with fittings for mild steel panels coated with 5 wt % SiC-incorporated commercial alkyd paint film (50 μm thick) at different immersion times in 3% NaCl solution.

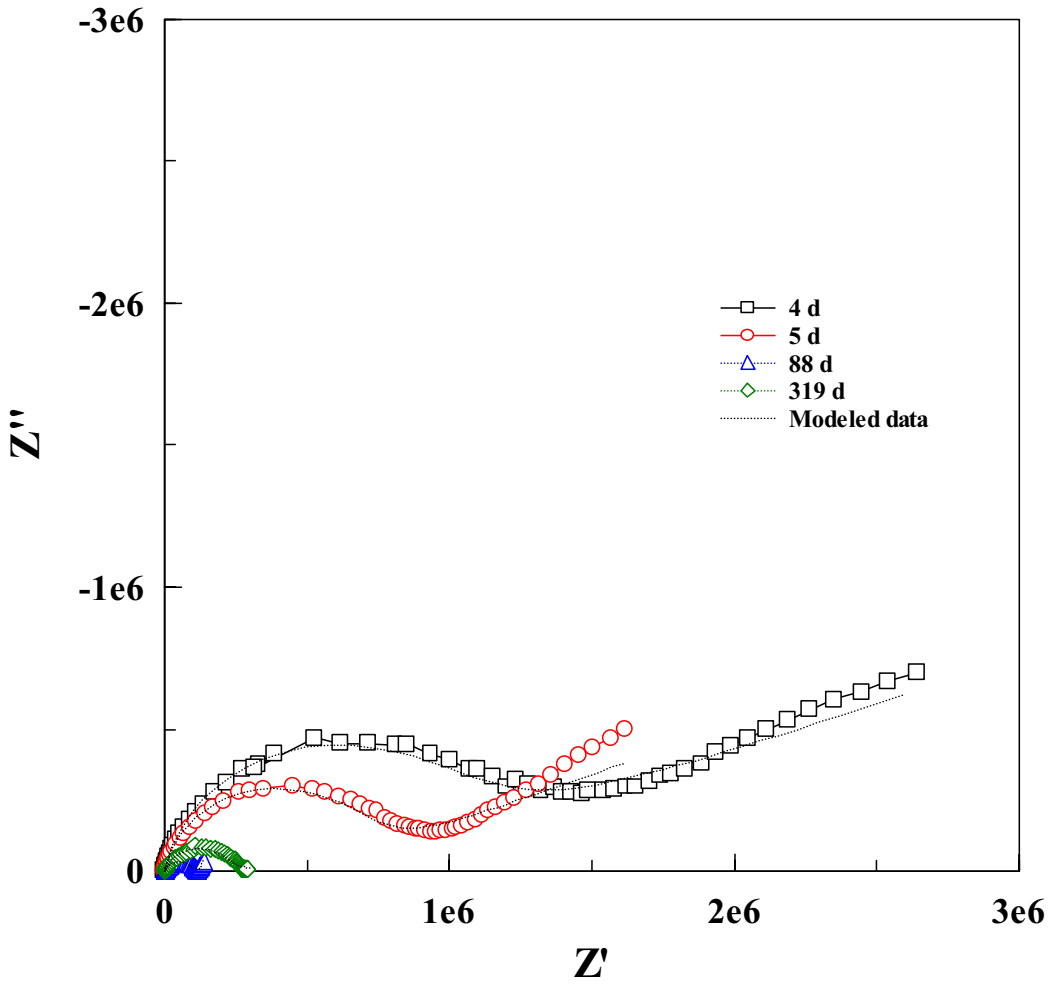

(b)

Figure 4.13 Continued.

On the other hand, in the first day of immersion in the electrolyte, the Nyquist plots in Figures 4.7 through 4.13 show either a capacitive semi-circle or a capacitive arc in the higher frequency region indicating an insulated substrate. The shape of the plot then changes to a capacitive semi-circle in the HF region followed by a diffusion tail in the LF region in agreement with the literature.[69] As shown in the Figures, the capacitive semi-circle progressively decreases as the immersion time increases indicating degradation of the paint coating and the diffusion tail starts at a higher frequency indicating a higher rate of electrolyte diffusion through the paint film.

Figures 4.14 through 4.17 show the effect of the film thickness on the behavior of the paint coatings in the corrosive electrolyte solution. As depicted in the figures, at any immersion time, compared to thin coatings, thicker coatings have higher $|Z|$ values at 1×10^{-2} Hz in the Bode plot and larger capacitive semi-circles in the Nyquist plots indicating the better insulation properties of the latter coatings.

Figures 4.18 through 4.22 show the effect of the SiC content on the behavior of the alkyd paint coating. The results depicted in Figures 4.18, 4.21, and 4.22 show that, within the first 100 d of immersion, the performance of the coatings containing 1 wt % SiC is better than that of the coatings containing 5 wt % SiC as reflected from the $|Z|$ values at 1×10^{-2} Hz in the Bode plots. However, for immersion times longer than 100 d (Figures 4.19 and 4.20), the 5 wt % SiC-reinforced coatings showed better stability with higher and more stable $|Z|$ values at 1×10^{-2} Hz and larger capacitive semi-circles in the Bode and Nyquist plots, respectively.

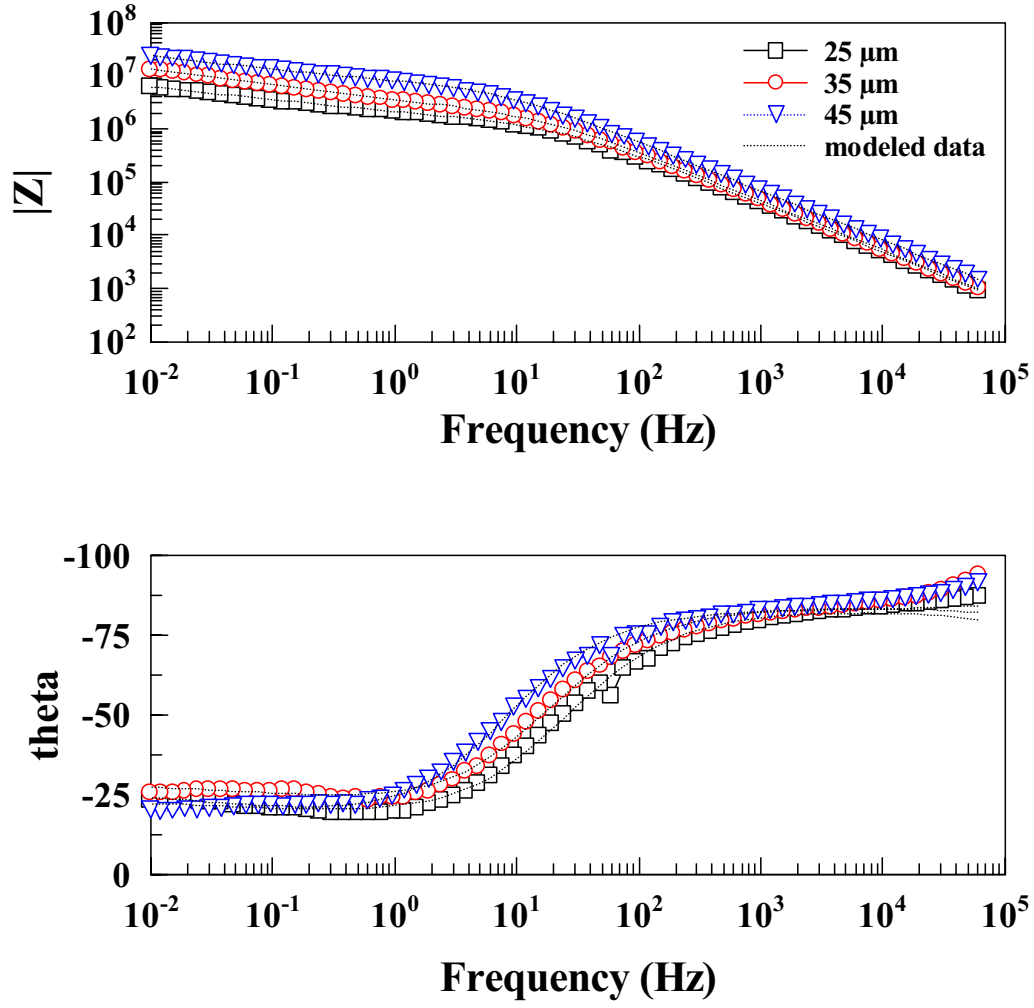

Figure 4.14 Bode (a) and Nyquist (b) plots with fittings for mild steel panels coated with 1 wt % SiC-incorporated commercial alkyd paint film (with different film thicknesses) after 6 d of immersion in 3% NaCl solution. The coatings specifications are shown in the legend.

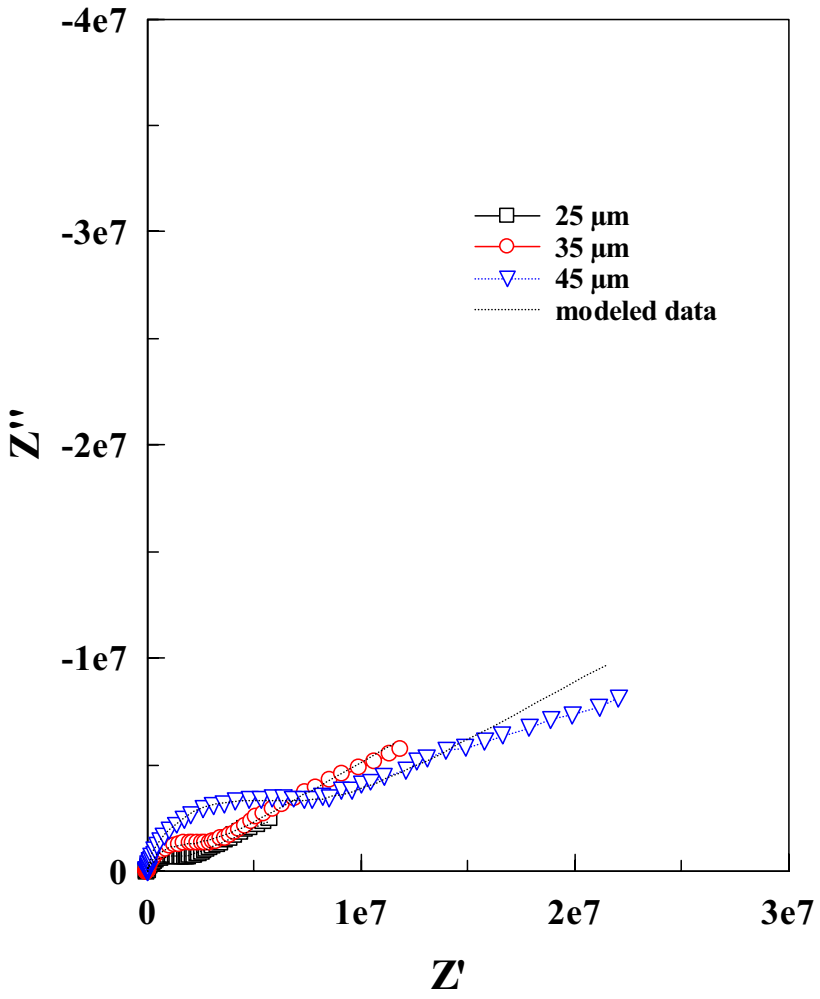

(b)

Figure 4.14 Continued.

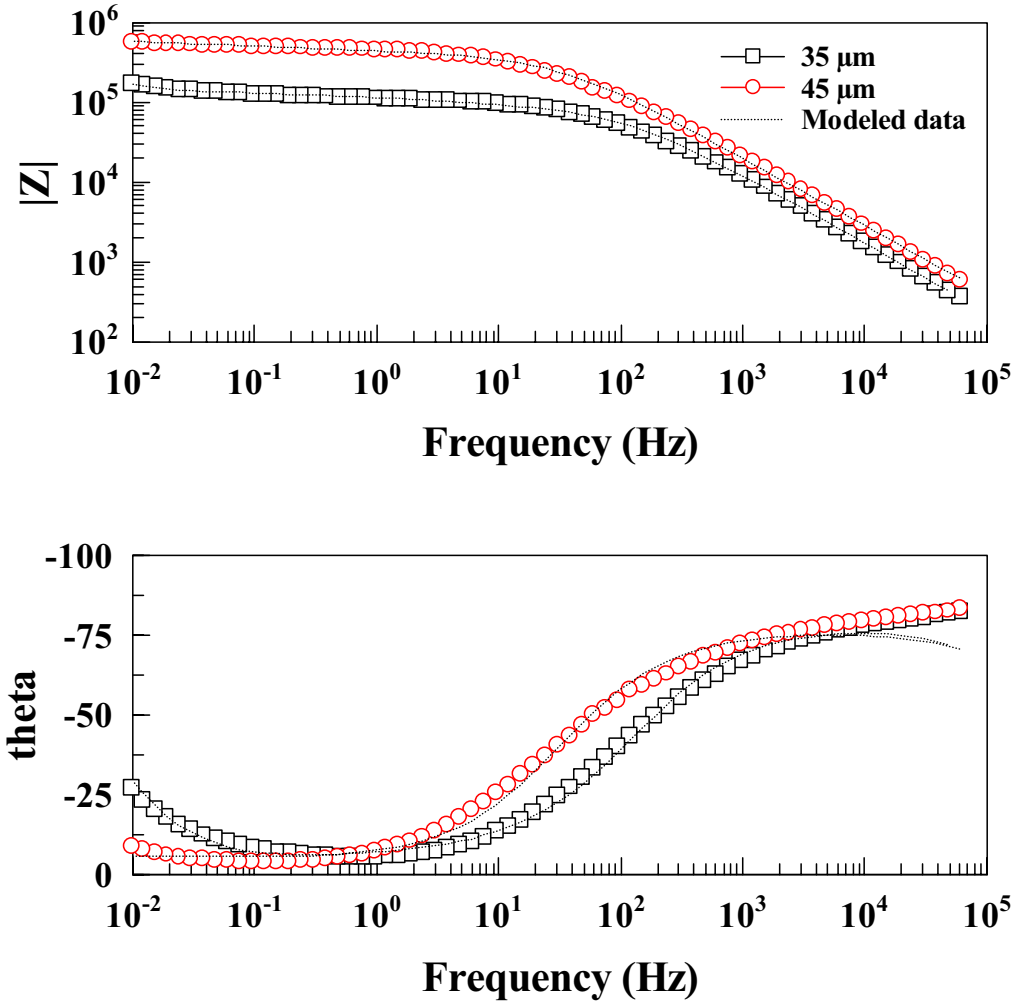

Figure 4.15 Bode (a) and Nyquist (b) plots with fittings for mild steel panels coated with 1 wt % SiC-incorporated commercial alkyd paint film (with different film thicknesses) after 100 d of immersion in 3% NaCl solution. The coatings specifications are shown in the legend.

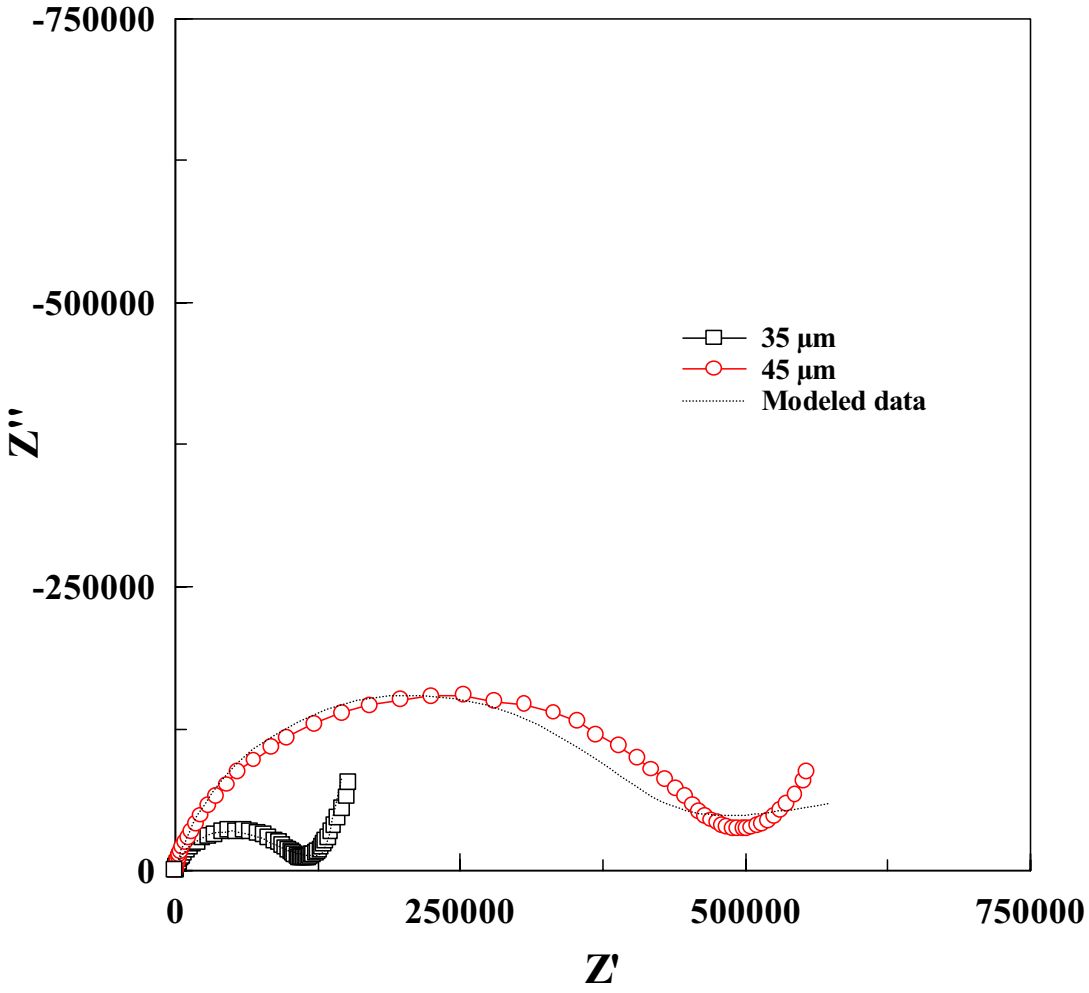

(b)

Figure 4.15 Continued.

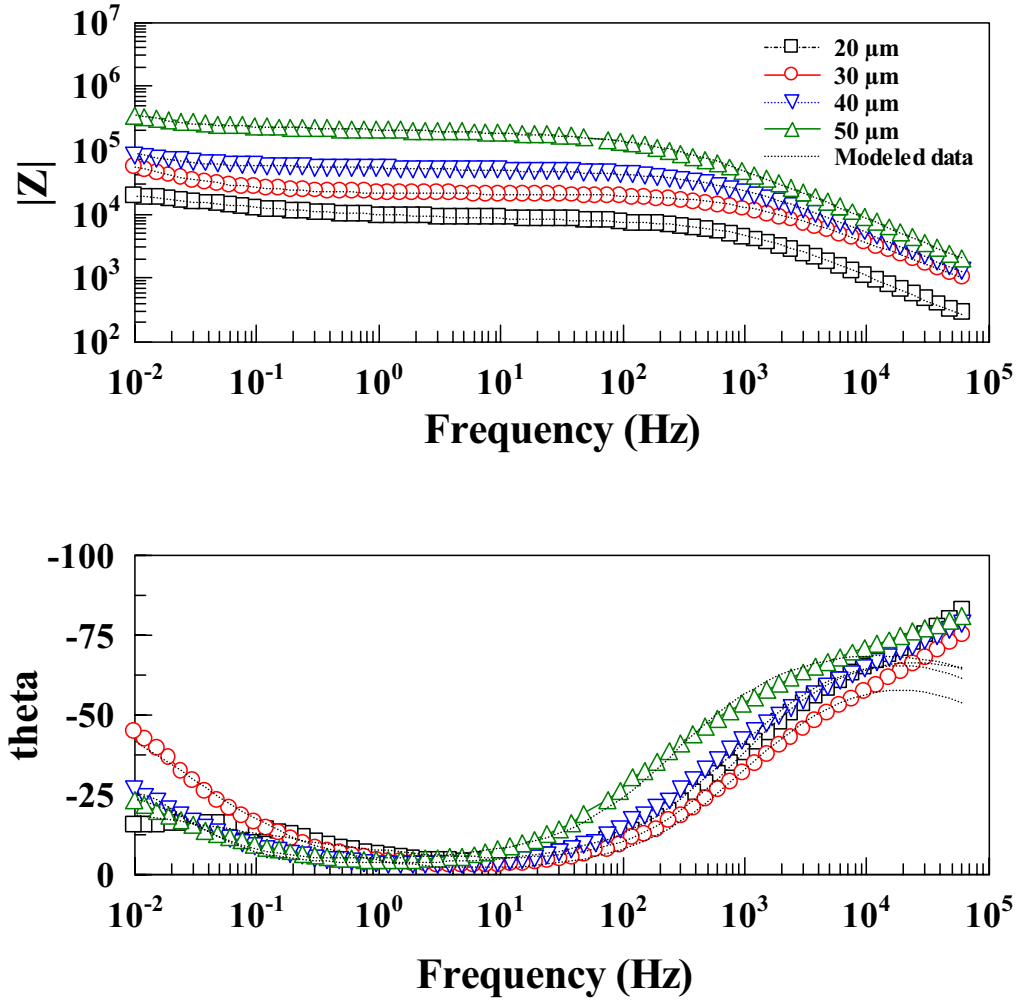

(a)

Figure 4.16 Bode (a) and Nyquist (b) plots with fittings for mild steel panels coated with 5 wt % SiC-incorporated commercial alkyd paint film (with different film thicknesses) after 20 d of immersion in 3% NaCl solution. The coatings specifications are shown in the legend.

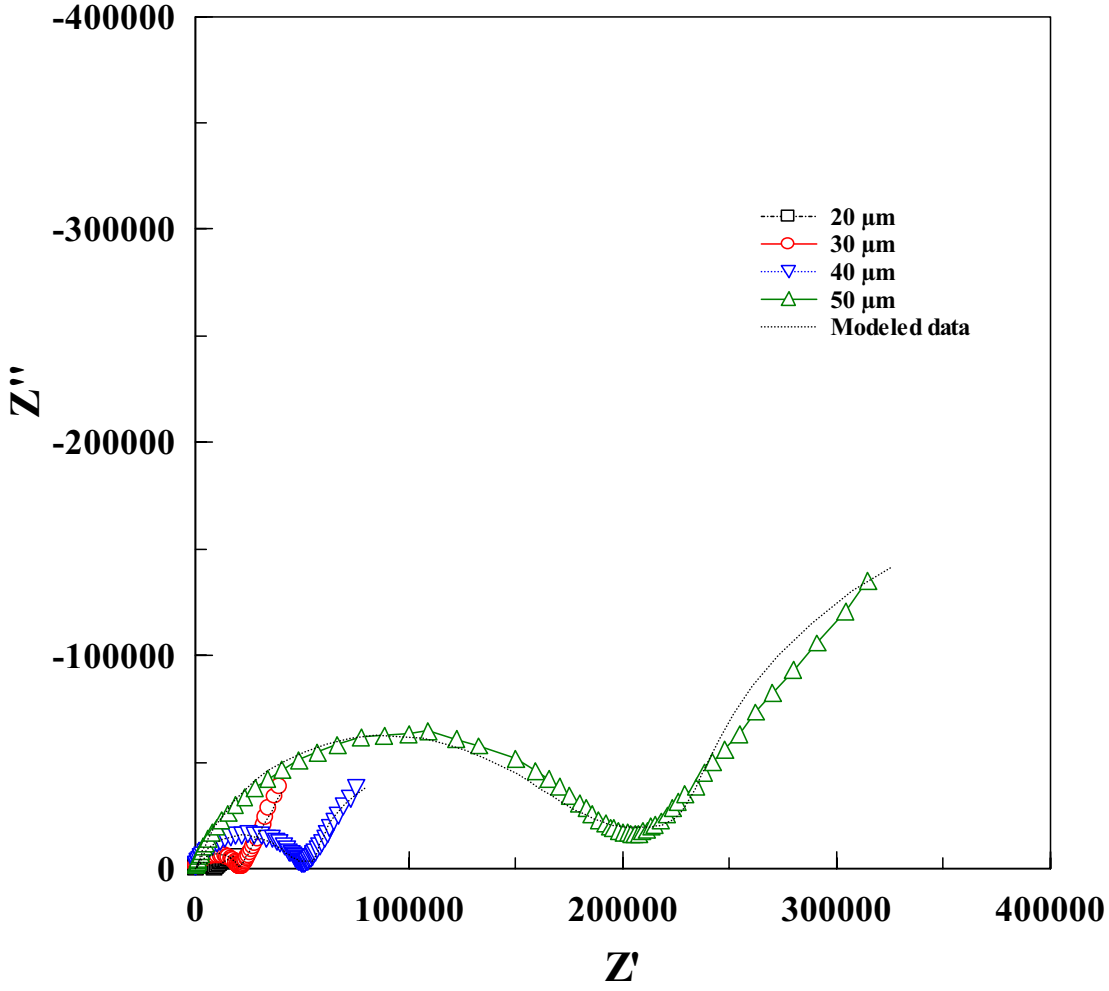

(b)

Figure 4.16 Continued.

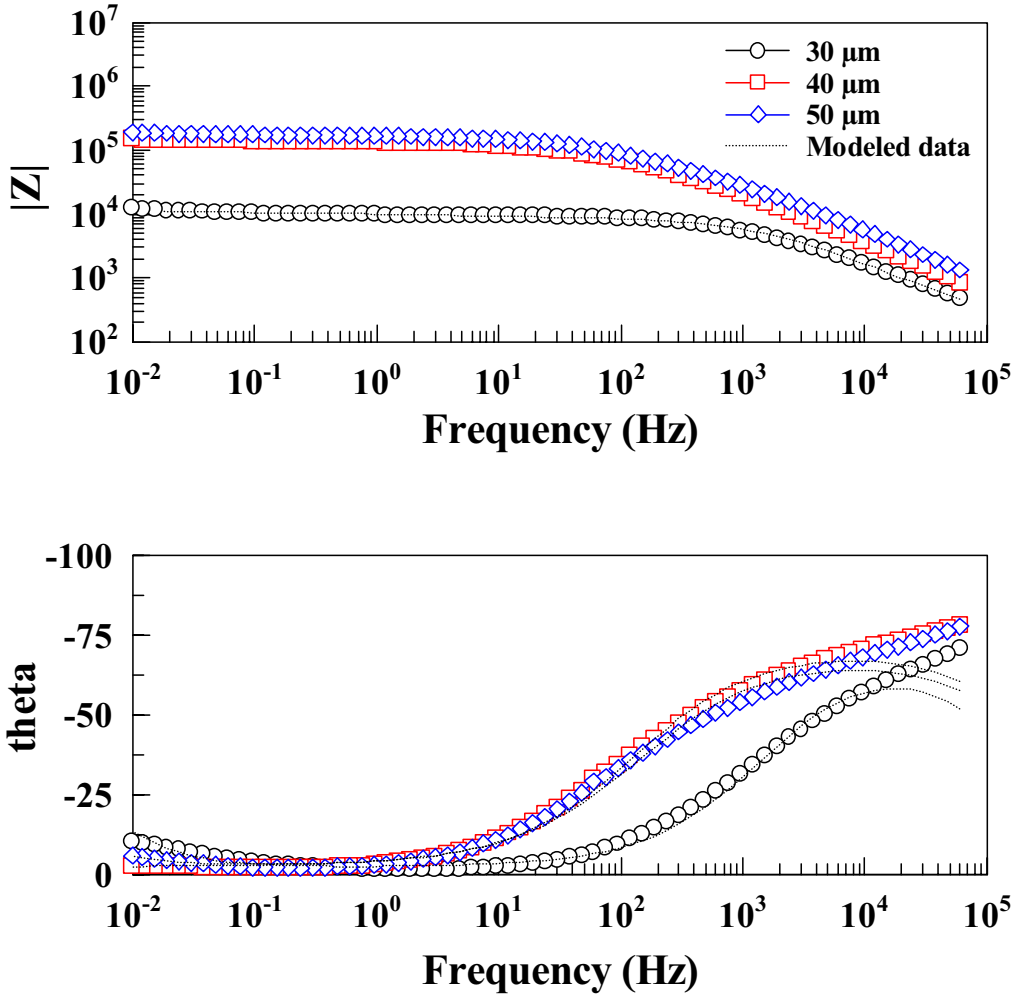

(a)

Figure 4.17 Bode (a) and Nyquist (b) plots with fittings for mild steel panels coated with 5 wt % SiC-incorporated commercial alkyd paint film (with different film thicknesses) after 180 d of immersion in 3% NaCl solution. The coatings specifications are shown in the legend.

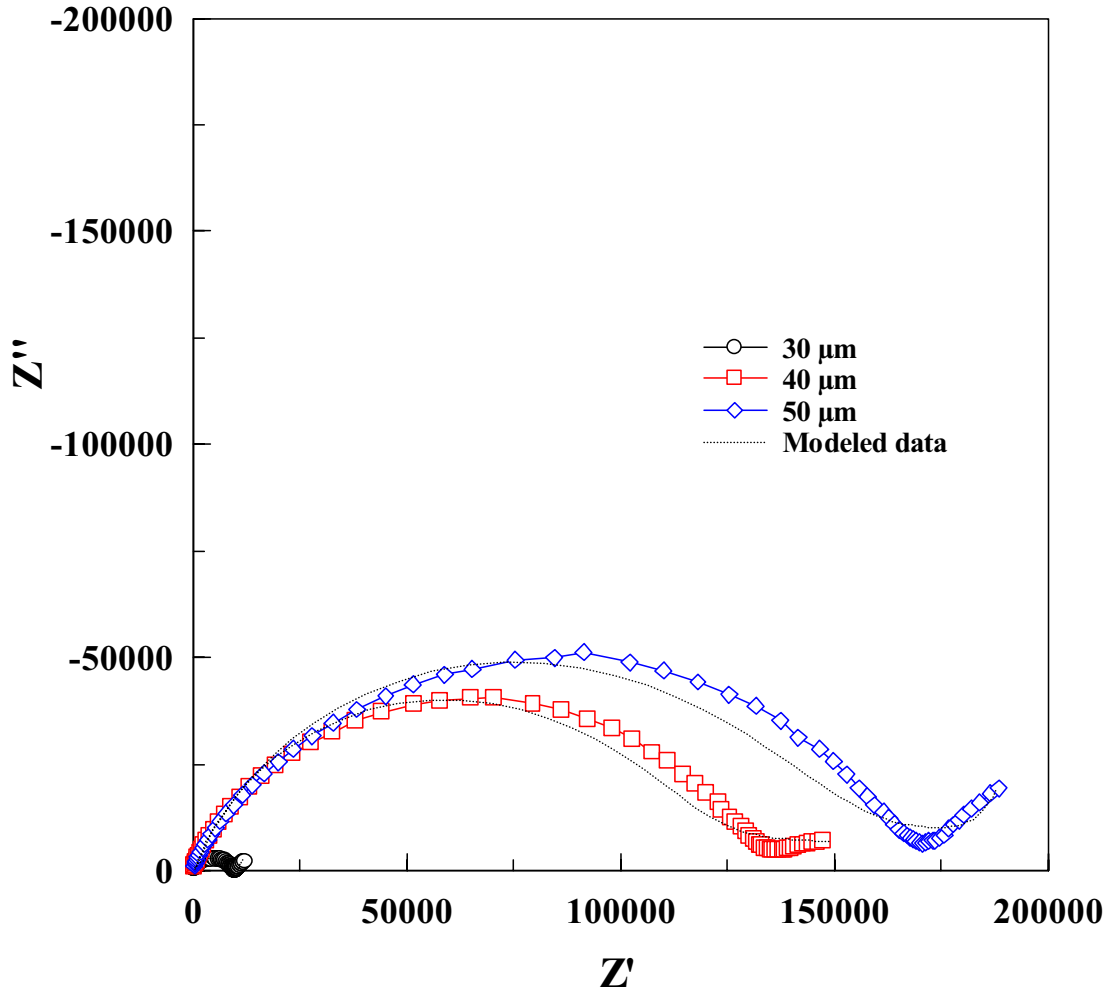

(b)

Figure 4.17 Continued.

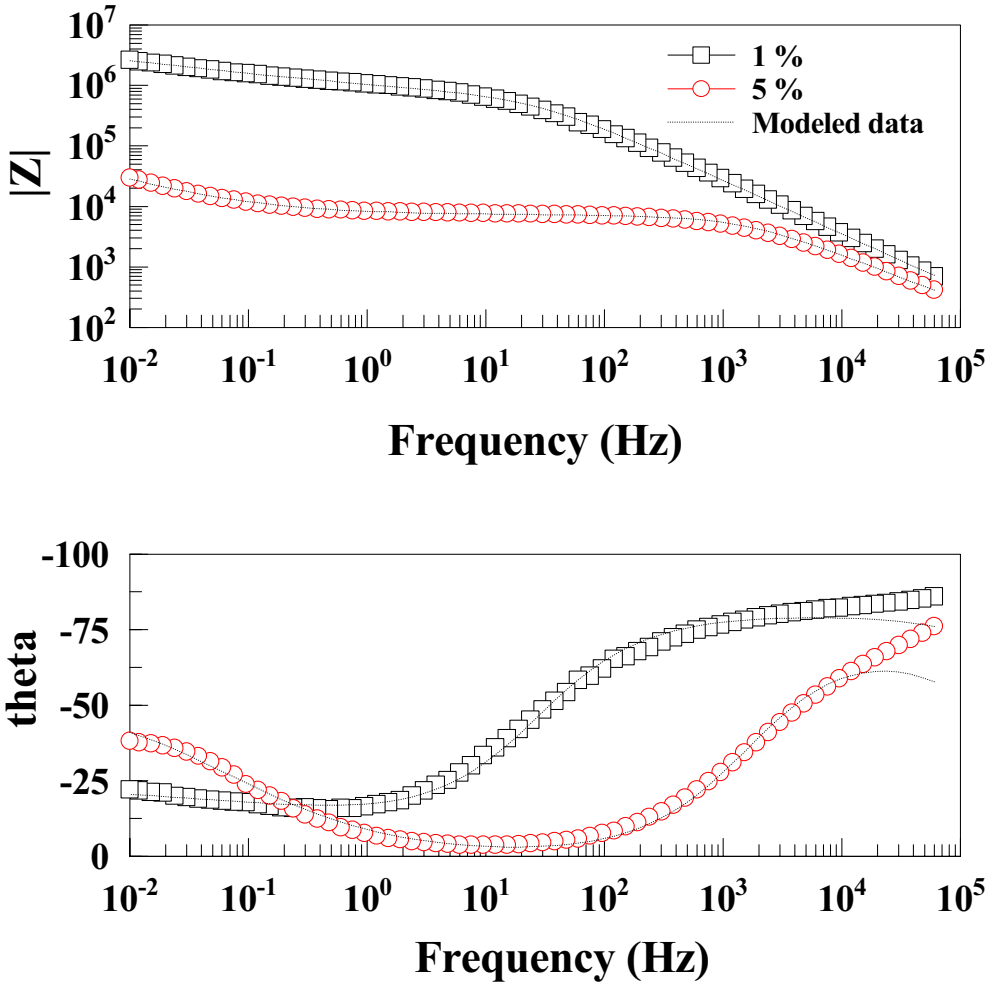

(a)

Figure 4.18 Bode (a) and Nyquist (b) plots with fittings for mild steel panels coated with SiC-incorporated commercial alkyd paint film (20 μm thick) with different SiC loadings after 10 d of immersion in 3% NaCl solution. The coatings specifications are shown in the legend.

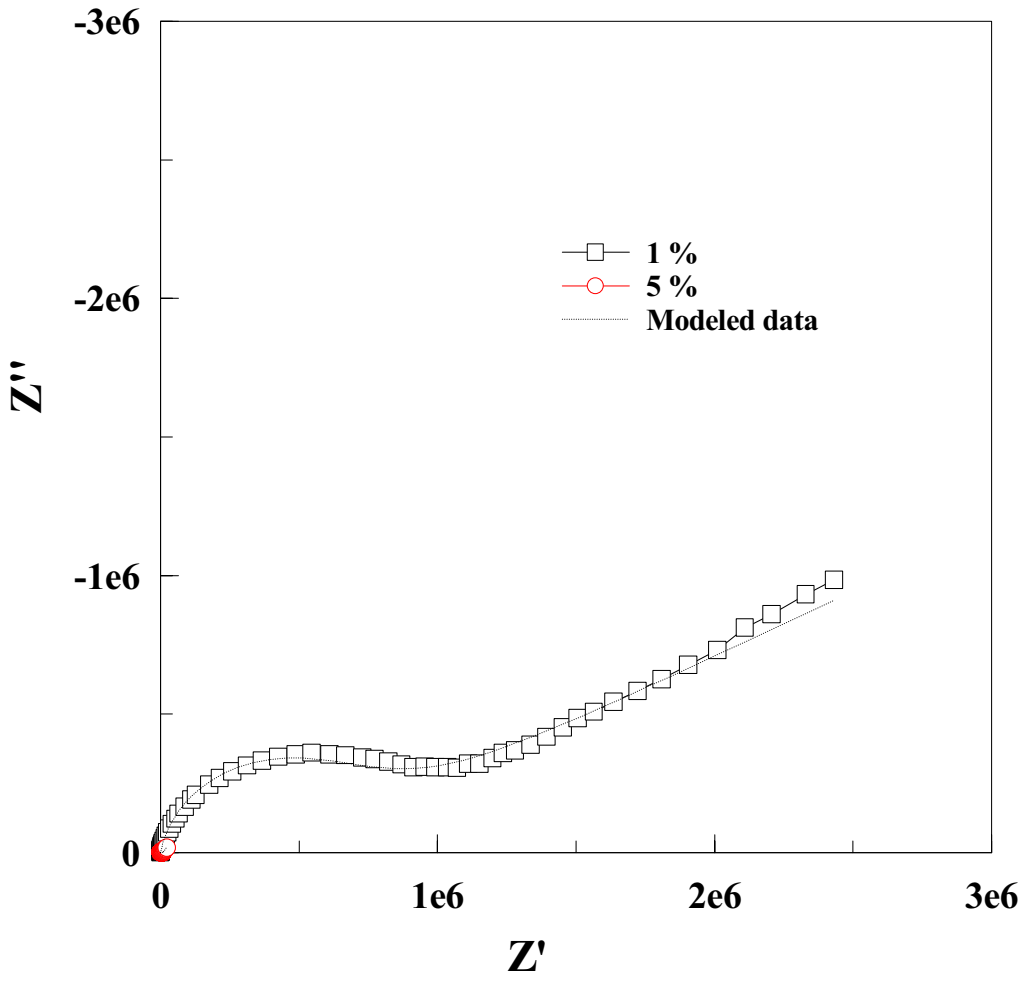

(b)

Figure 4.18 Continued.

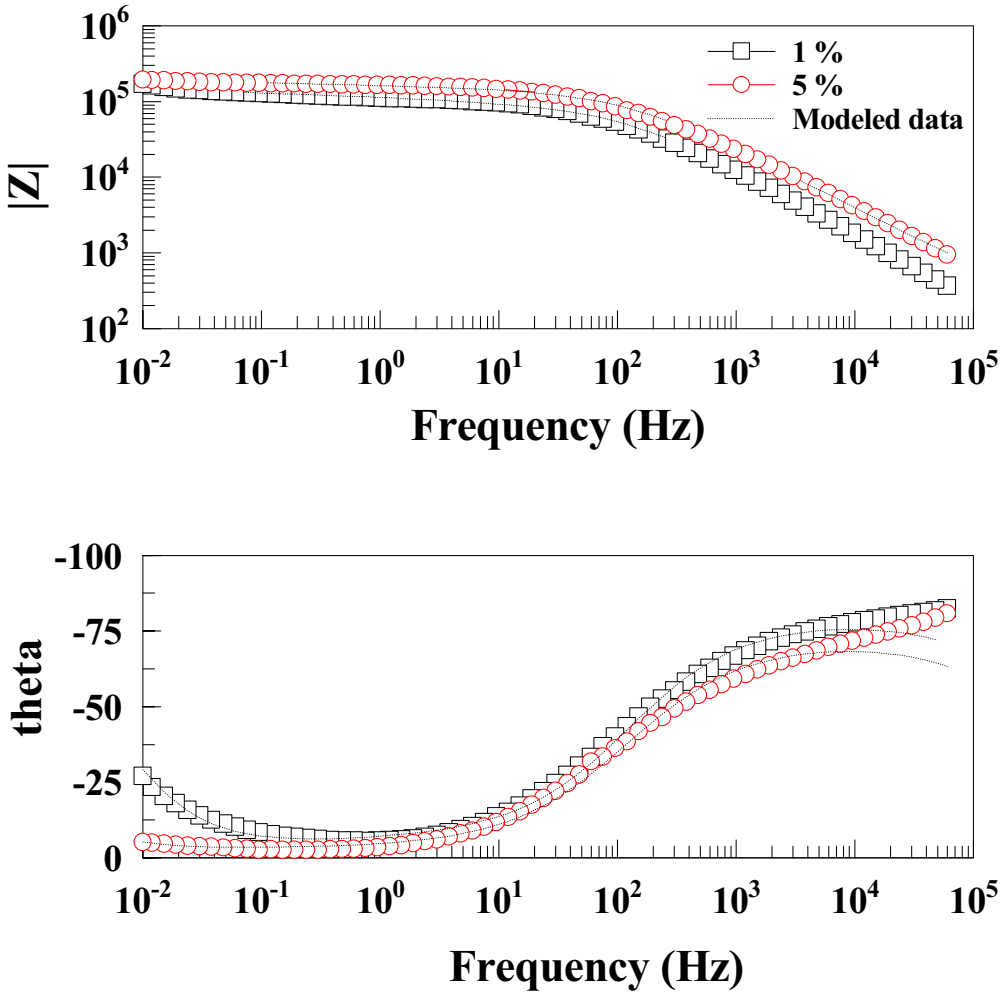

(a)

Figure 4.19 Bode (a) and Nyquist (b) plots with fittings for mild steel panels coated with SiC-incorporated commercial alkyd paint film (40 μm thick) with different SiC loadings after 100 d of immersion in 3% NaCl solution. The coatings specifications are shown in the legend.

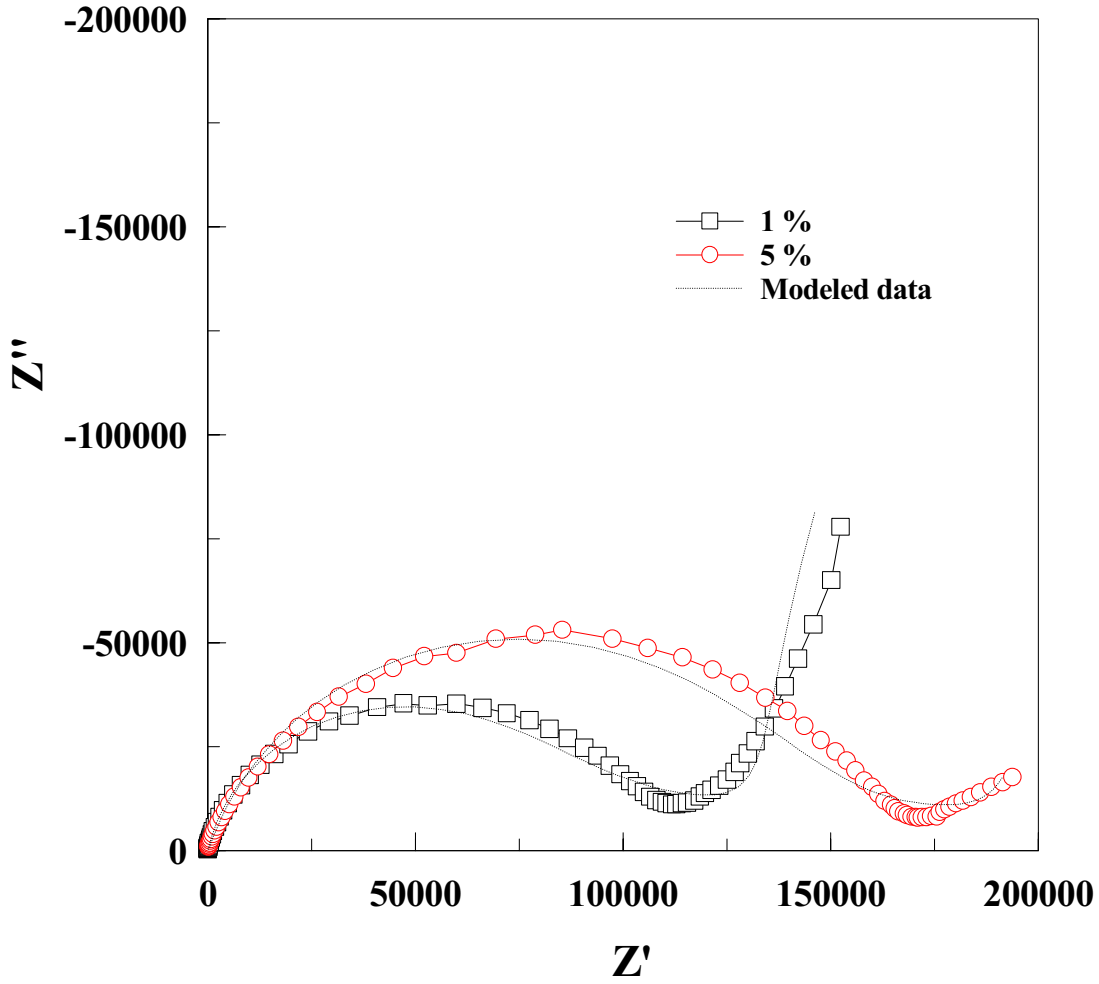

(b)

Figure 4.19 Continued.

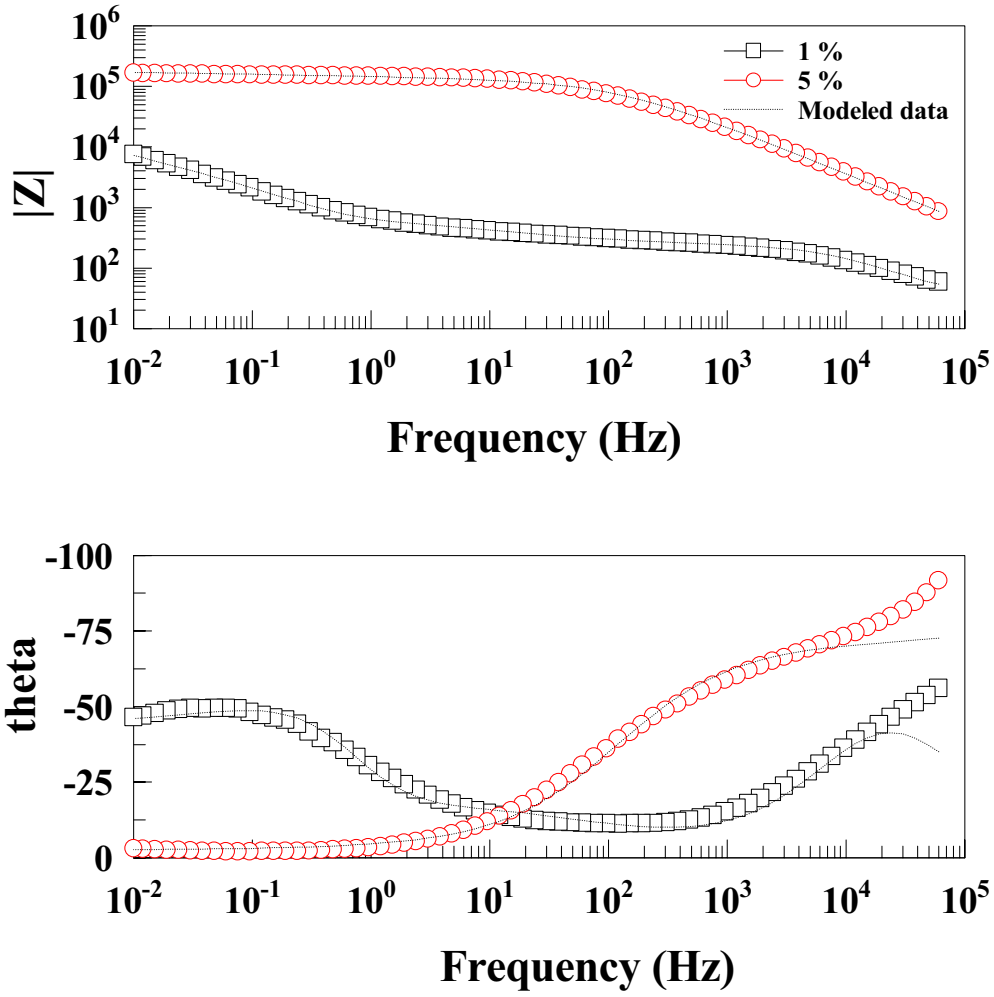

(a)

Figure 4.20 Bode (a) and Nyquist (b) plots with fittings for mild steel panels coated with SiC-incorporated commercial alkyd paint film (40 μm thick) with different SiC loadings after 160 d of immersion in 3% NaCl solution. The coatings specifications are shown in the legend.

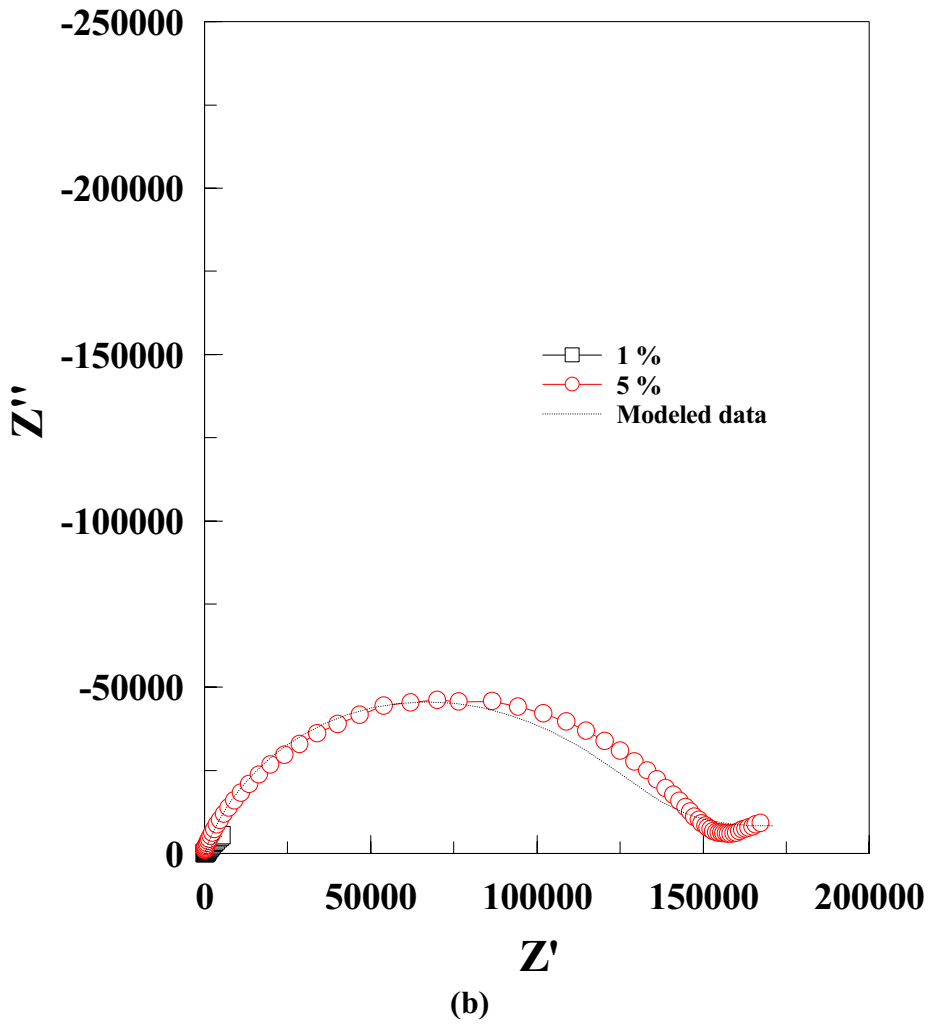

Figure 4.20 Continued.

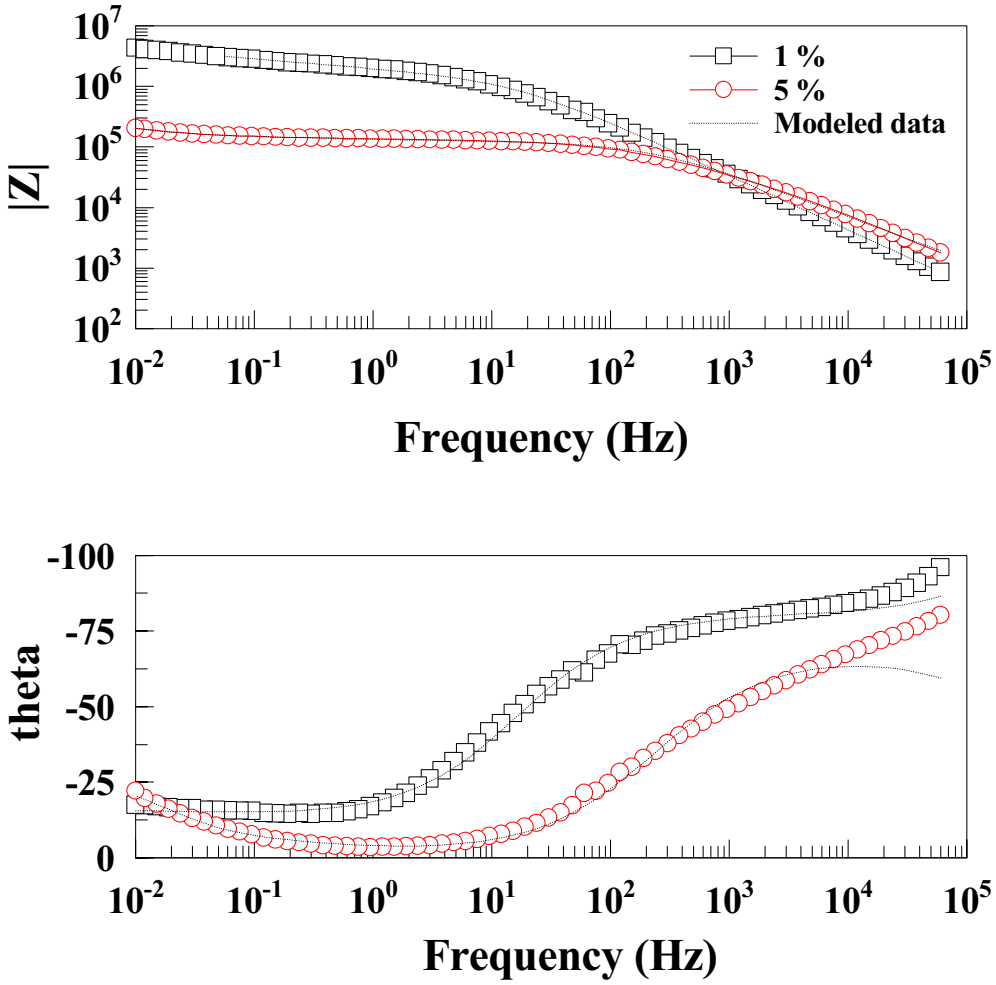

(a)

Figure 4.21 Bode (a) and Nyquist (b) plots with fittings for mild steel panels coated with SiC-incorporated commercial alkyd paint film (50 μm thick) with different SiC loadings after 30 d of immersion in 3% NaCl solution. The coatings specifications are shown in the legend.

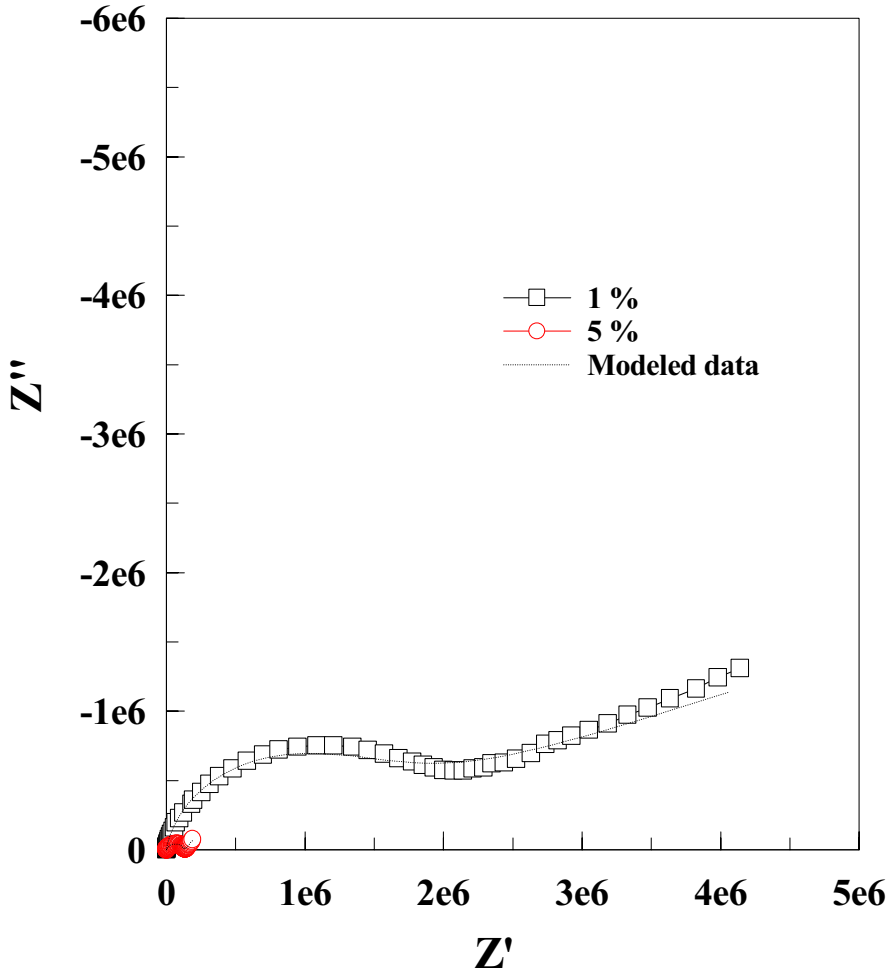

(a)

Figure 4.21 Continued.

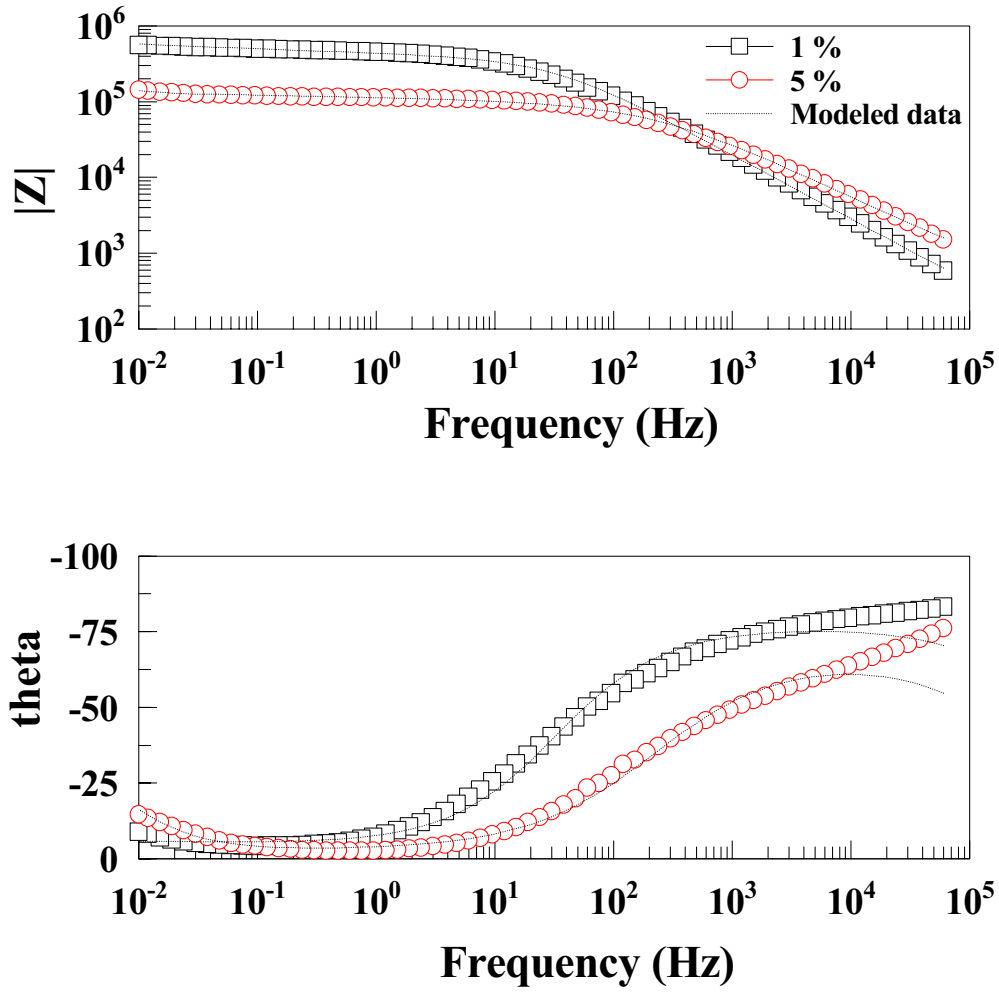

(a)

Figure 4.22 Bode (a) and Nyquist (b) plots with fittings for mild steel panels coated with SiC-incorporated commercial alkyd paint film (50 μm thick) with different SiC loadings after 90 d of immersion in 3% NaCl solution. The coatings specifications are shown in the legend.

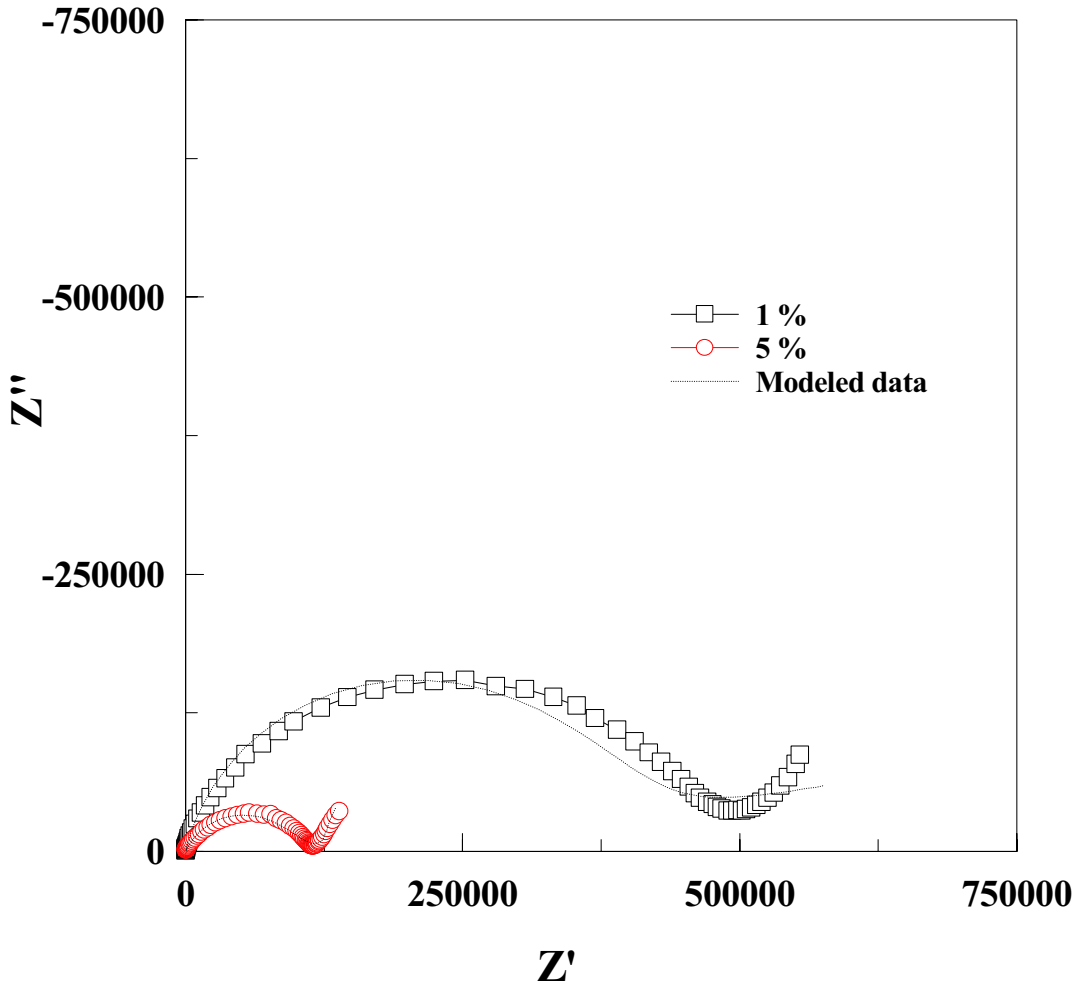

(b)

Figure 4.22 Continued.

4.3.3 Equivalent Electrical Circuits and Data Fitting

Figure 4.23 shows the equivalent electrical circuit model used to analyze the behavior of the SiC-incorporated alkyd paint coatings applied to the surface of mild steel samples immersed in 3% NaCl solution. The elements in that circuit are the Ohmic (solution) resistance (R); the electrode double layer capacitance (C_{dl}); the coating capacitance (C_c); the coating resistance (R_c); the polarization (charge transfer) resistance (R_p); the Warburg diffusional impedance (Z_w); and the constant phase element (*CPE*). The values of system parameters were calculated based on this equivalent circuit model (vide infra).

As depicted in Figures 4.7 through 4.22, the suggested fitting model (Figure 4.23) reproduced fitting spectra that are almost superimposed on the experimental spectra for all of the systems studied.

Plots of variation of the calculated values of system parameters such as the impedance modulus ($|Z|$), the polarization resistance (R_p), the double layer capacitance (C_{dl}), the coating resistance (R_c), the coating capacitance (C_c), the percent water uptake, and the delaminated area (A_d) with exposure time are presented in Figures 4.24 through 4.51.

4.3.4 Total Impedance ($|Z|$) Measurements

Figures 4.24 through 4.27 show the variation of $|Z|$ values measured at 1.0×10^{-2} Hz with immersion time for SiC-reinforced alkyd coatings with different film thicknesses. The data show high $|Z|$ values for all coatings upon initial immersion in the NaCl solution in the range of 10^4 to 10^7 Ω which decrease with immersion time due to

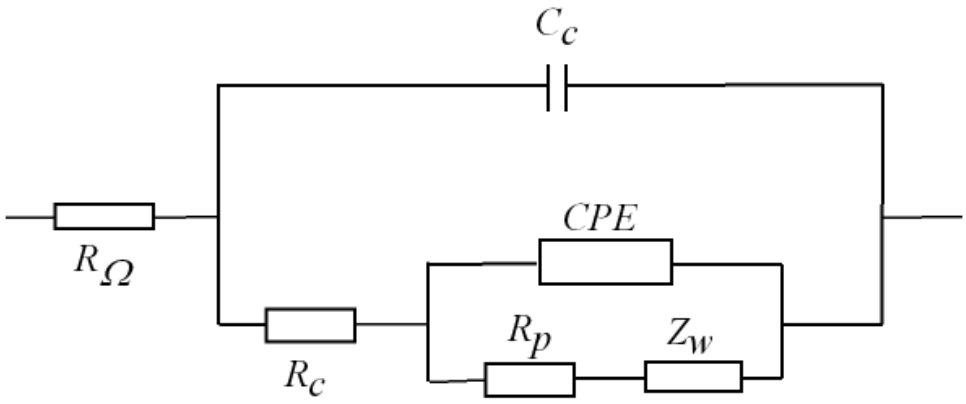

Figure 4.23 The electrical equivalent circuits used to fit the experimental data for SiC-incorporated alkyd paint coatings applied to the surface of mild steel coupons immersed in 3% NaCl solution. R = Ohmic (solution) resistance, C_{dl} = the electrode double layer capacitance, C_c = coating capacitance, R_c = coating pore resistance, R_p = polarization (charge transfer) resistance, Z_w = Warburg diffusional impedance, and CPE = constant phase element.

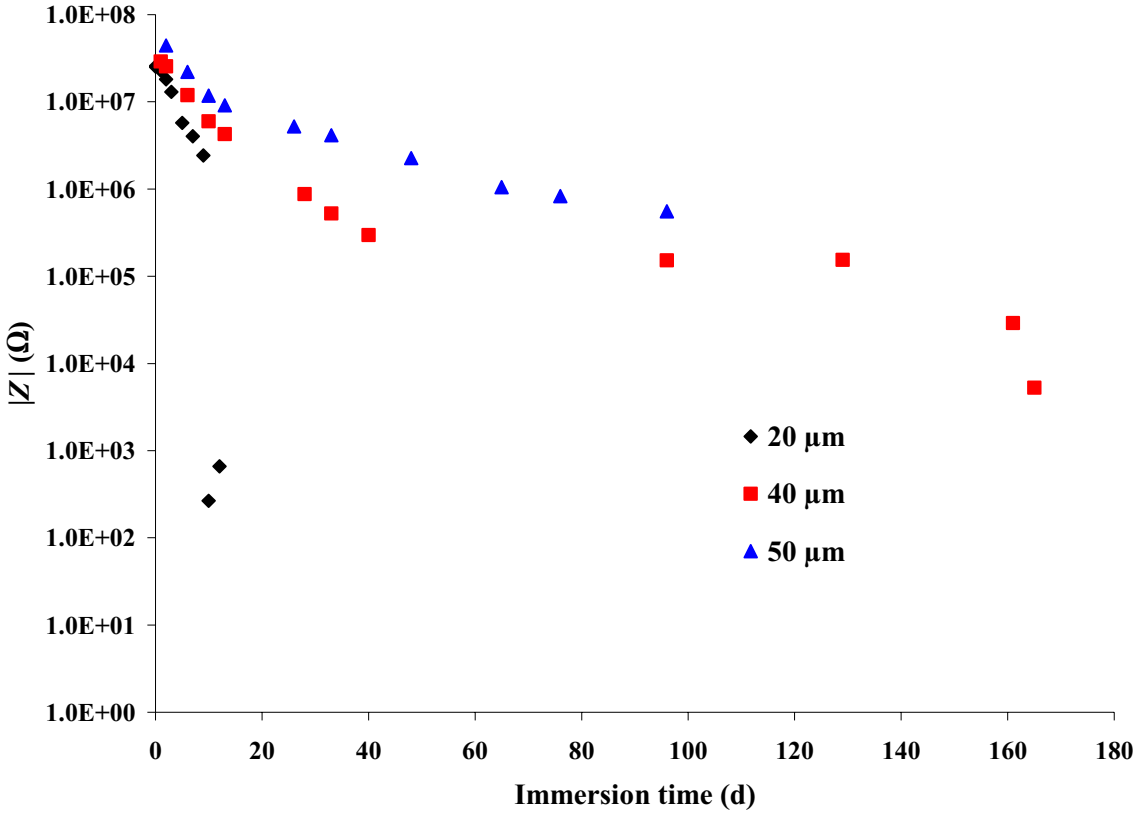

Figure 4.24 Variation of the absolute impedance ($|Z|$), measured at 1.0×10^{-2} Hz, with immersion time for mild steel panels coated with a commercial alkyd paint film containing 1 wt % SiC and exposed to 3% NaCl solution. ◆ = 20 µm, ■ = 40 µm, and ▲ = 50 µm.

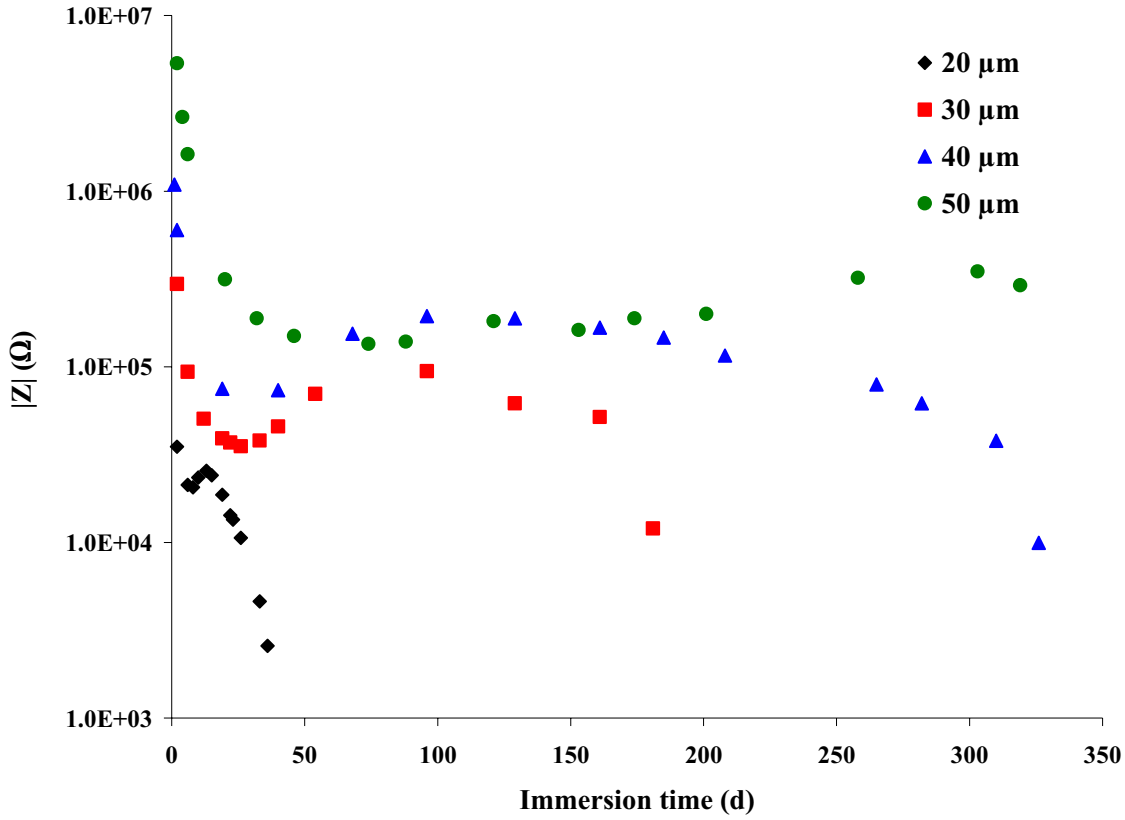

Figure 4.25 Variation of the absolute impedance ($|Z|$), measured at 1.0×10^{-2} Hz, with immersion time for mild steel panels coated with a commercial alkyd paint film containing 5 wt % SiC and exposed to 3% NaCl solution. ◆ = 20 µm, ■ = 30 µm, ▲ = 40 µm, and ● = 50 µm.

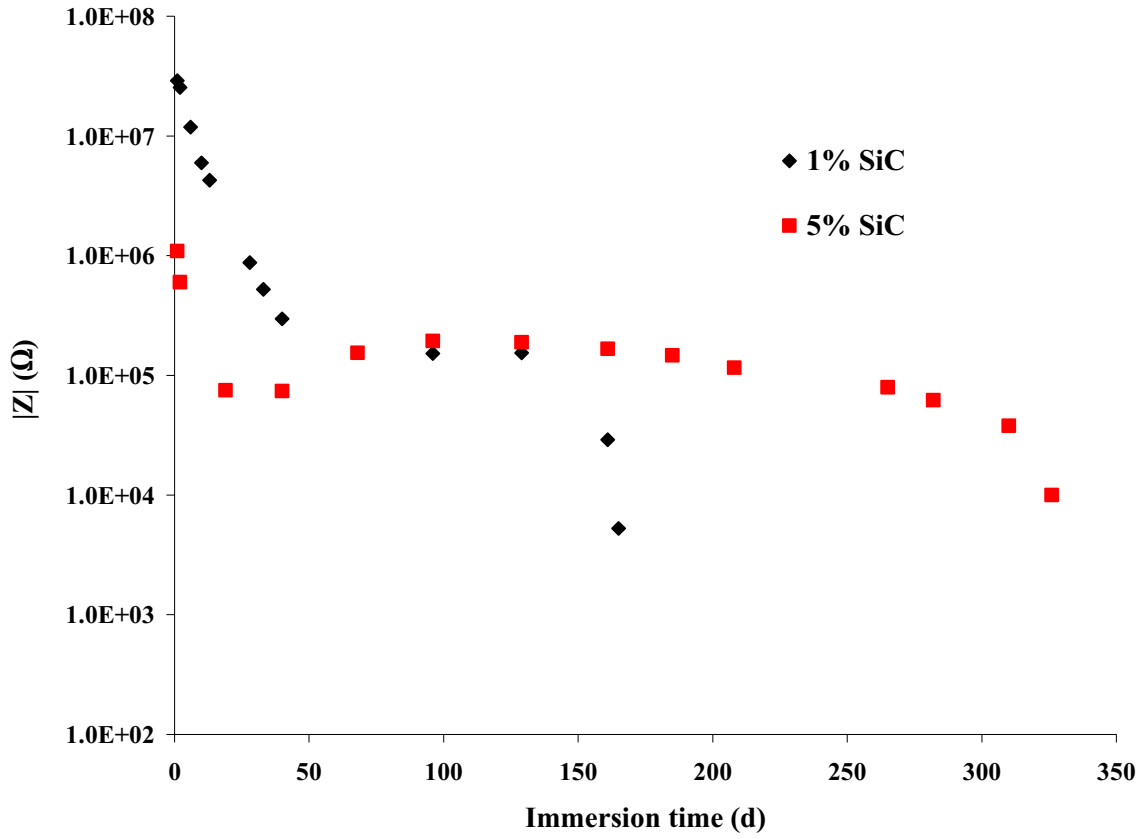

Figure 4.26 Variation of the absolute impedance ($|Z|$), measured at 1.0×10^{-2} Hz, with immersion time for mild steel panels coated with a SiC-incorporated commercial alkyd paint film (40 μm thick) and exposed to 3% NaCl solution. ◆ = paint + 1% SiC, and ▲ = paint + 5% SiC.

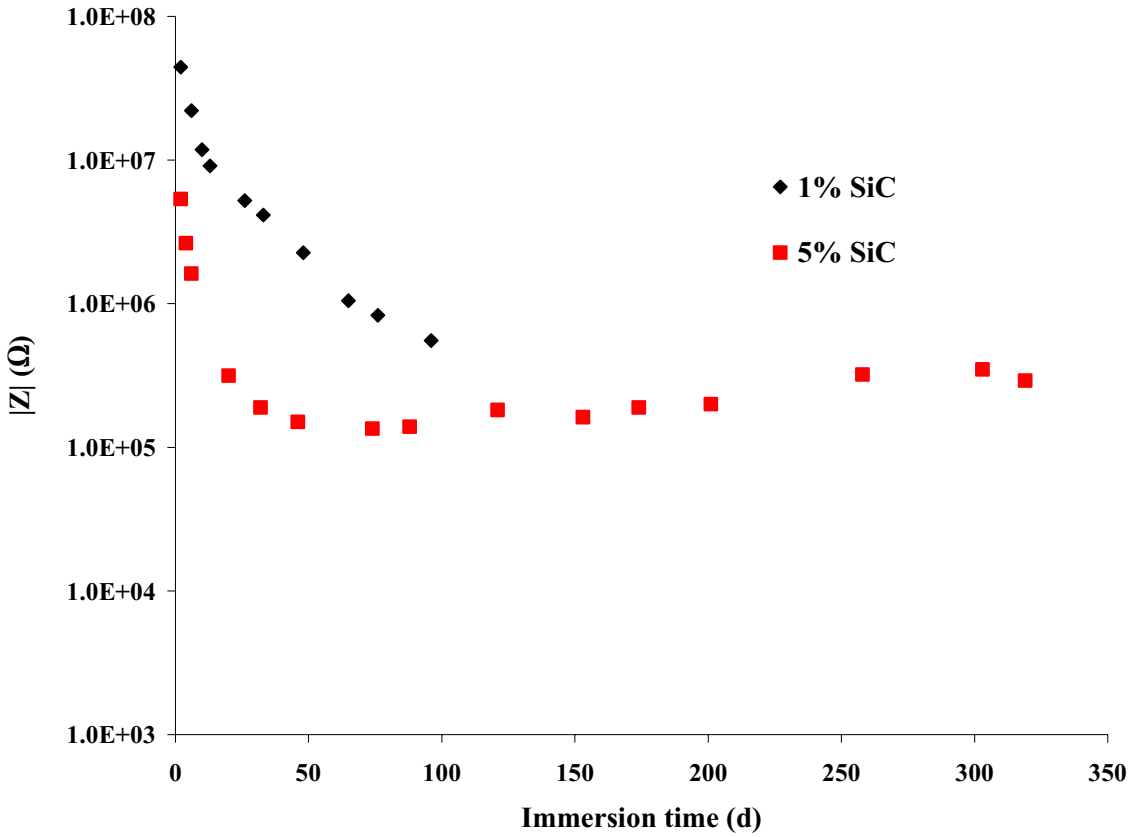

Figure 4.27 Variation of the absolute impedance ($|Z|$), measured at 1.0×10^{-2} Hz, with immersion time for mild steel panels coated with a SiC-incorporated commercial alkyd paint film (50 μm thick) and exposed to 3% NaCl solution. ◆ = paint + 1% SiC, and ▲ = paint + 5% SiC.

the degradation of the coating film in the corrosive solution. These results are consistent with those in the literature.[53, 58, 70-75]

As shown in Figures 4.24 through 4.27, thin coatings are less stable and fail much earlier than thick ones. In addition, as mentioned above, paint containing 1 wt % SiC have higher initial impedance values than 5 wt % SiC (Figures 4.26 and 4.27). However, as shown in the figures, the rate of drop in the impedance in the coatings containing 1% SiC is much faster than that in the coatings containing 5 % SiC. Thus, as shown in Figures 4.26 and 4.27, after ~ 170 d, the 5% SiC-containing coatings appear more protective (with stable and higher $|Z|$ values) than coatings containing 1% SiC.

4.3.5 Polarization Resistance (R_p) Measurements

The polarization resistance (R_p) is one of the parameters used to determine the rate of corrosion of any electrochemical system. R_p is inversely proportional to the corrosion rate and its value is determined from the LF limit of the real part in the Nyquist plot.[76, 77]

Figures 4.28 through 4.31 show the variation of R_p with immersion time for mild steel coupons spin-coated with SiC-incorporated commercial alkyd paint with different thicknesses and SiC loadings. As shown in the figures, for all of the tested coatings, depending on the film thickness and composition, the initial R_p values are in the range of 10^4 to $10^8\ \Omega$ and decrease with immersion time. The relatively high initial R_p values imply that the coatings are initially largely intact and stable. However, as the immersion time increases, defects and pores in the coating initiate and grow in number and size. The

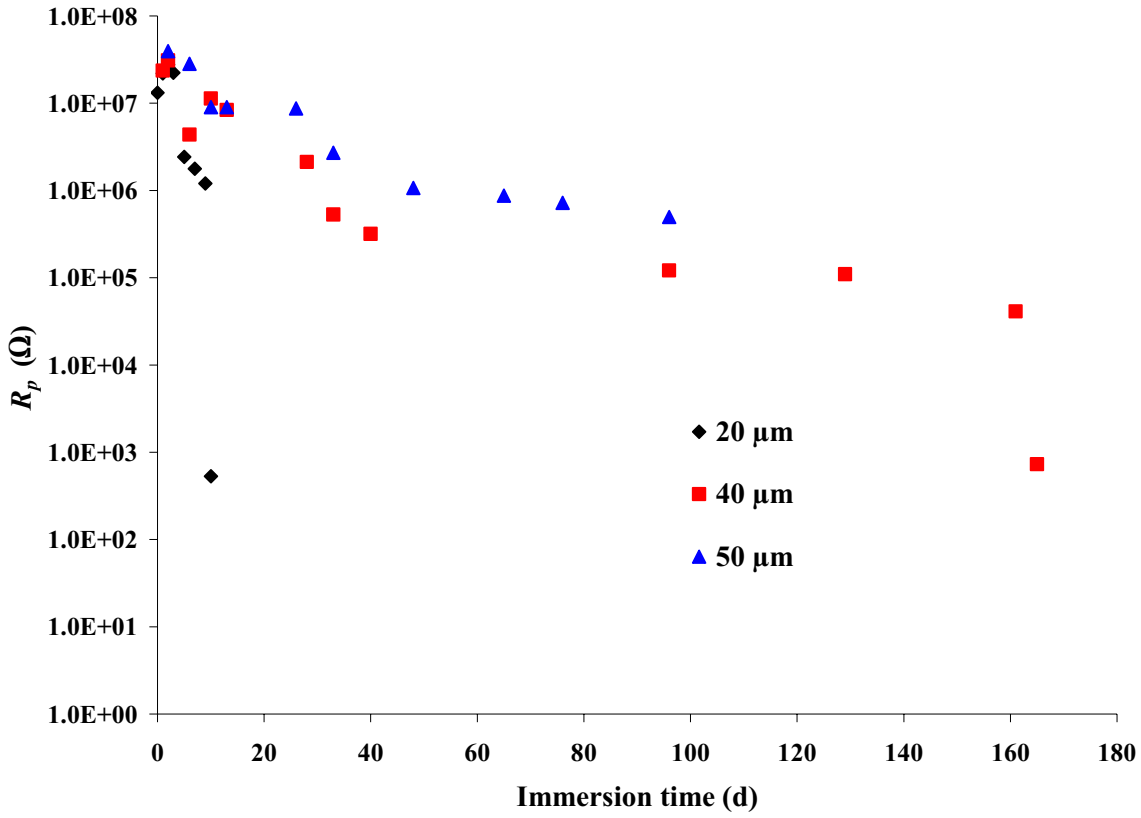

Figure 4.28 Variation of the polarization resistance (R_p) with immersion time for mild steel panels coated with a commercial alkyd paint film containing 1 wt % SiC in 3% NaCl solution. ◆ = 20 µm, ■ = 40 µm, and ▲ = 50 µm.

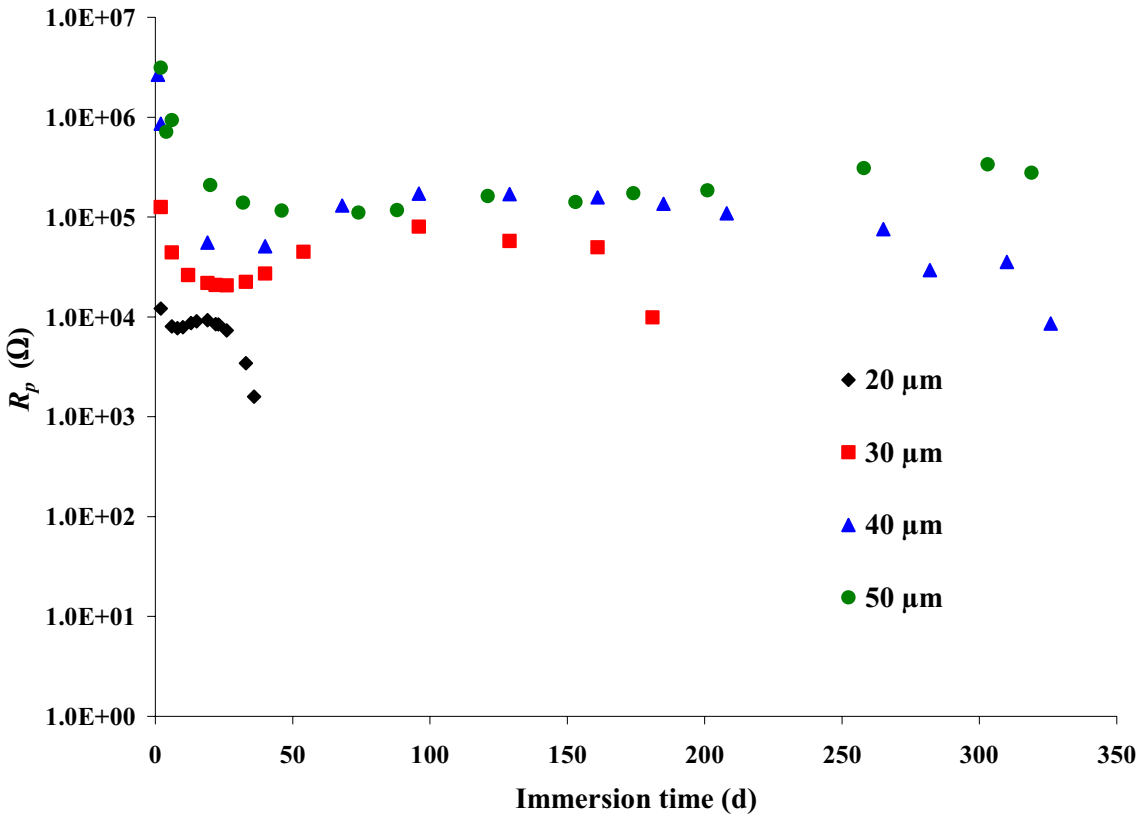

Figure 4.29 Variation of the polarization resistance (R_p) with immersion time for mild steel panels coated with a commercial alkyd paint film containing 5 wt % SiC in 3% NaCl solution. ◆ = 20 µm, ■ = 30 µm, ▲ = 40 µm, and ● = 50 µm.

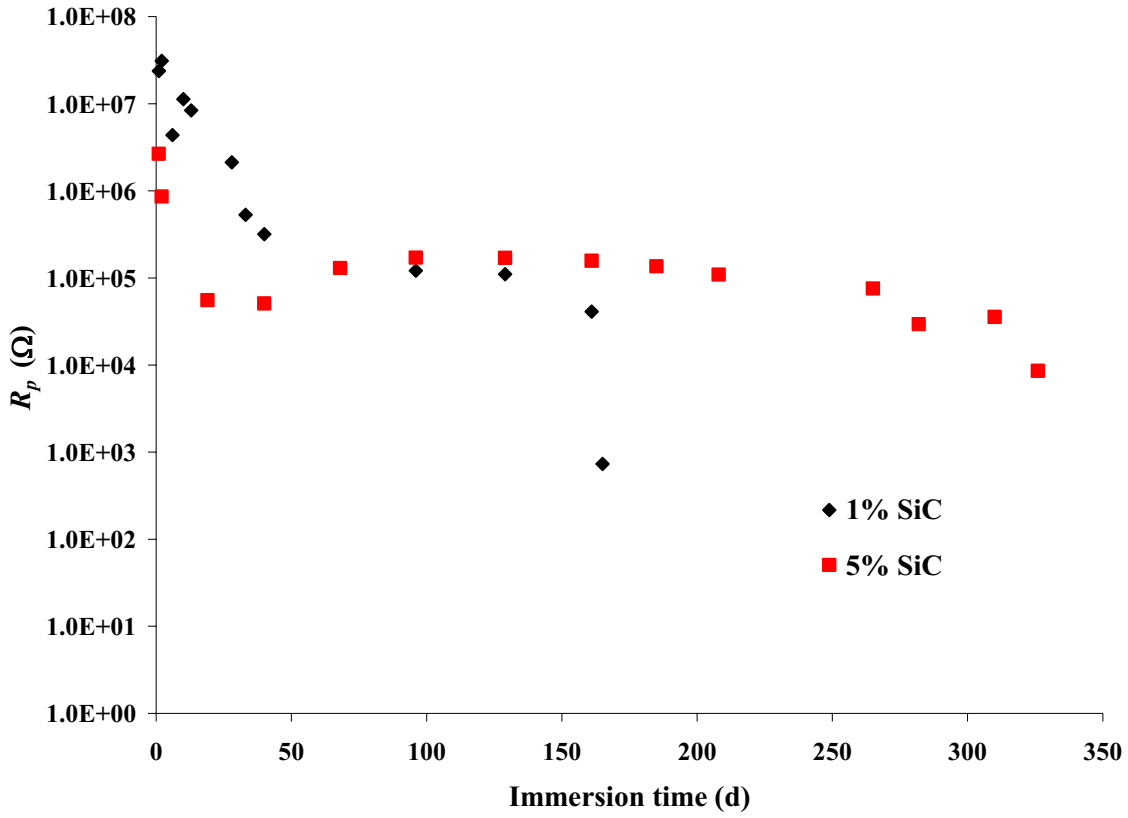

Figure 4.30 Variation of the polarization resistance (R_p) with immersion time for mild steel panels coated with a SiC-incorporated commercial alkyd paint film (40 μm thick) and exposed to 3% NaCl solution. ◆ = paint + 1% SiC, and ▲ = paint + 5% SiC.

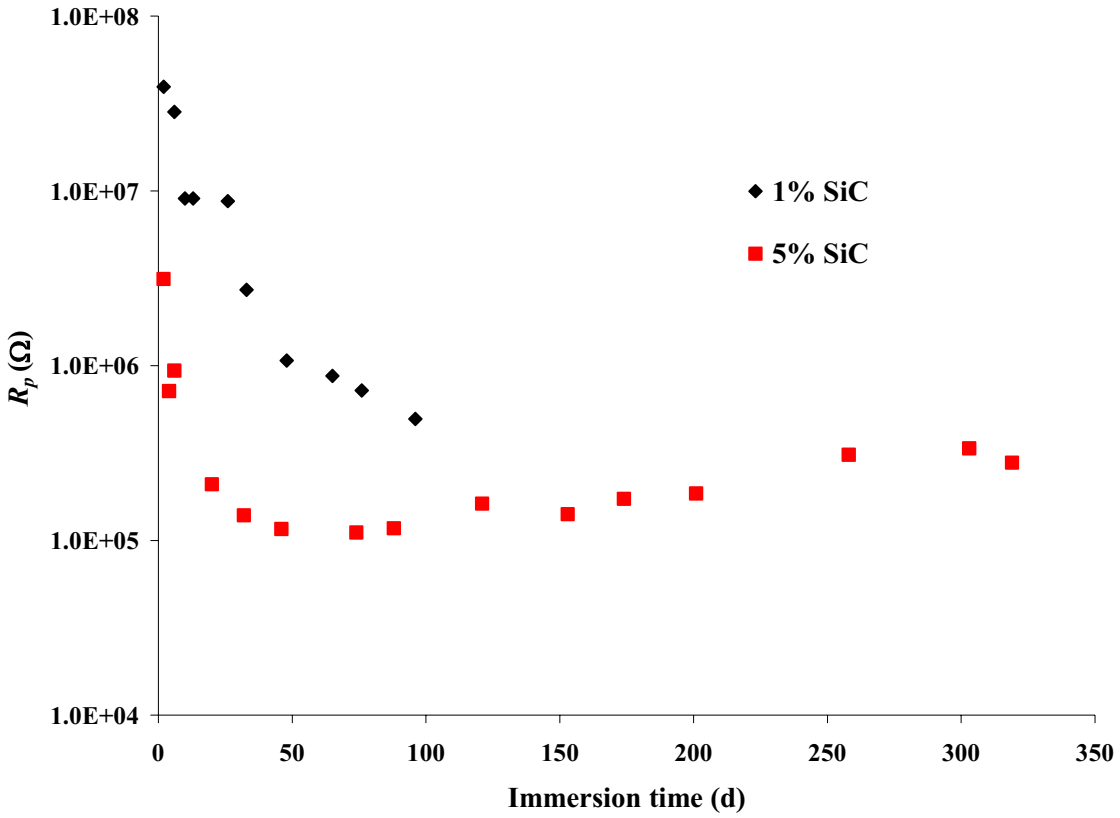

Figure 4.31 Variation of the polarization resistance (R_p) with immersion time for mild steel panels coated with a SiC-incorporated commercial alkyd paint film (50 μm thick) and exposed to 3% NaCl solution. ◆ = paint + 1% SiC, and ▲ = paint + 5% Si.

growth of these active sites is accompanied by significant decrease in the R_p of the system and hence an increase in the corrosion rate.

The data depicted in Figures 4.28 and 4.29 show that, for film coatings having the same SiC wt %, the thicker the coating film, the higher the initial R_p value and the slower the rate of decrease in R_p with immersion time and hence the longer the time needed for the coating film to breakdown. In addition, the data show that the steepest decrease in R_p, and the fastest corrosion rate occurs for thin coatings (20 μm). This indicates a fast diffusion of the electrolyte through thin coatings and hence a fast degradation of the paint films.

For thick coating films (30-50 μm) and coatings containing 5 wt % SiC, the results shown in Figures 4.28 through 4.31 show an initial decrease in R_p followed by a plateau for a long period of immersion, then followed by a sudden decrease of R_p indicating the film breakdown. The results also show that the thicker the coating, the longer the plateau region.

For coatings having the same film thickness (Figures 4.30 and 4.31), the initial R_p values for coatings containing 5 wt % SiC are at least one order of magnitude less than the corresponding values for coatings containing 1 wt % SiC. However, after an initial period of ~ 100 d of immersion, the R_p values for the former coatings remain almost unchanged at values than those of the latter coatings indicating a better stability for the coatings containing 5 wt % SiC.

4.3.6 Double-Layer Capacitance (C_{dl}) Measurements

Figures 4.32 through 4.35 display the variation of C_{dl} with the immersion time for some coating systems with different thicknesses and SiC wt %. An increase in the C_{dl} with immersion time indicates an increase of the detached area on the substrate surface under the coating.[68] As shown in the figures, depending on the paint film composition and thickness, the initial C_{dl} values are low (as low as 7.0×10^{-8} F/cm^2) and increase with immersion time. The relatively low initial C_{dl} values imply that the coatings are initially largely bonded to the substrate surface. However, as the immersion time increases the value of C_{dl} increase for a short period of time, denoting the entry of the electrolyte into the paint coating. After that initial period of increase, the value of C_{dl} remain unchanged for the long exposure time until the film finally fails and corrosion occurs at the steel substrate surface and the value of C_{dl} increases rapidly.

As shown in Figures 4.32 and 4.33, for coatings having the same SiC content, the thicker the coating film, the lower the initial value of the C_{dl} indicating a good protective film with greater corrosion stability. On the other hand, Figures 4.34 and 4.35 show that the paint coating containing 5 wt % SiC has a higher initial C_{dl} value than a coating containing 1 wt % SiC with the same film thickness. Nevertheless, it can be noticed that after ~ 50 d of immersion, the value of C_{dl} for the former coating decreases to a stable value and remains unchanged for a long period of immersion in the corrosive solution while the latter coating fails earlier. These results are also in good agreement with the R_p measurements (vide supra).

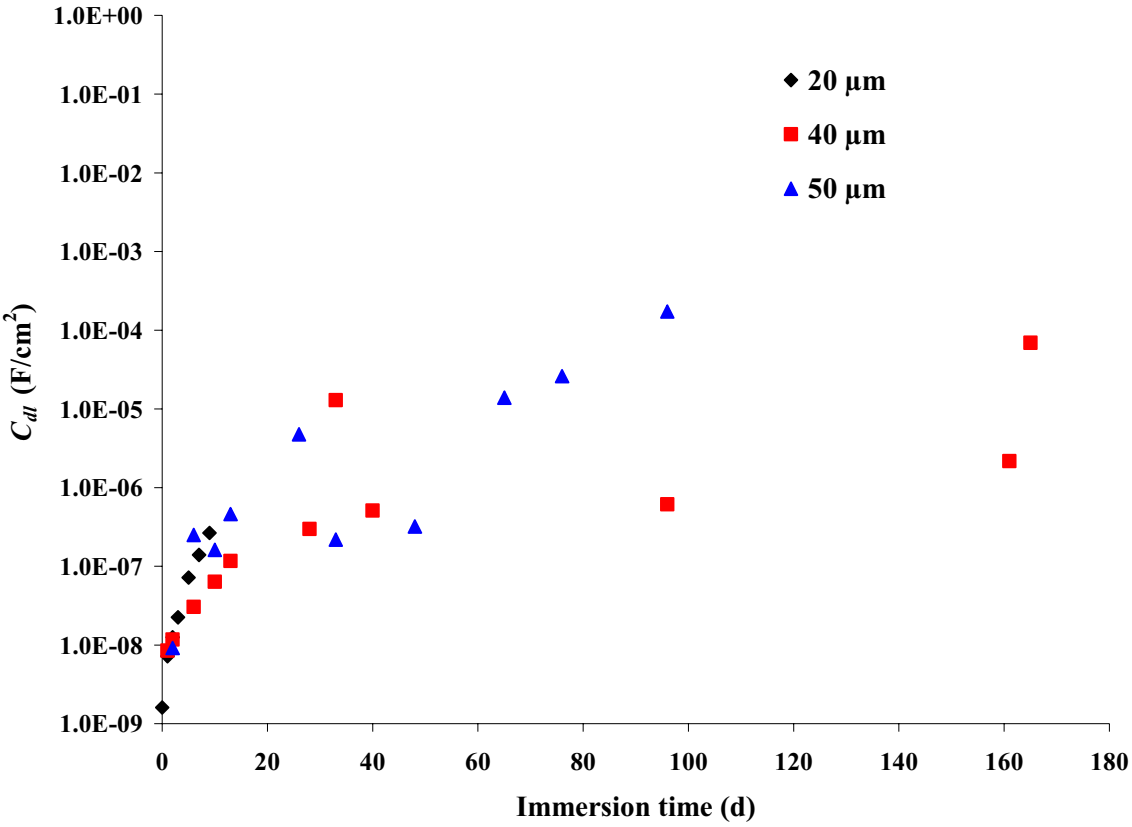

Figure 4.32 Variation of the double layer capacitance (C_{dl}) with immersion time for mild steel panels coated with a commercial alkyd paint film containing 1 wt % SiC in 3% NaCl solution. ◆ = 20 µm, ■ = 40 µm, and ▲ = 50 µm.

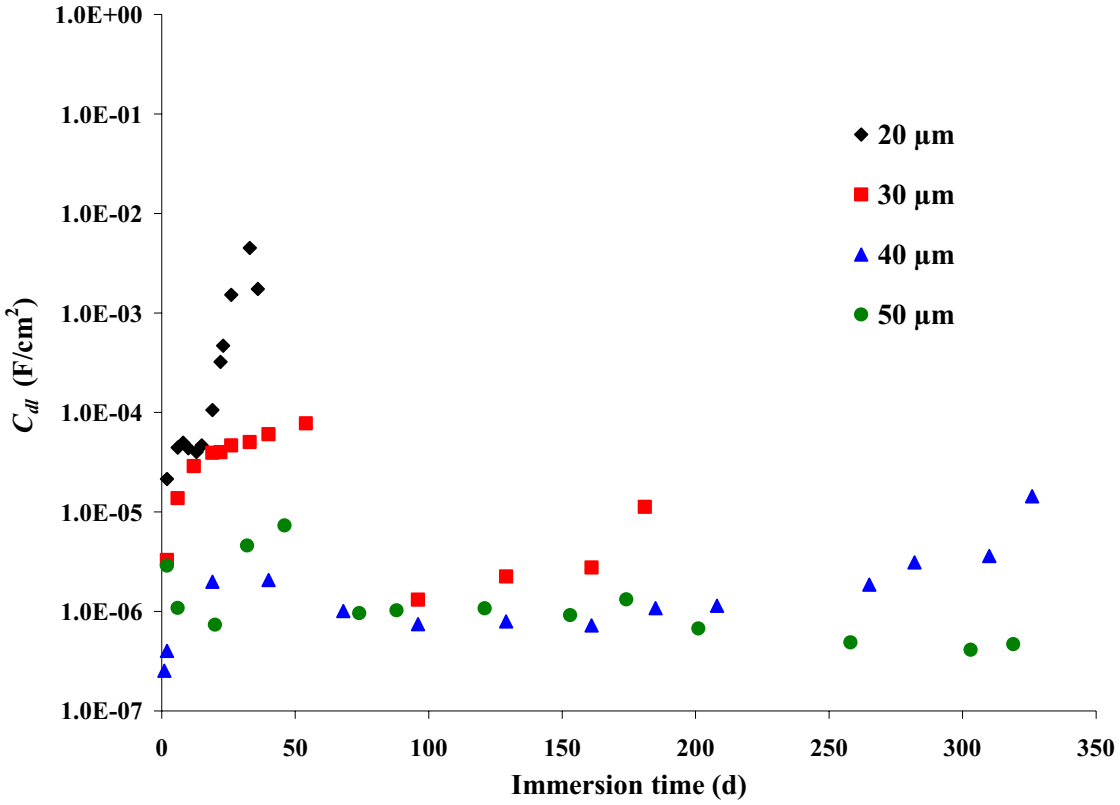

Figure 4.33 Variation of the double layer capacitance (C_{dl}) with immersion time for mild steel panels coated with a commercial alkyd paint film containing 5 wt % SiC in 3% NaCl solution. ◆ = 20 µm, ■ = 30 µm, ▲ = 40 µm, and ● = 50 µm.

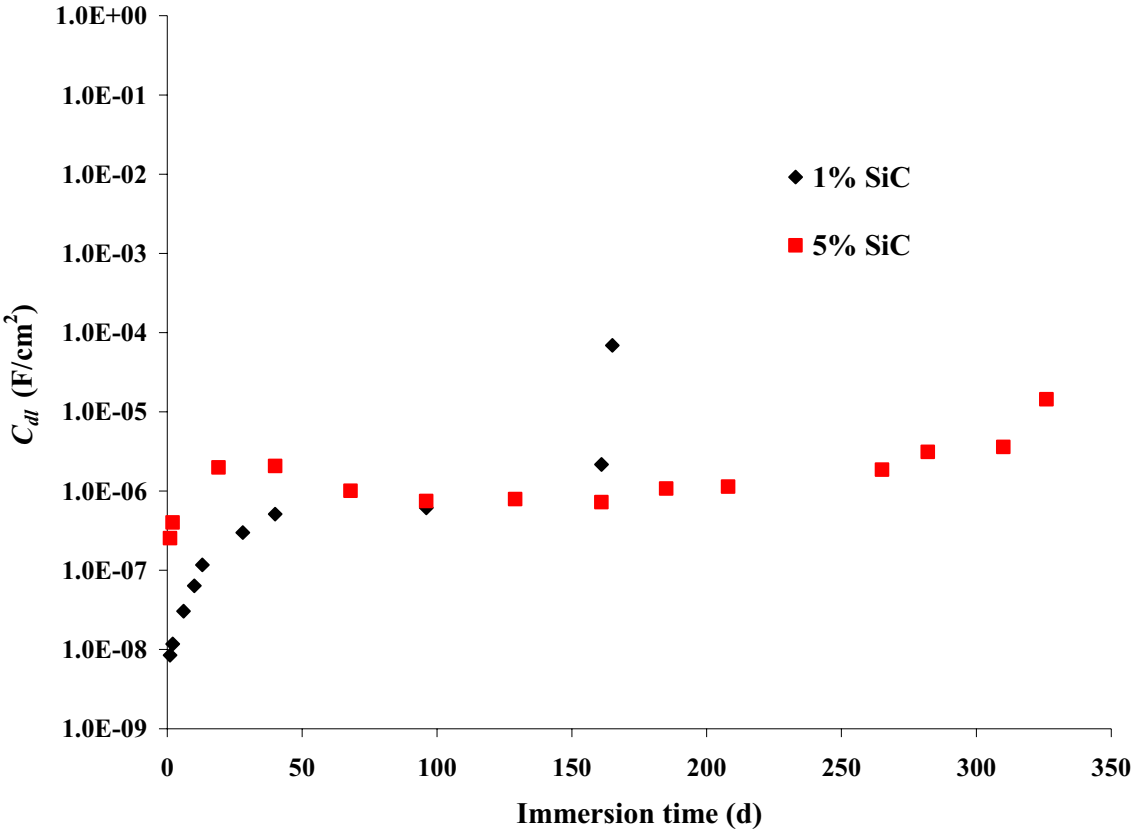

Figure 4.34 Variation of the double layer capacitance (C_{dl}) with immersion time for mild steel panels coated with a Si-incorporated commercial alkyd paint film (40 μm thick) and exposed to 3% NaCl solution. ◆ = paint + 1% SiC, and ■ = paint + 5% SiC.

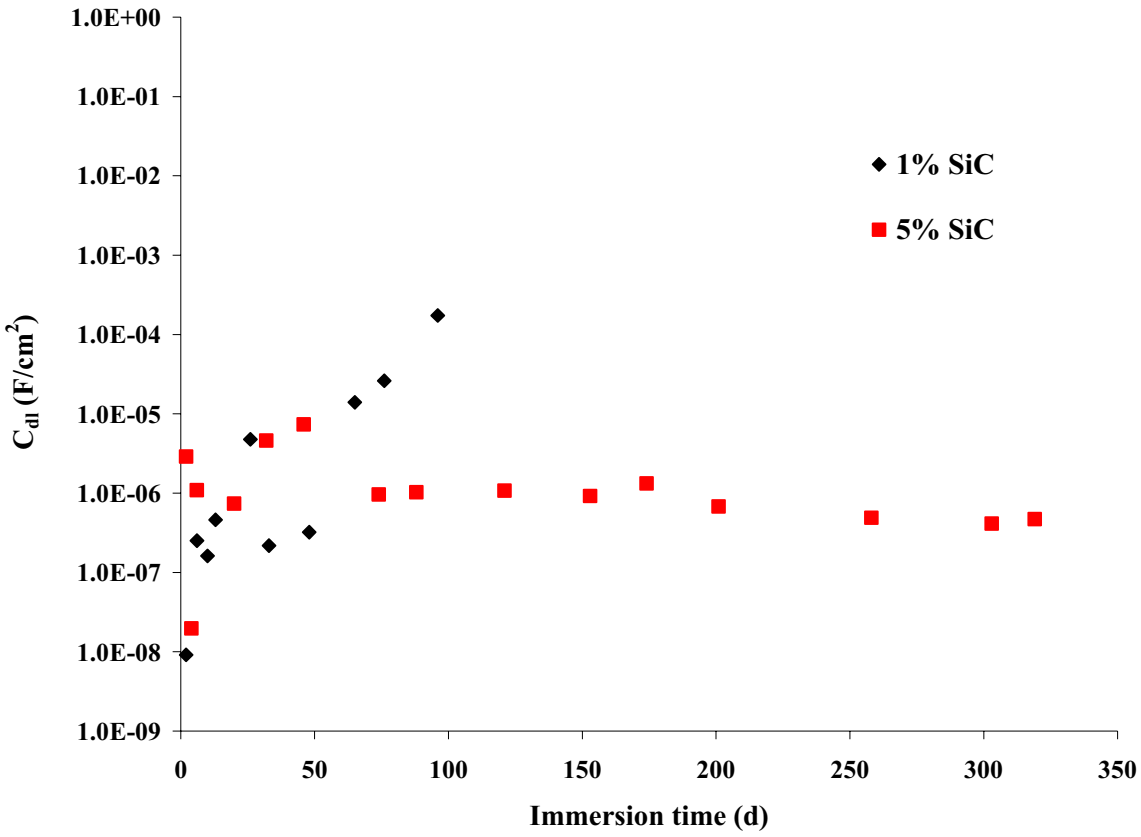

Figure 4.35 Variation of the double layer capacitance (C_{dl}) with immersion time for mild steel panels coated with a Si-incorporated commercial alkyd paint film (50 μm thick) and exposed to 3% NaCl solution. ◆ = paint + 1% SiC, and ■ = paint + 5% SiC.

4.3.7 Coating Resistance (R_c) Measurements

As mentioned in Chapter 3, the coating resistance (R_c) along with the coating capacitance (C_c) are considered the best measures for the stability of any organic coatings applied to the surface of a metal substrate.[73, 78] For a coated substrate exposed to an aqueous solution of a corrosive electrolyte, a decrease in R_c and increase in C_c imply degradation of the coating.[79, 80]

The variation of the R_c with immersion time is shown in Figures 4.36 through 4.39 for SiC-incorporated alkyd paint coatings applied to mild steel substrates with different coating thicknesses and SiC loadings. The data show that, depending on the coating thickness and the SiC wt %, the initial R_c values for all coatings are in the range of 10^4 to 10^7 Ω. As shown in the figures, the value of R_c which decreases in the first few days of exposure to NaCl solution, denoting the entry of the electrolyte into the alkyd paint coating. After this initial period, the value of R_c reaches a plateau and remains almost constant over a long immersion time period before R_c significantly drops indicating a film breakdown and corrosion of the metallic substrate. The length of the immersion time before film breakdown occurs is an indication of the stability of the coating. The longer the immersion time before film breakdown, the greater the insulation protection properties of the coating film. In addition, as shown in Figures 4.36 and 4.37, for coatings having the same SiC loading, the thicker the coating, the higher the initial R_c value.

For coatings having the same film thickness (Figures 4.38 and 4.39), the initial R_c values for coatings containing 5 wt % SiC are at least one order of magnitude less than the corresponding values for coatings containing 1 wt % SiC. However, after an initial

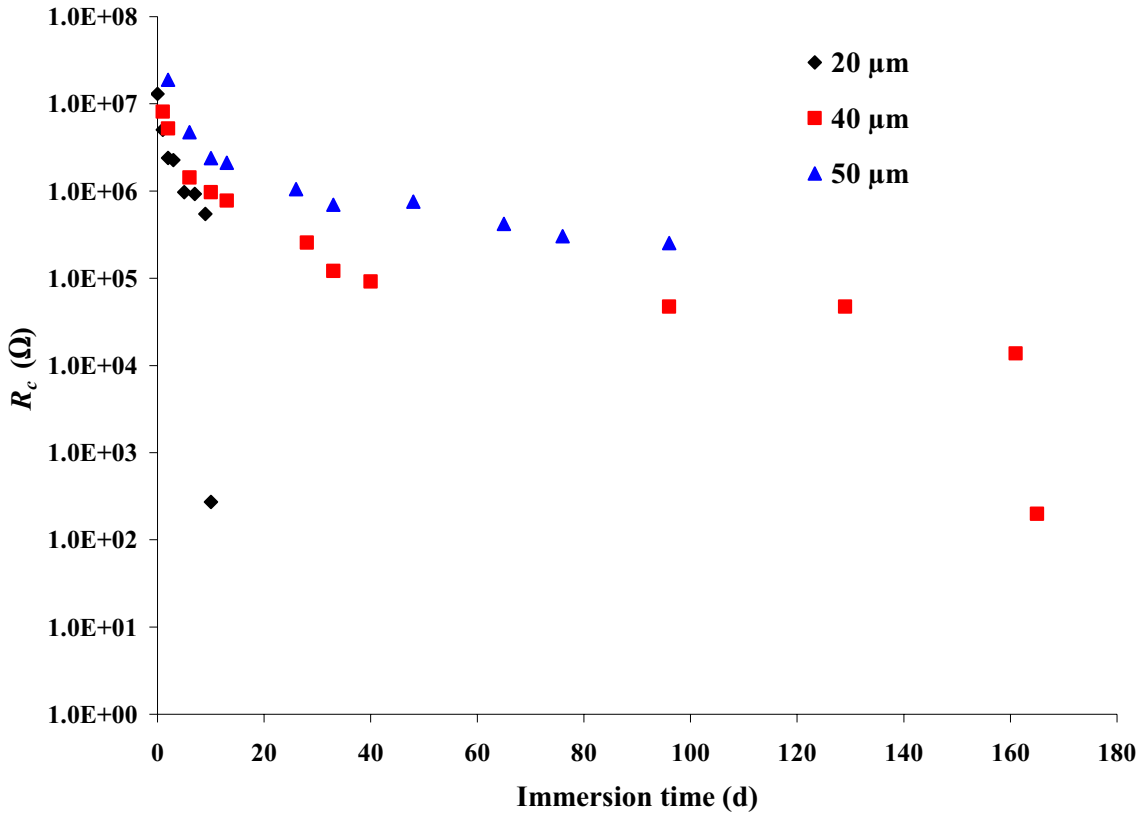

Figure 4.36 Variation of the coating resistance (R_c) with immersion time for mild steel panels coated with a commercial alkyd paint film containing 1 wt % SiC in 3% NaCl solution. ■ = 20 µm, ◆ = 40 µm, and ▲ = 50 µm.

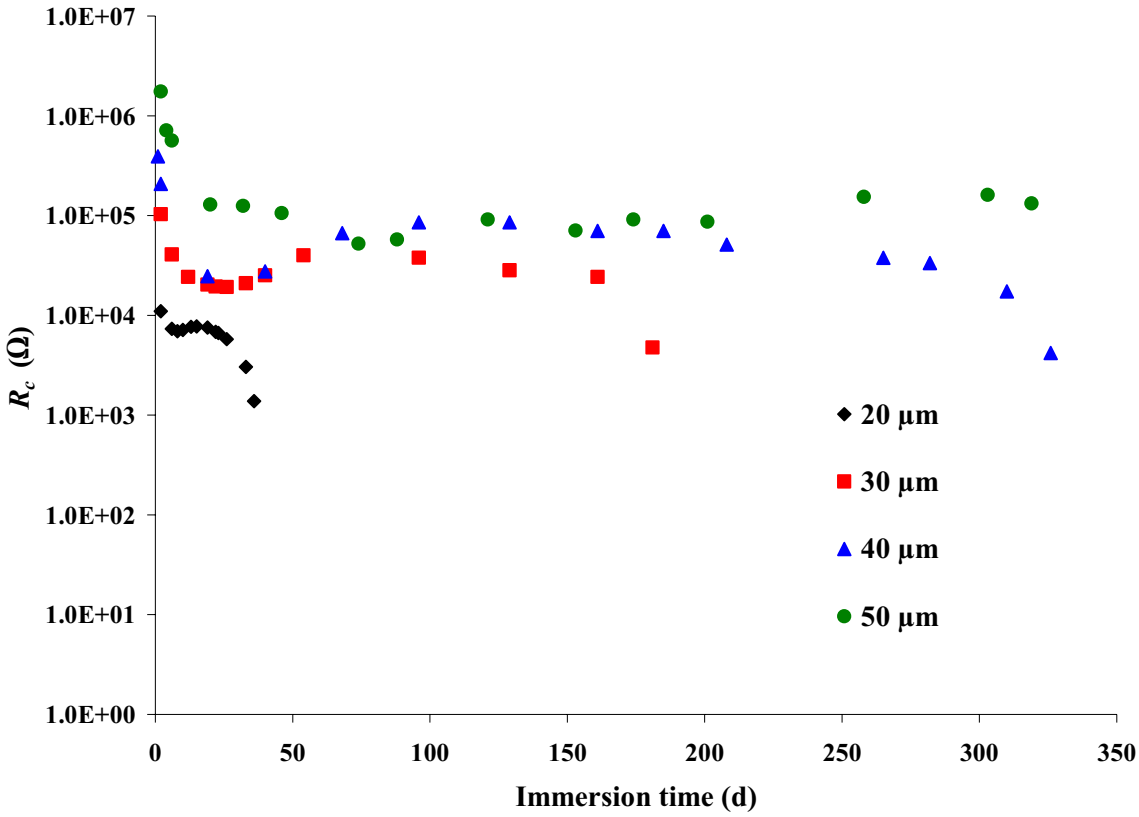

Figure 4.37 Variation of the coating resistance (R_c) with immersion time for mild steel panels coated with a commercial alkyd paint film containing 5 wt % SiC in 3% NaCl solution. ■ = 20 µm, ◆ = 30 µm, ▲ = 40 µm, and ● = 50 µm.

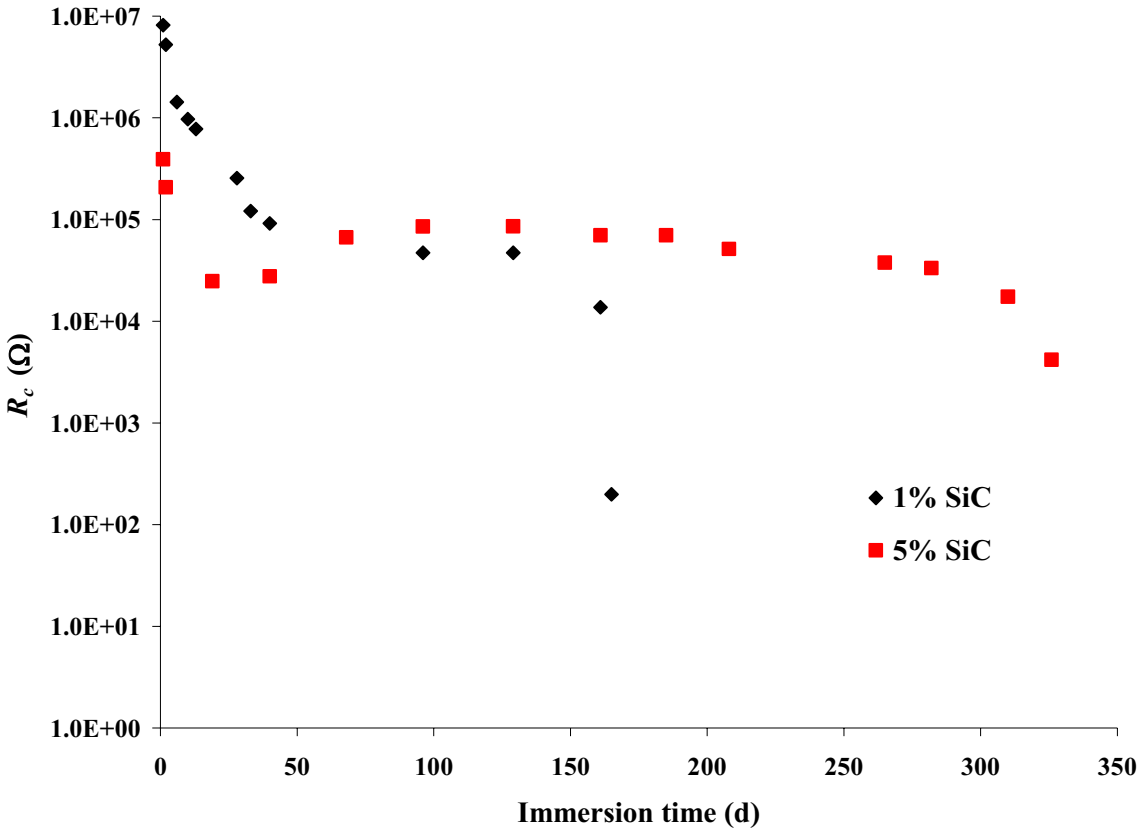

Figure 4.38 Variation of the coating resistance (R_c) with immersion time for mild steel panels coated with a SiC-incorporated commercial alkyd paint film (40 μm thick) and exposed to 3% NaCl solution. ◆ = paint + 1% SiC, and ■ = paint + 5% SiC.

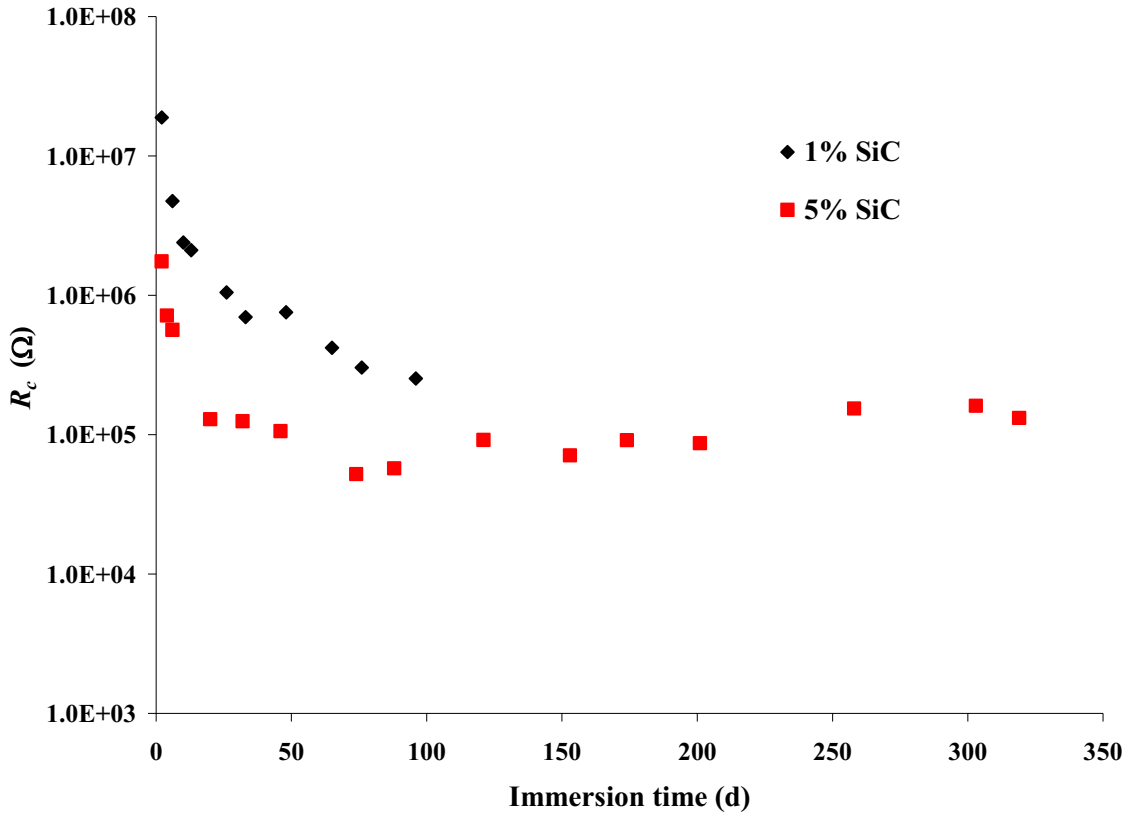

Figure 4.39 Variation of the coating resistance (R_c) with immersion time for mild steel panels coated with a SiC-incorporated commercial alkyd paint film (50 μm thick) and exposed to 3% NaCl solution. ◆ = paint + 1% SiC, and ■ = paint + 5% SiC.

period of 50-100 d of immersion, the R_c values for the former coatings remain almost unchanged at values higher than those of the latter coatings. It is also notable from Figures 4.38 and 4.39 that the plateau region for the 5 wt % SiC-reinforced coatings is longer than that for the 1 wt % coatings indicating a better stability for the former coating. These results are consistent with the R_p and C_{dl} results (vide supra).

4.3.8 Coating Capacitance (C_c) Measurements

As mentioned before, the value of the coating capacitance (C_c) reflects the total amount of water in the coating and its value is expected to increase with immersion time.[81-83] Figures 4.40 through 4.43 display the variation of C_c with immersion time for SiC-reinforced paint coatings applied to the surface of mild steel samples with different film thicknesses and SiC loadings. As shown in the figures, depending on the paint film composition and thickness, the initial C_c values are low (as low as 5.0×10^{-9} F/cm^2) and increase with immersion time. As with the C_{dl}, the relatively low initial C_c values imply that the coatings are initially largely bonded to the substrate surface. However, as the immersion time increases the value of C_c increase for a short period of time, denoting the entry of the electrolyte into the paint coating. After that initial period of increase, the value of C_c remain unchanged for the long exposure time until the film finally fails and corrosion occurs at the steel substrate surface and the value of C_c increases rapidly.

As shown in Figures 4.40 and 4.41, for coatings having the same SiC content, the thicker the coating film, the lower the initial value of the C_c indicating a good protective film with greater corrosion stability. On the other hand, Figures 4.42 and 4.43 show that the paint coating containing 5 wt % SiC has a slightly higher initial C_c value than a

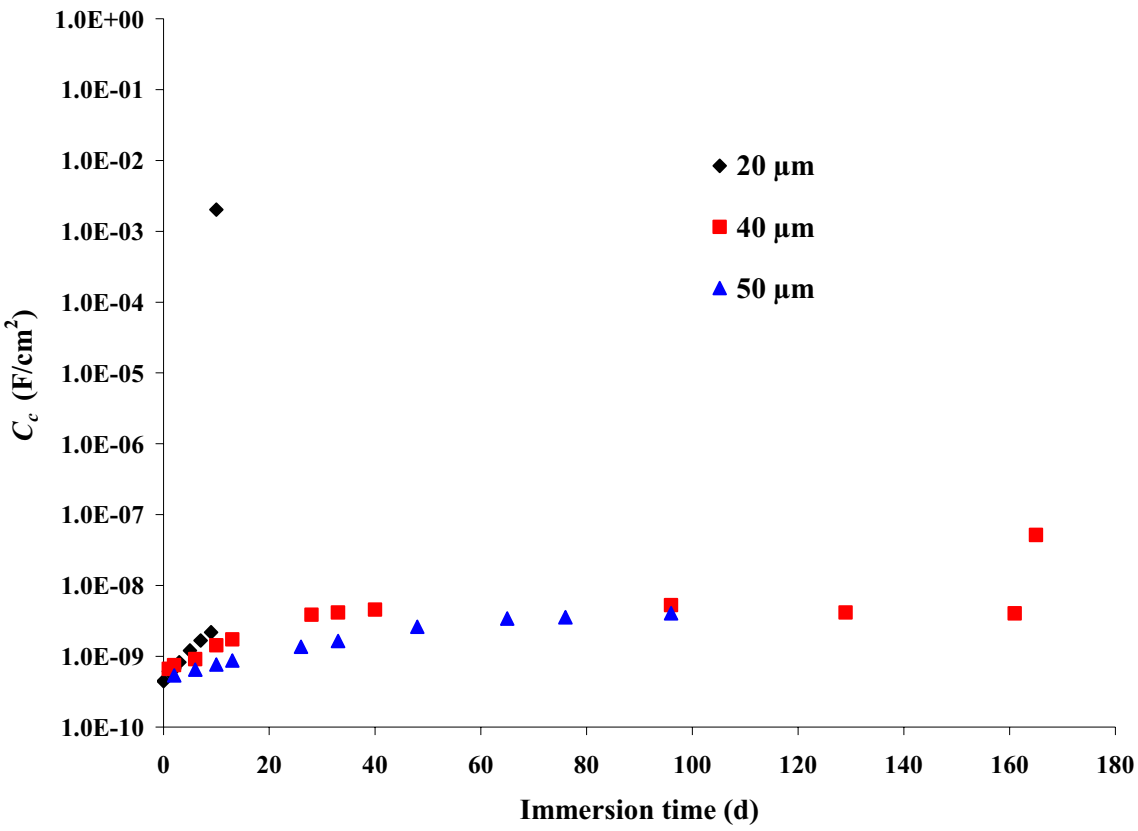

Figure 4.40 Variation of the coating capacitance (C_c) with immersion time for mild steel panels coated with a commercial alkyd paint film containing 1 wt % SiC in 3% NaCl solution. ◆ = 20 µm, ■ = 40 µm, and ▲ = 50 µm.

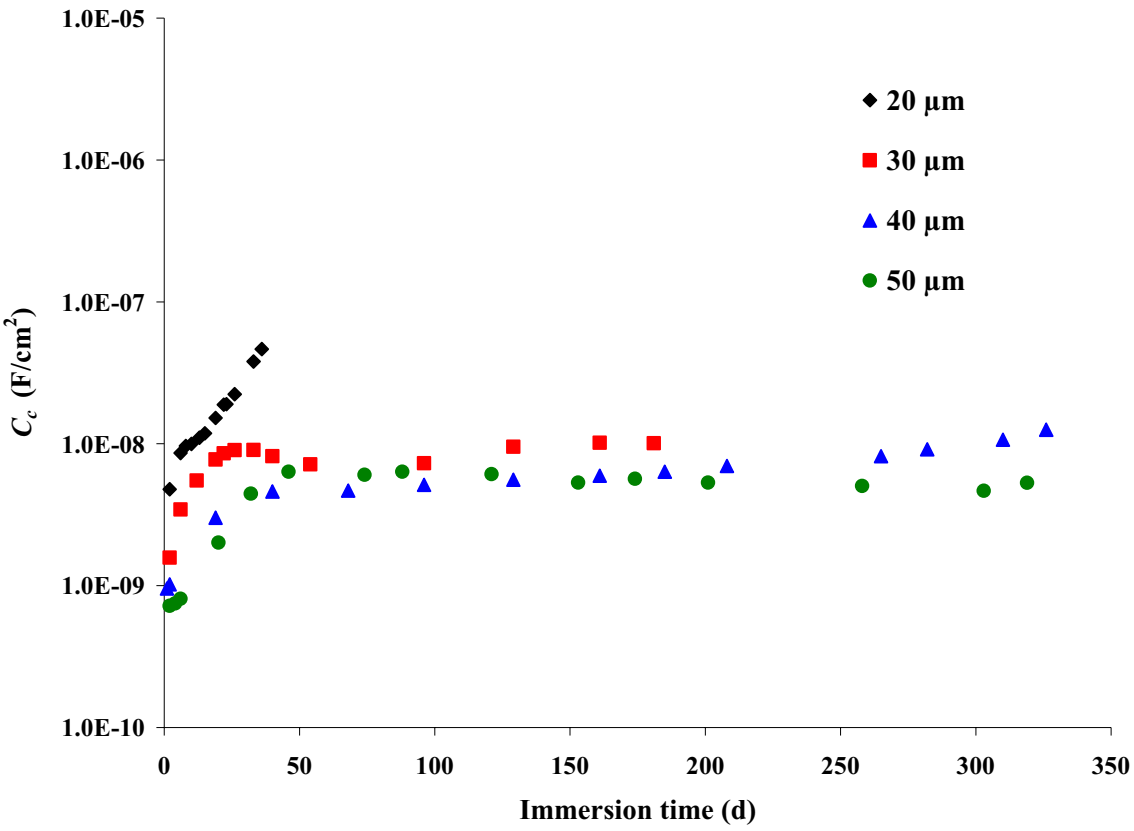

Figure 4.41 Variation of the coating capacitance (C_c) with immersion time for mild steel panels coated with a commercial alkyd paint film containing 5 wt % SiC in 3% NaCl solution. ■ = 20 µm, ◆ = 30 µm, ▲ = 40 µm, and ● = 50 µm.

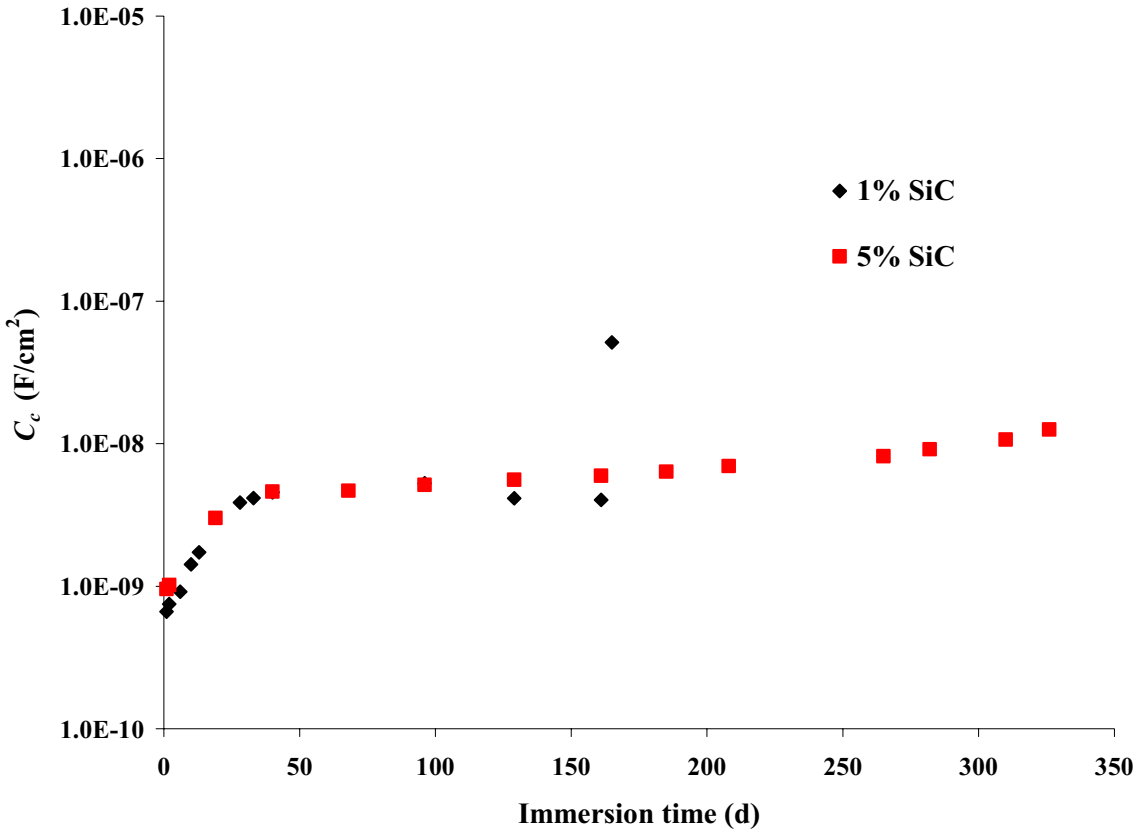

Figure 4.42 Variation of the coating capacitance (C_c) with immersion time for mild steel panels coated with a Si-incorporated commercial alkyd paint film (40 μm thick) and exposed to 3% NaCl solution. ◆ = paint + 1% SiC, and ■ = paint + 5% SiC.

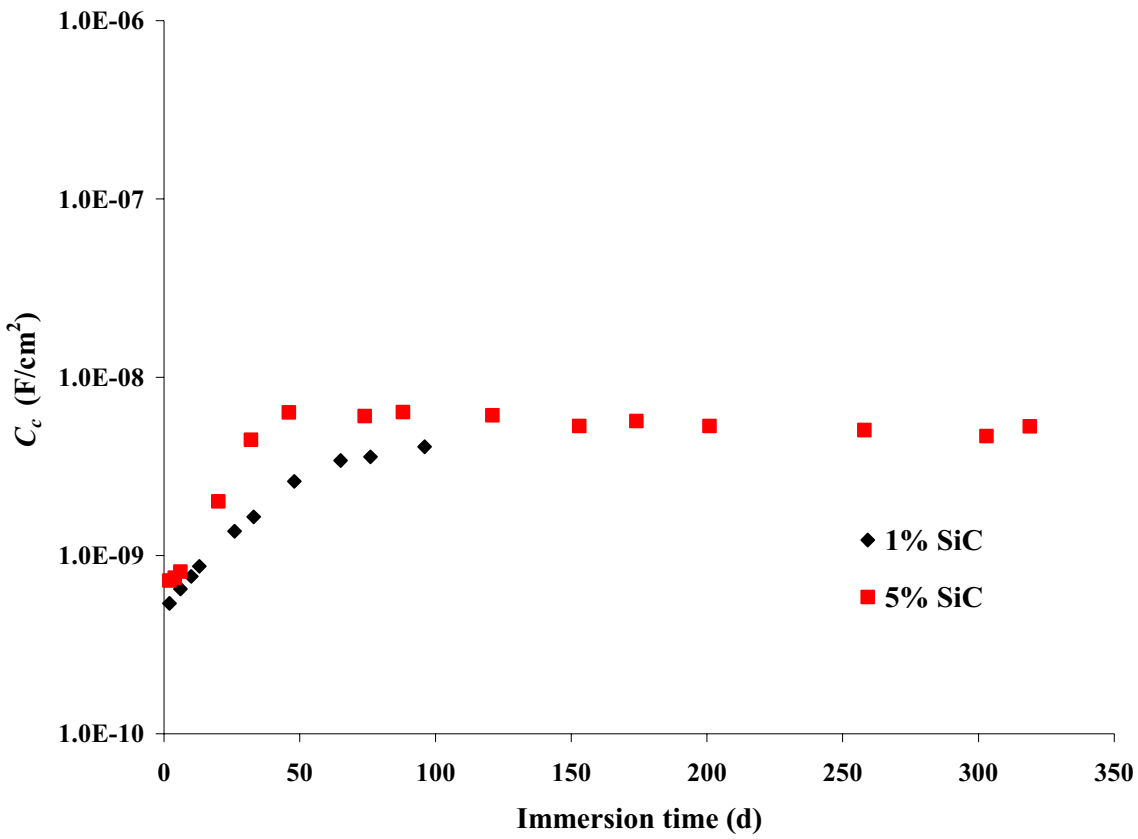

Figure 4.43 Variation of the coating capacitance (C_c) with immersion time for mild steel panels coated with a Si-incorporated commercial alkyd paint film (50 μm thick) and exposed to 3% NaCl solution. ◆ = paint + 1% SiC, and ■ = paint + 5% SiC.

coating containing 1 wt % SiC with the same film thickness. However, it can be noticed that after ~ 100 d of immersion, the value of C_c for the former coating decreases to a stable value and remains unchanged for a long period of immersion in the corrosive solution while the latter coating fails earlier. These results are also consistent with the R_p, C_{dl} and R_c results (vide supra).

4.3.9 Water Uptake Measurements

As mentioned in Chapter 3, water uptake is considered the primary factor that governs the service life of any coating. Degradation of a coating is accompanied by an increase in the percent water uptake and decrease in the coating resistance.[84] Percent water uptake values were calculated from the coating capacitance (C_c) using Equation 3.3 (Chapter 3).

Figures 4.44 through 4.47 show the variation of the percent water uptake with immersion time for SiC-containing alkyd paint samples, with different thicknesses and SiC loadings, applied to the surface of mild steel substrates. The results show that the initial percent water uptake for all studied samples is less than 10%. As the exposure time increases, the percent water uptake increases until the coating film is totally destroyed where the electrolyte reaches the substrate surface and corrosion products are formed. As shown in Figures 4.44 through 4.47, the increase in water uptake starts gradually for all of the tested panels followed by a rapid increase that corresponds to the complete loss of adhesion and onset of blistering in the coating films.

The data depicted in Figures 4.44 and 4.45 show that the thicker the coating film, the lesser percent of water absorbed, the slower the permeability of the electrolyte, and

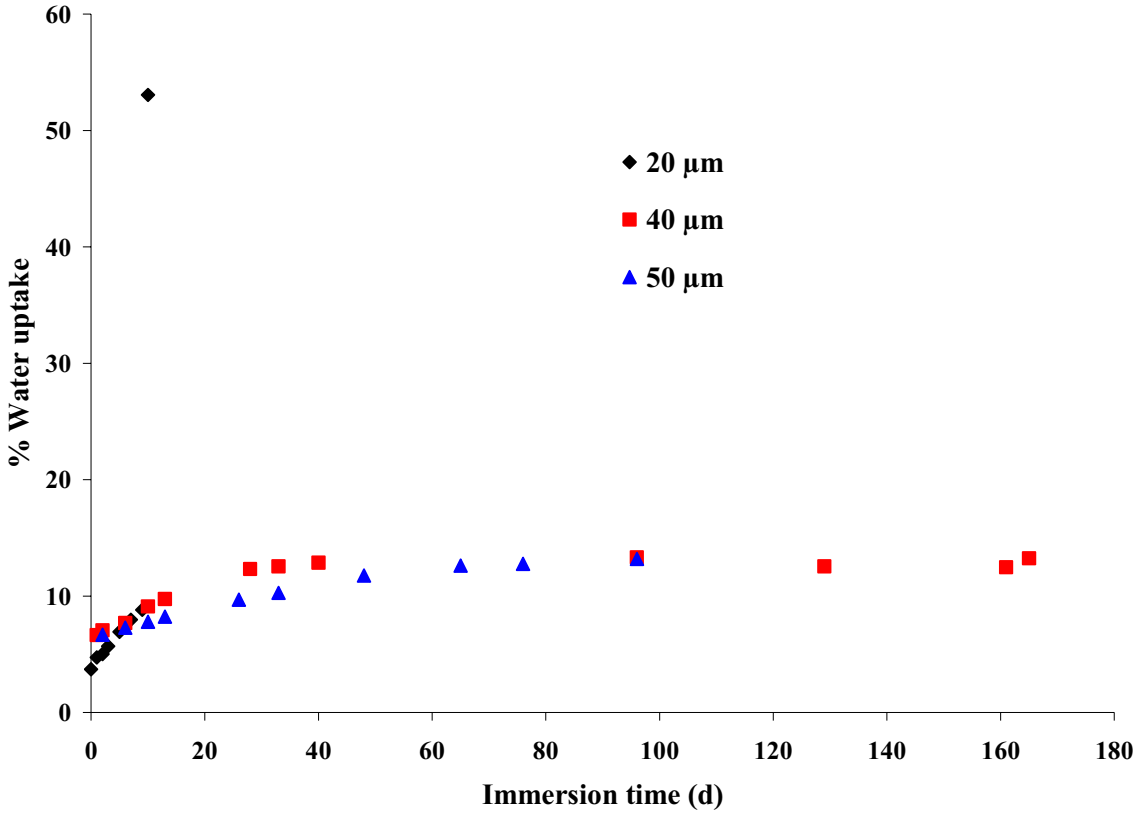

Figure 4.44 Variation of % water uptake with immersion time for mild steel panels coated with a commercial alkyd paint film containing 1 wt % SiC and exposed to 3% NaCl solution. ◆ = 20 µm, ■ = 40 µm, and ▲ = 50 µm.

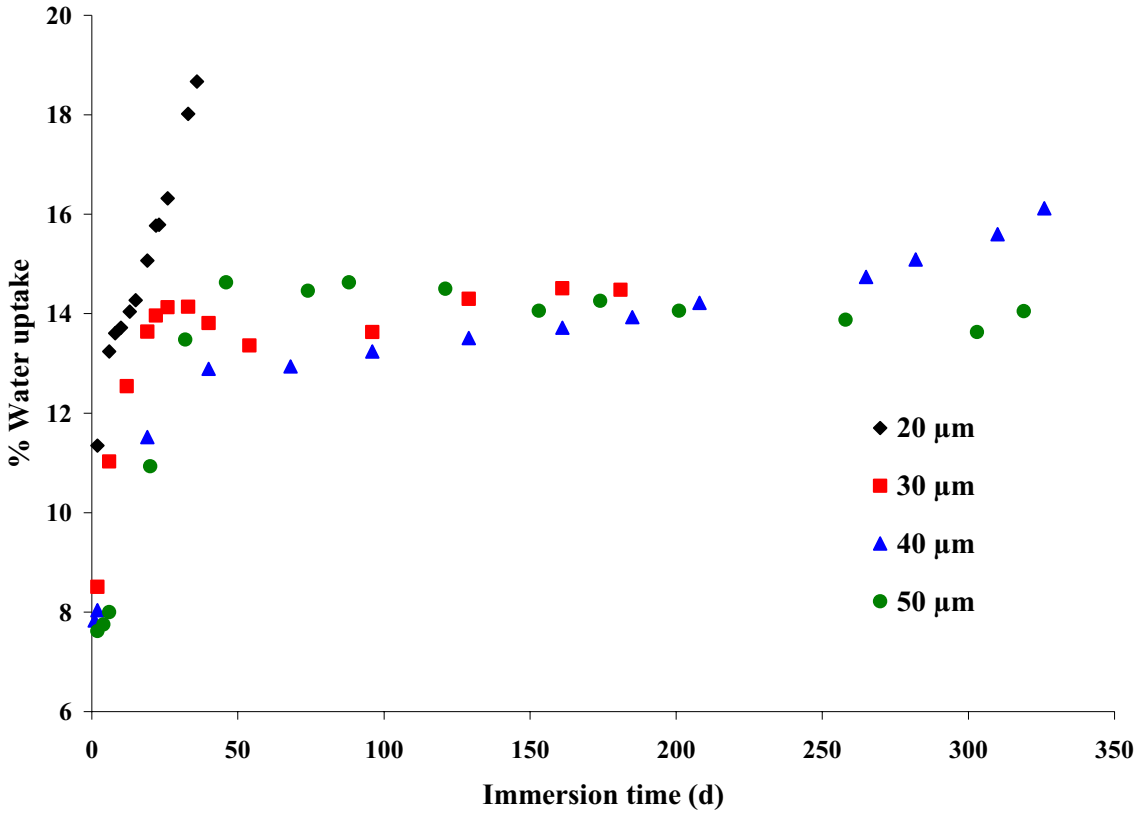

Figure 4.45 Variation of % water uptake with immersion time for mild steel panels coated with a commercial alkyd paint film containing 5 wt % SiC and exposed to 3% NaCl solution. ■ = 20 µm, ◆ = 30 µm, ▲ = 40 µm, and ● = 50 µm.

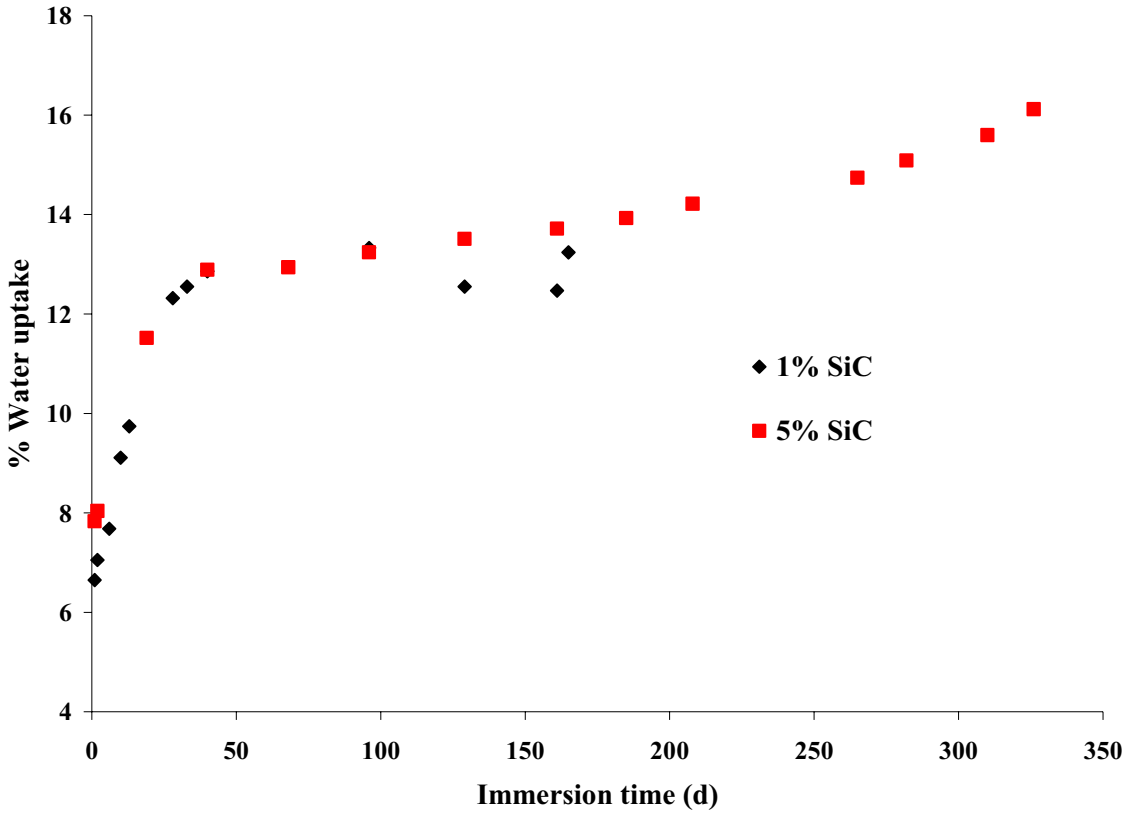

Figure 4.46 Variation of % water uptake with immersion time for mild steel panels coated with a SiC-incorporated commercial alkyd paint film (40 μm thick) in 3% NaCl solution. ◆ = paint + 1% SiC, and ■ = paint + 5% SiC.

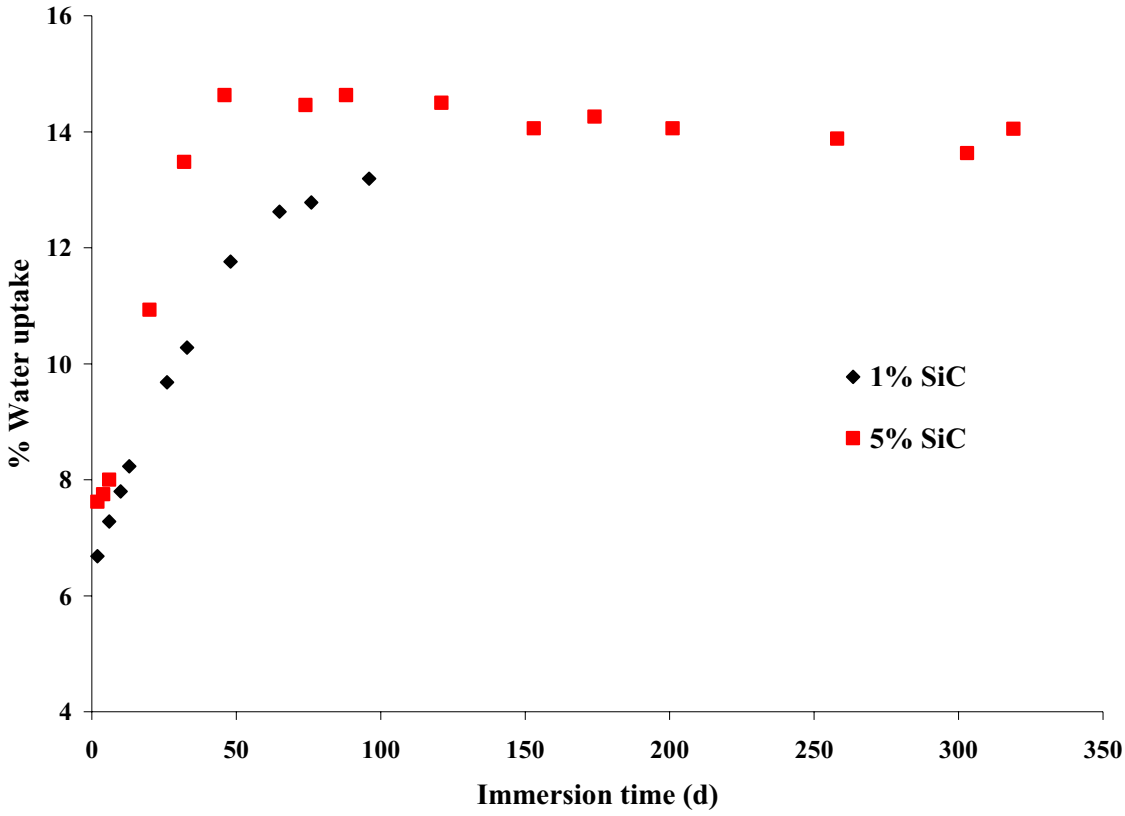

Figure 4.47 Variation of % water uptake with immersion time for mild steel panels coated with a SiC-incorporated commercial alkyd paint film (50 μm thick) in 3% NaCl solution. ◆ = paint + 1% SiC, and ■ = paint + 5% SiC.

hence the longer the time needed for the coating breakdown. Moreover, Figures 4.46 and 4.47 show that, for film coatings of the same thickness, the immersion time elapsed before the coating film breakdown occurs is longer for coatings containing 5 wt % SiC than that for coatings containing 1 wt % SiC.

4.3.10 Delaminated Area (A_d) Measurements

As mentioned before, delamination in coatings is the detachment of the coating film from a substrate surface due to the diffusion of water, ions, and dissolved oxygen through the coating when the coated substrate is exposed to aqueous solutions.[85] Delamination leads to loss of the adhesion and protective properties of the coating. The electrochemically active area beneath the coating is known as the area of delamination or delaminated area (A_d).[86-88] In the current investigation, $\%A_d$ values for all samples investigated were determined using Equation 3.4 and 3.5 (Chapter 3).

Figures 4.48 through 4.51 present the variation of $\%A_d$ with immersion time for SiC-incorporated paint coatings. As shown in the figures, the value of $\%A_d$ increases with increased immersion time indicating the absorption of water in the coatings. As shown in Figures 4.48 and 4.49, for very thin coatings (20 μm), the increase in the value of $\%A_d$ is very fast and the coatings failed in ≤ 40 d. On the other hand, for thick coatings (≥ 40 μm), after an initial increase, $\%A_d$ remains more or less constant for a period of time followed by a rapid increase that corresponds to the complete loss of adhesion and onset of blistering in the coating films. The longer the period in which the value of $\%A_d$ remains unchanged, the more stable the coating is. Accordingly, the data depicted in

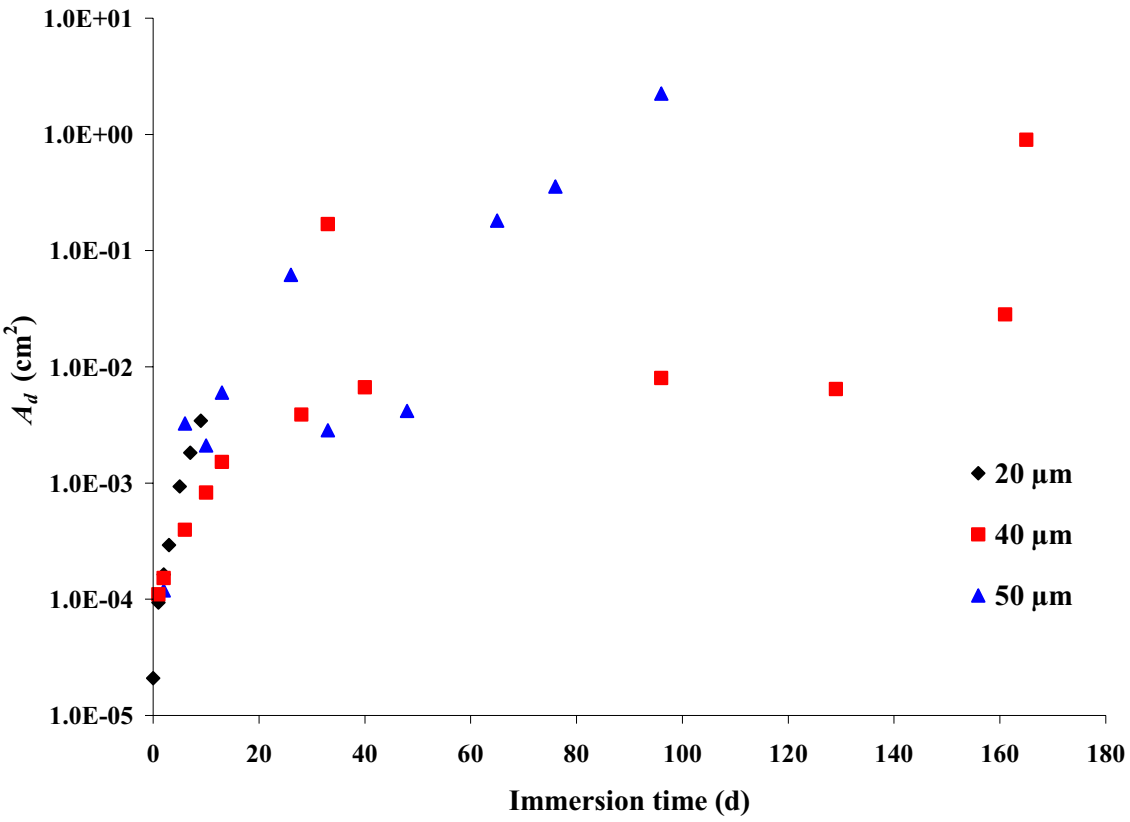

Figure 4.48 Variation of the percent delaminated area (%A_d) with immersion time for mild steel panels coated with a commercial alkyd paint film containing 1 wt % VGCNF and exposed to 3% NaCl solution. ◆ = 20 µm, ■ = 40 µm, and ▲ = 50 µm.

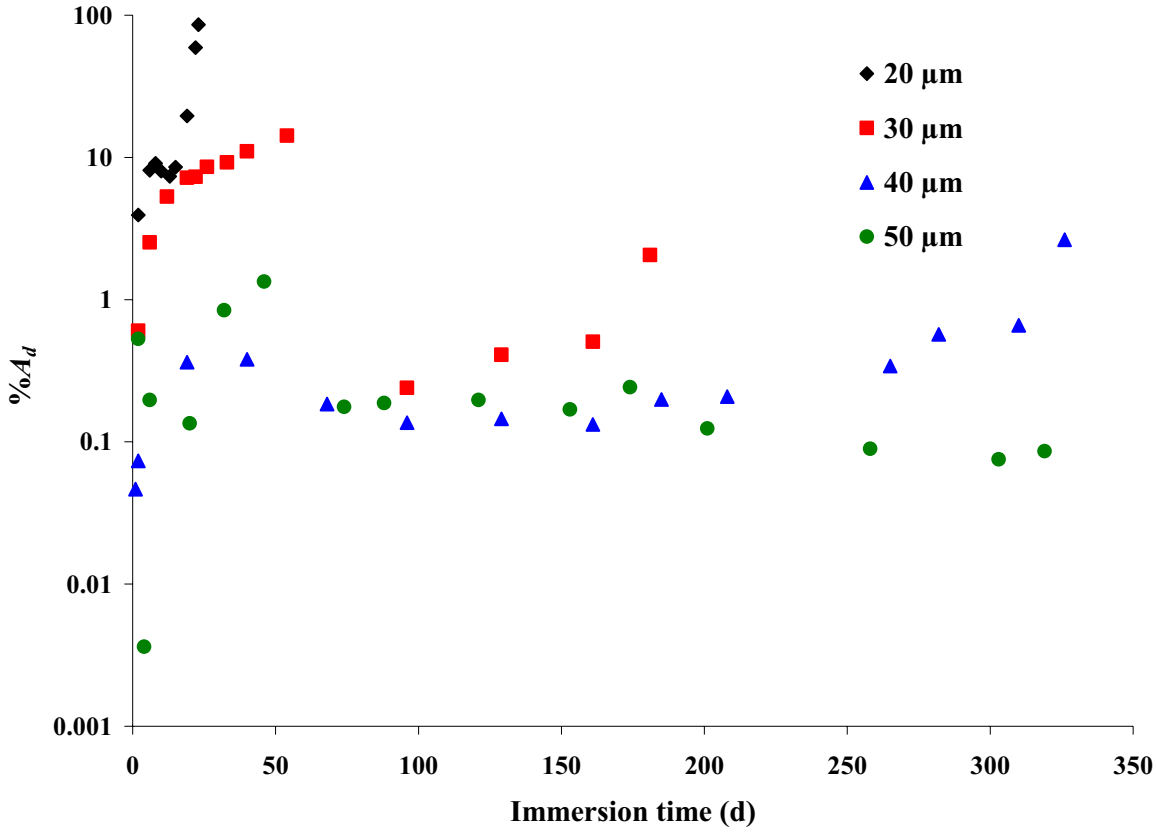

Figure 4.49 Variation of the percent delaminated area (%A_d) with immersion time for mild steel panels coated with a commercial alkyd paint film containing 5 wt % VGCNF and exposed to 3% NaCl solution. ■ = 20 µm, ◆ = 30 µm, ▲ = 40 µm, and ● = 50 µm.

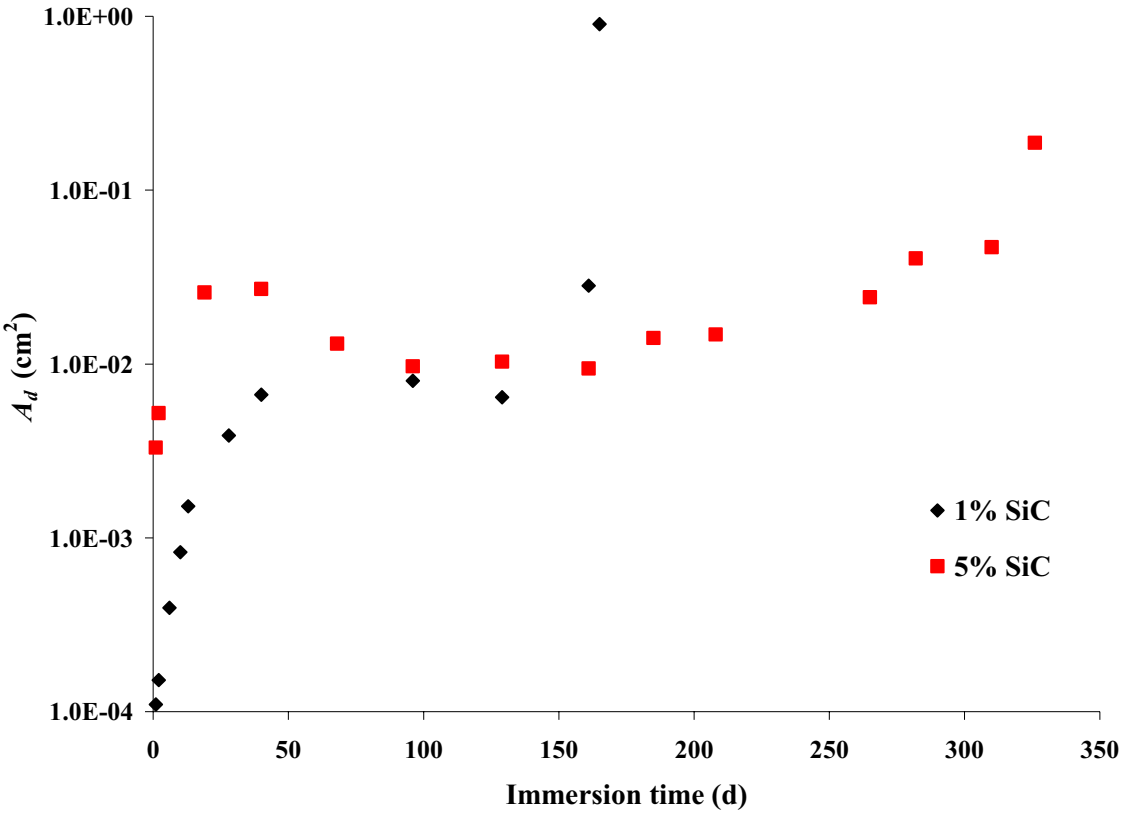

Figure 4.50 Variation of the percent delaminated area (%A_d) with immersion time for mild steel panels coated with a SiC-incorporated commercial alkyd paint film (40 μm thick) and exposed to 3% NaCl solution. ◆ = paint + 1% SiC, and ■ = paint + 5% SiC.

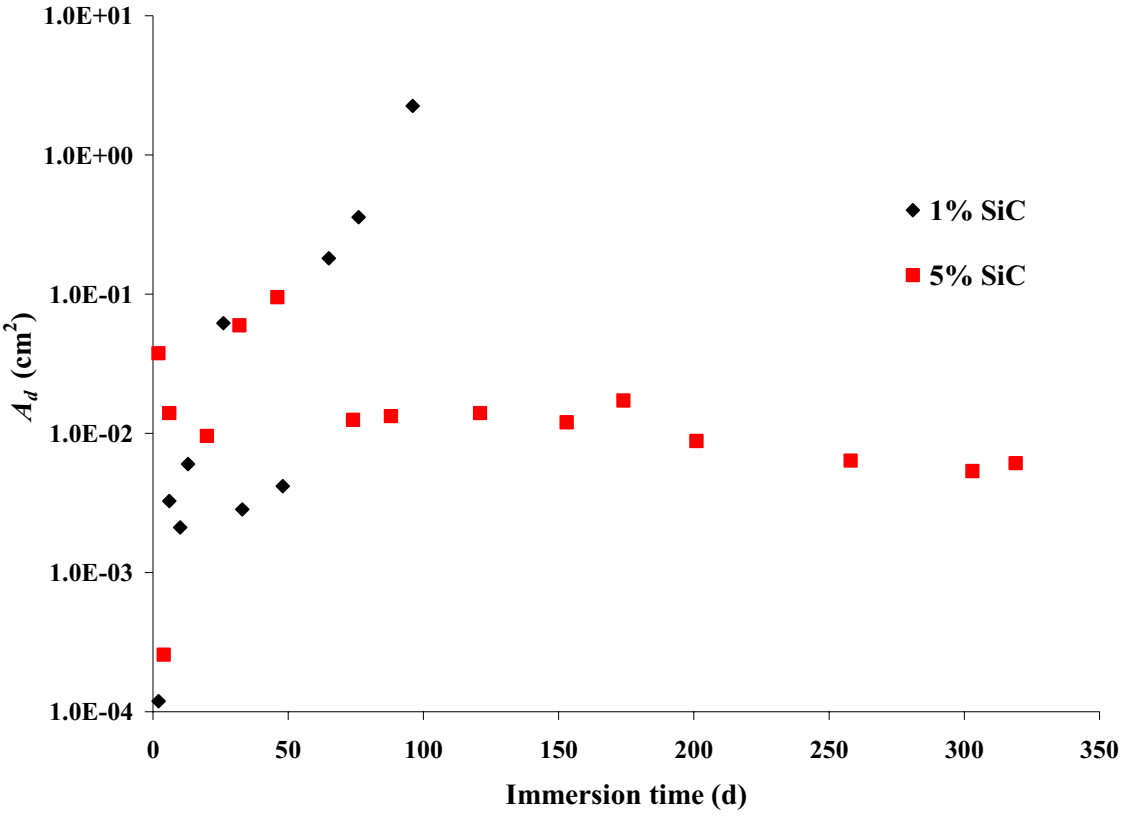

Figure 4.51 Variation of the percent delaminated area (%A_d) with immersion time for mild steel panels coated with a SiC-incorporated commercial alkyd paint film (50 μm thick) and exposed to 3% NaCl solution. ◆ = paint + 1% SiC, and ■ = paint + 5% SiC.

Figures 4.50 and 4.51 show that paint coatings containing 5 wt % SiC are more stable and have longer service lives than coatings containing 1 wt % SiC. These results are in accordance with the water uptake measurements (vide supra).

4.3.11 SiC Microparticles vs. VGCNFs

The main goal of the investigation in this chapter was to compare the effect of the SiC particles with that of VGCNF on the corrosion protection properties of the alkyd paint applied to the surface of mild steel substrates. Accordingly, the EIS behavior of alkyd paint coatings having the same thickness and wt % of either SiC or VGCNF was compared.

Figures 4.52 through 4.55 show a comparison between the EIS behavior (Bode and Nyquist plots) for mild steel samples coated with SiC- and VGCNF-reinforced paint coatings with the same coating thickness and loadings immersed in 3% NaCl solution. The Bode plots in Figures 4.52 through 4.55 show that paint coatings containing VGCNF have higher and stable LF $|Z|$ values than the corresponding coatings containing SiC. On the other hand, the Nyquist plots in Figures 4.52 through 4.55 show, for both SiC- and VGCNF-reinforced coatings, a capacitive semi-circle in the HF region and a diffusion tail in the LF region. As shown in the figures, the semi-circles for paint coatings containing VGCNF are much bigger than those for paint coatings containing SiC. The behavior shown in Figures 4.52 through 4.55, for at all immersion times, indicate that VGCNF-incorporated paint coatings are more stable and have better corrosion protection performance than SiC-incorporated coatings.

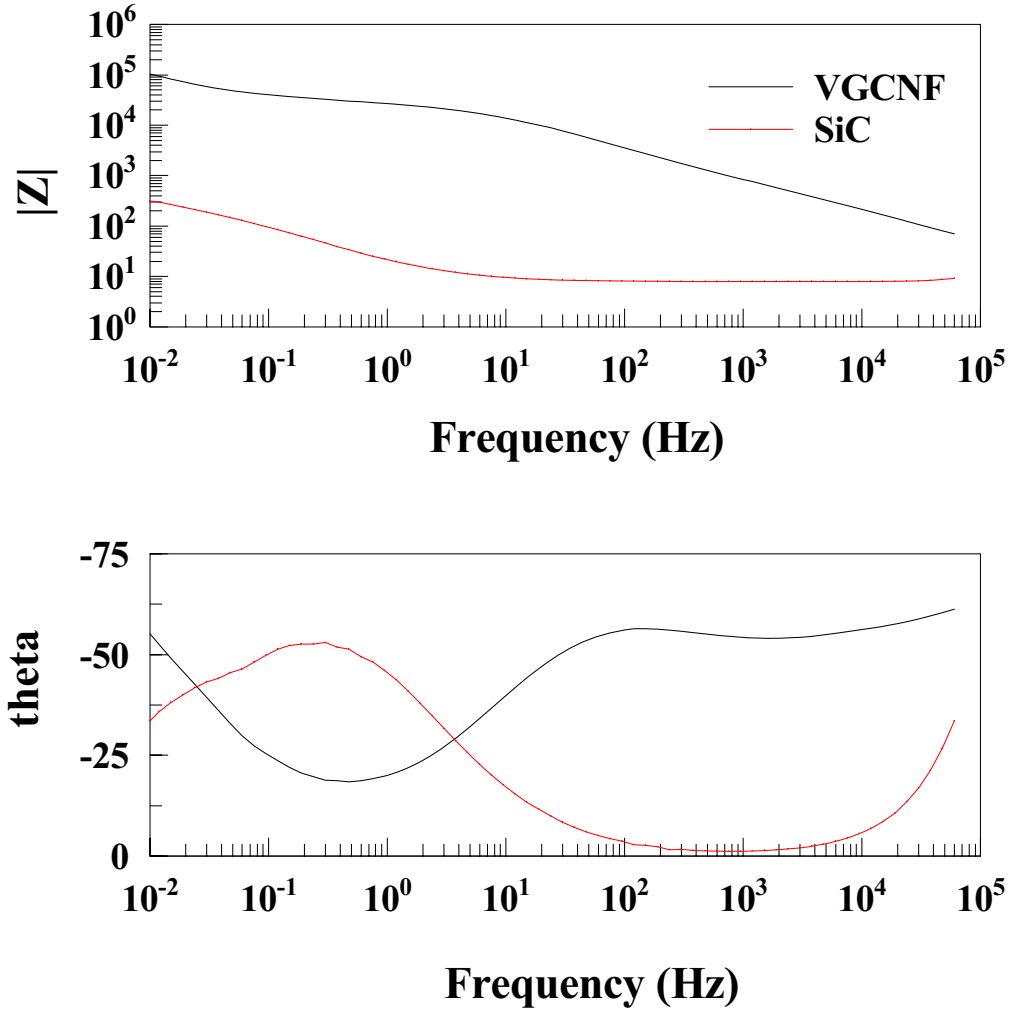

Figure 4.52 Bode (a) and Nyquist (b) plots for mild steel panels coated with 1 wt % VGCNF- and 1 wt % SiC-incorporated commercial alkyd paint film (20 μm thick) after 10 d of immersion in 3% NaCl solution. The coating specification is shown in the legend.

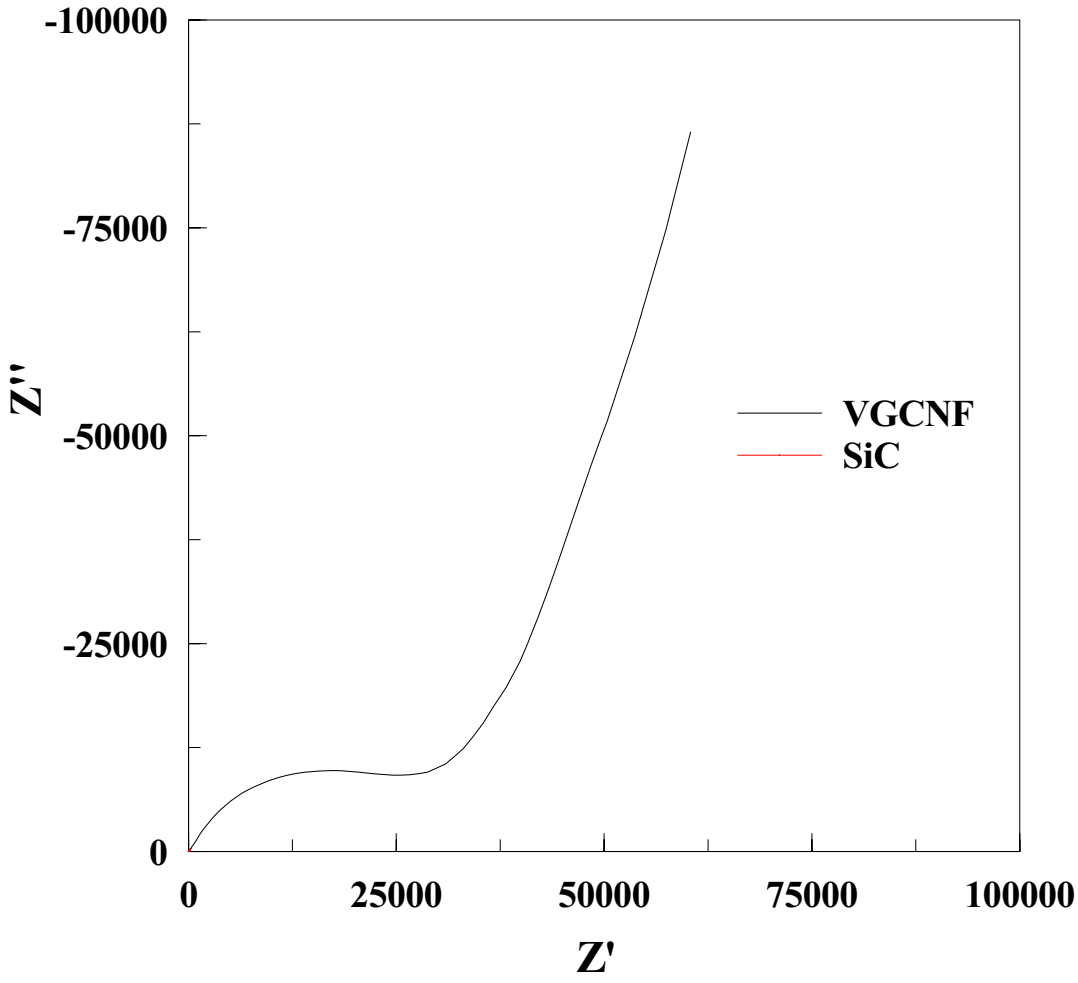

Figure 4.52 Continued.

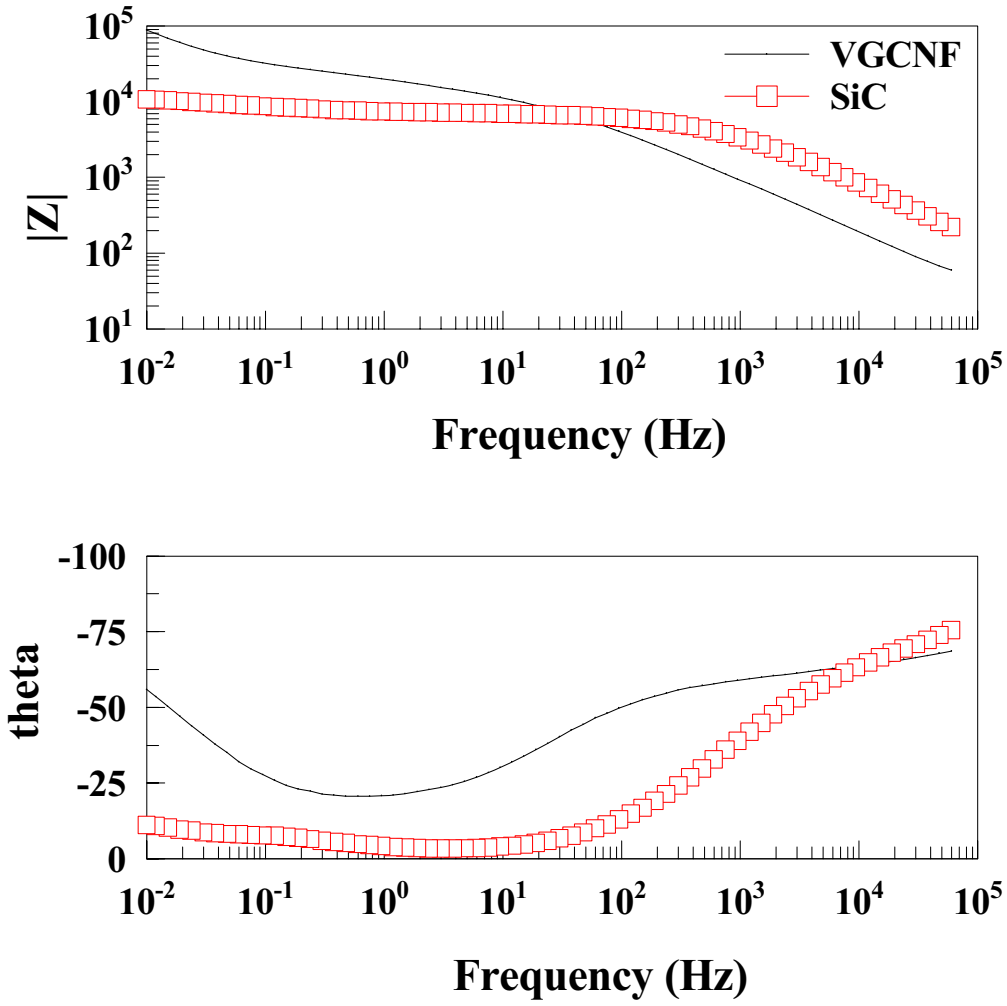

Figure 4.53 Bode (a) and Nyquist (b) plots for mild steel panels coated with 5 wt % VGCNF- and 5 wt % SiC-incorporated commercial alkyd paint film (20 μm thick) after 25 d of immersion in 3% NaCl solution. The coating specification is shown in the legend.

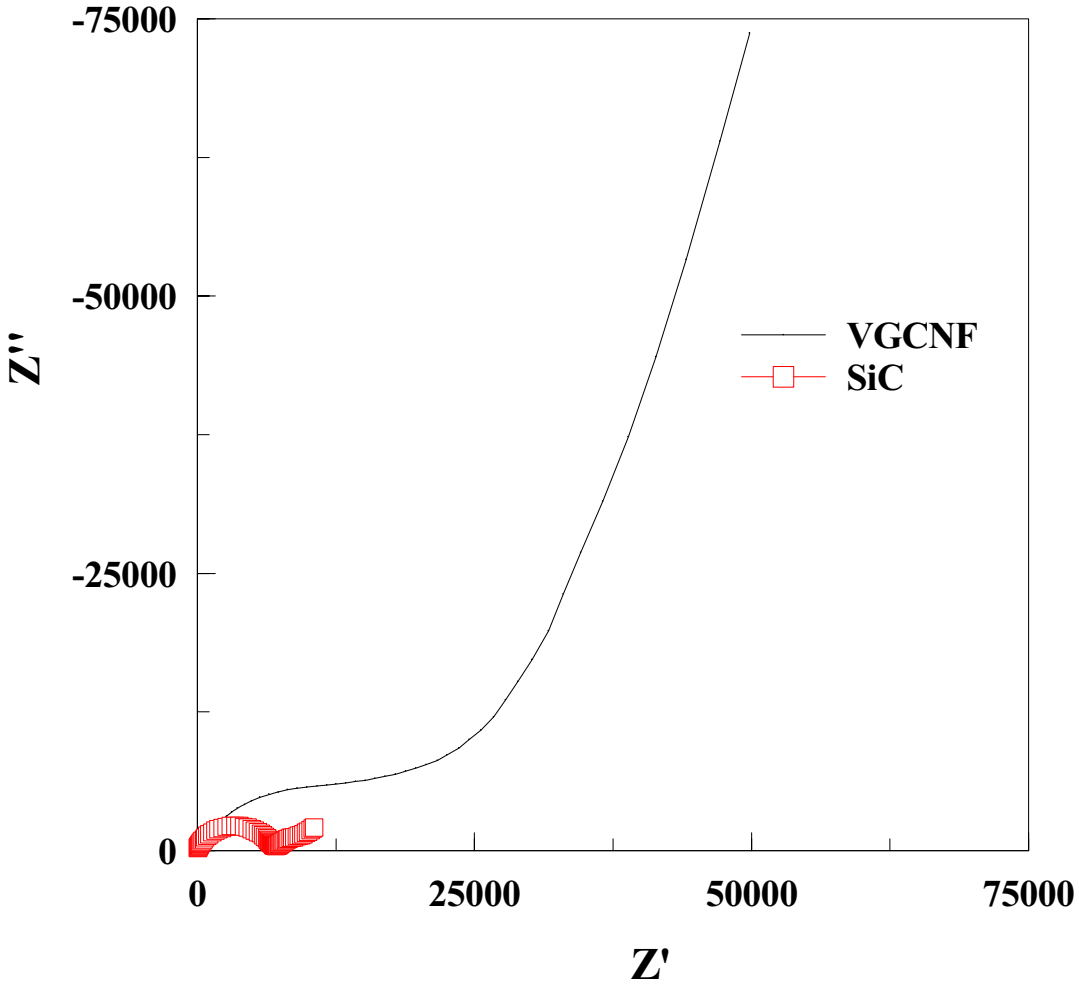

Figure 4.53 Continued.

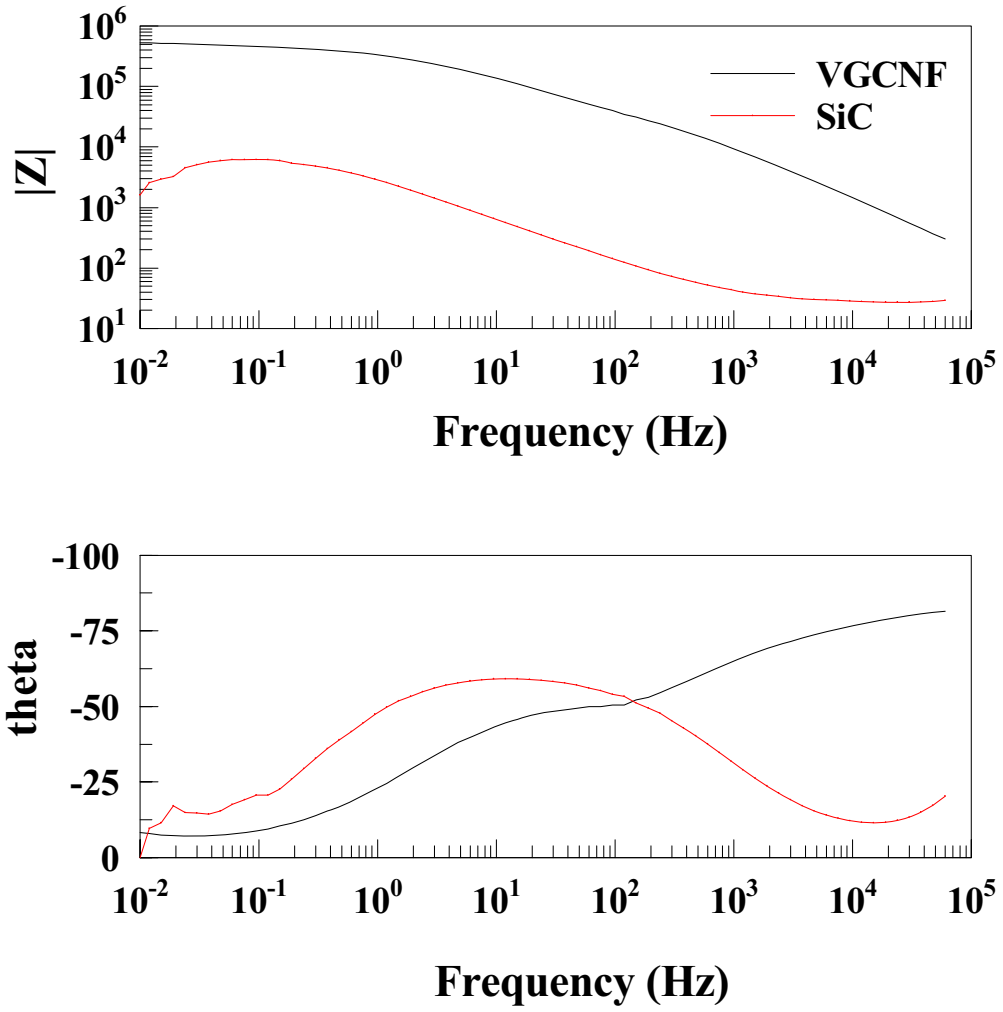

Figure 4.54 Bode (a) and Nyquist (b) plots for mild steel panels coated with 1 wt % VGCNF- and 1 wt % SiC-incorporated commercial alkyd paint film (50 μm thick) after 129 d of immersion in 3% NaCl solution. The coating specification is shown in the legend.

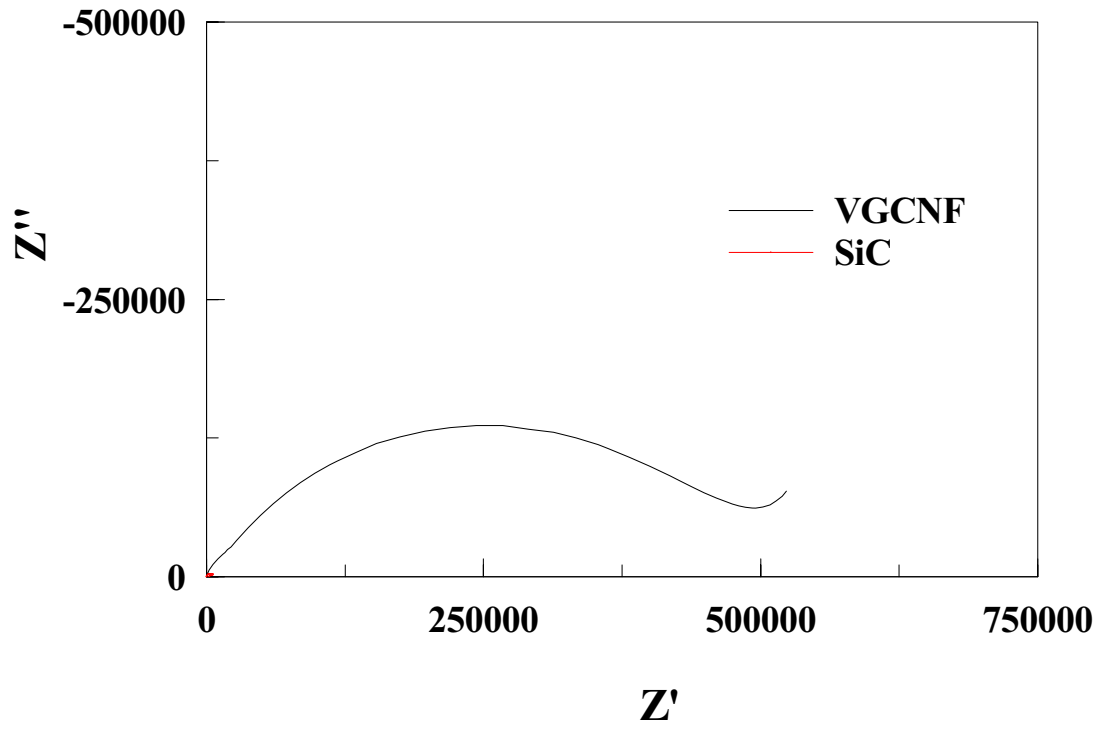

Figure 4.54 Continued.

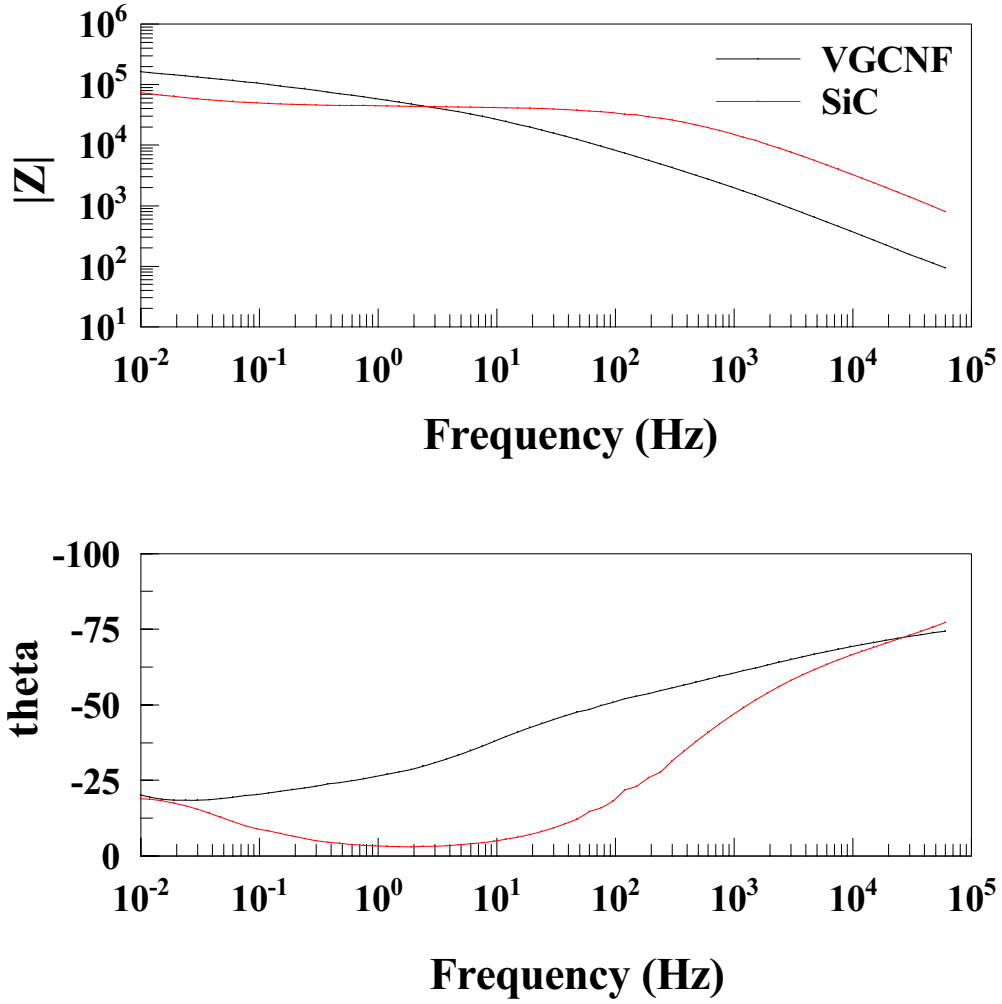

Figure 4.55 Bode (a) and Nyquist (b) plots for mild steel panels coated with 5 wt % SiC-, and 5 wt % VGCNF-incorporated commercial alkyd paint film (30 μm thick) after 50 d of immersion in 3% NaCl solution. The coating specification is shown in the legend.

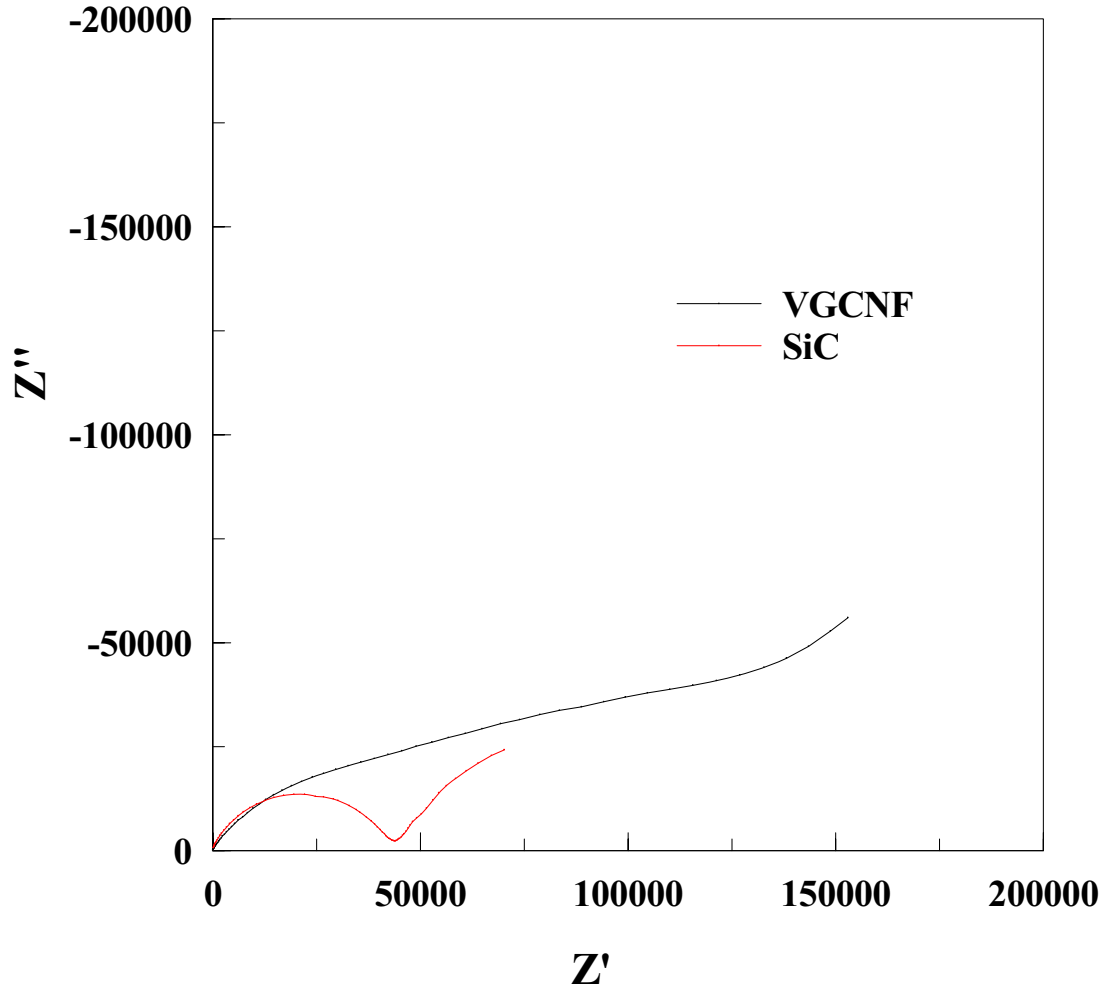

Figure 4.55 Continued.

In order to rank the coatings based on their anticorrosive properties, the OCP as well as the EIS behavior of 50 μm thick paint coatings containing 5 wt % of either SiC or VGCNF is compared with the behavior of pure paint having the same thickness is shown in Figures 4.56 through 4.62. Figure 4.56 shows the variation of the OCP with immersion time for the three coatings systems. As shown in the figure, the initial OCP for the pure paint coating is the most positive among the three coatings. However, it is clear that, among the three coating systems, the rate of decrease in the OCP is the highest and the steady-state potential (E_{ss}) of the bare steel alloy is reached in the shortest time for the pure paint coating (failed after 200 d) indicating poor anticorrosive properties for the pure coating. On the other hand, after 650 d of immersion, the OCP of VGCNF-incorporated coating is still positive (~ +0.1 V), thus reflecting the higher stability of the coating. It is also evident that the SiC-incorporated coating is more stable than the pure paint but less stable than the VGCNF-incorporated coating.

The Bode plots in Figures 4.57 and 4.58 show that paint coatings containing VGCNF have the highest initial LF $|Z|$ values among the three coatings. In addition, the Nyquist plots in the figures show that the capacitive semi-circles for VGCNF-incorporated coatings are the largest in size among the three coatings indicating the higher stability of the VGCNF-reinforced coatings.

Figures 4.59 through 4.62 show the variation of some of the corrosion parameters ($|Z|$, R_p, R_c, and A_d, respectively) for the three coating systems with immersion time for the three coatings. As shown in these figures, the VGCNF-incorporated coating shows the longest period of stable performance while immersed in the corrosive electrolyte. In

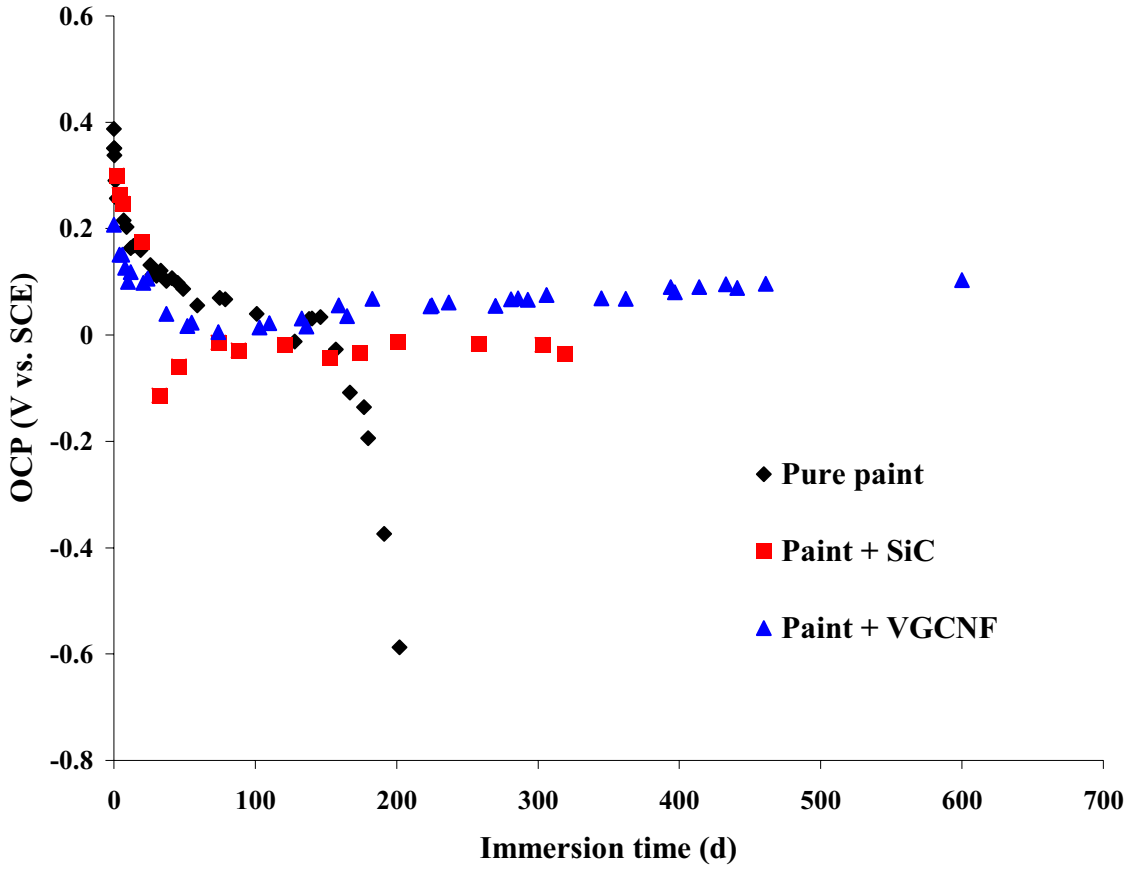

Figure 4.56 Long term OCP-immersion time curves for mild steel panels coated with pure, 5 wt % SiC-, and 5 wt % VGCNF-incorporated commercial alkyd paint film (50 μm thick) and exposed to 3% NaCl solution. ◆ = pure paint, ■ = paint + SiC, and ▲ = paint + VGCNF.

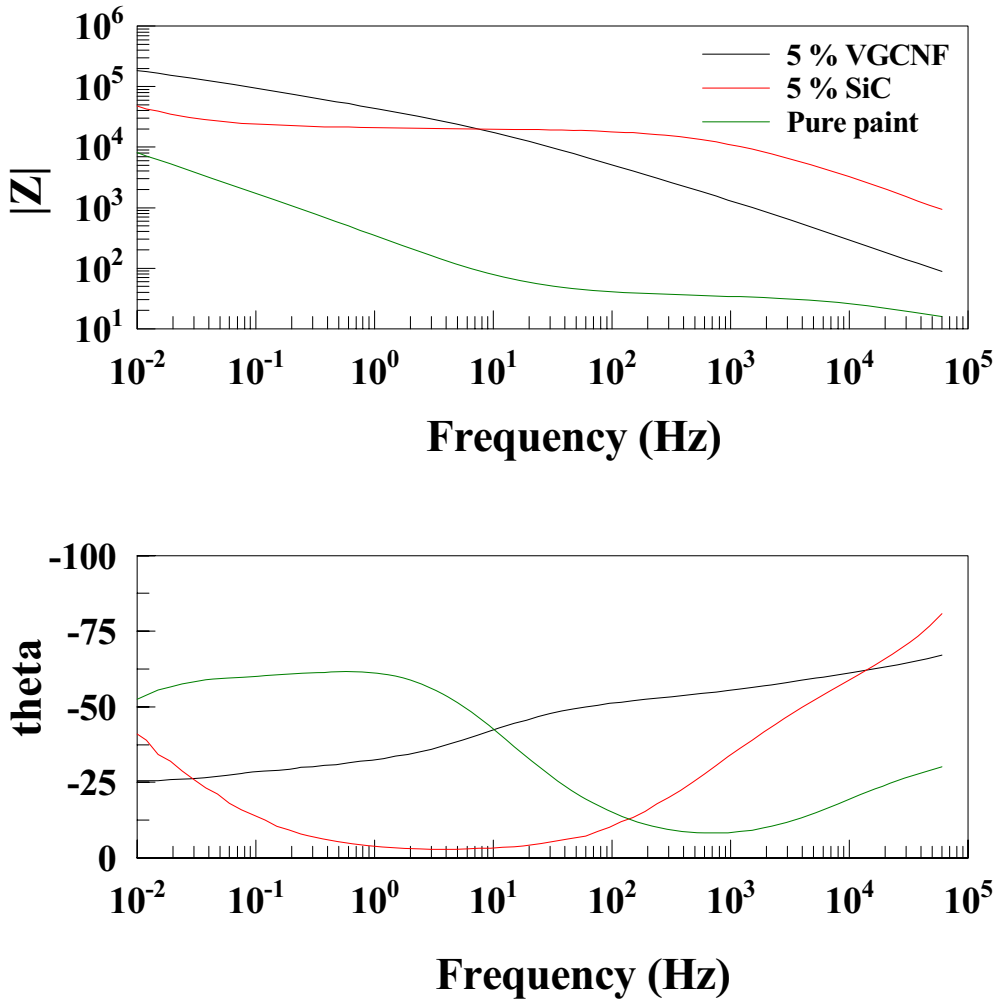

Figure 4.57 Bode (a) and Nyquist (b) plots for mild steel panels coated with pure, 5 wt % SiC-, and 5 wt % VGCNF-incorporated commercial alkyd paint film (30 μm thick) after 30 d of immersion in 3% NaCl solution. The coatings specifications are shown in the legend.

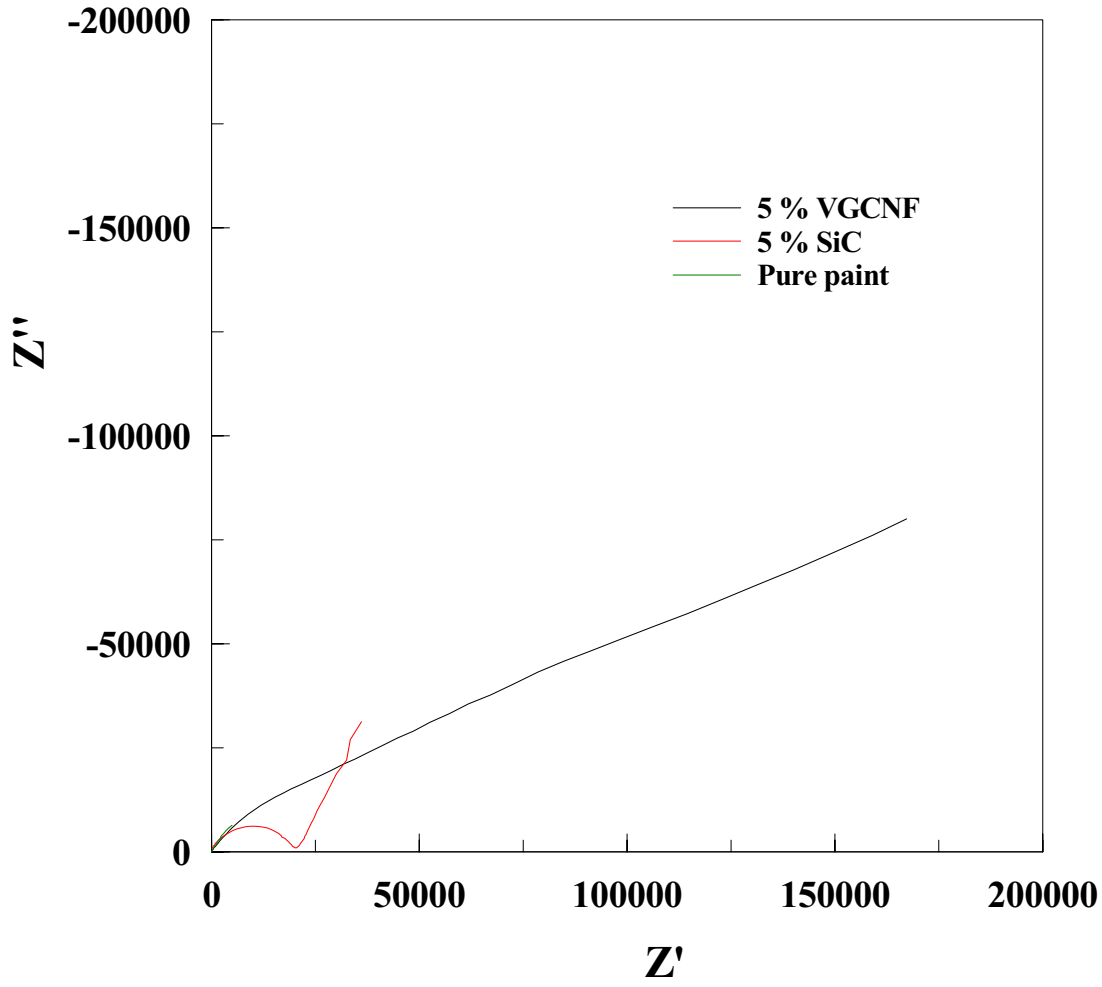

Figure 4.57 Continued.

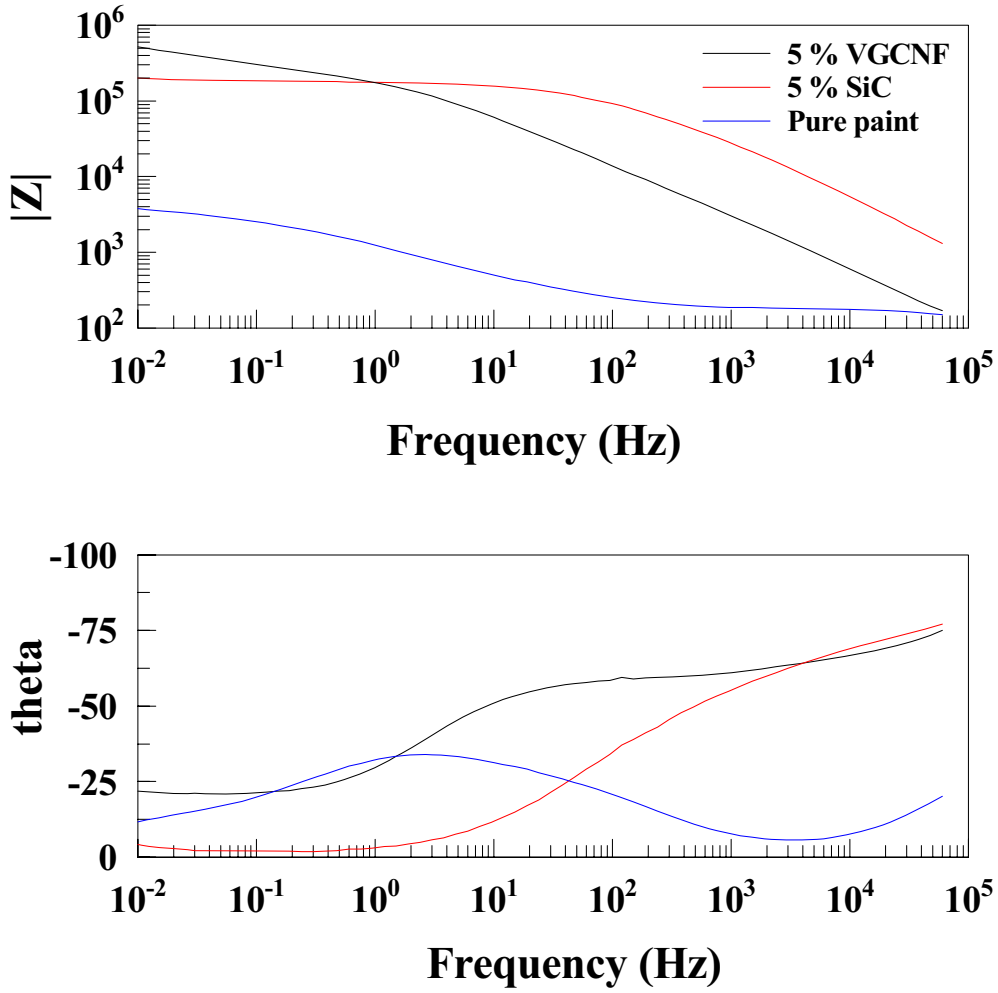

Figure 4.58 Bode (a) and Nyquist (b) plots for mild steel panels coated with pure, 5 wt % SiC-, and 5 wt % VGCNF-incorporated commercial alkyd paint film (50 μm thick) after 200 d of immersion in 3% NaCl solution. The coatings specifications are shown in the legend.

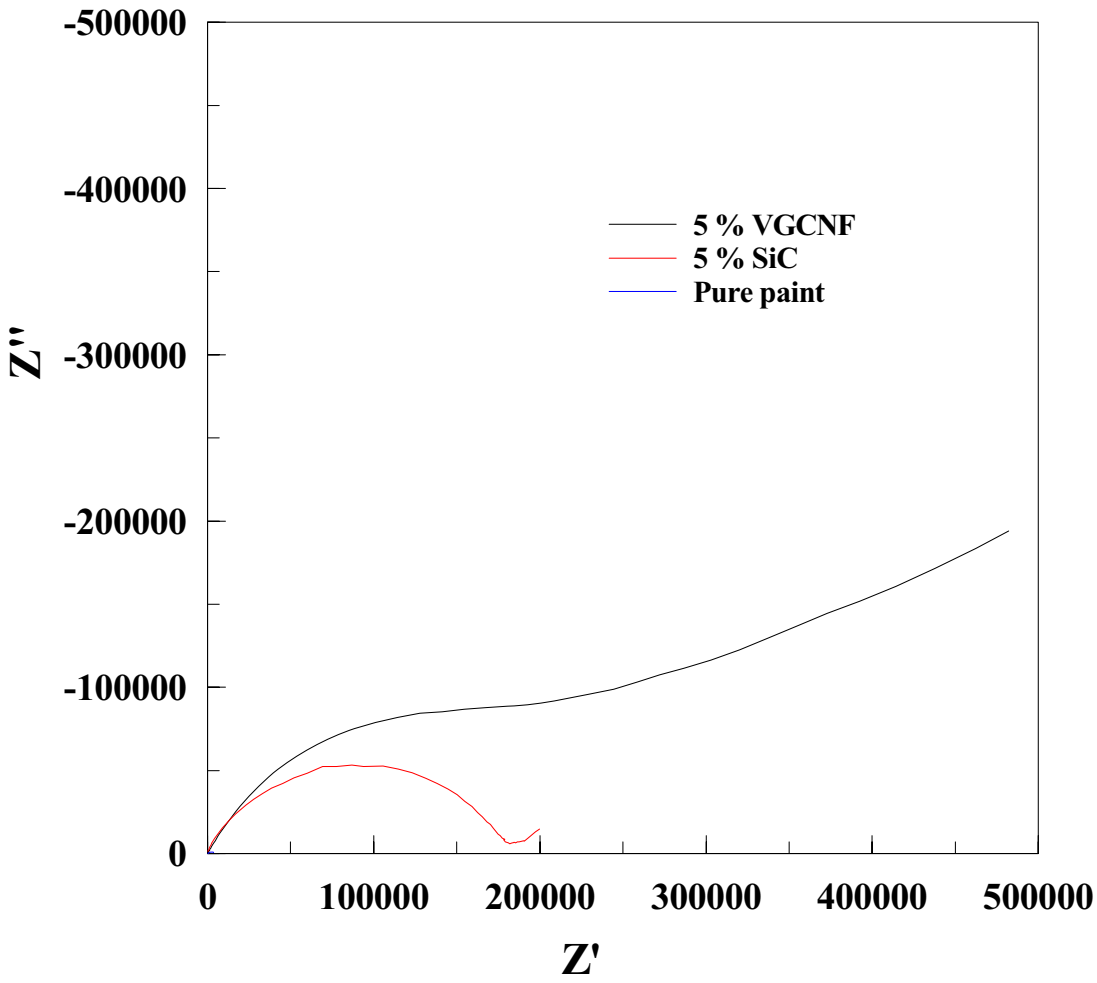

Figure 4.58 Continued.

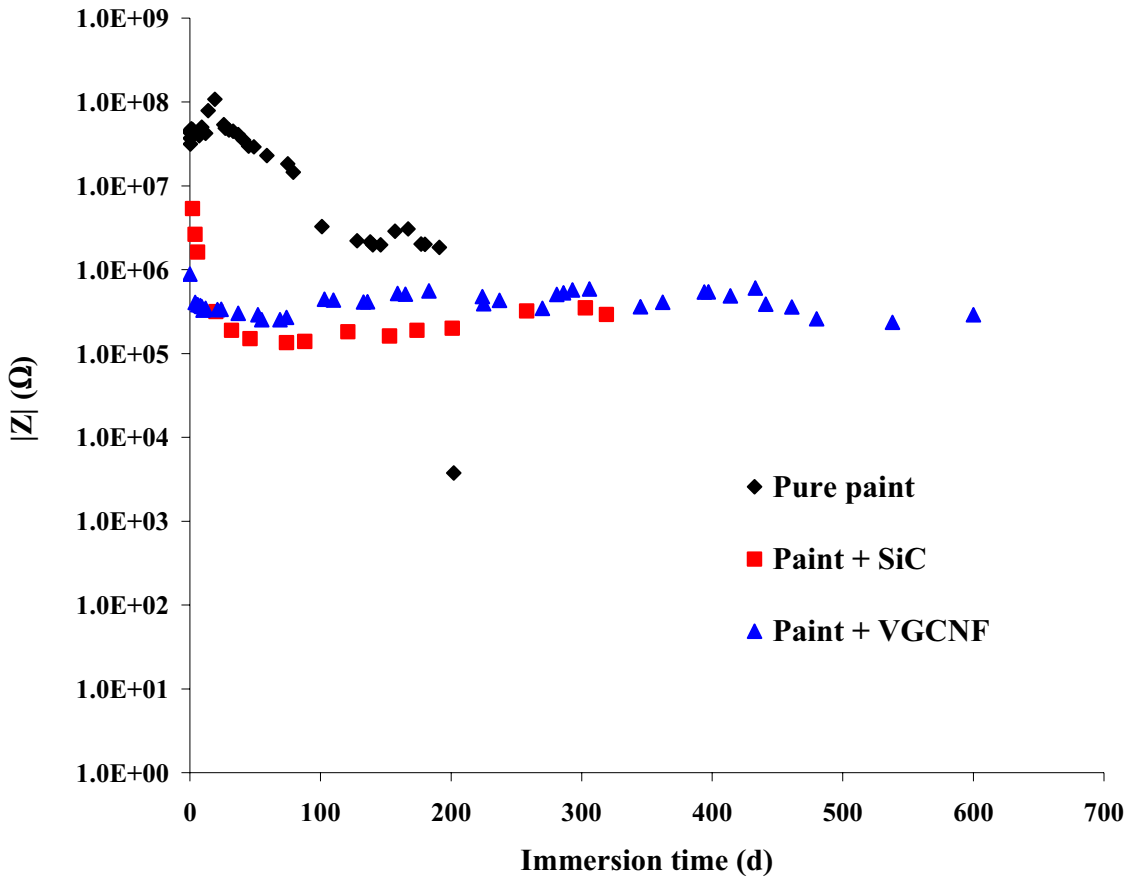

Figure 4.59 Variation of the absolute impedance (|*Z*|), measured at 1.0×10^{-2} Hz, with immersion time for mild steel panels coated with pure, 5 wt % SiC-, and 5 wt % VGCNF-incorporated commercial alkyd paint film (50 μm thick) and exposed to 3% NaCl solution. ◆ = pure paint, ■ = paint + SiC, and ▲ = paint + VGCNF.

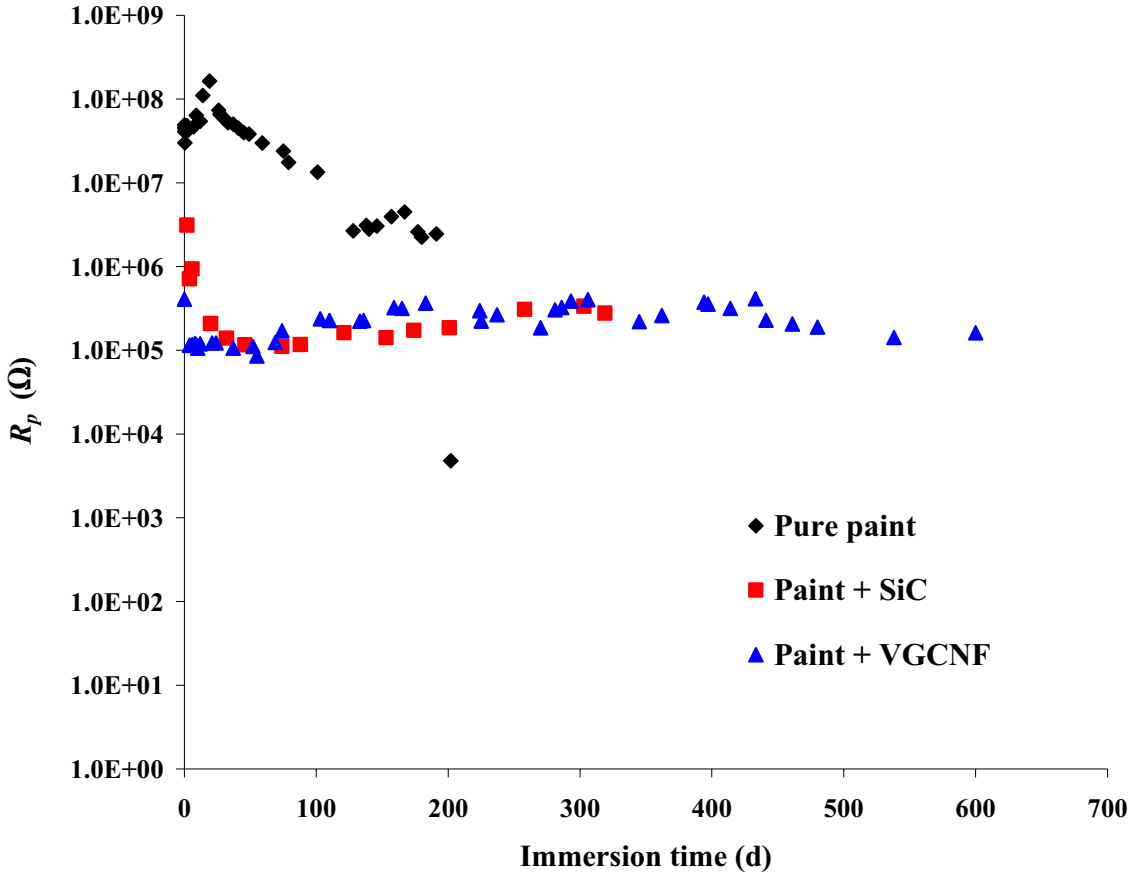

Figure 4.60 Variation of the polarization resistance (R_p) with immersion time for mild steel panels coated with pure, 5 wt % SiC-, and 5 wt % VGCNF-incorporated commercial alkyd paint film (50 μm thick) and exposed to 3% NaCl solution. ◆ = pure paint, ■ = paint + SiC, and ▲ = paint + VGCNF.

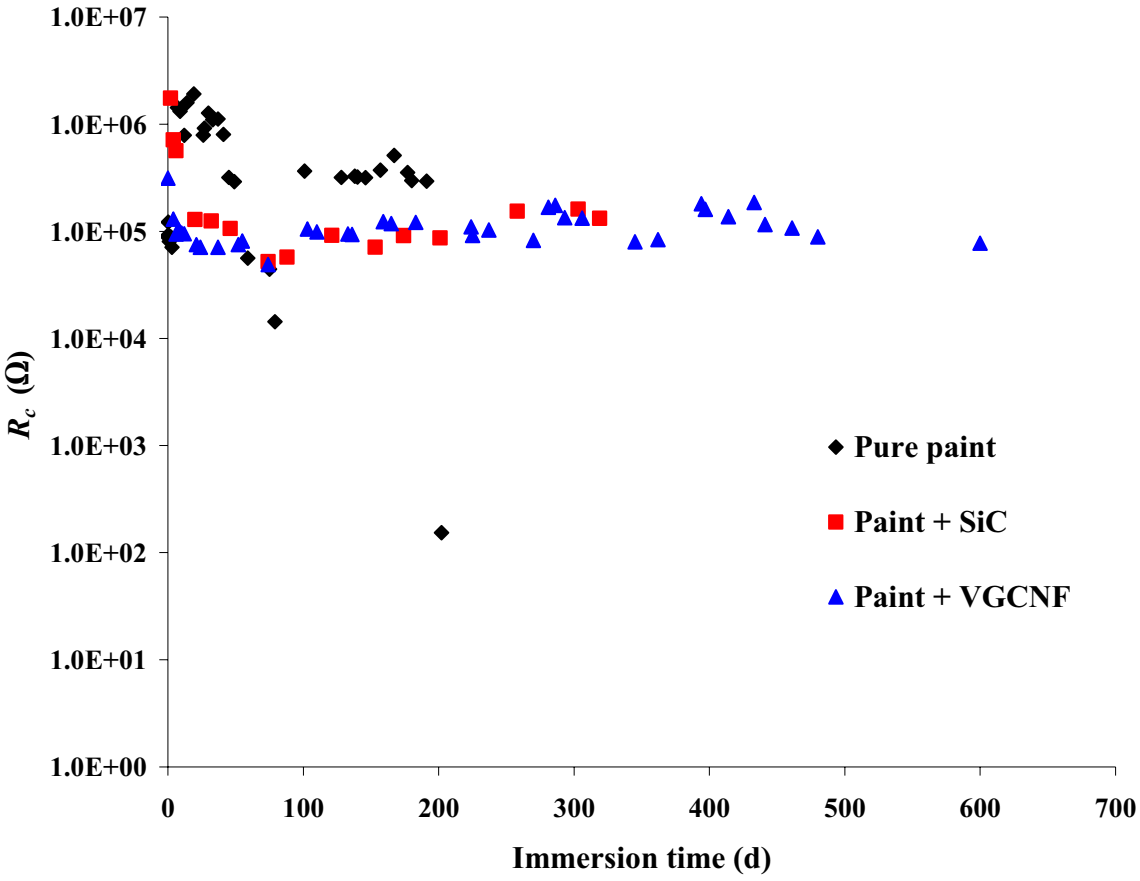

Figure 4.61 Variation of the coating resistance (R_c) with immersion time for mild steel panels coated with pure, 5 wt % SiC-, and 5 wt % VGCNF-incorporated commercial alkyd paint film (50 μm thick) and exposed to 3% NaCl solution. ◆ = pure paint, ■ = paint + SiC, and ▲ = paint + VGCNF.

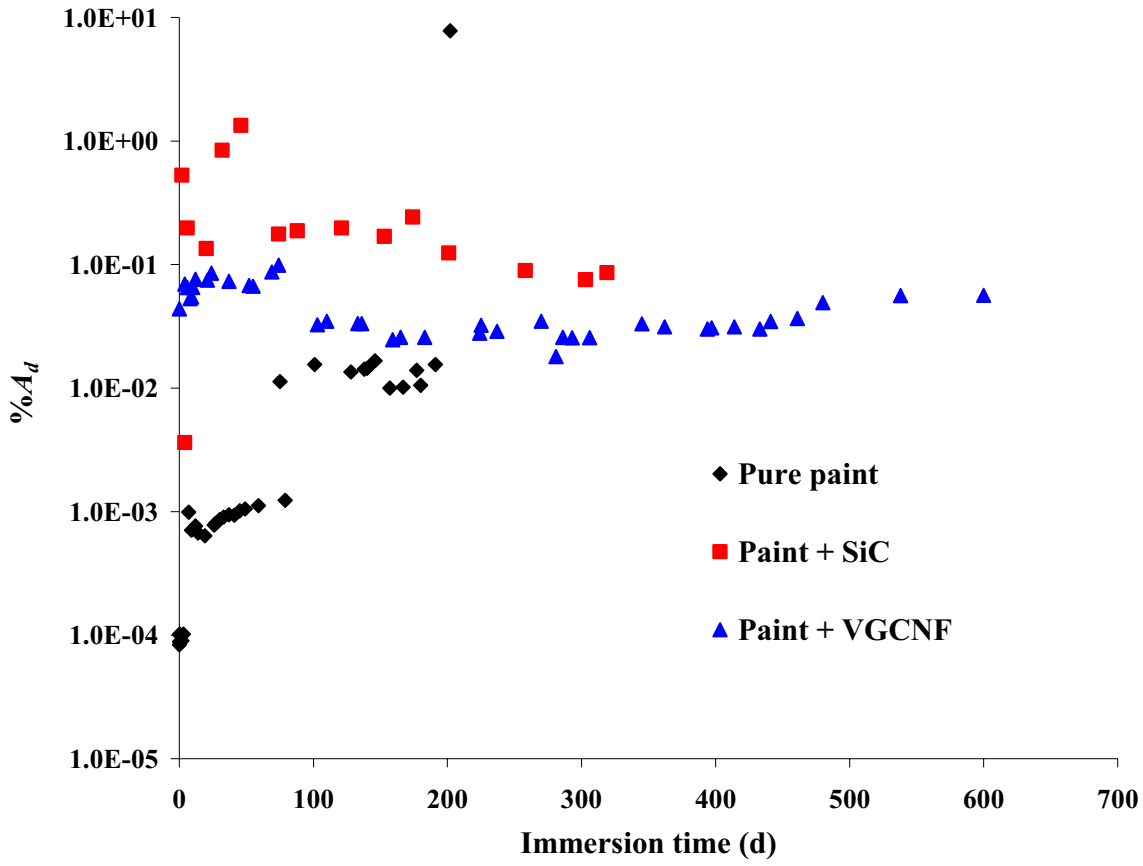

Figure 4.62 Variation of the percent delaminated area (%A_d) with immersion time for mild steel panels coated with pure, 5 wt % SiC-, and 5 wt % VGCNF-incorporated commercial alkyd paint film (50 μm thick) and exposed to 3% NaCl solution. ◆ = pure paint, ■ = paint + SiC, and ▲ = paint + VGCNF.

conclusion, Figures 4.52 through 4.62 collectively show that the incorporation of SiC or VGCNF improves the insulating properties of the pure paint. In addition, it is evident that VGCNF is a better additive and produces superior corrosion protection properties and hence lower corrosion rates relative to the SiC particles.

4.4 Conclusions

In this chapter, the OCP and the EIS behavior of mild steel coupons coated with a commercial alkyd paint containing 1 and 5 wt % of SiC with different film thicknesses in 3% NaCl solution was investigated. The results showed that the incorporation of the SiC in the alkyd paint matrix enhances the anticorrosive properties imparted by the coating. However, compared to VGCNF-reinforced coatings with the same loading and thickness, the results showed that SiC-incorporated coatings are inferior with lower barrier properties and higher corrosion rates.

4.4 References

(1) Pensl, G.; Ciobanu, F.; Frank, T.; Krieger, M.; Reshanov, S.; Schmid, F.; Weidner, M. *International Journal of High Speed Electronics and Systems* **2005**, *15*, 705-745.

(2) Zhao, J. H. *MRS Bulletin* **2005**, *30*, 293-298.

(3) Rea, L. S. *International SAMPE Symposium and Exhibition* **2003**, *48*, 62-69.

(4) Cadady, J. B.; Johnson, R. W. *Solid-State Electronics* **1996**, *39*, 1409-1422.

(5) Carter, C. H., Jr.; Edmond, J. A.; Palmour, J. W. *International SAMPE Electronics Conference* **1994**, *7*, 8-17.

(6) Morkoc, H.; Strite, S.; Gao, G. B.; Lin, M. E.; Sverdlov, B.; Burns, M. *Journal of Applied Physics* **1994**, *76*, 1363-1398.

(7) Feitknecht, J. *Springer Tracts in Modern Physics* **1971**, *58*, 48-118.

(8) Ptnaik, P. *Handbook of Inorganic Chemicals*; McGraw-Hill Professional: New York, 2002.

(9) Saddow, S. E.; Cordina, O. In *Advances in Silicon Carbide Processing and Applications*; Saddow, S. E., Agarwal, A., Eds.; Artech House, Inc.: Norwood, MA, 2004, pp 1-28.

(10) Dong, J.; Chen, A. B. *Springer Series in Materials Science* **2004**, *73*, 63-87.

(11) Lambrecht, W. R. L.; Albanesi, E. A.; Segall, B. *Institute of Physics Conference Series* **1994**, *137*, 457-460.

(12) Pensl, G.; Choyke, W. J. *Physica B: Condensed Matter* **1993**, *185*, 264-283.

(13) Helbig, R. *Physica Scripta, T* **1991**, *T35*, 194-200.

(14) Vashishath, M.; Chatterjee, A. K. *Maejo International Journal of Science and Technology* **2008**, *2*, 444-470.

(15) Tan, L.; Allen, T. R.; Barringer, E. *Journal of Nuclear Materials* **2009**, *394*, 95-101.

(16) Zacharias, P. *Materials Science Forum* **2009**, *615-617*, 889-894.

(17) Park, Y.-H.; Hinoki, T.; Kohyama, A. *Journal of Nuclear Materials* **2009**, *386-388*, 1014-1017.

(18) Henager, C. H.; Shin, Y.; Blum, Y.; Giannuzzi, L. A.; Kempshall, B. W.; Schwarz, S. M. *Journal of Nuclear Materials* **2007**, *367-370*, 1139-1143.

(19) Agarwal, A.; Burk, A.; Callanan, R.; Capell, C.; Das, M.; Haney, S.; Hull, B.; Jonas, C.; O'Loughlin, M.; O'Neil, M.; Palmour, J.; Powell, A.; Richmond, J.; Ryu, S.-H.; Stahlbush, R.; Sumakeris, J.; Zhang, J. *Materials Science Forum* **2009**, *600-603*, 895-900.

(20) Johnson, C. M. *International Journal of Electronics* **2003**, *90*, 667-693.

(21) Sriram, S.; Siergiej, R. R.; Clarke, R. C.; Agarwal, A. K.; Brandt, C. D. *Physica Status Solidi A: Applied Research* **1997**, *162*, 441-457.

(22) Kellerman, D.; Begeau, J.; Huang, Q.; Ono, K. *Proceedings of SPIE-The International Society for Optical Engineering* **1995**, *2649*, 72-76.

(23) Jiang, L.; Cheung, R. *International Journal of Computational Materials Science and Surface Engineering* **2009**, *2*, 227-242.

(24) Henry, A.; Janzen, E.; Mastropaolo, E.; Cheung, R. *Materials Science Forum* **2009**, *615-617*, 625-628.

(25) Foerster, C.; Cimalla, V.; Brueckner, K.; Hein, M.; Pezoldt, J.; Ambacher, O. *Materials Science & Engineering, C: Biomimetic and Supramolecular Systems* **2005**, *C25*, 804-808.

(26) Dunning, J.; Fu, X. A.; Rajgopal, S.; Mehregany, M.; Zorman, C. A. *Materials Science Forum* **2004**, *457-460*, 1523-1526.

(27) Zorman, C. A.; Mehregany, M. *Materials Science Forum* **2004**, *457-460*, 1451-1456.

(28) Lopin, A. V.; Semenov, A. V.; Puzikov, V. M.; Trushkovsky, A. G.*:Functional Materials* **2006**, *13*, 631-636.

(29) Ulph, E. *Proceedings of SPIE-The International Society for Optical Engineering* **1989**, *966*, 116-121.

(30) Kelner, G.; Shur, M. *EMIS Datareviews Series* **1995**, *13*, 270-272.

(31) Badila, M.; Brezeanu, G.; Millan, J.; Godignon, P.; Locatelli, M. L.; Chante, J. P.; Lebedev, A.; Lungu, P.; Dinca, G.; Banu, V.; Banoiu, G. *Diamond and Related Materials* **2000**, *9*, 994-997.

(32) Chinthavali, M.; Ozpineci, B.; Tolbert, L. M.; Zhang, H. *Materials Science Forum* **2009**, *600-603*, 1239-1242.

(33) Natarajan, N.; Vijayarangan, S.; Rajendran, I. *Science and Engineering of Composite Materials* **2008**, *15*, 21-30.

(34) Martinez, J. L., Jr.; Fusaro, J. M.; Romero, G. L.; Humbert, D.; Hooser, D. *International SAMPE Symposium and Exhibition* **1996**, *41*, 1417-1426.

(35) Hooker, J. A.; Doorbar, P. J. *Materials Science and Technology* **2000**, *16*, 725-731.

(36) Weiss, D.; Chamberlain, B.; Bruski, R. *Engineered Casting Solutions* **2001**, *3*, 38-40.

(37) Rajan, T. P. D.; Pillai, R. M.; Pai, B. C. *Journal of Materials Science* **1998**, *33*, 3491-3503.

(38) Stott, F. H.; Ashby, D. J. *Corrosion Science* **1978**, *18*, 183-198.

(39) Greene, H. J.; Mansfeld, F. *Corrosion* **1997**, *53*, 920-927.

(40) Chen, C.; Mansfeld, F. *Corrosion Science* **1997**, *39*, 1075-1082.

(41) Gladkovas, M.; Medeliene, V.; Samuleviciene, M.; Juzeliunas, E. *Chemija* **2002**, *13*, 36-40.

(42) Palanikumar, K.; Karthikeyan, R. *Multidiscipline Modeling in Materials and Structures* **2008**, *4*, 345-358.

(43) Brendel, A.; Paffenholz, V.; Koeck, T.; Bolt, H. *Journal of Nuclear Materials* **2009**, *386-388*, 837-840.

(44) Yu, E.; Sun, J.-Y.; Chung, H.-S.; Oh, K. H. *International Journal of Modern Physics B* **2008**, *22*, 6167-6172.

(45) Bhat, M. S. N.; Surappa, M. K.; Nayak, H. V. S. *Journal of Materials Science* **1991**, *26*, 4991-4996.

(46) Sun, H.; Koo, E. Y.; Wheat, H. G. *Corrosion* **1991**, *47*, 741-753.

(47) Ozben, T.; Kilickap, E.; Cakir, O. *Journal of Materials Processing Technology* **2008**, *198*, 220-225.

(48) Chawla, N. *Advanced Materials & Processes* **2006**, *164*, 29-31.

(49) Hou, K. H.; Ger, M. D.; Wang, L. M.; Ke, S. T. *Wear* **2002**, *253*, 994-1003.

(50) Garcia, I.; Fransaer, J.; Celis, J. P. *Surface and Coatings Technology* **2001**, *148*, 171-178.

(51) Lewinsohn, C. A.; Singh, M.; Henager, C. H., Jr. *Ceramic Transactions* **2003**, *138*, 201-208.

(52) Mansfeld, F. *Electrochimica Acta* **1990**, *35*, 1533-1544.

(53) Simpson, T. C.; Moran, P. J.; Hampel, H.; Davis, G. D.; Shaw, B. A.; Arah, C. O.; Fritz, T. L.; Zankel, K. L. *ASTM Special Technical Publication* **1990**, *1000*, 397-412.

(54) Mansfeld, F. In *Analytical Methods in Corrosion Science and Engineering*; Marcus, P., Mansfeld, F., Eds.; CRC Press: Boca Raton, FL, 2006, pp 463-505.

(55) Orazem, M. E.; Tribollet, B. *Electrochemical Impedance Spectroscopy*; John Wiley & Sons, Inc.: Hoboken, NJ, 2008.

(56) Lasia, A. *Modern Aspects of Electrochemistry* **1999**, *32*, 143-248.

(57) Vogelsang, J.; Strunz, W. *Materials and Corrosion* **2001**, *52*, 462-469.

(58) Loveday, D.; Peterson, P.; Rodgers, B. *Journal of Coatings Technology* **2004**, *1*, 88-93.

(59) Loveday, D.; Peterson, P.; Rodgers, B. *Journal of Coatings Technology* **2004**, *1*, 46-52.

(60) Aslanyan, I. R.; Bonino, J. P.; Celis, J. P. *Surface and Coatings Technology* **2006**, *200*, 2909-2916.

(61) Dikici, B.; Tekmen, C.; Yigit, O.; Gavgali, M.; Cocen, U. *Corrosion Science* **2009**, *51*, 469-476.

(62) Surviliene, S.; Cesuniene, A.; Jasulaitiene, V.; Bucinskiene, D. *Transactions of the Institute of Metal Finishing* **2008**, *86*, 308-314.

(63) Surviliene, S.; Lisowska-Oleksiak, A.; Jasulaitiene, V.; Cesuniene, A. *Transactions of the Institute of Metal Finishing* **2005**, *83*, 130-136.

(64) Pardo, A.; Merino, M. C.; Mohedano, M.; Casajus, P.; Coy, A. E.; Arrabal, R. *Surface and Coatings Technology* **2009**, *203*, 1252-1263.

(65) Pardo, A.; Merino, M. C.; Viejo, F.; Feliu, S., Jr.; Carboneras, M.; Arrabal, R. *Journal of the Electrochemical Society* **2005**, *152*, B198-B204.

(66) Pardo, A.; Merino, S.; Merino, M. C.; Barroso, I.; Mohedano, M.; Arrabal, R.; Viejo, F. *Corrosion Science* **2009**, *51*, 841-849.

(67) Malfatti, C. F.; Zoppas Ferreira, J.; Santos, C. B.; Souza, B. V.; Fallavena, E. P.; Vaillant, S.; Bonino, J. P. *Corrosion Science* **2005**, *47*, 567-580.

(68) Chaudhari, S.; Patil, P. P. *Journal of Applied Polymer Science* **2007**, *106*, 400-410.

(69) Liu, J.; Gong, G.; Yan, C. *Electrochimica Acta* **2005**, *50*, 3320-3332.

(70) Deflorian, F.; Fedrizzi, L. *Journal of Adhesion Science and Technology* **1999**, *13*, 629-645.

(71) Bonnel, K.; Le Pen, C.; Pebere, N. *Electrochimica Acta* **1999**, *44*, 4259-4267.

(72) Kendig, M. W.; Jeanjaquet, S.; Lumsden, J. *ASTM Special Technical Publication* **1993**, *STP 1188*, 407-427.

(73) Scully, J. R. *Journal of the Electrochemical Society* **1989**, *136*, 979-990.

(74) Carbonini, P.; Monetta, T.; Nicodemo, L.; Mastronardi, P.; Scatteia, B.; Bellucci, F. *Progress in Organic Coatings* **1996**, *29*, 13-20.

(75) Itagaki, M.; Ono, A.; Watanabe, K.; Katayama, H.; Noda, K. *ECS Transactions* **2006**, *1*, 215-222.

(76) Stern, M. *Journal of the Electrochemical Society* **1957**, *104*, 559-563.

(77) Stern, M.; Geavy, A. L. *Journal of the Electrochemical Society* **1957**, *104*, 56-63.

(78) Kendig, M.; Mansfeld, F. *Materials Research Society Symposium Proceedings* **1988**, *125*, 293-320.

(79) Amirudin, A.; Thierry, D. *Progress in Organic Coatings* **1995**, *26*, 1-28.

(80) Amirudin, A.; Thierry, D. *British Corrosion Journal* **1995**, *30*, 128-134.

(81) Bellucci, F.; Nicodemo, L. *Corrosion* **1993**, *49*, 235-247.

(82) Brasher, D. M.; Kingsbury, A. H. *Journal of Applied Chemistry* **1954**, *4*, 62-72.

(83) Lindqvist, S. A. *Corrosion* **1985**, *41*, 69-75.

(84) Deflorian, F.; Fedrizzi, L.; Bonora, P. L. *British Corrosion Journal* **1997**, *32*, 145-149.

(85) Leng, A.; Streckel, H.; Stratmann, M. *Corrosion Science* **1999**, *41*, 547-578.

(86) Deflorian, F.; Fedrizzi, L.; Bonora, P. L. *Electrochimica Acta* **1993**, *38*, 1609-1613.

(87) Jorcin, J.-B.; Aragon, E.; Merlatti, C.; Pebere, N. *Corrosion Science* **2006**, *48*, 1779-1790.

(88) Bastos, A. C.; Simoes, A. M.; Ferreira, M. G. *Key Engineering Materials* **2002**, *230-232*, 361-364.

CHAPTER 5

ACCELERATED CORROSION (SALT-FOG) TESTING OF VGCNF- AND SiC-REINFORCED ALKYD PAINT-COATED MILD STEEL PANNELS IN 5% NaCl

5.1 Introduction

Protective coatings applied to the surfaces of metals and alloys are expected to last for up to two decades in service. To evaluate the corrosion protection of any coating applied to a metal or alloy three general ways are used. These are outdoor (real life) tests; indoor tests in presence of water or water vapor by immersion or humidification; and the use of accelerated corrosion tests. Each of these different methods has its own advantages and limitations.[1]

The current demand in corrosion studies, especially for industrial manufacturers and coatings designers, is towards the use of accelerated, but reliable, test methods to evaluate the stability and predict the expected life of a protective coating in a short period of time.[2] Among the accelerated atmospheric corrosion tests used are the salt spray tests which are based on the ASTM B117 test (hot 5% NaCl spray).[3]

The salt spray tests are generally run at high temperature. A test that runs at a high temperature will greatly increase the rate of diffusion of the electrolyte into the coating, reducing the barrier properties of the coating, and hence accelerating the degradation of

the coating film.[4-6] The salt spray tests, have been in use for almost a century now, were originally designed to test the stability and degree of degradation of different inhibitive pigments, organic and inorganic protective coatings on metals and alloys.[7-9] Soon after that, the salt spray tests became widely used for the evaluation of the corrosion resistance of bare metals and alloys especially in marine service or on exposed shore locations.[2, 10, 11]

The ASTM B117 test offers simple and easy to apply standard protocols for the preparation, exposure, and evaluation of the results. However, this test has been criticized because it does not simulate real conditions (its results show poor correlation to the results of real-world testing for certain metals and alloys).[10, 12-14] Moreover, the test results are not consistent among different equipment.[10, 12, 13] Accordingly, some researchers consider the salt spray test an arbitrary performance test.[10, 15] However, despite all of these limitations, the salt spray test is very popular and is favored by several automotive and aircraft manufacturers and several other finishing industries that use the test as the standard end-item test for screening and ranking candidate coating systems on many metals and alloys.[16-18] The test sorts out bad coatings and accepts good ones for further evaluation.[19, 20] Moreover, sometimes, the results of the salt spray test are used as the only criterion to evaluate the performance of protective coating systems. Furthermore, certain materials are sometimes designed based solely on the results of the salt spray test without paying attention to the real-world performance of the product.[21]

In the current investigation, the ASTM B117 protocol was used to compare the anticorrosion stabilities of pure paint, VGCNF/alkyd paint, and SiC/alkyd paint coatings applied to mild steel panels with different thicknesses and wt % of VGCNF and SiC.

5.2 Experimental

5.2.1 Chemicals and Reagents

Sodium chloride, hydrochloric acid, and sodium hydroxide were purchased from Fisher Scientific (Pittsburgh, PA). All solutions were prepared as needed using 18 MΩ-cm ultra-pure water (Milli-Q, Millipore Corp., Bedford, MA).

5.2.2 Electrodes and Instrumentation

The accelerated corrosion test was performed according to the specifications given in the ASTM B117 protocol.[3] The test was performed in a warm (35 ºC) 5% NaCl solution in a Q-FOG Cyclic Corrosion Tester (Model CCT 600 , Q-Panel Lab Products, Cleveland, OH) (Figure 5.1). The salt spray test was conducted using square-shaped mild steel panels (8 cm × 8 cm × 1.5 mm) coated with either a pure alkyd paint film or a paint film containing fixed weight percents of either VGCNF or SiC. To avoid the corrosion of the back sides of the panels due to the spray, these sides were also coated with thick layers of paint. In addition, to minimize the corrosion of the samples due to the edge effects, the samples edges were covered with a commercial electrical tape.[22] As illustrated in Figure 5.2, the samples were then mounted on the hanging holders of the test rack in the spray chamber at a 30º angle to the horizontal, such that the coated surfaces face the source of corrosive electrolyte (NaCl solution). The coated panels were arranged on the test rack such that drip from neighboring panels did not contaminate any of them.

Figure 5.1 Q-Fog cyclic corrosion tester used in the current study.

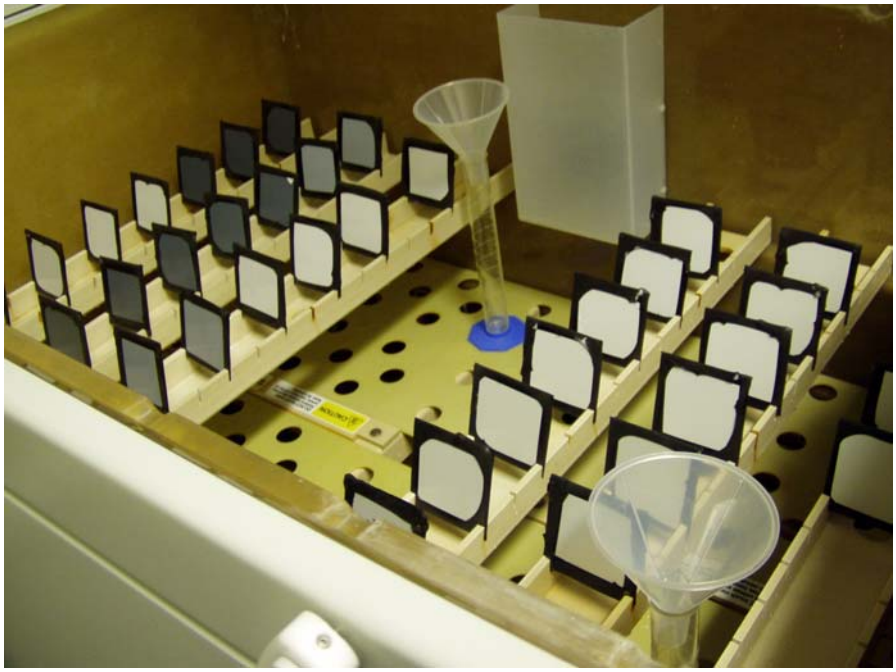

(a)

(b)

Figure 5.2 Digital photos showing the arrangement of a set of coated steel coupons in the salt spray cabinet (a) before the test, and (b) at the end of the test.

The electrolyte (5% NaCl) was added to the tester reservoir and the pH was adjusted to pH 7.2 before starting the experiment. The pH of the electrolyte solution changes during the process of fog generation, heating, and collection. Accordingly, the pH must be adjusted on daily basis using super-saturated solution of NaOH and/or concentrated HCl. The pH was adjusted using a pH meter (Checker pH tester, Model HI 98103, Hanna Instruments, Woonsocket, RI). The test was run at a spray flow rate of 0.5 L/h for 720 h (30 d). The level of the electrolyte in the tester reservoir was adjusted on daily basis using a freshly prepared 5% NaCl solution adjusted to pH 7.2.

The uniformity of fog dispersion (fallout) throughout the chamber should be verified before and throughout the test period. For this purpose, a fog collection kit made up of two graduated measuring cylinders and two funnels were used to collect electrolyte samples during the spraying. The cylinders were placed in the tester cabinet such that one of them is ~ 15 cm from the tester nozzle and the other at the furthest possible distance from the jet. According to the ASTM B117, the collection rate should be between 1.0 and 2.0 mm of solution per hour (averaged over not less than 16 hours) per 80 cm^2 of area. Other practices that contribute to reproducible results have been followed as mentioned in the literature.[23, 24]

5.2.3 Visual Assessments

Before being placed in the corrosion cabinet, the coated mild steel panels were assessed both visually and using a digital camera. During the cyclic test, the coupons were periodically removed from the cabinet and the extent of degradation (rusting) and blistering were also assessed both visually and using the digital camera for corrosion and

delamination/blistering on daily basis until the panels failed. Figure 5.2 shows digital photos for the arrangement of the tested samples in the salt spray cabinet before (Figure 5.2.a) and after (Figure 5.2.b) the test.

5.3 Results and Discussions

The salt spray test was performed twice with duplicate samples in each run. The investigated coating samples had different thicknesses and wt % of either VGCNF or SiC nanoparticles. The results obtained from the two tests are photographically and graphically represented in Figures 5.3 through 5.10. The average results are also summarized in Table 5.1.

All the coatings studied were white to gray in color and therefore it was possible to observe the corrosion products on the surface with naked eye. The results of both runs indicate a very good reproducibility and offer an excellent indication of the anti-corrosive properties offered by all of the alkyd paint coating systems under investigation.

As displayed in Figures 5.3 through 5.9, all the coating systems failed after different time intervals of salt fog exposure depending on the coating thickness, the type of reinforcing material, and its weight percent. As the exposure time increases, the water uptake increases and the coating film starts to swell and detach from the steel surface. Accordingly, with increased exposure time, adhesion loss increases with increased permeation of electrolytes through the coating to the metal surface.[25, 26] It is also apparent in all of the figures that the corrosion products start to appear as red-black (iron oxides)

(a) Before exposure

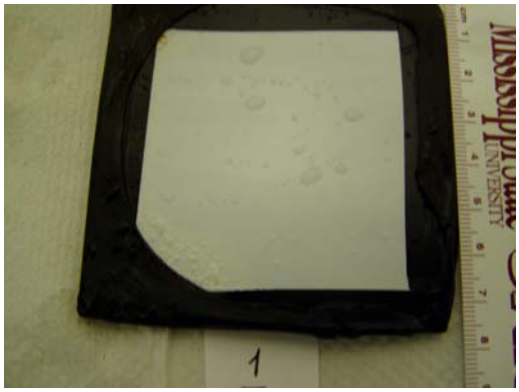

(b) After 96 h

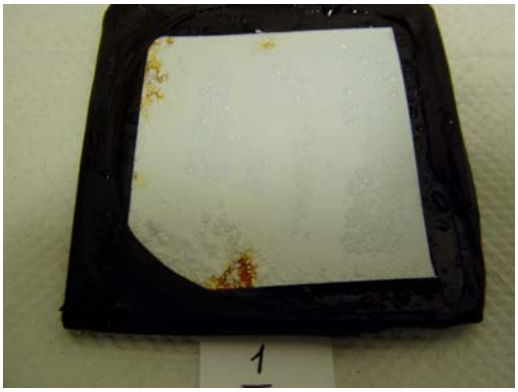

(c) After 120 h

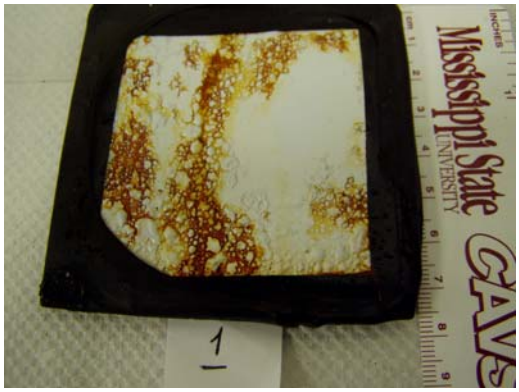

(d) After 168 h

Figure 5.3 Digital photos, recorded at different time intervals of salt fog exposure, for mild steel panels coated with a pure commercial alkyd paint film (film thickness is ~ 20 μm).

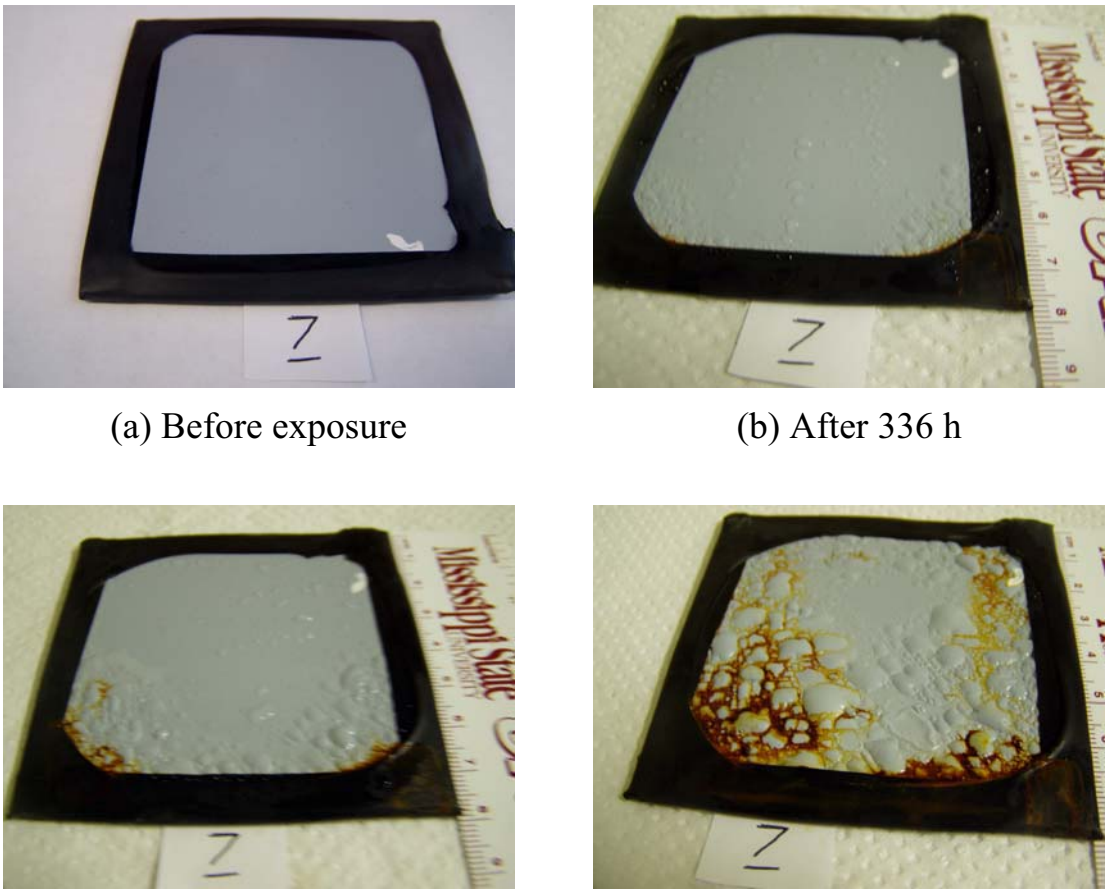

(a) Before exposure (b) After 336 h

(c) After 384 h (d) After 480 h

Figure 5.4 Digital photos, recorded at different time intervals of salt fog exposure, for mild steel panels coated with a commercial alkyd paint film containing 1 wt % VGCNF (film thickness is ~ 40-50 μm).

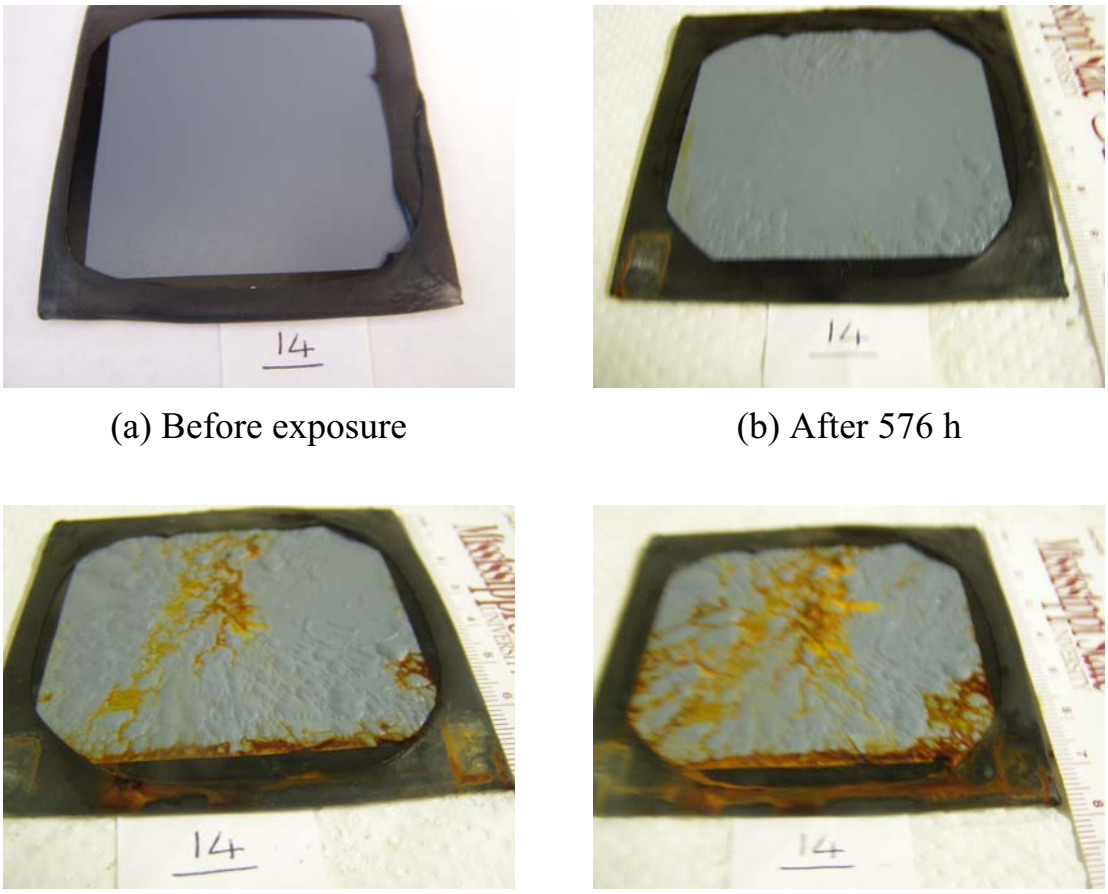

(a) Before exposure (b) After 576 h

(c) After 600 h (d) After 648 h

Figure 5.5 Digital photos, recorded at different time intervals of salt fog exposure, for mild steel panels coated with a commercial alkyd paint film containing 3 wt % VGCNF (film thickness is ~ 40-50 μm).

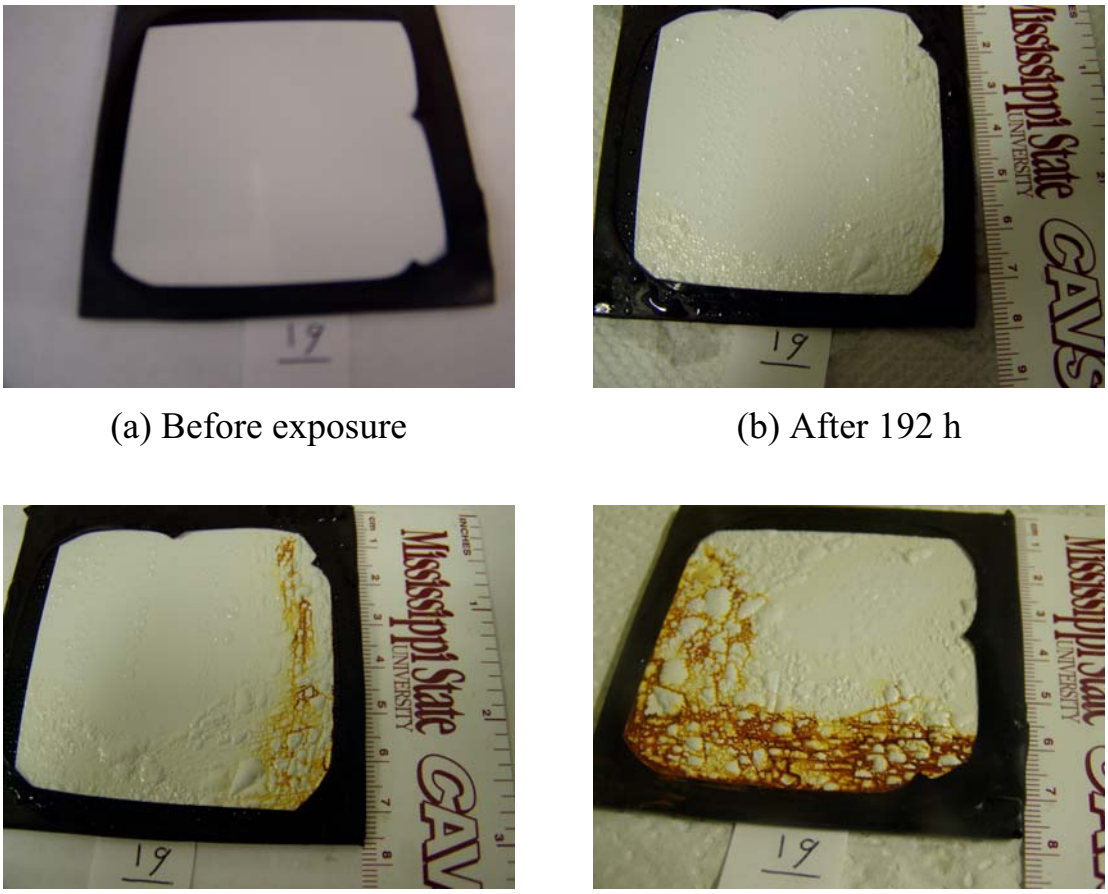

(a) Before exposure (b) After 192 h

(c) After 216 h (d) After 264 h

Figure 5.6 Digital photos, recorded at different time intervals of salt fog exposure, for mild steel panels coated with a commercial alkyd paint film containing 1 wt % SiC (film thickness is ~ 30 μm).

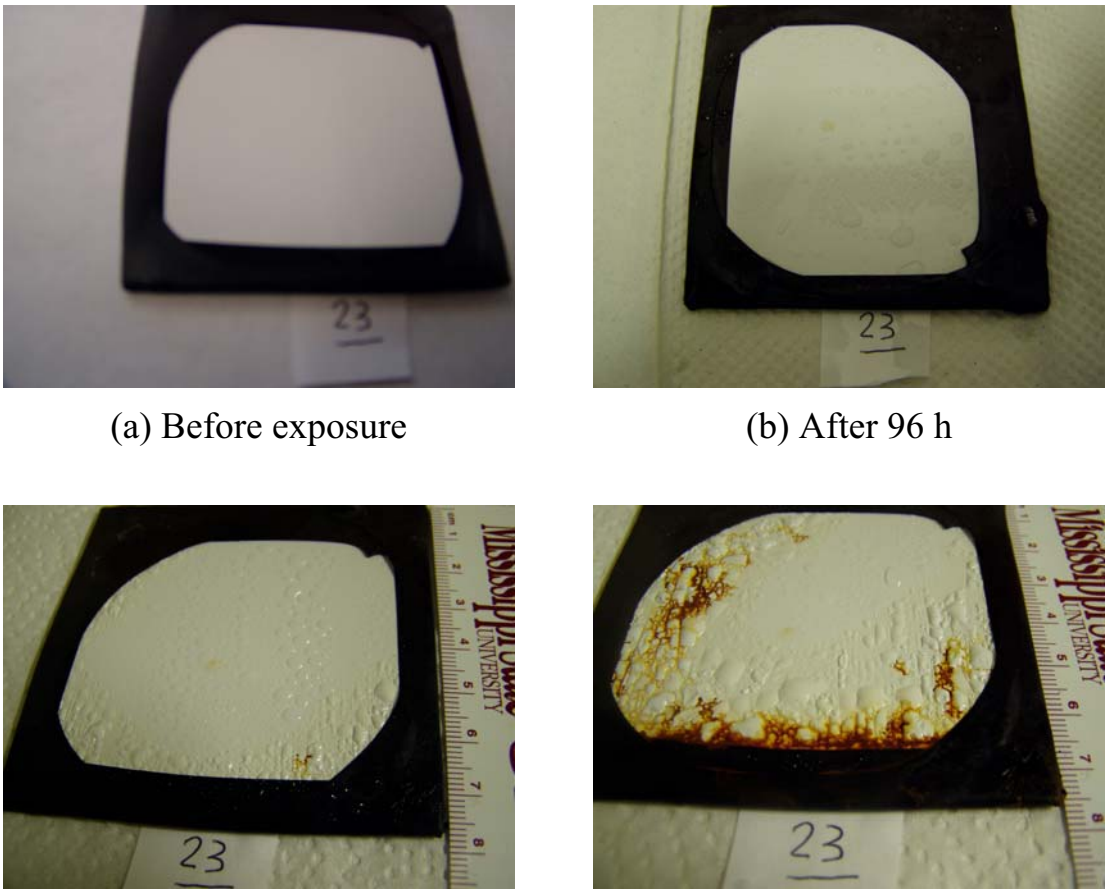

(a) Before exposure (b) After 96 h

(c) After 240 h (d) After 312 h

Figure 5.7 Digital photos, recorded at different time intervals of salt fog exposure, for mild steel panels coated with a commercial alkyd paint film containing 1 wt % SiC (film thickness is ~ 40-50 μm).

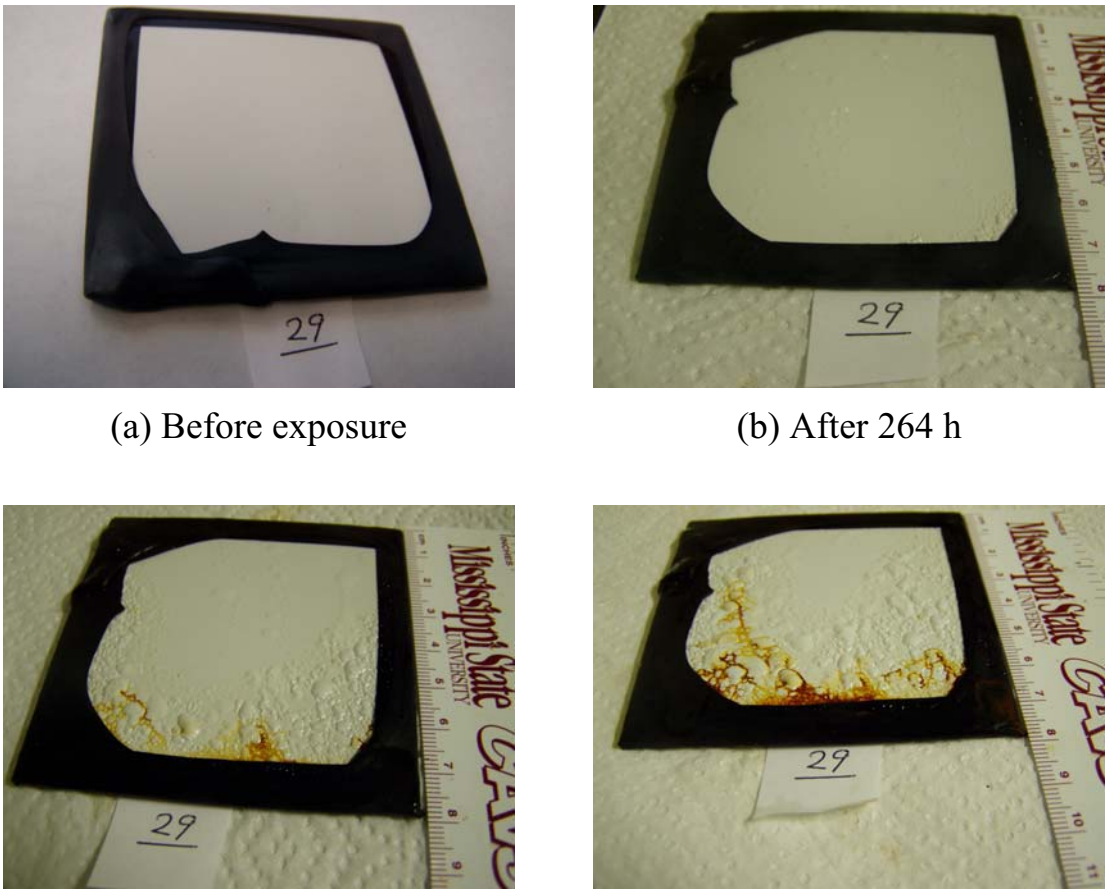

(a) Before exposure (b) After 264 h

(c) After 372 h (d) After 384 h

Figure 5.8 Digital photos, recorded at different time intervals of salt fog exposure, for mild steel panels coated with a commercial alkyd paint film containing 5 wt % SiC (film thickness is ~ 40-50 μm).

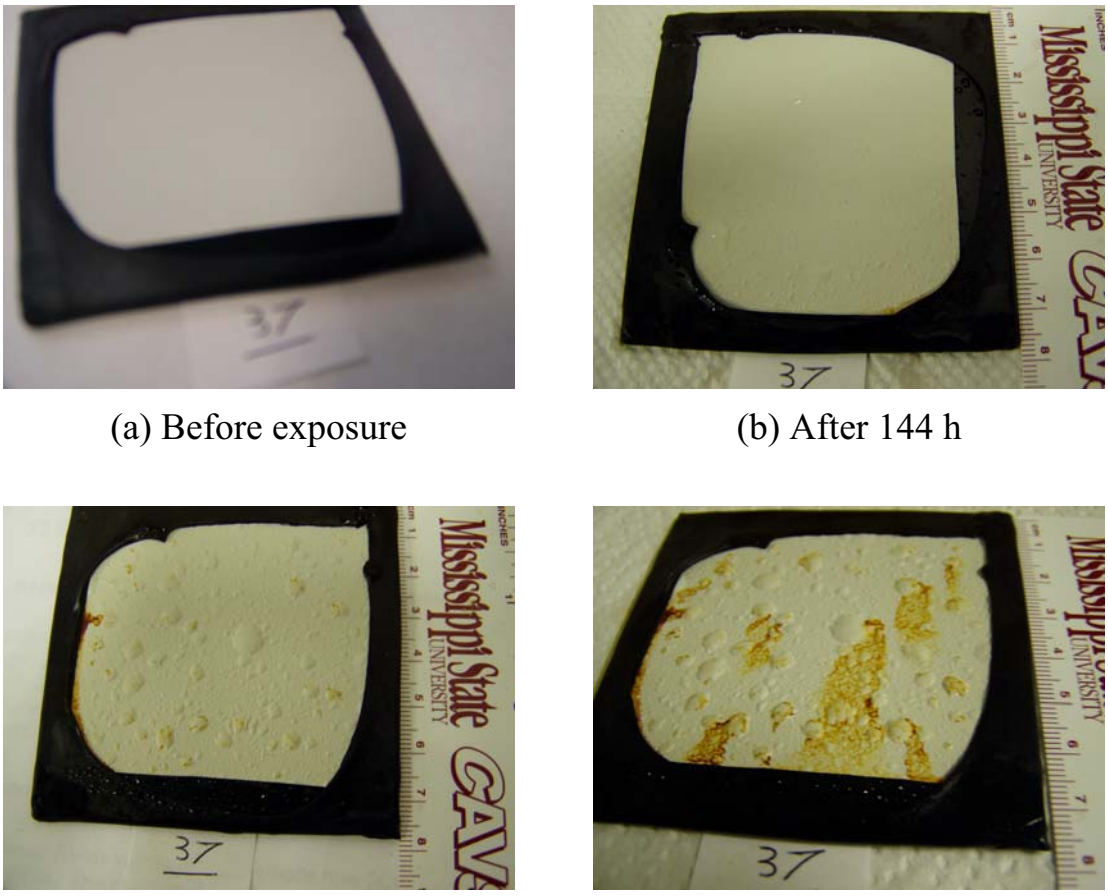

(a) Before exposure (b) After 144 h

(c) After 216 h (d) After 240 h

Figure 5.9 Digital photos, recorded at different time intervals of salt fog exposure, for mild steel panels coated with a commercial alkyd paint film containing 10 wt % SiC (film thickness is ~ 40-50 μm).

Table 5.1 Specifications of the coating systems assessed for anti-corrosive protection using the salt spray method.

Coating specifications	Film thickness (μm)	Average time elapsed before corrosion onset (h)
Pure paint	20	120
	40-50	168
Paint + 1% VGCNF	40-50	384
	60	480
	70	720*
Paint + 3% VGCNF	20-30	264
	40-50	576
Paint + 1% SiC	30	204
	40-50	240
Paint + 3% SiC	30	168
	40-50	468
Paint + 5% SiC	30	228
	40-50	372
Paint + 10% SiC	30	120
	40-50	216

*Testing ended with no failure.

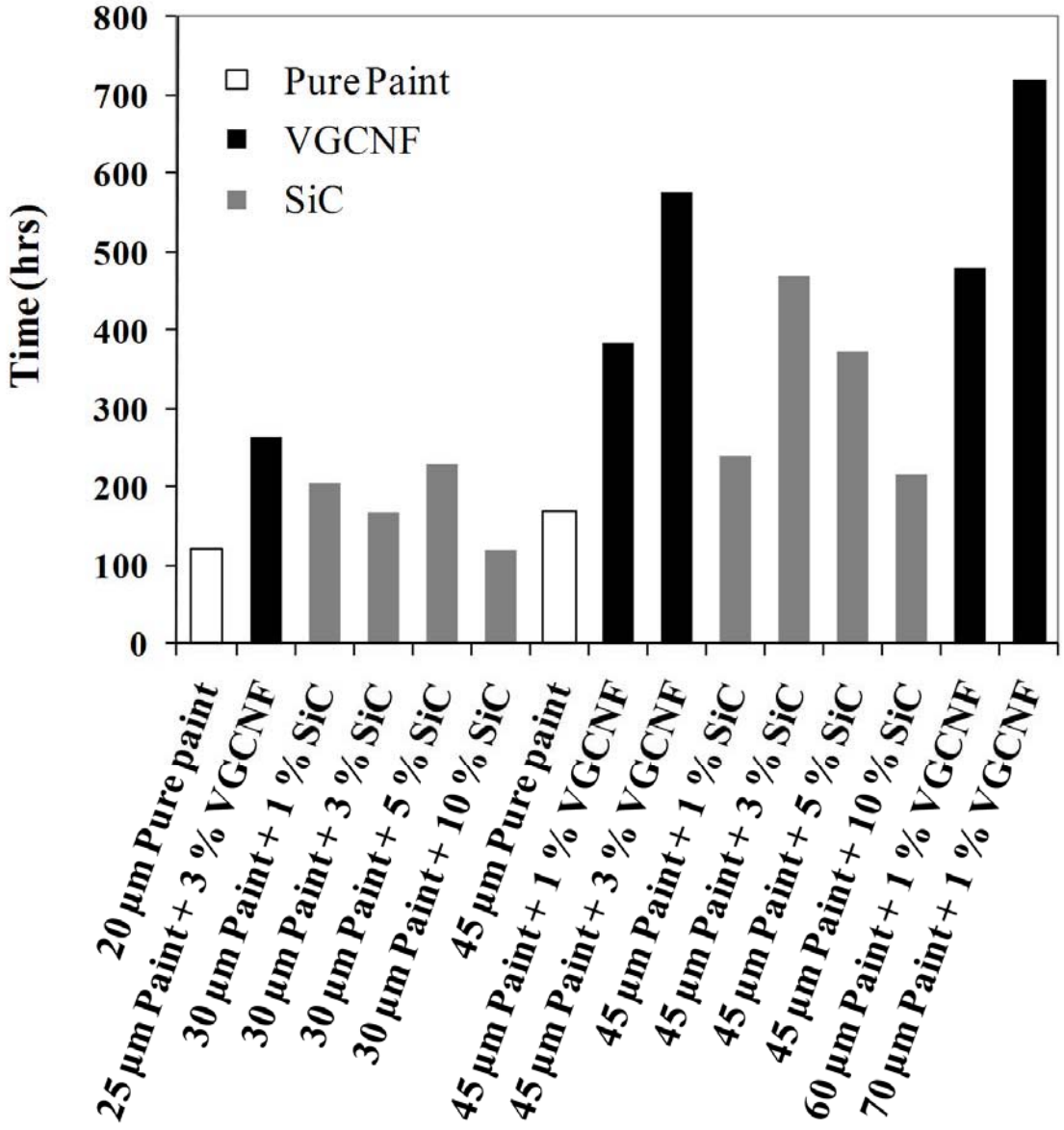

Figure 5.10 Variation of the average time elapsed before corrosion onset with the wt % of VGCNF and SiC and film thickness of the alkyd paint coatings for all tested panels.

or red (iron hydroxide) tiny spots before they spread to cover the whole surface with red iron hydroxide (rust).

The results depicted in Figure 5.10 indicate that the anti-corrosive properties of the VGCNF-reinforced and SiC-reinforced coating systems are far better than those of the unmodified coating of the same film thickness. In addition, the results also show that the thicker the coating, the longer the time elapsed before corrosion onset. It is also clear from Figure 5.10 that the VGCNF-modified coatings are the best corrosion resistant systems and were last to fail. The data also indicate the higher the wt % of the VGCNF, the longer the time elapsed before the onset of corrosion. However, for SiC-incorporated coatings, the data presented in Figure 5.10 indicate that systems with SiC loadings higher than 3% show a shorter lifetime and hence worse anti-corrosive protection properties.

Looking at the results depicted in Table 5.1 and Figures 5.3 through 5.10 vs. the EIS results for the same paint coating systems presented in Chapters 3 and 4, one can notice that the salt spray test correlates very well with the EIS results.

5.4 Conclusions

Despite its limitations, the salt spray test provided an excellent qualitative evaluation of the corrosion resistance of the pure, VGCNF-reinforced, and SiC-reinforced alkyd paint coatings applied to the surface of mild steel specimens. The results of the accelerated corrosion tests showed that all coating systems with and without VGCNF or SiC provide efficient corrosion protection for the mild steel substrate. In addition, the incorporation of VGCNF and SiC in the paint matrix greatly enhanced the corrosion protection properties and hence increased the lifetime of the coating systems relative to

the unmodified (pure) systems. The results also showed that the VGCNF-modified coatings have better stabilities and longer lifetimes in comparison to the SiC-modified coatings. Moreover, the results presented in this chapter are in agreement with the EIS results presented in Chapters 3 and 4.

5.5 References

(1) Funke, W. *Journal of the Oil and Colour Chemists' Association* **1979**, *62*, 63-67.

(2) Koleske, J. V., Ed. *Paint and Coating Testing Manual: Fourteenth Edition of the Gardner-Sward Handbook*; ASTM: Philadelphia, PA, 1995.

(3) American Society for Testing and Materials (ASTM), ASTM B-117-97 Standard Practice for Operating Salt Spray (Fog) Apparatus.

(4) Bierwagen, G. P.; He, L.; Li, J.; Ellingson, L.; Tallman, D. E. *Progress in Organic Coatings* **2000**, *39*, 67-78.

(5) Loveday, D.; Peterson, P.; Rodgers, B. *Journal of Coatings Technology* **2005**, *2*, 22-27.

(6) Mayne, J. E. O. *British Corrosion Journal* **1970**, *5*, 106-111.

(7) Capp, J. A. *Proceedings, American Society for Testing of Materials* **1914**, *14*, 474-481.

(8) Finn, A. N. *Proceedings, American Society for Testing of Materials* **1918**, *18*, 237-238.

(9) Merica, P. D.; Waltenberg, R. G.; Finn, A. N. *Bulletin of the American Institute of Mining and Metallurgical Engineers* **1919**, 1051-1062.

(10) Roberge, P. R. *ASTM Special Technical Publication* **1995**, *STP 1238*, 18-30.

(11) Davis, J. R., Ed. *Carbon and Alloy Steels*; ASM International: Materials Park, OH, 1996.

(12) LaQue, F. L. *Materials and Methods* **1952**, *35*, 77-81.

(13) LaQue, F. L. *Marine Corrosion: Causes and Prevention*; John Wiley & Sons, Inc.: New York, 1975.

(14) Skerry, B. S.; Simpson, C. H. *Corrosion* **1993**, *49*, 663-674.

(15) Sample, C. H. *Proceedings, American Society for Testing and Materials Bulletin* **1943**, *123*, 19-22.

(16) Forshee, A. G. *Metal Finishing* **1991**, *89*, 45-47.

(17) Forshee, A. G. *Metal Finishing* **1991**, *89*, 13-14.

(18) Mills, D. J.; Boden, P. J. *Corrosion Science* **1993**, *35*, 1311-1318.

(19) Brasunas, A. D., Ed. *NACE Basic Corrosion Course*, 2nd ed.; NACE: Houston, TX, 1971.

(20) Mohler, J. B. *Metal Finishing* **1975**, *73*, 48-50.

(21) Austin, M. J. In *Paint and Coating Testing Manual: Fourteenth Edition of the Gardner-Sward Handbook*; Koleske, J. V., Ed.; ASTM: Philadelphia, PA, 1995, pp 238-251.

(22) Wessling, B.; Posdorfer, J. *Electrochimica Acta* **1999**, *44*, 2139-2147.

(23) Altmayer, F. *Plating and Surface Finishing* **1985**, *72*, 36-40.

(24) Altmayer, F. *Metal Finishing* **1985**, *83*, 57-60.

(25) Funke, W. *ACS Symposium Series* **1986**, *322*, 222-228.

(26) Funke, W. *Journal of the Oil and Colour Chemists' Association* **1985**, *68*, 229-232.

CHAPTER 6

CONCLUSIONS

6.1 Summary of This Work

In the preceding chapters, the corrosion-protection of commercial alkyd paint coatings with different film thicknesses either in the pure state or containing a known amount of vapor grown carbon nanofibers (VGCNFs) or silicon carbide (SiC) particles applied to the surface of mild steel substrates in aqueous 3% NaCl solution were investigated with several electrochemical and surface analysis techniques. The paint coatings, containing different weight percents of VGCNF or SiC, were applied to the mild steel coupons using the spin-coating techniques. Open circuit potential (OCP), electrochemical impedance spectroscopy (EIS), cyclic voltammetry (CV), accelerated corrosion test (salt spray test), optical profilometry, atomic force microscopy (AFM), microhardness and nanoindentation, scanning electron microscopy (SEM), and electrical conductivity measurements were performed.

Chapter 1 provides an overview of the importance of the corrosion and corrosion control studies as well as the economic importance of iron and steel alloys. It also provides a brief discussion on the importance of organic coatings as materials for the protection of metals and alloys against atmospheric corrosion. In addition, it presents a short discussion on the EIS technique, its importance, merits, and its applications especially in the field of corrosion. Moreover, the chapter provides a brief discussion on

the corrosion protection mechanism offered by organic coatings. The chapter also includes a section devoted to VGCNFs; their physical, electrical, and mechanical properties; and their applications especially as a reinforcing material in polymer matrix composites. The chapter ends with a section on the aims and scope of the current research project.

Chapter 2 was devoted to studying the mechanical and electrical properties of dry alkyd coatings with different thicknesses and VGCNF weight percent. The coatings were deposited on mild steel and poly(methyl methacrylate) (PMMA) substrates. In addition, the chapter involved some surface analysis measurements such as optical profilometry, SEM, and AFM measurements. The electrical conductivity measurements showed that the incorporation of the VGCNF in the alkyd paint matrix improves the electrical conductivity of the pure paint. On the other hand, the nanoindentation measurements showed that the incorporation of VGCNF in the paint matrix improves the hardness up to 3 wt % and then its hardness deteriorates for VGCNF content higher than 3%.

In Chapter 3, the EIS, along with other electrochemical techniques, such as OCP and CV measurements, were used to investigate the effect of VGCNF incorporation in an alkyd paint film applied to the surface of mild steel substrates on the corrosion protection properties of the coating film when exposed to 3% NaCl solutions. The experimental EIS data were fitted to electrical equivalent circuits. Several electrochemical parameters such as the impedance modulus ($|Z|$), the polarization resistance (R_p), the double layer capacitance (C_{dl}), the coating resistance (R_c), the coating capacitance (C_c), the percent water uptake, the delaminated area (A_d), the VGCNF resistance (R_f), and the VGCNF capacitance (C_f) were calculated for paint coatings with different thicknesses and

VGCNF loadings in the 0-10 wt % range. The results were then graphed vs. the immersion time in 3% NaCl solution. VGCNF-reinforced alkyd paint coatings provided excellent barrier and corrosion properties in comparison to unmodified paint coatings. The chapter ends by discussing the role of the VGCNF, as a conductive material, in the corrosion protection mechanism of the alkyd paint coatings.

In Chapter 4, the EIS behavior of SiC-incorporated alkyd paint coated mild steel samples in 3% NaCl solution under the same conditions used in Chapter 3 was investigated. The main objective of the work presented in this chapter was to compare the corrosion protection properties of SiC-reinforced coatings with those of VGCNF-reinforced coatings of the same thickness. After a brief introduction on the importance of SiC and its applications, the EIS results are presented. This work showed that the incorporation of the SiC particles in the paint matrix does improve the corrosion protection properties. The chapter ends with a section comparing the effect of SiC and VGCNF incorporation in the alkyd paint matrix on the barrier properties (corrosion protection) properties of the pure paint matrix. The barrier properties of SiC-reinforced coatings are superior to those of pure paint coatings but inferior to the barrier properties of VGCNF-reinforced coatings.

In Chapter 5, accelerated salt fog tests were used to evaluate and compare the stability and corrosion resistance of unmodified, VGCNF-reinforced, and SiC-reinforced alkyd paint coatings, applied to mild steel coupons. The goal of this study is to rank the three coating systems in order of their anticorrosive properties. The chapter starts with a brief introduction on the importance, merits, and applications of the salt spray test as a desirable accelerated corrosion test. The discussion is followed by a short section on the

experimental setup used to perform the salt spray test based on the guidelines given in the ASTM B117 protocol. Digital photos, tables, and graphs showed the gradual change in the morphology of the paint film layer, the extent of degradation, and the time elapsed before the coating films failed and the corrosion products were visual. The stability, barrier properties, and service life, had the following order; VGCNF-reinforced coatings > SiC-reinforced coatings > pure (unmodified) paint coatings.

Overall, the incorporation of a small amount (0.5-5 wt %) of VGCNF leads to significant improvements in the corrosion resistance, barrier properties, and mechanical properties of the paint matrix. In addition, the higher the VGCNF loading, up to 5 wt %, the better the corrosion protection properties of the coating become and hence the longer its lifetime. Moreover, the measurements showed that VGCNF is better at improving the barrier properties of commercial alkyd paint coatings applied to the surface of mild steel coupons than SiC particles.

6.2 The Mechanism of Protection

Incorporating VGCNFs or SiC particles into the paint matrix improved the barrier (anticorrosion) and electrical properties of the unmodified alkyd paint matrix. In this section, the role of the additives (VGCNF and SiC) in improving the properties of the host paint is discussed.

Paints and organic coatings are the most commonly used materials for the corrosion protection of a wide range of metals and engineering alloys in many industries.[1-8] These materials not only inhibit the transport of corrodents (water, oxygen, and ions) to the metallic substrate, but also decrease electrical transport between anodic

and cathodic sites on the metal substrate.[9, 10] However, as mentioned in Chapter 1, pure paints and coatings are not perfect barriers against corrosion because these materials are porous. They contain microvoids, defects; and are permeable to oxygen and water to some degree.[11-14] Accordingly, one of the current trends in the fields of organic coatings and composites is the incorporation of nano-sized pigments to block the microvoids and defect sites, thus reducing the permeability of the coating to the corrodents (oxygen, water, and ions). This includes conductive or nonconductive particles such as platy talcs, mica, glass flakes, micaceous iron oxides such as Fe_2O_3, leafed or regular Al, graphite, carbon black, TiO_2 nanoparticles, steel nanoparticles, Pb dust, Ca ferrite, Zn nanoparticles, SiC nanoparticles, and other metal flake pigments.[15-30] Dispersion of pigments with platelet-shaped particles in a paint matrix can reduce the permeability rates for corrodents as much as five fold when the pigment particles are aligned parallel to the coating surface.[26, 27] Since the corrodents cannot pass through the pigment particles, the presence of aligned particles can reduce the diffusion rates of the corrodents through the paint coating matrix.[6] Bentz and Nguyen have devised a simulation model for the effect of several variables (including pigmentation parameters such as pigment particle geometry, pigment volume concentration, and pigment absorption characteristics) on the diffusion of environmental species through coatings reinforced with pigments.[31] This model showed that, regardless of the conductivity of the particles, well dispersed, lamellar pigment particles at concentrations near, but below, the percolation limit (see below) give the best barrier performance.

Dispersing a conductive material into a nonconductive matrix can render the matrix conductive.[6, 16, 32-39] The properties of the host matrix depends on several

parameters including the particle size, shape, morphology, orientation in the paint matrix, and the weight percent of the added conductive filler.[34, 40-43] A threshold weight percent for the filler exists (known as the percolation limit or threshold), above which the properties (e.g., the electrical conductivity) of the host matrix deteriorate.[32] This threshold value depends on both the type of the conductive filler and the polymeric composite in which the filler is dispersed.[34] For example, the threshold value is about 7.5% for epoxy resins containing Fe[34] and 20-40% for epoxy resins reinforced with Ag, Sn, Pb, Cu, or Al.[35, 36] The threshold value is 5-6% for Cu particles in polyvinyl chloride[37] and Ni in polyethylene[38] while it is 1% and 8% for carbon black (CB) in polyvinyl alcohol,[16] and Araldite D,[44] respectively. The threshold value is 37% for Ag particles in Bakelite powder[45] while the value for VGCNFs in vinyl ester composites is 2-3%.[39]

Carbon blacks (CBs) are a family of small size colloidal spheres (typically 13-100 nm in diameter) of hexagonal planar structures of elemental carbon that are produced by the incomplete combustion or thermal decomposition of gaseous or liquid hydrocarbons.[46-48] The spheres further fuse together to form aggregates (with a normal size in the 200-1000 nm).[49, 50] CB aggregates are produced in a variety of particle size and shape, porosity, and surface chemistry.[51, 52] They are electrically conductive materials with conductivity in the range of 0.1 to 10^2 S/cm at room temperature.[53] Insulating polymers and polymer composites filled with CBs at the percolation threshold become conductive.[54-58] When incorporated in a polymer matrix, CBs tend to fill the pores in the polymer matrix and form a conductive network with short distances between the particles. This conductive network allows the transfer of electrons among the particles

throughout the whole polymer matrix.[59-62] Therefore, the dispersion of the CB particles enhances the electrical conductivity of the host matrix.[16, 63-65] According to El-Tantaway et al.,[58] the dispersion of 7% CB (the percolation threshold) into an epoxy, fills the free volume in the epoxy matrix, thus reducing the gap between the polymeric chains in the epoxy. Therefore, the electrical conductivity of the epoxy matrix is increased from 3.4×10^{-7} ($\Omega^{-1}.cm^{-1}$) for an epoxy composite containing 4 wt % CB to 3.4×10^{-3} ($\Omega^{-1}.cm^{-1}$) for an epoxy composite containing 7 wt % CB. In addition, the presence of CB particles improves the stiffness as well as the thermal stability of the polymer matrix. Accordingly, CBs are widely used as reinforcing fillers, conductive fillers, UV light stabilizers, and pigments for a range of applications including packagings for electronic components and electrical cables, electrical heaters, electrical screening materials, inks, plastics, rubbers, and paints.[53, 56, 63, 66-80]

Zhang et al. studied the effect of CB nanoparticle-modified polyvinyl alcohol lacquer coatings on the corrosion behavior of steel in 3.5% NaCl solution.[16] The incorporation of the CB nanoparticles in the lacquer matrix up to 1 wt % greatly decreases the rate of corrosion of steel. The authors suggested that the CB nanoparticles improve the corrosion protection properties of the pure lacquer matrix through filling the pores in the matrix.

Sujith and Unnikrishnan[81] studied the barrier properties of composites based on natural rubber, ethylene vinyl acetate and three different types of CBs having different particle sizes in a solvent mixture of crude oil products (petrol, kerosene and diesel). The authors showed that the smaller the size of the CB particles, the lower the rate of diffusion of the solvent (crude oil products) through the composite. The authors attributed

the decrease in the diffusion rate to the degree of CB reinforcement. According to the literature, maximum reinforcement is attained if the filler particles are of comparable size (either the same or smaller than) the polymer chain end-to end distance.[82] The extent of filler reinforcement depends on both the size and surface area of the filler. In general, small filler particles with large surface area usually provide maximum reinforcement and rigidity to the polymer coating or composite material.[81] Accordingly, pigment fillers with large sizes are usually less efficient than pigments with small sizes in extending the diffusion path taken by the corrodents to reach the coating/metal substrate interface. Therefore, composites reinforced with the smallest CB particles are expected to have the longest and indirect pathways, maximum reinforcement, highest rigidity, and hence the lowest rate of solvent diffusion. On the other hand, for composites containing large size CB particles, the corrodents encounter shorter diffusion paths. Accordingly, these composites are expected to be less compact, have lower filler density, and hence have higher rates of solvent diffusion.

Rwei et al. investigated the effect of dispersing CB aggregates into various polymeric materials (including polydimethylsiloxane (PDMS), silicon rubber, and epoxy) on the electrical conductivity of the host matrix.[83]. The electrical conductivity of the paint matrix increases from 10^{-9} to 10^{-4} $\Omega^{-1}.cm^{-1}$ when less than 3% CB aggregates were dispersed into the PDMS matrix. The authors attributed this enhancement in the conductivity to the formation of a CB "aggregate-network" structure when CB particles are dispersed in the PDMS matrix.

Praveen et al. studied the addition of CNTs to zinc coatings showing that the incorporation of CNTs into a zinc composite coating increases the corrosion resistance of

the zinc coating.[25] The authors suggested that the CNTs fill the active sites (microvoids) in the zinc composite coating and hence provide a physical barrier to the corrosive medium.

VGCNFs are smaller in size and have larger aspect ratio than CB. Accordingly, many studies have shown that VGCNFs can form conductive (percolation) networks while maintaining the intrinsic properties of the host polymer matrix.[84-89] In this regard, a study conducted by Pittman et al.[84] showed that the incorporation of VGCNFs along with CB in a polystyrene matrix improves the conductivity of the composite at low VGCNF loading because their aspect ratio allows percolation path at low wt % values. This countered by their tendency to partially nest and entangle in the composite matrix.

Choi et al.[85] investigated the influence of the incorporation of VGCNFs on the electrical and mechanical properties of a polycarbonate composite matrix. Incorporating VGCNFs decreased the electrical resistivity of the composite. The authors attributed this decrease in electrical resistivity to a good VGCNF network. In a comprehensive study on the development of VGCNF-reinforced polymer composites for electrostatic discharge (ESD) materials and structural composites, Lozano et al.[86, 87, 89] investigated the effect of addition of VGCNFs on the properties of polypropylene (PP) matrix. The ESD measurements showed the formation of highly dispersed VGCNF networks which led to a percolation threshold at 9-18 wt % in the PP matrix. In another investigation, Li and Luo[90] studied the mechanical properties of CNF-reinforced carbon/carbon composites. The authors showed that a CNF loading up to 5 wt % enhances the mechanical properties (e.g., flexure strength and modulus). The authors attributed this improvement in mechanical properties to the formation of a CNF network or web in the composite matrix

which results in an improvement in the interfacial adhesion between the CNFs and the host matrix. According to the authors, the CNFs act as a bridge in the pores in the host matrix and make it difficult for cracks to initiate or form in the matrix.[90]

Conducting polymers (CPs) such as polyaniline (PANI), polypyrrole (PPy), polythiophene, and their derivatives are widely used for corrosion protection of many metals and engineering alloys.[30, 91-117] Other application areas for CPs include chemical sensors, bioimplants, electronic and optical materials, energy storage and solar cells, memory devices, electrocatalysis, rechargeable batteries, and actuators.[118-124]

The availability of π electrons in CPs enables them to be good corrosion inhibitors. CPs have switchable properties because they can exist in various interchangeable stable oxidation states.[100, 125-127] They are usually applied to metallic surfaces either alone as film forming corrosion inhibitors[92, 93, 95, 128-133] or as additives in a protective coating matrix.[91, 99, 134-136]

When applied to metallic surfaces, CPs promote corrosion protection in different ways depending on the nature of the substrate. For example, when applied to metals sensitive to passivation, such as iron and steel alloys, CPs shift the corrosion potential of the metallic substrate to more noble values where the corrosion rate is lower.[137-143] In this case, the metal substrate is protected by a passivation mechanism provided by the redox properties of the CP. In this regard, Lee et al. investigated the corrosion protection properties of mild steel coated with a layer of PANI.[144] The authors reported that PANI acts as a redox mediator where it passivates the metal at the metal/polymer interface and reoxidizes itself by dissolved oxygen at the polymer/solution interface. Other researchers also reported that metal passivation occurs through the formation of iron oxide (γ-Fe_2O_3

and Fe_3O_4) surface layers.[92, 135, 138, 145] Moreover, Kinlen et al. reported the formation of an insoluble Fe-PANI complex at the metal surface when iron was coated with a PANI film. The complex catalytically reduces oxygen and hence lowers the rate of Fe corrosion.[142, 146] For these CP/steel systems, the presence of microscopic voids or imperfections in the coating matrix does not have appreciable effect on the stability of the coating system because the CP has the capacity to provide the charge necessary to allow self healing for the metal surface through the reoxidation of the metal in the defected areas.[141] For these systems, the degree of corrosion protection afforded by the CP depends on the structure and electronic properties of the CP, the coating thickness, and the nature of the corrosion medium.[127, 137, 147-149] On the other hand, for metals such as zinc, CPs can only protect the metallic surface by a barrier effect that isolates the metal substrate from the corrosive medium by the formation of an adherent oxide layer.

Among the currently used CPs, PANI and its derivatives are the most widely used for corrosion protection of metals and alloys.[30, 94, 99, 105, 129, 134, 137, 150-161] For example, Wessling reported that copper, mild steel, and stainless steel passivate when they are dipped in solutions of doped PANI.[162] For mild steel, passivation occurs through the formation of a dense layer of γ-iron oxide beneath the PANI coating (at the PANI/steel interface). The authors also showed that PANI is reduced from the emeraldine salt to leucoemeraldine at the polymer/solution interface. The oxidation half reaction is the formation of passive oxide on the steel substrate. Within 24 h, leucoemeraldine was reoxidized back to emeraldine by oxygen in air.[162] Purging oxygen into the system can accelerate the latter oxidation reaction. However, the latter oxidation step is responsible for the catalytic action of PANI because it results in the regeneration of the oxidizing

power of PANI.[11] It is worth mentioning here that, for any CP to provide a stable passivating layer on a steel substrate, the CP should have high oxidizing power to oxidize iron directly to Fe^{3+} and not Fe^{2+} (which will result in the dissolution of the substrate.[11]

The hypothesis of the current investigation, mentioned in Chapter 2, was that, when mixed with the paint matrix, VGCNF would show an inhibiting (blocking) effect to the corrosion reaction of the coated substrate in a way similar to that afforded by CPs. However, compared to CPs, all carbon materials including CBs, VGCNFs, and CNTs cannot switch between different redox states to any extent when the corrosion conditions are changed. Moreover, there is no study that reported the formation of a passive oxide layer at the polymer/substrate interface for organic coatings reinforced with CB, VGCNFs, or CNTs. Accordingly, the proposed hypothesis was incorrect.

6.3 The Proposed Corrosion Protection Mechanism

Chapter 1 noted that iron and steel alloys corrode when oxygen and water are in direct contact with the metallic surface. When applied to the surface of a metallic substrate, paints and organic coatings retard corrosion by acting as a barrier to prevent oxygen and water from reaching the substrate surface. However, organic coatings are not perfect corrosion barriers and have a limited service life. They are permeable to water, oxygen, and ions to some extent.[6, 163] In practice, an organic coating exposed to atmospheric conditions is saturated with water at least half its service life.[164, 165] When a coated metal is exposed to a neutral electrolyte (e.g., NaCl solution), water and oxygen diffuse to the metal surface through the weak real (microscopic) points in the coating (such as pores, voids, inhomogeneities, cracks, defects, scratches, and areas of poor

adhesion) and/or virtual pores in regions of low crosslinking and therefore high transport in the coating matrix.[166, 167] Corrosion usually starts at or near these weak points in the coating film. This results in swelling of the coating due to water uptake, formation of blisters, the onset of underfilm corrosion, delamination (loss of adhesion), and ultimately complete disbondment and degradation of the coating film.[6, 163-165, 168, 169] The presence of an electrolyte (e.g., NaCl) also increases the solubility of water in coatings and hence accelerates the rate of coating degradation and substrate corrosion.[6]

When a coated metal is immersed in an aqueous solution, water permeation, and to a lesser extent oxygen permeation, through the organic coating occurs via diffusion mainly due to the concentration gradient.[163] In addition to diffusion, there are at least two more driving forces for water permeation, namely (i) capillary forces in the coating due to presence of residual solvent molecules, entrapped air bubbles during coating application, and poor coating curing, and (ii) osmosis due to the presence of impurities.[164] Water diffusion causes swelling of the coating. Eventually, water molecules will reach the coating/substrate interface and interfere with the adhesion between the coating and metal surface. At the end, adhesion is lost and an electrochemical double layer is established at the metal surface and corrosion initiation occurs at the metallic substrate.[168-170]

Leidheiser and Funke[171] proposed two different mechanisms for loss of adhesion, and hence coating film damage and degradation: (i) chemical disbondement due to chemical reactions between water molecules and the different polymer-metal bonds, and (ii) mechanical or hydrodynamic disbondement due to accumulation of water molecules in local sites of bad adhesion in the coating and build up of osmotic pressures (due to the

presence of inhomogeneities in the metal surface, soluble salts as impurities at the metal surface, and/or the accumulation of corrosion products such as Fe^{2+} and OH^- ions). As a result of these reactions, blisters form and expand, exposing more of the bare metal substrate.[172, 173] Thus, delamination of the organic coating takes place which results in the disbondment of the coating film and hence corrosion of the bare metallic substrate.[6]

Based on the above discussion along with the Section 6.2, we strongly believe that, when added to the alkyd paint matrix, the nano-sized VGCNFs fill in the polymer matrix including the voids, pores, and imperfections in the matrix and form a network-like structure in the host paint matrix that reduces the porosity of the coating film and act as a barrier for water, oxygen, and ions in solution (the corrodents). Since the corrodents cannot pass through the VGCNFs in the paint matrix, the presence of the VGCNFs can reduce the rate of diffusion through a coating. Thus, the presence of VGCNFs blocks the voids in the paint matrix and acts as a barrier or obstacle for the diffusion of corrodents, thus, leading to an extended diffusive double layer and creating longer and indirect pathways for the corrodents to go through before reaching the metal surface. As a result, the rate of corrosion of the metal decreases.[164, 174] In addition, being a conductive material in the form of a network-like structure, the VGCNFs enhance the electrical conductivity of the paint matrix.[175] Moreover, increasing the VGCNF loading up to the percolation limit increases the density of the nanofibers in the paint matrix and makes the coating more impervious.[11] Accordingly, the incorporation of VGCNF into the alkyd paint matrix improves the barrier properties and reduces the permeability of the paint coating in a way similar to that afforded by CB nanoparticles, CNTs, VGCNFs, platy talcs, mica, and glass flakes when added to paint and coating systems.[16, 25, 81, 83-87, 89, 90, 176, 177]

Adhesion of the coating to its substrate is considered one of the most crucial factors that determine the stability and the service lifetime of any coating.[178] In addition to their rule as a blocking pigment, VGCNFs, with their unique size, aspect ratio, and physical properties, can also act as a promoter for the adhesion forces between the coating film and the metallic substrate. Accordingly, the presence of the VGCNFs in the paint matrix would increase the time needed for the delamination and degradation of the paint coating.

The above mechanism is supported by the electrical conductivity, electrochemical (CV and EIS), and chemical (salt spray) measurements presented in Chapters 2, 3, and 5. For example, the electrical conductivity measurements showed that the incorporation of the VGCNFs enhances the electrical conductivity of the alkyd paint matrix. This increase in the electrical conductivity is expected and can be explained as follows; the incorporation of the VGCNFs in the paint matrix generates a network-like structure of the nanofibers in the paint matrix. The presence of the conductive VGCNF network not only blocks the defects in the paint matrix and hinders the diffusion of the corrodents through the paint film, but also renders the paint matrix conductive. So, the increased conductivity of the host paint matrix is a result of the dispersion of the VGCNFs in the coating matrix. Moreover, both the electrochemical and electrical conductivity measurements showed that VGCNFs provide better enhancement in both the corrosion protection and electrical conductivity properties than SiC microparticles. This is normal and expected because the nano-sized VGCNFs with their higher aspect ratio are smaller in size than the SiC microparticles and according to the literature, the smaller the size of the pigment particles, the better the reinforcement and barrier properties of the host coating.[82]

Accordingly, dispersion of nano-sized particles in a coating matrix provides a longer and more tortuous diffusion path for the corrodents to go through before reaching the metal substrate. This leads to slower rates of corrosion for VGCNF-reinforced coatings than those for SiC-reinforced coatings.[82] On the other hand, VGCNFs are inherently more conductive than SiC microparticles. Accordingly, it is expected that, for paint coatings containing the same amount of either additives, VGCNFs-reinforced coating systems are more electrically conductive that SiC-reinforced coating systems.

The OCP measurements showed that the incorporation of VGCNFs in the alkyd paint matrix has a significant effect on the rate of decrease of the OCP with immersion time. When dispersed in the paint matrix, VGCNFs hinder the permeability of the coating to oxygen and water. Thus, the presence of VGCNFs in the paint matrix reduces the rate of oxygen and water diffusion, and improves the adhesion properties of the paint film, thus increases the service lifetime of the paint film. Accordingly, the OCP values for VGCNF-reinforced coatings are expected to remain positive (noble) for a longer period of immersion time compared to the OCP value for a pure paint coating film which decreases and reaches the steady state potential (E_{ss}) of the bare substrate in a short period of immersion time.

The CV measurements also showed distinct redox peaks for $Ru(NH_3)_6Cl_3$ and $K_3Fe(CN)_6$ (the mediators) for paint coatings containing 3 or more wt % VGCNF. These results are also expected. The pure paint matrix is insulating and hence the CVs are expected to show redox peaks of the mediators. On the other hand, VGCNF is a conductive material and hence the mediators can undergo redox reactions at their surfaces. Thus, redox peaks are expected to appear for VGCNF-reinforced paint coatings.

In addition, based on the proposed mechanism, increasing the VGCNF content in the matrix increases the density of the conductive VGCNF network and hence assures efficient transport of electrons in the redox reactions taking place when the voltammograms are collected.[179] Accordingly, the higher the VGCNF in the paint matrix, the better and well distinct the peaks are in the voltammograms as shown in Chapter 3.

The EIS and salt spray measurements showed that alkyd paint coatings having higher VGCNF content and very thick are much more stable (retard the onset of metal corrosion and film blistering) than thin paint coatings with or without VGCNF. Thicker films with higher VGCNFs wt % have higher nanofiber density and, as long as the VGCNF content is below the percolation limit, these coating are expected to increase the time necessary for permeation of the corrodents through the coating thus delaying the arrival of the corrodents at the coating/metal substrate interface.[6] For paint coatings with VGCNF above the percolation limit, barrier properties are low because more fibers make the diffusion of the corrodents faster and also lowers the electrical resistivity of the coating.

Figure 6.1 shows the variation of time to coating failure based on the salt fog and OCP measurements with coating thickness for pure alkyd paint coatings applied to the surface of mild steel samples in NaCl solutions. As mentioned in Chapter 5, the salt fog test has been criticized because the experimental conditions as well as the test results show poor correlation to the real-world conditions and results.[180-183] Due to these limitations, the results of the accelerated salt fog test are usually used as a qualitative estimate of the service lifetime of a coating. Thus, the results of the salt fog test can be used as a qualitative prediction for the electrochemical measurements (such as the OCP

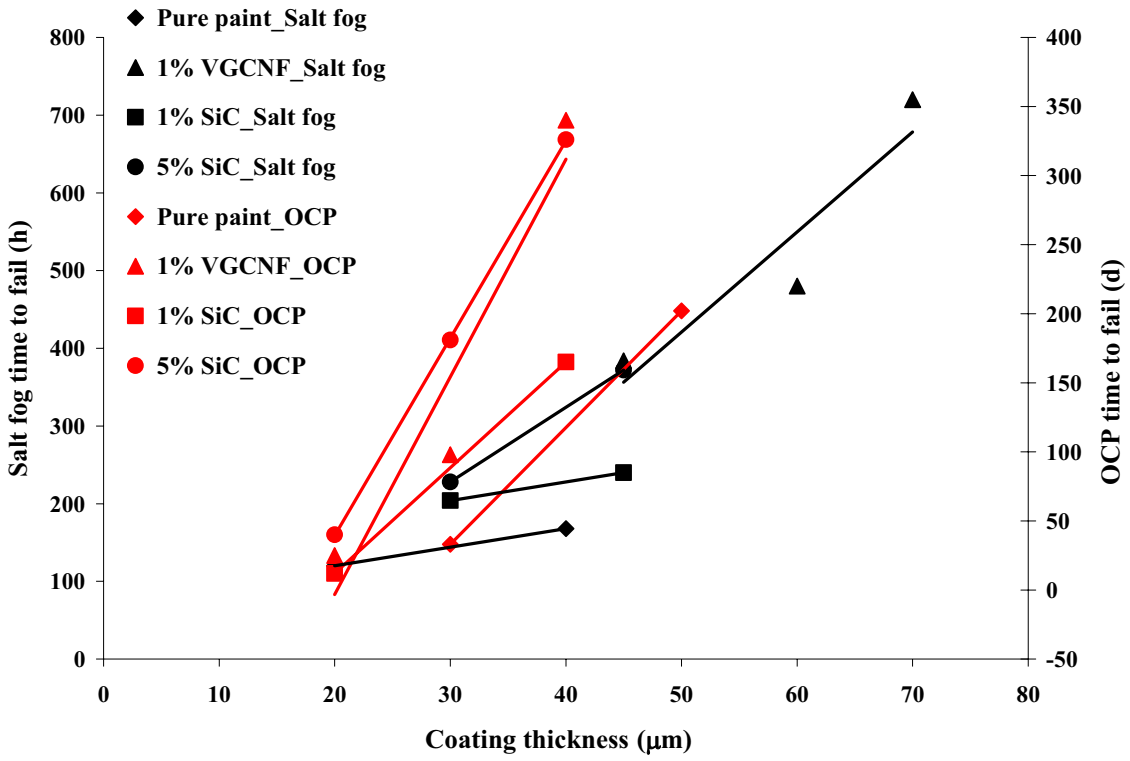

Figure 6.1 Variation of time to coating failure based on salt fog and open circuit potential (OCP) measurements with coating thickness for alkyd paint coatings containing different wt % of either VGCNFs or SiC microparticles applied to the surface of mild steel samples in NaCl solutions. ◆, ◆ = pure paint, ▲, ▲ = paint + 1% VGCNF, ●, ● = paint + 1% SiC, and ■, ■ = paint + 5% SiC.

measurements) of the coatings under normal conditions but are not expected to have a perfect correlation with the electrochemical measurements.

As shown in Figure 6.1, the straight lines for the OCP results are more or less parallel to each other indicating a good correlation among the OCP results for the paint coatings with and without VGCNFs or SiC. On the other hand, the correlation among the salt results is not as good as it is for the OCP measurements. Nevertheless, it is obvious from Figure 6.1 that for both OCP and salt fog measurements, there is a linear relationship between the film thickness and the coating film time to fail. The thicker the coating film, the longer the time needed for the metal to fail (corrode).

Table 6.1 shows the variation of the time to coating failure slope based on the salt fog and open circuit potential (OCP) measurements presented in Figure 6.1. The results in Table 6.1 show a good agreement between the salt fog and OCP measurements. For both tests, the incorporation of 1% VGCNFs in the paint matrix increases the value of the slope relative to its value for the pure paint coating. The slope values in Table 6.1 also show that the dispersion of 5% SiC particles in the paint matrix also increases the value of the slope. The values of these slopes can be taken as a measure for the stability of the coating films. The larger the value of the slope is, the higher the stability, and hence the longer the service lifetime, of the coating film. It is also clear from Table 6.1 that the presence of 1% VGCNFs in the paint matrix increased the time required for the degradation and failure of the coating film (i.e., increased the coating film stability) as reflected by the higher slopes value for this coating system (12.88 h/μm, and 15.78 d/μm) compared to the value of the slopes for the pure paint coating (2.40 h/μm, and 8.45 d/μm). Moreover, the results in Table 6.1 show that a paint coating containing 1%

Table 6.1 Variation of time to coating failure slope based on salt fog and open circuit potential (OCP) measurements for alkyd paint coatings containing different wt % of either VGCNFs or SiC microparticles applied to the surface of mild steel samples in NaCl solutions.

Coating Specification	Salt Fog		OCP	
	Slope (h/μm)	R^2	**Slope (d/μm)**	R^2
Pure paint	2.40	–*	8.45	–*
Paint + 1% VGCNF	12.88	0.88	15.75	0.91
Paint + 1% SiC	2.40	–*	7.65	–*
Paint + 5% SiC	9.60	–*	14.3	–*

*n = 2 for these curves

VGCNFs is more stable and has a longer time to fail than a paint coating containing 5% SiC microparticles. The increase in the value of the slope can be explained as follows: the dispersion of the VGCNFs or the SiC particles fill the paint matrix, act as a barrier for the diffusion of the corrodents, and hence delay the arrival of the corrodents to the metal surface through enlarging the path taken by the corrodents. As a result of this delay, the slope increases when VGCNFs or SiC particles are incorporated in the paint matrix indicating good protective properties.

Tables 6.2 through 6.4 show the variation of some of the calculated corrosion parameters (OCP, $|Z|$, R_p, C_{dl}, R_c, and A_d) for 30 μm thick pure, 5% VGCNF- and 5% SiC-reinforced alkyd paint coatings for selected time intervals of immersion in 3% NaCl. For the complete set of results, Chapters 3 and 4 should be consulted. The data shown in these figures support the proposed mechanism as explained below.

As discussed by Haruyama et al.[184] and expanded by Mansfeld and Tsai[185, 186], the following relationships apply for a coated metal

$$R_c \quad \frac{R_c^\circ}{A_d} \quad \frac{R_c^\circ}{AD} \tag{6.1}$$

$$R_c^\circ \quad \rho.d \tag{6.2}$$

$$D \quad \frac{A_d}{A} \tag{6.3}$$

$$R_p \quad \frac{R_p^\circ}{A_d} \quad \frac{R_p^\circ}{AD} \tag{6.4}$$

$$C_{dl} \quad (\varepsilon\varepsilon^\circ / d) \quad C_{dl}^\circ A_d \quad C_{dl}^\circ AD \tag{6.5}$$

$$C_c \quad C_c^\circ (A - A_d) \quad C_c^\circ A(1-D) \tag{6.6}$$

Table 6.2 Variation of the open circuit potential (OCP) and total impedance (|*Z*|) with immersion time for pure, VGCNF-, and SiC-reinforced alkyd paint-coated mild steel coupons (30 μm thick) in 3% NaCl solution.

	Pure paint		**Paint + 5% VGCNF**		**Paint + 5% SiC**	
Immersion time (d)	**OCP (V vs. SCE)**	**|*Z*| (kΩ)**	**OCP (V vs. SCE)**	**|*Z*| (kΩ)**	**OCP (V vs. SCE)**	**|*Z*| (kΩ)**
1	0.235	5560	0.127	462		
3	0.084	550	0.099	379	0.261	296
5	0.005	113	0.073	333	0.160	94
8	-0.052	59	0.047	319		
11	-0.074	56	0.032	290	0.069	51
19	-0.050	41	0.018	256	0.025	39
20	-0.078	41	0.017	254	0.021	37
24	-0.059	42	0.019	202	-0.015	35
29	-0.305	13	-0.018	185		
33	-0.589	1	-0.010	196	-0.032	38
40			-0.001	192	-0.063	46
50			-0.002	163	-0.085	70
70			-0.014	329		
80			0.070	504		
90			0.068	508		
96			0.046	558	-0.049	95
98			0.050	562		
127			0.059	467	-0.058	62
159			-0.054	390	-0.089	52

Table 6.3 Variation of the polarization resistance (R_p) and double layer capacitance (C_{dl}) with immersion time for pure, VGCNF-, and SiC-reinforced alkyd paint-coated mild steel coupons (30 μm thick) in 3% NaCl solution.

Immersion time (d)	Pure paint (30 μm thick)		Paint + 5% VGCNF (30 μm thick)		Paint + 5% SiC (30 μm thick)	
	R_p (kΩ)	C_{dl} (μF/cm²)	R_p (kΩ)	C_{dl} (μF/cm²)	R_p (kΩ)	C_{dl} (μF/cm²)
1	7300	0.01	94	0.55		
3	574	0.09	101	0.56	126	4.70
5	814	0.17	82	0.55	44	13.70
8	24	0.33	84	0.52		
11	10	0.62	94	0.57	26	28.90
19	5	1.59	106	0.69	22	39.30
20	5	2.21	121	0.71	21	39.90
24	5	3.56	111	0.79	21	46.90
29	0.1	54.10	111	0.76		
33		413.00	115	0.54	22	50.40
40			119	0.50	27	60.30
50			106	0.45	45	77.60
70			245	0.41		
80			478	0.33		
90			450	0.35		
96			418	0.36	50	1.30
98			475	0.35		
127			354	0.41	58	2.24
159			387	0.53	50	2.76

Table 6.4 Variation of the coating resistance (R_c) and percent delaminated area (%A_d) with immersion time for pure, VGCNF-, and SiC-reinforced alkyd paint-coated mild steel coupons (30 μm thick) in 3% NaCl solution.

Immersion time (d)	Pure paint (30 μm thick)		Paint + 5% VGCNF (30 μm thick)		Paint + 5% SiC (30 μm thick)	
	R_c (kΩ)	%A_d	R_c (kΩ)	%A_d	R_c (kΩ)	%A_d
1	6.27	0.019	87.9	0.101		
3	1.22	0.016	70.6	0.102	103.0	0.604
5	1.11	0.031	80.2	0.100	40.7	2.521
8	0.97	0.059	74.9	0.095		
11	1.17	0.114	89.2	0.105	24.3	5.295
19	0.88	0.293	68.9	0.126	20.3	7.197
20	0.94	0.406	72.2	0.130	19.4	7.310
24	0.85	0.653	55.2	0.145	19.2	8.563
29	0.07	9.915	48.6	1.383		
33	0.02	75.634	56.3	0.099	21.0	9.239
40			51.7	0.091	25.1	11.042
50			39.0	0.083	40.0	14.225
70			75.5	0.075		
80			94.3	0.065		
90			87.4	0.066		
96			121.0	0.065	37.8	0.239
98			125.0	0.067		
127			105.0	0.075	28.2	0.410
159			85.8	0.097	24.3	0.506

where R_c is the coating resistance which is related to the paths of ionic conductivity in the coating (Ω), C_{dl} is the double layer at the coating/metal interface where corrosion occurs (F), ρ is the coating resistivity (Ω.cm), ϵ is the relative dielectric constant of the coating, ϵ^o is the dielectric constant of the vacuum (8.85×10^{-14} F.cm^{-1}), D is the delaminated area ratio, $D = A_d/A$, A_d is the delaminated area (cm^2), A is the total coating area (cm^2), d is coating thickness (cm), and R^o_c, R^o_p, C^o_{dl}, and C^o_c are area-normalized (specific) resistances (Ω.cm^2) and capacitances (F.cm^{-2}), respectively.[185-187] As the immersion time increases, water, oxygen, and electrolyte entry into the epoxy increases, A_d increases and hence the value of D increases and the resistivity (ρ) decreases.[187, 188]

As shown in Table 6.2, the initial OCP for the three coating systems (pure paint, VGCNF-containing and SiC-containing paint) were positive values (about +0.3 to +0.2 V vs. SCE). The steady-state potential (E_{ss}) of the bare mild steel in the same electrolyte solution is about -0.6 V (vs. SCE)[189] Accordingly, it is clear that the application of the coating, with or without VGCNF or SiC, shifts the initial OCP of the bare substrate to a more positive value indicating the protective characters of the coatings. As shown in Table 6.2, as the immersion time increased, the OCP of the coated substrates shifted toward more negative values before it reached the E_{ss} value of the bare steel alloy when the coating fails. Table 6.2 also shows that after 33 d of immersion in the corrosive medium, the pure paint coating totally degraded (OCP = -0.589 V) while the value for the VGCNF- and SiC-reinforced coatings having the same thickness are still far more positive (-0.010, and -0.032 V, respectively) indicating the better stability and barrier properties of the modified paint matrixes. These results could also be explained based on the adhesion properties of the VGCNF- and SiC-modified paint coatings. In this regard,

the improved adhesion properties of the modified coating delay the shift of the OCP to more negative values. The OCP values show that after 159 d of immersion, the OCP of VGCNF-reinforced coating (-0.054 V) is still more positive than the value for the SiC-reinforced coating (-0.089 V), thus indicating better barrier properties for the former coating. This result is expected and consistent with the literature where the smaller size and larger aspect ratio VGCNFs have better barrier properties in blocking the voids and defects in the paint matrix than the larger SiC microparticles.[81]

Table 6.2 also presents the variation of the total impedance ($|Z|$) with immersion time for the three coating systems for the same period of time. As shown in Table 6.2, for the three coating systems, the value of $|Z|$ decreases with immersion time indicating that coating degradation and loss of corrosion protection. This decrease of impedance with time is primarily due to a decrease of the coating resistance (R_c) as D increases and/or ρ decreases (Equations 6.1 through 6.3). As shown in Table 6.2, the rate of drop of $|Z|$ with immersion time is higher for the pure paint system .After 33 d of immersion in the corrosive solution; the $|Z|$ value for the pure paint coating is at least two orders of magnitude less than that of VGCNF- or SiC-containing coatings. This behavior can be explained based on the suggested mechanism as follows; the presence of the VGCNFs or the SiC particles in the alkyd paint matrix blocks the imperfections or weak points in the paint matrix (such as pores, voids, inhomogeneities, cracks, defects, scratches, and areas of poor adhesion) and act as barriers for the transport of the corrodents through the coating film to the metal/coating interface, thus increasing the total impedance of the paint film compared to the pure paint matrix.[190]

The polarization resistance (R_p) and the double layer capacitance (C_{dl}) are two of the important parameters used in the characterization of any electrochemical system under corrosion. As shown in Chapter 3, R_p is inversely proportional to the rate of corrosion. Degradation of organic coatings in corrosive media is always accompanied by a decrease in R_p and an increase in C_{dl} as the immersion time. As the immersion time increases, the water uptake increases, A_d increases, and thus D increases. Accordingly, as shown in Equation 6.4, the value of R_p is expected to decrease with increasing immersion time. Table 6.3 shows a continuous decrease in R_p for the pure paint coating and the coating failed in 29 d. On the other hand, for a paint coating containing either 5% VGCNFs or SiC microparticles, the R_p values showed some fluctuations (decrease, followed by increase, and finally decrease) with immersion time. Although the increase in R_p is not expected, it is common in the literature and is attributed to various reasons including the blockage of a pore or a defect in the coating by corrosion products.[191, 192] Nevertheless, the data presented in Table 6.3 show that after ~159 d of immersion in the corrosive electrolyte, the values of R_p for a paint coating containing 5% SiC starts to decrease and the paint failed after ~180 d of immersion (see Figure 4.29 in Chapter 4). For the corresponding VGCNF-reinforced paint coating, the results in Chapter 3 (Figure 3.45) show that after 600 d of immersion, the value of R_p is still very high indicating the stability of the coating film. These results clearly indicate the improvement of the corrosion protection properties of the paint matrix when VGCNFs or SiC microparticles are dispersed in the paint matrix.

Table 6.3 also shows the variation of C_{dl} for the three coating systems with time. The values of C_{dl} are taken as a measure of the area over which the coating has

disbonded.[193] The increase in C_{dl} with immersion time indicates an increase of the disbonded area (wet area) over the substrate surface under the coating. As shown in Equation 6.5, C_{dl} is directly proportional to A_d which increases with immersion time. The data presented in Table 6.3 indicate that the initial C_{dl} values for the three coating systems are low and increase with immersion time. The relatively low initial C_{dl} values imply that the coatings are initially largely bonded to the substrate surface. However, as the immersion time increases the values of C_{dl} increase for a short period of time, denoting the entry of the electrolyte into the paint coating. After that initial period of increase, the value of C_{dl} remain unchanged for the long exposure time until the film finally fails and corrosion occurs at the steel substrate surface and the value of C_{dl} increases rapidly. Table 6.3 shows that the C_{dl} values for VGCNF- and SiC-reinforced coating systems are lower and stable for longer periods of time than the pure coating system. This also reflects the greater stability and improved barrier properties of the paint matrix due to the dispersion of the VGCNFs or SiC microparticles in the paint matrix.

The R_p and C_{dl} data presented in Table 6.3 along with Figures 3.45 (Chapter 3) and 4.29 (Chapter 4) show another effect of the incorporation of VGCNFs on the properties of the host paint matrix. The results show that the R_p values for the VGCNF-reinforced coating are higher than the corresponding values for SiC-reinforced coatings. Similarly, the C_{dl} values for the VGCNF-reinforced coating system are smaller than the corresponding values for SiC-reinforced coating system. These results reflect the better reinforcement effect of the VGCNFs. Also, the formation of an oxide coating, which would occur only on the VGCNF-reinforced paint samples, would increase R_p and decrease C_{dl}.

The estimated values of the coating resistance (R_c) along with the coating capacitance (C_c) are generally considered the best measures for the stability of the organic coatings.[194, 195] It is well known that a decrease in R_c and increase in C_c during exposure to the corrosive medium imply degradation of the coating. Thus, the magnitude of Rc at a given immersion time is an indicative of the degree of degradation of the coating film by the ingress of the corrodents through the film.[167, 196-198] As shown in Equations 6.1 and 6.6, as the immersion time increases, the water uptake of the coating increases, the values of ϵ and D increase wile ρ decreases as conductive paths and defects (blisters) develop in the coating.[166, 185, 197, 199, 200] Accordingly, as the immersion time increases, R_c decreases while C_c increases. The data shown in Table 6.4 depict that, for the three coating systems, R_c slightly decreases in the first few days of exposure to NaCl solution, denoting the entry of the electrolyte into the alkyd paint coating. This is the first step of electrolyte diffusion through an organic coating.[7, 188, 201] After this initial period, the value of R_c reaches a plateau and remains almost constant over a period of immersion time before R_c significantly drops indicating a film breakdown and corrosion of the metallic substrate. The length of the immersion time before film breakdown occurs is an indication of the stability of the organic coating. The longer the length of this plateau, the greater the corrosion protection properties of the coating film. As shown in Table 6.4, for the pure paint system, the length of the plateau is very short, the R_c value decreased appreciably in a very short time, and the paint film was damaged in 33 d indicating that this coating system is the least stable and most susceptible to corrosion.[197] On the other hand, for VGCNF- and SiC-reinforced coating systems, the plateau region is longer and the R_c values are higher than the corresponding values for the pure paint system. These

results clearly indicate that the incorporation of the VGCNFs or the SiC microparticles into the alkyd paint matrix improves the corrosion protection properties of the film coating. In a very recent publication, Deflorian et al. showed the incorporation of TiO_2 + CB in an epoxy/phenolic paint matrix increases the length of the plateau region in the R_c-immersion time graphs for paint coatings as thin as 29.2 mm immersed in 0.35 wt % NaCl solutions.[7] The authors attributed the improvement in the barrier properties of the paint coating to the presence of the pigments (TiO_2 and CB). Table 6.4 also shows that the length of the plateau region is bigger, with higher R_c value, for VGCNF-reinforced coating system than with the SiC-incorporated coating system. This indicates that VGCNFs, with their smaller size and higher aspect ratio, have a better effect in improving the barrier properties of the paint matrix than SiC microparticles.

The delaminated area (A_d) is the electrochemically active area under the coating. Delamination of a coated metal substrate immersed in an electrolyte solution occurs as a result of the diffusion of water, oxygen and ions in the electrolyte solution, through the polymer coating until it finally gets in direct contact with the bare metal substrate where the electrochemical corrosion reactions take place at the bare metal/electrolyte interface. Accordingly, delamination leads to loss of the adhesion and protective properties of the coating.[202-204] Due to all of these processes, delamination will occur and, in theory, A_d is expected to increase with immersion time. Table 6.4 presents the variation of A_d with immersion time for the three coating systems. As shown in the table, the value of A_d increases with increased immersion time indicating the absorption of water in the coatings. The A_d data in Table 6.4 clearly show that the fastest increase in the value of A_d occurs for the pure paint coating system. On the other hand, for VGCNF- and SiC-

reinforced coating systems, A_d is more or less stable over a long period of immersion in the corrosive medium indicating more stable coatings. Table 6.4 also shows that the A_d values for the VGCNF-reinforced coating system are lower than the corresponding values for the SiC-reinforced coating system. This is also due to the difference in size and surface area between the two fillers. These results are also in accordance with the literature results.[205]

Figures 6.2 and 6.3 show the effect of the VGCNF wt % on the values of the VGCNF resistance (R_f) and capacitance (C_f) in the coating film, respectively. It can be see from both figures that R_f decreases and C_f increases for the first few days of immersion denoting the entry of water and NaCl into the coating film. This initial behavior is also common in the literature for the variation R_c and C_c with immersion time.[40] Several reasons have been suggested for this initial behavior including the following: changes in the dielectric properties of the coating due to water uptake, local concentration of water in the coating film, and a decrease in the dielectric permittivity due to the generation of internal stresses in the coating film.[40, 167]

Examining Figure 6.2 clearly shows that a paint coating containing 5% VGCNFs is less resistive (more conductive) than a coating having 1% VGCNFs. As shown in the figure, for a paint coating containing 1% VGCNFs, as the immersion time increases, the water uptake in the coating film increases and the value of R_f fluctuates while the coating film swells and blisters spread in the coating. When the film is completely degraded, the value of R_f drops. On the other hand, for a paint coating containing 5% VGCNFs, after an initial period of decrease in R_f and increase in C_f, the values of the fiber resistance and capacitance reach a plateau and remain almost unchanged over a long period of

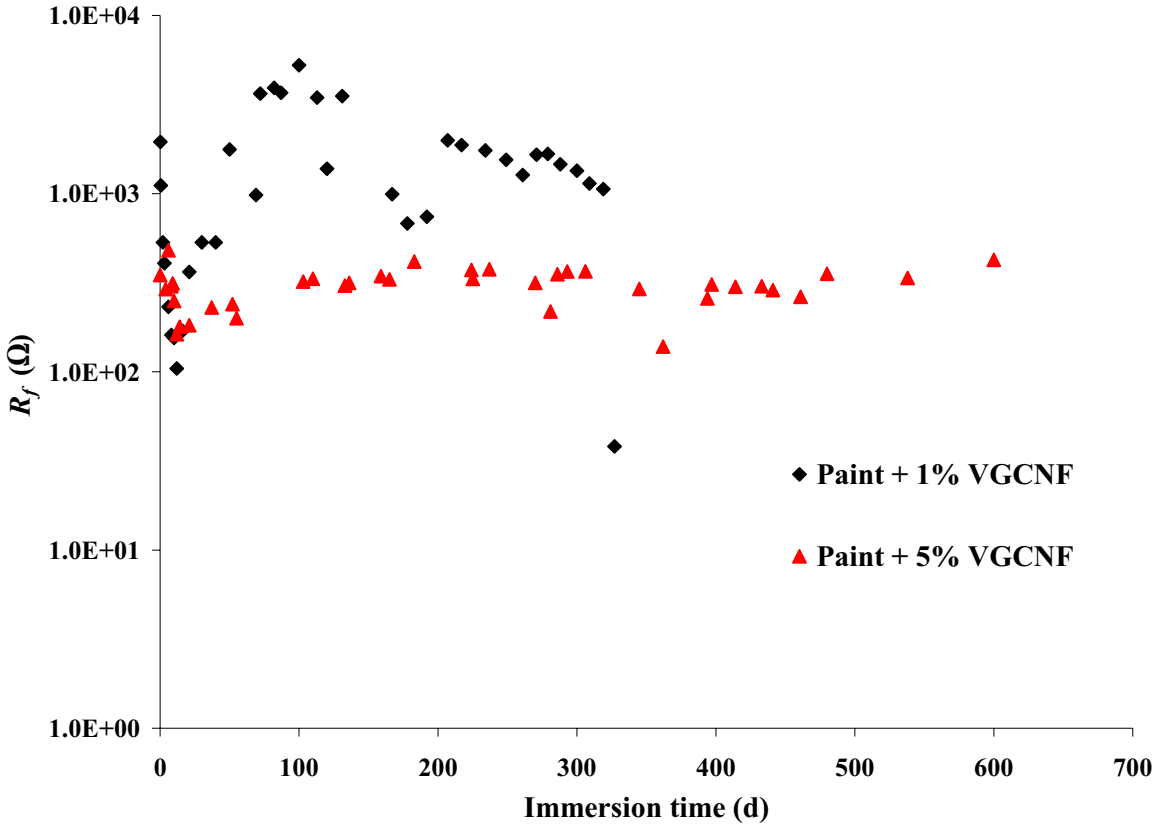

Figure 6.2 Variation of the VGCNF resistance (R_f) with immersion time for mild steel panels coated with a VGCNF-incorporated commercial alkyd paint film (40 μm thick) and exposed to 3% NaCl solution. ◆ = paint + 1% VGCNF, and ▲ = paint + 5% VGCNF.

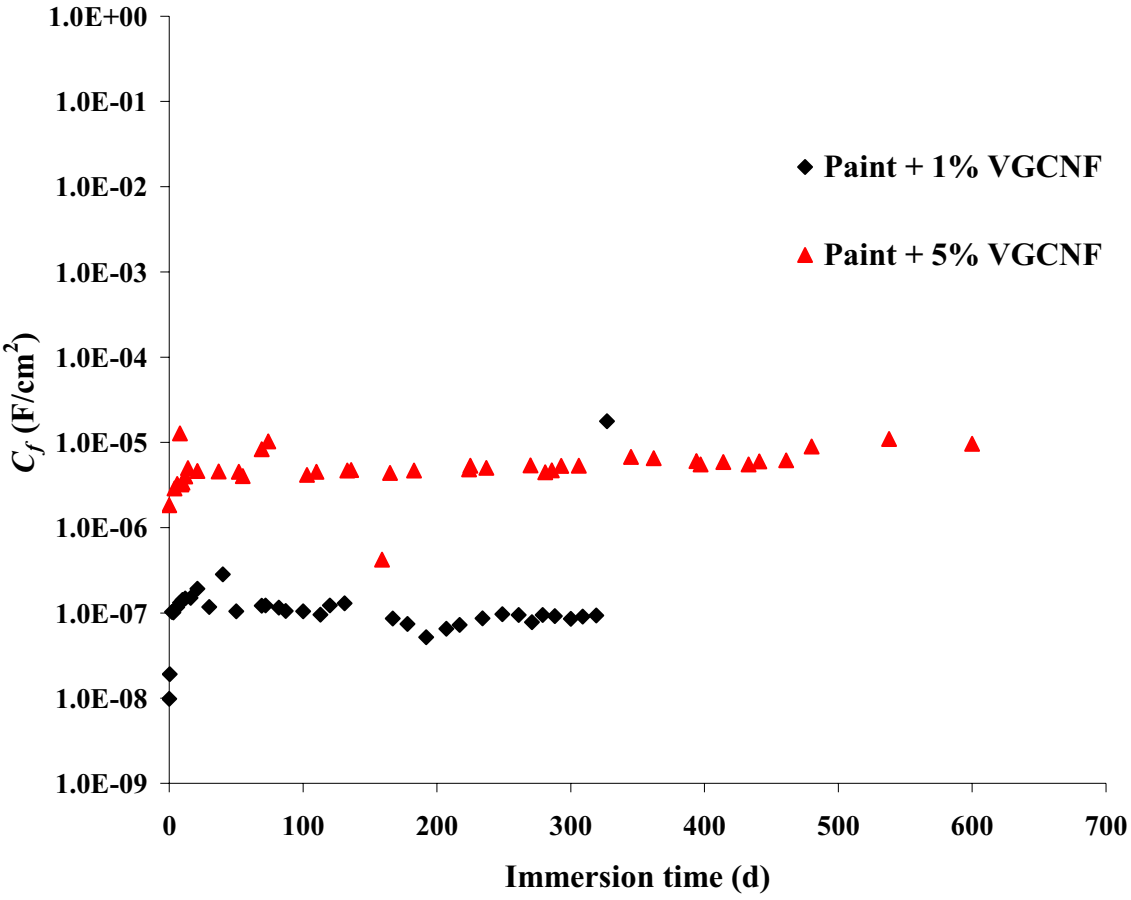

Figure 6.3 Variation of the VGCNF capacitance (C_f) with immersion time for mild steel panels coated with a VGCNF-incorporated commercial alkyd paint film (40 μm thick) and exposed to 3% NaCl solution. ◆ = paint + 1% VGCNF, and ▲ = paint + 5% VGCNF.

immersion in the corrosive medium, indicating the maintenance of good barrier coating. This result is consistent with the nature of VGCNF as a conductive material. The result is also consistent with the electrical conductivity measurements presented in Chapter 2 as well as the literature.[84, 175, 206-208]

Based on the above discussion, it can be clearly stated that, when added to the alkyd paint matrix, VGCNFs act as barrier (inhibitive) pigment and improves the barrier properties of the host matrix through blocking the defective sites and microvoids in the paint matrix and creating longer paths for the corrodents to go through before they reach the metal substrate surface.

The mechanism of corrosion protection offered by SiC-reinforced alkyd paint coating is similar to that mentioned above for VGCNF-reinforced alkyd paint coatings. The mechanism is also consistent with the proposed equivalent electrical circuit as well as the electrical, mechanical, and electrochemical measurements. A comparison between the behavior of SiC microparticles (1.5 μm in diameter) vs. VGCNFs (120 – 200 nm) showed that, although the incorporation of SiC in the paint matrix improves the properties of the paint matrix, the barrier properties of VGCNF-reinforced alkyd paint coatings are better than those of the SiC-reinforced coatings. This can be attributed to the size difference between the SiC microparticles and the VGCNFs. The larger size SiC particles have a higher possibility to agglomerate than the VGCNFs. According to the literature, the mechanical properties of the coating or composite containing SiC particles become worse with increasing the reinforcing particle size.[209-211]

6.4 Future Work

Coating film homogeneity and integrity is an important parameter that affects the chemical, physical, electrical, mechanical, and electrochemical properties, and hence the service life of the coating.[4-6, 174, 212-217] Accordingly, a coating film with uniform distribution of the incorporated particles throughout the matrix is required to enhance the quality of the coating film.[218] As with any other nano-sized material, the small size of the VGCNFs makes the formation of aggregates in the coating matrix practically inevitable.[68, 219-221] Accordingly, one of the immediate goals to complete this investigation is to seek different methods to mix the VGCNFs in the alkyd paint matrix to produce a coating mixture with uniform dispersion of the VGCNFs without destroying the integrity of the VGCNFs or reducing their aspect ratio.

As mentioned above, there is a threshold wt % for any added conductive filler above which the barrier properties as well as the mechanical properties of the host coating deteriorate. This threshold depends on both the type of the conductive filler and the host matrix.[34] So, another future goal of this line of research is to determine the exact threshold VGCNF and SiC wt % in the commercial alkyd paint used in this investigation.

As mentioned above, adhesion is one of the important parameters that greatly determine the stability and lifetime of any organic coating.[178] Accordingly, another immediate goal for this study is to investigate the adhesion properties and the type of bonding between the alkyd paint coatings, with and without VGCNF or SiC, and steel. In this regard, mechanical tests such as cross-cut test, indentation debonding, tensile methods, delamination tests, knife cutting methods, and peel tests will be performed and compared.[178]

Another future goal to complete this study is to accelerate the degradation of the paint coating through techniques, other than the salt spray, that are likely to occur when the paint coatings are in use. Among these accelerated techniques are increasing the temperature and/or changing the pH of the corrosive environment.[222-224] Another technique for accelerating the degradation of organic coatings is the formation of a physical defect (e.g., a pinhole, pore, a scratch, discontinuity, a mechanical damage or deformation) in the paint film, where corrosion would preferentially occur.[225-229] This study would be closer to the actual behavior of organic coatings applied to metallic structures where defects in the coatings could be introduced either during production or generated during the lifetime of the coating.

Another objective to complete this study is to apply the VGCNF-and SiC-modified coatings to mild steel coupons exposed to different real-life (outdoor) atmospheric conditions and follow the long-term corrosion behavior of these substrates. In this regard, coated samples would be mounted in different local sites with different degrees of weather conditions and aggressiveness (temperature, relative humidity, air pollutants, etc) and the EIS measurements are conducted on regular bases for a long period of exposure.[230]

As mentioned above, organic coatings are one of the most economic and effective corrosion resistant materials that are extensively used for the protection and/or decoration of a wide range of substrates including metals and engineering alloys in various environments. According to the U.S. Department of Commerce Census Bureau, the total amount of organic coating material sold in the United States in 1997 was 5.56 billion liters**,** at a value of **$**16.56 billion**.**[231] These figures are increasing annually. Accordingly,

the search for newer inexpensive additives that can improve the barrier properties, and hence the lifetime, of organic coatings will never stop.

Among the factors affecting the corrosion protection performance of any organic coating is the nature (e.g., the electrical properties) of the additives as well as the adhesion properties of the substrate-paint matrix. This makes VGCNF, with its unique properties, an ideal candidate for incorporation in other paints applied to several metals and substrates. Based on this discussion, one of the future goals of this work is to compare the barrier properties as well as the electrical and mechanical properties of a series of commercial paints containing VGCNF and applied to the same metallic substrate.

Another future goal of this line of research is to modify the paint matrix with other powdered materials (such as carbon black, Au, Pt, Al, and Zn powders) and compare the effect of the incorporation of these materials on the corrosion performance of the paint matrix, relative to the unmodified paint when applied on the surface of mild steel samples immersed in 3% NaCl solutions.

6.5 References

(1) Hare, C. H. In *Coatings Technology Handbook* 3rd ed.; Tracton, A. A., Ed.; CRC Press: Boca Raton, FL, 2006, pp 102/101-102/109.

(2) Leidheiser, H., Jr., Ed. *Corrosion Control by Organic Coatings*; NACE: Houston, TX, 1981.

(3) Forsgren, A. *Corrosion Control Through Organic Coatings* CRC Press: Boca Raton, FL, 2006.

(4) Carruth, G. F., Ed. *Organic coatings*; Marcel Dekker, Inc.: New York, 1979.

(5) de Wit, J. H. W.; van der Weijde, D. H.; Ferrari, G. In *Corrosion Mechanisms in Theory and Practice* 2nd ed.; Marcus, P., Ed.; Marcel Dekker, Inc.: New York, 2002, pp 683-729.

(6) Wicks, Z. W. J.; Jones, F. N.; Pappas, S. P. *Organic Coatings - Science and Technology Vol 2. Applications, Properties and Performance* 3rd ed.; John Wiley & Sons, Inc.: Hoboken, NJ, 2007.

(7) Deflorian, F.; Rossi, S.; Vadillo, M. D. C.; Fedel, M. *Journal of Applied Electrochemistry* **2009**, *39*, 2151-2157.

(8) Khanna, A. S., Ed. *High-Performance Organic Coatings: Selection, Application and Evaluation*; CRC Press: Boca Raton, FL, 2008.

(9) Mayne, J. E. O. In *Corrosion,* 2nd ed.; Shreir, L. L., Ed.; Newnes Butterworths: Boston, MA, 1976; Vol. 2, pp 15:24-15:37.

(10) Kendig, M.; Scully, J. *Corrosion* **1990**, *46*, 22-29.

(11) Lu, W.-K.; Basak, S.; Elsenbaumer, R. L. In *Handbook of Conducting Polymers,* 2nd ed.; Skotheim, T. A., Elsenbaumers, R. L., Reynolds, J. R., Eds.; Marcel Dekker, Inc.: New York, 1998, pp 881-920.

(12) Taylor, S. R. *IEEE Transactions on Electrical Insulation* **1989**, *24*, 787-806.

(13) Wittmann, M. W.; Leggat, R. B.; Taylor, S. R. *Journal of the Electrochemical Society* **1999**, *146*, 4071-4075.

(14) Uhlig, H. H.; Revie, R. W. *Corrosion and Corrosion Control: An Introduction to Corrosion Science and Engineering*, 3rd ed.; John Wiley & Sons, Inc.: New York, 1985.

(15) Praveen, B. M.; Venkatesha, T. V. *Journal of Alloys and Compounds* **2009**, *482*, 53-57.

(16) Zhang, W.-G.; Li, L.; Yao, S.-W.; Zheng, G.-Q. *Corrosion Science* **2007**, *49*, 654-661.

(17) Ataee-Esfahani, H.; Vaezi, M. R.; Nikzad, L.; Yazdani, B.; Sadrnezhaad, S. K. *Journal of Alloys and Compounds* **2009**, *484*, 540-544.

(18) Ramalingam, S.; Muralidharan, V. S.; Subramania, A. *Journal of Solid State Electrochemistry* **2009**, *13*, 1777-1783.

(19) Ma, J.; Shi, Y.; Di, J.; Yao, Z.; Liu, H. *Materials and Corrosion* **2009**, *60*, 274-279.

(20) Zamblau, I.; Varvara, S.; Bulea, C.; Muresan, L. M. *Chemical and Biochemical Engineering Quarterly* **2009**, *23*, 43-52.

(21) Wang, S.-C.; Tseng, C.-H. *Advanced Materials Research* **2008**, *51*, 131-139.

(22) Zhou, Y. B.; Qian, B. Y.; Zhang, H. J. *Thin Solid Films* **2009**, *517*, 3287-3291.

(23) Xu, J.; Tao, J.; Jiang, S. *Materials Chemistry and Physics* **2008**, *112*, 966-972.

(24) Chu, X. Y.; Hong, X.; Zhang, X. T.; Zou, P.; Liu, Y. C. *Journal of Physical Chemistry C* **2008**, *112*, 15980-15984.

(25) Praveen, B. M.; Venkatesha, T. V.; Arthoba Naik, Y.; Prashantha, K. *Surface and Coatings Technology* **2007**, *201*, 5836-5842.

(26) Bieganska, B.; Zubielewicz, M.; Smieszek, E. *Progress in Organic Coatings* **1988**, *16*, 219-229.

(27) Funke, W. *Journal of Coatings Technology* **1983**, *55*, 31-38.

(28) Gonzalez, S.; Mirza Rosca, I. C.; Souto, R. M. *Progress in Organic Coatings* **2001**, *43*, 282-285.

(29) Kalendova, A.; Snuparek, J. *FATIPEC Congress* **2000**, *25th*, 21-42.

(30) Kalendova, A.; Sapurina, I.; Stejskal, J.; Vesely, D. *Corrosion Science* **2008**, *50*, 3549-3560.

(31) Bentz, D. P.; Nguyen, T. *Journal of Coatings Technology* **1990**, *62*, 57-63.

(32) Li, C.; Thostenson, E. T.; Chou, T.-W. *Composites Science and Technology* **2008**, *68*, 1227-1249.

(33) Bueche, F. *Journal of Applied Physics* **1972**, *43*, 4837-4838.

(34) Kouloumbi, N.; Tsangaris, G. M.; Skordos, A.; Kyvelidis, S. *Progress in Organic Coatings* **1996**, *28*, 117-124.

(35) De Araujo, F. F. T.; Rosenberg, H. M. *Journal of Physics D: Applied Physics* **1976**, *9*, 1025-1030.

(36) Aharoni, S. M. *Journal of Applied Physics* **1972**, *43*, 2463-2465.

(37) Bhattacharyya, S. K.; De, S. K.; Basu, S. *Polymer Engineering and Science* **1979**, *19*, 533-539.

(38) Malliaris, A.; Turner, D. T. *Journal of Applied Physics* **1971**, *42*, 614-618.

(39) Xu, J.; Donohoe, J. P.; Pittman, C. U., Jr. *Composites, Part A* **2004**, *35A*, 693-701.

(40) Kouloumbi, N.; Tsangaris, G. M.; Kyvelidis, S. T. *Journal of Coatings Technology* **1994**, *66*, 83-88.

(41) Brooman, E. W. *Metal Finishing* **2002**, *100*, 104-110.

(42) Brooman, E. W. *Metal Finishing* **2002**, *100*, 48-52.

(43) Brooman, E. W. *Metal Finishing* **2002**, *100*, 42, 44-47, 49-53.

(44) Miane, J. L.; Achour, M. E.; Carmona, F. *Physica Status Solidi A: Applied Research* **1984**, *81*, K71-K76.

(45) Gurland, J. In *Powder metallurgy in the nuclear age* Metallwerk Plansee AG & Co.: Reutte/Tyrol, Austria, 1962; Vol. 1962, pp 507-518.

(46) Donnet, J. B.; Bansai, R. C.; Wang, M. J., Eds. *Carbon Black: Science and Technology*, 2nd ed.; Marcel Dekker: New York, 1993.

(47) Wissler, M. *Journal of Power Sources* **2006**, *156*, 142-150.

(48) Pandolfo, A. G.; Hollenkamp, A. F. *Journal of Power Sources* **2006**, *157*, 11-27.

(49) Brewer, S. A. In *Coloring of Plastics: Fundamentals,* 2nd ed.; Charvat, R. A., Ed.; John Wiley & Sons, Inc.: Hoboken, NJ, 2004, pp 159-174.

(50) Li, Q.; Yu, N.; Qiu, Z.; Zhou, X.; Wu, C. F. *Colloids and Surfaces, A: Physicochemical and Engineering Aspects* **2008**, *317*, 87-92.

(51) Aoki, Y. *Colloids and Surfaces, A: Physicochemical and Engineering Aspects* **2007**, *308*, 79-86.

(52) Aoki, Y. *Journal of Applied Polymer Science* **2008**, *108*, 2660-2666.

(53) Spain, I. L. In *Chemistry and physics of carbon*; Walker Jr., P. L., Thrower, P. A., Eds.; Marcel Dekker, Inc. : New York 1981; Vol. 16, pp 119-304.

(54) Das, N. C.; Chaki, T. K.; Khastgir, D. *Journal of Polymer Engineering* **2002**, *22*, 115-136.

(55) Das, N. C.; Chaki, T. K.; Khastgir, D.; Chakraborty, A. *Advances in Polymer Technology* **2001**, *20*, 226-236.

(56) Huang, J.-C. *Advances in Polymer Technology* **2002**, *21*, 299-313.

(57) Wang, Y.-J.; Pan, Y.; Zhang, X.-W.; Tan, K. *Journal of Applied Polymer Science* **2005**, *98*, 1344-1350.

(58) El-Tantawy, F.; Kamada, K.; Ohnabe, H. *Materials Letters* **2002**, *56*, 112-126.

(59) Kotsilkova, R.; Nesheva, D.; Nedkov, I.; Krusteva, E.; Stavrev, S. *Journal of Applied Polymer Science* **2004**, *92*, 2220-2227.

(60) Lux, F. *Journal of Materials Science* **1993**, *28*, 285-301.

(61) Chekanov, Y.; Ohnogi, R.; Asai, S.; Sumita, M. *Journal of Materials Science* **1999**, *34*, 5589-5592.

(62) Medalia, A. I. *Rubber Chemistry and Technology* **1986**, *59*, 432-454.

(63) Al-Saleh, M. H.; Sundararaj, U. *Composites, Part A: Applied Science and Manufacturing* **2008**, *39A*, 284-293.

(64) Achour, M. E.; El Malhi, M.; Miane, J. L.; Carmona, F. *Journal of Applied Polymer Science* **1996**, *61*, 2009-2013.

(65) Bigg, D. M. *Polymer Engineering and Science* **1977**, *17*, 842-847.

(66) Dannenberg, E. M. In *Kirk-Othmer Encyclopedia of Chemical Technology,* 3rd ed.; Grayson, M., Ed.; John Wiley & Sons, Inc.: New York, 1978; Vol. 4, pp 631-666.

(67) Pfaff, G.; Buxbaum, G., Eds. *Industrial Inorganic Pigments, Completely Revised and Extended* 3rd ed.; Wiley-VCH Verlag GmbH: Weinheim, Germany, 2005.

(68) Andrews, R.; Jacques, D.; Minot, M.; Rantell, T. *Macromolecular Materials and Engineering* **2002**, *287*, 395-403.

(69) Donnet, J.-B. *Carbon* **1994**, *32*, 1305-1310.

(70) Bourrat, X. *Carbon* **1993**, *31*, 287-302.

(71) Mozetic, M.; Zalar, A.; Panjan, P.; Bele, M.; Pejovnik, S.; Grmek, R. *Thin Solid Films* **2000**, *376*, 5-8.

(72) Heithaus, M.; Foster, J. *Modern Paint and Coatings* **1996**, *86*, 28-33.

(73) Johnson, J. E.; Wnek, W. J. *PPCJ, Polymers Paint Colour Journal* **1995**, *185*, 21, 24, 27.

(74) Calahorra, A.; Aharoni, D.; Dodiuk, H. *Journal of Coatings Technology* **1992**, *64*, 27-31.

(75) Cole, C. A.; Blatt, R. G.; Odell, A. G.; Ruch, E. J. *Proceedings of the Industrial Waste Conference* **1992**, *46th*, 801-810.

(76) Crnjak Orel, Z.; Jerman, R.; Hodoscek, M.; Orel, B. *Solar Energy Materials* **1990**, *20*, 435-454.

(77) Burton, L. C.; Hwang, K.; Zhang, T. *Rubber Chemistry and Technology* **1989**, *62*, 838-849.

(78) Calahorra, A. *Journal of Coatings Technology* **1988**, *60*, 25-30.

(79) Smith, T. *Polymers Paint Colour Journal* **1984**, *174*, 342, 344.

(80) Hess, W. M.; Garret, M. D. *Journal of the Oil and Colour Chemists' Association* **1971**, *54*, 24-83.

(81) Sujith, A.; Unnikrishnan, G. *Journal of Materials Science* **2005**, *40*, 4625-4640.

(82) Manson, J. A.; Sperling, L. H. *Polymer Blends and Composites*; Plenum Press: New York, 1976.

(83) Rwei, S. P.; Ku, F. H.; Cheng, K. C. *Colloid and Polymer Science* **2002**, *280*, 1110-1115.

(84) Zhang, B.; Fu, R.; Zhang, M.; Dong, X.; Zhao, B.; Wang, L.; Pittman, C. U. *Composites, Part A: Applied Science and Manufacturing* **2006**, *37A*, 1884-1889.

(85) Choi, Y.-K.; Sugimoto, K.-I.; Song, S.-M.; Endo, M. *Composites, Part A: Applied Science and Manufacturing* **2006**, *37A*, 1944-1951.

(86) Lozano, K. *JOM* **2000**, *52*, 34-36.

(87) Lozano, K.; Bonilla-Rios, J.; Barrera, E. V. *Journal of Applied Polymer Science* **2001**, *80*, 1162-1172.

(88) Bhattacharyya, S.; Subramanyam, S. V. *Plastics Engineering* **1998**, *45*, 201-296.

(89) Lozano, K.; Yang, S.; Zeng, Q. *Journal of Applied Polymer Science* **2004**, *93*, 155-162.

(90) Li, J.; Luo, R. *Composites, Part A: Applied Science and Manufacturing* **2008**, *39A*, 1700-1704.

(91) Armelin, E.; Aleman, C.; Iribarren, J. I. *Progress in Organic Coatings* **2009**, *65*, 88-93.

(92) Kalendova, A.; Vesely, D.; Sapurina, I.; Stejskal, J. *Progress in Organic Coatings* **2008**, *63*, 228-237.

(93) Fang, J.; Xu, K.; Zhu, L.; Zhou, Z.; Tang, H. *Corrosion Science* **2007**, *49*, 4232-4242.

(94) Yagan, A.; Pekmez, N. O.; Yildiz, A. *Progress in Organic Coatings* **2007**, *59*, 297-303.

(95) Nguyen, T. D.; Nguyen, T. A.; Pham, M. C.; Piro, B.; Normand, B.; Takenouti, H. *Journal of Electroanalytical Chemistry* **2004**, *572*, 225-234.

(96) Vang, C.; Dewald, M.; He, J.; Richter, A.; Tallman, D. E.; Bierwagen, G. P. *Polymer Preprints* **2002**, *43*, 401-402.

(97) Ahmad, N.; MacDiarmid, A. G. *Synthetic Metals* **1996**, *78*, 103-110.

(98) Kendig, M.; Hon, M.; Warren, L. *Progress in Organic Coatings* **2003**, *47*, 183-189.

(99) Talo, A.; Passiniemi, P.; Forsen, O.; Ylaesaari, S. *Synthetic Metals* **1997**, *85*, 1333-1334.

(100) Tallman, D. E.; Spinks, G.; Dominis, A.; Wallace, G. G. *Journal of Solid State Electrochemistry* **2002**, *6*, 73-84.

(101) Colak, N.; Oezyilmaz, A. T. *Polymer-Plastics Technology and Engineering* **2005**, *44*, 1547-1558.

(102) Ding, K.; Jia, Z.; Ma, W.; Jiang, D.; Zhao, Q.; Cao, J.; Tong, R. *Protection of Metals* **2003**, *39*, 71-76.

(103) Tsuchiya, S.; Ueda, M.; Ohtsuka, T. *ISIJ International* **2007**, *47*, 151-156.

(104) Garcia, M. A. L.; Smit, M. A. *Journal of Power Sources* **2006**, *158*, 397-402.

(105) Entezami, A. A.; Massoumi, B. *Current Trends in Polymer Science* **2004**, *9*, 81-89.

(106) Bonastre, J.; Garces, P.; Huerta, F.; Quijada, C.; Andion, L. G.; Cases, F. *Corrosion Science* **2006**, *48*, 1122-1136.

(107) Branzoi, V.; Pilan, L.; Golgovici, F.; Branzoi, F. *Molecular Crystals and Liquid Crystals* **2006**, *446*, 305-318.

(108) Huer, E.; Bereket, G.; Sahin, Y. *Materials Chemistry and Physics* **2006**, *100*, 19-25.

(109) Musiani, M. M. *Electrochimica Acta* **1990**, *35*, 1665-1670.

(110) Rahman, S. U.; Abul-Hamayel, M. A.; Aleem, B. J. A. *Surface and Coatings Technology* **2006**, *200*, 2948-2954.

(111) Tueken, T.; Yazic, B.; Erbil, M. *Materials & Design* **2006**, *28*, 208-216.

(112) Tueken, T.; Yazici, B.; Erbil, M. *Progress in Organic Coatings* **2004**, *51*, 205-212.

(113) Selvaraj, M.; Palraj, S.; Maruthan, K.; Rajagopal, G.; Venkatachari, G. *Synthetic Metals* **2008**, *158*, 888-899.

(114) Gelling, V. J.; Vetter, C.; Somayajula, S. V. K.; Qi, X. *Polymer Preprints* **2008**, *49*, 642-643.

(115) Tueken, T.; Yazici, B.; Erbil, M. *Progress in Organic Coatings* **2005**, *53*, 38-45.

(116) Grgur, B. N.; Krstajic, N. V.; Vojnovic, M. V.; Lacnjevac, C.; Gajic-Krstajic, L. *Progress in Organic Coatings* **1998**, *33*, 1-6.

(117) Tueken, T. *Surface and Coatings Technology* **2006**, *200*, 4713-4719.

(118) Ponce de Leon, C.; Campbell, S. A.; Smith, J. R.; Walsh, F. C. *Transactions of the Institute of Metal Finishing* **2008**, *86*, 34-40.

(119) Leclerc, M.; Najari, A.; Beaupre, S. *Canadian Journal of Chemistry* **2009**, *87*, 1201-1208.

(120) Li, C.; Bai, H.; Shi, G. *Chemical Society Reviews* **2009**, *38*, 2397-2409.

(121) Karyakin, A. A. *Encyclopedia of Sensors* **2006**, *1*, 329-351.

(122) Pringle, J. M.; Forsyth, M.; MacFarlane, D. R. *Electrodeposition from Ionic Liquids* **2008**, 167-211.

(123) Wallace, G. G.; Spinks, G. M. *Chemical Engineering Progress* **2007**, *103*, S18-S24.

(124) Skotheim, T. A.; Reynolds, J. R., Eds. *Handbook of Conducting Polymers, Third Edition: Conjugated Polymers, Theory, Synthesis, Properties, and Characterization*; CRC Press: Boca Raton, FL, 2007.

(125) Stejskal, J.; Kratochvil, P.; Jenkins, A. D. *Polymer* **1996**, *37*, 367-369.

(126) Barisci, J. N.; Lewis, T. W.; Spinks, G. M.; Too, C. O.; Wallace, G. G. *Journal of Intelligent Material Systems and Structures* **1999**, *9*, 723-731.

(127) Nguyen, T. D.; Keddam, M.; Takenouti, H. *Electrochemical and Solid-State Letters* **2003**, *6*, B25-B28.

(128) Sitaram, S. P.; Stoffer, J. O.; O'Keefe, T. J. *Journal of Coatings Technology* **1997**, *69*, 65-69.

(129) Kraljic, M.; Zic, M.; Duic, L. *Bulletin of Electrochemistry* **2004**, *20*, 567-570.

(130) Bernard, M. C.; Hugot-LeGoff, A.; Joiret, S.; Dinh, N. N.; Toan, N. N. *Synthetic Metals* **1999**, *102*, 1383-1384.

(131) Camalet, J. L.; Lacroix, J. C.; Aeiyach, S.; Chane-Ching, K.; Lacaze, P. C. *Synthetic Metals* **1998**, *93*, 133-142.

(132) Kalendova, A.; Vesely, D.; Stejskal, J.; Nemec, P. *Materials Research Innovations* **2009**, *13*, 295-297.

(133) Lu, J. L.; Liu, N. J.; Wang, X. H.; Li, J.; Jing, X. B.; Wang, F. S. *Synthetic Metals* **2003**, *135-136*, 237-238.

(134) McAndrew, T. P. *Trends in Polymer Science* **1997**, *5*, 7-11.

(135) Lu, W.-K.; Elsenbaumer, R. L.; Wessling, B. *Synthetic Metals* **1995**, *71*, 2163-2166.

(136) Adhikari, A.; Claesson, P.; Pan, J.; Leygraf, C.; Dedinaite, A.; Blomberg, E. *Electrochimica Acta* **2008**, *53*, 4239-4247.

(137) Herrasti, P.; Ocon, P.; Ibanez, A.; Fatas, E. *Journal of Applied Electrochemistry* **2003**, *33*, 533-540.

(138) DeBerry, D. W. *Journal of the Electrochemical Society* **1985**, *132*, 1022-1026.

(139) Krstajic, N. V.; Grgur, B. N.; Jovanovic, S. M.; Vojnovic, M. V. *Electrochimica Acta* **1997**, *42*, 1685-1691.

(140) Iroh, J. O.; Su, W. *Electrochimica Acta* **2000**, *46*, 15-24.

(141) Martins, J. I.; Reis, T. C.; Bazzaoui, M.; Bazzaoui, E. A.; Martins, L. *Corrosion Science* **2004**, *46*, 2361-2381.

(142) Kinlen, P. J.; Silverman, D. C.; Jeffreys, C. R. *Synthetic Metals* **1997**, *85*, 1327-1332.

(143) Reut, J.; Opik, A.; Idla, K. *Synthetic Metals* **1999**, *102*, 1392-1393.

(144) Li, P.; Tan, T. C.; Lee, J. Y. *Synthetic Metals* **1997**, *88*, 237-242.

(145) Zhong, L.; Zhu, H.; Hu, J.; Xiao, S.; Gan, F. *Electrochimica Acta* **2006**, *51*, 5494-5501.

(146) Kinlen, P. J.; Ding, Y.; Silverman, D. C. *Corrosion* **2002**, *58*, 490-497.

(147) Williams, G.; McMurray, H. N. *Electrochemical and Solid-State Letters* **2005**, *8*, B42-B45.

(148) Ocon, P.; Cristobal, A. B.; Herrasti, P.; Fatas, E. *Corrosion Science* **2005**, *47*, 649-662.

(149) Rammelt, U.; Nguyen, P. T.; Plieth, W. *Electrochimica Acta* **2003**, *48*, 1257-1262.

(150) de Souza, S. *Surface and Coatings Technology* **2007**, *201*, 7574-7581.

(151) Ogurtsov, N. A.; Shapoval, G. S. *Russian Journal of Applied Chemistry* **2006**, *79*, 605-609.

(152) Spinks, G. M.; Dominis, A. J.; Wallace, G. G.; Tallman, D. E. *Journal of Solid State Electrochemistry* **2002**, *6*, 85-100.

(153) McAndrew, T. P.; Miller, S. A.; Gilicinski, A. G.; Robeson, L. M. *Polymeric Materials Science and Engineering* **1996**, *74*, 204-206.

(154) Araujo, W. S.; Margarit, I. C. P.; Ferreira, M.; Mattos, O. R.; Lima Neto, P. *Electrochimica Acta* **2001**, *46*, 1307-1312.

(155) Bernard, M. C.; Hugot-Le Goff, A.; Joiret, S.; Dinh, N. N.; Toan, N. N. *Journal of the Electrochemical Society* **1999**, *146*, 995-998.

(156) de Souza, S.; Pereira da Silva, J. E.; Cordoba de Torresi, S. I.; Temperini, M. L. A.; Torresi, R. M. *Electrochemical and Solid-State Letters* **2001**, *4*, B27-B30.

(157) Fenelon, A. M.; Breslin, C. B. *Surface and Coatings Technology* **2004**, *190*, 264-270.

(158) Jeyaprabha, C.; Sathiyanarayanan, S.; Venkatachari, G. *Journal of Applied Polymer Science* **2006**, *101*, 2144-2153.

(159) Oezyilmaz, A. T.; Tueken, T.; Yazici, B.; Erbil, M. *Progress in Organic Coatings* **2005**, *52*, 92-97.

(160) Ogurtsov, N. A.; Pud, A. A.; Kamarchik, P.; Shapoval, G. S. *Synthetic Metals* **2004**, *143*, 43-47.

(161) Brusiz, V.; Angelopoulos, M.; Graham, T. *Journal of the Electrochemical Society* **1997**, *144*, 436-442.

(162) Wessling, B. *Advanced Materials* **1994**, *6*, 226-228.

(163) Sangaj, N. S.; Malshe, V. C. *Progress in Organic Coatings* **2004**, *50*, 28-39.

(164) de Wit, J. H. W. In *Corrosion Technology Volume 8: Corrosion Mechanisms in Theory and Practice*; Marcus, P., Oudar, J., Eds.; Marcel Dekker, Inc.: New York, 1995, pp 581-628.

(165) Dickie, R. A.; Floyd, F. L., Eds. *Polymeric Materials for Corrosion Control*; American Chemical Society: Washington, DC, 1986.

(166) Mansfeld, F.; Kendig, M. W. *ASTM Special Technical Publication* **1985**, *866*, 122-142.

(167) Amirudin, A.; Thierry, D. *Progress in Organic Coatings* **1995**, *26*, 1-28.

(168) Nguyen, T.; Hubbard, J. B.; Pommersheim, J. M. *Journal of Coatings Technology* **1996**, *68*, 45-56.

(169) Dickie, R. A. *Progress in Organic Coatings* **1994**, *25*, 3-22.

(170) Leidheiser, H., Jr. *ACS Symposium Series* **1986**, *322*, 124-135.

(171) Leidheiser, H.; Funke, W. *Journal of the Oil and Colour Chemists' Association* **1987**, *70*, 121-132.

(172) Perera, D. Y. *Progress in Organic Coatings* **1996**, *28*, 21-23.

(173) Chuang, T. J.; Nguyen, T.; Lee, S. *Journal of Coatings Technology* **1999**, *71*, 75-85.

(174) Grundmeier, G.; Schmidt, W.; Stratmann, M. *Electrochimica Acta* **2000**, *45*, 2515-2533.

(175) Wu, M.-S.; Lee, J.-T.; Chiang, P.-C. J.; Lin, J.-C. *Journal of Materials Science* **2007**, *42*, 259-265.

(176) Nowacki, L. J. *Paint, Oil and Colour Journal* **1967**, *152*, 211-241.

(177) Dhage, D. In *High Performance Organic Coatings: Selection, Application And Evaluation*; Khanna, A. S., Ed.; CRC Press: Boca Raton, FL, 2008, pp 388-406.

(178) Schweitzer, P. A., Ed. *Paint and Coatings: Applications and Corrosion Resistance*; CRC Press: New York, 2006.

(179) Kalendova, A.; Vesely, D.; Stejskal, J.; Trchova, M. *Progress in Organic Coatings* **2008**, *63*, 209-221.

(180) LaQue, F. L. *Materials and Methods* **1952**, *35*, 77-81.

(181) LaQue, F. L. *Marine Corrosion: Causes and Prevention*; John Wiley & Sons, Inc.: New York, 1975.

(182) Roberge, P. R. *ASTM Special Technical Publication* **1995**, *STP 1238*, 18-30.

(183) Skerry, B. S.; Simpson, C. H. *Corrosion* **1993**, *49*, 663-674.

(184) Haruyama, S.; Asari, M.; Tsuru, T. *Proceedings of the Electrochemical Society* **1987**, *87-2*, 197-207.

(185) Mansfeld, F.; Tsai, C. H. *Corrosion* **1991**, *47*, 958-963.

(186) Tsai, C. H.; Mansfeld, F. *Corrosion* **1993**, *49*, 726-737.

(187) Xiao, H.; Hansfeld, F. *Journal of the Electrochemical Society* **1994**, *141*, 2332-2337.

(188) Lazarevic, Z. Z.; Miskovic-Stankovic, V. B.; Kacarevic-Popovic, Z.; Drazic, D. M. *Corrosion Science* **2005**, *47*, 823-834.

(189) Chaudhari, S.; Patil, P. P. *Journal of Applied Polymer Science* **2007**, *106*, 400-410.

(190) Girardi, F.; Graziola, F.; Aldighieri, P.; Fedrizzi, L.; Gross, S.; Di Maggio, R. *Progress in Organic Coatings* **2008**, *62*, 376-381.

(191) Compere, C.; Frechette, E.; Ghali, E. *Corrosion Science* **1993**, *34*, 1259-1274.

(192) McIntyre, J. F.; Leidheiser, H., Jr. *Journal of the Electrochemical Society* **1986**, *133*, 43-48.

(193) Bajat, J. B.; Dedic, O. *Journal of Adhesion Science and Technology* **2007**, *21*, 819-831.

(194) Kendig, M.; Mansfeld, F. *Materials Research Society Symposium Proceedings* **1988**, *125*, 293-320.

(195) Scully, J. R. *Journal of the Electrochemical Society* **1989**, *136*, 979-990.

(196) Walter, G. W. *Corrosion Science* **1991**, *32*, 1059-1084.

(197) Kendig, M.; Mansfeld, F.; Tsai, S. *Corrosion Science* **1983**, *23*, 317-329.

(198) Amirudin, A.; Thierry, D. *British Corrosion Journal* **1995**, *30*, 128-134.

(199) Mansfeld, F.; Kendig, M. W.; Tsai, S. *Corrosion* **1982**, *38*, 478-485.

(200) Mansfeld, F. *Corrosion* **1988**, *44*, 856-868.

(201) Miskovic-Stankovic, V. B.; Drazic, D. M.; Teodorovic, M. J. *Corrosion Science* **1995**, *37*, 241-252.

(202) Leng, A.; Streckel, H.; Hofmann, K.; Stratmann, M. *Corrosion Science* **1999**, *41*, 599-620.

(203) Leng, A.; Streckel, H.; Stratmann, M. *Corrosion Science* **1999**, *41*, 579-597.

(204) Leng, A.; Streckel, H.; Stratmann, M. *Corrosion Science* **1999**, *41*, 547-578.

(205) Kousik, G.; Pitchumani, S.; Renganathan, N. G. *Progress in Organic Coatings* **2001**, *43*, 286-291.

(206) Al-Saleh, M. H.; Sundararaj, U. *Carbon* **2009**, *47*, 2-22.

(207) Guo, H.; Kumar, S. *PMSE Preprints* **2006**, *94*, 492-493.

(208) Zhang, B.; Fu, R.; Zhang, M.; Dong, X.; Wang, L.; Pittman, C. U. *Materials Research Bulletin* **2006**, *41*, 553-562.

(209) Ahlatci, H.; Candan, E.; Cimenoglu, H. *Zeitschrift fuer Metallkunde* **2002**, *93*, 330-333.

(210) Candan, S. *Materials Letters* **2004**, *58*, 3601-3605.

(211) Ravi, V. A.; Frydrych, D. J.; Nagelberg, A. S. *Transactions of the American Foundrymen's Society* **1995**, *102*, 891-895.

(212) Stratmann, M.; Feser, R.; Leng, A. *Electrochimica Acta* **1994**, *39*, 1207-1214.

(213) Buchheit, R. G. In *Handbook of Environmental Degradation of Materials*; Kutz, M., Ed.; William Andrew, Inc.: Norwich, NY, 2005, pp 367-385.

(214) Suzuki, I. *Corrosion-Resistant Coatings Technology*; CRC Press: Boca Raton, FL, 1989.

(215) Roberge, P. R. *Handbook of Corrosion Engineering*; McGraw-Hill: New York, 2000.

(216) DeRenzo, D. J., Ed. *Handbook of Corrosion Resistant Coatings*; Noyes Data Corporation/Noyes Publications: Park Ridge, NJ, 1986.

(217) Perez, C.; Izquierdo, M.; Abreu, C. M.; Collazo, A.; Merino, P. *Recent Research Developments in Electrochemistry* **2002**, *5*, 115-144.

(218) Choi, Y.-K.; Sugimoto, K.-I.; Song, S.-M.; Gotoh, Y.; Ohkoshi, Y.; Endo, M. *Carbon* **2005**, *43*, 2199-2208.

(219) Liu, L.; Huang, Z. M.; He, C. L.; Han, X. J. *Materials Science & Engineering, A: Structural Materials: Properties, Microstructure and Processing* **2006**, *A435-A436*, 309-317.

(220) Jen, M.-H. R.; Tseng, Y.-C.; Wu, C.-H. *Composites Science and Technology* **2005**, *65*, 775-779.

(221) Breuer, O.; Sundararaj, U. *Polymer Composites* **2004**, *25*, 630-645.

(222) Van der Weijde, D. H.; Van Westing, E. P. M.; De Wit, J. H. W. *Materials Science Forum* **1998**, *289-292*, 237-245.

(223) Angeles, M. E.; Magana, C. R.; Rodriguez, F. J. *Anti-Corrosion Methods and Materials* **2009**, *56*, 154-161.

(224) Oliveira, C. G.; Ferreira, M. G. S. *Corrosion Science* **2002**, *45*, 123-138.

(225) Deflorian, F.; Fedrizzi, L.; Rossi, S.; Bonora, P. L. *Journal of Applied Electrochemistry* **2002**, *32*, 921-927.

(226) Le Thu, Q.; Takenouti, H.; Touzain, S. *Electrochimica Acta* **2006**, *51*, 2491-2502.

(227) Le Pen, C.; Pebere, N.; Lacabanne, C. *Proceedings - Electrochemical Society* **2001**, *2000-24*, 39-49.

(228) Lavaert, V.; Moors, M.; Wettinck, E. *Journal of Applied Electrochemistry* **2002**, *32*, 853-857.

(229) Funke, W. *Special Publication - Royal Society of Chemistry* **1993**, *126*, 179-190.

(230) Palma, E.; Puente, J. M.; Morcillo, M. *Corrosion Science* **1997**, *40*, 61-68.

(231) Corrosion-Doctors Home Page. http://corrosion-doctors.org/PaintCoatings/Frames.htm (accessed Dec 2009)